Fossil

Record

27 (3) 2024

MUSEUM FÜR
NATURKUNDE
BERLIN

PENSOFT

Fossil Record
An International Journal of Palaeontology

Editor-in-Chief

Editorial Secretary

Editorial Board

Fossil Record

2024. Volume 27. Issue 3

ISSN: 2193-0066 (print), 2193-0074 (online)

In Focus

Summary of the changes in composition of the median and temporal series in tetrapods.

See the paper by **Kean KJ, Danto M, Pérez-Ben C, Fröbisch NB** "Evolution of the tetrapod skull: a systematic review of bone loss".

Cover design

PENSOFT®

Fossil Record
An International Journal of Palaeontology

Content of volume **27** (**3**) 2024

Abstract & Indexing Information

Biological Abstracts® (Thompson ISI)
BIOSIS Previews® (Thompson ISI)
Camgridge Scientific Abstracts (CSA/CIG)
Web of Science® (Thompson ISI)
Zoological Record™ (Thompson ISI)

Fossil Record 27 (3) 2024, 289–289 | DOI 10.3897/fr.27.142092

Welcoming address of the Director General

Johannes Vogel[1]

1 *Museum für Naturkunde, Leibniz Institute for Evolution and Biodiversity Science, Invalidenstraße 43, D-10115 Berlin, Germany*

https://zoobank.org/C2BD2083-E38F-4761-825D-EF9F33E8EA68

Corresponding author: Johannes Vogel (johannes.vogel@mfn.berlin)

Published 30 December 2024

Since its foundation in 1998 Fossil Record has found its place in the palaeontological scientific community. Fossil Record has come a long way in the past quarter of a century. The journal has become very visible in the scientific community and is now firmly established in the top quartile of palaeontological journals worldwide. Its impact factor is currently 1.9.

In the beginning a lot of manuscripts were submitted by authors affiliated with the Museum für Naturkunde Berlin (MfN) but today most submissions come from abroad and from authors not affiliated with the MfN. In 2014, a new chapter in the history of Fossil Record began: in consultation with stakeholders the journal was transformed into an open access journal. With this important step, the Museum für Naturkunde Berlin wanted to set an example for the open availability of research results. And our subsequent success proves us right! Furthermore, Fossil Record is one of the few open access journals that does not request article processing charges from the authors. Such costs have been covered by the MfN.

Today, the MfN is very proud to present a special volume to mark the anniversary of its palaeontological journal. Its theme, ‘The fish-to-tetrapod transition and the conquest of land by vertebrates’, fits in perfectly with one of the museum’s main areas of research, in which various research groups are working on the evolution of early land vertebrates. An active and intense excavation and research program is being carried out in Thuringia at the ‘Bromacker’ in close collaboration with Jena University, Stiftung Schloss Friedenstein in Gotha and the UNESCO Geopark Drei Gleichen.

I would particularly like to thank the editorial board of Fossil Record and the publication office of the MfN for their tireless efforts to improve the quality and visibility of the journal. We are proud to have a deep and very trusting cooperation between the Directorate, the MfN publication management team and the editors of Fossil Record. This team approach has certainly contributed to the success of the journal. But my particular thanks go to the three editors of this special volume, who have published a very interesting and diverse cross-section of modern research articles on early tetrapods. I would like to congratulate the journal on its anniversary and wish it all the best for the future. The MfN is very proud of Fossil Record and its other two scientific journals!

Fossil Record 27 (3) 2024, 291–293 | DOI 10.3897/fr.27.143987

Editorial: 25 years of ‘Fossil Record, an International Journal of Palaeontology’

Florian Witzmann[1], Marcello Ruta[2], Nadia Fröbisch[1,3], Stefanie Paß[1], Elisa Herrmann[1]

1 *Museum für Naturkunde, Leibniz-Institut für Evolutions- und Biodiversitätsforschung, Berlin, Germany*
2 *Department of Life Sciences, University of Lincoln, Joseph Banks Laboratories, Green Lane, Lincoln, LN6 7DL, UK*
3 *Institut für Biologie, Humboldt Universität zu Berlin, Berlin, Germany*

https://zoobank.org/0194BBA0-D9D4-43B7-9A93-5E87A5736850

Corresponding author: Florian Witzmann (florian.witzmann@mfn.berlin)

Published 30 December 2024

In his editorial accompanying the first issue of ‘Mitteilungen aus dem Museum für Naturkunde, geowissenschaftliche Reihe’ on 19 November 1998, Prof. Hans Peter Schultze – the journal’s founder and director of the former Institute of Palaeontology at the Museum für Naturkunde Berlin – wrote: ‘I wish for the journal a good start and a successful commencement, with high recognition from the scientific community’. In 2006 the journal was renamed ‘Fossil Record, an International Journal of Palaeontology’ and in 2023 it celebrated its 25th anniversary. Fulfilling Prof. Schultze’s vision and expectations, ‘Fossil Record’ has steadily gained a solid reputation as a well-established, modern scientific outlet, currently ranked within the top quartile of palaeontological journals. The journal attracts a broad international readership and features research in all fields of palaeontology. Paving the way for its success were the tireless efforts of the early editors, Professor Gloria Arratia and Dr. Dieter Korn, who put exacting rules firmly in place in terms of article quality and impact, ultimately leading to the ‘Fossil Record’ being SCIE-listed in 2014. The journal has adhered to its tradition of publishing articles in English, with two volumes released every year, and with a minimum of two international reviewers selected for each article. In a continuous effort of the journal to stay modern, it has now become an international open access journal, a success that has been greatly supported by the Coordination Office for Scientific Publishing as part of the Library. As a key driver of the museum’s Open Access strategy, the Coordination Office plays a crucial role in ensuring that the museum’s Open Access journals, including ‘Fossil Record’, achieve wide visibility and make a meaningful impact within the global scientific community. We extend our heartfelt thanks to our colleagues, as well as the numerous contributors and referees, whose dedication and expertise have significantly contributed to the rapid growth and success of ‘Fossil Record’. Our gratitude also goes to the Museum für Naturkunde and its Directorate General for generously covering the author page charges, and to the Library for their steadfast commitment to promoting Open Access at the museum.

This special issue celebrates the 25th anniversary of ‘Fossil Record’. We chose ‘The fish-to-tetrapod transition and the conquest of land by vertebrates’ as its overarching topic. This research topic has a long tradition at the Museum für Naturkunde, starting with contributions by the eminent palaeoichthyologist and histologist, Walter Gross (1903–1974), to whom we owe the discovery and first description of the Devonian tetrapod-like fish *Panderichthys rhombolepis*, the holotype of which is kept at the Museum für Naturkunde. Hans-Peter Schultze and his working group continued Gross’ work and amplified its scope. Schultze published important new findings on *Elpistostege*, a relative of *Panderichthys* that is even closer to tetrapods than the latter and conducted research on the phylogenetic status of tetrapods as a monophyletic group and the environmental conditions accompanying the transition from fishes to tetrapods. For short intervals, distinguished early tetrapod-researchers, including Michel Laurin (from 1997 to 1998) and Rainer Schoch (from 2001 to 2002) worked at the Museum für Naturkunde. Today, the long tradition of early tetrapod research at the Museum continues with the activities of the research groups led by Nadia Fröbisch and Florian Witzmann, with primary focus on temnospondyl amphibians.

Vertebrate terrestrialization is a major chapter in animal evolution. Following the conquest of the land, vertebrates evolved a remarkable diversity of body proportions and a wide array of feeding, locomotory, and sensory adaptations. Early tetrapods are of great interest to the scientific community because they illuminate the rise of modern terrestrial ecosystems and the deep roots of much of today's terrestrial vertebrate diversity. Last but not least, this topic is of great interest for the public at large, because it is one of the major evolutionary transitions and research on early tetrapods is also the study of our own remote ancestry.

We are delighted to present this special volume to mark the achievements of 'Fossil Record' and the increasing importance and reach of early tetrapod studies. The volume features a welcoming address by Prof. Johannes Vogel, the Director General of the MfN, followed by a contribution by Prof. Hans-Peter Schultze, who provides an account of the founding of the journal in 1998 and the difficulties it faced in the beginning. The centerpiece of the volume consists of eight original research articles written by 18 international authors, both established scientists and young researchers. The articles cover a wide range of topics such as the palaeoecology of the fish-tetrapod transition, morphology and phylogeny of stem tetrapods, phylogeny and morphology of temnospondyls, the convergent evolutionary simplification of the tetrapod skull, and biomechanics of the skull in semiaquatic and terrestrial tetrapods.

The first article, by Michel Laurin, examines the extent to which the habitats of the early tetrapods revealed a marine influence, a question that has long been controversial. Originally it was assumed, by analogy with modern amphibians, that early tetrapods inhabited freshwater environments, where they had originated from fish-like ancestors. Accordingly, most early tetrapods were thought to be unable to tolerate brackish or marine environments. Based on a vast compendium of data and a literature survey, Michel Laurin builds upon his earlier study on this topic that he undertook with Rodrigo Soler-Gijón in 2010. Following different lines of evidence, he shows that many early tetrapods were euryhaline and lived in brackish waters or even marine settings and concludes that tetrapods originated in marine environments.

The first body fossils of stem-tetrapods with limbs are known from the Late Devonian. In the first 15 million years of the subsequent Carboniferous Period (the Tournaisian and parts of the Viséan), only very few remains of tetrapods have been found worldwide, a circumstance to which this time interval owes its name, "Romer's Gap". In recent years, however, new finds from the Early Carboniferous, particularly from Scotland and Canada, have begun to close this gap. In the second article, Tim Smithson and Marcello Ruta – along with the late Jenny Clack – redescribe one of the recently discovered Tournaisian tetrapods, *Ossirarus kierani* from Scotland, which shows a mosaic of plesiomorphic and derived characters. Their phylogenetic results strengthen the hypothesis that the morphological and taxonomic diversity of early tetrapods in the lowermost Carboniferous were greater than previously assumed.

Different groups of tetrapods independently showed a reduction and loss of skull roof bones, attaining a simpler skull morphology relative to tetrapodomorph fishes and various Devonian and later Paleozoic groups. In the third article, Kim Kean, Marylène Danto, Celeste Pérez-Ben and Nadia Fröbisch provide an overview of the groups of tetrapods in which a reduction of the cranial bones took place and how this occurred. Interestingly, the loss of individual bones was very variable and cannot be correlated with a particular lifestyle or body size, suggesting complex and as yet poorly understood morphogenetic patterns.

The eryopids are a diverse group of Permo-Carboniferous temnospondyls that had transitioned from the strictly aquatic existence of their ancestors to a more amphibious mode of life. While the phylogenetic position of eryopids within temnospondyls is well established, the relationships within the group are controversial. The affinities of three taxa from the Middle Permian of Russia, *Clamorosaurus borealis*, *C. nocturnus* and *Syndyodosuchus*, have remained elusive so far. In the fourth article, Ralf Werneburg and Florian Witzmann undertake a detailed redescription of their anatomy and lifestyle, and present a comprehensive phylogenetic analysis of eryopids. They retrieve no support for the previously held hypothesis that the Russian eryopids were terrestrial animals and argue that a semiaquatic lifestyle is more probable.

In the fifth article, Raphael Moreno, Sanjukta Chakravorti, Samuel Cooper and Rainer Schoch address the taxonomic diversity and palaeobiogeographic and stratigraphic distribution of temnospondyls in the partially marine Grabfeld Formation (Gipskeuper) of southwestern Germany, straddling the Ladinian-Carnian boundary. Although the frequent occurrences of sabkha and playa deposits suggest arid environmental conditions, the authors demonstrate a surprising diversity of temnospondyls belonging to at least three families, including the oldest occurrence of a metoposaurid. This work presents important palaeobiogeogaphic data on temnospondyls in the Ladinian and Carnian and provides evidence that many members of this group were euryhaline.

The ontogeny of Palaeozoic temnospondyls included a larval phase similar to that of modern salamanders and has been studied for more than 150 years. In contrast, the ontogeny of the predominantly Mesozoic stereospondyls remains poorly understood. In the sixth article of this volume, Rainer Schoch, Florian Witzmann, Raphael Moreno, Ralf Werneburg and Eudald Mujal describe for the first time the ontogeny of the largest known temnospondyl, the capitosaurian stereospondyl *Mastodonsaurus giganteus* from the Middle Triassic of Germany, with preserved skulls ranging between 12–15 mm and 1200 mm. In contrast to the larval ontogenies of Palaeozoic forms, *Mastodonsaurus* attained adult morphological characteristics of its skull and postcranium early in ontogeny, with juvenile and adult skulls differing mainly in overall proportions. The findings broaden our knowledge of stereospondyl ontogeny and indicate a major shift in the developmental mode of stereospondyls relative to their Palaeozoic relatives.

The seventh article, by Pummy Roy, Sanjukta Chakravorti and Dhurjati Prasad Sengupta, expands our knowledge of Gondwanan tetrapod assemblages throughout the Triassic. Based on newly found and hitherto undescribed material, the authors address the taxonomy and morphology of an apex predator, the giant capitosaur *Cherninia denwai* from the middle Triassic Denwa Formation of central India. In addition to cranial material, they also document several postcranial bones for the first time.

The eighth article, by Ingmar Werneburg, discusses the biomechanical basis for the formation of cranial openings in tetrapods, including temporal fenestrae, palatal vacuities and squamosal embayments, during the evolutionary transition from water to land. The author documents differences in the mode of feeding and body posture in two semi-aquatic early tetrapods (a stereospondyl amphibian and a stem-amniote) and two terrestrial amniotes (an early archosaur and a dinosaur), and concludes that the formation or closure of skull openings is tightly correlated with the bite force exerted by the jaw adductors as well as with the presence of cranial weapons (e.g., horns, frills, protuberances). Additionally, the author shows how the stress induced by the neck musculature may have an impact on the skull architecture. Finally, he provides a new hypothesis for the evolution of skull openings, especially in the temporal region, based on biomechanical considerations.

We hope that this special issue will stimulate further discussions and scientific work in the field of early tetrapods. Special thanks go to go to the Department Service Development and Impact whose generous financial support made this special issue possible. We would also like to express our sincere thanks to Pensoft Publishers for the excellent cooperation. Last but not least, we wish to thank all the authors of this special issue for their contributions, and the numerous reviewers whose expertise greatly enhanced the quality of the articles.

Fossil Record 27 (3) 2024, 295–297 | DOI 10.3897/fr.27.141907

The start of the scientific journal ‘Fossil Record’

Hans-Peter Schultze[1]

1 *Biodiversity Institute, University of Kansas, Dyche Hall, Lawrence, Kansas 66045, USA*

https://zoobank.org/4861F867-3EA9-4D3F-82A6-50486F475C73

Corresponding author: Hans-Peter Schultze (hp1937@ku.edu)

Academic editor: Florian Witzmann ♦ **Received** 15 November 2024 ♦ **Accepted** 13 December 2024 ♦ **Published** 30 December 2024

Abstract

This article describes the early years of the journal Fossil Record and the circumstances at the Museum für Naturkunde and the Humboldt University Berlin under which the foundation of the journal took place. The former Department of Palaeontology of the Museum für Naturkunde had a strong interest to publish its own scientific journal, and this led to the foundation of the journal in 1998 which is known today as Fossil Record. For reasons of a corporate similar appearance it was decided that the new journal as well as the two older scientific journals of the Museum für Naturkunde use the common title Mitteilungen aus dem Museum für Naturkunde in Berlin (Communications from the Museum of Natural History in Berlin) with subtitles for all three journals: Geowissenschaftliche Reihe for the palaeontological journal, Zoologische Reihe for the zoological journal and Deutsche Entomologische Zeitschrift for the entomological journal. With volume 9 (2006), the palaeontological journal appeared under the new title Fossil Record. From the beginning it was a goal of the editors to reach the international community by opening the journal to authors outside the museum and by publishing mainly in English. The palaeontological journal Fossil Record has developed from an in-house journal with international contributions to an internationally well cited journal.

Key Words

Department of Palaeontology, Humboldt University, Mitteilungen aus dem Museum für Naturkunde in Berlin, Museum für Naturkunde

The precursors of the Museum für Naturkunde (= Museum of Natural History), Berlin were the nucleus of the Universität zu Berlin at its founding in 1810 (Hoppe 1998, 1999). Geosciences were represented by the mineralogist Christian Samuel Weiss (Hoppe 2000). In 1889 the collections moved location from the main building of the university at Unter den Linden 6 to Invalidenstr. 43, which is still the present address of the museum. Only the departments of Mineralogy, Geology/Palaeontology and Zoology were established in the new building (Hoppe 2003). Palaeontology dominated geoscience over the next 43 years until the arrival of the tectonic geologist Hans Stille, who put emphasis on geology in the broad sense (Gross and Schultze 2004). The Department of Geology survived WWII, but not the university reform of the GDR (Deutsche Demokratische Republik) in 1968, when it lost its independence as a department, although the curatorships continued to exist as part of the Humboldt Universität, the new name of the Friedrich-Wilhelm-Universität after WWII.

After the German reunification in 1990, three scientific departments, Palaeontology, Mineralogy and Zoology, were reestablished at the Museum für Naturkunde; Palaeontology as Palaeobiology - and unique for Germany - with teaching duties in the Department of Biology of the Humboldt Universität (with the argument that classical geology/palaeontology already existed at the Freie Universität in Berlin and applied geology at the Technische Universität also in Berlin).

All three departments, Zoology, Palaeontology and Mineralogy, belonged to the Humboldt Universität, with one of the three directors as general director of the Museum für Naturkunde (the mineralogist Prof. Dr. Dieter Stöffler in the first years 1993–1999, followed by Hans-Peter Schultze from 1999 to 2004). The budget of the museum had to be decided between the three directors, and one item concerned publications. The Department of Zoology published three scientific journals (Mitteilungen aus der Zoologischen Sammlung des Museums für Naturkunde in

Berlin since 1898; Deutsche Entomologische Zeitschrift since 1857 [1875]; and Annalen für Ornithologie since 1977), whereas the other two departments published none. The Department of Palaeontology had a strong interest to change that deficiency to be able to publish monographs and volumes dedicated to single subjects like Tendaguru, whereas the Department of Mineralogy preferred to not publish in an in-house journal. The director of Zoology, Prof. Ulrich Zeller was willing to integrate the Annalen für Ornithologie with the Mitteilungen aus der Zoologischen Sammlung des …. (Zeller et al. 1998), and consequently, there was basic funding available for a geoscience journal. During the discussions concerning a name of the geoscience journal, having a corporate similar appearance was the argument of the director Stöffler to use the common title Mitteilungen aus dem Museum für Naturkunde in Berlin (= Communications from the Museum of Natural History in Berlin; Fig. 1A–C) with subtitles for all three journals.

Figure 1. Publications of the Museum für Naturkunde in Berlin. **A–C.** Mitteilungen aus dem Museum für Naturkunde in Berlin in 1998; **A.** Deutsche Entomologische Zeitschrift; **B.** Zoologische Reihe; **C.** Geowissenschaftliche Reihe; **D.** Fossil Record vol. 11(1) in 2008.

The Mitteilungen aus dem Museum für Naturkunde in Berlin, Geowissenschaftliche Reihe contain only palaeontological papers and the history of the two geoscience departments (Hoppe 1998, 1999, 2000, 2001, 2003; Gross and Schultze 2004). It was a goal to reach the international community by opening the journal to authors outside the museum and by publishing mainly in English. Managing editor Prof. Dr. Gloria Arratia worked hard towards the internationalization by approaching and inviting colleagues outside of the museum and explaining advantages to publish in the journal. A little more than half the authors were not members of the Palaeontology Department. On the other side, the assistant editor Mrs. Petra Keßling helped old colleagues of the GDR adapt to the modern publication requirements, apart from continuing to publish in German. From 1998 (volume 1) until 2005 (volume 8), 97 papers were published under the journal name Mitteilungen aus dem Museum für Naturkunde in Berlin. Geowissenschaftliche Reihe. Volume 2 contains 14 papers on fossils from Tendaguru collected before WWI. Volume 5 is the Festband for the 65th birthday of the director of the Department of Palaeontology, Hans-Peter Schultze; it contains 21 papers.

For volume 8 (2005), the new managing editor Dr. Dieter Korn prepared the journal for acceptance in the citation index with articles assigned a doi number available on line; with volume 9 (2006), the volumes appeared in two issues per year under the new title Fossil Record, a name suggested by Dr. Wolfgang Kiessling, and, starting with volume 11 (2008, Fig. 1D), a new color and changing design from issue to issue (Aberhan 2008). A new name and design were also given to the zoological journal (Zoosystematics and Evolution; Glaubrecht et al. 2008). The corporate title was omitted with the change to the new publisher Pensoft in 2014 for the Deutsche Entomologische Zeitschrift (Zimmermann and Paß 2022) and Zoosystematics and Evolution and in 2021 for the Fossil Record. The palaeontological journal Fossil Record has developed from an in-house journal with international contributions to an internationally well cited journal.

References

Aberhan M (2008) Address by the Editor-in-Chief. Mitteilungen aus dem Museum für Naturkunde in Berlin, Fossil Record 11(1): 5. https://doi.org/10.1002/mmng.200700007

Glaubrecht M, Bartsch P, Ohl M (2008) Editorial. Zoosystematics and Evolution – an evolving journal. Mitteilungen aus dem Museum für Naturkunde in Berlin, Zoosystematics and Evolution 84(1): 5–8. https://doi.org/10.1002/zoos.200700009

Gross W, Schultze H-P (2004) Zur Geschichte der Geowissenschaften im Museum für Naturkunde zu Berlin. Teil 6: Geschichte des Geologisch-Paläontologischen Instituts und Museums der Universität Berlin 1910–2004. Mitteilungen aus dem Museum für Naturkunde in Berlin, Geowissenschaftliche Reihe 7: 5–43. https://doi.org/10.1002/mmng.4860070103

Hoppe G (1998) Zur Geschichte der Geowissenschaften im Museum für Naturkunde zu Berlin Teil 1: Aus der Vorgeschichte bis zur Gründung der Berliner Bergakademie im Jahre 1770. Mitteilungen aus dem Museum für Naturkunde in Berlin, Geowissenschaftliche Reihe 1: 5–19. https://doi.org/10.1002/mmng.4860010102

Hoppe G (1999) Zur Geschichte der Geowissenschaften im Museum für Naturkunde zu Berlin Teil 2: Von der Gründung der Bergakademie zur Gründung der Universität 1770–1810. Mitteilungen aus dem Museum für Naturkunde in Berlin, Geowissenschaftliche Reihe 2: 3–24. https://doi.org/10.5194/fr-2-3-1999

Hoppe G (2000) Zur Geschichte der Geowissenschaften im Museum für Naturkunde zu Berlin Teil 3: Von A. G. Werner und R. J. Haüy zu C. S. Weiss – Der Weg von C. S. Weiss zum Direktor des Mineralogischen Museums der Berliner Universität. Mitteilungen aus dem Museum für Naturkunde in Berlin, Geowissenschaftliche Reihe 3: 3–25. https://doi.org/10.1002/mmng.4860030102

Hoppe G (2001) Zur Geschichte der Geowissenschaften im Museum für Naturkunde zu Berlin Teil 4: Das Mineralogische Museum der Universität Berlin unter Christian Samuel Weiss von 1810 bis 1856. Mitteilungen aus dem Museum für Naturkunde in Berlin, Geowissenschaftliche Reihe 4: 3–27. https://doi.org/10.1002/mmng.4860040102

Hoppe G (2003) Zur Geschichte der Geowissenschaften im Museum für Naturkunde zu Berlin Teil 5: Vom Mineralogischen Museum im Hauptgebäude der Universität zu den zwei geowissenschaftlichen Institutionen im Museum für Naturkunde – 1856 bis 1910. Mitteilungen aus dem Museum für Naturkunde in Berlin, Geowissenschaftliche Reihe 6: 3–51. https://doi.org/10.1002/mmng.4860060102

Zeller U, Ade M, Bartsch P, Glaubrecht M (1998) Editorial. A century of scientific publication continued. Mitteilungen aus dem Museum für Naturkunde in Berlin, Zoologische Reihe 74(1): 3–4. https://doi.org/10.1002/mmnz.4850740102

Zimmermann D, Paß S (2022) Editorial Response to a proposed name change for our journal. Mitteilungen aus dem Museum für Naturkunde in Berlin, Deutsche Entomologische Zeitschrift 69(2): 123–124. https://doi.org/10.3897/dez.69.89973

Fossil Record 27 (3) 2024, 299–332 | DOI 10.3897/fr.27.123291

PENSOFT.

für Natur MUSEUM FÜR NATURKUNDE BERLIN

Habitat of early stegocephalians (Chordata, Vertebrata, Sarcopterygii): a little saltier than most paleontologists like?

Michel Laurin[1]

1 *CR2P (Centre de Recherches en Paléontologie – Paris), CNRS/MNHN/Sorbonne Université, Muséum national d'Histoire naturelle, 75231 Paris cedex 05, France*

https://zoobank.org/467D5A67-9D29-44FB-8AB8-3003D6C2635F

Corresponding author: Michel Laurin (michel.laurin@mnhn.fr)

Academic editor: Florian Witzmann ♦ **Received** 17 March 2024 ♦ **Accepted** 9 May 2024 ♦ **Published** 30 December 2024

Abstract

A controversy on the degree of marine influence in the paleoenvironments represented by many Paleozoic stegocephalian-bearing fossiliferous localities has persisted for decades. Many authors have equated the absence of a typical stenohaline marine fauna with freshwater environments, but this ignores continental salt lakes and the many transitional environments (deltaic, estuarine, lagoonal, and some epicontinental seas that receive much freshwater influx, like the Baltic Sea) that separate typical marine environments from freshwater environments. This is problematic because it seems plausible that many of the late Paleozoic sediments that have been preserved were deposited on coasts in deltas and estuaries. The author had compiled a dataset of paleoenvironmental interpretations of Devonian to Early Permian stegocephalian ("tetrapod")-bearing fossiliferous localities in 2010. How have these interpretations withstood the test of time, especially in the face of new results from different kinds of evidence? An updated dataset and a new literature review show that the case for a marine origin of stegocephalians has strengthened, especially through additional discoveries or reinterpretations of fossils that suggest marine influence in various classical vertebrate-bearing Permo-Carboniferous localities traditionally interpreted as freshwater, and a recent analysis of stable isotopes in Late Devonian localities.

Key Words

Amphibians, brackish, Carboniferous, Devonian, epicontinental seas, freshwater, marine environment, paleoenvironments, Permian, tetrapods

Introduction

Most early studies on Paleozoic stegocephalians have assumed that these taxa normally inhabited freshwater or dry land, unless their remains were clearly associated with typically marine fossils. This is exemplified by this quote from Milner (1987: 497):

> *"Most of the British and North American tetrapod localities represent water bodies within non-marine swamps and have generally been assumed to be in the freshwater regions of fluviodeltaic systems,* ***not least because of the presence of amphibians as presumed freshwater indicators*** *together with the absence of unambiguously marine organisms."* (Emphasis mine in all quotes unless stated otherwise.)

Thus, the fact that most of the Devonian and Carboniferous stegocephalians were called "amphibians" (in the paraphyletic sense of "anamniotic limbed vertebrate") probably played a role in this, even though parsimony does not validate the inference that these were freshwater taxa (Laurin and Soler-Gijón 2010).

This quote highlights the need for a precise nomenclature. Indeed, if the word "amphibians" had been consistently used in the sense that is now established under the PhyloCode (Cantino and de Queiroz 2020), as the lissamphibian total-group (Laurin et al. 2020), it is possible that the paleoenvironment of many Permo-Carboniferous localities would have been interpreted more cautiously. Similarly, it may be useful to mention here the difference between Tetrapoda (or “tetrapods”), and Stegocephali (or “stegocephalians”) as used in this report. Both terms are here used as established under the PhyloCode. Namely, Stegocephali is defined as “The largest clade that includes *Eryops megacephalus* Cope 1877 (Temnospondyli) but not *Tiktaalik roseae* Daeschler et al. 2006, *Panderichthys rhombolepis* Gross 1930 (Panderichthyidae), and *Eusthenopteron foordi* Whiteaves 1881 (Osteolepiformes).” As such, it includes all known limbed vertebrates, and may conceivably contain some finned tetrapodomorphs, given that the fragmentary remains of the basalmost members of that clade, like *Elginerpeton* and *Ventastega*, cast doubt on the nature of their paired appendages (Laurin 2010). Tetrapoda is defined as the crown-group of limbed vertebrates, or the smallest clade that includes lissamphibians and amniotes, to simplify the definition provided by Laurin (2020a). As such, Tetrapoda is less inclusive than Stegocephali; it minimally excludes Devonian limbed vertebrates like *Acanthostega*, *Ichthyostega* and *Tulerpeton*, and under some phylogenies (e.g., Marjanović and Laurin 2019: fig. 14), it also excludes temnospondyls, embolomeres and seymouriamorphs. This review focuses on all stegocephalians, not only on tetrapods.

Many late Paleozoic fossiliferous localities lacking fossils of stenohaline, strictly marine organisms (such as echinoderms, cephalopods and coral reefs) have been interpreted as freshwater habitats, or the marine influence on such habitats has been minimized. However, factors other than low and fluctuating salinity may explain the absence of many stenohaline marine taxa; these include high sedimentation rates and turbidity (Feldman et al. 1993: 494), which are deleterious to filter-feeding, sessile organisms, as well as photosynthetic ones. Most contemporary estuaries and possibly tide-dominated deltas are precisely zones of maximal turbidity, because of tidal circulation and coagulation of clays resulting from mixing of fresh and salt water (Feldman et al. 1993: 494). This makes such environments difficult to recognize in the fossil record; the absence of typical marine taxa therein may well lead to erroneous interpretations of a freshwater environment.

Taxa found in these localities were often assumed to have been stenohaline, freshwater forms. Carpenter et al. (2011: 639) summarized this potential source of bias thus: “Traditionally, Pennsylvanian fishes have been classified either as marine or nonmarine (Calder 1998), the latter often taken to mean freshwater (Dick 1998).” Worse, they pointed out that “In very many cases, the mere absence of an associated stenohaline fauna and the co-occurrence of plant fossils have been cited as sure evidence for a freshwater habitat”. This comment could apply to the classical Texas Cisuralian redbeds, which include many of the most fossiliferous stegocephalian-bearing localities (Fig. 1). Yet, brackish water is not uncommon, especially along the coasts in deltas, estuaries, lagoons, and large epicontinental seas, such as the Baltic Sea, and it seems that brackish habitats were widespread in the past too (Buatois et al. 1998, 2005; Falcon-Lang 2005). Furthermore, most sediments ultimately end up in the seas and oceans, with the continents providing only temporary storage (Hay 1998). Some rivers flow toward internal basins without connection to the seas, but these basins represent a small proportion of the emerged lands, and their main water bodies (e.g., Great Salt Lake in the USA, Dead Sea in the Middle East, etc.) typically contain saltwater (Moscatello and Belmonte 2009; Pagaling et al. 2009: 5751), which implies that the deltas and estuaries of rivers that flow into these salt lakes are brackish. Given that most sedimentation occurs in deltas and estuaries along the coasts (Peters and Husson 2017: 323) and that these environments are among the most favorable for fossilization, it seems plausible that most vertebrate fossils might come from such environments. However, the literature suggests that most Permo-Carboniferous stegocephalians that left a fossil record inhabited freshwater bodies, which may seem anomalous given where most of the long-term sedimentation occurs.

Determining the habitat of long-extinct taxa is difficult because sedimentation and regression/transgression cycles cause shorelines to move quickly in geological terms (Carpenter et al. 2011 and references therein), and carcasses can be transported before being buried and fossilized. Thus, progress on this front will ultimately require detailed inventories of taxa occurring in fairly narrow strata and with good geographic data. The literature is not as rich as we would like in such detailed studies, but the review below tries to summarize a representative sample of the data currently available, especially in the Famennian and Carboniferous and, to a lesser extent, in the Cisuralian.

Fortunately, some studies considered brackish habitats in their assessment of paleohabitats, but often still seem to have minimized the marine influence. This can be illustrated by the “Birthday Bonebed” of the Permo-Carboniferous Halgaito Formation (Utah), which was studied recently by Huttenlocker et al. (2018), who suggested (p. 87) that

> *Within the bonebed, microconchids, xenacanths, actinopterygians, and the lungfish* Sagenodus *suggest an assemblage that was to some degree dependent on permanent standing water. We interpret these stream systems, particularly those associated with the major tiered channel bodies, as* ***primarily freshwater with little marine influence****, though the microconchids and xenacanths potentially leave open the possibility of proximity to marine-influenced channel reaches (Carpenter et al., 2015; Ó Gogáin et al., 2016).*

However, Huttenlocker et al. (2018: 87) concluded that the aquatic fauna preserved in the bonebed included “**freshwater** xenacanths, actinopterygians, and lungfish” (in addition to the aquatic to amphibious temnospondyl *Eryops* and some presumably more terrestrial

Figure 1. A *Dimetrodon grandis* chases an *Eryops megacephalus* and an *Edaphosaurus pogonias* through a *Sigillaria* forest. In the foreground, a *Meganeuropsis* flies near strobili of *Equisetum hyemale*; the ground is covered by mosses. Reconstruction of the Artinskian (Early Permian) in what is now Texas, USA. Drawing by Ruben Koops (Haarlem, Netherlands), Rafael Albo (Corumbá, Brazil), Jacek Major (Starachowice, Poland), and Amin Khaleghparast (a biologist from Tehran, Iran); coloring by Ruben Koops. Advisors for *Dimetrodon*: Tracy Lee Ford (San Diego, California, USA) and Russell J. Hawley (Casper, Wyoming, USA). Advice on plants was provided by Ryan Thummel and Paige K. Wilson Deibel (both at U. of Washington).

eupelycosaur amniotes). As this quote shows, a primarily freshwater interpretation is favored, despite the presence of microconchids, xenacanths, and dipnoans, three clades of marine origin. Of these, only diponans are still extant, and may thus have played a greater role, historically, in inferring paleoenvironments. Extant dipnoans inhabit freshwater and by the Carboniferous, some had already invaded freshwater environments, but other remained marine (Schultze and Soler-Gijón 2004: 341); thus, their presence in a Carboniferous locality does not resolve the degree of marine influence. Microconchids and xenacanths are frequently associated with early stegocephalians, which justifies a short review of their probable paleoenvironment (in dedicated sections below). The predominantly freshwater interpretation of the Halgaito Formation by Huttenlocker et al. (2018) is surprising given that they indicated (pp. 73–74) interfingering with a marine facies in the lower half of the formation. Given that the "Birthday Bonebed" is precisely in the lower half of this formation, the open sea (preserved in the marine facies) was presumably not far. Similarly, Huttenlocker et al. (2018: 86) reported results of their strontium isotopic analyses, and concluded that "These results are consistent with the hypothesis that tooth formation occurred in an environment with **some freshwater-influence**, supporting that the xenacanths associated with the bonebed were either occasional or permanent residents of these **freshwater systems**." Note how the indication of freshwater influence was used to infer that the xenacanths lived in freshwater. Why could the "Birthday Bonebed" not represent a marginal-marine, brackish-water environment? As we will see below, interpreting the isotopic signatures is not always straightforward.

I studied the problematic paleoenvironments inhabited by Permo-Carboniferous stegocephalians before (Laurin and Soler-Gijón 2010), but some important empirical studies were published since then, and my earlier study did not cover (or only superficially) some relevant topics, such as the probable habitat of some taxa frequently associated with Paleozoic stegocephalians; this new review attempts to fill some of these gaps, especially the probable habitat of various taxa frequently associated with stegocephalians, in the same temporal interval (Famennian to Kungurian). This paper first presents (below) evidence that marine influenced has been minimized in many earlier studies, as shown for three examples; it then surveys briefly the main isotopic methods that have been used to assess paleosalinity. This is followed by sections on the paleoenvironmental significance of several taxa that are often associated with early stegocephalians. All of these data are then used to review the paleoenvironments of a few Famennian and Carboniferous localities that have yielded stegocephalians; Cisuralian localities would be relevant too, but could not be included for lack of time and space.

Biased interpretation in favor of freshwater?

Unrecognized tidal deposits?

There are reasons to believe that the extent of marine influence in the habitat of early stegocephalians has been significantly under-estimated in the literature (see below). A similar bias against marginal-marine environments has recently been argued to be present in the paleobotanical literature, at least in the Carboniferous. DiMichele et al. (2023: 14) stated:

> *“Tidal environments have been identified in other areas, including in European basinal settings (e.g. Fossil Grove: Gastaldo 1986, reinterpreted as a tidal setting).* ***Such deposits are likely much more widespread than recognized because of the difficulty of identifying tidalites in their nascent, very finely laminated stages****, particularly in mudrocks (most likely to be encountered in the basal coal-roof transition strata found in mines close to channel environments, see Fig. 10a). However,* ***the limited recognition of tidal-flat settings also may reflect that most palaeobotanists are generally unfamiliar with these kinds of strata”***

This is hardly a new claim, though it remains highly relevant. Kuecher et al. (1990: 211) had already concluded, in their study of the Francis Creek Shale (in which the Mazon Creek biota is preserved) that “evidence of Westphalian tides may have been misinterpreted or overlooked in field studies elsewhere.” One of the reasons is that weathering can obscure the fine laminations; Kuecher et al. (1990: 212) indicated that cores were better for such studies, but most paleontological prospection or excavation does not entail coring. Kuecher et al. (1990: 219) observed that many Late Carboniferous coal deposits from Europe and North America were associated with fluvio-delatic sediments interbedded with marine sediments, and that tidal rythmites should be common in such deposits, and conjectured that many tidal rythmites had been misinterpreted by previous authors as fluviatile. The fact that the tidal rhytmites of Mazon Creek went unnoticed for about 30 years despite intensive geological field work there supports this suggestion (Kuecher et al. 1990: 219). Indeed, tidal rhythmites are now known from other Eastern Interior Coal Basin localities that were initially interpreted as non-marine (Archer et al. 1995: 408).

Schultze (2009: 127) had similarly pointed out that features typically interpreted as fluvial “can be produced by the extension of rivers into the intertidal area”, and indeed, recent research has shown previously unrecognized similarities between sedimentary structures left by tidal channels and meanders formed by rivers (Finotello et al. 2018). More generally, Feldman et al. (1993: 485) stated that “Alternative interpretations are possible because nearly identical, varve-like, normally graded laminations can be produced in environments ranging from deep marine to shallow lagoons and freshwater lakes.” What characterizes tidal deposits is the cycles of thickness variation linked to tides and neap-spring cycles (Feldman et al. 1993: 494), but without thorough analysis, this cyclicity may go unnoticed. However, tidal currents can propagate far upstream of deltas, so that the presence of tidal rhythmites alone does not guarantee that water was brackish or of regular marine salinity (Feldman et al. 1993: 495).

Old Red Sandstone

This bias in favor of a freshwater interpretation is not restricted to formations and sites that have yielded early stegocephalians. Even older strata have arguably been affected by a similar interpretation bias. A good example is provided by the Old Red Sandstone (ORS from here on; this ranges from late Silurian to Early Carboniferous in age), which yielded many early vertebrates. Janvier (2007: 41) explained why the ORS was initially interpreted as a freshwater deposit:

> *“The first Silurian and Devonian fish remains described in the beginning of the nineteenth century were preserved in sandstones (e.g., the “Old Red Sandstone” of Britain and the Baltic States) and generally associated with plant remains, but rarely with marine invertebrates. In addition, these heavily armored fishes were regarded as “ganoids,” a group which classically included living bichirs, gars, and catfishes, all reputedly freshwater. Progressively, the received wisdom became that all these early fishes lived in freshwater and occasionally passed into the sea, when found in marine sediments.”*

This may explain why Boucot and Janis (1983: 262) interpreted the “Vertebrate-eurypterid fauna” of the “Lyne Water Fish Beds” (Wenlock/Ludlow, Silurian) as non-marine (brackish or freshwater).

However, subsequent findings showed that some ORS was almost certainly deposited in a marginal marine environment as had been suspected already by some authors in the 1970s (e.g., Goujet and Blieck 1977). For some deposits, marine influence seems certain. Thus, Goujet and Emig (1985) described *Lingula* fossils from the top of the Wood Bay Formation (Emsian, Early Devonian) of Spitzbergen, in levels above those that yielded a diversified fauna of gnathostomes and jawless vertebrates. These deposits had previously been interpreted, based on sedimentological data and the absence of typically marine metazoans, as freshwater sediments (Friend and Moody-Stuart 1970), but

Goujet and Emig (1985) interpreted them as marine and suggested that the *Lingula* fossils represented individuals killed by a catastrophic event, such as a massive influx of freshwater following a storm or sudden short-term increase of water discharged by one of the nearby rivers. They also noted that the absence of brachiopods from the lower, vertebrate-bearing levels was not anomalous because shells of *Lingula* are fragile and are seldom preserved (Emig 1981). One of the earliest Sr isotopic studies of the ORS also concluded that at least some of its deposits seemed to be marine (Schmitz et al. 1991: 793).

Janvier (2007: 42–43) remained cautious about the paleoenvironment in which the ORS was deposited; he mentioned that some paleontologists considered that it had been deposited in marginal marine environments, whereas others viewed it as composed of freshwater deposits. Subsequently, isotopic analyses documented additional instances (in addition to the case reported by Goujet and Emig 1985) of ORS strata deposited in marginal-marine environments (Goedert et al. 2018; see section "Devonian localities").

Escuminac Formation

The bias against marine influence is not restricted to vertebrate paleontologists. In her monograph on freshwater ecosystems in the fossil record, Gray (1988: 24) sharply criticized previous suggestions that the Escuminac Formation was deposited in a marginal marine (probably estuarine and brackish) environment:

> *"Similar in its* ***defective logic*** *and* ***willingness to ignore the impressive data gathered by others*** *concerning both depositional environment and characteristics of the biota, is Schultze's (1972; Schultze and Arsenault, 1985) conclusion that the Late Devonian, freshwater-lacustrine, vertebrate faunas of the Escuminac Formation, Miguasha, Quebec, Canada are "coastal marine, based on the fauna present" merely because some of the genera are also found in undoubted marine deposits elsewhere in the world. Unwillingness to consider that any Devonian vertebrate might have been able to flourish in both marine and freshwater environments, as is the case with many taxa today, is biologically, as well as geologically,* ***so unrealistic as scarcely to merit serious attention****. With regard to the locality at Miguasha,* ***the nearest known marine Upper Devonian beds are no closer than the Hudson Bay region****, Canada,* ***central New York****, U.S.A., and the* ***south of England****."*

Yet, shortly after, a study based on isotopes of several chemical elements concluded that the *Bothriolepis canadensis* sample that they had included yielded "a strong marine signal" (Schmitz et al. 1991: 793). Similarly, Matton et al. (2012) showed that isotopic data from specimens of several taxa (in addition to *B. canadensis*, these include the finned tetrapodomorph *Eusthenopteron foordi*, the dipnoan *Scaumenacia curta*, the actinopterygian *Cheirolepis canadensis*, and the acanthodian *Homalacanthus concinnus*) indicate significant marine influence, and this formation is now interpreted as a brackish estuarine environment, an interpretation supported by other types of data, notably the fossil record (Cloutier 2013).

These developments illustrate the danger of relying on previous reconstructions of ancient coastlines to assess local paleoenvironments (Schultze 1995, 2009: 129); if previous paleoenvironmental interpretations were erroneous, subsequent ones risk reinforcing previous misinterpretations, which hampers scientific progress. Another spectacular case of a marine-influenced paleoenvironment recognized far from the closest reconstructed paleo-coast is the Early Carboniferous Ducabrook Formation, where Parker and Webb (2008: 525) documented estuarine conditions about 400 km from the nearest open marine sediments.

El Cobre Canyon

A possible bias against even the presence of a modest marine influence may be visible in previous works on the Permo-Carboniferous El Cobre Canyon in New Mexico, which is typically considered to be a freshwater (fluvial) environment (Fracasso 1980; Lucas and Lerner 2010). Contrary to the few cases examined above, possible marine influence in El Cobre has not been evoked in the recent literature as far as I know. Yet, in one of the earliest studies of this locality, Williston and Case (1912) reported the presence of a brachiopod (initially called *Spirifer*, but later re-named *Anthracospirifer*), a typically marine taxon. This was dismissed by Langston (1953: 412), who stated that "It is unfortunate that the material of which Case's specimen was composed was not recorded. Had it been limestone the question might have been resolved quickly since the only limestone in El Cobre Canyon is of Jurassic age (Todilto)." Because of this, Langston (1953) considered this brachiopod fossil "as intrusive and therefore of no stratigraphic [or paleoenvironmental] significance" for the vertebrate fauna preserved in El Cobre. There are several problems with this reasoning. First, the brachiopod fossil suggests a Pennsylvanian age, not Jurassic, so Langston's (1953) assumption about the origin of the fossil does not seem plausible. Second, brachiopods need not come from limestone; they also occur in sandstone. In fact, some brachiopods, such as orthoids, are typically associated with siliciclastic environments, even though these environments are negatively correlated with brachiopod diversity (e.g., Jakobsen et al. 2014: 196). Third, Langston summarily dismissed a finding to which Williston and Case (1912) seemed to attach great importance; it is worth quoting the short passage on this topic (Williston and Case 1912: 6–7):

> *"At the south side of the cañon, the junior author found a* ***perfect cast*** *of a* Spirifer*, identified by Professor Schuchert as* S. rockymontanus *Marcou, a form occurring in Colorado in the Pennsylvanian. Though the specimen was found free, so that its exact horizon could not be determined, its* ***excellent preservation proves conclusively that it had not been carried far from its original bed****, and inasmuch as vertebrate fossils are found in the deepest strata of the cañon* ***it seems quite certain that the specimen came from an intercalated bed among those yielding so-called Permian vertebrates****.* ***No other explanation seems possible.****"*

One might tend to prefer the opinion of more recent studies that benefited from additional decades of research, but the statements by Langston (1953: 412) suggest that he did not see the brachiopod fossil; how should this be weighted against the fact that Williston and Case (1912) found and saw the fossil?

The presence of this sole brachiopod fossil does not imply that sediments of all levels of the El Cobre Canyon were deposited in a marine-influenced environment; some data suggest otherwise. For instance, Utting and Lucas (2010: 73) reported that "No evidence was found of any marine palynomorphs such as acanthomorph acritarchs or scolecodonts." However, their sample was restricted to "a 2 m shale bed in the middle part of the El Cobre Canyon Formation", so their findings represent a small proportion of the deposits found in the canyon and are not incompatible with marine influence in other levels of the locality.

Other evidence suggests that there might be marine influence in El Cobre Canyon. Lucas and Lerner (2010) thus reported the presence of ichnofossils attributed to cf. *Paleohelcura tridactyla*, which may have been produced by scorpions, other arachnids, or eurypterids. In their discussion of the eurypterid prosoma assigned to *Adelophthalmus* from El Cobre canyon, Lucas and Lerner (2010: 40–41) stated: "These eurypterids inhabited shallow ponds or enclosed lagoons on the deltaic plain adjacent to the ancestral Cañon del Cobre area". Lagoons and deltas may be brackish environments, and indeed, *Adelophthalmus* from the Red Tanks Member of the Madera Formation, a few tens of km away (Kues and Kietzke 1981; Braddy et al. 2021), is clearly from a marginal-marine, brackish environment (see below, section on eurypterids). While Lucas and Lerner (2010) clearly preferred to interpret the ichnofauna that they described as a freshwater assemblage, their reference to lagoons and a deltaic plain suggests that the sea was not far. Another quote from Lucas and Lerner (2010: 41) reinforces this impression: "There is a single prior Pennsylvanian record [of cf. *Paleohelcura tridactyla*], which comes from a **tidal flat** setting in the McAlester Formation of Oklahoma (Lucas et al. 2004). There are no previous North American records of *Paleohelcura* from lacustrine settings." One might add that the McAlester Formation of Oklahoma in which *Paleohelcura tridactyla* was reported also yielded "a few impressions of the shells of marine gastropods" (Lucas et al. 2004: 45). Could at least some levels of El Cobre Canyon document brackish water assemblages?

Autochtonous or allochtonous stegocephalian remains?

An important consideration in paleoenvironmental studies is the autochtonous or allochtonous nature of the fossils preserved in a given locality. Only autochtonous fossils are informative in this respect. Allochtonous fossils provide information about more distant environments. In most cases, only fairly long-distance transport (several km) can be easily detected, through wear marks (erosion) on the surface of fossils, disarticulation, and the fragmentary nature of specimens (for instance, only a few isolated bones, rather than a nearly complete, articulated skeleton). Abundance of material can also be used, to an extent, in combination with quality of preservation (Bennett et al. 2021: 15), because erratics are likely to be allochtonous. However, even for localities that have been subjected to detailed taphonomic studies, such as Jarrow, it is difficult to know if the stegocephalians are preserved in their environment or if they were transported over relatively short distances (Ó Gogáin et al. 2022: 15). In other cases, it looks like some fossils are allochtonous, whereas others (including vertebrates) seem to be autoctonous (Bennett et al. 2021: 18). When there is evidence of transportation, it is generally assumed that carcasses have been carried by rivers from a more continental environment, although the possibility that it was washed in by tides or storms from a more marine environment, while less likely, cannot be ruled out either, as emphasized by Gierlowski-Kordesch and Cassle (2015: 210–211).

In a few cases, transportation can be ruled out, even for fairly short distances. Some fossils of sessile organisms are obviously preserved in situ; this may occur for brachiopods, coral-forming organisms (especially cnidarians), some echinoderms and some mollusks, among others, but not vertebrates, unless they are found in burrows (a few examples are known, notably for dipnoans). Other compelling but rarer cases are found when evidence of predation is encountered, which suggests, minimally, that predator and prey occupied the same habitat, although this does not rule out transport of the bodies over a short distance. An example is described below, of a shark (*Triodus sessilis*) that ate a temnospondyl that had eaten an acanthoderm (Kriwet et al. 2008). Such fossils provide excellent information on the local paleoenvironment, and such examples are described in a few localities below.

Another type of fossil that nearly always reflects local paleoenvironments are ichnofossils. The identity of the trackmakers is often poorly constrained, but some ichnofossils are associated with specific paleoenvironments and as such, they may be informative. They are even more useful when the identity of the trackmaker is reasonably well-constrained. An example is provided by the ichnofossils of Puertollano (Spain), which includes an interesting assemblage of trackways left by a stegocephalian and traces left by a finned vertebrate that swam above the substrate. The trackway, called *Puertollanopus microdactylus*, was left by a small stegocephalian, tentatively identified as an amphibian (a "microsaur") or, less probably, an amniote. The traces left by a gnathostome that swam above the substrate, presumably in shallow water, are called *Undichna britannica*, and they were probably left by the xenacanthid chondrichtyan *Orthacanthus*, which is also known by skeletal remains from the locality (Soler-Gijón 1997). Several instances of superposition of both tracks are explained by tides, with the stegocephalian footprints being left at low tide, while the swimming traces were left at high tide (Soler-Gijón and Moratalla 2001).

Isotopic signal and paleosalinity

Basic principles and limits of isotopic methods to assess paleosalinity

The isotopic ratios of various elements have been used to assess paleoenvironments, notably to shed new light on the degree of marine influence and paleosalinity in various fossiliferous localities. We saw above that Huttenlocker et al. (2018: 86) concluded, from their strontium isotopic analyses, that the Halgaito Formation had formed in a freshwater environment. Earlier, Fischer et al. (2013) had also concluded, based on isotopic analyses of oxygen and strontium, that many vertebrate-bearing European Permo-Carboniferous localities (including, among others, Buxières-les-Mines and Nýřany) represented freshwater environments lacking any detectable marine influence. Similar conclusions, following similar reasoning but based on isotopes of other elements (carbon, oxygen and sulfur), were drawn about the Bourbon-l'Archambault Basin, which contains xenacanthiform chondrichthyans, by Luccisano et al. (2023: 8).

As we will see below, some of these conclusions may rest on tenuous ground because the isotopic signature of strontium reflects freshwater input and flux between a given water body and the ocean, rather than salinity; a similar phenomenon has been documented for neodymium by Woodard et al. (2013: 57) and (to a lesser extent) for carbon by Quinton and Rygel (2023). However, a conclusion based on recent analyses of isotopes of other elements (especially on sulfur) might be more robust (Luccisano et al. 2023: 8). Strontium (Sr) has been the most intensively studied element in this respect, so to an extent, the discussion below will emphasize this, but other elements, such as carbon (C), oxygen (O) and sulfur (S), which were used in some recent studies, are also discussed below.

The ^{87}Sr/^{86}Sr ratio (^{87}Sr being the radiogenic isotope) has varied through time, but oceanic mixing appears to have resulted in fairly homogeneous world-wide ^{87}Sr/^{86}Sr oceanic values at any given time. By contrast, freshwater bodies have much more variable ratios at any given time because these ratios depend on the ^{87}Sr/^{86}Sr signature of the soil and bedrock in the drainage basins. Thus, if the ^{87}Sr/^{86}Sr ratio of a given sediment matches the contemporary oceanic ratio, the sediments were probably deposited in oceans, although in a small minority of cases, the similarity might be coincidental. Conversely, a significant departure from the coeval ^{87}Sr/^{86}Sr oceanic ratio (beyond measurement error and outside two standard deviations) indicates that the Sr in the water body in which the sediments were deposited was not at equilibrium with oceanic values. This indicates that little or no exchange with the ocean took place. Several studies have interpreted such cases as representing freshwater, but this is only one of several other possibilities; the others include brackish water, which may be purely continental, far from the coasts, but also coastal (ponds, lagoons, estuaries and deltas), and even some epicontinental seas, such as the Baltic Sea.

Thus, interpreting the isotopic signature of Sr in terms of salinity is not straightforward. Purely continental saltwater lakes have a Sr isotopic signature that reflects that of the rivers that flow into it, and brackish coastal environments, such as the Baltic Sea, show strong deviations from oceanic signatures, especially where the freshwater influx is greatest; for instance, Andersson et al. (1992) reported a value as high as 0.709718±41 in the most freshwater part of the Baltic (Gulf of Bothnia, close to the deltas of the Kalix and Kemi rivers), which is about 0.000568 (568 parts per million) higher than their measured value for the Atlantic Ocean (0.709150±24). Fairly strong departures from the marine Sr isotopic ratio (and presumably in isotopic ratios of other elements) can occur in marginal marine basins when limited flux occurs between that basin and the ocean, especially when much of the water outflow is through evaporation; in this respect, the Baltic Sea is probably not the most spectacular example. This occurred in the Mediterranean, in the Messinian salinity crisis, and Flecker et al. (2002: 227) concluded that "excluding net evaporation from the hydrologic budget of the Mediterranean could result in an **order of magnitude error** in the palaeosalinities inferred from Sr isotope data." Furthermore, many parts of the Mediterranean developed their own Sr isotopic signature shortly before the Messinian salinity crisis (Flecker et al. (2002: 228). This is surprising because Sr concentration in oceans is about 7.7 ppm (parts per million), which is over a hundred times more than in freshwater (Andersson et al. 1994). This great disparity in abundance should make the ^{87}Sr/^{86}Sr ratio efficient to detect even a small amount of marine influence, but as shown by Flecker et al. (2002), under even moderate restriction of water flux and fairly strong evaporation, sharp departures from oceanic values can be observed.

Epeiric seas may not reflect oceanic isotopic values, as exemplified by the extant Baltic Sea (Andersson et al. 1992, 1994; Carpenter et al. 2011: 650). Large inland seas may also form, as shown by the fate of the Paratethys, which remains in a much-reduced state as the brackish Black, Caspian, and Aral seas, and in which typically marine faunal components have fluctuated over time, depending on the opening and closing of connections with the ocean (Richards et al. 2018; Dewaele et al. 2022). Even basins located far from any coast and without any link to the sea may be brackish or even hypersaline, and in these cases, Sr isotopic values may not reflect paleosalinity. Salt lakes are not rare in deserts, and even occur in moderately dry environments (e.g., Moscatello and Belmonte 2009; Borzenko 2020). Hypersaline lakes may occur at high altitude, very far from the nearest sea; for instance, the hypersaline lake Salar Guayatayoc in Argentina is located at 3432 m above sea level (Pagaling et al. 2009: 5751). A large, perennial salt lake was present in what is now northern Germany in the Rotliegend, at least by the Guadalupian (Gast 1991), or perhaps toward the end of the Cisuralian (Verdier 1996), and smaller salt lakes may have occurred elsewhere in the Carboniferous and the Permian. The isotopic signatures of such water bodies may differ substantially from marine levels, but they are not freshwater environments.

Sulfur (S) has also been uses as a paleosalinity indicator in some recent studies. As for Sr, S is highly variable in freshwater environments, with δ^{34}S values ranging from − 20.0 to + 20.0‰, whereas current oceans have a δ^{34}S value of about + 21.0‰ (Goedert et al. 2020). δ^{34}S values are very useful paleosalinity indicators because S is much more abundant (about a hundred times) in the oceans and seas than in freshwater, so even a little oceanic water diluted in much freshwater should leave an isotopic signature. However, the same argument can be made for Sr, which does not prevent significant deviations from oceanic isotopic ratios in basins with limited (or no) exchange with the ocean, especially when much evaporation occurs (see above). The δ^{34}S values of a water body also depend on the source of S, which can come from dissolution of evaporites in a drainage basin. In that case, the δ^{34}S values would reflect those of the oceans in which the evaporites precipitated, which may be much older than the salt or brackish lake, and this creates an additional difficulty given the fluctuation of the δ^{34}S oceanic values over time, which have varied between about 10 and 40‰ just in the Phanerozoic, and with uncertainties for some ages in of up to 10‰ (Wu et al. 2014). These phenomena complicate interpretation of δ^{34}S values because atypical cases of freshwater rivers with fairly high δ^{34}S values and saline springs with fairly low δ^{34}S values have been documented even in Canada (Hitchon and Krouse 1972). Thus, purely continental, but brackish or salty lakes, can have non-marine δ^{34}S values. A well-known example is the Great Salt Lake, which is strongly hypersaline and for which δ^{34}S values of +14.6 and +17.1‰ have been reported (for different dates) by Mayo and Klauk (1991: table 4). Numerous saltwater lakes (some of which are hypersaline) in Eastern Transkaibalia have been studied by Borzenko (2020), who showed that their δ^{34}S display a great range of values, from –8.4 to 27.4‰. Such environments, which must have existed in a distant past, might be challenging to model using δ^{34}S data. Thus, as for Sr, S isotopic data is more useful to assess the degree of marine influence than for paleosalinity.

A third element that has been used to assess paleosalinity is oxygen (O). Current oceanic seawater has a relatively uniform δ18O value of 0 ± 1‰, although it is lower at high latitudes, ranging from about −3 to −1‰ (Goedert et al. 2020), and this value has changed over time (Veizer et al. 1999). Current freshwater δ18O is more variable and ranges from −6 and −2‰ at low latitudes to about −15‰ at high latitudes. Hypersaline water (in lakes, lagoons and sabkhas) can have δ18O values higher than 2‰. Thus, comparing the δ18O inferred for an ancient water body to that inferred for the contemporary oceanic values, and considering the inferred paleolatitude of the water body, the δ18O can provide valuable data about whether that water body was part of a sea, an estuary, or a purely continental environment. However, contrary to Sr and S, there is as much O in freshwater as in marine water, so the δ18O should be less sensitive to detect a small proportion of seawater in a water body than methods based on Sr and S. Thus, the δ18O may be less useful to assess presumed brackish environments than δ^{34}S and the ^{87}Sr/^{86}Sr ratio. Also, the δ18O value of apatite (found in bone, dentin and enamel) differs from that of the ambient water, but there is a linear relationship between the δ18O of both substances (ambient water and apatite of animals living therein). Additional factors complicate further interpretation of apatite δ18O values because it is also affected by thermo-metabolism (thus differing between ectotherms and endotherms), evaporative transcutaneous water loss, and varies among taxa (Goedert et al. 2020: fig. 1).

Paleosalinity assessed through isotopic methods: a few case studies

Isotopic analyses have been used to assess the paleoenvironment of many fossiliferous localities, but their relevance in this context can be analyzed through the example of the Joggins Formation, which has yielded a rich metazoan fauna, including many vertebrates, including some stegocephalians. On the basis of isotopic analyses, Brand (1994: 314) concluded that “The higher Sr ratio of the Joggins bivalves relative to its marine counterparts **unequivocally proves** the non-marine (continental) affinity of these fossils and their enclosing sediments.” His analyses were based on *Naiadites* bivalves, which are often interpreted as a freshwater taxon (see below, section on xiphosurans). This is not necessarily incongruent with more recent interpretations (see below), given that Brand (1994) sampled one of the most freshwater-adapted faunal elements from one of the levels with the least marine influence, but these results may not be as robust as initially suggested. For instance, in the graph of the δ^{13}C vs. δ^{18}O (Brand 1994: fig. 6), the *Naiadites* samples fall close to the marine (brachiopod) samples, but a «mineralogical adjustment» to correct for assumed diagenesis is invoked (especially for the δ^{13}C) to interpret these bivalves as freshwater forms, which suggests that diagenetic effects may hamper straightforward interpretation of these results. In any case, many factors influence carbon isotopic ratios, and their effect is neither simple nor fully understood (Quinton and Rygel 2023), and various studies have shown that carbon isotopic ratios are not suitable to discriminate between marine and freshwater environments (Luccisano et al. 2023: 10). Thus, carbon isotopes are not discussed further in this review. Similarly, Brand (1994: 314) reported a ^{87}Sr/^{86}Sr ratio of >0.7093 from "two well-preserved bivalves from the uppermost unit of the Joggins Formation", and indicated that these "are at variance with that of coeval data (<0.7085) based on marine invertebrates." However, his graph of the ^{87}Sr/^{86}Sr ratio over time (Brand 1994: fig. 7) shows a spike in the late Westphalian A at >0.7091, which is close to the Joggins sample both temporally and in isotopic value (the difference is less than the observed range within the Baltic Sea; see above). Brand (1994) did not seriously consider the implications of this spike (which is briefly evoked in his text), probably because the spike was located, in Brand's (1994) figure, slightly earlier than Joggins. However, considering stratigraphic uncertainties in such cases is critical, and indeed, Joggins is now considered a little older than previously thought (Carpenter et al. 2015 ; Rygel et al. 2015). Thus, the Sr isotopic signal found by Brand (1994) seems to give a weaker, less convincing continental signal than initially suggested, and as explained above, "continental" does not necessarily imply "freshwater". Through comparisons with the Baltic Sea, Falcon-Lang (2005: 491) interpreted Brand's (1994) results more categorically as "entirely consistent with brackish-water conditions." Carpenter et al. (2015: 681) reached similar conclusions based on new analyses of two specimens.

Isotopic data are also directly relevant to assess the habitat of early stegocephalians and their associated fauna. Among the latter, xenacanthiform chondrichthyans are especially relevant and are discussed below. Some xenacanthids were found in marine sediments (Hampe and Ivanov 2007), but most were found in localities that have traditionally been interpreted as freshwater environments as suggested by Luccisano et al. (2023), who performed isotopic analyses by of the localities of Buxières-les-Mines (Bourbon-l'Archambault Basin, Allier) and the Muse (Autun Basin). These sites probably both date from the Asselian (Pellenard et al. 2017; Luccisano et al. 2022; Mercuzot et al. 2022).

Luccisano et al. (2023: 8) reported that the δ^{34}S values of the xenacanthiforms and other vertebrates from Buxières-les-Mines are "lower than 12‰ with variations from -6.0‰ to 9.6‰ for unaltered samples", whereas those from the Muse "range from 1.2‰ to 6.9‰" and concluded that "Those samples are depleted in heavy isotope by at least 3‰ and on average by 10‰ compared to seawater." The samples that displayed the highest δ^{34}S values (the closest to contemporary marine values) and might have inhabited brackish water for at least part of the time (according Luccisano et al. 2023) belong to an actinopterygian and two temnospondyl samples. Luccisano et al. (2023) based their estimate of a marine water δ^{34}S close to 12‰ near the Carboniferous-Permian transition on Claypool et al. (1980), which is a fairly old study. Nevertheless, the more recent isotopic curves by Wu et al. (2014) yield similar values, while showing also substantial uncertainty on the estimates. The analyses of Fischer et al. (2013) also suggested a fairly continental habitat for most of the European localities that they studied, and for the chondrichthyans (hybodontiforms and xenacanthiforms) that inhabited them. To sum up, these δ^{34}S results show deviations from the inferred coeval marine values, which implies negligible water exchange with the marine environment and suggest freshwater environments, but this does not necessarily rule out purely continental brackish environments.

The δ^{18}O values obtained by Luccisano et al. (2023) from Buxières-les-Mines are less convincing. The δ^{18}O values from the Muse xenacanthiforms range from 17.3‰ to 25.1‰, whereas vertebrates from Buxières-les-Mines yielded values around 17.0‰. Permian conodonts, which are thought to be representative of contemporary seawater, have a δ^{18}O is in the range of 21‰–23‰, an interval that is encompassed by the δ^{18}O values of Buxières-les-Mines xenacanthiforms. Luccisano et al. (2023: 10) nevertheless concluded that their results "may reflect ^{18}O-enriched water due to large evaporation rates that commonly take place in arid environments." This is plausible, but these δ^{18}O values (contrary to the δ^{34}S values) are not independent evidence that the Buxières-les-Mines xenacanthiforms had not ventured in marine-influenced environments, and large evaporation rates are compatible with continental brackish lakes. These results are not entirely congruent with those of Fischer et al. (2013) on Buxières-les-Mines, which appeared to be one of the most continental localities, with a δ^{18}O of 16.6‰. By contrast, shark teeth from Puertollano, which is probably a paralic, brackish environment (Soler-Gijón and Moratalla 2001; Laurin and Soler-Gijón 2006; Soler-Gijón and López-Martínez 2008), yielded an average δ^{18}O of 18.5‰ (with a single value at 20.2‰), and shark teeth from the marine locality of Kalinovskie Vyselki quarry of the Moscow region yielded only a slightly higher δ^{18}O of 19.6‰ (Fischer et al. 2013: table 1). The lack of discriminating power in the δ^{18}O values obtained by Luccisano et al. (2023) is unsurprising because extant taxa display considerable variability in this respect, with some significant habitat-related differences, but also some overlap between freshwater, marine and terrestrial taxa (Goedert et al. 2020: fig. 1). There is also some uncertainty about the value of oceanic δ^{18}O over time; Luccisano et al. (2023: 9) disagreed with Fischer et al. (2013) about the minimal $\delta^{18}O_p$ (the lowerscript "p" stands for "phosphate") value (22‰ vs 18‰) that would suggest a truly marine signal. However, the fact that Fischer et al. (2013:50) reported mean values of $\delta^{18}O_p$ of 19.6‰ for shark teeth and 21.1‰ for conodonts from the "unequivocal marine facies" of the Kalinovskie Vyselki quarry near Moscow supports Fisher's (2013) use of their lower threshold (18‰) for a marine signal.

Luccisano et al. (2023: 8) concluded that "In light of the bioapatite $\delta^{34}S$ values, the environment of Buxières-les-Mines and the Muse OSB do not seem to have been subjected to significant marine influences contrary to what was assumed in previous studies". While this seems plausible, especially in light of the findings of Fischer et al. (2013), this only implies that Buxières-les-Mines appears to represent a continental locality, plausibly freshwater, but possibly also a brackish basin with little or no water flux with the ocean. It also suggests that the vertebrates that lived there, including the xenacanthids, appeared not to have ventured into the oceans.

A slightly different picture emerges for the xenacanthiforms from Joggins; the few Sr isotopic analyses performed by Carpenter et al. (2015), on two specimens (a xenacanthid tooth and a sarcopterygian scale) suggested that the $^{87}Sr/^{86}Sr$ ratio of 0.710338 ± 83 (cf. *Xenacanthus*) and 0.7097772 ± 300 (cf. *Rhizodopsis*) was slightly higher than that of the Pennsylvanian oceans, which they considered to be typically ≤ 0.7083, and this implies at least a major freshwater contribution to the environment. However, Carpenter et al. (2015: 680) noted that higher values for Pennsylvanian epicontinental seas had also been reported. Indeed, Woodard et al. (2013) reported values of up to 0.7105 for Patlanoaya (for a sample dated from about 306 Ma), but suggested that these high values reflected alteration, as suggested by the "conodont color alteration index". Carpenter et al. (2015: 681) concluded that these results for a xenacanthid from Joggins were "equivocal, merely indicating that the environment was unlikely to have been fully marine", which is consistent with a restricted, brackish sea similar to the Baltic Sea, when taking into consideration other sources of information, such as the fossil community found at Joggins (see section on Joggins below). Isotopic works on the habitat of the xenacanthiforms from Buxières-les-Mines and the Muse suggests a much more continental and much less salty environment, plausibly freshwater; hence, isotopic data suggest that xenacanthiforms occupied various habitats, and other lines of evidence support this conclusion (see next section).

Taxa associated with Permo-Carboniferous stegocephalians and their paleoenvironmental significance

Freshwater chondrichthyans?

Today, the vast majority of extant chondrichthyans are strictly marine; only 43 species (less than 4% of elasmobranch species currently recognized) venture into freshwater (Carpenter et al. 2011: 651 and references cited therein). Fewer still reproduce there (Feitosa et al. 2016, 2020); all of these are viviparous, as extensively documented in the only extant strictly freshwater chondrichthyans, the Potamotrygonidae, also known as freshwater stingrays (Charvet-Almeida et al. 2005). This may not be a coincidence because only about 40% of the extant chondrichthyan species are viviparous (Dulvy and Reynolds 1997). Thus, no extant chondrichthyan lays eggs in freshwater environments. This raises doubts about the traditional interpretation of various Permo-Carboniferous localities that have yielded fossilized chondrichthyan eggs but were nevertheless interpreted as freshwater paleoenvironments. These include the Mazon Creek Lagerstätte (Schultze 2009), in which a range of marine to freshwater paleoenvironments were recognized until recently (Baird et al. 1985). However, the presence of chondrichtyan eggs, among others, suggests that there was no freshwater fauna there (Clements et al. 2019).

Xenacanthiforms are the chondrichthyans most frequently associated with Permo-Carboniferous stegocephalians (Fig. 2). They apparently lived in the same environments at least occasionally, as shown by a spectacular discovery of a *Triodus sessilis* specimen that had ingested two temnospondyls (*Cheliderpeton* [now *Glanochthon*] *latirostre* and *Archegosaurus decheni*); these temnospondyls were apparently not washed-in carcasses because the *Glanochthon* specimen had remains of *Acanthodes bronni* in its abdominal region, which suggests that all these taxa shared the same habitat (Kriwet et al. 2008). For the reassignment of *Cheliderpeton latirostre* to the more recent taxon *Glanochthon* that was erected partly for this purpose, see Schoch and Witzmann (2009). Xenacanthiforms have long been interpreted as freshwater sharks (Jain 1980; Kohring 1995: 263; Dick 1981, 1988; Kriwet et al. 2008), and would then be the first freshwater chondrichthyans (Compagno 1990). This once-widespread opinion may have resulted from their frequent occurrence in Pennsylvanian Coal Measures (Hampe 2003; Carpenter et al. 2011: 650) and with stegocephalians, which are often called (inappropriately) "amphibians". The latter is not a good argument, but some isotopic data support this interpretation, as mentioned above (Fischer et al. 2013; Luccisano et al. 2023). However, occurrences in marine environments were subsequently documented by many studies. In fact, *Diplodoselache woodi*, which may well be one of the earliest and most basal xenacanthiform, was found in what Dick (1981: 111) interpreted as a large lagoon that was frequently isolated from the open sea by a sand bar, and *D. woodi* appears to have inhabited the lagoon (rather than representing an allochtonous element). This suggests a brackish environment. Hampe and Ivanov (2007) described xenacanthiform teeth for which they erected the nominal species *Triodus teberdaensis* in marine carbonates from the Pennsylvanian Tolstiy Bugor Formation (Moscovian) of Karachay-Cherkess Republic (Russia), and geologically older marine occurrences had been documented earlier, as in the Middle Devonian limestones of the Rhenish Schiefergebirge (Stritzke 1986). Similarly, the basal conglomerate of the Hamilton quarry has yielded teeth of *Xenacanthus*, *Orthacanthus* and a cochliodontid chondrichthyan, in a clearly marine association that includes echinoderm ossicles, brachiopods

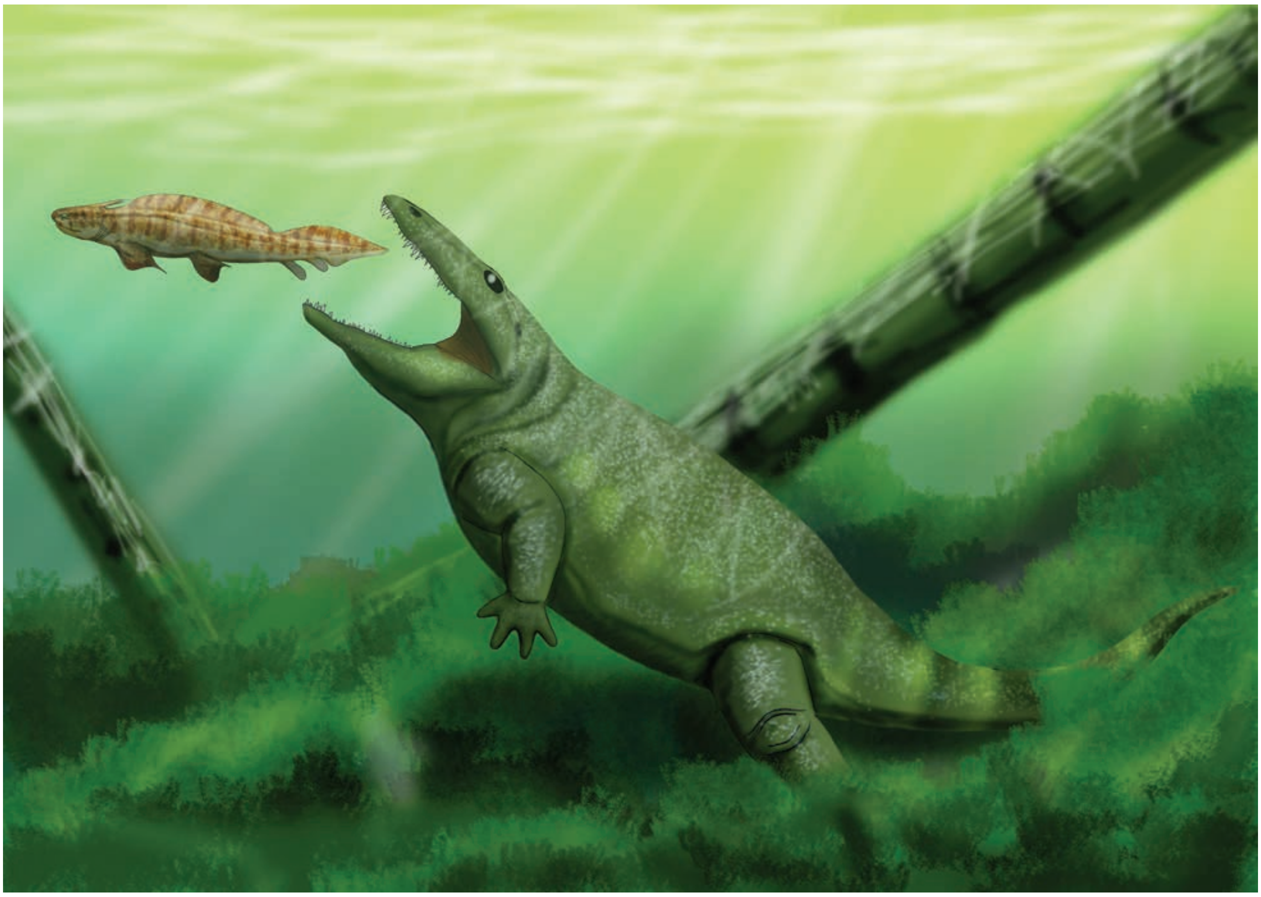

Figure 2. The temnospondyl *Eryops megacephalus* leaps to seize a small chondrichthyan (*Xenacanthus*). While the co-existence of both taxa is well established, the environment that they occupied (freshwater, brackish water, or even a marginal marine environment) remains enigmatic. Amin Khaleghparast (a biologist from Tehran, Iran) drew the figure, which was colored by Dmitry Bogdanov (a cardiologist and paleo-artist from Chelyabinsk, Russia); Roman Yevseyev (Moscow) adjusted the legs. Anatomical advice was provided by Tracy Lee Ford (San Diego, California, USA) and Bryan Riolo (Ocala, Florida, USA).

(some of which are in growth position), fusulinids and corals (Cunningham et al. 1993). Xenacanthiforms have also been documented in coastal, probably brackish environments, such as the Kasimovian Cohn Coal Member of the Mattoon Formation in Illinois (Carpenter et al. 2011). In the Cohn Coal Member, xenacanthiforms co-occur with microconchids, often called "*Spirobis*" or "spirorbids" in the older literature, which were probably euryhaline organisms living mostly in brackish water (see below). Carpenter et al. (2011: 650) listed several other reports that showed that xenacanthiforms are "intimately associated with brackish and marine fauna". In fact, many xenacanthiforms seem to have disappeared from the British Coal Measures in the Bolsovian substage (Hampe 2003), in which the last marine incursion in the British Pennsylvanian occurred (Waters and Davies 2006). Carpenter et al. (2011) suggested that these events are causally related; the extinctions would then imply that few xenacanthiforms could survive in freshwater. Furthermore, growth patterns in *Orthacanthus* from Spain have been interpreted as reflecting tidal cycles (Soler-Gijón 1999).

As we saw above (isotopic section), the δ34S results on xenacanthiform bioapatite obtained by Luccisano et al. (2023) from the localities of Buxières-les-Mines (Bourbon-l'Archambault Basin, Allier) and the Muse (Autun Basin) implied that these taxa did not venture into the open ocean. This suggests that at least some xenacanthiform populations lived far from the open ocean. However, note that other studies have not excluded the possibility of at least temporary marine influence in the Bourbon-l'Archambault Basin. For instance, Steyer et al. (2012: 514) speculated that the mass mortality of the seymouriamorph *Discosauriscus* in the Franchesse locality (about 20 km North-North-East from Buxières) might have resulted from temporary and sudden flooding, potentially of salty water from the North Sea, which is plausible according to some paleogeographical reconstructions.

Collectively, xenacanthiforms appear to have inhabited both continental, plausibly freshwater (at Buxière-les-Mines and the Muse) and marine environments (represented in other localities), and most frequently environments transitional between these, but this does not imply that each xenacanthiform species inhabited all these environments. Perhaps, as in extant teleosts, there may have been freshwater, marine, and euryhaline taxa, but so far, we have a highly incomplete picture of xenacanthiform environmental preferences.

Freshwater microconchids?

Microconchids (often called "*Spirorbis*" in the older literature) are often associated with Permo-Carboniferous stegocephalians. Their paleoenvironmental significance is thus relevant to assess the habitat of early stegocephalians. Note that microconchids have often been called "*Spirorbis*" in the older literature, but the latter is an extant marine annelid, and the coiled calcitic tubes encountered in fossiliferous localities older than the Cretaceous were not formed by annelids, but rather, by microconchids (Taylor and Vinn 2006). The fossil record of microconchids extends from the Late Ordovician to the Middle Jurassic (Zatoń et al. 2012: 603). They originated in the marine environment, but subsequently became adapted to other habitats (Zatoń et al. 2012: 604). What these habitats were is to an extent controversial. Microconchids undoubtedly occurred in brackish, marine-influenced coastal environments, but their presence in truly freshwater environments is contentious. Some authors seem certain that microconchids inhabited freshwater for part of their evolutionary history, from the early Devonian to the Late Triassic (Zatoń et al. 2012: 606), but others suggested that they are not found in freshwater, but only in brackish, marine-influenced environments, such as estuaries and deltas (Gierlowski-Kordesch and Cassle 2015). A vigorous exchange took place recently between the proponents of these opposing points of view (Gierlowski-Kordesch et al. 2016; Zatoń et al. 2016).

To assess the validity of these opposing claims, I checked the most relevant data presented by Zatoń et al. (2012: table S1, appendix A). I restricted my scrutiny to the interval ranging from the Middle Devonian to the Early Permian because this is the temporal interval relevant to the origin of stegocephalians and to their great evolutionary radiation that gave rise to the first amphibians (the total clade of lissamphibians; Laurin et al. 2020) and amniotes. In that interval, four occurrences were listed as fresh to brackish water (hence, uncertain salinity), but only two (both from the Late Carboniferous, one in Ohio and the other one from England) were indicated to be freshwater (rather than brackish). These two cases should thus provide the strongest evidence supporting the presence of microconchids in freshwater and will be examined critically.

The Ohio occurrence is justified by a conference abstract (Lewis and Dunagan 2000), which indicates that this occurrence is from the Conemaugh Group. However, in a more recent assessment of this occurrence, Martino (2016: 142) interpreted the significance of microconchids differently:

> *"Their presence indicates a marine connection and probable brackish influence (Schultz[e], 2009; Gierlowski-Kordesch and Cassle, 2015). Two occurrences of microconchid-bearing 'nonmarine' limestones in the Glenshaw Formation have been re-interpreted as brackish, clear water, nearshore facies (Morris, 1967; Busch and West, 1987)"*

Indeed, Busch and West (1987) had previously indicated that the microconchids, which he called "spirorbid annelids", occurred during a major transgression, in "intertidal-supratidal ponds". Thus, this record, rather than supporting the occurrence of microconchids in freshwater, suggests that these records occurred in a marginal-marine, brackish environment.

To support the presence of "freshwater" microconchids in the Westphalian (Late Carboniferous) of England, Zatoń et al. (2012: table S1, appendix A) cited a book on British regional geology to which I have no access. However, Lomax et al. (2016) described Westphalian microconchids from Yorkshire, which I will consider representative of the record alluded to by Zatoń et al. (2012). In that locality, microconchids co-occur with xiphosurans and shark egg capsules, both of which (especially the latter) suggest a significant marine influence (see section "Freshwater chondrichthyans"). Thus, neither of these supposedly freshwater occurrences of microconchids stands up to scrutiny.

Before closing this section, it may be useful to discuss a recent study that clearly sides with the interpretation that some microconchids occurred in freshwater, even though this concerns taxa that occur after the temporal interval considered in this paper (namely, in the latest Permian and early Triassic). Shcherbakov et al. (2021) interpreted the Early Triassic Petropavlovka Lagerstätte as a freshwater ecosystem, but its fauna includes xiphosurans, which, as I demonstrate below, (next section) suggest marine influence. They did not completely rule out the possibility that the Petropavlovka Lagerstätte represented a brackish water assemblage, but they seemed to prefer a freshwater interpretation (p. 1345) because several temnospondyls (which they call "amphibians") "have never been recorded in assemblages with marine fossils" and because dipnoans are also present in the Lagerstätte. About the latter, they stated that "the overwhelming majority of the Permian and later dipnoans were restricted to freshwater". This may not be entirely correct; the present study aims at demonstrating that many temnospondyls lived in brackish, coastal environments (in addition to presumably occurring in freshwater), as I previously suggested (Laurin and Soler-Gijón 2010), and Permian dipnoans frequently occurred in the same environments as early stegocephalians and xenacanthiform chondrichtynans. For instance, *Gnathorhiza* occurs in the Cisuralian Jemez Springs locality of the Cutler Group (formerly Abo Formation), along with *Xenacanthus* and a great diversity of stegocephalians (Berman 1993: 16). Furthermore, some Permian dipnoans appear to have been euryhaline (McCahon and Miller 2015). A xiphosuran head shield is encrusted with microconchids, which thus probably lived in the same environment. The Petropavlovka Lagerstätte may well represent a brackish water assemblage.

The case for a freshwater community in the latest Permian Tunguska Basin, also described by Shcherbakov et al. (2021), seems at first more convincing because it has yielded fossils of aquatic insect larvae, namely mayfly nimphs of the taxon *Khungtukunia sibirica* (Sinitshenkova

2013), and extant mayfly nimphs require a salinity inferior to 8‰ (Chadwick et al. 2002), though not necessarily freshwater. The Tunguska Basin also yielded lepisosteiforms and amiiforms, which Shcherbakov et al. (2021: 1344) interpreted as "relict freshwater" taxa, citing for this Arratia (2004). However, Arratia (2004: 306) stated, on the contrary, that early actinopterygians, including early stem- and crown-teleosts, were overwhelmingly marine, with invasions of freshwater occurring in some lineages in the Middle and Late Jurassic. The traditional interpretation of lepisosteiforms and amiiforms being adapted to freshwater is based only on extant taxa, and it has been refuted by more recent research; Guinot and Cavin (2018: 580) concluded that "Our results indicate a marine ancestry for the entire actinopterygian clade. Basal-most clades such as Cladistia, Chondrostei, Lepisosteiformes, Amiiformes, whose living representatives are known from freshwater or mixed environments all arose from a marine ancestry." The slightly earlier study by Betancur-R et al. (2015) is congruent on this point. The "relict freshwater" neopterygian taxa mentioned by Shcherbakov et al. (2021: 1344) include *Tungusichthys acentrophoroides*, *Arctosomus sibiricus*, *Evenkia eunotoptera* and *Eoperleidus bergi*. Surprisingly, three of these taxa (*Tungusichthys*, *Arctosomus*, and *Evenkia*) are included in Sepkoski's (2002) monograph "A compendium of fossil marine animal genera", and thus presumably occur in marine environments. The distribution of *Eoperleidus* seems to be far more limited and I could not find more information about its habitat (beyond its occurrence in the Tunguska Basin), but the three other taxa hardly constitute convincing evidence of a freshwater habitat.

Shcherbakov et al. (2021) also discussed other Permo-Triassic assemblages that contained what they interpreted as possibly freshwater microconchids. The interpretation of these assemblages is more complex than they suggest, and this will be exemplified by their discussion of the Grès à Voltzia, in which they recognize some marine influence. They report that the assemblage includes, among others, egg capsules (probably from chondricthyans), limnomedusae, horseshoe crabs, euthycarcinoids, gilled mayfly, aquatic beetle larvae, aquatic insect egg clutches, lingulids and temnospondyls, in addition to microconchids (Shcherbakov et al. 2021: 1347). It is possible that this assemblage reflects more than one community because many (perhaps most) insect larvae normally develop in a salinity inferior to 8‰ (Chadwick et al. 2002) whereas lingulid brachiopods normally live in a much greater (at least 30‰) salinity (Hammond 1983). However, even this surprising assemblage could possibly reflect a single community because many insect larvae tolerate brackish water and occur in estuaries (Williams and Williams 1998), and a few even live in hypersaline environments (Pallares et al. 2015). That assemblage would then have to be coastal and brackish because there are no freshwater brachiopods. To sum up, the case for the Permo-Triassic microconchids described by Shcherbakov et al. (2021) as freshwater (rather than brackish water) taxa is not entirely convincing.

Thus, in this paper, I will consider that the presence of microconchids implies marine influence. Bennett et al. (2021: 17), in their analysis of the palaeoenvironment of Mississippian coastal lakes of the Ballagan Formation, likewise accepted the conclusions of Gierlowski-Kordesch and Cassle (2015) that microconchids are marine organisms and concluded that larval spirorbids are "readily transported into non-marine environments by tidal currents or storm deposits"; this may explain the occurrence of a few scattered microconchids in assemblages that show little other evidence of marine influence, but that must nevertheless have formed near the coast.

Xiphosuran habitat through time

The habitat of Permo-Carboniferous xiphosurans, which are sometimes associated with early stegocephalians, has proven particularly controversial. Extant xiphosurans (only four currently recognized species) are basically marine, even though they frequently enter brackish estuaries and less frequently, rivers where the water is almost fresh; this is documented, for *Carcinoscorpius rotundicauda* (named *Limulus rotundicauda*, in the older literature), in the Hughli river at least as far as Calcutta (Annandale 1909, 1922). This is a bit less than 100 km (as the crow flies) from the coast, but only about 40 km from the proximal part of the Hughli estuary. Størmer (1952: 630) even stated that this species can "migrate up rivers into perfectly fresh water", but provided no reference to support this statement. However, given the obviously extreme osmotic tolerance of *C. rotundicauda*, Størmer's (1952: 630) statement may well be correct. The three other extant xiphosuran species seem to be less euryhaline and inhabit the seas, including coasts and estuaries.

Some paleontologists argued for an early invasion of freshwater habitats by xiphosurans. For instance, Gray (1988: 60) concluded that "The Rudstangen record suggests freshwater limuloids in the Late Silurian." Similarly, Gray (1988: 58) indicated that their occurrence in the ORS led Størmer to infer that some xiphosurans invaded brackish or fresh waters, and that by the Carboniferous, most limuloids lived in these environments. Notably, Gray (1988: 57) concluded that the xiphosuran *Kodymirus* lived in freshwater, or perhaps brackish water, because of similarities between its depositional environment and the Old Red Sandstone facies. However, the ORS no longer appears to be a freshwater deposit (Janvier 2007), partly because of marine fossils found in some strata (Goujet and Emig 1985) and because recent isotopic analyses of East Greenland ORS deposits show significant marine influence (Goedert et al. 2018). Thus, the occurrence of xiphosurans in ORS only supports presence of some xiphosurans in brackish (rather than fresh) water.

Xiphosurans occur in what was once called the Braidwood Mazon Creek fauna (Schultze 2009: 127), which was thought to include a freshwater fauna, whereas the Essex fauna from Mazon Creek was recognized to show strong marine influence. Gray (1988: 58) considered, as was common at the time, that the Braidwood was a freshwater fauna, and concluded, on the basis of such arguments, that "There seems **no doubt** that some of the most characteristic and common limuloids in Carboniferous coal swamp assemblages of Europe and North America", namely, the euproopaceans which occur in Mazon Creek, were "associated with **freshwater** habitats". However, Schultze and Maples (1992: 234) concluded that the "Braidwood fauna" inhabited a "tidally influenced coastal or estuarine" environment, and more recently, Schultze (2009: 127) mentioned the presence of the brachiopod *Lingula* in the Mazon Creek biota. Clements et al. (2019: 5) went further and argued that Mazon Creek preserves faunae located at various distances from the shore but that it lacks a discrete freshwater fauna, and that "Most of the major groups found in the Mazon Creek could tolerate varying degrees of salinity". Among these, they listed both "horseshoe crabs" (xiphosurans) and eurypterids.

Lamsdell (2016: 185) also claimed that "Colonization of the freshwater realm is shown to have occurred at least five times" in xiphosurans, and this is summarized neatly in his figure 2, which optimizes xiphosuran habitat (binary, marine vs. non-marine) onto a timetree. However, a closer look at the supporting data leads to qualify these claims. The most speciose of these putative freshwater xiphosuran clades is Belinurina. The habitat of the terminal taxa shown in the tree (Lamsdell 2016: fig. 2) is indicated, along with supporting references, in Lamsdell's (2016) tables 1–3, and these indicate that for all taxa in Belinurina, the habitat is freshwater/brackish. Thus, there is no firm evidence that any of these taxa were truly adapted to freshwater, rather than being euryhaline, like some extant xiphosurans (Annandale 1909). The second speciose clade of "non-marine" xiphosurans, Austrolimulidae, originated in the Paleozoic but radiated in the Mesozoic. For this review, I consider only Paleozoic taxa, and extant ones, for the information that they provide about habitat. The Paleozoic austrolimulids (solely represented by *'Paleolimulus' longispinus* in Lamsdell's analysis), "are known from marginal marine, fluvially influenced environments". Lamsdell (2016: 185) indicated that "Aside from these two clades [Belinurina and Austrolimulidae], xiphosurids are shown to have invaded the freshwater realm twice in the Palaeozoic (Schimper 1853; Anderson and Horrocks 1995) and once in the Mesozoic (Riek and Gill 1971)." These two additional Paleozoic "freshwater" invasions deserve additional scrutiny. Schimper (1853) reported the presence of "*Limmulites Bronnii*", subsequently renamed *Limulites bronni* by Størmer (1952), in the "grès bigarré" near Wasselonne (about 20 km W-NW of Strasbourg), which is Triassic, as reported in Lamsdell (2016: fig. 2), rather than Paleozoic. Presumably, Lamsdell (2016: 185) considered that this represented a Paleozoic freshwater invasion because the ghost lineage of *Limulites bronni* extends into the Permian. Of all the Paleozoic xiphosurans listed by Lamsdell (2016) in his table 1, *L. bronni* is the only one listed as freshwater, rather than marine or freshwater/brackish. However, we know little about the paleoenvironmental conditions of the deposits. Schimper (1853) described no other fossil from the locality that yielded *L. bronni*, but he did report an ammonite, also from the "grès bigarré" from the quarry in Soultz-les-Bains, barely 10 km south of the *L. bronni* locality; this does not suggest a freshwater environment! The last putative Paleozoic freshwater xiphosuran mentioned by Lamsdell (2016) is *Valloisella lievinensis*. However, Anderson and Horrocks (1995) did not indicate that this was a freshwater taxon; they only indicated that "The arthropod was found associated with non-marine bivalves and the other, more commonly encountered, Coal Measures xiphosuran, *Bellinurus* [often spelled *Belinurus*] PICTET, 1846." However, non-marine does not mean "freshwater"; brackish environments are also typically considered non-marine, and indeed, *Bellinurus* is listed in Lamsdell (2016: table 1) as freshwater/brackish. Furthermore, little is known about the fauna and stratigraphic context associated with *Valloisella lievinensis*. Anderson and Horrocks (1995) described two specimens of this taxon. For the first one, BU (University of Birmingham) 2466, Anderson and Horrocks (1995: 648) indicated:

> *"it was collected from a Coal Measures site near Dudley, Worcs. The Coal Measures strata in this area are Westphalian B in age (Upper Carboniferous) but unfortunately, **this is the only stratigraphic detail available**. The **nearby site** of Coseley (Westphalian B) has yielded Bellinurus koenigianus WOODWARD, 1872, Bellinurus bellulus KONIG 1851 (see SCHULTKA 1994: 347), and Pringlia birtwelli (WOODWARD, 1872)."*

Thus, the locality data for this specimen are vague, stratigraphy is worse, and there is no associated fauna. The other specimen, LL 11133, has fairly precise locality data (the Bickershawe Complex colliery tip near Leigh, Wigan), but the reported associated fauna (mostly terrestrial, with the exception of the bivalve *Naiadites*) is only moderately reliable because "Unfortunately, the material is not preserved in situ, however all of the material listed above comes from a single, constrainable area of the spoil tip, and as such is likely to reflect original association." (Anderson and Horrocks 1995: 649). Note that the bivalve *Naiadites* is usually called "non-marine", but its distribution does not seem to fully support this assertion. At Joggins, it occurs, along with other bivalves, throughout the geological section of the coastal site of Joggins (Nova Scotia), even in the lowest levels of the section (though it is less abundant there than in higher levels), which show strong marine influence, as shown by the occurrence of punctate brachiopods and echinoderm fragments (Grey et al. 2011). Thus, the paleoenvironment of *V. lievinensis* is poorly documented, and all that can be stated about it is that it was most likely not typically marine, but it may have been either freshwater or brackish.

What should we conclude from all this? What seems to be reasonably well-established is that chelicerates most likely originated in the marine environment (Aria 2022), like most ancient metazoan taxa. Extant xiphosurans are marine and at least some taxa are euryhaline, with abilities to tolerate very low salinities, but they never venture very far from the sea. The fossil record shows that Permo-Carboniferous xiphosurans inhabited marginal-marine, probably brackish environments. They may possibly have invaded freshwater environments, but there is currently no solid evidence of this; on the contrary, when associated with early stegocephalians, it is typically in localities that show some marine influence, as in Mazon Creek and Montceau-les-Mines (which is discussed below). Given their marine origin in the early Paleozoic, parsimony suggests that until convincing proof of truly freshwater Paleozoic xiphosurans is produced, this taxon should be considered to have inhabited marine and marine-influenced environments; the burden of the proof is on authors who claim truly freshwater occurrences of xiphosurans in the Paleozoic. Goldring and Seilacher (1971: 440) reached this conclusion long ago and stressed that

> *"The main habitats of limulids have always been in the shallow sea; but the fossilization potential for both, carcasses and tracks, was so much lower in the true biotope than in marginal and partly nonmarine environments that the fossil representation of the limulids is now stronger in these than in their main biotopes".*

Eyrypterids, marine, brackish or freshwater?

Eurypterids are rare, but a good proportion of the known Permo-Carboniferous specimens have been found in localities that yielded stegocephalians, like Joggins (Carpenter et al. 2015), the Hamilton quarry (Cunningham et al. 1993), Mazon Creek (Clements et al. 2019), and Kinney Quarry (Hunt et al. 1992; Braddy et al. 2021, 2023). A specimen was even found in the El Cobre Canyon (New Mexico), in locality 4564, low in the canyon (Hannibal et al. 2005).

The habitat of eurypterids, as for several other extinct taxa, has proven difficult to assess. Gray (1988: 62) indicated that "Much the same kind of controversy evoked in discussion of limuloid habitats has been raised with regard to eurypterids although these animals have no modern analogues." Indeed, the fact that eurypterids are extinct adds to the difficulty in inferring their paleoenvironment. Some authors (cited in Gray 1988: 62) suggested that the first ones, in the Ordovician (Fig. 3), were marine, and many of the first discovered eurypterids were found in limestone, associated with a fairly typical marine fauna (Lebrun and Pylypenko 2023), but after that, as the group diversified taxonomically and presumably ecologically as well, the story becomes more complex. Indeed, Boucot and Janis (1983: 260) suggested that the Fish Bed Formation (Ludlow, Silurian) was "Non-marine as suggested by the eurypterid fauna" (note that in this context, "non-marine" more likely means brackish coastal than freshwater). Kjellesvig-Waering (1958: 1108) suggested that from the Pennsylvanian on, they were restricted to freshwater. However, Kjellesvig-Waering later rejected the idea of non-marine eurypterids (Gray 1988: 62).

Nevertheless, Permo-Carboniferous eurypterids have often been interpreted as freshwater taxa (Lamsdell et al. 2019). This fact does not seem to be well-supported, as demonstrated by the citation chain that links papers that indicate that eurypterids, after the Devonian, were restricted to freshwater habitats: Lamsdell and Selden (2017: 104) cited Lamsdell and Braddy (2010) for this (in addition to an old paper from 1916 that I was unable to obtain), but the latter cited Braddy (2001) to justify the claim (and made no new contributions to this question). Braddy (2001) reanalyzed data from Plotnick (1999), which did not tackle Permo-Carboniferous eurypterids, as reflected by its title, "Habitat of Llandoverian-Lochkovian eurypterids". It seems dangerous to conclude, from a study based on Silurian to Early Devonian eurypterids, that all post-Devonian taxa were freshwater forms!

Furthermore, Plotnick's (1999) interpretations seem to minimize marine influence. To demonstrate this, his ecological classification scheme needs to be explained. Plotnick (1999) classified the biofacies assemblages from least (BA0) to most marine (BA6). This was a slight modification of a scheme developed by Boucot and summarized in Boucot and Janis (1983: 252):

> *1 corresponds to the intertidal environment, as well as the brackish plus estuarine; 2 to the high subtidal; 3 to the remainder of the subtidal photic-phytal zone; 4 and 5 to the mid- and outer-shelf zone; and 6 to the shelf margin to upper bathyal region.*

To this, Plotnick added BA0, for "probable nonmarine occurrences". The faunal composition of some of the localities seems to match imperfectly the assigned assemblage. Out of the 94 localities, 8 are scored as BA 0, sometimes "or BA 1", and 46 are classified as possibly BA 1, sometimes "or BA 2", which reflects substantial uncertainty. The localities classified as BA 0 (including those that might be BA1) exhibit some signs of marine influence; some localities (like no. 2) have no associated fauna, or only plants, presumably terrestrial (like no. 62), some are associated with vertebrates (ex. localities 1, 17, 51, 54, 64), and only one (71) is associated with a more diversified biota, which includes xiphosurans. But note that while these vertebrates were once considered freshwater because they occur in the Old Red Sandstone (then considered to represent freshwater deposits), the argument no longer holds because many authors consider the ORS as a marginal marine environment (Janvier 2007), as mentioned above (section on the ORS). Thus, most of the localities classified as BA0 (non-marine) by Plotnick (1999) are ecologically difficult to assess, and rather than truly freshwater, they could well

Figure 3. *Pentecopterus*, one of the oldest (Darriwilian, mid-Ordovician) eurypteryds. Drawing by Patrick Lynch, published on Wikimedia commons (https://en.wikipedia.org/wiki/Eurypterid#/media/File:Eurypterids_Pentecopterus_Vertical.jpg) under the CC0 1.0 DEED licence.

represent marginal-marine environments, such as proximal, low-salinity deltaic areas, bays where freshwater discharge is important, and low-salinity lagoons. A more thorough ecological assessment of these localities would be worthwhile.

The localities classified as BA 1 show stronger marine influence, like brachiopods, mostly inarticulate, especially lingulids, or more rarely, articulate brachiopods like *Hindella*, *Atrypa*, *Dalejina* (like localities 7, 18, 26, 27, etc.). Some, like localities 26–30, 32–35, 38, 48, even yielded cephalopods, which suggests a fairly typical marine environment (see below). Some have corals, in addition to cephalopods, like localities 3,2 68, and 79, or crinoids, like localities 37, 48. A few BA 1 localities have acritarchs (no 42), stromatolites (66), trilobite fragments (88), or possible cirripedes (92). Some BA 1 localities are hypersaline (91). Thus, most of the localities considered BA1 by Plotnick (1999) seem to represent the marine end of the spectrum encompassed by this category, namely, intertidal environments, as well as fairly salty brackish and the distal estuarine, rather than the proximal, low-salinity estuarine environments.

Last but not least, paleobiogeographic data show that at least some eurypterids, namely, the pterygotoids "apparently could cross open oceans, and are found throughout the world in the short time span of their existence (~40 Ma)", as Tetlie (2007: 559) concluded. However, examination of the paleobiogeographical distribution patterns of some of the geologically most recent eurypterids, namely the Adelophthalmoidea, shows that they were at least able to disperse in coastal areas, given that by the Permian, they were present in the South China Block, in addition to the core area of eurypterids in former Laurentia and Baltica (Tetlie 2007: fig. 5C). Indeed, (Tetlie 2007: 572) admitted that adelophthalmoids and pterygotoids were "the most dispersed [eurypterids] throughout the world." Adelophthalmoids are also among the eurypterids most frequently associated with Permo-Carboniferous stegocephalians. For instance, *Adelophthalmus brasdorensis* occurs at Joggins, *Adelophthalmus mazonensis* occurs at Mazon Creek, *Adelophthalmus sellardsi* is found in the Hamilton Quarry (in the marginal marine ostracode wackestone that also yielded rhynchonellid and productid brachiopods), and *Adelophthalmus* sp. is found in El Cobre Canyon (Cunningham et al. 1993; Hannibal et al. 2005; Tetlie 2007: table 5). More importantly, nearly 200 specimens of *Adelophthalmus luceroensis* have been found in the nearby Red Tanks Member of the Bursum Formation (Kues and Kietzke 1981; Braddy et al. 2021), which also yielded a diverse vertebrate fauna (Harris et al. 2004). These deposits are from a marine embayment, and the levels that produce *A. luceroensis* also yield microconchids, which reflect marine influence (Braddy et al. 2021:112).

Thus, the case for a freshwater interpretation of some eurypterids seems to be weak. Braddy (2001: 120) wrote "No marine fauna has ever been reported from this assemblage [Early Devonian Midland Valley of Scotland] and the presence of terrestrial plants and invertebrates indicates a freshwater lacustrine setting." I did not try to reassess the paleoenvironment of these Early Devonian deposits because this paper focuses on the Frasnian to the Kungurian, but note that none of the three arguments given in this quote is fully satisfactory. The most convincing, the absence of marine faunas, is negative evidence, and given the controversial environmental tolerances of many Devonian taxa (such as microconchids, xiphosurans and eurypterids; see below), it is of limited value because some taxa that actually lived in marginal-marine, brackish environments may have been misinterpreted as freshwater forms. The presence of terrestrial plants (or any terrestrial organism) is irrelevant, as pointed out by Schultze (2009: 127); such plants do grow on coasts of seas and oceans, so they only indicate that land was nearby, but give no information about paleosalinity. Last but not least, "invertebrates" are a huge paraphyletic group that is found in all environments, and if the author meant "terrestrial invertebrates" (the sentence is ambiguous on this point), just like land plants, they only indicate that the shore was nearby.

Some bias in favor of a freshwater interpretation was built into Braddy's (2001) study. He classified benthic assemblages (B.A.) into the categories B.A. 0, "non-marine (e.g. lacustrine and fluvial settings)", B.A. 1, for "marginal settings (e.g. lagoons, hypersaline environments, littoral settings and mud flats)", B.A. 2, for "shallow marine settings", and B.A. 3 +, which designates "deeper marine settings". Braddy (2001 121) indicated (p. 121) that "In the case of disputed environmental settings the lowest B.A [most continental] is used, for consistency." Using this logic, with the data then available, would have led to consider the entire ORS freshwater, and indeed, a locality with no paleoenvironmental data would be considered freshwater. A similar bias seems to occur in the eurypterid literature cited by Braddy (2001). Thus, in his discussion of the Upper Silurian Bertie Waterlimes, Braddy (2001: 124) indicated that it had been

> *"variously interpreted as representing an upper intertidal portion of a sabkha to subtidal sequence (Hamell, 1982), a near shore lagoon showing fluctuating salinity (Heckel, 1972; Copeland and Bolton, 1985), a wide lagoonal system behind a reef (Ruedemann, 1925; Monahan, 1931), a* ***brackish to freshwater lagoon or estuarine*** *deposit (Kindle, 1934), or a* ***deltaic*** *environment (O'Connell, 1916)."*

Yet, Braddy (2001: 124) indicated that evaporites occur in the Bertie Waterlimes, which "contains a diverse eurypterid fauna (Clarke and Ruedemann 1912) associated with a rare marine fauna, including **cephalopods**, bivalves, **lingulid brachiopods**, worms, gastropods, xiphosurans…"!

The eurypterids that co-occur with microconchids probably inhabited marine-influenced habitats (see above, section on microconchids). One such co-occurrence with microconchids (reported erroneously as "*Spirorbis*") is in the Middle Devonian Gaspé Sandstone Series of New Brunswick and Québec provinces, in Canada (Gray 1988: 37). Similarly, one of the sites that yielded the most abundant and best-preserved eurypterid remains, in the Red Tanks member of the Madera Formation, contains microconchids, which were called "spirorbid worms" by Kues and Kietzke (1981: 709). This abundance and good preservation is not entirely consistent with Lamsdell et al.'s (2019: 1713) conclusion that "the eurypterid material [in coastal deposits; not specifically from the Red Tanks] was swept in from continental settings". The Red Tanks member also includes fusulinids and some marine and "non-marine" (possibly brackish or freshwater) strata.

More importantly, at least four specimens (at least one of which belongs to the mycteropoid *Mycterops whitei*) have been found in three Late Pennsylvanian localities in two formations (Hushpuckney Shale, Swope Formation, Iowa, and Stark Shale Member, Dennis Formation, Nebraska) that have yielded "abundant conodonts" (Schram 1984). These specimens are fairly well-preserved because Schram (1984: 208) indicated that "the holotype alone is more complete than the known specimens of *M. ordinatus* Cope, 1886; *M. mathieui* (Pruvost), 1923; or *M.* (*?*) *blairi* Waterston, 1968." Thus, these mycteropoid remains must not have been carried far from their habitat, which suggests that they were marine.

Gray (1988: 62) cautiously concluded that she could not dismiss the possibility "that there were marine, brackish and freshwater taxa throughout eurypterid history", but some more recent studies suggest a shift in opinion about eurypterid habitat. Thus, Tetlie and Poschmann (2008: 241) argued, after a "critical review" of this topic, that "There is much more of a marine influence in many of the sections yielding *Adelophthalmus* than has previously been acknowledged." More precisely, they suggested that "adelophthalmoids as a whole, throughout the history of the clade, inhabited environments situated near the coastal realm, predominantly those with reduced salinities, such as lagoons, estuaries or deltas", while recognizing that "some basal forms are known from fully marine deposits." Tetlie and Poschmann (2008: 241) suggested that *Adelophthalmus* was found in habitats with less salinity than other adelophthalmoids, especially in freshwater. However, this apparently referred to a brief episode of eurypterid history, "during Bashkirian and Moscovian times, when they are usually encountered within **coal-bearing strata** and associated with **terrestrial organisms** and 'freshwater bivalves'." Terrestrial organisms cannot indicate paleosalinity, and the coal-bearing strata have recently been reinterpreted as displaying marine influence (e.g., Carpenter et al. 2015; Ó Gogáin et al. 2016). Tetlie and Poschmann (2008: 242) admitted that "These horizons were usually interpreted as reflecting freshwater conditions, but nevertheless a marine influence is commonly, but not always, encountered within the respective sequences", and they concluded that "*Adelophthalmus* seems to be mainly confined to paralic or lowland basins, in depositional environments that had a close connection to the marginal marine realm." This interpretation differs only slightly from my interpretation of the habitat that I infer from the associated fauna, such as microconchids, xiphosurans, and xenacanthiforms, and from more recent literature about the relevant localities. The habitats of *Adelophthalmus*, which is arguably the most "freshwater" eurypterid, were obviously close to the sea, and Tetlie and Poschmann (2008) interpret them as freshwater, whereas I suspect, based on other associated faunal elements, that they were more likely to have been brackish environments, although perhaps with a fairly low salt content.

More recent research suggests that Permo-Carboniferous eurypterids may have lived closer to the seas than previously thought. Thus, Braddy et al. (2023), in their study of *Hibbertopterus* (Mycteropoidea, Stylonurina) from the Carboniferous of Kinney Quarry (New Mexico), indicated that this site included sediments from "non-marine to shallow marine settings", but as in most other studies, "non-marine" only indicates an environment other than a typical marine setting in which coral reefs and echinoderms (among others) occur; this does not rule out brackish estuaries, deltas and lagoons. But more marine conditions were suggested by Feldman et al. (1993: 489–491) because brachiopods and crinoid debris occur there. Indeed, Braddy et al. (2023: 261) concluded that "The Kinney Quarry rocks represent a marine embayment" and that *Hibbertopterus* probably lived there (rather than the carcasses having been washed in). In light of their findings, and of a trackway of *Cyrtoctenus* reported from the Ecca Group in a paleoenvironment with possibly high salinity, Braddy et al. (2023: 261) admitted that previous ideas on Permo-Carboniferous eurypterid habitats "may need to be re-evaluated" and that they were probably euryhaline.

I conclude from the above that the presence of eurypterids in the seas and marginal-marine environments is much better established than in truly freshwater deposits; I have not seen a single solid case for the latter, although localities where *Adelophthalmus* occurs without any other faunal element suggesting marine influence (if such localities exist) could plausibly represent a freshwater environment. However, I have not studied all eurypterid-bearing localities, so my conclusions on Permo-Carboniferous eurypterid paleoenvironments remain tentative; as Tetlie and Poschmann (2008: 242) admitted, our understanding of eurypterid paleoecology "is still in its infancy", and "only detailed examinations, i.e. bed-by-bed excavations of eurypterid-bearing sequences, may further improve our knowledge". Nevertheless, this interpretation of the habitat of eurypterids is not new. In his summary of the three main schools of thought on this topic, Plotnick (1999: 107) indicated that according to the "facies School" (one of the three main schools), first proposed by Kjellesvig-Waering (1961), eurypterids occurred in three facies: biofacies 1, fully marine; biofacies 2, near-shore, epeiric seas and lagoons, presumed to be somewhat hypersaline; biofacies 3, presumed "near-shore, brackish, deltaic environments. Note that even biofacies 3 is considered brackish, rather than truly freshwater. Kjellesvig-Waering (1961:794) explained that it included "the more brackish part of bays, and estuaries." This is further confirmed by Plotnick (1999: 107), who clarified that "Biofacies 3 of that school (not of his own scheme) was considered to be brackish water and landward of BA [Biofacies Assemblage] 1." This still seems to reflect the habitat of the most continental eurypterids; I have seen no evidence of eurypterids living far from the seas, in mid- to high-altitude, freshwater lakes and rivers.

Euthycarcinoids

These enigmatic arthropods of uncertain affinities (Ortega-Hernández et al. 2010; Giribet and Edgecombe 2019) occur in some Permo-Carboniferous localities that yielded stegocephalians, like Mazon Creek and Montceau-les-Mines (Rolfe 1985; Schram and Rofle 1994). The literature suggests that they inhabited a wide range of habitats from marine to freshwater, but this literature arguably displays the same problems in paleoenvironmental interpretation as that of eurypterids. Thus, Schram and Rolfe (1994: 142) indicated that while many euthycarcinoids seem to have been marine, those from Montceau-les-Mines "are thought to have inhabited fresh water (Rolfe 1985)." However, Rofle (1985) may have suggested that the Montceau euthycarcinoids were freshwater inhabitants only because they were associated with "amphibians", which is not a good justification (Laurin and Soler-Gijón 2010). Simultaneously, he admitted that at Mazon Creek, they occur "only in the Essex fauna, i.e. with the most marine animals, in the distal region of the delta" (my translation throughout this paper, unless indicated otherwise). Neither paper explains why the Mazon Creek euthycarcinoids are marine, whereas the same taxa in Montceau should be considered freshwater. The euthycarcinoids of both localities are thought to be closely related; *Schramixerxes gerem* in Montceau is closely related to *Kottixerxes gloriosus* from Mazon Creek, whereas *Sottixerxes multiplex* from Montceau is related to *Pieckoxerxes pieckoae* from Mazon Creek, according to Schram and Rolfe (1994: 142). Indeed, Poplin and Heyler (1994) provide a different, arguably better-justified interpretation of the same findings:

> *"Fossil remains of these animals were found in many regions of the world, generally in rocks derived from marine or coastal environments, such as Mazon Creek for instance. Thus their presence in the intermontane basin of Montceau-les-Mines poses a problem."*

Similarly, Racheboeuf et al. (2008: 12) interpreted the euthycarcinoids from Montceau as freshwater organisms, partly based on comparisons with euthycarcinoids from the "non-marine Braidwood facies of Mazon Creek" (p. 23). However, this quote raises two problems: first, it places these Mazon Creek euthycarcinoids in a different facies than Rofle (1985), and second, as discussed above (section on xiphosurans), Mazon Creek apparently lacks a freshwater fauna; it preserves aquatic, presumably euryhaline taxa, and terrestrial organisms (Clements et al. 2019). Furthermore, Racheboeuf et al. (2008: 14) mentioned that Schram and Rolfe (1997: 211) considered euthycarcinoids to be marine.

Brachiopods

Brachiopods occasionally co-occur with stegocephalians in Permo-Carboniferous localities. Extant brachiopods are exclusively marine animals, with a fairly low tolerance to salinity variations. Some studies have suggested that in the Paleozoic, they may have lived in slightly hypersaline or slightly brackish water (Fürsich and Hurst 1980). However, among extant brachiopods, even lingulids, which are probably the most tolerant brachiopods to salinity variations, are "only moderately euryhaline, and optimally marine", as shown by experimental studies (Hammond 1983: 1311). They normally live in a salinity of at least 30‰ (Hammen and Lum 1977), even though lower salinities may be tolerated for short periods. The paleoenvironmental significance of lingulids has often been misinterpreted, according to Cherns (1979). In his study of two nominal species of *Lingula* from the Lower Leintwardine Beds (LLB), Ludlow, late Silurian, Cherns (1979: 42) stated that "Fossil lingulids, by analogy with modem forms, are often inferred to have lived in shallow water", but after analyzing his data, he concluded (p. 45) that "Neither LLB species conforms to the commonly held view of *Lingula* as an intertidal, very nearshore, or even brackish water, indicator." Thus, the presence of any brachiopod in a locality indicates a marine, fairly saline environment, contrary to what has often been suggested.

Echinoderms

Echinoderms are infrequently associated with stegocephalians, but a few such associations are mentioned below, so it is worth reviewing briefly their osmotic tolerance. This taxon is overwhelmingly marine, a constraint probably linked to the fact that echinoderms have poorly developed circulatory, excretory, and gas exchange systems (Turner 2007: 464). Very few extant echinoderms, like *Ophiura albida*, *Amphiura chiajei* and *Asterias rubens*, have adapted to brackish waters (Cognetti and Maltagliati 2000: 9). Turner and Meyer (1980: 249) reported that "brackish-water populations of at least 22 species of echinoderms" were known, but more appeared to be discovered subsequently because Turner (2007: 464) reported that about 40 species of echinoderms occur in estuaries. This is a tiny proportion of the 7584 currently recognized extant echinoderm species (as of 3 march, 2024) by the WORMS (World Register of Marine Species). Even the most euryhaline extant echinoderm (and the only one endemic to brackish water), the ophiuroid *Ophiophragmus filograneus*, which has been found occasionally in brackish water that had (momentarily) very low salinities, showed physiological stress when subjected to salinities below about 17‰ (Turner and Meyer 1980: 252), and experiments showed exposure to 8‰ salinity is deadly within 17 days (Turner 2007: 467). A record for echinoderms is a naturally-occurring population in Florida that was observed in a bay at 7.7‰ salinity in summer of 1958, but in that season, salinity fluctuated between 7.7 and 14‰ salinity, and after 1959, a subsequent study failed to recover any individuals (Turner 2007: 471), so it is possible that this bout of low salinity proved fatal for this population. Furthermore, some estuarine populations of echinoderms are sterile and continue to exist only through immigration from more marine environments. Thus, the presence of echinoderms is strong evidence that a truly marine environment either prevailed locally, or occurred in the vicinity, and that the salinity was probably above 15‰ on average, on a yearly basis, although it may have occasionally fluctuated down to a minimum of about 8‰, below which even the most osmotolerant echinoderms are quickly killed.

Cephalopods

Extant cephalopods are among the most strictly marine mollusks. Parsimony suggests that crown-cephalopods in general were also marine, and this crown-group is ancient, given that the divergence between nautilids and coleoids harks back deep into the Paleozoic. Indeed, some molecular studies placing it around the Late Devonian (Stöger et al. 2013), which is plausible because coleids are known from the Carboniferous at least (Klug et al. 2019) and nautiloids are much older still. What we know of the cephalopod fossil record (Leonova 2011) also suggests that they have always been exclusively marine forms. Unsurprisingly, cephalopods only infrequently co-occur with stegocephalians in Permo-Carboniferous localities, but several such examples are mentioned in this paper. Most extant cephalopod taxa tolerate only mild salinity fluctuations (Jereb and Roper 2016: 6). The most euryhaline taxa, like the squid *Lolliguncula brevis*, can survive in water that has at least 17.9‰ salinity (Bartol et al. 2002), which is about half of the normal sea water salinity (about 35‰); they die in about 48 h in water that has 16.5‰ salinity (Hendrix et al. 1981). Thus, the presence of cephalopods in a locality indicates strong marine influence, unless there is evidence of long-distance transportation.

Freshwater jellyfish?

Many articles that describe supposedly fully continental (i.e., without any marine influence) deposits reported “freshwater jellyfishes” (e.g., Poujol et al. 2023: 5). Yet, an overwhelming majority of extant cnidarians are marine, with only fewer than 35 nominal species documented in freshwater habitats (Jankowski et al. 2008), as compared to over 12 000 nominal extant cnidarian species, according to the WORMS registry (https://www.marinespecies.org/ consulted on October 3, 2023). This amounts to 0.3% of the extant cnidarian specific biodiversity in freshwater ecosystems. In Permo-Carboniferous localities, putative “freshwater jellyfishes” and other cnidarians have been reported in sites that are now known to show strong marine influence. Most interesting is the case of Mazon Creek, which has yielded a variety of cnidarians (Clements et al. 2019: table 1), including medusae and the hydroid *Devotella* (Schultze 2009: 127). The most common cnidarian at Mazon Creek is *Essexella asherae* (Baird et al. 1985), which is a sea anemone, rather than a medusa (Plotnick et al. 2023). *Essexella asherae* appears to be autochtonous at Mazon Creek because of its abundance and its benthic lifestyle, and it was presumably a euryhaline, coastal marine taxon (Plotnick et al. 2023: 24) because Baird et al. (1986: fig. 2) showed that it is most abundant in the deepest, most marine (offshore) facies.

Devonian localities

Established ideas and recent isotopic analyses

Most Devonian localities that have yielded stegocephalians were long interpreted as freshwater by most authors. Thus, Long and Gordon (2004: 703) stated that “A reasonable generalization is that they [Devonian stegocephalians] most likely inhabited large **freshwater river and lake systems**, environments similar to those inhabited by the East Greenland forms [*Ichthyostega* and *Acanthostega*].” However, Schultze (2009: 128) argued that “The most parsimonious interpretation of the environment of the earliest (Devonian) tetrapods is coastal marine”. Subsequent isotopic study of *Ichthyostega* remains, and those of other Devonian tetrapodomorphs from East Greenland (Upper Devonian Celsius Bjerg group, *Remigolepis* series) and from the Zhongning Formation of Ningxia Hui (China), which has yielded the stegocephalian *Sinostega pani*, confirmed that these taxa “were euryhaline and inhabited transitional aquatic environments subject to high-magnitude, rapid changes in salinity, such as estuaries or deltas” (Goedert et al. 2018: 68). This result is particularly interesting because my earlier review (Laurin and Soler-Gijón 2010: fig. 4) accepted *Ichthyostega* and *Acanthostega* as the only Devonian stegocephalians for which the traditional freshwater habitat interpretation was not contradicted by indicators of marine influence; I now stand corrected! It would be interesting to perform similar analyses on other Devonian localities and formations, such as the Red Hill locality of the Catskill Formation, which yielded the stegocephalian *Hynerpeton*, and which was long interpreted as a freshwater taxon, but which might possibly have been euryhaline (Broussard et al. 2018).

Strud (Belgium)

The Famennian Strud locality (Belgium), which recently yielded a stegocephalian (Clément et al. 2004), has been interpreted as “one of the oldest continental – probably fresh-water – ecosystems” (Denayer et al. 2016). However, this hides considerable variability in the salinity of the environments represented in the strata of Strud, as the authors recognized:

> *“The depositional setting approximately corresponds to a ramp with both an increase in the marine influence and a deepening southwards (Thorez et al. 1977). The proximal facies (northwards) frequently*

> *show a continental influence and are thus dominantly sandy and silty, whereas the distal facies (southwards) are more mixed with frequent carbonate intercalations (Ciney area and southwards) indicating deposition in a 'deeper' part of the basin (c. 50 m deep after Thorez & Dreesen, 1986)."*

Indeed, faunal elements that indicate a fairly typical marine environment occur at various levels of the Strud succession and more generally, in the Dinant Synclinorium (Thorez et al. 1977). These will be reviewed from the base to the top. In the late Fransian/early Famennian Fasiole Formation, Denayer et al. (2016: 113, 116, 121) report spiriferid brachiopods and a sandy crinoidal limestone. The overlying Bois-des-Mouches/Citadelle de Huy Formation includes, near its top, a "coarse crinoidal limestone" (Denayer et al. 2016: 115), as well as "rhynchonellid brachiopods, locally abundant but not broken", which "suggest a more marine environment" (Denayer et al. 2016: 123). The late Famennian Poulseur Member of the Comblain-la-Tour Formation contains "some brachiopod shells, often dissolved" (Denayer et al. 2016: 115), and a "bioturbated marine sandstone" (Denayer et al. 2016: 123). Finally, near the top of the succession, the Complain-au-Pont Formation contains a crinoidal limestone (Denayer et al. 2016: 115). Lamsdell et al. (2019: 1709) indicated that the 1.4 m thick channel-filling succession in which they found eurypterid material displayed "no evidence for marine influence". This may have been true of the 1.4 m section, but is this a large enough area to expect to find traces of marine influence in what was apparently a deltaic or estuarine environment? And eurypterids only indicate that the sea was near (see above).

The stegocephalian from Strud was found in beds B and D of the Royseux Member of the Evieux Formation (Clément et al. 2004; Denayer et al. 2016: 114), which did not yield typical marine fossils. Because of this, these beds of the Royseux Member have been interpreted as a freshwater to brackish, fluviatile to estuarine environment. However, this member is between the Poulseur Member and the Complain-au-Pont Formation, both of which contain marine fossils. Thus, the open sea was probably not very far from the habitat of the Stud stegocephalian. Indeed, Denayer et al. (2016: 123) interpreted the Royseux Member of the Evieux Formation) as "a lagoonal deposit in a back-barrier position. It consists of fining-upwards sequences associated with red beds, evaporitic dolomite (sabkha sequence) and anhydrite pseudomorphs, locally with dark shale". The presence of evaporitic dolomite and of anhydrite pseudomorphs implies saline (plausibly brackish) water, which became hypersaline at least occasionally. Were the scant remains of the stegocephalians washed in, which would be compatible with a freshwater habitat, or did this stegocephalian inhabit the estuary and other marginal-marine habitats, as apparently did the other Devonian stegocephalians? In this case, the fragmentary nature of the specimen does not preclude the possibility that it represents an allochtonous taxon.

Carboniferous localities and formations

Minto Formation (New Brunswick)

The early Moscovian (Pennsylvanian) Minto Formation of New Brunswick has yielded an interesting metazoan fauna that includes a few stegocephalian remains, including a jaw that plausibly belongs to a colosteid, small limb bones, and a vertebral centrum that has been plausibly attributed to an embolomere, in addition to finned tetrapodomorph material, mostly assigned to *Megalichthys* (Ó Gogáin et al. 2016). While the stegocephalian material is scant (15 specimens, out of the total of 722 vertebrate specimens), Ó Gogáin et al. (2016: 713) suggested that the vertebrate remains had undergone "minimal transportation". Nevertheless, the possibility that the fragmentary stegocephalian remains of this locality represent para-autochtonous occurrences cannot be dismissed. This site is interesting because the paleoenvironment appears to represent marginal-marine environments with a salinity gradient that ranges from open marine shallow environments to tidal estuaries. This interpretation is supported by framboidal pyrite, sponge spicules, spirorbiform microconchids, echinoid spines, bioclasts of punctate brachiopods in the most marine facies, and spirorbiform microconchids, along with the bivalve *Naiadites*, in the brackish embayment facies. The xenacanthiform remains occur in all facies (salinities), which is consistent with their inferred broad osmotic tolerance, which appears to have ranged from fully marine to freshwater (see above). Other taxa appear to have displayed osmotic preferences: dipnoans, some rhizodonts (*Archichthys*, *Strepsodus*) and *Megalichthys* occur mostly in the open marine facies, whereas *Rhizodus* and *Rhizodopsis* are most common in brackish tidal estuaries (Ó Gogáin et al. 2016: 714). The stegocephalians are most abundant in the brackish embayment. Ó Gogáin et al. (2016: 717) suggested that euryhaline habit could explain why many Permo-Carboniferous gnathostome remains "show enriched strontium isotope values indicative of continental or freshwater influences".

Joggins

Joggins has yielded many stegocephalian remains, including the oldest known amniotes (Carroll 1964; Archer et al. 2015: 662). The diversity, abundance, and quality of preservation of stegocephalian remains (e.g., Godfrey et al. 1991), many of which are articulated (Holmes et al. 1998) or at least composed of many clearly associated skeletal elements (Mann et al. 2020), suggests that little transport had occurred (Falcon-Lang et al. 2006: 561). This locality has long been interpreted as an intra-montane, freshwater basin (Carroll 1970: 17), and some isotopic analyses support this interpretation (Brand 1994). As we saw above (isotopic section), Brand (1994) suggested that the Joggins Formation sediments were non-marine (continental), but the few Sr isotopic analyses performed by Carpenter et al. (2015) led them to conclude that these results were equivocal, and only indicated that the environment was probably not fully marine. Indeed, Carpenter et al. (2015) concluded, based on faunal data, that the marine influence at Joggins was fairly strong, at least at several stratigraphic levels.

Other recent studies support marine influence in the Joggins Formation (Davies et al. 2005), and similar conclusions had been reached much earlier by Duff and Walton (1973). The Joggins cliffs preserve a variety of habitats that reflect 14 or 15 cyclothems (probably linked to regressions and transgressions), with some levels representing marginal marine levels, and other levels that exhibit less marine influence (Grey et al. 2011; Carpenter et al. 2015). The marine levels are represented by the open water (OW) facies that contains limestone and coal; other facies include poorly drained floodplain units (PDF) and well-drained alluvial plain units (WDF). The presence of framboidal pyrite in the most marine levels also indicate normal marine salinity levels (Grey et al. 2011: 262), and agglutinating foraminifers, which are characteristic of shallow marine environments, occur both in Joggins and the nearby Sydney basin, where the Florence locality is located (Schultze 2009: 127–128).

The OW facies has been interpreted as reflecting a “brackish sea” in recent studies (e.g., Carpenter et al. 2015), but it yields fossils that show that a stenohaline, marine fauna was present nearby; these include echinoderm fragments (from blastoids, crinoids, or both), fragments of punctate brachiopods (Grey et al. 2011: 260), and actinistian scales (Schultze 2009: 127). In addition, the OW facies yields other taxa that may have been euryhaline rather than frankly marine, including microconchid tubes, chondrichthyan scales and teeth, and a lungfish tooth plate. Grey et al. (2011: 262) concluded that «The Joggins Formation records a waning marine influence over time» and that at some point (at least in the OW facies showing the strongest marine influence, especially near the base of the formation), it was close to the Paleo-Tethys Ocean. Grey et al. (2011: 262) noted “antithetic abundances of brackish ostracodes and freshwater bivalves”, but at Joggins, bivalves are present even in layers that produced fragments of punctate brachiopods (Grey et al. 2011: 260), so without a finer analysis that discriminates between the bivalve taxa present at various levels, it is unclear that these are indeed freshwater (rather than brackish water, or even marine) bivalves. Grey et al. (2011: 262) supported earlier conclusions that the Joggins Formation represents “fluvial deposition into shallow brackish waters” and suggested that this brackish environment was inhabited only by euryhaline organisms. In extant ecosystems, typical brackish faunae composed primarily of taxa with marine relatives inhabit waters where the salinity is between 5‰ and 30‰, and especially in the upper half of this salinity range (Cognetti and Maltagliati 2000). Carpenter et al. (2015: 662) suggested that a western extension of the Tethys Ocean had spread through a hypothetical mid-Euramerican seaway and reached the area of Joggins at highstand of cyclical transgressions possibly driven by Milankovitch-scale orbital cycles. They also suggested that the brackish waters present at Joggins “probably represent the distal extension of the marine bands that characterize coal measure successions in north-west Europe”, which suggests marine influence in many other Permo-Carboniferous localities that have yielded stegecephalians. These interpretations are supported by the reinterpretation of supposedly endemic gnathostome taxa (*Ctenoptychius cristatus*, actually a synonym of the chondrichthyan *Ageleodus pectinatus*; *Gyracanthus duplicatus*, actually an undetermined gyracanthid acanthodian; *Conchodus plicatus*, actually an indeterminate *Sagenodus* dipnoan) as fairly cosmopolitan taxa that also occur in fully marine environments. Thus, Carpenter et al. (2015: 682) interpreted the Joggins aquatic gnathostome fauna “as having a distinctly euryhaline or diadromous mode of life”, and they even suggested (p. 683) that in the Pennsylvanian, a much greater proportion of gnathostomes were euryhaline than today (only 3–5% now), and that this represented an important intermediate step toward the subsequent establishment of vertebrates in freshwater habitats. Carpenter et al. (2015: 683) interpreted this as resulting from important glacio-eustatic fluctuations that resulted in the “widespread development of brackish estuaries and epeiric seaways”. Ironically, these recent works suggest that Dawson’s (1865) much earlier interpretation of Joggins as a coastal deposit was correct, after all.

Hamilton fossil-Lagerstätte

This fossil Konservat-Lagerstätte from Kansas preserves a Stephanian coastal community (Cunningham et al. 1993). The stegocephalian fauna includes temnospondyls (Trimerorhachoidea, Dissorophoidea, the second-most frequently represented vertebrate taxon, and Eryopoidea), some of which are represented by larvae, as well as amniotes (Captorhinomorpha, Diapsida, Edaphosauridae, and Ophiacodontidae). Other vertebrates include the acanthodian *Acanthodes*, which is the most common vertebrate, Xenacanthida (*Expleuracanthus?*, *Orthacanthus*, and *Xenacanthus*), Hybodontoidea (*Hamiltonichthys*), Actinopterygii (‘*Elonichthys*’ and other), Dipnoi (*Gnathorhiza*, *Sagenodus*), Actinistia, and Tetrapodomorpha (Megalichthyinae). Eurypterids and numerous remains of “spirorbids” (actually microconchids) from Hamilton may represent euryhaline forms (see above), but brachiopods and echinoderms provide the best evidence of normal marine conditions in at least some levels (in the marine limestone and mudstone), which also yielded temnospondyls. Many of the vertebrates are articulated and fairly well-preserved, which suggests that they have not been transported far from where they lived, although others show signs of flotation. Furthermore, vertebrate coprolites include remains of marine metazoans

(Cunningham et al. 1993: 230), which shows that they fed in a marine environment. Much of the local fauna appears to have been preserved in its environment; Cunningham et al. (1993: 227) stated that "Some productid brachiopods, for example, are preserved in apparent growth position, nested between clasts, with their delicate spines intact. Additionally, some colonies of an encrusting cystoporate bryozoan (*Fistulipora*?) apparently are in growth position". Other fossils from Hamilton, such as bryozoans, echinoderms, and fusulinids, are fragmented, abraded, and micritized and may be reworked from older sediments (Cunningham et al. 1993: 227). These could have been transported (not necessarily far), but they are easily distinguishable from the much better-preserved autochtonous elements. Schultze et al. (1994: 443) interpreted the temnospondyls as autochtonous and concluded that they "retained their tolerance to salinity from their marine ancestors and were able to spawn in near-shore environments."

The Hamilton locality displays three main lithologies: a conglomerate, an ostracode wackestone, and an assemblage of laminated limestones and mudstones. Most marine and brackish fossils mentioned above occur in all three lithologies, except for the echinoderms, which may occur only as lithoclasts of wackestone, in the laminated limestones and mudstones, which also includes the vertebrate fossils. Patterns in the lamination suggest that the limestones and mudstones were deposited in a tidal environment, and Cunningham et al. (1993: 235) suggested that the high sedimentation rate and variable salinity may have enhanced fossilization. The deposits probably formed in a lagoon or estuary and some tidal creeks. Cunningham et al. (1993: 234) concluded that despite the fact that previous studies had "emphasized the freshwater nature of the laminated limestones from the Main Quarry based on some faunal elements, systematic sieving of the fossil-bearing beds has revealed the presence of marine invertebrate fossils throughout the sequence" and suggested that "The mixed composition of the fossil assemblage is interpreted as indicative of brackish or, most probably, variable paleosalinity." Thus, the vertebrates that inhabited this locality were plausibly euryhaline, coastal forms. Hamilton is among the most marine-influenced Permo-Carboniferous localities (all of which yielded stegocephalians) compared by Schultze and Maples (1992).

Mazon Creek

Much has been written about the biota and paleoenvironment of this locality, including in various sections (above) of the present paper. Here, only a few additional points need to be added. Above, I indicated that many taxa found in Mazon Creek may have been euryhaline, but exceptions exist. Beyond the obvious case of allochtonous (mostly terrestrial) taxa, a fairly diverse cephalopod assemblage is documented (Saunders and Richardson 1979), and this even includes coleoids (Doguzhaeva et al. 2007), which have a poor fossil record. As mentioned above, the vast majority of cephalopods are stenohaline, marine forms, and only a few taxa, like the extant squid *Lolliguncula brevis* are moderately euryhaline (Bartol et al. 2002). Shark egg capsules are also present, and this also suggests strong marine influence because extant chondrichthyans lay eggs only in the marine environment, including along the coasts, notably in estuaries, but never in freshwater (Schultze and Soler-Gijón 2004: 326; Schultze 2009: 127). Holothurians, which also occur (Baird et al. 1986), are another typically marine taxon, like most other echinoderms.

Thus, Mazon Creek undoubtedly exhibits a stronger degree of marine influence than most other classical Permo-Carboniferous stegocephalian-bearing localities. This is paradoxical because a detailed study of tidal rhythmites of various Carboniferous and Holocene localities led Archer et al. (1995: 411) to conclude that "the Francis Creek rhythmites [in the area of Mazon Creek] may have formed in a **significantly inland** setting with a **strong fluvial influence** and overprinting on the tidal cycles." Thus, the sedimentological data point at a brackish-water estuarine environment where stenohaline marine forms could not have lived. The cephalopods documented from Mazon Creek may have ventured there at high tide when salinity was the highest and may have made only brief incursions there.

Other than the cephalopods, the obviously allochtonous elements include the remains of terrestrial embryophytes and of terrestrial arthropods, such as myriapods, arachnids (including scorpions), and insects (Clements et al. 2019: 5). The possibility that some bivalves and stegocephalians were washed-in freshwater faunal elements was considered briefly by Clements et al. (2019: 5) based on the previously assumed habitats of these taxa, but these authors admitted that the occurrence of these bivalves with "polychaetes" raised serious doubts about this interpretation, and that the habitat of the stegocephalians was equally poorly constrained. The exceptionally good preservation of these stegocephalian remains, with dermal scales (e.g., Mann et al. 2021), skin and toepads (Mann and Gee 2020) suggests that they have not been transported far, without guaranteeing that they were truly autochtonous.

Red Tanks Member of the Bursum Formation

Although not among the classical stegocephalian-bearing Permo-Carboniferous localities, the Red Tanks Member of the Bursum Formation recently yielded a fairly diversified assemblage of late Pennsylvanian stegocephalians (the temnospondyls *Eryops*, *Trimerorhachis* and an undetermined taxon, the embolomere *Archeria*, a diadectid, a caseid, *Edaphosaurus* and *Dimetrodon* cf. *D. milleri*) and other vertebrates (the chondrichtyans *Petalodus* and *Deltodus*, undetermined actinopterygians, as well as the dipnoan *Gnathorhiza bothrotreta*) from "mixed marine-nonmarine sequences" (Harris et al. 2004: 267). The presence of typically marine levels in limestone layers of this member is demonstrated by the presence of conodonts and fusulinids, among others. In addition to this limestone, the Red Tanks Member includes “nonmarine mudstones and siltstones of a coastal plain environment”, “mudstones of a brackish to freshwater environment”, “nearshore and fluvial sandstones, limestone conglomerates of a high-energy nearshore environment, limestone horizons composed of different types of bioclastic wackestones and mudstones, and rare packstones indicating deposition in an open to restricted shallow marine shelf environment” (Harris et al. 2004: 267–268). Thus, this member seems to preserve several paleoenvironments, most of which show some marine influence, as well as some freshwater environments. The stegocephalians and other vertebrates were found in several lithologies, mostly in mudstones, siltstones, sandstones and conglomerates, but also, more rarely, in shales and in the limestone levels, as in localities 4640 and 5349 (Harris et al. 2004: fig. 2, appendix). Thus, the vertebrate community preserved in the Red Tanks Member plausibly inhabited a variety of habitats, ranging from freshwater to brackish, possibly even marine. However, given their rather fragmentary nature, some or all of these might represent allochtonous elements.

Montceau-les-Mines

Montceau-les-Mines has been considered by many authors to represent an intramontane, freshwater basin (e.g., Perrier and Charbonnier 2014). Thus, Racheboeuf et al. (2008: 12) indicated that the Montceau biota “is a mixture of both strictly aquatic, **freshwater** faunal components and terrestrial ones”. Also, they argued that “the closest Upper Carboniferous marine deposits were located at least several hundred kilometres SW of Montceau”. However, this argument rests on previous paleoenvironmental interpretations that allowed reconstructing ancient coastlines, which is weak given the numerous changes in interpretation over the years, such as those concerning the Old Red Sandstone. This paleogeographic argument was criticized long ago by Schultze (1995: 258) who pointed out that “This method stacks one interpretation on another (the palaeogeographic position on an assumed distinction of marine from freshwater, the questioned palaeoenvironment)”. Furthermore, Schultze (2009: 130) pointed out that many taxa (conchostracans, ostracodes, the bivalve *Anthraconaia*, eurypterids, *Acanthodes*, chondrichthyans, and actinopterygians) interpreted as freshwater indicators in Montceau also occur in the clearly strongly marine-influenced environment of Mazon Creek. Schultze (2009: 133) went further and stated that “The lack of undoubtedly freshwater forms in the Paleozoic is a specific problem.” This may be slightly overstated because aquatic insect larvae, though uncommon, do suggest freshwater or low salinity, if autochtonous, despite the few exceptions consisting in extant insect larvae that can develop in hypersaline water (Pallares et al. 2015).

The isotopic analyses by Fischer et al. (2013) and Luccisano et al. (2023) suggested that some localities in the area (Buxières-les-Mines, and the Muse) represent continental environments with little or no marine influence (see section “Freshwater chondrichthyans?”), but these studies did not sample Montceau, and I am unaware of relevant isotopic analyses on that locality. Montceau is about 40 km South of the Muse, and about 110 km East of Buxières-les-Mines, so Montceau would have been a little closer to the Paleotethys than Buxières and the Muse (Schultze 2009; Mercuzot et al. 2022), and this is consistent with the presence of taxa that suggest marine influence and that have not been described from Buxières and the Muse. These include acritarchs, the annelid *Palaeocampa anthrax* (Pleijel et al. 2004), which belongs to the marine taxon Amphinomida, and abundant remains of the xiphosuran *Liomesaspis* (Anderson 1997; Racheboeuf et al. 2002). As mentioned above (section on xiphosurans), even the most euryhalie extant xiphosuran does not venture more than about 100 km from the seas. All of these were dismissed by Racheboeuf et al. (2008: 13) as indicators of marine influence, but accepted as such by Pleijel et al. (2004).

Another possible indicator of marine influence is *Myxineidus gononorum*, based on a fossil that was initially described as a hagfish, even though a more recent study raised doubts about its identity and suggested that it might be a lamprey (Germain et al. 2014). Hagfishes are purely marine, but lampreys inhabit both the seas and freshwater. The fossil displays two rows of denticles forming a chevron pattern, which is characteristic of hagfishes and what appears to be an impression of a wrinkled skin, which is reminiscent of a dead hagfish, but a faint halo around the head looks like the peculiar mouth of lampreys (though it appears to be devoid of the keratinous denticles present on the mouth of extant lampreys). However, Germain et al. (2014: 133) wondered if “this pattern [reminiscent of a lamprey’s mouth] somewhat reflects the original body shape of the animal, or is merely and incidental artefact due to the distribution of microbially induced films during the decay of the animal”, and they also admitted that “Quite a similar halo is sometimes observed in other fossiliferous nodules from Montceau-les-Mines, not necessarily associated with soft tissue preservations.” In the end, their suggestion that the fossil represented a lamprey seemed to depend as much on the presumed freshwater habitat of Montceau as on its morphology, because they stated that their new interpretation “would perhaps resolve the controversial problem of the presence of a hagfish in the reputedly fresh-water, intramontane basin of Montceau-les-Mines”. Indeed, Germain et al. (2014: 134) stated that the Montceau basin “provides no clear evidence for any marine influence, be it temporarily.” Given the evidence mentioned above that suggests marine influence in that basin, especially the annelid *Palaeocampa* and the xiphosuran *Liomesaspis*, it seems better to base a taxonomic assignment of *Myxineidus* on its morphology, which unfortunately leaves serious doubts about its affinities.

Stegocphalians are represented by temnospondyls (*Branchiosaurus petrolei*, *Micromelerpeton boyi*, and fragments of *Actinodon*), nectrideans (*Sauravus costei*, *S. spinosus*, and *Montcellia longicaudata*), the aistopod *Phlegethontia longissima*, and fragments of a synapsid (*Stereorachis? blanziacensis*); none of these are very well-preserved, even though several specimens preserve traces of soft tissues (Perrier and Charbonnier 2014). It is thus unclear if this fauna was autochtonous; significant transport cannot be excluded.

German basins

In my previous review (Laurin and Soler-Gijón 2010), I presented various arguments supporting marine influence in the Saar-Nahe basin. These obviate the need for a detailed treatment of this basin, but a few additional points can be made. The presence of glauconite in that basin also supports marine influence (Schultze 2009: 131) because it normally forms in the marine environment (Baldermann et al. 2013). In addition, microconchids are present in various horizons in the basin (Schultze 2009: 131 and references cited therein), and as indicated above (section "Freshwater microconchids?"), these indicate marine influence.

In the central German basins, which extend from the Thüringer Wald Permo-Carboniferous basins to the Döhlen Basin farther east, Schultze (2009: 132) reported the presence of chondrichthyan egg capsules. As indicated above (section on Mazon Creek), these suggest fairly strong marine influence. In addition, xiphosurans (the limulid *Euproops*) occur there, in several levels, and they can be locally abundant given that Schultka (2000) described 45 individuals from at least four levels of a single locality. As explained in the section "Xiphosuran habitat through time", this suggests at the very least proximity to the sea. In north-east Germany, the Rotliegend has yielded "hydromedusas" (Legler et al. 2004), which also suggests marine influence (Schultze 2009: 132).

It is impossible to assess the allochtonous or autochtonous nature of all stegocephalian remains found in all localities of the German basins, but the *Glanochthon latirostre* and *Archegosaurus decheni* found in a shark (*Triodus sessilis*) in the Lower Permian Lake Humberg, in the Saar-Nahe Basin, probably all lived in the same environment and there is no reason to infer significant transport (Kriwet et al. 2008).

Bohemia

The Bohemian basins in the Czech Republic were already discussed by Laurin and Soler-Gijón (2010), so only a few comments are needed here. These basins are best known for the famous Late Carboniferous (Westphalian D, Kasimovian) Nýřany locality (Schoch 2022: 14) in the Plzeň-Manětín Basin (Klembara et al. 2014). Nýřany yielded a great diversity of stegocephalians: temnospondyls, such as *Cochleosaurus bohemicus* (Sequeira 2003), *Cheliderpeton vranyi* (Werneburg and Steyer 2002), *Anthracobamus fritschi*, *Branchiosaurus salamandroides*, *'Platyrhinops' fritschi*, *Mordex calliprepes*, *Mattauschia laticeps* (Schoch 2022), the baphetid *Loxomma bohemicum* (Fritsch 1883), the enigmatic *Gephyrostegus bohemicus* (Godfrey and Reisz 1991), which has long been considered an anthracosaur, although some analyses suggest a more crownward position (Marjanović and Laurin 2019), amphibians that are still often referred to as "microsaurs" (a paraphyletic group), such as *Microbrachis pelikani* (Vallin and Laurin 2004), *Crinodon limnophyes*, *Ricnodon copei*, *Sparodus validus*, *Hyloplesion longicostatum* (Carroll and Gaskill 1978), as well as other amphibians, such as the nectrideans *Sauropleura scalaris* and *Urocordylus angustatus* (Fritsch 1883), and some amniotes, among others. Nýřany and other nearby Carboniferous strata have typically been interpreted as freshwater environments (Sequeira 2003: 21; Opluštil et al. 2005), but Laurin and Soler-Gijón (2010) presented an alternative interpretation. In addition to the presence of chondrichthyan egg capsules and microconchids already evoked by Laurin and Soler-Gijón (2010), the presence of limulid xiphosurans and of the eurypterid *Adelophthalmus* (Schultze 2009: 132) suggest marine influence in at least some parts of the basin and some horizons. Medusae have been described there; they have been interpreted as freshwater taxa (Kozur 1984), but see above (section "Freshwater jellyfish?") for reasons to question this interpretation. The taxonomic diversity suggests that most stegocephalians found in that locality were probably amphibious or aquatic. The Nýřany assemblage has been interpreted as representing a brief, local accumulation, which seems plausible given the good preservation of most specimens (Sequeira 2003: 21). Ichnofossils also show that temnospondyls occurred locally (Turek 1989). All of this supports the hypothesis that most of these specimens were not carried far.

Conclusion

This literature survey illustrates a recurring theme that pervades the history of paleontological research on the Paleozoic paleoenvironments. The absence of typically marine indicators, such as coral reefs, echinoderms, and a diversified brachiopod fauna has been interpreted as indicating a "non-marine environment", which was often implicitly or explicitly assumed to be freshwater. However, "non-marine environments" thus defined (very broadly) include estuaries, deltas, coastal mangroves, lagoons and salt marshes, which occur between truly marine and freshwater environments on, or near the coast, as well as brackish or salt lakes, which occur even far from coasts. This seems to have been too often forgotten. Thus, the paleoenvironment of many Permo-Carboniferous localities that have yielded stegocephalians need to be reassessed, even in the comparatively well-studied Permian redbeds of Texas (Fig. 1).

Freshwater ecosystems may well be very ancient; Gray (1988: 1) even boldly suggested that “The freshwater ecosystem may be as old as most life.” That may well be, but various factors may have conspired to yield a very fragmentary picture of the history of freshwater ecosystems. The ichnofossil record, which is more abundant than body fossils for many taxa, suggests a marine origin of early life; Buatois et al. (2005: 322) stated that “Virtually all Precambrian ichnofaunas represent the activity of open-marine biotas that presumably inhabited nearshore to deep-marine areas under normal salinity conditions”. Oceans and seas cover more of the Earth’s surface than continents, and more importantly, most sediments are deposited by the largest, most powerful rivers, in deltas that are predominantly located at the edge of seas (including epicontinental seas) and oceans. In fact, Peters and Husson (2017: 323) concluded that “Most of the surviving volume of sedimentary rock (~75%) was deposited in and adjacent to shallow seas on continental crust”. By contrast, non-marine sediments decrease in quantity with increasing age. This implies that in the Permo-Carboniferous, we expect far more fossiliferous localities (though not necessarily those that yielded stegocephalians) to represent marine and coastal (plausibly brackish) environments than freshwater ones. These factors, plus the higher erosion rates of high-altitude deposits compared to low-altitude sediments that we can expect from basic physical principles, may result in a low fossilization potential of freshwater organisms, especially ancient ones, except for those living close to the seas, where their remains may be carried after death.

On the contrary, marginal-marine environments, where much sedimentation occurs, should be fairly well-represented in the fossil record, but they may be difficult to interpret because coastlines can vary quickly, especially in deltas, and even on a daily basis, tides result in short-term salinity variations in some coastal habitats. Thus, the exact environmental preferences and tolerances of long-extinct organisms that inhabited these coastal environments are difficult to assess. These organisms appear to have included many Paleozoic stegocephalians. Of course, this does not mean that all Paleozoic stegocephalians lived in brackish or normal-marine salt water. Like extant teleosts that occupy a great range of aquatic environments, many stegocephalians may have been adapted to freshwater habitats, and in some cases, independent evidence exists for this (e.g., Witzmann and Brainerd 2017).

Above, I raised the question of a bias in favor of freshwater interpretation of localities devoid of typically marine fossils, and discussed some cases for which marginal-marine, brackish environments seem more plausible. While I focused on the body fossil record which I know best, I note that Buatois et al.’s (2005) review of the ichnological record suggests a similar pattern. Localities or formations that were initially interpreted as freshwater and now seem to more plausibly represent brackish environments include the Sequatchie Formation (Upper Ordovician) from Georgia and Tennessee (p. 325), the Kanawa Formation (Middle Pennsylvanian) from West Virginia (p. 327), the Permian Rio Bonito Formation from southern Brazil (p. 328), “many Cretaceous units” (p. 331), and the Ekalaka Member of the Paleocene Fort Union Formation in Montana (p. 334), just to mention the cases reported by Buatois et al. (2005). Furthermore, “in virtually every case, ichnological interpretations were supported fully by the companion microfossil studies” (Buatois et al. 2005: 331), as well as by neoichnological studies (p. 337).

This review mostly supports the preliminary conclusions that I presented more than a decade ago (Laurin and Soler-Gijón 2010). For most of the localities that I had discussed earlier, like Joggins, my suspicions of some marine influence have been strengthened by this new literature review. One notable exception is the habitat of some Famennian (Late Devonian) stegocephalians from Greenland. At that time, nothing suggested marine influence, so I had accepted the freshwater habitat that had been inferred in the literature, even though it appeared anomalous in an optimization of habitat use in early stegocephalians (Laurin and Soler-Gijón 2010: fig. 4), in which *Ichthyostega* and *Acanthostega* displayed an acquisition of a freshwater lifestyle from an ancestor that was inferred to have lived in brackish water. The isotopic analyses performed by Goedert et al. (2018) show that there is no need to invoke such transitions to a freshwater habitat in these Devonian taxa, which appear to have inhabited brackish, coastal marine environments. A new optimization of lifestyle on a stegocephalian phylogeny (Fig. 4) shows the updated scores for *Ichthyostega* and *Acanthostega*. Laurin and Soler-Gijón (2010: table 2) had also considered Strud to be a freshwater locality, and while the recent literature still interprets it this way (Denayer et al. 2016), most levels in the Dinant Synclinorium are clearly marine (Thorez and Dreesen 1986), and even in the more continental strata (on the northern edge of the basin) that have yielded stegocephalian remains, the sea could not have been far. More research on the habitat of Devonian stegocephalians would be useful.

The picture that emerges from all this is that early stegocephalian diversification seems to have occurred to a large extent close to coasts, including those of epicontinental seas, and to a lesser extent farther inland, and on land and possibly in freshwater. Is this pattern genuine, or does it reflect a taphonomic artefact that reflects the extent of sedimentation in deltas of the largest rivers on the coasts, along with erosion of sediments deposited farther from the coasts? If the latter is correct, a large evolutionary radiation of stegocephalians may have occurred in freshwater habitats but be poorly known because of taphonomic bias. Some localities, like Buxière-les-Mines, the Muse and Nýřany, may represent these freshwater localities, as suggested by the traditional interpretations. What was the salinity of the coastal environments in which stegocephalians diversified? As we saw above, the mere fact that tides occurred, as shown by tidal rhythmites, does not necessarily indicate brackish water because tidal effects can propagate inland along rivers (Feldman et al. 1993: 495), but most localities

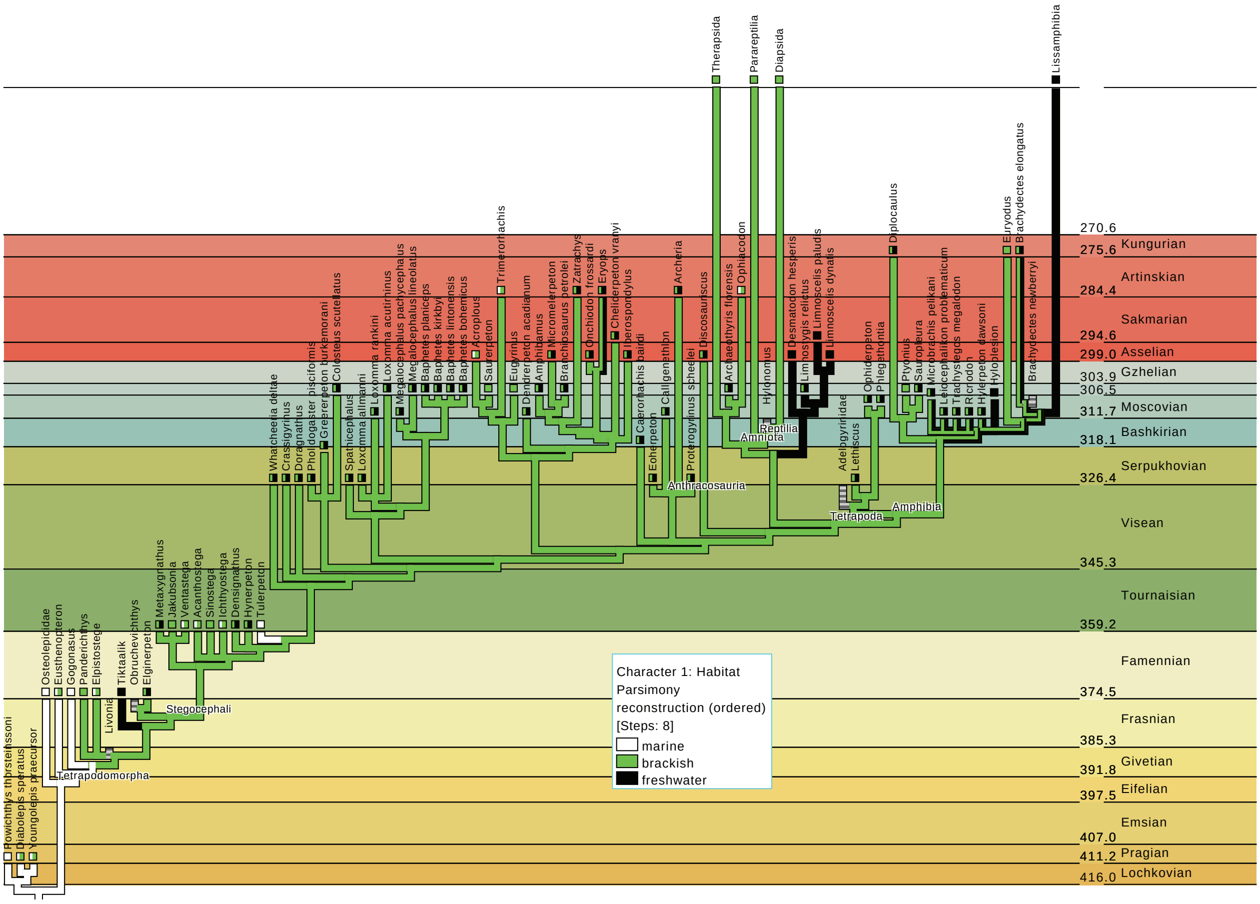

Figure 4. Optimization of habitat in stegocephalians (with a few other sarcopterygians provided to better optimize near the base of Stegocephali) on a phylogeny. This figure is slightly updated from Laurin and Soler-Gijón (2010: fig. 4), which represented the interpretations of the authors at the time. For the data shown, only the habitat of *Ichthyostega* and *Acanthostega* has been updated to reflect the findings of Goedert et al. (2018), along with the geological age of *Sinostega*. To facilitate comparisons, the phylogeny was kept the same as in Laurin and Soler-Gijón (2010: fig. 4); in any case, minor changes in the phylogeny of various taxa would not change the overall pattern, and the relationships between the main clades have been confirmed by two recent studies based on extensive datasets (Marjanović and Laurin 2019; Laurin et al. 2022). The geological timescale, shown only from the Devonian through the Cisuralian, has been colored using the RGB Color Code provided by the Commission for the Geological Map of the World.

where tidal rhythmites have been recognized yielded fossils of taxa of marine origin, which suggests brackish water.

This survey may have raised more problems than it has solved, and unfortunately, time constraints prevented me from reassessing the paleoenvironment of the many Carboniferous stegocephalian-bearing localities and formations, such as the Garnett quarry, and of the more numerous Cisuralian localities. Hopefully, this review has shown that it is time to have a fresh look at the development of continental ecosystems from the Late Devonian through the Cisuralian.

Acknowledgments

I thank Amin Khaleghparast (Tehran, Iran) for sending me two images that he had contributed to create to use as figures, Jean Goedert (CR2P, Paris) for information about isotopic methods to assess paleosalinity, Gloria Arratia (U. of Kansas, Lawrence) for commenting on the short section of the draft on the habitat of early actinopterygians, and Simon Braddy (Manorbier, U.K.) for sending one of his papers on eurypterids and providing the e-mail address of a retired colleague. Two reviewers and the editor, Florian Witzmann, provided feedback that improved the paper. However, the opinions expressed in this paper and the errors that the text may contain are my sole responsibility.

References

Anderson LI (1997) The xiphosuran *Liomesaspis* from the Montceau-les-Mines Konservat-Lagerstätte, Massif Central, France. Neues Jahrbuch für Geologie und Paläontologie-Abhandlungen 204: 415–436. https://doi.org/10.1127/njgpa/204/1997/415

Anderson LI, Horrocks C (1995) *Valloisella lievinensis* Racheboeuf, 1992 (Chelicerata: Xiphosura) from the Westphalian B of England. Neues Jahrbuch für Geologie und Paläontologie, Monatshefte 1995: 647–658. https://doi.org/10.1127/njgpm/1995/1995/647

Andersson PS, Wasserburg G, Ingri J (1992) The sources and transport of Sr and Nd isotopes in the Baltic Sea. Earth and planetary science letters 113: 459–472. https://doi.org/10.1016/0012-821X(92)90124-E

Andersson PS, Wasserburg G, Ingri J, Stordal MC (1994) Strontium, dissolved and particulate loads in fresh and brackish waters: the Baltic Sea and Mississippi Delta. Earth and Planetary Science Letters 124: 195–210. https://doi.org/10.1016/0012-821X(94)00062-X

Annandale N (1909) Xiphosura–The habits of Indian King Crabs. Records of the Zoological Survey of India 3: 294–295. https://doi.org/10.26515/rzsi/v3/i3/1909/163288

Annandale N (1922) The marine element in the fauna of the Ganges. Bijdragen tot de Dierkunde 22: 143–154. https://doi.org/10.1163/26660644-02201020

Archer AW, Kuecher GJ, Kvale EP (1995) The role of tidal-velocity asymmetries in the deposition of silty tidal rhythmites (Carboniferous, Eastern Interior Coal Basin, USA). Journal of Sedimentary Research 65: 408–416. https://doi.org/10.1306/D42680D6-2B26-11D7-8648000102C1865D

Aria C (2022) The origin and early evolution of arthropods. Biological Reviews 97: 1786–1809. https://doi.org/10.1111/brv.12864

Arratia G (2004) Mesozoic halecostomes and the early radiation of teleosts. In: Arratia G, Tintori A (Eds) Mesozoic fishes. Dr. Friedrich Pfeil, Munich, 279–315.

Baird GC, Sroka S, Shabica C, Kuecher G (1986) Taphonomy of Middle Pennsylvanian Mazon Creek area fossil localities, northeast Illinois: significance of exceptional fossil preservation in syngenetic concretions. Palaios 1: 271–285. https://www.jstor.org/stable/3514690

Baird GC, Sroka SD, Shabica CW, Beard TL (1985) Mazon Creek-type fossil assemblages in the U.S. midcontinent Pennsylvanian: their recurrent character and palaeoenvironmental significance. Philosophical Transactions of the Royal Society of London, Series B 311: 87–99. https://doi.org/10.1098/rstb.1985.0141

Baldermann A, Warr LN, Grathoff GH, Dietzel M (2013) The rate and mechanism of deep-sea glauconite formation at the Ivory Coast–Ghana Marginal Ridge. Clays and Clay Minerals 61: 258–276. https://doi.org/10.1346/CCMN.2013.0610307

Bartol I, Mann R, Vecchione M (2002) Distribution of the euryhaline squid *Lolliguncula brevis* in Chesapeake Bay: effects of selected abiotic factors. Marine Ecology Progress Series 226: 235–247. https://doi.org/10.3354/meps226235

Bennett C, Kearsey T, Davies S, Leng M, Millward D, Smithson T, Brand P, Browne M, Carpenter D, Marshall J (2021) Palaeoecology and palaeoenvironment of Mississippian coastal lakes and marshes during the early terrestrialisation of tetrapods. Palaeogeography, Palaeoclimatology, Palaeoecology 564: 110194. https://doi.org/10.1016/j.palaeo.2020.110194

Berman DS (1993) Lower Permian vertebrate localities of New Mexico and their assemblages. New Mexico Museum of Natural History and Science Bulletin 2: 11–21.

Betancur-R R, Ortí G, Pyron RA (2015) Fossil-based comparative analyses reveal ancient marine ancestry erased by extinction in ray-finned fishes. Ecology Letters 18: 441–450. https://doi.org/10.1111/ele.12423

Borzenko S (2020) Principal parameters controlling water composition in saline and brackish lakes in Eastern Transbaikalia. Geochemistry International 58: 1356–1373. https://doi.org/10.1134/S0016702920090037

Boucot AJ, Janis C (1983) Environment of the early Paleozoic vertebrates. Palaeogeography, Palaeoclimatology, Palaeoecology 41: 251–287. https://doi.org/10.1016/0031-0182(83)90091-3

Braddy SJ (2001) Eurypterid palaeoecology: palaeobiological, ichnological and comparative evidence for a 'mass–moult–mate' hypothesis. Palaeogeography, Palaeoclimatology, Palaeoecology 172: 115–132. https://doi.org/10.1016/S0031-0182(01)00274-7

Braddy SJ, Lerner AJ, Lucas SG (2021) A new specimen of *Adelophthalmus luceroensis* (Eurypterida: Chelicerata) from the late Carboniferous (middle Missourian; Kasimovian) Kinney Quarry Lagerstätte of New Mexico. Neues Jahrbuch für Geologie und Paläontologie-Abhandlungen 302: 105–115. https://doi.org/10.1127/njgpa/2021/1021

Braddy SJ, Lerner AJ, Lucas SG (2023) A new species of the eurypterid *Hibbertopterus* from the Carboniferous of New Mexico, and a review of the Hibbertopteridae. Historical Biology 35: 257–263. https://doi.org/10.1080/08912963.2022.2032690

Brand U (1994) Continental hydrology and climatology of the Carboniferous Joggins Formation (lower Cumberland Group) at Joggins, Nova Scotia: evidence from the geochemistry of bivalves. Palaeogeography, Palaeoclimatology, Palaeoecology 106: 307–321. https://doi.org/10.1016/0031-0182(94)90016-7

Broussard DR, Trop JM, Benowitz JA, Daeschler EB, Chamberlain Jr JA, Chamberlain RB (2018) Depositional setting, taphonomy and geochronology of new fossil sites in the Catskill Formation (Upper Devonian) of north-central Pennsylvania, USA, including a new early tetrapod fossil. Palaeogeography, Palaeoclimatology, Palaeoecology 511: 168–187. https://doi.org/10.1016/j.palaeo.2018.07.033

Buatois LA, Gingras MK, MacEachern J, Mángano MG, Zonneveld J-P, Pemberton SG, Netto RG, Martin A (2005) Colonization of brackish-water systems through time: evidence from the trace-fossil record. Palaios 20: 321–347. https://doi.org/10.2110/palo.2004.p04-32

Buatois LA, Mangano MG, Maples CG, Lanier WP (1998) Ichnology of an Upper Carboniferous fluvio-estuarine paleovalley: The Tonganoxie Sandstone, Buildex Quarry, eastern Kansas, USA. Journal of Paleontology 72: 152–180. https://doi.org/10.1017/S0022336000024094

Busch R, West R (1987) Hierarchal genetic stratigraphy: a framework for paleoceanography. Paleoceanography 2: 141–164. https://doi.org/10.1029/PA002i002p00141

Cantino PD, de Queiroz K (2020) International Code of Phylogenetic Nomenclature (PhyloCode): A Phylogenetic Code of Biological Nomenclature. CRC Press, Boca Raton, Florida, [xl +] 149 pp. http://phylonames.org/code/

Carpenter D, Falcon-Lang HJ, Benton MJ, Nelson WJ (2011) Fishes and tetrapods in the Upper Pennsylvanian (Kasimovian) Cohn Coal member of the Mattoon formation of Illinois, United States: systematics, paleoecology, and paleoenvironments. Palaios 26: 639–657. http://www.bioone.org/doi/full/10.2110/palo.2010.p10-121r

Carpenter DK, Falcon-Lang HJ, Benton MJ, Grey M (2015) Early Pennsylvanian (Langsettian) fish assemblages from the Joggins Formation, Canada, and their implications for palaeoecology and palaeogeography. Palaeontology 58: 661–690. https://doi.org/10.1111/pala.12164

Carroll RL (1964) The earliest reptiles. Zoological Journal of the Linnean Society 45: 61–83. https://doi.org/10.1111/j.1096-3642.1964.tb00488.x

Carroll RL (1970) The Earliest Known Reptiles. Yale Scientific Magazine: 16–23.

Carroll RL, Gaskill P (1978) The order Microsauria. American Philosophical Society, Philadelphia, 211 pp.

Chadwick MA, Hunter H, Feminella JW, Henry RP (2002) Salt and water balance in *Hexagenia limbata* (Ephemeroptera: Ephemeridae) when exposed to brackish water. Florida Entomologist 85: 650–651. https://doi.org/10.1653/0015-4040(2002)085[0650:SAWBIH]2.0.CO;2

Charvet-Almeida P, Araújo Md, Almeida MPd (2005) Reproductive aspects of freshwater stingrays (Chondrichthyes: Potamotrygonidae) in the Brazilian Amazon Basin. Journal of Northwest Atlantic Fishery Science 35: 165–171. https://doi.org/10.2960/J.v35.m502

Cherns L (1979) The environmental significance of *Lingula* in the Ludlow Series of the Welsh Borderland and Wales. Lethaia 12: 35–46. https://doi.org/10.1111/j.1502-3931.1979.tb01240.x

Claypool GE, Holser WT, Kaplan IR, Sakai H, Zak I (1980) The age curves of sulfur and oxygen isotopes in marine sulfate and their mutual interpretation. Chemical Geology 28: 199–260. https://doi.org/10.1016/0009-2541(80)90047-9

Clément G, Ahlberg EP, Blieck A, Blom H, Clark JA, Poty E, Thorez J, Janvier P (2004) Devonian tetrapod from western Europe. Nature 427: 412–413. https://doi.org/10.1038/427412a

Clements T, Purnell M, Gabbott S (2019) The Mazon Creek Lagerstätte: a diverse late Paleozoic ecosystem entombed within siderite concretions. Journal of the Geological Society 176: 1–11. https://doi.org/10.1144/jgs2018-088

Cloutier R (2013) Great Canadian Lagerstätten 4. The Devonian Miguasha biota (Québec): UNESCO world heritage site and a time capsule in the early history of vertebrates. Geoscience Canada 40: 149–163. https://doi.org/10.12789/geocanj.2013.40.008

Cognetti G, Maltagliati F (2000) Biodiversity and adaptive mechanisms in brackish water fauna. Marine Pollution Bulletin 40: 7–14. https://doi.org/10.1016/S0025-326X(99)00173-3

Compagno LJ (1990) Alternative life-history styles of cartilaginous fishes in time and space. Environmental Biology of Fishes 28: 33–75. https://doi.org/10.1007/BF00751027

Cunningham CR, Feldman HR, Franseen EK, Gastaldo RA, Mapes G, Maples CG, Schultze H-P (1993) The Upper Carboniferous Hamilton fossil-Lagerstätte in Kansas: a valley-fill, tidally influenced deposit. Lethaia 26: 225–236. https://doi.org/10.1111/j.1502-3931.1993.tb01524.x

Davies S, Gibling M, Rygel MC, Calder JH, Skilliter D (2005) The Pennsylvanian Joggins Formation of Nova Scotia: sedimentological log and stratigraphic framework of the historic fossil cliffs. Atlantic Geology 41: 115–142. https://id.erudit.org/iderudit/ageo41_2_3art03

Dawson JW (1865) On the conditions of the deposition of coal, more especially as illustrated by the coal-formation of Nova Scotia and New Brunswick. Quarterly Journal of the Geological Society of London 22: 95–169. https://doi.org/10.1144/GSL.JGS.1866.022.01-02.12

Denayer J, Prestianni C, Gueriau P, Olive S, Clement G (2016) Stratigraphy and depositional environments of the Late Famennian (Late Devonian) of Southern Belgium and characterization of the Strud locality. Geological Magazine 153: 112–127. https://doi.org/10.1017/S001675681500031X

Dewaele L, Gol'din P, Marx FG, Lambert O, Laurin M, Obadă T, de Buffrénil V (2022) Hypersalinity drives convergent bone mass increases in Miocene marine mammals from the Paratethys. Current Biology 32: 248–255. https://doi.org/10.1016/j.cub.2021.10.065

Dick JR (1981) *Diplodoselache woodi* gen. et sp. nov., an early Carboniferous shark from the Midland Valley of Scotland. Earth and Environmental Science Transactions of The Royal Society of Edinburgh 72: 99–113. https://doi.org/10.1017/S0263593300009937

Dick JRF (1998) *Sphenacanthus*, a Palaeozoic freshwater shark. Zoological Journal of the Linnean Society 122: 9–25. https://doi.org/10.1111/j.1096-3642.1998.tb02523.x

DiMichele WA, Eble CF, Pfefferkorn HW, Elrick SD, Nelson WJ, Lucas SG (2023) Kasimovian floristic change in tropical wetlands and the Middle–Late Pennsylvanian Boundary Event. Geological Society, London, Special Publications 535: SP535-2022-2228. https://doi.org/10.1144/SP535-2022-228

Doguzhaeva LA, Mapes RH, Mutvei H (2007) A Late Carboniferous coleoid cephalopod from the Mazon Creek Lagerstätte (USA), with a radula, arm hooks, mantle tissues, and ink. In: Landman NH, Davis RA, Mapes RH (Eds) Cephalopods Present and Past New Insights And Fresh Perspectives. Springer, Dordrecht, The Netherlands, 121–143. https://doi.org/10.1007/978-1-4020-6806-5_6

Duff P, Walton E (1973) Carboniferous sediments at Joggins, Nova Scotia. Septième Congrès International de Stratigraphie et de Géologie du Carbonifère, Krefeld, Compte Rendu 2: 365–379.

Dulvy NK, Reynolds JD (1997) Evolutionary transitions among egg-laying, live-bearing and maternal inputs in sharks and rays. Proceedings of the Royal Society of London, Series B 264: 1309–1315. https://doi.org/10.1098/rspb.1997.0181

Emig CC (1981) Observations sur l'écologie de *Lingula reevei* Davidson (Brachiopoda: Inarticulata). Journal of Experimental Marine Biology and Ecology 52: 47–61. https://doi.org/10.1016/0022-0981(81)90170-2

Falcon-Lang HJ (2005) Small cordaitalean trees in a marine-influenced coastal habitat in the Pennsylvanian Joggins Formation, Nova Scotia. Journal of the Geological Society 162: 485–500. https://doi.org/10.1144/0016-764904-080

Falcon-Lang HJ, Benton MJ, Braddy SJ, Davies SJ (2006) The Pennsylvanian tropical biome reconstructed from the Joggins Formation of Nova Scotia, Canada. Journal of the Geological Society 163: 561–576. https://doi.org/10.1144/0016-764905-063

Feitosa LM, Martins APB, Nunes JLS (2016) New record of *Carcharhinus leucas* (Valenciennes, 1839) in an equatorial river system. Marine Biodiversity Records 9: 1–4. https://doi.org/10.1186/s41200-016-0094-6

Feitosa LM, Nunes JLS (2020) A new record of *Carcharhinus leucas* in an Amazonian River system. Boletim do Laboratório de Hidrobiologia 30: 62–67. https://doi.org/10.18764/1981-6421e2020.6

Feldman HR, Archer AW, Kvale EP, Cunningham CR, Maples CG, West RR (1993) A tidal model of Carboniferous Konservat-Lagerstätten formation. Palaios 8: 485–498. https://doi.org/10.2307/3515022

Finotello A, Lanzoni S, Ghinassi M, Marani M, Rinaldo A, D'Alpaos A (2018) Field migration rates of tidal meanders recapitulate fluvial morphodynamics. Proceedings of the National Academy of Sciences 115: 1463–1468. https://doi.org/10.1073/pnas.1711330115

Fischer J, Schneider JW, Voigt S, Joachimski MM, Tichomirowa M, Tütken T, Götze J, Berner U (2013) Oxygen and strontium isotopes from fossil shark teeth: Environmental and ecological implications for Late Palaeozoic European basins. Chemical Geology 342: 44–62. https://doi.org/10.1016/j.chemgeo.2013.01.022

Flecker R, De Villiers S, Ellam R (2002) Modelling the effect of evaporation on the salinity–87Sr/86Sr relationship in modern and ancient marginal-marine systems: the Mediterranean Messinian Salinity Crisis. Earth and Planetary Science Letters 203: 221–233. https://doi.org/10.1016/S0012-821X(02)00848-8

Fracasso MA (1980) Age of the Permo-Carboniferous Cutler Formation vertebrate fauna from El Cobre Canyon, New Mexico. Journal of Paleontology 54: 1237–1244. https://www.jstor.org/stable/1304247

Friend P, Moody-Stuart M (1970) Carbonate deposition on the river floodplains of the Wood Bay Formation (Devonian) of Spitsbergen. Geological Magazine 107: 181–195. https://doi.org/10.1017/S0016756800055655

Fritsch A (1883) Fauna der Gaskohle und der Kalksteine der Permformation Böhmens. Fr. Rivnac, Prague, 182 pp. https://doi.org/10.5962/bhl.title.61450

Fürsich FT, Hurst JM (1980) Euryhalinity of Palaeozoic articulate brachiopods. Lethaia 13: 303–312. https://doi.org/10.1111/j.1502-3931.1980.tb01055.x

Gast R (1991) The perennial Rotliegend saline lake in NW Germany. Geologisches Jahrbuch 119: 25–59.

Germain D, Sanchez S, Janvier P, Tafforeau P (2014) The presumed hagfish *Myxineidus gononorum* from the Upper Carboniferous of Montceau-les-Mines (Saône-et-Loire, France): New data obtained by means of Propagation Phase Contrast X-ray Synchrotron Microtomography. Annales de Paléontologie 100: 131–135. https://doi.org/10.1016/j.annpal.2013.12.003

Gierlowski-Kordesch EH, Cassle CF (2015) The '*Spirorbis*' problem revisited: sedimentology and biology of microconchids in marine-nonmarine transitions. Earth-Science Reviews 148: 209–227. https://doi.org/10.1016/j.earscirev.2015.04.010

Gierlowski-Kordesch EH, Falcon-Lang HJ, Cassle CF (2016) Reply to comment on the paper of Gierlowski-Kordesch and Cassle "The '*Spirorbis*' problem revisited: Sedimentology and biology of microconchids in marine-nonmarine transitions" [Earth-Science Reviews, 148 (2015): 209–227]. Earth Science Reviews 152: 201–204. https://doi.org/10.1016/j.earscirev.2015.11.011

Giribet G, Edgecombe GD (2019) The phylogeny and evolutionary history of arthropods. Current Biology 29: R592–R602. https://doi.org/10.1016/j.cub.2019.04.057

Godfrey SJ, Reisz RR (1991) The vertebral morphology of *Gephyrostegus bohemicus* Jaekel 1902, with comments on the atlas-axis complex in primitive tetrapods. Historical Biology 5: 27–36. https://doi.org/10.1080/10292389109380386

Godfrey S, Holmes RB, Laurin M (1991) Articulated remains of a Pennsylvanian embolomere (Amphibia: Anthracosauria) from Joggins, Nova Scotia, Canada. Journal of Vertebrate Paleontology 11: 213–219. https://www.jstor.org/stable/4523372

Goedert J, Amiot R, Berthet D, Fourel F, Simon L, Lécuyer C (2020) Combined oxygen and sulphur isotope analysis—a new tool to unravel vertebrate (paleo)-ecology. The Science of Nature 107: 1–9. https://doi.org/10.1007/s00114-019-1664-3

Goedert J, Lécuyer C, Amiot R, Arnaud-Godet F, Wang X, Cui L, Cuny G, Douay G, Fourel F, Panczer G, Simon Laurent, Steyer Jean.-Sébastien, Min Z (2018) Euryhaline ecology of early tetrapods revealed by stable isotopes. Nature 558: 68–72. https://doi.org/10.1038/s41586-018-0159-2

Goldring R, Seilacher A (1971) Limulid undertracks and their sedimentological implications. Neues Jahrbuch für Geologie und Paläontologie, Abhandlungen 137: 422–442.

Goujet D, Blieck A (1977) La faune de Vertébrés de l'horizon «Vogti» (Groupe de Red Bay, Spitsberg). Comparaison avec les autres faunes ichthyologiques du Dévonien inférieur européen. Comptes Rendus de l'Académie des Sciences de Paris D284: 1513–1515.

Goujet D, Emig C (1985) Des *Lingula* fossiles, indicateurs de modifications de l'environnement dans un gisement du Dévonien inferieur du Spitsberg. Comptes rendus de l'Académie des sciences Série 2, Mécanique, Physique, Chimie, Sciences de l'univers, Sciences de la Terre 301: 945–948.

Gray J (1988) Evolution of the freshwater ecosystem: the fossil record. Palaeogeography, Palaeoclimatology, Palaeoecology 62: 1–214. https://doi.org/10.1016/0031-0182(88)90054-5

Grey M, Pufahl PK, Aziz AA (2011) Using multiple environmental proxies to determine degree of marine influence and paleogeographical position of the Joggins Fossil Cliffs, UNESCO World Heritage Site. Palaios 26: 256–263. https://doi.org/10.2110/palo.2010.p10-118r

Guinot G, Cavin L (2018) Body size evolution and habitat colonization across 100 million years (Late Jurassic–Paleocene) of the actinopterygian evolutionary history. Fish and Fisheries 19: 577–597. https://doi.org/10.1111/faf.12275

Hammen C, Lum SC (1977) Salinity tolerance and pedicle regeneration of *Lingula*. Journal of Paleontology 51: 548–551. https://www.jstor.org/stable/1303685

Hammond L (1983) Experimental studies of salinity tolerance, burrowing behavior and pedicle regeneration in *Lingula anatina* (Brachiopoda, Inarticulata). Journal of Paleontology 57: 1311–1316.

Hampe O (2003) Revision of the Xenacanthida (Chondrichthyes: Elasmobranchii) from the Carboniferous of the British Isles. Earth and Environmental Science Transactions of the Royal Society of Edinburgh 93: 191–237. https://doi.org/10.1017/S0263593300000419

Hampe O, Ivanov A (2007) First xenacanthid shark from the Pennsylvanian (Moscovian) of the Northern Caucasus (Russia). Fossil Record 10: 179–189. https://doi.org/10.1002/mmng.200700004

Hannibal JT, Lucas SG, Lerner AJ, Caney DS (2005) An eurypterid (*Adelophthalmus* sp.) from a plant-rich lacustrine facies of Upper Pennsylvanian strata in El Cobre Canyon, New Mexico. New Mexico Museum of Natural History and Science Bulletin 31 The Permian of Central New Mexico: 34–37.

Harris SK, Lucas SG, Berman DS, Henrici A (2004) Vertebrate fossil assemblage from the Upper Pennsylvanian Red tanks member of the Bursum Formation, Lucero Uplift, central New Mexico. New Mexico Museum of Natural History and Science Bulletin 25: 267–283.

Hay WW (1998) Detrital sediment fluxes from continents to oceans. Chemical geology 145: 287–323. https://doi.org/10.1016/S0009-2541(97)00149-6

Hendrix Jr J, Hulet W, Greenberg M (1981) Salinity tolerance and the responses to hypoosmotic stress of the bay squid *Lolliguncula brevis*, a euryhaline cephalopod mollusc. Comparative Biochemistry and Physiology, A 69: 641–648. https://doi.org/10.1016/0300-9629(81)90150-X

Hitchon B, Krouse H (1972) Hydrogeochemistry of the surface waters of the Mackenzie River drainage basin, Canada—III. Stable isotopes of oxygen, carbon and sulphur. Geochimica et Cosmochimica Acta 36: 1337–1357. https://doi.org/10.1016/0016-7037(72)90066-X

Holmes RB, Carroll RL, Reisz RR (1998) The first articulated skeleton of *Dendrerpeton acadianum* (Temnospondyli, Dendrerpetontidae) from the Lower Pennsylvanian locality of Joggins, Nova Scotia, and a review of its relationships. Journal of Vertebrate Paleontology 18: 64–79. http://www.jstor.org/stable/4523873

Hunt AP, Lucas SG, Berman DS (1992) The Late Pennsylvanian amphibian fauna of the Kinney Quarry, central New Mexico. New Mexico Bureau of Mines & Mineral Resources Bulletin 138: 211–220.

Huttenlocker AK, Henrici A, Nelson WJ, Elrick S, Berman DS, Schlotterbeck T, Sumida SS (2018) A multitaxic bonebed near the Carboniferous–Permian boundary (Halgaito Formation, Cutler Group) in Valley of the Gods, Utah, USA: vertebrate paleontology and taphonomy. Palaeogeography, Palaeoclimatology, Palaeoecology 499: 72–92. https://doi.org/10.1016/j.palaeo.2018.03.017

Jain S (1980) Freshwater xenacanthid (= pleuracanth) shark fossils from the Upper Triassic Maleri Formation, India. Geological Society of India 21: 39–47.

Jakobsen KG, Brock GA, Nielsen AT, Topper TP, Harper DA (2014) Middle Ordovician brachiopods from the Stairway Sandstone, Amadeus Basin, central Australia. Alcheringa 38: 190–208. https://doi.org/10.1080/03115518.2013.858204

Jankowski T, Collins AG, Campbell R (2008) Global diversity of inland water cnidarians. Hydrobiologia 595: 35–40. https://doi.org/10.1007/s10750-007-9001-9

Janvier P (2007) Living primitive fishes and fishes from deep time. Fish Physiology 26: 1–51. https://doi.org/10.1016/S1546-5098(07)26001-7

Jereb P, Roper CF (2016) Cephalopods of the world-an annotated and illustrated catalogue of cephalopod species known to date. Fao, Rome, [xviii +] 352 pp.

Kjellesvig-Waering EN (1958) The genera, species and subspecies of the family Eurypteridae, Burmeister, 1845. Journal of Paleontology: 1107–1148. https://www.jstor.org/stable/1300776

Kjellesvig-Waering EN (1961) The Silurian Eurypterida of the Welsh Borderland. Journal of Paleontology 35: 789–835. https://www.jstor.org/stable/1301214

Klembara J, Clack JA, Milner AR, Ruta M (2014) Cranial anatomy, ontogeny, and relationships of the Late Carboniferous tetrapod *Gephyrostegus bohemicus* Jaekel, 1902. Journal of Vertebrate Paleontology 34: 774–792. https://doi.org/10.1080/02724634.2014.837055

Klug C, Landman NH, Fuchs D, Mapes RH, Pohle A, Guériau P, Reguer S, Hoffmann R (2019) Anatomy and evolution of the first Coleoidea in the Carboniferous. Communications Biology 2: 280. https://doi.org/10.1038/s42003-019-0523-2

Kohring RR (1995) Reflections on the origin of the amniote egg in the light of reproductive strategies and shell structure. Historical Biology 10: 259–275. https://doi.org/10.1080/10292389509380524

Kozur H (1984) Die Verbreitung der limnischen Meduse *Medusina limnica* Müller 1978 im Rotliegenden Mitteleuropas. Paläontologische Zeitschrift 58: 41–50. https://doi.org/10.1007/BF02990326

Kriwet J, Witzmann F, Klug S, Heidtke UHJ (2008) First direct evidence of a vertebrate three-level trophic chain in the fossil record. Proceedings of the Royal Society of London, Series B 275: 181–186. https://doi.org/10.1098/rspb.2007.1170

Kuecher GJ, Woodland BG, Broadhurst FM (1990) Evidence of deposition from individual tides and of tidal cycles from the Francis Creek Shale (host rock to the Mazon Creek Biota), Westphalian D (Pennsylvanian), northeastern Illinois. Sedimentary Geology 68: 211–221. https://doi.org/10.1016/0037-0738(90)90113-8

Kues BS, Kietzke KK (1981) A large assemblage of a new eurypterid from the Red Tanks Member, Madera Formation (late Pennsylvanian-early Permian) of New Mexico. Journal of Paleontology 55: 709–729. https://www.jstor.org/stable/1304420

Lamsdell JC (2016) Horseshoe crab phylogeny and independent colonizations of fresh water: ecological invasion as a driver for morphological innovation. Palaeontology 59: 181–194. https://doi.org/10.1111/pala.12220

Lamsdell JC, Braddy SJ (2010) Cope's Rule and Romer's theory: patterns of diversity and gigantism in eurypterids and Palaeozoic vertebrates. Biology Letters 6: 265–269. https://doi.org/10.1098/rsbl.2009.0700

Lamsdell JC, Lagebro L, Edgecombe GD, Budd GE, Gueriau P (2019) Stylonurine eurypterids from the Strud locality (Upper Devonian, Belgium): new insights into the ecology of freshwater sea scorpions. Geological Magazine 156: 1708–1714. https://doi.org/10.1017/S0016756818000936

Lamsdell JC, Selden PA (2017) From success to persistence: identifying an evolutionary regime shift in the diverse Paleozoic aquatic arthropod group Eurypterida, driven by the Devonian biotic crisis. Evolution 71: 95–110. https://doi.org/10.1111/evo.13106

Langston Jr W (1953) Permian amphibians from New Mexico. University of California Publications in Geological Sciences 29: 349–416.

Laurin M (2010) How Vertebrates Left the Water. University of California Press, Berkeley, [xv +] 199 pp. https://doi.org/10.1525/9780520947986

Laurin M (2020a) *Stegocephali*. In: de Queiroz K, Cantino PD, Gauthier JA (Eds) Phylonyms: A companion to the PhyloCode. CRC Press, Boca Raton, Florida, 741–745. https://www.routledge.com/Phylonyms-A-Companion-to-the-PhyloCode-1st-Edition/de-Queiroz-Cantino-Gauthier/p/book/9781138332935

Laurin M (2020b) *Tetrapoda*. In: de Queiroz K, Cantino PD, Gauthier JA (Eds) Phylonyms: A companion to the PhyloCode. CRC Press, Boca Raton, Florida, 759–764. https://www.routledge.com/Phylonyms-A-Companion-to-the-PhyloCode-1st-Edition/de-Queiroz-Cantino-Gauthier/p/book/9781138332935

Laurin M, Arntzen JW, Báez AM, Bauer AM, Damiani R, Evans SE, Kupfer A, Larson A, Marjanović D, Müller H, Olsson L, Rage J-C, Walsh D (2020) *Amphibia*. In: de Queiroz K, Cantino PD, Gauthier JA (Eds) Phylonyms: A companion to the PhyloCode. CRC Press, Boca Raton, Florida, 765–771. https://doi.org/10.1201/9780429446276

Laurin M, Soler-Gijón R (2006) The oldest known stegocephalian (Sarcopterygii: Temnospondyli) from Spain. Journal of Vertebrate Paleontology 26: 284–299. https://doi.org/10.1671/0272-4634(2006)26[284:TOKSST]2.0.CO;2

Laurin M, Soler-Gijón R (2010) Osmotic tolerance and habitat of early stegocephalians: indirect evidence from parsimony, taphonomy, paleobiogeography, physiology and morphology. In: Vecoli M, Clément G (Eds) The Geological Society of London, London, 151–179. https://doi.org/10.1144/SP339.13

Laurin M, Lapauze O, Marjanović D (2022) What do ossification sequences tell us about the origin of extant amphibians? Peer Community Journal 2: 1–35. https://doi.org/10.24072/pcjournal.89

Lebrun P, Pylypenko D (2023) Des euryptérides dans le Silurien (Wenlock) de la Podolie ukrainienne. Fossiles, 5–22.

Legler B, Schneider J, Gand G, Körner F (2004) Playa and sabkha environments from Northern Germany and Southern France. In: Environmental reconstruction and stratigraphy in the Palaeozoic. Bergakademie Freiberg, 64–82.

Leonova T (2011) Permian ammonoids: biostratigraphic, biogeographical, and ecological analysis. Paleontological Journal 45: 1206–1312. https://doi.org/10.1134/S0031030111100029

Lewis H, Dunagan S (2000) Depositional environments and paleoclimate of the Upper Pennsylvanian lacustrine limestones of the Conemaugh Group (eastern Ohio). In: Geological Society of America, Abstracts with Programs, 58 pp.

Lomax DR, Robinson P, Cleal CJ, Bowden A, Larkin NR (2016) Exceptional preservation of Upper Carboniferous (lower Westphalian) fossils from Edlington, Doncaster, South Yorkshire, UK. Geological Journal 51: 42–50. https://doi.org/10.1002/gj.2602

Long JA, Gordon MS (2004) The greatest step in vertebrate history: a paleobiological review of the fish-tetrapod transition. Physiological and Biochemical Zoology 77: 700–719. https://doi.org/10.1086/425183

Lucas SG, Lerner AJ (2010) Pennsylvanian lake-margin ichnoassemblage from Cañon del Cobre, Rio Arriba county, New Mexico. New Mexico Museum of Natural History and Science Bulletin 49: 37–48.

Lucas SG, Lerner AJ, Bruner M, Shipman P (2004) Middle Pennsylvanian ichnofauna from eastern Oklahoma, USA. Ichnos 11: 45–55. https://doi.org/10.1080/10420940490442322

Luccisano V, Cuny G, Pradel A, Fourel F, Lécuyer C, Pouillon J-M, Lachat K, Amiot R (2023) Palaeoenvironmental and palaeoecological reconstructions based on oxygen, carbon and sulfur isotopes of Early Permian shark spines from the French Massif central. Palaeogeography, Palaeoclimatology, Palaeoecology 628: 111760. https://doi.org/10.1016/j.palaeo.2023.111760

Luccisano V, Pradel A, Amiot R, Pouillon JM, Kindlimann R, Steyer JS, Cuny G (2022) Systematics, ontogeny and palaeobiogeography of the genus *Orthacanthus* (Diplodoselachidae, Xenacanthiformes) from the lower Permian of France. Papers in Palaeontology 8: e1470. https://doi.org/10.1002/spp2.1470

Mann A, Gee BM (2020) Lissamphibian-like toepads in an exceptionally preserved amphibamiform from Mazon Creek. Journal of Vertebrate Paleontology 39: e1727490. https://doi.org/10.1080/02724634.2019.1727490

Mann A, Calthorpe AS, Maddin HC (2021) *Joermungandr bolti*, an exceptionally preserved ‘microsaur’ from the Mazon Creek Lagerstätte reveals patterns of integumentary evolution in Recumbirostra. Royal Society Open Science 8: 210319. https://doi.org/10.1098/rsos.210319

Mann A, Gee BM, Pardo JD, Marjanović D, Adams GR, Calthorpe AS, Maddin HC, Anderson JS (2020) Reassessment of historic ‘microsaurs’ from Joggins, Nova Scotia, reveals hidden diversity in the earliest amniote ecosystem. Papers in Palaeontology 6: 605–625. https://doi.org/10.1002/spp2.1316

Marjanović D, Laurin M (2019) Phylogeny of Paleozoic limbed vertebrates reassessed through revision and expansion of the largest published relevant data matrix. PeerJ 6: e5565. https://doi.org/10.7717/peerj.5565

Martino RL (2016) Sequence stratigraphy of fluvially-dominated strata of the Mid-Late Pennsylvanian Conemaugh Formation, central Appalachian Basin. International Journal of Coal Geology 154: 136–154. https://doi.org/10.1016/j.coal.2015.12.016

Matton O, Cloutier R, Stevenson R (2012) Apatite for destruction: Isotopic and geochemical analyses of bioapatites and sediments from the Upper Devonian Escuminac Formation (Miguasha, Québec). Palaeogeography, Palaeoclimatology, Palaeoecology 361: 73–83. https://doi.org/10.1016/j.palaeo.2012.08.004

Mayo AL, Klauk RH (1991) Contributions to the solute and isotopic groundwater geochemistry, Antelope Island, Great Salt Lake, Utah. Journal of Hydrology 127: 307–335. https://doi.org/10.1016/0022-1694(91)90120-7

McCahon TJ, Miller KB (2015) Environmental significance of lungfish burrows (Gnathorhiza) within Lower Permian (Wolfcampian) paleosols of the US midcontinent. Palaeogeography, Palaeoclimatology, Palaeoecology 435: 1–12. https://doi.org/10.1016/j.palaeo.2015.05.032

Mercuzot M, Bourquin S, Pellenard P, Beccaletto L, Schnyder J, Baudin F, Ducassou C, Garel S, Gand G (2022) Reconsidering Carboniferous–Permian continental paleoenvironments in eastern equatorial Pangea: facies and sequence stratigraphy investigations in the Autun Basin (France). International Journal of Earth Sciences 111: 1663–1696. https://doi.org/10.1007/s00531-022-02200-6

Milner AR (1987) The Westphalian tetrapod fauna; some aspects of its geography and ecology. Journal of the Geological Society 144: 495–506. https://doi.org/10.1144/gsjgs.144.3.0495

Moscatello S, Belmonte G (2009) Egg banks in hypersaline lakes of the South-East Europe. Saline Systems 5: 1–7. http://www.salinesystems.org/content/5/1/3

Ó Gogáin A, Falcon-Lang HJ, Carpenter DK, Miller RF, Benton MJ, Pufahl PK, Ruta M, Davies TG, Hinds SJ, Stimson MR (2016) Fish and tetrapod communities across a marine to brackish salinity gradient in the Pennsylvanian (early Moscovian) Minto Formation of New Brunswick, Canada, and their palaeoecological and palaeogeographical implications. Palaeontology 59: 689–724. https://doi.org/10.1111/pala.12249

Ó Gogáin A, O’Sullivan G, Clements T, Hoare BC, Murray J, Wyse Jackson PN (2022) Metamorphism as the cause of bone alteration in the Jarrow assemblage (Langsettian, Pennsylvanian) of Ireland. Palaeontology 65: e12628. https://doi.org/10.1111/pala.12628

Opluštil S, Martínek K, Tasáryová Z (2005) Facies and architectural analysis of fluvial deposits of the Nýřany Member and the Týnec Formation (Westphalian D–Barruelian) in the Kladno-Rakovník and Pilsen basins. Bulletin of Geosciences 80: 45–66.

Ortega-Hernández J, Legg DA, Tremewan J, Braddy SJ (2010) Euthycarcinoids. Geology Today 26: 195–198. https://doi.org/10.1111/j.1365-2451.2010.00770.x

Pagaling E, Wang H, Venables M, Wallace A, Grant WD, Cowan DA, Jones BE, Ma Y, Ventosa A, Heaphy S (2009) Microbial biogeography of six salt lakes in Inner Mongolia, China, and a salt lake in Argentina. Applied and environmental microbiology 75: 5750–5760. https://doi.org/10.1128/AEM.00040-09

Pallares S, Arribas P, Bilton DT, Millan A, Velasco J (2015) The comparative osmoregulatory ability of two water beetle genera whose species span the fresh-hypersaline gradient in inland waters (Coleoptera: Dytiscidae, Hydrophilidae). PLOS ONE 10: e0124299. https://doi.org/10.1371/journal.pone.0124299

Parker KE, Webb JA (2008) Estuarine deposition of a mid-Viséan tetrapod unit, Ducabrook Formation, central Queensland: implications for tetrapod dispersal. Australian Journal of Earth Sciences 55: 509–530. https://doi.org/10.1080/08120090801888644

Pellenard P, Gand G, Schmitz M, Galtier J, Broutin J, Stéyer J-S (2017) High-precision U-Pb zircon ages for explosive volcanism calibrating the NW European continental Autunian stratotype. Gondwana Research 51: 118–136. https://doi.org/10.1016/j.gr.2017.07.014

Perrier V, Charbonnier S (2014) The Montceau-les-Mines Lagerstätte (Late Carboniferous, France). Comptes rendus Palevol 13: 353–367. https://doi.org/10.1016/j.crpv.2014.03.002

Peters SE, Husson JM (2017) Sediment cycling on continental and oceanic crust. Geology 45: 323–326. https://doi.org/10.1130/G38861.1

Pleijel F, Rouse GW, Vannier J (2004) Carboniferous fireworms (Amphinomida: Annelida), with a discussion of species taxa in palaeontology. Invertebrate Systematics 18: 693–700. https://doi.org/10.1071/IS04003

Plotnick R (1999) Habitat of Llandoverian-Lochkovian eurypterids. In: Boucot AJ, Lawson JD (Eds) Paleocommunities: a case study from the Silurian to the Lower Devonian. Cambridge University Press, Cambridge, 106–131.

Plotnick RE, Young GA, Hagadorn JW (2023) An abundant sea anemone from the Carboniferous Mazon Creek Lagerstätte, USA. Papers in Palaeontology 9: e1479. https://doi.org/10.1002/spp2.1479

Poplin C, Heyler D (1994) Les eurhycarcinoïdes [Euthycarcinoids]. In: Poplin C, Heyler D (Eds). CTHS, Paris, 137.

Poujol M, Mercuzot M, Lopez M, Bourquin S, Bruguier O, Hallot E, Beccaletto L (2023) Insights on the Permian tuff beds from the Saint-Affrique Basin (Massif Central, France): an integrated geochemical and geochronological study. Comptes Rendus Géoscience 355: 1–25. https://doi.org/10.5802/crgeos.184

Quinton PC, Rygel MC (2023) Is there a link between carbon isotopes and sea level in epicontinental carbonate settings? Evolving Earth 1: 100016. https://doi.org/10.1016/j.eve.2023.100016

Racheboeuf PR, Vannier J, Anderson LI (2002) A New Three-Dimensionally Preserved Xiphosuran Chelicerate from the Montceau-Les-Mines Lagerstätte (Carboniferous, France). Palaeontology 45: 125–147. https://doi.org/10.1111/1475-4983.00230

Racheboeuf PR, Vannier J, Schram FR, Chabard D, Sotty D (2008) The euthycarcinoid arthropods from Montceau-les-Mines, France: functional morphology and affinities. Earth and Environmental Science Transactions of the Royal Society of Edinburgh 99: 11–25. https://doi.org/10.1017/S1755691008006130

Richards K, van Baak CG, Athersuch J, Hoyle TM, Stoica M, Austin WE, Cage AG, Wonders AA, Marret F, Pinnington CA (2018) Palynology and micropalaeontology of the Pliocene-Pleistocene transition in outcrop from the western Caspian Sea, Azerbaijan: Potential links with the Mediterranean, Black Sea and the Arctic Ocean? Palaeogeography, Palaeoclimatology, Palaeoecology 511: 119–143. https://doi.org/10.1016/j.palaeo.2018.07.018

Rolfe WI (1985) Les euthycarcinoides de Montceau et Mazon Creek. Bulletin trimestriel de la Société d'histoire naturelle et des amis du Muséum d'Autun 115: 71–73.

Rygel MC, Lally C, Gibling MR, Ielpi A, Calder JH, Bashforth AR (2015) Sedimentology and stratigraphy of the type section of the Pennsylvanian Boss Point Formation, Joggins Fossil Cliffs, Nova Scotia, Canada. Atlantic Geology 51: 1–43. https://doi.org/10.4138/atlgeol.2015.001

Saunders WB, Richardson Jr ES (1979) Middle Pennsylvanian (Desmoinesean) Cephalopoda of the Mazon Creek Fauna, Northeastern Illinois. In: Mazon Creek Fossils. Elsevier, 333–359. https://doi.org/10.1016/B978-0-12-519650-5.50020-5

Schimper W-P (1853) Paleontologica alsatica ou fragments paléontologiques des différents terrains stratifiés qui se recontrent en Alsace. Mémoires de la Société du Muséum d'Histoire Naturelle de Strasbourg 4: 1–10.

Schmitz B, Aberg G, Werdelin L, Forey PL, Bendix-Almgreen SE (1991) ^{87}Sr/^{86}Sr, Na, F, Sr, and La in skeletal fish debris as a measure of the paleosalinity of fossil-fish habitats. Geological Society of America Bulletin 103: 786–794. https://doi.org/10.1130/0016-7606(1991)103%3C0786:SSNFSA%3E2.3.CO;2

Schoch RR (2022) Phylogeny of the amphibamiform temnospondyls: the relationship of taxa known by adults, larvae and neotenes. Journal of Systematic Palaeontology 20: 1–30. https://doi.org/10.1080/14772019.2022.2113831

Schoch RR, Witzmann F (2009) The temnospondyl *Glanochthon* from the Lower Permian Meisenheim Formation of Germany. Special Papers in Palaeontology 81: 121–136.

Schram FR (1984) Upper Pennsylvanian arthropods from black shales of Iowa and Nebraska. Journal of Paleontology 58: 197–209. https://www.jstor.org/stable/1304745

Schram FR, Rolfe WDI (1994) The Stephanian (Late Carboniferous) Euthycarcinoidea from the Montceau-les-Mines basin (Massif Central - France). In: Poplin C, Heyler D (Eds). CTHS, Paris, 139–144.

Schram FR, Rolfe WI (1997) Euthycarcinoids and Thylacocephalans. In: Shabica CW, Hay A (Eds) Richardson's guide to the fossil fauna of Mazon Creek. Northeastern Illinois University, Chicago, 211–214.

Schultka S (2000) Zur Palökologie der Euproopiden im Nordwestdeutschen Oberkarbon. Fossil Record 3: 87–98. https://doi.org/10.1002/mmng.20000030105

Schultze H-P (1995) Terrestrial biota in coastal marine deposits: fossil-Lagerstätten in the Pennsylvanian of Kansas, USA. Palaeogeography, Palaeoclimatology, Palaeoecology 119: 255–273. https://doi.org/10.1016/0031-0182(95)00011-9

Schultze H-P (2009) Interpretation of marine and freshwater paleoenvironments in Permo–Carboniferous deposits. Palaeogeography, Palaeoclimatology, Palaeoecology 281: 126–136. https://doi.org/10.1016/j.palaeo.2009.07.017

Schultze H-P, Maples CG (1992) Comparison of the Late Pennsylvanian faunal assemblage of Kinney Brick Company quarry, New Mexico, with other Late Pennsylvanian Lagerstätten. New Mexico Bureau of Mines & Mineral Resources Bulletin 138: 231–242.

Schultze H-P, Maples CG, Cunningham CR (1994) The Hamilton Konservat-Lagerstätte: Stephanian biota in a marginal-marine setting. Transactions of the Royal Society of Edinburgh 84: 443–451. https://doi.org/10.1017/S0263593300006246

Schultze H-P, Soler-Gijón R (2004) A xenacanth clasper from the ?uppermost Carboniferous-Lower Permian of Buxières-les-Mines (Massif central, France) and the palaeoecology of the European Permo-Carboniferous basins. Neues Jahrbuch für Geologie und Paläontologie Abhandlungen 232: 325–363. https://doi.org/10.1127/njgpa/232/2004/325

Sepkoski Jr JJ (2002) A compendium of fossil marine animal genera. Bulletins of American paleontology 363: 1–560.

Sequeira SEK (2003) The skull of *Cochleosaurus bohemicus* Frič, a temnospondyl from the Czech Republic (Upper Carboniferous) and cochleosaurid interrelationships. Transactions of the Royal Society of Edinburgh: Earth Sciences 94: 21–43. https://doi.org/10.1017/S0263593300000511

Shcherbakov DE, Vinn O, Zhuravlev AY (2021) Disaster microconchids from the uppermost Permian and Lower Triassic lacustrine strata of the Cis-Urals and the Tunguska and Kuznetsk basins (Russia). Geological Magazine 158: 1335–1357. https://doi.org/10.1017/S0016756820001375

Sinitshenkova N (2013) New mayflies (Insecta: Ephemerida= Ephemeroptera) from the intertrappean deposits of the Tunguska Basin, Siberia. Paleontological Journal 47: 84–88. https://doi.org/10.1134/S0031030113010127

Soler-Gijón R (1997) *Orthacanthus meridionalis*, a new xenacanth shark (Elasmobranchii) from the Upper Carboniferous of the Puertollano basin, Spain. Neues Jahrbuch für Geologie und Paläontologie, Abhandlungen 204: 141–169. https://doi.org/10.1127/njgpa/204/1997/141

Soler-Gijón R (1999) Occipital spine of *Orthacanthus* (Xenacanthidae, Elasmobranchii): structure and growth. Journal of Morphology 242: 1–45. https://doi.org/10.1002/(SICI)1097-4687(199910)242:1%3C1::AID-JMOR2%3E3.0.CO;2-9

Soler-Gijón R, López-Martínez N (2008) Tidal rythmites in Upper Carboniferous deposits from Puertollano (Central Spain): Palaeoenvironmental implications. In: Stamberg S, Zajic J (Eds) Faunas and Palaeoenvironments of the late Paleozoic. Czech National Committe for IGCP, Hradec Králové, 43–44.

Soler-Gijón R, Moratalla JJ (2001) Fish and tetrapod trace fossils from the Upper Carboniferous of Puertollano, Spain. Palaeogeography, Palaeoclimatology, Palaeoecology 171: 1–28. https://doi.org/10.1016/S0031-0182(01)00257-7

Steyer J-S, Sanchez S, Debriette PJ, Valli AM, Escuille F, Pohl B, Dechambre R-P, Vacant R, Spence C, de Ploeg G (2012) A new vertebrate Lagerstätte from the Lower Permian of France (Franchesse, Massif Central): palaeoenvironmental implications for the Bourbon-l'Archambault basin. Bulletin de la Société géologique de France 183: 509–515. https://doi.org/10.2113/gssgfbull.183.6.509

Stöger I, Sigwart J, Kano Y, Knebelsberger T, Marshall B, Schwabe E, Schrödl M (2013) The continuing debate on deep molluscan phylogeny: evidence for Serialia (Mollusca, Monoplacophora+ Polyplacophora). BioMed Research International 2013: 407072. https://doi.org/10.1155/2013/407072

Størmer L (1952) Phylogeny and taxonomy of fossil horseshoe crabs. Journal of Paleontology 26: 630–640. https://www.jstor.org/stable/1299851

Stritzke R (1986) Xenacanthid shark teeth in Middle Devonian limestones of the Rhenish Schiefergebirge, West Germany. Journal of Paleontology 60: 1134–1135. https://doi.org/10.1017/S0022336000022678

Taylor PD, Vinn O (2006) Convergent morphology in small spiral worm tubes ('*Spirorbis*') and its palaeoenvironmental implications. Journal of the Geological Society 163: 225–228. https://doi.org/10.1144/0016-764905-145

Tetlie OE (2007) Distribution and dispersal history of Eurypterida (Chelicerata). Palaeogeography, Palaeoclimatology, Palaeoecology 252: 557–574. https://doi.org/10.1016/j.palaeo.2007.05.011

Tetlie OE, Poschmann M (2008) Phylogeny and palaeoecology of the Adelophthalmoidea (Arthropoda; Chelicerata; Eurypterida). Journal of Systematic Palaeontology 6: 237–249. https://doi.org/10.1017/S1477201907002416

Thorez J, Dreesen R (1986) A model of a regressive depositional system around the Old Red Continent as exemplified by a field trip in the Upper Famennian "Psammites du Condroz" in Belgium. Annales de la Société géologique de Belgique 109: 283–323. https://popups.uliege.be/0037-9395/index.php?id=2507

Thorez J, Streel M, Bouckaert J, Bless M (1977) Stratigraphie et paléogéographie de la partie orientale du Synclinorium de Dinant (Belgique) au Famennien Supérieur: un modèle de bassin sédimentaire reconstitué par analyse pluridisciplinaire sédimentologique et micropaléontologique. Mededelingen-Rijks Geologische Dienst 28: 17–28.

Turek V (1989) Fish and amphibian trace fossils from Westphalian sediments of Bohemia. Palaeontology 32: 623–644.

Turner R, Meyer C (1980) Salinity tolerance of the brackish-water echinoderm *Ophiophragmus filograneus* (Ophiuroidea). Marine Ecology Progress Series 2: 249–256. https://www.jstor.org/stable/24813186

Turner RL (2007) Effects of long-term exposure to low salinity on the brackish-water amphiurid brittlestar *Ophiophragmus filograneus* (Lyman, 1875) from the Indian River Lagoon System, Florida. Florida Scientist 70: 464–475. https://www.jstor.org/stable/24321672

Utting J, Lucas SG (2010) Palynological investigation of the Upper Pennsylvanian (Carboniferous) El Cobre Canyon Formation, Cutler Group, Canon del Cobre, Rio Arriba County, New Mexico, U.S.A. New Mexico Museum of Natural History and Science Bulletin 49: 71–74.

Vallin G, Laurin M (2004) Cranial morphology and affinities of *Microbrachis*, and a reappraisal of the phylogeny and lifestyle of the first amphibians. Journal of Vertebrate Paleontology 24: 56–72. https://doi.org/10.1671/5.1

Veizer J, Ala D, Azmy K, Bruckschen P, Buhl D, Bruhn F, Carden GA, Diener A, Ebneth S, Godderis Y (1999) 87Sr/86Sr, δ13C and δ18O evolution of Phanerozoic seawater. Chemical Geology 161: 59–88. https://doi.org/10.1016/S0009-2541(99)00081-9

Verdier J (1996) The Rotliegend sedimentation history of the southern North Sea and adjacent countries. In: Geology of Gas and Oil under the Netherlands: Selection of papers presented at the 1983 International Conference of the American Association of Petroleum Geologists, held in The Hague. Springer, 45–56. https://doi.org/10.1007/978-94-009-0121-6_6

Waters C, Davies S (2006) Carboniferous: extensional basins, advancing deltas and coal swamps. In: Brenchley PJ, Rawson PF (Eds) The Geology of England. Geological Society, London, 173–223. https://doi.org/10.1144/GOEWP.9

Werneburg R, Steyer J-S (2002) Revision of *Cheliderpeton vranyi* Fritsch, 1877 (Amphibia, Temnospondyli) from the Lower Permian of Bohemia (Czech Republic). Paläontologische Zeitschrift 76: 149–162. https://doi.org/10.1007/BF02988193

Williams DD, Williams NE (1998) Aquatic insects in an estuarine environment: densities, distribution and salinity tolerance. Freshwater Biology 39: 411–421. https://doi.org/10.1046/j.1365-2427.1998.00285.x

Williston S, Case E (1912) The Permo-Carboniferous of northern New Mexico. The Journal of Geology 20: 1–12. https://doi.org/10.1086/621924

Witzmann F, Brainerd E (2017) Modeling the physiology of the aquatic temnospondyl *Archegosaurus decheni* from the early Permian of Germany. Mitteilungen aus dem Museum für Naturkunde in Berlin Fossil Record 20: 105. https://doi.org/10.5194/fr-20-105-2017

Woodard SC, Thomas DJ, Grossman EL, Olszewski TD, Yancey TE, Miller BV, Raymond A (2013) Radiogenic isotope composition of Carboniferous seawater from North American epicontinental seas. Palaeogeography, Palaeoclimatology, Palaeoecology 370: 51–63. https://doi.org/10.1016/j.palaeo.2012.11.018

Wu N, Farquhar J, Strauss H (2014) δ34S and Δ33S records of Paleozoic seawater sulfate based on the analysis of carbonate associated sulfate. Earth and Planetary Science Letters 399: 44–51. https://doi.org/10.1016/j.epsl.2014.05.004

Zatoń M, Vinn O, Tomescu AM (2012) Invasion of freshwater and variable marginal marine habitats by microconchid tubeworms–an evolutionary perspective. Geobios 45: 603–610. https://doi.org/10.1016/j.geobios.2011.12.003

Zatoń M, Wilson MA, Vinn O (2016) Comment on the paper of Gierlowski-Kordesch and Cassle "The '*Spirorbis*' problem revisited: Sedimentology and biology of microconchids in marine–nonmarine transitions" [Earth-Science Reviews, 148 (2015): 209–227]. Earth-Science Reviews 152: 198–200. https://doi.org/10.1016/j.earscirev.2015.11.012

Fossil Record 27 (3) 2024, 333–352 | DOI 10.3897/fr.27.126410

On *Ossirarus kierani*, a stem tetrapod from the Tournaisian of Burnmouth, Berwickshire, Scotland, and the phylogeny of early tetrapods

Timothy R. Smithson[1], Marcello Ruta[2], Jennifer A. Clack[1†]

1 *University Museum of Zoology Cambridge, Downing Street, Cambridge, CB2 3EJ, UK*
2 *Department of Life Sciences, University of Lincoln, Joseph Banks Laboratories, Green Lane, Lincoln, LN6 7DL, UK*

https://zoobank.org/95419035-67A1-4977-908F-2B426C42E0DC

Corresponding author: Timothy R. Smithson (ts556@cam.ac.uk)

Academic editor: Nadia Fröbisch ♦ **Received** 28 April 2024 ♦ **Accepted** 7 October 2024 ♦ **Published** 30 December 2024

Abstract

Recent discoveries in the Scottish Borders have greatly expanded our knowledge of post-Devonian tetrapods. Six new taxa have been named and briefly described so far. One of these, *Ossirarus kierani*, is represented by a single specimen from the coastal section of the Tournaisian Ballagan Formation at Burnmouth. It comprises the disarticulated bones of the posterior half of the skull, the anterior portion of the axial skeleton, and parts of the pectoral girdle and forelimbs. It is relatively small, with an estimated skull length of 54 mm. Like some Devonian tetrapods it has a preopercular and a lateral line system represented by pores. It shares with embolomeres, a tabular-parietal suture, an intertemporal and a long tabular horn. The gastrocentrous vertebrae resemble those of *Caerorhachis* and the brachial foramen pierces the humerus through the posterior edge, as in *Mesanerpeton*. Phylogenetic analyses place *Ossirarus* on the tetrapod stem, crownward of some – but not all – Devonian taxa. The topology of the tetrapod stem suggests that numerous lineages of Carboniferous tetrapods extended back into the Devonian.

Key Words

Carboniferous, Ballagan Formation, flood plain, tabular horn, gastrocentrous

Introduction

The recent discovery of a diverse vertebrate fauna in the Ballagan Formation in the earliest Carboniferous of the Tweed Basin in the Scottish Borders (Smithson et al. 2012, 2015; Clack et al. 2016, 2018, 2019a; Smithson and Clack 2018; Otoo et al. 2019) has shown that vertebrates recovered quickly following the end-Devonian extinction event and that the early Carboniferous was a period of innovation, diversification and evolutionary change (Lloyd et al. 2011; Smithson et al. 2015; Clack et al. 2016). So far, among the numerous fossil sites discovered in the Scottish Borders (Smithson et al. 2015, fig. 1), six tetrapod horizons have been found at Burnmouth on the coast, three in the bed of Whiteadder Water at Willie's Hole, and one in the bank of the River Tweed near Coldstream. The age of these beds extend from the *Vallatisporites verrucosus* – *Retusotriletes incohatus* (VI) palynozone at the base of the Tournaisian to the *Schopfites claviger* – *Aurospora macra* (CM) zone at the top (Clack et al. 2016, 2019a; Ross et al. 2018; Marshall et al. 2019; Otoo et al. 2019). Most are flood plain deposits (Bennett et al. 2016) closely associated with palaeosols (Kearsey et al. 2016) and dolostones (Bennett et al. 2021), but at least one is a conglomerate lag at the base of a channel sandstone (Clack et al. 2018, 2019a). So far, six new tetrapods have been named and briefly described (Clack et al. 2016; Smithson and Clack 2018), while others have been figured but not yet named

---

† Deceased.

(Smithson et al. 2012; Clack et al. 2016, 2018, 2019a). Initial phylogenetic analyses have found that all the named taxa show no close relationship to one another and suggest a deep split between stem amphibians and stem amniotes in the early Carboniferous (Clack et al. 2016).

The early tetrapod *Ossirarus kierani* from Burnmouth was named, diagnosed and briefly described by Clack et al. (2016). Here we give a full description of the available material and reconsider its phylogenetic relationships.

Material and methods

Ossirarus kierani is represented by a single specimen (UMZC 2016.3) in the University Museum of Zoology, Cambridge (Fig. 1). It comprises the disarticulated bones of the posterior half of the skull (Figs 1–4; skull reconstruction, Fig. 5; comparisons with other tetrapod skulls Fig. 6) and an incomplete postcranium (Fig. 7), including the anterior portion of the axial skeleton, and parts of the pectoral girdle and forelimbs (Figs 8–12; reconstruction of anterior half of skeleton, Fig. 13). The specimen was collected by TRS in 2010 from the cliffs at the Ross end of Burnmouth, Scottish Borders (Grid reference NT964606), 340.5 m above the base of the Ballagan Formation (Clack et al. 2016; Otoo et al. 2019). It was preserved in a thin layer of clay immediately above a palaeosol (Otoo et al. 2019, figs 2, 3).

The specimen was prepared mechanically under a binocular microscope. The clay matrix was moistened with water and then removed with either a fine camel-hair brush or a mounted needle. The bones were strengthened with paraloid B72 dissolved in acetone. Most of the photographs were taken with a Sony DCS-W830 camera, but the photographs of the right humerus (Fig. 11A–E) were taken with a Dino-Lite Pro/Pro2 Digital Microscope, and that of the ventral scale (Fig 12C) was taken with a GXCAM-U3 Series 5MP USB-3 C-Mount Camera. The figures were prepared using Microsoft Paint and Adobe PowerPoint.

Phylogenetic analysis

Ossirarus kierani was coded into a data matrix consisting of 64 taxa and 275 characters. The matrix (PAUP*-readable Nexus file in Suppl. material 1) is largely based upon the dataset in Clack et al. (2016), with additions of

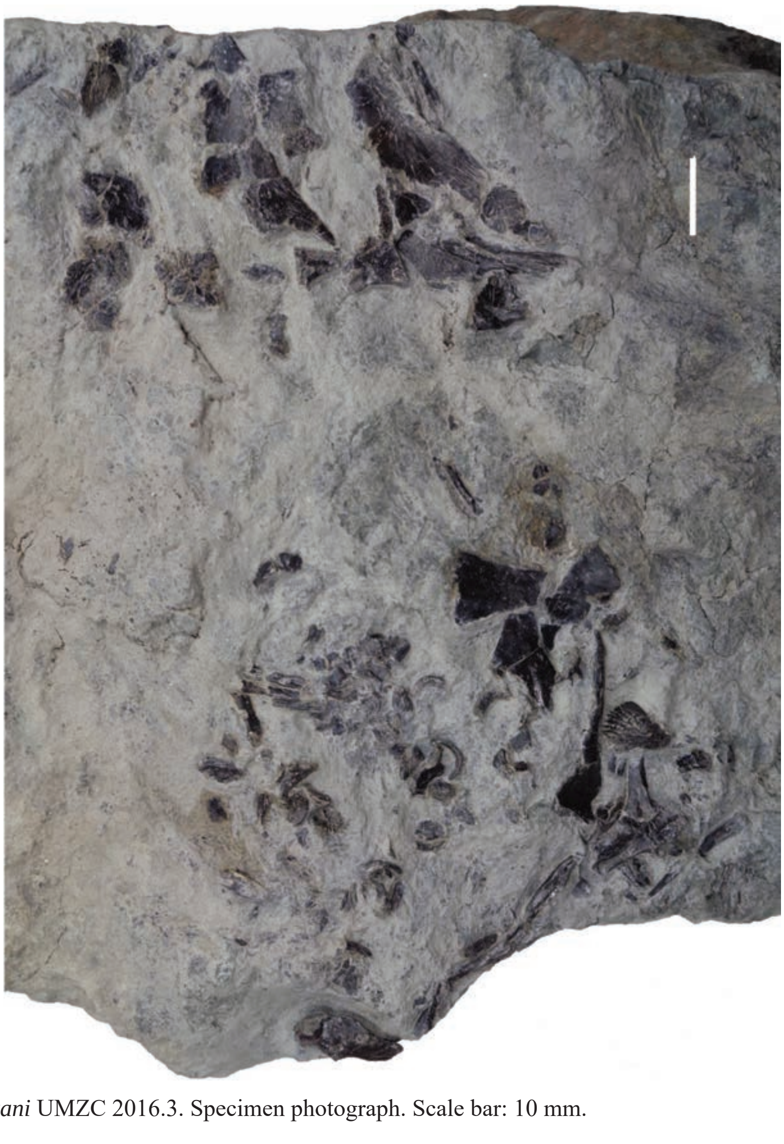

Figure 1. *Ossirarus kierani* UMZC 2016.3. Specimen photograph. Scale bar: 10 mm.

taxa and characters (character list in Suppl. material 2). As part of ongoing investigations into the tetrapod fauna from the Scottish Borders, we are conducting a re-assessment of several recently published phylogenies of early tetrapods, with an aim to provide a comprehensive review of character formulations and codings. Therefore, the phylogenetic results presented in this paper should only be regarded as provisional.

We carried out maximum parsimony tree searches in PAUP* (version 4.0a.169; Swofford 1998), with all characters treated as unordered and, initially, as having equal unit weight. The initial, equal-weights analysis exploited heuristic searches with the tree bisection-reconnection branch-swapping algorithm and 5×10^4 random stepwise taxon addition sequences. We used the “amb-” option to collapse tree branches if the minimum retrieved length of any branch was zero. During the searches, one tree was kept in memory. The trees saved from this round of branch-swapping were used in a new branch-swapping round, saving multiple trees. Lastly, the trees retrieved from this second round were subjected to ten additional branch swapping iterations. An additional parsimony analysis used characters re-weighted according to the best-fit value of their rescaled consistency indexes from the ‘unweighted’ analysis. A third parsimony analysis employed the implied weighting strategy of Goloboff (1993), with a value of 12 for the constant of concavity *K* (Goloboff et al. 2018). As the implied-weighted analysis proved to be memory-intensive, we used 3×10^3 random stepwise taxon addition sequences. Where multiple equally parsimonious trees were found, we summarised alternative branching patterns using strict, 50% majority-rule and Adams consensus topologies. Node support for the equal-weights analysis was evaluated through bootstrapping (Felsenstein 1985) and jackknifing (Farris et al. 1996), in each case using 3×10^5 replicates of character resampling under the ‘fast’ stepwise addition option in PAUP*. For jackknifing, we set a threshold value of 50% character deletion. For both resampling methods, we retained groups with support equal to, or greater than, 50%.

Results

Systematic Palaeontology

Ossirarus kierani **Clack & Smithson, 2016**

Holotype. UMZC 2016.3. A single block containing scattered skull and postcranial remains.

Locality. Ross cliffs, Burnmouth, Scottish Borders Region, Scotland. National grid reference NT964606.

Horizon. 340.5 m above the base of the Ballagan Formation. CM palynozone, mid-Tournaisian, Mississippian.

Emended diagnosis. Autapomorphies: tabular elongate triangle forming a conspicuous tabular horn with a convex lateral margin.

Derived characters present in several stem amniotes: tabular-parietal contact; exoccipital separate from basioccipital; multipartite gastrocentrous vertebrae with widely notochordal centra.

Plesiomorphies and characters of uncertain polarity: jugal with extensive postorbital component, with anteriorly placed shallow contribution to orbit; preopercular and intertemporal present; cleithrum with long, narrow, curved stem and expanded dorsal blade; diamond-shaped interclavicle lacking parasternal process; humerus with elongate and oblique pectoralis process comparable with the ventral humeral ridge of elpistostegalians and *Acanthostega*; brachial foramen piercing posterior edge of humerus at the base of entepicondyle as in *Mesanerpeton*; radius c. 60% the length of humerus; neural arches as unfused bilateral halves.

Description.

Skull. ***General skull preservation.*** The bones are generally well preserved. They are disarticulated and have drifted apart slightly, so that sutural overlap areas are often very clear. The pre-orbital region is missing, and the lower jaws and other tooth bearing bones are not preserved apart from a fragment of maxilla or premaxilla (Fig. 2). We estimate that the skull was 54 mm long and the preserved region made up approximately two thirds of its length. Apart from the tabular and squamosal, which show some ornamentation, the skull roofing bones are essentially smooth. The lateral line system is represented by pores in the jugal, postorbital, postfrontal and preopercular; there are no open lateral line canal grooves.

Cheek region. Much of the right cheek is preserved. It comprises the jugal, postorbital, an incomplete right squamosal and a preopercular. The left cheek is represented by the posterior part of the jugal.

The jugal is a large bone. It is c. 25 mm long, including an extensive area overlapped by the quadratojugal, and has a maximum depth of c. 7 mm behind the orbit margin (Fig. 2). The orbit margin is shallow and below it the bone is relatively deep and posteriorly elongated. It most closely resembles the jugal of *Acanthostega* (Clack 2002) and colosteids (Smithson 1982; Hook 1983). It lacks the tall, vertical orbital margin seen in *Diploradus* (Clack et al. 2016), *Pederpes* (Clack and Finney 2005) and *Whatcheeria* (Lombard and Bolt 1995; Rawson et al. 2021). The suture with the lacrimal is vertical and judging by the shape of the orbit margin sits under the centre of the orbit. The area behind the orbit is gently concave. It is unclear if this depression is natural or the result of crushing. The dorsal edge of the bone behind the orbit margin is damaged but it appears to have overlapped the ventral edge of the postorbital. The posterior portion of the jugal bears numerous fine ridges and furrows and was probably overlapped by the quadratojugal. This area is large and represents approximately one sixth of the area of the jugal. A much smaller area of ridges and furrows on the posterodorsal edge of the jugal probably formed part of the area overlapped by the squamosal. The incomplete left jugal is represented by the posterior portion bearing the ridges and furrows of the quadratojugal overlap area.

The postorbital is almost rectangular in outline with a gently concave orbital margin anteriorly. Its sutural

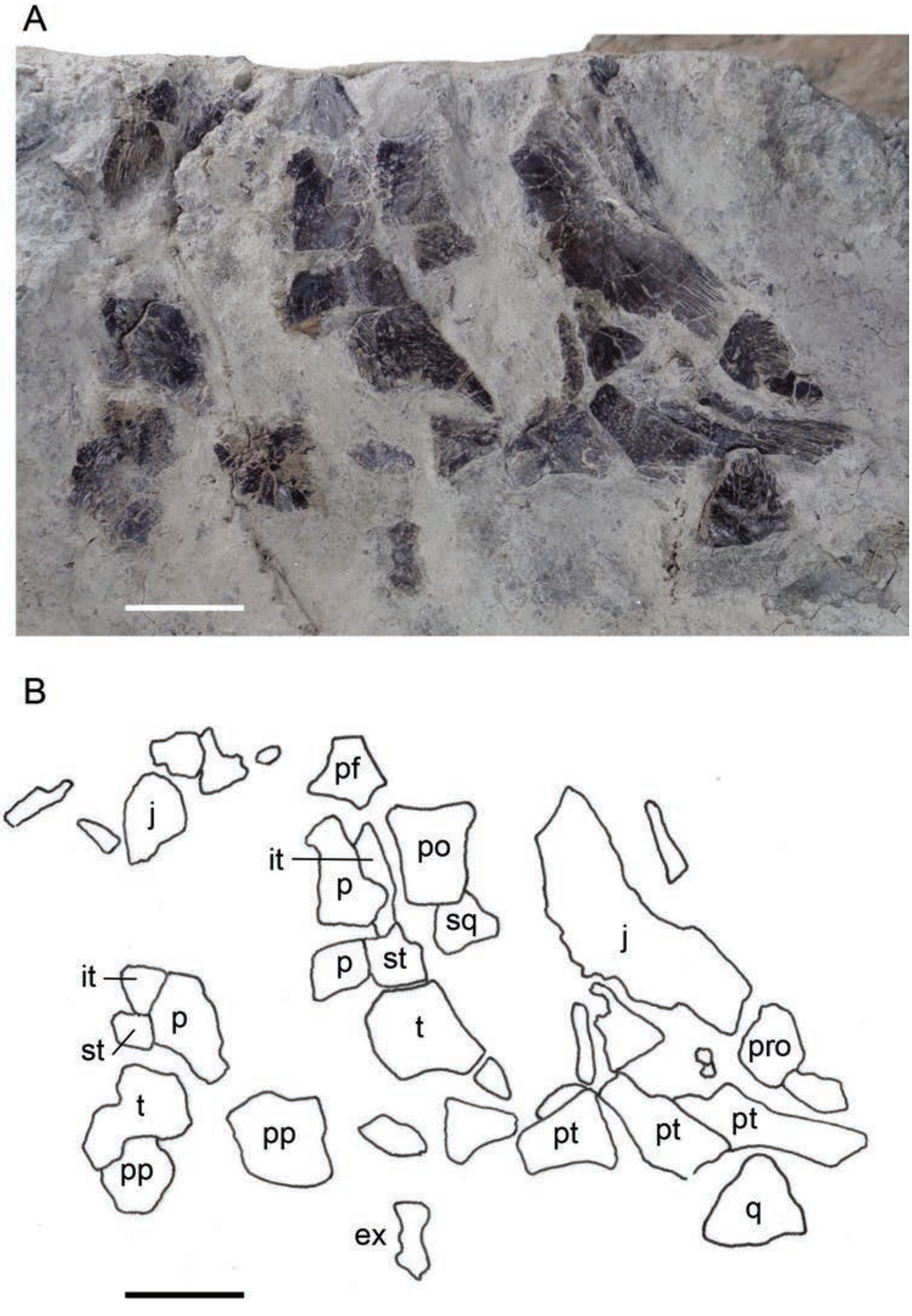

Figure 2. *Ossirarus kierani* UMZC 2016.3. Skull bones. **A.** Specimen photograph; **B.** Interpretive drawing. Scale bars: 10 mm. Abbreviations: c.r, conical recess; ex, exoccipital; j, jugal; p, parietal, pf, postfrontal; pin, pineal; po, postorbital; pp, postparietal; pro, preopercular; pt, pterygoid; q, quadrate; sq, squamosal; t, tabular.

contacts with surrounding bones are well preserved. Ventrolaterally, there is a shallow step from the smooth external surface to an area of fine ridges and grooves marking the area of overlap by the jugal. The ridges and grooves continue onto the posterior edge marking the area of overlap by the squamosal. These ridges and grooves are also found at the anterolateral corner of the postorbital where it was overlapped by the postfrontal. The medial margin of the postorbital is damaged but appears to have formed a thin lamina that overlapped the lateral edge of the intertemporal.

The squamosal is incomplete and appears to have broken into several pieces, most of which have been lost. Two fragments make up part of the posterior edge of the bone and a third formed the anterodorsal portion of the squamosal between the jugal and skull roof, behind the postorbital (Fig 2). The external surface of the bone bears a fine reticulate ornament in contrast with the smooth surface of the jugal.

The preopercular lies behind the jugal (Fig. 2). We initially thought it was part of the quadratojugal but the presence of a lateral line pore and the extent and orientation of the area of sutural overlap, as well as comparisons with the preopecular of *Acanthostega* (Porro et al. 2015) and *Whatcheeria* (Rawson et al. 2021), convinced us it is the preopercular. The bone is roughly triangular-shaped. It is c. 7 mm long and c. 6 mm high. Approximately two thirds of the surface is covered with the fine ridges and grooves that mark the area of overlap with the quadratojugal (Fig. 2) with only about one third exposed on the surface of the skull. The exposed area is roughly quadrangular, and bears a single lateral line canal sulcus in the posteroventral corner. One side of the quadrangle forms part of the posterodorsal edge of the suspensorium. The anterodorsal edge formed a suture with the squamosal and the anteroventral and posteroventral areas were overlapped by the quadratojugal. The preopercular is hypothesized to have occupied a position on the edge of the suspensorium, above the quadratojugal, in a similar position to the preopercular in *Ichthyostega* (Clack and Milner 2015, fig. 8), *Pederpes* (Clack and Finney 2006) and *Whatcheeria* (Rowson et al. 2021), rather than forming the posteroventral corner of the suspensorium as found in *Acanthostega* (Porro et al. 2015).

Skull table. Much of the right side of the skull table is preserved (Fig. 3) and comprises the parietal, postparietal, postfrontal, intertemporal, supratemporal and tabular. On the left, parts of the parietal, postparietal, supratemporal and tabular are preserved.

The parietals have separated along the midline and the left has drifted back relative to the right. The bones are thin and incomplete. The thickened area around the pineal is preserved on both sides. Using information from each bone gives a minimum anteroposterior length of 15 mm. The incomplete lateral edge of the parietal is thin and appears to have had a broad overlapping suture with the bones of the temporal series. On the right, the parietal appears to be partially overlying the supratemporal.

The incomplete postparietals have separated and drifted backwards. Each is poorly preserved with a fractured dorsal surface and little if any true edge around the bones. The right is the more complete and appears to be approximately square in outline. They are much smaller than the parietals and have an anteroposterior length of c8 mm.

The tabular is well preserved on the right. It is a relatively large, approximately triangular-shaped bone and its surface is ornamented with pits and grooves. The anterior edge, where the tabular meets the supratemporal is straight, the medial edge which contacts the midline bones is convex, the posterolateral edge is slightly concave and extends well beyond the posterolateral corner to produce a prominent tabular horn. There is no evidence of sutural contact with the squamosal, the lateral edge of the bone is gently rounded and smooth. The areas of sutural contact with the midline bones are very clear. Along most of the medial edge there is a shallow step down from the external surface to a broad area of ridges and grooves that would have been overlapped by the midline bones. At the posteromedial corner the tabular is thickened and the ridges and grooves form a sloping shelf which extends around on to the posterior edge. This posterior shelf probably marks the area of contact with the postparietal, while the broad flat area probably formed the suture with the overlying parietal. This arrangement suggests that *Ossirarus* had a tabular-parietal suture and is the earliest record of this feature in early tetrapods. The incomplete left tabular shows part of the tabular horn and the two discrete areas of sutural overlap along the medial edge. The pattern of ornament is similar to that on the right.

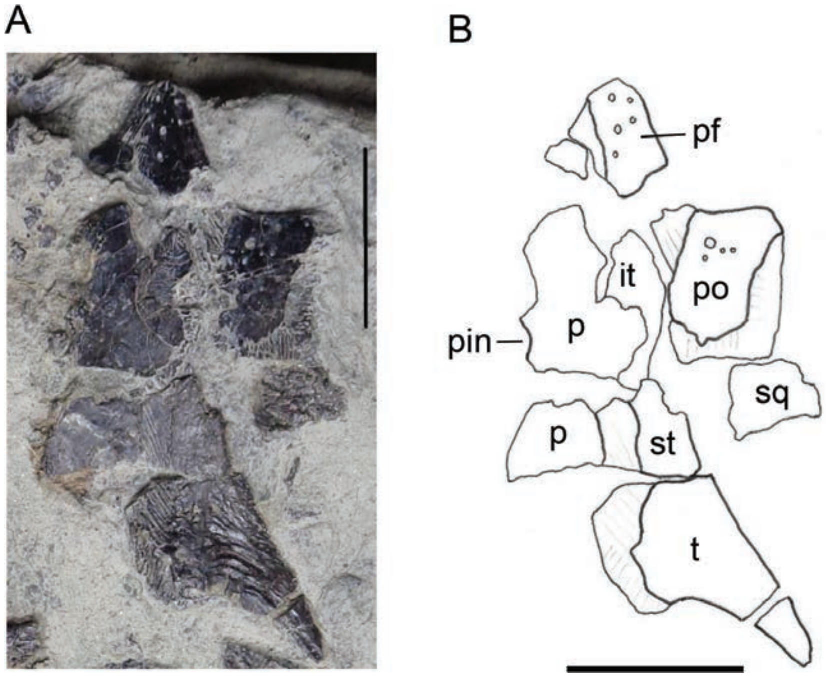

Figure 3. *Ossirarus kierani* UMZC 2016.3. Right skull table. **A.** Specimen photograph; **B.** Interpretive drawing. Scale bars: 10 mm. Abbreviations: see Fig. 2.

The supratemporal is well preserved on the right. It has separated slightly from the tabular and is partially overlapped by the parietal. It is incomplete anteriorly where it meets the intertemporal. The external surface is smooth. The posterior part of the lateral edge is gently rounded and shows no evidence of sutural contact with the squamosal. The anterior part is incomplete. As on the tabular, the exposed part of the medial edge bears a shallow step down from the external surface to a broad area of ridges and grooves that would have been overlapped by the parietal. On the left, the supratemporal has separated from the tabular. It is incomplete anteriorly and damaged along the lateral edge, but the straight, butt suture with the tabular is preserved posteriorly, together with an area of ridges and grooves on the medial edge originally overlapped by the right parietal.

The intertemporal appears to be present on the right between the supratemporal and postorbital and partially overlain posteriorly by the parietal. It is a relatively long bone, c. 9 mm is exposed, but its width cannot be determined, because of the overlying parietal. It is incomplete with damaged edges. There appears to be a small area of sutural overlap ridges and grooves at the anterior tip of the bone.

The posterior part of the postfrontal is preserved. The slightly concave lateral edge forms part of the orbit margin. The surface of the bone is smooth and shows a number of pores of the lateral line canal system. The thickened medial edge bears the characteristic ridges and grooves of sutural contact with the midline bones and there is a small area of ridges and grooves on the posteromedial edge suggesting it was overlapped by the intertemporal.

Palate. Very little of the palate is preserved. Part of the quadrate ramus of the right pterygoid and the right quadrate are present (Fig. 4).

The quadrate ramus is represented by a number of pieces which have been displaced posteriorly beyond the tabular horn and squamosal, and medial to the jugal and quadratojugal (Fig. 4). The pieces include an anterior portion bearing the conical recess, a central portion with a finished lateral edge marking part of the rim of the adductor fossa, and a posterior portion folded along a crack. This last piece has a ventrolateral part that would have sutured with the quadrate and a dorsomedial part that would have contributed to the medial wall and roof of the adductor chamber, and sutured with the squamosal. All the pieces of the pterygoid, apart from that forming the rim of the adductor fossa, have broken edges. The pieces bearing the conical recess and rim of the adductor fossa have broken along a simple crack and can readily be restored into their relative positions (Fig. 4). The other pieces are more difficult to align.

The surface of the bone behind the conical recess is lightly pitted. The surface of other broken pieces of the pterygoid is smooth, apart from the posterior-most portion, which is striated and probably represents an overlap area with the quadrate. None of the pieces of pterygoid bear denticles.

The right quadrate is preserved in internal view. It is roughly triangular-shaped with a central concavity. The lateral edge appears to be broken rather than sutural, and halfway up the medial edge is a notch, which presumably formed the quadrate contribution to the paraquadrate foramen that pierces the quadrate-pterygoid suture in some early tetrapods (Beaumont 1977, p. 52: Clack 2003, p. 488). The ventral edge is unfinished and forms the articulating surface with the articular of the lower jaw. The articulating surface is c. 8 mm long, well ossified and has a complicated shape. It is superficially screw-shaped with the axis running along the length of the articulating surface from the lateral to medial edges. It starts on the lateral edge as a ridge, followed by a furrow, and then a larger rounded ridge, followed by a deeper furrow and terminating on the medial edge with a rounded ridge.

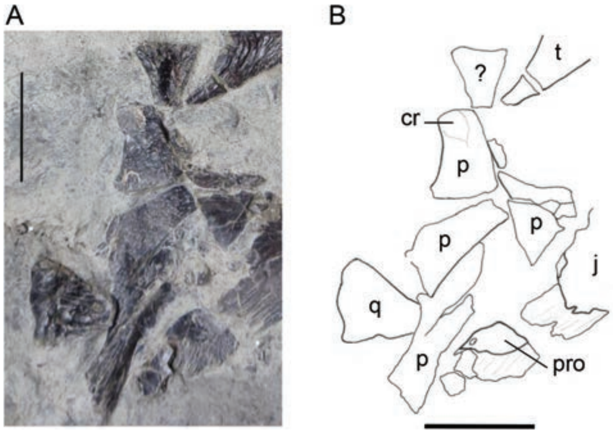

Figure 4. *Ossirarus kierani* UMZC 2016.3. Right suspensorium. **A.** Specimen photograph; **B.** Interpretive drawing. Scale bars: 10 mm. Abbreviations: see Fig. 2.

Despite its relatively small size (skull length c. 54 mm) the degree of ossification of the quadrate and the form of the sutures suggest that this was a mature individual.

Braincase. The only part of the braincase that is preserved is a small dumb-bell shaped bone lying behind the right tabular which we interpret as an exoccipital (Fig. 2). For a while we debated whether it might be a stapes, but eventually concluded that it is more likely to be part of the occipital arch.

The bone is c. 6.5 mm high with expanded ends. The end nearest to the tabular is considered to be the dorsal end, the exposed surface is the posterior side of the bone and it is interpreted as the left exoccipital. The dorsal surface is slightly damaged while the central portion is covered with smooth periosteal bone and is pierced on the lateral side by a foramen for the hypoglossal nerve (XII). The ventral end is a triangular-shaped area of unfinished bone which probably formed part of the occipital condyle for articulation with the atlas vertebra. Above and alongside the unfinished area the medial edge is gently curved and formed part of the boundary of the foramen magnum.

Restoration of the skull. The preservation of the skull of *Ossirarus* is unusual. The separation of the individual bones and exposure of the sutural overlap areas is rare and the result of its unusual preservation (see below: Discussion). This displacement of the bones has added an extra challenge to the preparation of a reconstruction

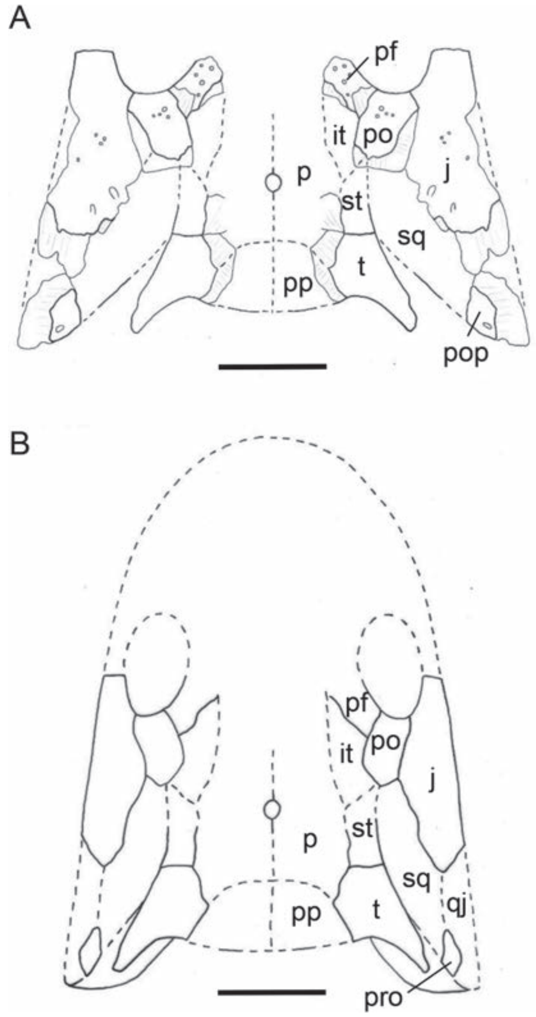

Figure 5. *Ossirarus kierani* UMZC 2016.3. Reconstruction of the skull. **A.** Restoration of the bones of the postorbital region in the horizontal plane; **B.** Reconstruction of the skull in dorsal view. Scale bars: 10 mm. Abbreviations: see Fig. 2.

of the skull (Fig. 5). Here, the patterns of sutural overlap revealed in µct scanning studies of the skulls of *Acanthostega* (Porro et al. 2015) and *Whatcheeria* (Rawson et al. 2021) have been used as a guide to the relationship between individual bones. We have also tried to take account of the incomplete preservation on some bones like the parietal and jugal, where the areas of overlap are thin and have been damaged and where the full extent of the bone is not preserved. Fig. 5A shows the relationships of the preserved bones on the right side of the skull (mirrored on the left) in the horizontal plane, with the sutures shown as thick lines and the areas of overlap shown as thinner lines. Fig. 5B is a partial reconstruction of the skull in dorsal view, based on a model prepared by folding a tracing of the bones in the horizontal plane over a moulded block of plasticine.

In Fig. 6 we compare the reconstruction of the skull of *Ossirarus* with those of a representative sample of tetrapods from the Upper Devonian and early Carboniferous. All are drawn to the same scale. In comparison with many early tetrapods, *Ossirarus* was relatively small. Upper Devonian tetrapods were typically quite large animals with some exceeding one metre in length (Clack and Milner 2015). Many early Carboniferous tetrapods were equally large. The whatcheeriid *Pederpes* from the Ballagan Formation near Dumbarton in Scotland was approximately one metre long (Clack and Finney 2005), and *Crassigyrinus*, which may be represented at Burnmouth by an incomplete lower jaw (Clack et al. 2018), attained a length of nearly two metres (Panchen 1985). In contrast, *Ossirarus* was probably little more than 300 mm long, and much more similar in size to the late Viséan tetrapods from East Kirkton like the temnospondyl *Balanerpeton* (Milner and Sequeira 1994) and the stem amniotes *Eldeeceon* (Ruta et al. 2020) and *Silvanerpeton* (Ruta and Clack 2006). However, although

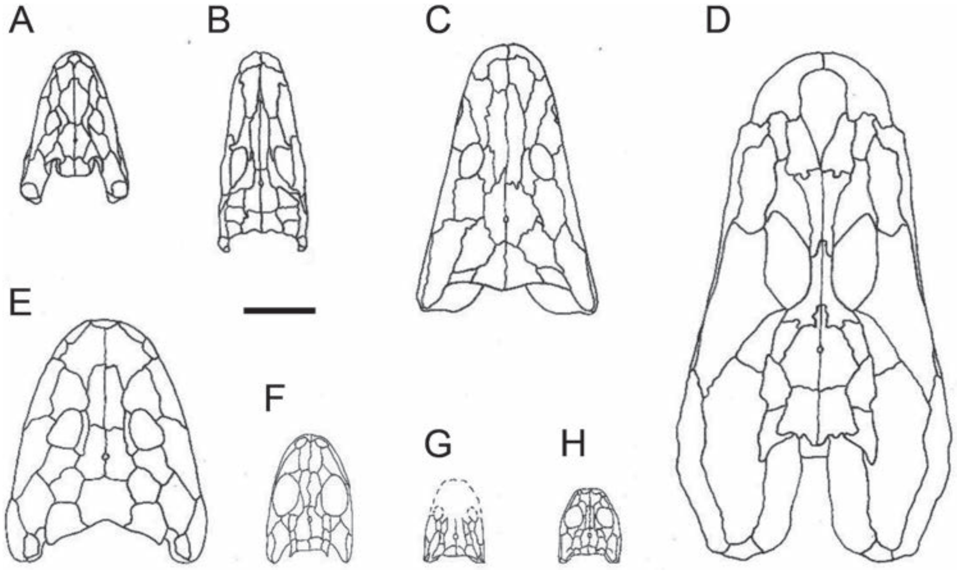

Figure 6. Skulls of tetrapods from the Upper Devonian and early Carboniferous. **A.** *Acanthostega gunnari* after Porro et al. (2015); **B.** *Whatcheeria deltae* after Rawson et al. (2021); **C.** *Greererpeton burkemorani* after Smithson (1982); **D.** *Crassigyrinus scoticus* after Porro et al. (2023); **E.** *Ichthyostega watsoni* after Clack and Milner (2015); **F.** *Silvanerpeton miripedes* after Ruta and Clack (2006); **G.** *Ossirarus kierani*; **H.** *Balanerpeton woodi* after Milner and Sequeira (1994). Scale bar: 50 mm.

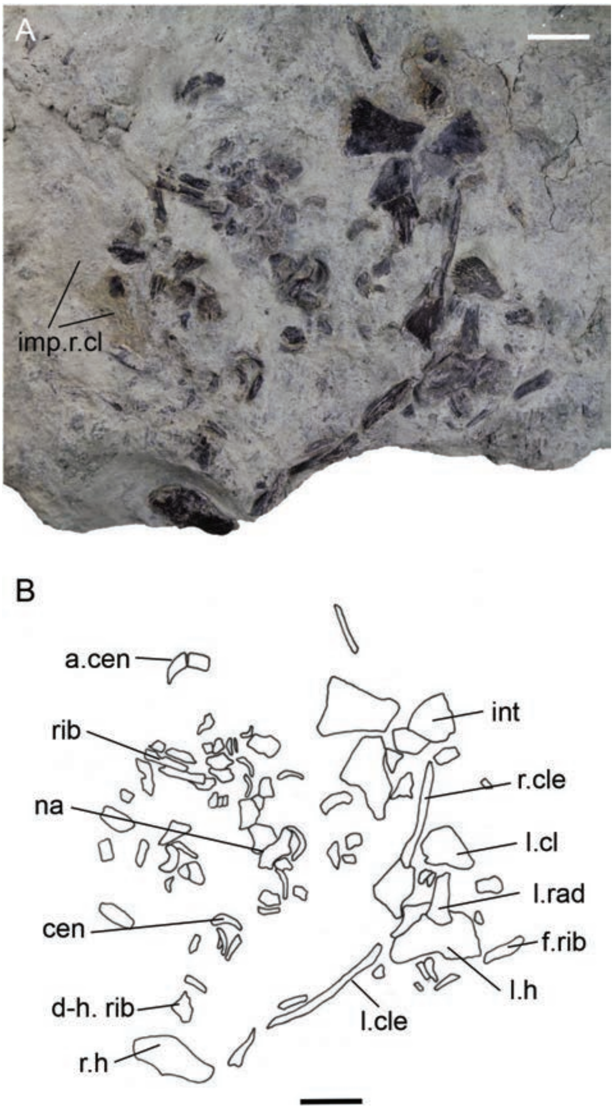

Figure 7. *Ossirarus kierani* UMZC 2016.3. Postcranial skeleton. **A.** Specimen photograph; **B.** Interpretive drawing. Scale bars: 10 mm. Abbreviations: a.cen, atlas intercentrum; cen, centrum; d-h.rib, double-headed rib; f.rib, flattened rib; imp.r.cl, impression of right clavicle; int, interclavicle, l.cl, left clavicle; l.cle, left cleithrum; l.h, left humerus; l.rad, left radius; na, neural arch; r.cle, right cleithrum; r.h, right humerus; rib, rib.

the skull of *Ossirarus* was similar in size to those of the East Kirkton tetrapods, there is one notable difference: the orbits of *Ossirarus* are much smaller. This was an unexpected variation but may be explained by differences in ecology. The East Kirkton tetrapods are generally considered to be the earliest known example of a terrestrial fauna (e.g. Clack 2017) whereas the presence of lateral line canals in *Ossirarus* suggest it was either aquatic or amphibious and less reliant on vision for prey capture.

Axial skeleton.

The axial skeleton of *Ossirarus* is represented by a number of disarticulated cervical and trunk centra, neural arches and ribs (Fig. 7). The vertebrae are multipartite and consist of four parts: two central elements and a neural arch in bilateral halves. None is preserved intact and parts of numerous vertebrae are scattered on the left side of the specimen with most of the bones of the pectoral girdle and forelimbs on the right (Fig. 7).

Centra. The most anterior centrum lies c. 36 mm behind the postparietals and adjacent to the interclavicle (Fig. 7). It is preserved largely in ventral view but with part of the posterior edge and 'aperture' for the notochord exposed. It is well preserved and appears to be uncrushed, but it is cracked along the ventral midline and one half has slightly overriden the other. The centrum forms a segment of a circle approximately 7 mm in diameter. It is c. 3 mm long, 2.5 mm high, and 0.5 mm thick. It would have surrounded a notochord c. 6 mm in diameter. The outer surface of the centrum is finished in periosteal bone. The centrum most closely resembles the atlas intercentrum of *Acanthostega* (Clack 1998, fig. 1) and given its position is most likely to be the atlas intercentum of *Ossirarus*.

Eleven cervical/trunk centra are preserved. The most complete are crescent-shaped in antero-posterior view and would have formed a thin husk of bone less than 1 mm thick around a notochord c. 6 mm in diameter (Fig. 8). In lateral view the centra are roughly triangular-shaped, c. 2.5 mm long, with the base the same length as the height of the sides. No facets are preserved for articulation with either the neural arch or the ribs, and there are no other features that may help distinguish the pleurocentra from the intercentra. Judging by the length of the neural arches, two centra would be accommodated beneath each arch, presumably with one occupying the position of the pleurocentrum the other the intercentrum. There is no evidence of paired pleurocentra typically found in rachitomous vertebrae or the dorsally fused pleurocentra of *Whatcheeria* (Lombard and Bolt 1995; Otoo et al. 2021). The centra of *Ossirarus* are probably the earliest known example of the gastrocentrous arrangement found in early tetrapods.

Parts of up to five neural arches are exposed (Fig. 7). They are preserved as bilateral halves, separated along the midline. They are approximately 6 mm long and the body of the neural arch is well ossified with short transverse processes projecting ventrolaterally from midway between the well-developed-zygapopheses (Fig. 8C). In all cases the neural spine has broken off and have failed to be identified amongst the vertebral fragments. Judging by the position and length of the breaks, the neural spines occupied a posterior position and had a basal length of c. 2 mm. On the underside of each half of the neural arch is an area of unfinished bone, approximately square-shaped (Fig. 8B), probably marking the area where the neural arch rested on the notochord. A similar scar is present on the neural arches of *Eoherpeton*, where the neural arch contacted the underlying pleurocentrum (Smithson 1985, fig 18).

Ribs. Some partial ribs are preserved (Fig. 7). Four at the anterior end on the scatter of post cranial bones are stout, straight rods c. 10 mm long, slightly expanded at their proximal ends but not obviously double-headed. There is no evidence of uncinate processes. Given their position behind the skull and beside the interclavicle, they are most probably cervical ribs. Immediately in

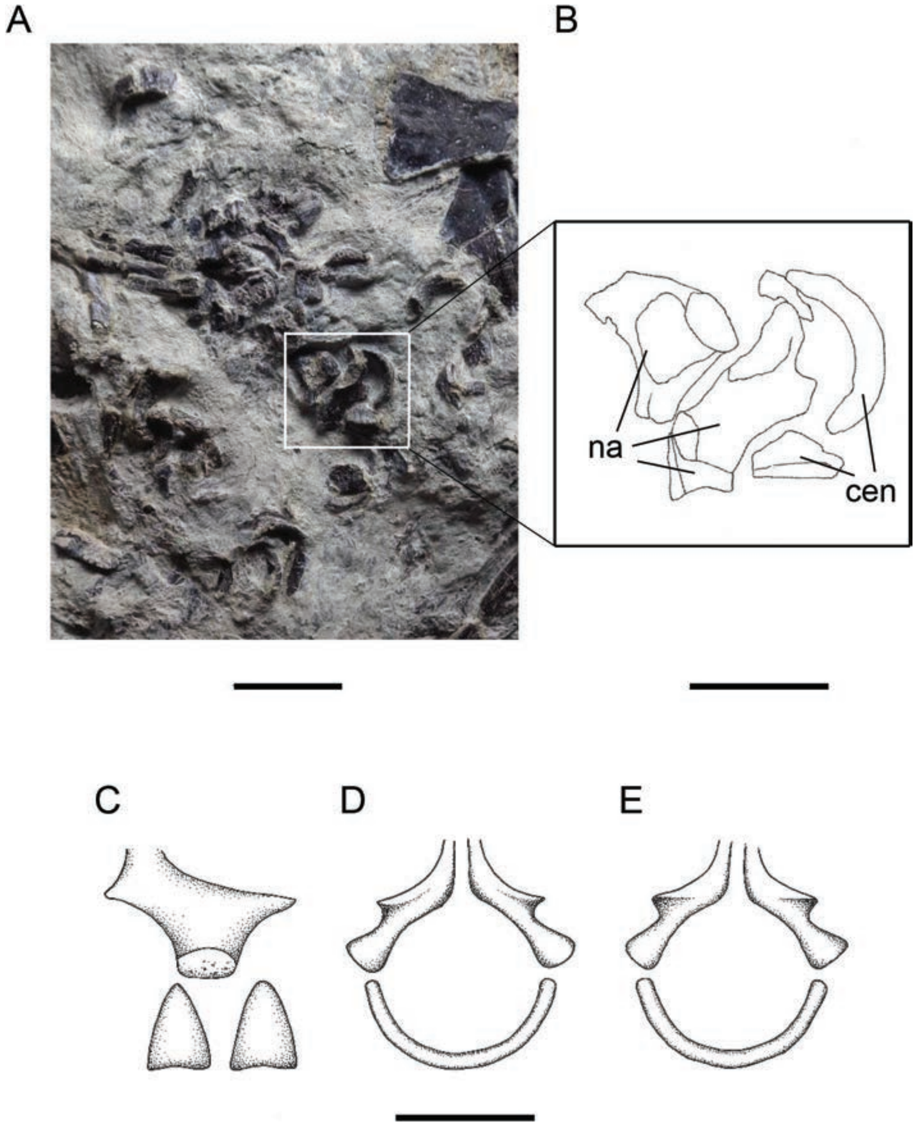

Figure 8. *Ossirarus kierani* UMZC 2016.3. Axial skeleton. **A.** Specimen photograph; **B.** Interpretive drawing of vertebral elements in box; **C–E.** Reconstruction of vertebra; **C.** Lateral view; **D.** Anterior view; **E.** Posterior view. Scale bars: 10 mm (**A**); 5 mm (**B, C**). Abbreviations: see Fig. 7.

front of the right humerus is the proximal end of a double-headed rib (Fig. 7). The rib head is clearly divided into dorsal tuberculum and ventral capitulum. The capitulum extends proximally beyond the tuberculum indicating the presence of a short transverse process on the corresponding vertebra (Fig. 8C). Beside the left humerus is a short piece of rib shaft (Fig. 7). It is c. 8 mm long and c. 3 mm wide and the exposed surface is gently convex. It probably formed part of the shaft of a broad, flattened rib, of the type found in the pectoral region of *Whatcheeria* (Otoo et al. 2021, figs 2, 3).

Appendicular skeleton. The appendicular skeleton is represented by much of the dermal pectoral girdle, the left and right humeri and the left radius (Figs 7, 9–12). All the bones are disarticulated and displaced, the interclavicle and cleithra are broken, and most of the left clavicle, the anterior portion of the interclavicle and the entepicondyles of each humerus are missing and represented by faint impressions in the matrix. The interclavicle is preserved in internal (dorsal) view, the right clavicle is preserved in external (ventral) view.

Cleithrum. The cleithrum is a long, narrow bone, approximately 30 mm in length, with an expanded dorsal blade (Fig. 10A). The right cleithrum is preserved in external view and broken into two pieces with the dorsal portion slightly overlying the ventral shaft. The posterior part of the dorsal blade is partially concealed by the left humerus. The left cleithrum is preserved in internal view and broken into three pieces slightly separated from one another. The dorsal blade is also partially concealed by the left humerus.

The cleithrum is divisible into two parts: a long narrow stem making up approximately two thirds of its length and an expanded dorsal blade. The stem is approximately 3 mm wide along most of its length but tapers slightly ventrally. In lateral view, it is gently bowed, with a convex posterior edge and a concave anterior edge. The internal surface carries a shallow central groove that fades out dorsally, where the stem expands to form

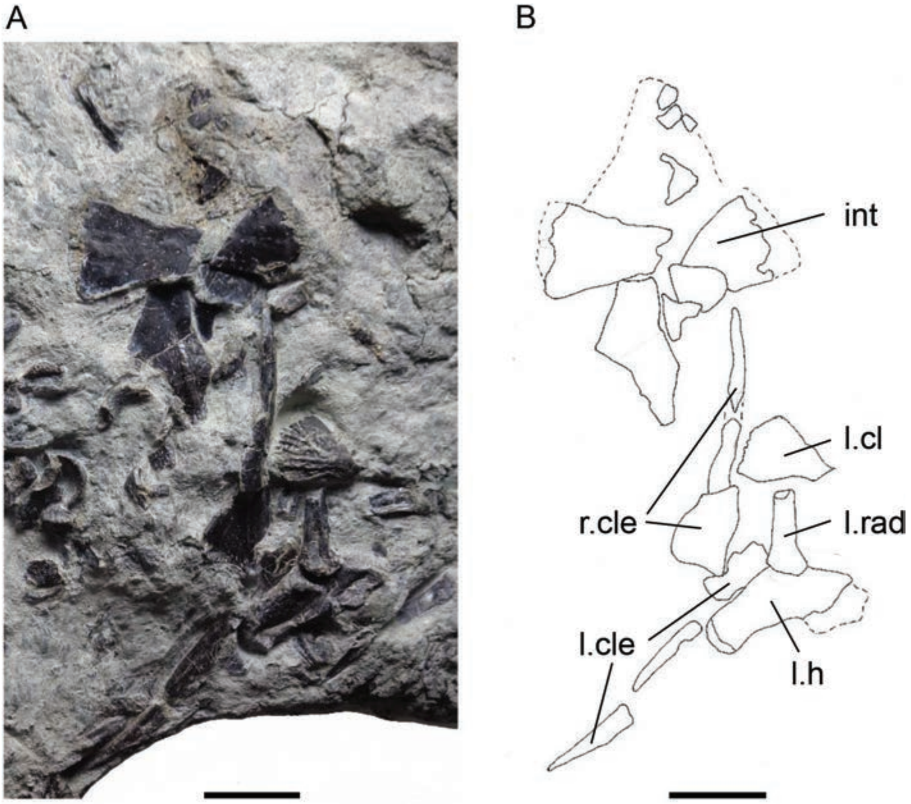

Figure 9. *Ossirarus kierani* UMZC 2016.3. Pectoral girdle and left forelimb. **A.** Specimen photograph; **B.** Interpretive drawing. Scale bars: 10 mm. Abbreviations: see Fig. 7.

the dorsal blade. The anterior edge is thin and sharp and may represent part of a post-branchial lamina (see Coates and Clack 1991; Coates 1996), but the posterior edge is gently rounded. Both diverge dorsally to produce the ventral portion of an expanded dorsal blade. The posterior edge of the blade is sinuous and terminates with a blunt dorsal process. In front of this process the dorsal edge is essentially straight and meets the anterior edge almost at right angles. It has a maximum anteroposterior length of c. 5 mm. The edges of the blade are gently rounded and the external surface of the right cleithrum is ornamented with a number of pits and grooves.

The cleithrum of *Ossirarus* is unlike that of most other early tetrapods in having a longer stem and a smaller and more angular dorsal blade. The cleithrum of the earliest known tetrapods *Acanthostega*, *Ichthyostega* and some specimens of *Whatcheria* is co-ossified with the scapulocoracoid (Otoo et al. 2021), but in *Pederpes* (Clack and Finney 2005) and in one specimen of *Whatcheria* (Otoo et al. 2021) the stem is broad and the dorsal blade more circular with a distinct notch on the posterior edge separating the blade from the stem. In *Ossinodus* (Warren and Turner 2004), the cleithrum is robust with distinct blade and stem, and it bears facets for articulation with the scapulocoracoid and clavicle. These facets are not developed on the cleithrum of *Ossirarus*. In colosteids like *Greererpeton* (Godfrey 1989), and in the baphetid *Eucritta* (Clack 2001), the cleithrum is gently curved and expands dorsally but lacks a distinct blade, while in the anthracosaur *Proterogyrinus* (Holmes 1984), the shaft is broad and straight with some slight widening dorsally.

Clavicle. The left clavicle is represented by impression of the ventral surface of the clavicular blade in the matrix in front of the right humerus (Fig. 7) together with a short piece of the clavicular stem. The right clavicle is partially exposed between the right cleithrum and left radius (Fig. 9). Much of the clavicular blade of the right clavicle is concealed beneath the right cleithrum and only the lateral part of the blade is visible. The base of the clavicular stem is preserved, but most of the stem is missing. The right clavicle is exposed in ventral view and the surface is ornamented with a well-developed reticulate pattern of ridges and grooves (Fig. 9A) that is also faintly visible in the impression of the left clavicle. This pattern of ornament has been found in a number of early tetrapods, including *Acanthostega* (Coates 1996), colosteids like *Greererpeton* (Godfrey 1989), *Doragnathus* (Smithson and Clack 2013) and many temnospondyls (Holmes 2000). The base of the clavicular stem is broad with laminae projecting from both the anterior and posterior edges. Together, these probably formed an open tube along the clavicular stem that received the stem of the cleithrum. Judging by the shape of the anterior portion of the interclavicle and the impression of the left clavicle, the clavicular blade was shaped like a long triangle, similar to those of *Doragnathus* (Smithson and Clack 2013) and *Greererpeton* (Godfrey 1989) (Fig. 10).

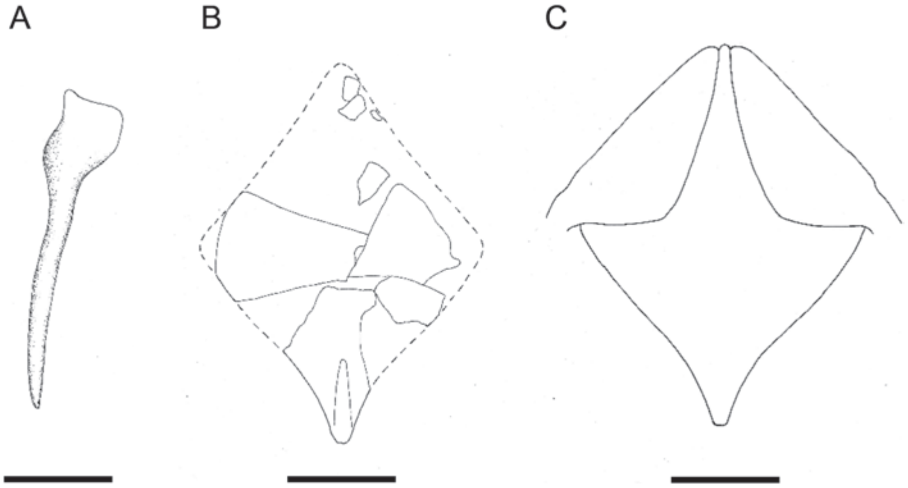

Figure 10. *Ossirarus kierani* UMZC 2016.3. Pectoral girdle. **A.** Recontruction of right cleithrum, lateral view; **B.** Outline reconstruction of interclavicle, dorsal view; **C.** Outline reconstruction of intercalvicle and clavicles, ventral view. Scale bars: 10 mm.

Interclavicle. The interclavicle is preserved in dorsal view (Figs 9, 10). Much of the anterior portion is missing and represented by impression in the surface of the matrix, but most of the posterior portion is preserved. It is broken into a number of pieces which have separated slightly, although part of the left lateral edge is missing. The interclavicle is approximately diamond-shaped, slightly longer than wide and lacks a parasternal process. As reconstructed (Fig. 10B), it is c. 36 mm long and c. 27 mm wide. Judging by the impression of the anterior portion, the ventral surface is ornamented with a reticulate pattern of ridges and grooves seen on the clavicle. The dorsal surface is smooth but not flat. Its contours are similar to those seen in the interclavicles attributed to *Doragnathus* (Smithson and Clack 2013). Extending laterally on either side from the centre of the interclavicle is a broad ridge. In *Doragnathus* this ridge corresponds with a groove on the ventral surface that accepts a ridge on the dorsal surface of the clavicular plate. Extending posteriorly from behind the centre of the interclavicle is a short midline ridge. This terminates at the posterior edge of the bone. A similar ridge is present on the interclavicles of *Doragnathus* as well as on an interclavicle described from Blue Beach, Nova Scotia (Anderson et al. 2015).

Humerus. Both left and right humeri are preserved (Figs 7, 11, 12). They are embedded in matrix and visible mainly in ventral view. The left humerus appears to have been flattened slightly, but the right is undistorted. The anterior edge and part of the posterior edge of the right humerus are exposed, and part of the dorsal surface was available for study after the bone was temporarily removed from the block. Much of the entepicondyle is missing in both humeri, but impression of the dorsal surface is preserved on the left. Each humerus is c. 17 mm long.

The humerus (Fig. 11) has the characteristic L-shape of early tetrapods. The proximal articulation is relatively broad and straight. Judging by the impression of the left entepicondyle this was well developed and square-shaped. The right humerus is twisted midway along the shaft and the angle of torsion is between 20–25 degrees. The insertions of the principal locomotory muscles from the shoulder to the proximal end of the humerus are clearly defined.

The proximal posterior edge is essentially straight and the pre-entepicondylar ridge is absent. The brachial foramen pierces the posterior edge of the humerus at the base of the entepicondyle, as it does in *Mesanerpeton* (Smithson and Clack 2018). The entrance of the foramen is not visible in dorsal view but it can be seen in ventral view (Fig. 11A, B, F). The exit is through the posterior part of the ventral ridge (see below). It is slightly concealed by this ridge and does not form a distinct opening on the ventral surface of the entepicondyle. The insertion for the coracobrachialis muscle is marked by a furrow on the posterior half of the ventral surface of the humeral head.

The ectepicondyle appears to be quite prominent, but the distal part of it is buried in the matrix. In the right humerus, it is visible in posterior view (Fig. 11A–C). It starts as a swelling level with the entrance of the brachial foramen and develops into a ridge that projects distally into the matrix. The latissimus dorsi process is borne on a low ridge which extends proximally from near the inception of the ectepicondyle.

The anterior edge of the right humerus is well preserved. The proximal end is marked by a fine ridge which extends distally from the articulating surface. There is no prepectoral space. The ridge swells to form the deltoid process on the anterodorsal surface and the pectoral process on the anteroventral surface. Beyond the pectoral process, the anterior edge bows dorsally and extends towards the radial condyle as a thin bony lamina, similar to that seen in *Acanthostega* (Smithson and Clack 2018, fig. 6). There is no distinct origin of the supinator muscle. The radial condyle is a relatively large, unfinished swelling on the anterodistal corner of the humerus, which is clearly visible in ventral and anterior views.

On the ventral surface, a ridge extends posterodistally from the distal edge of the pectoral process onto the entepicondyle. It consists of two parts, anteriorly

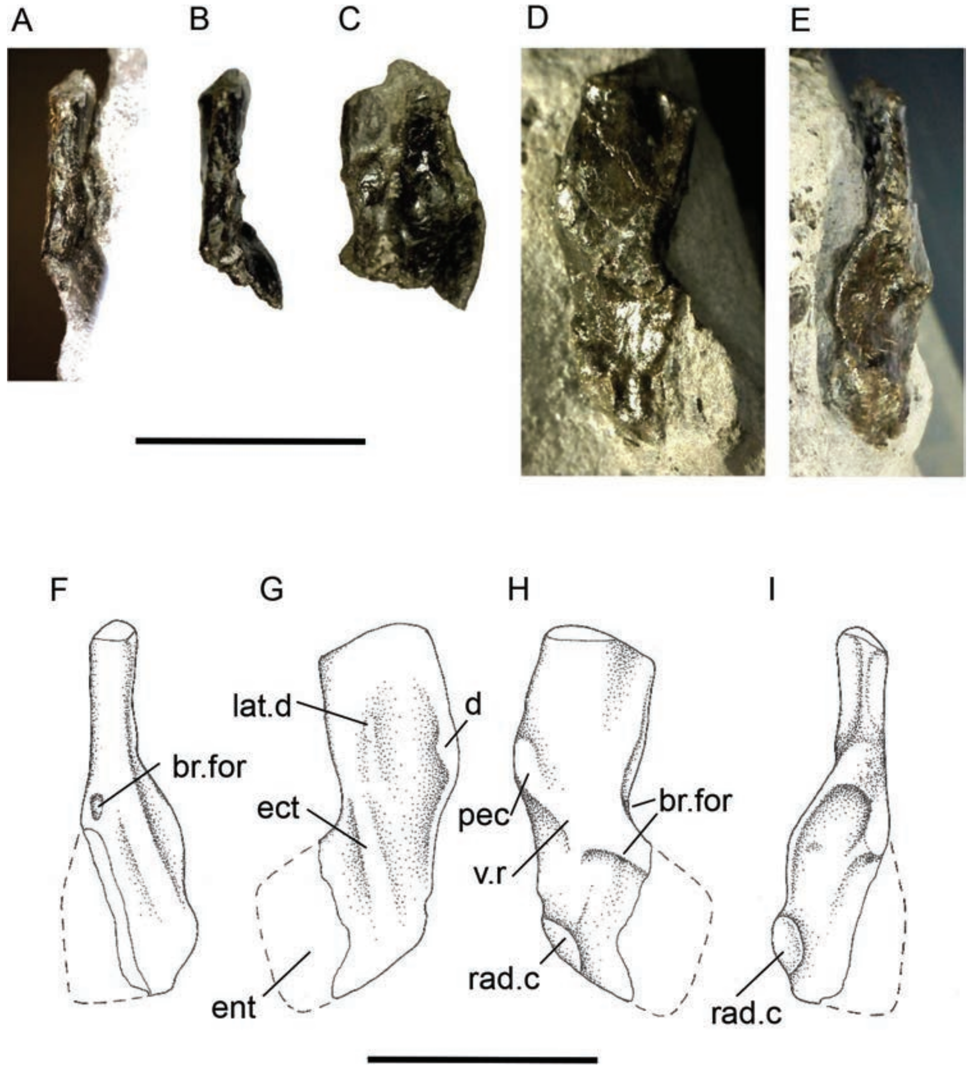

Figure 11. *Ossirarus kierani* UMZC 2016.3. Right humerus. **A–E.** Specimen photographs; **A.** Posterior view; **B.** Posterior view detached from the block; **C.** Dorsal view detached from the block; **D.** Ventral view; **E.** Anterior view; **F–I.** Restoration of right humerus; **F.** Posterior view; **G.** Dorsal view; **H.** Ventral view; **I.** Anterior view. Scale bars: 10 mm. Abbreviations: br.for, brachial foramen; d, deltoid process; ect, ectepicondyle; ent, entepicondyle; lat.d, latissimus dorsi; pec, pectoral process; rad, radius; rad.c, radial condyle; v.r, ventral ridge.

forming the smooth distal slope of the pectoral process and posteriorly the thickened proximal edge of the entepicondyle, pieced by the brachial foramen. The ridge fades between these two parts, turning distally towards the radial condyle. Presumably, it represents the vestige of the ventral ridge of tetrapodomorph fishes like *Tiktaalik* (Shubin et al. 2006) and *Gogonasus* (Holland 2013).

Radius. The left radius is preserved beside the left humerus (Fig. 12A, B). It is embedded in matrix and exposed in dorsomesial view. It is c. 10 mm long and approximately 60% the length of the left humerus. This compares with a radius–humerus ratio of 62% in *Pederpes* (Clack and Finney 2005), between 50% and 60% in *Whatcheeria* (Otoo et al. 2021, fig. 29A–C), 46% in *Proterogyrinus* (Holmes 1980, 1984) and 49% in *Baphetes* (Milner and Lindsey 1998). The ratio in *Acanthostega* is c. 53% (Coates 1996, fig. 15) and in *Crassigyrinus* is 72% (Panchen 1985).

The radius is approximately square-shaped in section with each of the sides being of similar dimensions. The faces of the exposed ventral and mesial sides are gently concave, and they meet at a sharp ridge. The ventral surface is further excavated below the proximal articulation to form a short groove. There is no evidence of the ventral radial crest figured by Coates (1996, fig 17) on the radius of *Acanthostega*. The junction between the medial surface and the concealed dorsal surface also forms a ridge. A similar ridge is present in *Archeria* (Romer 1957) and *Baphetes* (Milner and Lindsay 1998), but it is absent on the radius of *Crassigyrinus* (Panchen1985), *Pederpes* (Clack and Finney 2005) and *Whatcheeria* (Otoo et al. 2021). The proximal end of the radius of *Ossirarus* is gently rounded. The shaft tapers distally to an incompletely ossified or broken distal end. In its overall morphology the radius of *Ossirarus* is more like those of *Greererpeton* (Godfrey 1989) and *Proterogyrinus*

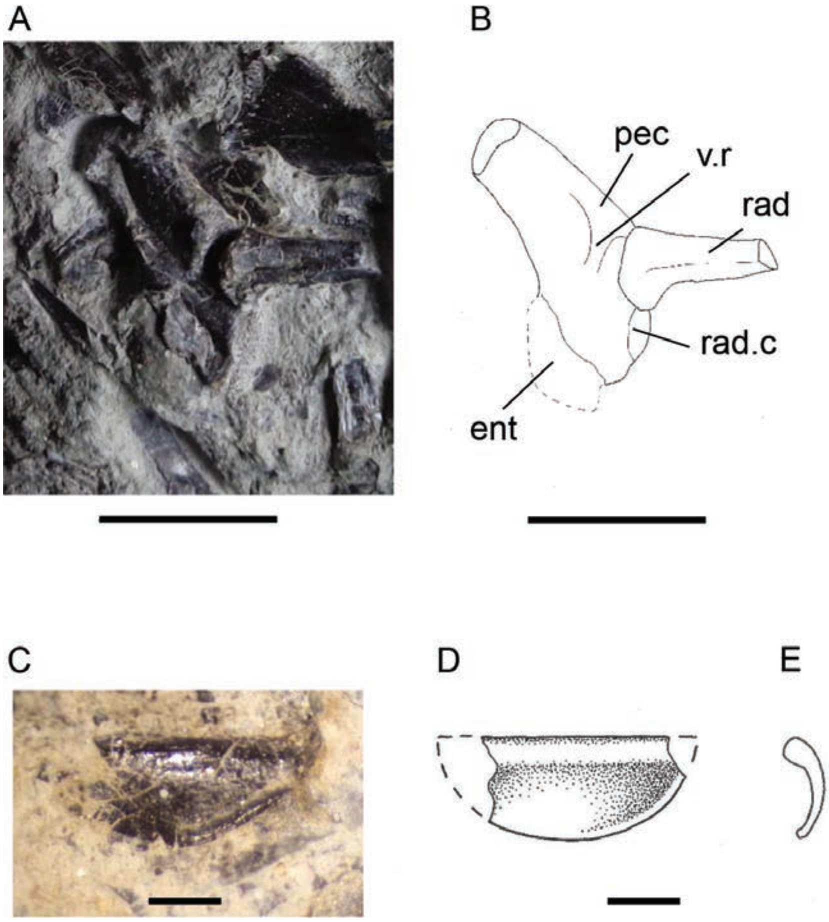

Figure 12. *Ossirarus kierani* UMZC 2016.3. Left humerus, left radius and ventral scale. **A.** Specimen photograph of left humerus and radius; **B.** Interpretive drawing of left humerus and radius; **C.** Specimen photograph of ventral scale; **D.** Interpretive drawing of ventral scale; **E.** Restoration of section through ventral scale. Scale bars: 10 mm (**A**, **B**); 1 mm (**C–E**). Abbreviations: see Fig. 11.

(Holmes 1980, 1984), where the four sides of the shaft have similar proportions, than those of *Acanthostega* (Coates 1996), *Baphetes* (Milner and Lindsay 1998), *Ossinodus* (Warren and Turner 2004), *Pederpes* (Clack and Finney 2005) and *Whatcheeria* (Otoo et al. 2021), where the dorsal (extensor) and ventral (flexor) surfaces are much broader than the anterior (mesial of Milner and Lindsay 1998) and posterior (lateral) surfaces, giving the radius a flattened appearance.

Scales. Most of the fragmentary scales were removed during preparation, but one slightly damaged example is preserved in internal view on the left side of the block near the right humerus. It is approximately semi-circular, with a straight side and a gently curved side (Fig. 12C, D). It is c. 2.5 mm long and c. 1.5 mm wide. The straight edge is thickened into a rounded ridge and the remainder of the scale is very thin apart from a narrow lip around the curved edge. In section the scale is gently curved with a concave internal surface and a convex external surface (Fig. 12E), a form described by Clack and Milner (2015, p. 23) as comma-shaped.

Ventral scales (gastralia) have been described in various early terapods, including *Acanthostega* (Coates 1996), *Crassigyrinus* (Panchen 1985), *Greererpeton* (Godfrey 1989) *Pederpes* (Clack and Finney 2005) and *Proterogyrinus* (Holmes 1984). None is triangular-shaped, but each has a rounded ventral ridge along their axis and, apart from the spindle-shaped scales of *Crassigyrinus*, each is externally convex.

Phylogenetic results

A maximum parsimony analysis with all characters equally weighted produced 1140 trees with a length of 1362 steps, an ensemble consistency index (CI) of 0.2676 (excluding two uninformative characters), and an ensemble retention index (RI) of 0.5799. The strict, 50% majority-rule and Adams consensus of those trees are shown in Suppl. material 3: fig. S1A–C. Re-weighting characters by the maximum value of their rescaled consistency indices from the previous analysis resulted in a single tree (length = 213.52943 steps; CI = 0.4524; RI = 0.7515) (Fig. 14). Lastly, the implied weights analysis yielded five trees (length = 1364 steps; Goloboff fit = -219.18765; CI = 0.2673; RI = 0.5791). The strict consensus of these five trees is shown in Fig. 15, and the 50% majority-rule and Adams consensus topologies are shown in Suppl. material 3: fig. S2A, B. Bootstrapping and jackknifing node support values feature in Suppl. material 3: fig. S3A, B.

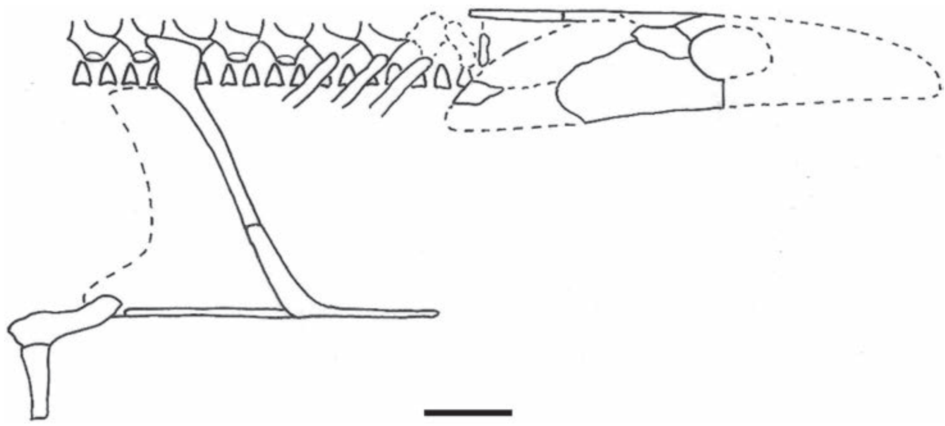

Figure 13. *Ossirarus kierani*. Reconstruction of anterior half of skeleton. Scale bar: 10 mm.

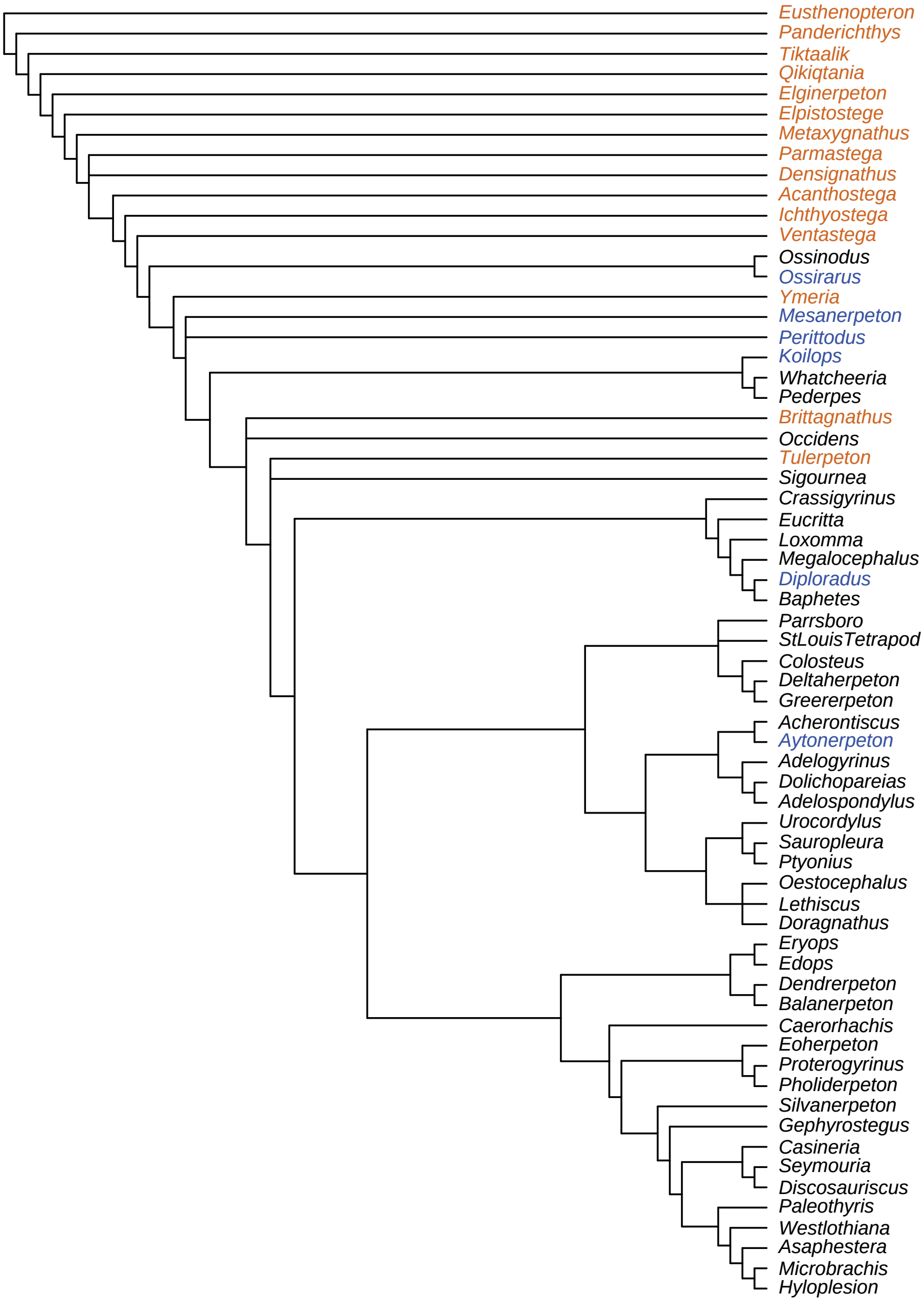

Figure 14. Single most parsimonious tree obtained after re-weighting characters by the maximum value (best fit) of their rescaled consistency indices from an unweighted analysis (see text for details). Taxa shown in brown text, Devonian; taxa shown in blue text, Tournaisian; taxa shown in black text, later Carboniferous and Permian.

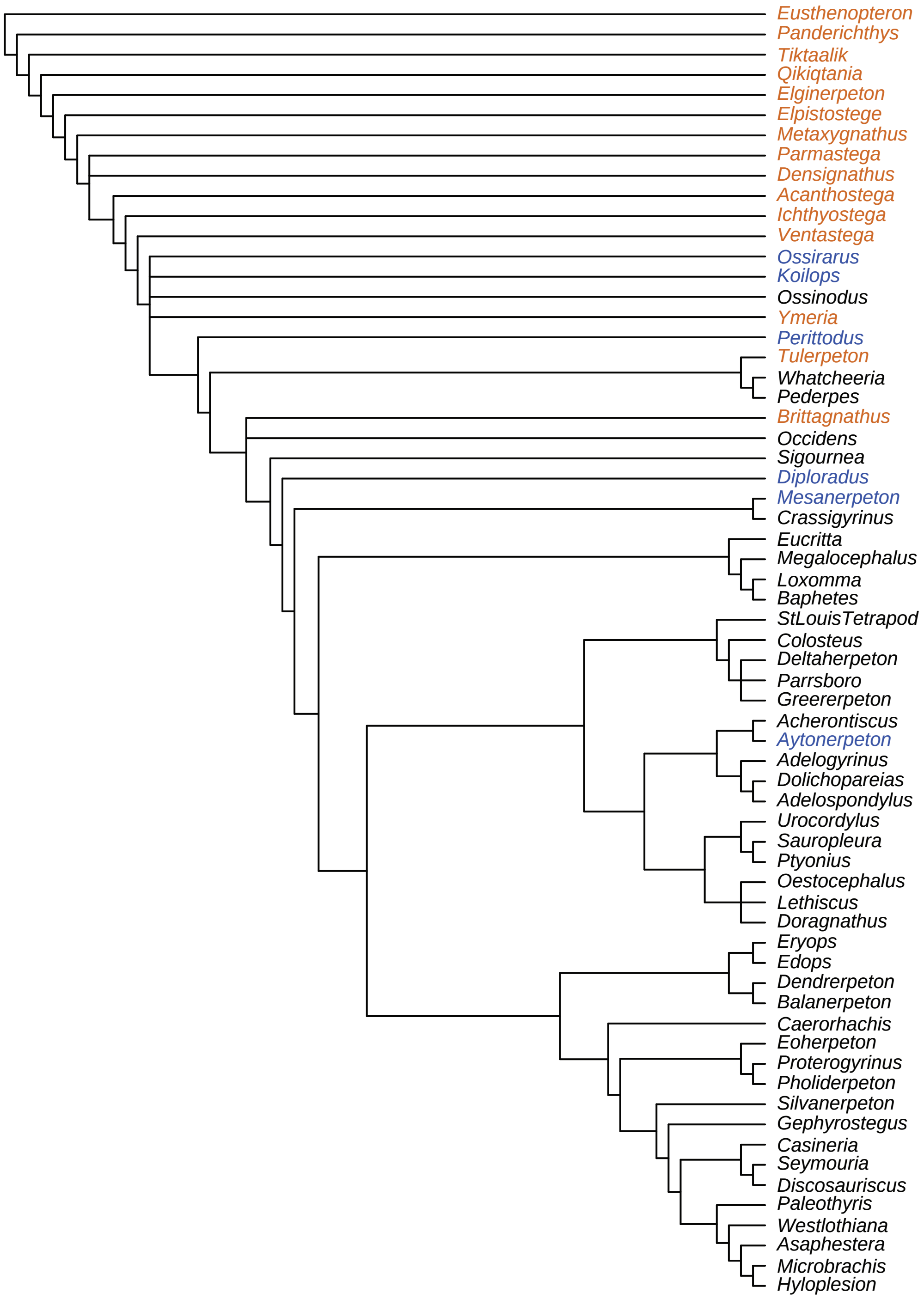

Figure 15. Strict consensus of nine most parsimonious trees obtained from an implied character weight analysis, with a value of 12 for the constant of concavity *K* (Goloboff et al. 2018). Taxa shown in brown text, Devonian; taxa shown in blue text, Tournaisian; taxa shown in black text, later Carboniferous and Permian

The branching patterns of trees obtained from the analyses with re-weighted and equal-weighted characters are broadly similar (Figs 14, 15). Some of the clades supported in those analyses also feature in the strict consensus topology from the analysis with equally weighted characters (Suppl. material 3: fig. S1A). Statistical support for most nodes in the equal weights analysis varies from weak to moderate (Suppl. material 3: fig. S3A, B). As in Clack et al.'s (2016, fig. 5) study, the taxa from the Ballagan Formation are interspersed with several Devonian and Carboniferous lineages, although their positions differ somewhat from those recovered in that study.

In all trees from the equal-weights analysis, in the single tree from the re-weighted analysis, and in three of the five trees from the implied-weights analysis, *Ossirarus* branches from the tetrapod stem as the most plesiomorphic of all Ballagan taxa, immediately crownward of *Ventastega* and anti-crownward of a diverse array of groups that includes all major post-Devonian clades and grades of early tetrapods as well as the Devonian *Ymeria*, *Brittagnathus* and *Tulerpeton*. In both the equal-weights and the re-weighted analyses, *Ossirarus* forms the sister taxon of *Ossinodus*.

Across all analyses, *Aytonerpeton* is the only Ballagan taxon showing a consistent phylogenetic placement, forming the sister taxon to *Acherontiscus* (Clack et al. 2019b). In all analyses, the (*Aytonerpeton* + *Acherontiscus*) clade forms the sister group to adelospondyls, and the group consisting of ((*Aytonerpeton* + *Acherontiscus*) + adelospondyls) joins (aïstopods + nectrideans). In turn, this broader clade is the sister group to colosteids, with the latter group also incorporating the enigmatic Parrsboro jaw (Godfrey and Holmes 1989; Ruta and Bolt 2008; Sookias et al. 2014).

In the equal-weights and re-weighted analyses, *Diploradus* is nested within baphetids (as sister taxon to *Baphetes*), with *Eucritta* and *Crassigyrinus* forming progressively more outlying sister taxa, in that order, to baphetids. In the strict consensus from the implied-weights analysis, *Diploradus* branches from the tetrapod stem-group between *Sigournea* and a clade of (*Crassigyrinus* + *Mesanerpeton*). In contrast, the equal-weights analysis shows *Mesanerpeton* in a polytomy with *Perittodus*, immediately crownward of *Ymeria*. In the strict consensus of trees from the equal-weights analysis, and immediately crownward of the (*Ossirarus* + *Ossinodus*) clade, is a large polytomy that subtends *Mesanerpeton*, *Ymeria*, *Perittodus*, a clade including *Koilops*, *Tulerpeton* and whatcheeriids in a trichotomy, and all more crownward taxa. Lastly, in the reweighted and equal-weights analyses, whatcheeriids form the sister group to *Koilops* and *Tulerpeton*, respectively.

In the remaining part of the phylogeny, all analyses reveal a consistent topology for the tetrapod crown-group. Thus, Temnospondyli ((*Balanerpeton* + *Dendrerpeton*) + (*Edops* + *Eryops*)) emerge as a holophyletic group. *Caerorhachis* is placed as the earliest-diverging stem-group amniote, while *Silvanerpeton* branches from the amniote stem crownward of (*Eoherpeton* + (*Pholiderpeton* + *Proterogyrinus*)) and anticrownward of *Gephyrostegus* (for a discussion of character polarity among stem-group amniotes, see also Ruta and Clack 2006; Ruta et al. 2020 and Clack et al. 2022). In both re-weighted and implied-weights analyses, *Casineria* is grouped with seymouriamorphs. In the same analyses, *Paleothyris* joins a clade of *Westlothiana* and 'microsaurs'. The topology of the tetrapod crown-group in the equal-weights analysis shows *Casineria* and seymouriamorphs collapsed in a trichotomy with the *Westlothiana*-*Palaeothyris*-'microsaur' clade. Within the latter clade, *Westlothiana* and *Paleothyris* are similarly collapsed in a trichotomy with 'microsaurs'.

Discussion

Preservation of *Ossirarus*

The skeleton of *Ossirarus* is preserved on the uneven surface of a palaeosol (Otoo et al. 2019, fig. 3A) that had developed on a flood plain (Kearsey et al. 2016). It was covered by a thin layer of clay during a flooding event which dispersed the bones such that while they are all clearly associated, none are articulated. Individual bones of the skull have separated from one another, exposing areas of sutural overlap. This suggests that the skeleton was well-rotted before the flooding event. Cracks on the surface of some of the bones, for example the postparietals (Fig. 2), may be the result of surface weathering (Behrensmeyer 1978), and may be evidence that the skeleton was exposed on a dry surface prior to burial. The bones have separated posteriorly suggesting that the flooding flowed from a single direction, at a velocity great enough to disturb the bones, but not to transport them very far.

Affinities

The results of the phylogenetic analysis underscore the conflict that pervades early tetrapod interrelationships and highlight areas where future efforts ought to be directed. One major result that emerges from comparisons between alternative tree topologies is that the six taxa currently named and described from the Ballagan Formation represent distinct and unrelated levels of morphological organization among the earliest known Carboniferous tetrapods. This finding is largely in agreement with some previous studies (e.g., Pardo et al. 2017) that have hypothesized greater bodyplan diversity among stem tetrapods than formerly surmised. A second result emerging from the phylogenetic analysis is that some well-established Carboniferous groups, such as colosteids and baphetids, may have originated earlier than formerly thought, either in the latest part of the Devonian or during the earliest part of the Carboniferous. Independent evidence in support of this hypothesis comes from recent fossil discoveries. Thus, the baphetoid *Spathicephalus marsdeni* pushes back the diversification of the baphetoid clade by approximately three million years (e.g., Smithson et al. 2017) and the discovery of a *Crassigyrinus*-like jaw at Burnmouth (Clack et al. 2018) and a *Crassigyrinus*-like fibula at Blue Beach (Lennie et al. 2020), may extend the origin of the genus from the late Viséan into the mid Tournaisian. In our analyses, evidence in favour of an earlier origin of several lineage comes from the diverse clade that comprises colosteids, *Aytonerpeton*, *Acherontiscus*, adelospondyls, aïstopods and nectrideans. The early Tournaisian age of *Aytonerpeton*, the clade in question may have originated some 360 Ma.. A third result from our investigation is that some Devonian taxa are interspersed among Carboniferous lineages, a result that supports the conclusions of some previous authors (e.g. Anderson et al. 2015; Clack et al. 2016).

It may be possible that such findings reflect the incomplete preservation of some taxa, but not all of them are necessarily implausible. A case in point is *Brittagnathus minutus*, a diminutive Devonian tetrapod known from a complete right lower jaw ramus (Ahlberg and Clack 2020), originally found to occur in proximity to the whatcheeriid

Pederpes finneyae. While we did not retrieve this arrangement, our results support the phylogenetic adjacency of *Brittagnathus* (as well as *Occidens*) to whatcheeriids.

Turning to *Ossirarus*, we were puzzled by the unusual mosaic of plesiomorphic and apomorphic traits in this taxon (see Diagnosis) and by the fact that seemingly 'reptiliomorph' (i.e., stem amniote-like) features, such as the occurrence presumed tabular-parietal contact, failed to retrieve a phylogenetically more derived position for this tetrapod. However, *Ossirarus* is also primitive in several respects. Thus, it exhibits an elongate suspensorium, resulting in a rather elongate cheek region. Furthermore, it shows a preopercular and intertemporal, a long- and narrow-stemmed cleithrum with an expanded dorsal blade, and a diamond-shaped interclavicle without a prolonged posterior process. In the appendicular skeleton, the elongate and oblique pectoralis process of the humerus is comparable with the ventral humeral ridge of elpistostegalians and *Acanthostega*, whereas the brachial foramen opening on the posterior edge of the humerus at the base of the entepicondyle mirrors the condition of *Mesanerpeton* (Smithson and Clack 2018).

In conclusion, whereas the evidence in support of stem-group tetrapod affinities for *Ossirarus* is backed up by a formal cladistic analysis, the placement of this taxon necessitates additional in-depth scrutiny. We are currently examining other tetrapods from the Ballagan Formation and we anticipate being able to provide a more comprehensive evaluation of their wider affinities in due course.

Acknowledgements

The study of *Ossirarus* began during the TW:eed Project, Tetrapod World: early evolution and diversification. It was supported by a NERC consortium grant NE/J022713/1. We thank members of the TW:eed Project for their support and encouragement, and especially for explaining the geology and palaeoenvironment of the Ballagan Formation at Burnmouth. We are grateful to Jason Head, Curator of Palaeontology and Matt Lowe, Collections Manager at the UMZC for access to, and permission to describe, *Ossirarus*. Tim Smithson thanks Jason Head and Rebecca Kilner, former Director, for access to research facilities in the UMZC. We are grateful to Jason Anderson (University of Calgary) and Nadia Fröbisch (Museum für Naturkunde Berlin) for their insightful remarks and constructive criticism.

References

Ahlberg PE, Clack JA (2020) The smallest known Devonian tetrapod shows unexpectedly derived features. Royal Society Open Science 7: 192117. https://doi.org/10.1098/rsos.192117

Anderson JS, Smithson T, Mansky CF, Meyer T, Clack JA (2015) A diverse tetrapod fauna at the base of 'Romer's Gap'. PLOS ONE 10(4): e0125446. https://doi.org/10.1371/journal.pone.0125446

Beaumount EH (1977) Cranial morphology of the Loxommatidae (Amphibia: Labyrinthodontia). Philosophical Transactions of the Royal Society, London, Series B 280: 29–101. https://doi.org/10.1098/rstb.1977.0099

Bennett CE, Kearsey TI, Davies SJ, Millward D, Clack JA, Smithson TR, Marshall JEA (2016) Early Carboniferous sandy siltstones deposited in seasonal flooding episodes preserve rare non-marine fossils. Sedimentology 63: 1677–1700. https://doi.org/10.1111/sed.12280

Bennett CE, Kearsey TI, Davies SJ, Leng MJ, Millward D, Smithson TR, Brand PJ, Browne MAE, Carpenter DK, Marshall JEA, Dulson H, Curry L (2021) Palaeontology and palaeoenvironment of Mississippian coastal lakes and marshes during the early terrestrialisation of tetrapods. Palaeogeography Palaeoclimatology Palaeoecology 564: 110194. https://doi.org/10.1016/j.palaeo.2020.110194

Behrensmeyer AK (1978) Taphonomic and ecologic information from bone weathering. Paleobiology 4: 150–162. https://doi.org/10.1017/S0094837300005820

Clack JA (1998) The neurocranium of *Acanthostega gunnari* and the evolution of the otic region in tetrapods. Zoological Journal of the Linnean Society 122: 61–97. https://doi.org/10.1111/j.1096-3642.1998.tb02525.x

Clack JA (2001) *Eucritta melanolimnetes* from the Early Carboniferous of Scotland, a stem tetrapod showing a mosaic of characteristics. Transactions of the Royal Society of Edinburgh: Earth Sciences 92: 75–95. https://doi.org/10.1017/S0263593300000055

Clack JA (2002) The dermal skull roof of *Acanthostega*, an early tetrapod from the Late Devonian. Transactions of the Royal Society of Edinburgh: Earth Sciences 93: 17–33. https://doi.org/10.1017/S0263593300000304

Clack JA (2003) A new baphetid (stem tetrapod) from the Upper Carboniferous of Tyne and Wear, UK, and the evolution of the tetrapod occiput. Canadian Journal of Earth Sciences 40: 483–498. https://doi.org/10.1139/e02-065

Clack JA (2017) The East Kirkton Lagerstätte: a window onto Early Carboniferous land ecosystems. In: Fraser NC, Sues HD (Eds) Terrestrial conservation lagerstätten: windows into the evolution of life on land. Dunedin Academic Press, Edinburgh, 39–64. https://doi.org/10.2307/jj.12638994.5

Clack JA, Finney SM (2005) *Pederpes finneyae*, an articulated tetrapod from the Tournaisian of western Scotland. Journal of Systematic Palaeontology 2: 311–346. https://doi.org/10.1017/S1477201904001506

Clack JA, Milner AR (2015) *Basal tetrapods*. Handbook of Paleoherpetology. Part 3A1. Friedrich Pfeil, Munich.

Clack JA, Bennett CE, Carpenter DK, Davies SJ, Fraser, NC, Kearsey TI, Marshall JEA, Millward D, Otoo BKA, Reeves EJ, Ross AJ, Ruta M, Smithson KZ, Smithson TR, Walsh SA (2016) Phylogenetic and environmental context of a Tournaisian tetrapod fauna. Nature Ecology & Evolution 1: 1–11. https://doi.org/10.1038/s41559-016-0002

Clack JA, Porro LB, Bennett CE (2018) A *Crassigyrinus*-like jaw from the Tournaisian (Early Mississippian) of Scotland. Earth and Environmental Science Transactions of the Royal Society of Edinburgh 108: 37–46. https://doi.org/10.1017/S1755691018000087

Clack JA, Bennett CE, Davies SJ, Scott AC, Sherwin JE, Smithson TR. (2019a) A Tournaisian (earliest Carboniferous) conglomerate-preserved non-marine faunal assemblage and its environmental and sedimentological context. PeerJ 6: e5972. https://doi.org/10.7717/peerj.5972

Clack JA, Ruta M, Milner AR, Marshall JE, Smithson TR, Smithson KZ (2019b) *Acherontiscus caledoniae*: the earliest heterodont and durophagous tetrapod. Royal Society Open Science 6: e182087. https://doi.org/10.1098/rsos.182087

Clack JA, Smithson TR, Ruta M (2022) A Mississippian (early Carboniferous) tetrapod showing early diversification of the hindlimbs. Communications Biology 5: 1–10. https://doi.org/10.1038/s42003-022-03199-x

Coates MI (1996) The Devonian tetrapod *Acanthostega gunnari* Jarvik: postcranial anatomy, basal tetrapod relationships and patterns of skeletal evolution. Transactions of the Royal Society of Edinburgh: Earth Sciences 87: 363–421. https://doi.org/10.1017/S0263593300006787

Coates MI, Clack JA (1991) Fish-like gills and breathing in the earliest known tetrapod. Nature 352: 234–236. https://doi.org/10.1038/352234a0

Farris JS, Albert VA, Källersjö M, Lipscomb D, Kluge AG (1996) Parsimony jackknifing outperforms neighbour-joining. Cladistics 12: 99–124. https://doi.org/10.1111/j.1096-0031.1996.tb00196.x

Felsenstein J (1985) Confidence limits on phylogenies: an approach using the bootstrap. Evolution 39: 783–791. https://doi.org/10.2307/2408678

Godfrey S (1989) The postcranial skeletal anatomy of the Carboniferous tetrapod *Greererpeton burkemorani*. Philosophical Transactions of the Royal Society, London, Series B 323: 75–133. https://doi.org/10.1098/rstb.1989.0002

Godfrey SJ, Holmes R (1989) A tetrapod lower jaw from the Pennsylvanian (Westphalian A) of Nova Scotia. Canadian Journal of Earth Sciences 26: 1036–1040. https://doi.org/10.1139/e89-084

Goloboff P (1993) Estimating character weighting during tree search. Cladistics 9: 83–91. https://doi.org/10.1111/j.1096-0031.1993.tb00209.x

Goloboff P, Torres A, Arias S (2018) Weighted parsimony outperforms other methods of phylogenetic inference under models appropriate for morphology. Cladistics 34: 407–437. https://doi.org/10.1111/cla.12205

Holland T (2013) Pectoral girdle and fin anatomy of *Gogonasus andrewsae* Long 1985: implications for tetrapodamorph limb evolution. Journal of Morphology 274: 147–164. https://doi.org/10.1002/jmor.20078

Holmes R (1980) *Proterogyrinus scheelei* and the early evolution of the labyrinthodont pectoral limb. In: Panchen AL (Ed.) The Terrestrial Environment and the Origin of Land Vertebrates. Academic Press, London, 351–376.

Holmes RB (1984) The Carboniferous amphibian *Proterogyrinus scheelei* Romer, and the early evolution of tetrapods. Philosophical Transactions of the Royal Society, London, Series B 306: 431–527. https://doi.org/10.1098/rstb.1984.0103

Holmes R (2000) Palaeozoic Temnospondyls. In: Heatwole H, Carroll RL (Eds) Amphibian Biology, Volume 4. Palaeontology. Surrey Beatty and Sons, Chipping Norton NSW, 1081–1120.

Hook RW (1983) *Colosteus scutellatus* (Newberry), a primitive temnospondyl amphibian from the Middle Pennsylvanian of Linton, Ohio. American Museum Novitates 2770: 1–41.

Kearsey TI, Bennett CE, Millward D, Davies SJ, Gowing CJB, Kemp SJ, Leng MJ, Marshall JEA, Browne MAE (2016) The terrestrial landscapes of tetrapod evolution in earliest Carboniferous seasonal wetlands of SE Scotland. Palaeogeography Palaeoclimatology Palaeoecology 457: 52–69. https://doi.org/10.1016/j.palaeo.2016.05.033

Lebedev OA, Clack JA (1993) Upper Devonian tetrapods from Andreyevka, Tula Region, Russia. Palaeontology 36: 721–734.

Lebedev OA, Coates MI (1995) The postcranial skeleton of the Devonian tetrapod *Tulerpeton curtum* Lebedev. Zoological Journal of the Linnean Society 114: 307–348. https://doi.org/10.1111/j.1096-3642.1995.tb00119.x

Lennie KI, Mansky CF, Anderson JS (2020) New *Crassigyrinus*-like fibula from the Tournaisian (earliest Carboniferous) of Nova Scotia. Canadian Journal of Earth Sciences 57: 1365–1369. https://doi.org/10.1139/cjes-2019-0128

Lloyd GT, Wang SC, Brusatte SL (2011) Identifying heterogeneity in rates of morphological evolution: discrete character change in the evolution of lungfish (Sarcopterygii; Dipnoi). Evolution 66: 330–348. https://doi.org/10.1111/j.1558-5646.2011.01460.x

Lombard RE, Bolt JR (1995) A new primitive tetrapod *Whatcheeria deltae* from the Lower Carboniferous of Iowa. Palaeontology 38: 471–494.

Marshall JEA, Reeves EJ, Bennett CE, Davies SJ, Kearney TI, Millward, Smithson TR, Brown MAE (2019) Reinterpreting the age of the uppermost 'Old Red Sandstone' and Early Carboniferous in Scotland. Earth and Environmental Science Transactions of the Royal Society of Edinburgh 109: 265–278. https://doi.org/10.1017/S1755691018000968

Milner AC, Lindsey W (1998) Postcranial remains of *Baphetes* and their bearing on the relationships of Baphetidae (= Loxommatidae). Zoological Journal of the Linnean Society 122: 211–235. https://doi.org/10.1111/j.1096-3642.1998.tb02530.x

Milner AR, Sequeira SEK (1994) The temnospondyl amphibians from the Viséan of East Kirkton, West Lothian, Scotland. Transactions of the Royal Society of Edinburgh, Earth Sciences 84: 331–361. https://doi.org/10.1017/S0263593300006155

Otoo BKO, Clack JA, Smithson TR, Bennett CE, Kearsey TI, Coates MI (2019) An early post-Devonian vertebrate fauna preserved in a Scottish floodplain deposit. Palaeontology 62: 225–253. https://doi.org/10.1111/pala.12395

Otoo BKO, Bolt JR, Lombard RE, Angielczyk KD, Coates MI (2021) The postcranial anatomy of *Whatcheeria deltae* and its implications for the family Watcheeriidae. Zoological Journal of the Linnean Society 182: 700–745. https://doi.org/10.1093/zoolinnean/zlaa182

Panchen AL (1985) On the amphibian *Crassigyrinus scoticus* Watson from the Carboniferous of Scotland. Philosophical Transactions of the Royal Society, London, Series B 309: 461–568. https://doi.org/10.1098/rstb.1985.0095

Pardo JD, Szostakiwskyj M, Ahlberg PE, Anderson JS (2017) Hidden morphological diversity among early tetrapods. Nature 546: 642–645. https://doi.org/10.1038/nature22966

Porro LB, Rayfield EJ, Clack JA (2015) Descriptive anatomy and three-dimensional reconstruction of the skull of the early tetrapod *Acanthostega gunnari* Jarvik, 1952. PLOS ONE 10: e0118882. https://doi.org/10.1371/journal.pone.0118882

Porro LB, Rayfield EJ, Clack JA (2023) Computed tomography and three-dimensional reconstruction of the skull of the stem tetrapod *Crassigyrinus scoticus* Watson, 1929. Journal of Vertebrate Paleontology 42: e2183134. https://doi.org/10.1080/02724634.2023.2183134

Rawson JRG, Porro LB, Martin-Silverstone E, Rayfield EJ (2021) Osteology and digital reconstruction of the skull of the early tetrapod *Whatcheeria deltae*. Journal of Vertebrate Paleontology 41: e1927749. https://doi.org/10.1080/02724634.2021.1927749

Romer AS (1957) The appendicular skeleton of the Permian embolomerous amphibian *Archeria*. Contributions to the Museum of Geology, University of Michigan 13: 103–159.

Ross AJ, Edgecombe GB, Clark N, Bennett CE, Carrio V, Contreras-Izquierdo R, Crighton B (2018) A new terrestrial millipede fauna of the earliest Carboniferous (Tournaisian) age from southeastern Scotland helps fill 'Romer's Gap'. Earth and Environmental Science Transactions of the Royal Society of Edinburgh 108: 99–110. https://doi.org/10.1017/S1755691018000142

Ruta M, Bolt JR (2008) The brachyopoid *Hadrokkosaurus bradyi* from the early Middle Triassic of Arizona, and a phylogenetic analysis of lower jaw characters in temnospondyl amphibians. Acta Palaeontologica Polonica 53: 579–592. https://doi.org/10.4202/app.2008.0403

Ruta M, Clack JA (2006) A review of *Silvanerpeton miripedes*, a stem amniote from the Lower Carboniferous of East Kirkton, West Lothian, Scotland. Transactions of the Royal Society of Edinburgh: Earth Sciences 97: 31–63. https://doi.org/10.1017/S0263593300001395

Ruta M, Clack JA, Smithson TR (2020) A review of the stem amniote *Eldeceeon rolfei* from the Viséan of East Kirkton, Scotland. Earth and Environmental Science Transactions of the Royal Society of Edinburgh 111: 173–192. https://doi.org/10.1017/S1755691020000079

Shubin NH, Daeschler EB, Jenkins FA (2006) The pectoral fin of *Tiktaalik roseae* and the origin of the tetrapod limb. Nature 440: 764–771. https://doi.org/10.1038/nature04637

Smithson TR (1980) A new labyrinthodont amphibian from the Carboniferous of Scotland. Palaeontology 23: 915–923.

Smithson TR (1982) The cranial morphology of *Greererpeton burkemorani* Romer (Amphibia: Temnospondyli). Zoological Journal of the Linnean Society 76: 29–90. https://doi.org/10.1111/j.1096-3642.1982.tb01955.x

Smithson TR (1985) The morphology and relationships of the Carboniferous amphibian *Eoherpeton watsoni* Panchen. Zoological Journal of the Linnean Society 85: 317–410. https://doi.org/10.1111/j.1096-3642.1985.tb01517.x

Smithson TR, Browne MA, Davies SJ, Marshall JE, Millward D, Walsh SA, Clack JA (2017) A new Mississippian tetrapod from Fife, Scotland, and its environmental context. Papers in Palaeontology 3: 547–557. https://doi.org/10.1002/spp2.1086

Smithson TR, Clack JA (2013) Tetrapod appendicular skeletal elements from the Early Carboniferous of Scotland. Comptes Rendus Palevol 12: 405–417. https://doi.org/10.1016/j.crpv.2013.06.006

Smithson TR, Clack JA (2018) A new tetrapod from Romer's Gap reveals an early adaptation for walking. Earth and Environmental Science Transactions of the Royal Society of Edinburgh 108: 89–97. https://doi.org/10.1017/S1755691018000075

Smithson TR, Wood SP, Marshall JEA, Clack JA (2012) Earliest Carboniferous tetrapod and arthropod faunas from Scotland populate Romer's Gap. Proceedings of the National Academy of Sciences 109: 4532–4537. https://doi.org/10.1073/pnas.1117332109

Smithson TR, Richards KR, Clack JA (2015) Lungfish diversity in Romer's Gap: reaction to the end-Devonian extinction. Palaeontology 59: 29–44. https://doi.org/10.1111/pala.12203

Sookias RB, Böhmer C, Clack JA (2014) Redescription and phylogenetic analysis of the mandible of an enigmatic Pennsylvanian (Late Carboniferous) tetrapod from Nova Scotia, and the lability of Meckelian jaw ossification. PLOS ONE 9: e109717. https://doi.org/10.1371/journal.pone.0109717

Swofford DL (1998) PAUP* Phylogenetic analysis using parsimony (*and other methods). Version 4. Sinauer Associates, Sunderland, MA.

Warren AA, Turner S (2004) The first stem tetrapod from the Early Carboniferous of Gondwana. Palaeontology 47: 151–184. https://doi.org/10.1111/j.0031-0239.2004.00353.x

Supplementary material 1

PAUP*-readable nexus file

Authors: Timothy R. Smithson, Marcello Ruta, Jennifer A. Clack
Data type: docx
Copyright notice: This dataset is made available under the Open Database License (http://opendatacommons.org/licenses/odbl/1.0). The Open Database License (ODbL) is a license agreement intended to allow users to freely share, modify, and use this Dataset while maintaining this same freedom for others, provided that the original source and author(s) are credited.
Link: https://doi.org/10.3897/fr.27.126410.suppl1

Supplementary material 2

List of characters used in phylogenetic analysis

Authors: Timothy R. Smithson, Marcello Ruta, Jennifer A. Clack
Data type: docx
Explanation note: Text.
Copyright notice: This dataset is made available under the Open Database License (http://opendatacommons.org/licenses/odbl/1.0). The Open Database License (ODbL) is a license agreement intended to allow users to freely share, modify, and use this Dataset while maintaining this same freedom for others, provided that the original source and author(s) are credited.
Link: https://doi.org/10.3897/fr.27.126410.suppl2

Supplementary material 3

Suppl. figures

Authors: Timothy R. Smithson, Marcello Ruta, Jennifer A. Clack

Data type: pdf

Explanation note: **fig. S1.** Results of parsimony analysis with all characters treated as having equal unit weight. **A.** Strict consensus of 1440 shortest trees. **B.** 50% majority-rule consensus of the same trees. **C.** Adams consensus of the same trees (see text for details). In the 50% majority-rule consensus, most branches receive 100% majority percentages, except for two branches within colosteids, both with 60%, as follows: (Parrsboro jaw, *Colosteus*, (*Greererpeton* + *Deltaherpeton*)) and (*Greererpeton* + *Deltaherpeton*). **fig. S2.** Results of parsimony analysis with implied character weighting. **A.** 50% majority-rule consensus of five shortest trees. **B.** Adams consensus of the same trees (see text for details). In the 50% majority-rule consensus, most branches receive 100% majority percentages, except for the two adjacent internal branches along the tetrapod stem-group between *Ymeria* and *Ossirarus*, both with 60%. **fig. S3.** Results of character resampling procedure, with percentage node support reported on relevant branches. **A.** Bootstrap 50% majority-rule consensus. **B.** Jackknife 50% majority-rule consensus (see text for details).

Link: https://doi.org/10.3897/fr.27.126410.suppl3

Fossil Record 27 (3) 2024, 353–380 | DOI 10.3897/fr.27.125460

The last eryopids: *Clamorosaurus* and *Syndyodosuchus* from the late Kungurian (Cisuralian, Permian) of Russia revisited

Ralf Werneburg[1], Florian Witzmann[2]

1 *NaturHistorisches Museum Schloss Bertholdsburg Schleusingen, Burgstrasse 6, D-98553 Schleusingen, Germany*
2 *Museum für Naturkunde, Leibniz Institute for Evolution and Biodiversity Science, Invalidenstraße 43, D-10115 Berlin, Germany*

https://zoobank.org/09729723-9CEC-4FBF-B0B1-FB8103534379

Corresponding author: Florian Witzmann (florian.witzmann@mfn.berlin)

Academic editor: Marcello Ruta ♦ **Received** 15 April 2024 ♦ **Accepted** 18 June 2024 ♦ **Published** 30 December 2024

Abstract

The three Permian (Cisuralian) temnospondyls *Syndyodosuchus tetricus*, *Clamorosaurus nocturnus* and *C. borealis* from the Pechora Coal Basin in Russia, are redescribed. The assignment of *Clamorosaurus* to the Eryopidae is confirmed, and several new characters are presented in detail. *Syndyodosuchus tetricus* is identified as an eryopid for the first time, as this taxon was previously regarded as a basal stereospondylomorph. In our phylogenetic analysis, *S. tetricus* forms a polytomy at the base of the Eryopidae together with *Actinodon frossardi* and *Osteophorus roemeri*. More crownward, *Glaukerpeton avinoffi* and *Onchiodon labyrinthicus* build a polytomy, followed by *O. thuringiensis* and *Stenokranio boldi* as successive sister taxa of a monophyletic *Clamorosaurus* plus *Eryops megacephalus*. A reweighted analysis finds *A. frossardi* at the base of Stereospondylomorpha; the Eryopidae is completely resolved and consists of *S. tetricus*, *O. roemeri*, *G. avinoffi*, *O. labyrinthicus*, *O. thuringiensis*, *S. boldi* and *E. megacephalus* as successive outgroups to *Clamorosaurus*. The phylogenetic position of *Clamorosaurus* among the most derived eryopids is congruent with its young stratigraphic age, whereas for *S. tetricus* as a basal eryopid a long ghost lineage has to be assumed. Although being coeval, the two genera occurred in different environments, with *Clamorosaurus* being preserved in lacustrine limestones wheras *S. tetricus* was found in a coal bed. The lifestyle of these eryopids can best be designated as semi-aquatic.

Key Words

Clamorosaurus, Eryopiformes, Inta Fauna, phylogeny, *Syndyodosuchus*, terrestrial adaptations, Ufimian

Introduction

Eryopid temnospondyls had a wide geographic distribution on northern Pangea, from the well-known occurrences in North America up to the eastern margin of Europe. This still enigmatic amphibian group has been of great importance in vertebrate paleontology, especially in the United States. The eponymous taxon *Eryops* whose skulls and even postcranial skeletons are extraordinarily common especially in the Texas Red Beds has served as the "generalized" temnospondyl for decades. *Eryops* and a second North American eryopid, *Glaukerpeton*, are well known from the latest Carboniferous to the early Permian in the US (Cope 1882; Case 1911; Miner 1925; Sawin 1941; Romer 1952; Moulton 1974; Pawley and Warren 2006; Werneburg et al. 2010; Werneburg and Berman 2012). Eryopids are widely distributed with few genera in several European localities: in Germany they are represented by *Onchiodon* and *Stenokranio* (Werneburg 1987; Boy 1990; Witzmann 2005a; Werneburg et al. 2023) as well as by indeterminate eryopid remains (Schoch and Hampe 2004; Witzmann 2013; Witzmann and Voigt 2014). *Actinodon* was found in France (Werneburg 1997; Werneburg and Steyer 1999), ?*Onchiodon* in the Czech Republic (Werneburg 1993), *Osteophorus* in Poland (Meyer 1860), and *Clamorosaurus* in the Pechora Basin in Russia (Gubin 1983). Gubin (1983) provided the original description of *Clamorosaurus* with two species as the first eryopids in the Far East of northern Pangea. Konzhukova (1956) had already described *Syndyodosuchus* from the same locality as an intasuchid stereospondylomorph and all later workers followed this assignment (e.g. Gubin 1984, 1991; Schoch and Milner 2000; Shishkin et al. 2000). However, Werneburg et al. (2020) suggested that *Syndyodosuchus* might be an eryopid temnospondyl, too. A detailed morphological revision of these two Russian genera was necessary to verify their phylogenetic position. This revision is even more interesting because *Clamorosaurus* and *Syndyodosuchus* from the Ufimian can be assigned to the late Kungurian (Cisuralian, Permian). This makes them the stratigraphically youngest eryopids in the world. The late Yuri Gubin once said to the senior author that 'the Russian eryopids have parents but no children'.

Occurrence, geological setting, and age

All eryopid material revised herein comes from Pechora and Inta in the Pechora Coal Basin of the East-European Platform in the northern Komi Republic of Russia (Fig. 1). This region lies just inside Europe to the NW of the northern Urals in the boreal region. Inta (66°05'N, 60°08'E) is located about 200 km southeast and Pechora (65°10'N, 57°15'E) about 300 km south of the Barents Sea. Both localities are about 180 km apart. *Clamorosaurus nocturnus* was found with several specimens far below the town of Pechora on the lower Pechora River. All other eryopids and *Intasuchus* were found near the town of Inta, which was founded in 1940 as a settlement in the wake of the coal mines there. *Syndyodosuchus* and *Intasuchus* were together discovered near the Large Inta River directly about 100 m deep in the coal layers of the mine by prisoners, as reported by the late Yuri Gubin from PIN Moscow (personal communication to the senior author, 1989). The only known specimen of *Clamorosaurus borealis* was collected 1961 in a limestone from coal mine number nine near the town of Inta.

Clamorosaurus nocturnus was found in the Sheshminskian Gorizont, the other eryopids are known from the Intinskaya Svita (Inta Formation). All these horizons belong to the

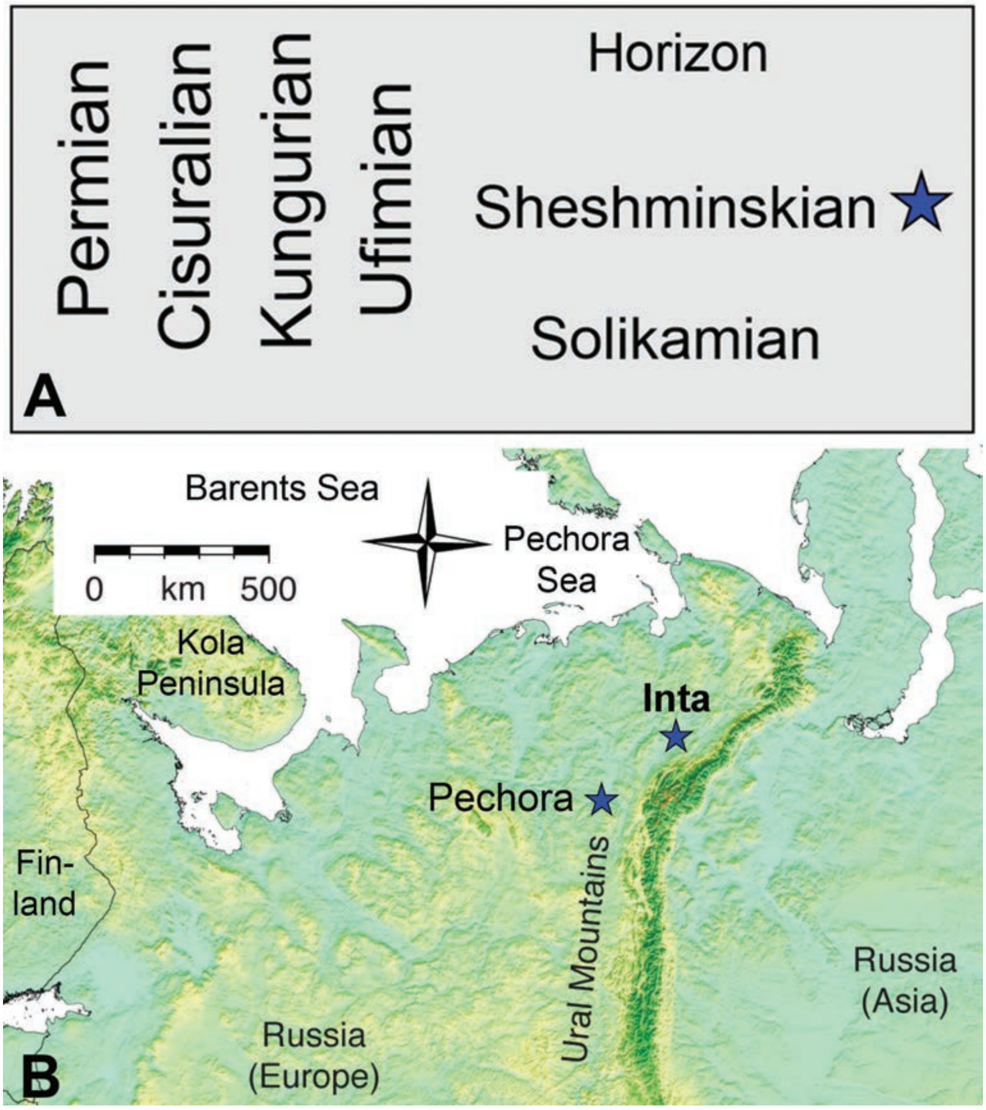

Figure 1. Stratigraphic position of the Sheshminskian horizon (**A**) and geographical map with the position of the locations Inta and Pechora at the NW-margin of the Ural Mountains in the Komi Republic of Russia (**B**).

Ufimian – well known in Russian stratigraphy – which is in correlation with the latest Kungurian of the international standard time scale (Cisuralian, Permian; Golubev 2005; Schneider et al. 2020). Therefore, the eryopids of the Pechora Basin lived about 274 million years ago.

Material and methods

This work is based on three eryopid species from the Ufimian-age Inta fauna discovered at the Pechora Coal Basin in the NW of the northern Urals, Russia. All fossil remains of these species are stored at the Paleontological Institute, Academy of Sciences, Moscow, Russia (PIN). A full drawer of skeletal remains exists from *Clamorosaurus nocturnus*: the holotype PIN 1582/1, a second and third anterior skull PIN 1582/4 + PIN 1582/6, as well as partial skeletal remains with scapulocoracoid and ribs (PIN 1582/2a), a clavicle (PIN 1582/2b), and a possible humerus-fragment in two parts (PIN 1582/2c). *Clamorosaurus borealis* is represented by the holotype and only specimen (PIN 3950/1) and consists of a complete skull together with isolated remains of the sphenethmoid and two stapes. The following parts of the third eryopid *Syndyodosuchus tetricus* are preserved: the nearly complete holotypic skull (PIN 570/40), isolated remains of a second skull with isolated right dentary (PIN 570/41) and an anterolateral skull fragment with premaxilla, maxilla, and vomer (PIN 570/6), a third, 17 cm long skull in poor preservation (PIN 570/2) as well as a fourth indeterminable skull fragment (PIN 570/3).

The sculpture density on the dorsal skull roof was measured by numbering the pits (p) per in^2 on the frontal and jugal (which are mostly well preserved), and it was quantified as the ratio of this number through the skull length (S_l in cm; see Table 1).

Preparation of the specimens was carried out mechanically by earlier colleagues from the PIN. Photographs were taken with a Nikon D5100 in 2002. Drawings were prepared from the A3-photographs and with a 'camera lucida' at a Motic binocular by RW in 2012, measurements realized on the reconstructed skull drawings – compare Fig. 2.

Table 1. Ranges of density counts of dermal sculpture pits (p) and valleys per in^2 (6.452 cm^2) of frontal and jugal in relation to the skull length (S_l in cm) given separately and combined for eryopids and grouped by genus, species, and maturity (Werneburg and Berman 2012; Werneburg et al. 2023).

Eryopids	frontal-p/S_l	jugal-p/S_l	range of p/S_l
Late Kungurian ***Clamorosaurus nocturnus*** (Pechora, Russia)	3.08	4.07	3.08–4.07
Late Kungurian ***Clamorosaurus borealis*** (Inta, Russia)	3.40	**5.23**	3.40–5.23 (prf: 7.84)
Late Kungurian ***Syndyodosuchus tetricus*** (Inta, Russia)	**5.00**	4.69	4.69–5.00
Late Pennsylvanian ***Glaukerpeton*** (Pennsylvania, West Virginia)	2.6–3.3	3.2–4.0	2.6–4.0
Pennsylvanian ***Eryops*** (El Cobre Canyon, New Mexico)	1.3	1.7	1.3–1.7
Early Permian ***Eryops grandis*** (New Mexico and Utah)	0.5–1.6	1.1	0.5–1.6
Adult Permian ***Eryops megacephalus***	**0.4**–1.1	**0.5**–1.0	0.4–1.1
subadult Permian ***Eryops*** (all Early Permian of Texas)	1.8	1.2–4.3	1.2–4.3
Early Permian ***Onchiodon thuringiensis*** (Germany)	1.0	-	1.0
Stenokranio boldi, Pennsylvanian-Permian boundary (Germany)	0.72–1.42	0.64–1.13	0.64–1.42

Results

Systematic paleontology

Tetrapoda Jaekel, 1909
Amphibia Linnaeus, 1758
Temnospondyli von Zittel, 1888

Eryopidae Cope, 1882

Diagnosis. Synapomorphies (from Werneburg et al. 2023, after Sawin 1941; Romer 1947; Boy 1990; Milner 1989, 1990; Werneburg and Steyer 1999; Schoch and Hampe 2004; Werneburg 2007; Werneburg and Berman 2012; Schoch and Milner 2014): (1) Enlarged choana medially wide; (2) Ectopterygoid, palatine and vomer only with two or three fangs (without subsequent smaller teeth); (3) Lacrimal reaches anteriorly to the naris or septomaxilla; (4) Enlarged posterior width of skull (pS_w/S_l=0.92–1.10; compare Fig. 2); (5) Posterior part of the cultriform process widened (partly); (6) Interclavicle of adults proportionally small and broadly-ovate in outline; (7) Ilium with vertically directed dorsal process, which is anteroposteriorly widened dorsally.

All three species to be revised, *Clamorosaurus nocturnus*, *C. borealis* and *Syndyodosuchus tetricus*, fulfill the first four criteria of the family diagnosis. The fifth diagnostic feature is not present in all eryopid genera, only in *Eryops* and *Onchiodon*. The sixth and seventh diagnostic features concern the interclavicle and ilium, which have not been recorded in all three species. In this respect, all these species can be assigned to the family Eryopidae.

***Clamorosaurus* Gubin, 1983**

Types species. *Clamorosaurus nocturnus* Gubin, 1983.

Diagnosis. Synapomorphy: (1) Very wide interpterygoid vacuities, with the orbitae not obscured in ventral view, in contrast to all other eryopids and shared with the stereospondylomorph *Intasuchus* (Konzhukova 1956; Werneburg et al. 2020), however, in contrast to *Intasuchus*, the interpterygoid vacuities of *Clamorosaurus* are unique in being anteriorly widened.

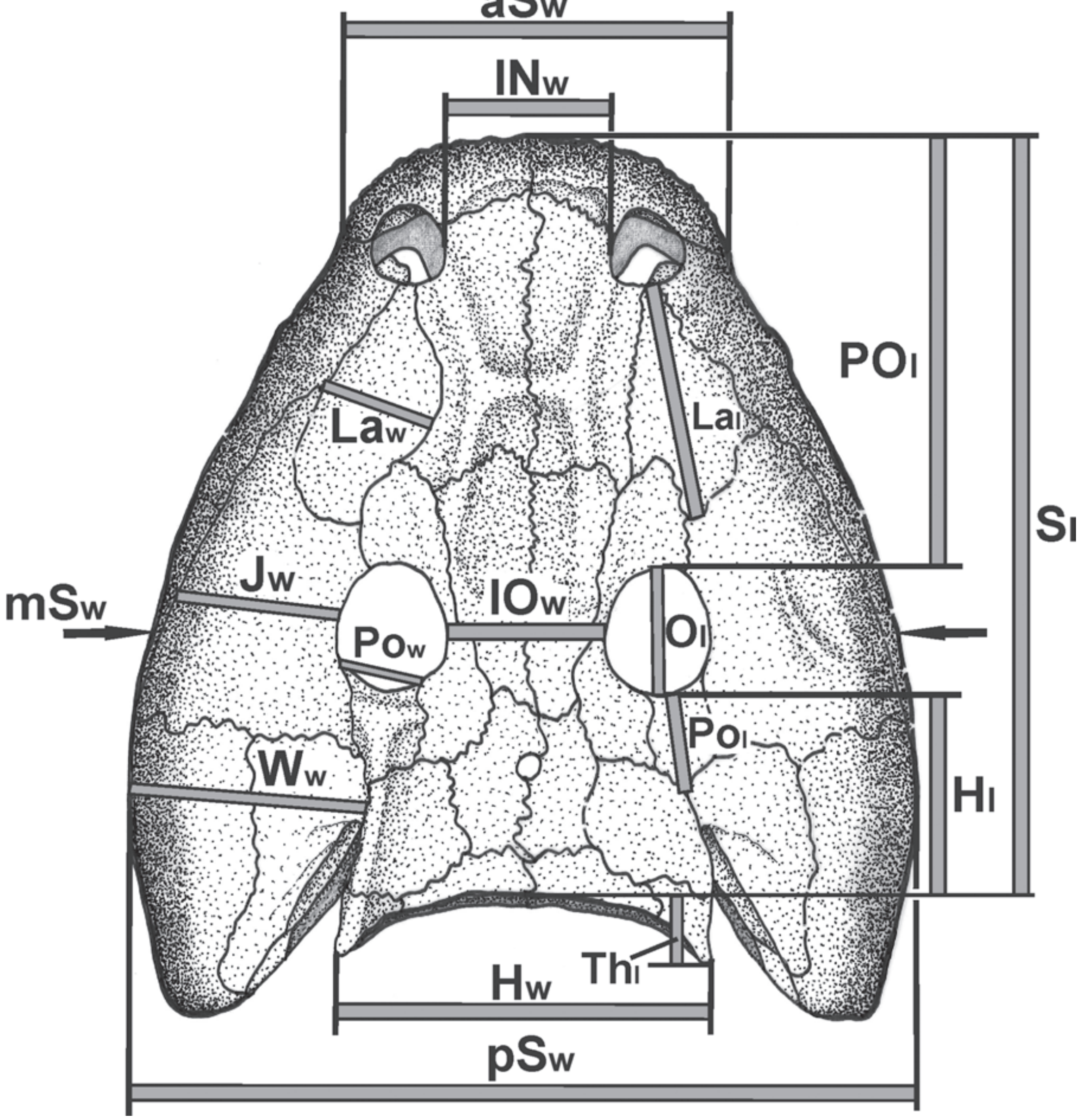

Figure 2. Reconstructed eryopid skull roof with measured distances. Abbreviations: aS_{w}, anterior width of skull at level of maxilla-premaxilla sutures; H_{l}, postorbital midline length of skull from level of posterior margins of orbits; H_{w}, postorbital width of skull between lateral margins of supratemporals; IN_{w}, minimum internarial width; IO_{w}, minimum interorbital width; J_{w}, transverse width of jugal at maximum lateral lacrimal extent of orbit; La_{l}, maximum length of lacrimal; La_{w}, maximum transverse width of lacrimal; mS_{w}, midlength width of skull at midlength level of orbits; O_{l}, maximum length of orbit; p, number of dermal skull pits or valleys per inch^2 (6.452 cm^2) mainly from frontal and jugal at midlength level of orbits; PO_{l}, preorbital midline length of skull from level of anterior margins of orbits; Po_{l}, maximum posterior length of postorbital from posteriormost extent of orbit; Po_{w}, maximum transverse width of postorbital at contribution to orbital margin; pS_{w}, maximum posterior width of skull at level of posterolateral margins of cheeks; S_{l} , midline skull length; Th_{l}, length of tabular horn region between levels of posterior tabular corner and occipital midline margin; W_{w}, maximum transverse width of cheek from lateral margin of supratemporal anterior to otic notch.

Characters shared with certain eryopids: (2) Premaxillary snout region laterally constricted at the level of the external naris, shared with *Eryops* and *Osteophorus*; (3) Skull very wide, shared with *Onchiodon*; (4) Fangs on the vomer located on two separate circular tooth pits, one medial to the anterior edge of the choanae and one medial to the choana at its midlength. Shared with *Syndyodosuchus*.

***Clamorosaurus nocturnus* Gubin, 1983**

Figs 3–6, 14A, B

Holotype. PIN 1582/1, consisting of the skull roof (skull length 18.2 cm), scapulocoracoid and ventral scales, together with undetermined bony remains, and a partly prepared section of the basal plate of the parasphenoid and the clavicle, both in ventral view.

Other material. PIN 1582/4, consisting of the anterior part of a skull with the skull roof in dorsal and the palate in ventral view; PIN 1582/6, consisting of the anterior part of a skull with the skull roof in dorsal view and the fangs of ectopterygoid, palatine and vomer of the palate in ventral view; PIN 1582/2a, consisting of a scapulacoracoid with ribs, PIN 1582/2b representing a clavicle, and PIN 1582/2c consisting of a possible humerus-fragment in two parts).

Occurrence. All this referred material was discovered near the town of Pechora on the lower Pechora River (Komi Republic, Russia) in the Sheshminskian Gorizont (Ufimian), late Kungurian (Cisuralian, Permian).

Diagnosis. *C. nocturnus* has no autapomorphies, but a unique combination of characters: (1) Density of sculpture pattern quantified as the number of pits per in^2 on frontal plus jugal range between 3.08 and 4.07, shared with *C. borealis*, *Glaukerpeton* and close to *Syndydosuchus*, but in contrast to all other eryopids; (2) Premaxillary and maxillary teeth are small and circular in cross section, in contrast to *C. borealis*, *O. labyrinthicus*, and *Eryops*; (3) Teeth no. 8 and 9 are the largest in the premaxilla, in contrast to *C. borealis* and many other eryopids; (4) Tooth no. 6 is the largest in the maxilla, in contrast to *C. borealis* and many other eryopids; (5) Equal internarial and interorbital width, in contrast to *C. borealis*, *Syndydosuchus*, *Glaukerpeton*, and *E. megacephalus*; (6) Narrow interorbital width, shared with *C. borealis*, *Syndydosuchus*, *Actinodon*, and *E. megacephalus*; (7) Jugal very wide, shared with *C. borealis*, *O. thuringiensis*, and *Eryops* sp. from the Moran Formation (MCZ1914; Werneburg 2008; Schoch and Milner 2014); (8) Septomaxilla is completely unsculptured and ventrally directed, shared with *C. borealis*, *Eryops*, and *Glaukerpeton*; (9) Short contact between jugal and prefrontal, shared with *Syndydosuchus*, *Glaukerpeton*, *Actinodon*, and *O. labyrinthicus*, but in contrast to *C. borealis*, *O. thuringiensis*, and *E. megacephalus*; (10) Supratemporal wide, but longer than wide, in contrast to *C. borealis*; (11) No interfrontal, in contrast to *Eryops* and *Osteophorus*; (12) No lateral

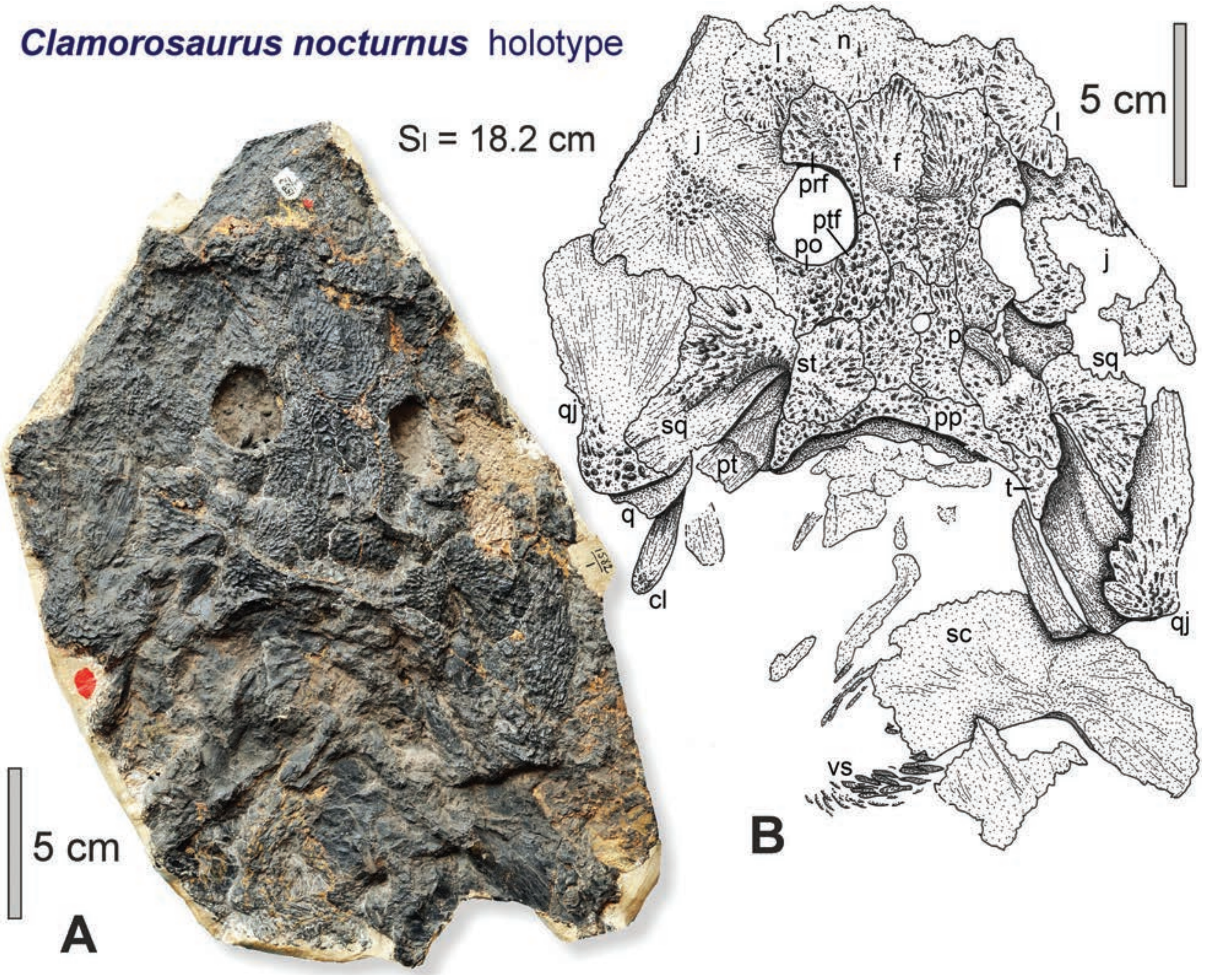

Figure 3. *Clamorosaurus nocturnus* Gubin, 1983, skull roof in dorsal view, with scapulocoracoid, clavicle and ventral scales (**A, B**), holotype PIN 1582/1, from the Sheshminskian Gorizont (late Kungurian, Permian) of the Pechora River (Komi Republic, Russia). Abbreviations: cl, clavicle; f, frontal; j, jugal; l, lacrimal; n, nasal; p, parietal; pm, premaxilla; po, postorbital; pp, postparietal; prf, prefrontal; pt, pterygoid; ptf, postfrontal; q, quadrate; qj, quadratojugal; sc, scapulocoracoid; sq, squamosal; st, supratemporal; t, tabular; vs, ventral scales.

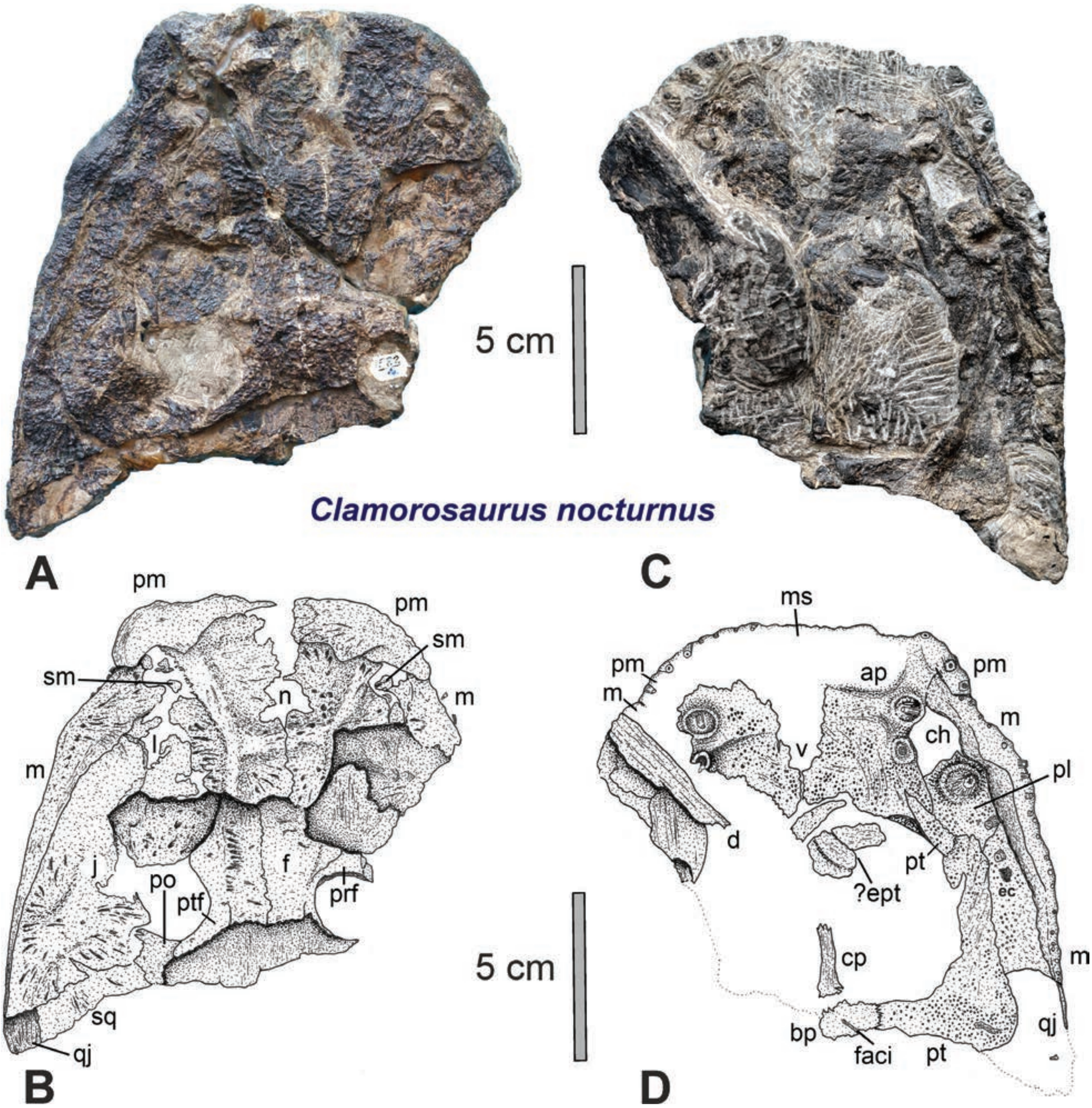

Figure 4. *Clamorosaurus nocturnus* Gubin, 1983, second specimen PIN 1582/4, with skull roof in dorsal view (**A, B**), and palate in ventral view (**C, D**), from the Sheshminskian Gorizont (late Kungurian, Permian) of the Pechora River (Komi Republic, Russia). Abbreviations: ap, anterior palatal depression; bp, basal plate of parasphenoid; ch, choane; cp, cultriform process; ec, ectopterygoid; ept, epipterygoid; f, frontal; faci, furrow for carotid artery; j, jugal; l, lacrimal; m, maxilla; n, nasal; pl, palatine; pm, premaxilla; po, postorbital; pt, pterygoid; ptf, postfrontal; qj, quadratojugal; sm, septomaxilla; sq, squamosal; v, vomer.

line sulci, in contrast to *Glaukerpeton* and *Actinodon*; (13) Interchoanal width is equal to internarial width, in contrast to *C. borealis*; (14) Short and wide palatine, only slightly longer than wide; (15) Ectopterygoid much longer than palatine; (16) Narrow basal plate of parasphenoid, in contrast to *C. borealis*, *Onchiodon*, *Stenokranio* and *Glaukerpeton*; (17) Cultriform process of parasphenoid longer than median length of vomer, shared with nearly all eryopids, but in contrast to *C. borealis*.

Comparative description. Three incompletely preserved skulls with median lengths of 16 to 18 cm show the skull roof in dorsal view and parts of the palate in ventral view. They have complementary, congruent features, such as a small, dense dermal sculpture, small, almost oval orbitae, a very narrow interorbital region (IOw/Sl=0.21), a very wide jugal, a wide lacrimal that reaches to the naris in front, and rather small teeth in the maxilla and premaxilla. Therefore, all these skulls belong to the same species.

General skull morphology. The dermal sculpture of the dorsal surface of the skull roof corresponds to the relatively fine sculpture pattern known from some eryopids such as *Clamorosaurus borealis*, *Syndyodosuchus tetricus* and *Glaukerpeton avinoffi* (Werneburg and

Berman 2012) (Table 1). It consists of a reticulated pattern of small pits and valleys separated by narrow ridges (Figs 1–3). The nasal, jugal and squamosal show much more radially directed ridges. The density of the sculpture pattern is quantified as the number of pits per in^2 (6.452 cm^2) on the frontal and jugal, which are typically well-preserved bones in eryopid skulls, and as a proportion of those counts to skull length. These intraspecific indices range between elements and specimens of *C. nocturnus* between 3.08 and 4.07, which are very similar in *C. borealis*, *S. tetricus* and *G. avinoffi* (Table 1). The dermal sculpture of the dorsal surface of the skull roof in other eryopid species has a much coarser pattern with indices from 0.4 up to 1.7. Higher indices between 1.2 and 4.3 occur only in the subadult *Eryops* (Table 1).

The dorsal strutting pattern with large ridges on the skull roof is well developed (Fig. 6A) and probably increased the mechanical stability of the skull (Sawin 1941; Boy 1990; Werneburg 2007; Schoch and Sobral 2021; Werneburg et al. 2023). A large longitudinal ridge extends from the lateral portion of the tabular and supratemporal to the postorbital. It then runs on the anterior skull table from the suture between prefrontal/frontal and on the lateral part of the nasal to the medial margin of the naris. Additional transverse ridges occur between the longitudinal ridges on frontals and nasals (Figs 3, 4A, B). The areas between these ridges are depressed. Additionally, a short ridge on the jugal is traceable (Fig. 4B). The degree of skull roof ossification appears to be relatively low and the bones may be intermediate between the normally thick bones as in most other eryopids and the 30–50% thinner skull roof bones of *Glaukerpeton* (Werneburg and Berman 2012).

The combination of the three known skulls of *C. nocturnus* allowed a tentative reconstruction of the skull roof in dorsal view and of the palate in ventral view (Fig. 6A, B). The skull is slightly wider than long (Table 2; $pS_w/S_l=1.04$). The lateral margin of the skull is convex in dorsal view. The snout margin is laterally constricted at the level of the naris like in *Eryops megacephalus*, *Osteophorus* and *C. borealis*. The postorbital region of the skull roof is relatively long ($H_l/S_l=0.26$) and wide ($H_w/S_l=0.50$) in contrast to that of *E. megacephalus* and *Stenokranio*. The preorbital skull is relatively elongate ($PO_l/S_l=0.57$). The internarial and interorbital width are nearly equal ($IN_w/S_l=IO_w/S_l=0.21–22$) as in many eryopids, but in contrast to *Glaukerpeton* in which the internarial width is smaller, and to *E. megacephalus*, *C. borealis* and *S. tetricus* with a smaller interorbital width (Table 2). The occipital margin of the skull roof is only slightly concave as in *Onchiodon thuringiensis* and *C. borealis*. The quadrate condyles lie distinctly posterior to the occipital condyles ($Qc_l/S_l=0.17$; Table 2). The long oval orbits are relatively small compared to other eryopids ($O_l/S_l=0.16$).

Growth stage. The three skulls of *Clamorosaurus nocturnus* (PIN 1582/1, 1582/4 and 1582/6) clearly belong to adult animals, as indicated by the following features: (a) The dermal sculpture consists of a reticulated pattern of small pits and valleys separated by narrow ridges; (b) The quadrate condyles lie distinctly posterior to the occipital condyles; (c) The quadrate is ossified dorsally; (d) The orbits are relatively small compared to other eryopids; (e) The pterygoid has a pronounced transverse process; (f) The scapulocoracoid is well ossified (Figs 3, 5F); (g) The skull length of 16–18 cm is relatively large and ranged in the middle-sized group in the family Eryopidae, and *Actinodon* and *Onchiodon labyrinthicus* have no larger skulls. However, the degree of ossification of the neurocranium indicates that the three specimens were early adults: (h) Sphenethmoid and basioccipital are not preserved and were probably not ossified in this stage.

Skull roof. The interpremaxillary suture is short and accounts for 7.4% of the midline length of the skull. The alary process of the premaxilla is wide and short. *C. borealis* and *Actinodon* have no alary process. The premaxillary tooth arcade has nine tooth loci (only six in *C. borealis*). The relatively small teeth have a circular cross-section, and only the two posteriormost teeth are slightly larger. This type of dentition contrasts with that of *C. borealis*, *E. megacephalus* and *O. labyrinthicus*, which consists of much larger teeth that are long-oval in cross-section.

The maxilla has a relatively narrow dorsal shelf and is ventrally in contact with the quadratojugal. Its tooth arcade has about 25 tooth loci (only 21 in *C. borealis*). The teeth have a circular cross-section and they are relatively small. Only the sixth tooth is slightly larger, similar in size to the two larger ones of the premaxilla. This type of dentition contrasts with that of *C. borealis*, *E. megacephalus* and *O. labyrinthicus*, which has much larger teeth that are long-oval in cross-section.

The circular naris is of similar proportional length as in *Glaukerpeton* or *E. megacephalus*, comprising 10% of the midline length of the skull. The small septomaxilla is not sculptured (Figs 4A, B, 5A, B) and may be ventrally directed inside the naris (shared with *Eryops*). The posterior margin of the naris is clearly formed by the nasal, lacrimal and maxilla (Fig. 5A, B).

The lacrimal is roughly diamond-shaped. It is separated from the orbit by a short contact between jugal and prefrontal. The medial part of the lacrimal is wide ($La_w/La_l=0.49$), and this bone participates in the posterolateral narial margin. The frontal is long and narrow like in most other eryopids and gets narrower in its posterior part where it is restricted by the medially expanding postfrontals.

The jugal is proportionally wider ($Ju_w/S_l=0.22$) than in all other eryopids apart from *Eryops* sp. (MCZ1914) from the Moran Formation (Table 2). The postorbital is triangular in outline. The postfrontal and prefrontal clearly contact one another as in all eryopids. The prefrontal is anteriorly relatively wide. The width of the supratemporal is striking; this bone is only 1.1 times longer than wide. Only in *C. borealis* the supratemporal is much wider than long (see below).

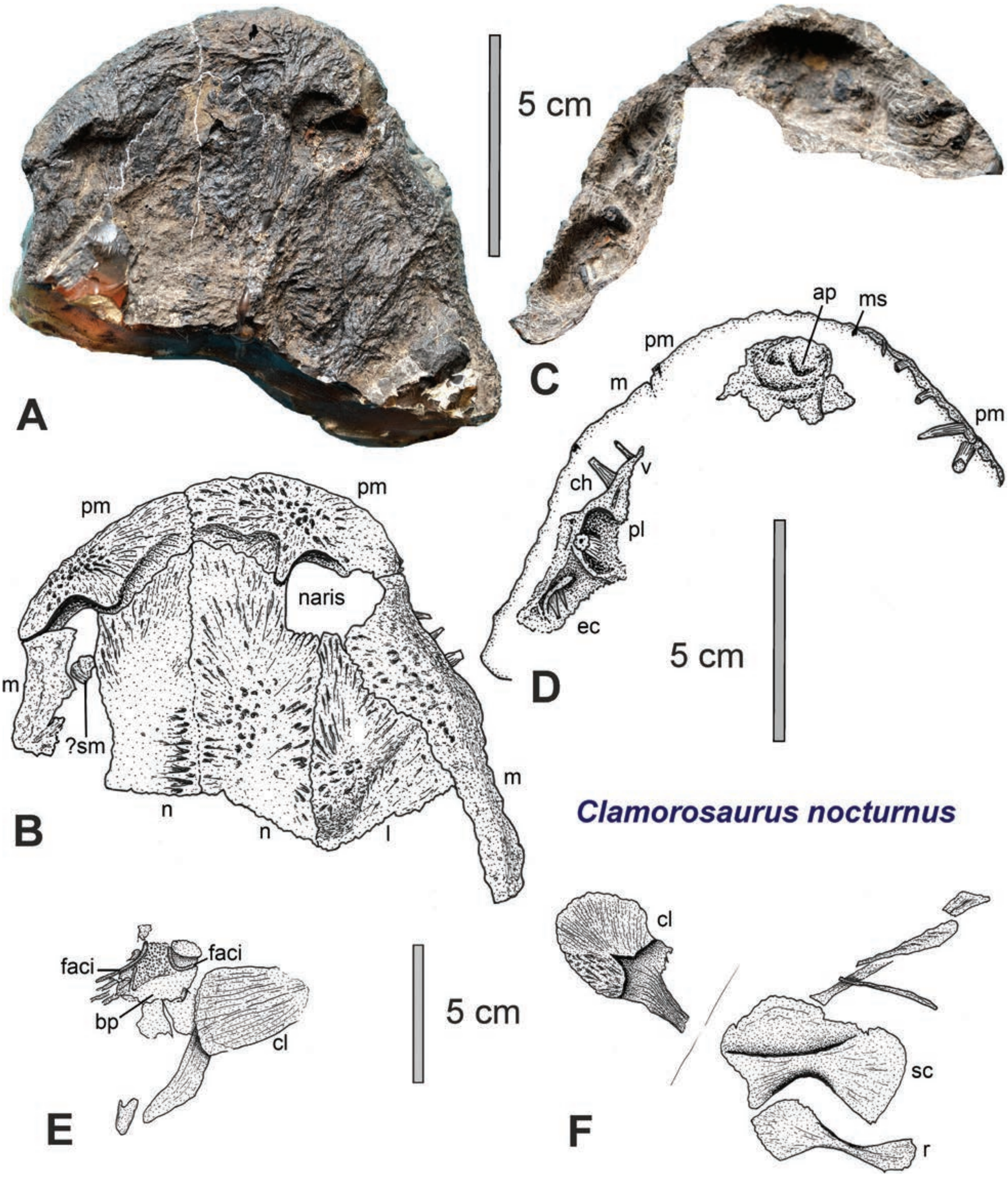

Figure 5. *Clamorosaurus nocturnus* Gubin, 1983, further specimens, an anterior skull (PIN 1582/6) with skull roof in dorsal view (**A, B**), and palatal remains in ventral view (**C, D**), basal plate of parasphenoid and clavicular blade of the holotype in ventral view (PIN 1582/1, **E**), and postcranial bones from an additional specimen (PIN 1582/2a–b, **F**) with remains of the scapulacoracoid, clavicle and ribs, all from the Sheshminskian Gorizont (late Kungurian, Permian) of the Pechora River (Komi Republic, Russia). Abbreviations: ap, anterior palatal depression; bp, basal plate of parasphenoid; ch, choane; cl, clavicle; ec, ectopterygoid; faci, furrow for carotid artery; l, lacrimal; m, maxilla; ms, median suture; n, nasal; pl, palatine; pm, premaxilla; r, rib; sc, scapulocoracoid; sm, septomaxilla; v, vomer.

The parietals anteriorly approach the level of the posterior orbital margin, and the postparietals and tabulars are comparatively short. The tabular horn is modestly elongated (Th_l/S_l=0.09), narrow and its rounded tip points posteriorly and slightly laterally. The width of the cheek is pronounced (W_w/S_l=0.30) and is only exceeded by the relative cheek width in *Onchiodon* (Table 2). The squamosal is relatively narrow and the quadratojugal is very wide,

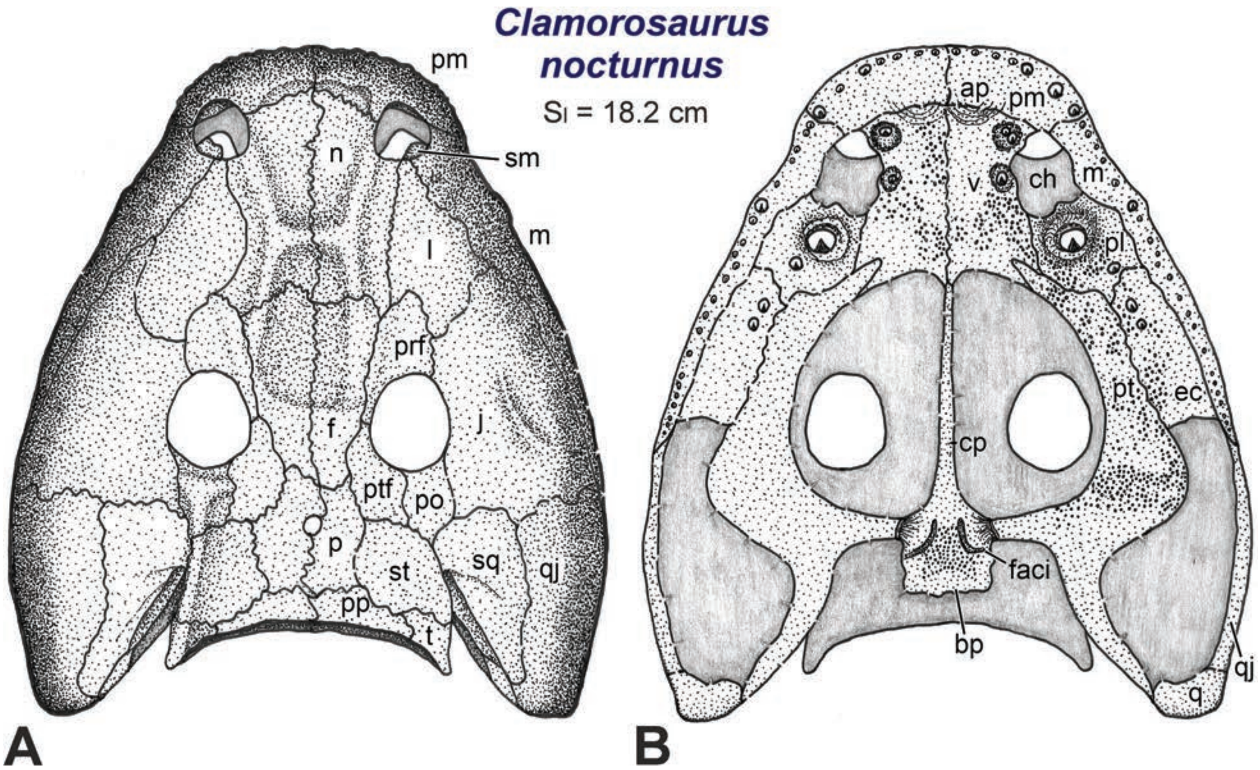

Figure 6. *Clamorosaurus nocturnus* Gubin, 1983, tentative reconstruction of the skull roof in dorsal view (**A**), and of the palate in ventral view (**B**). Abbreviations: ap, anterior palatal depression; bp, basal plate of parasphenoid; ch, choane; cp, cultriform process; ec, ectopterygoid; f, frontal; j, jugal; l, lacrimal; m, maxilla; n, nasal; p, parietal; pl, palatine; pm, premaxilla; po, postorbital; pp, postparietal; prf, prefrontal; pt, pterygoid; ptf, postfrontal; q, quadrate; qj, quadratojugal; sm, septomaxilla; sq, squamosal; st, supratemporal; t, tabular; v, vomer.

especially in its anterior part. The quadratojugal reaches far posterior so that its posterior end comes to lie posterior to the squamosal and roofs the quadrate (Fig. 6A, B).

The exposure of the quadrate on the occipital surface of the cheek (Fig. 1) consists of a narrow strip of bone that is directed anteromedially between the squamosal and the quadrate ramus of the pterygoid. A boss-like protuberance at the ventral margin of the dorsal quadrate process like in *Stenokranio* or *Glaukerpeton* might have been developed (Fig. 3B). Quadratojugal foramina cannot be determined with certainty. Like in most adult eryopids, lateral line sulci are not present (Witzmann et al. 2010; Werneburg et al. 2023).

Palate and braincase. From the palate, large parts of the vomers, palatines, ectopterygoids, pterygoids and the basal plate of the parasphenoid are preserved. Longitudinal ridges on the palatal bones are not developed. Immediately anterior to the level of the anterior vomerine tusks, the rounded posterior end of the anterior palatal fossae extends on the anterior part of the vomers (Fig. 4D) and probably on the dental shelf of the premaxilla.

The vomer is elongated and narrow. The smallest width of both vomers (=interchoanal width ICw/Sl=0.22) is equal to the smallest width between the narial openings (internarial width) and nearly the same as the interorbital width. The posterolateral corner of the vomer encloses the anterior tip of the pterygoid as in *Eryops*. The suture between vomer and palatine is much more elongated than in *C. borealis*, *Glaukerpeton* and *Actinodon*. The short palatine is only slightly longer than wide. The ectopterygoid is elongated and c. 1.5 times longer than the palatine. Its posteriormost part is equal in width to the medially neighbouring pterygoid.

The dentition of palatine and ectopterygoid is interesting. The palatine bears a conspicuous fang anteriorly and a much smaller one posteriorly, which has the same size as the two fangs on the anterior part of the ectopterygoid. The fangs on the vomer are of equal or smaller size than those on the ectopterygoid. They are located on two separate circular tooth pits; the slightly larger one is located medial to the anterior edge of the choanae and has space for two small fangs. On the right vomer, only one tooth is preserved in this pit, but there is space for another one. Two teeth have been recorded on the left vomer. A further, slightly smaller tooth pit with one tooth is positioned medial to the choana at its midlength. Apart from *C. nocturnus*, this second tooth pit on the vomer is only known in *C. borealis* (here with a pair of fangs) and *Syndyodosuchus*.

The relatively small choana is of irregular outline, medially expanded and slightly longer than wide. The choanae of *Glaukerpeton*, *Actinodon* and *Eryops* are larger and more elongate, and in the case of *Stenokranio* about as long as wide (Fig. 15).

The pterygoid has a narrow palatinal ramus; its most anterior part forms a narrow, anteromedially directed tip, which may overlap the posterolateral corner of the

Table 2. Comparative measurements of adult eryopid skulls (largest and smallest values in bold; after Boy 1990; Werneburg 1997, 2007; Werneburg and Berman 2012; Werneburg et al. 2023, and the present study). Institutional abbreviations.—CM, Carnegie Museum of Natural History, Pittsburgh, Pennsylvania; CMNH, Cleveland Museum of Natural History, Cleveland, Ohio; FMNH, Field Museum of Natural History, Chicago, Illinois; MCZ, Museum of Comparative Zoology of the Harvard University, Cambridge, Massachusetts; MHNA, Museum of Natural History, Autun, France; MMG, Museum für Mineralogie und Geologie, Dresden, Germany; NHMMZ/ LS, Natural History Museum Mainz/State Collection of Natural History of Rhineland–Palatinate, Germany; NHMS, Naturhistorisches Museum Schloss Bertholdsburg, Schleusingen, Germany; NMMNH, New Mexico Museum of Natural History, Albuquerque, New Mexico; PIN, Paleontological Institute, Academy of Sciences, Moscow, Russia; UGKU, Urweltmuseum GEOSKOP/Lichtenberg Castle near Kusel, Germany. For anatomical abbreviations, see Fig. 2.

	Stenokranio boldi	***Glaukerpeton avinoffi***	***Eryops* sp.- MCZ1914**	***Eryops megacephalus***	***Onchiodon thuringiensis***	***Onchiodon labyrinthicus***	***Actinodon frossardi***	***Clamorosaurus nocturnus***	***Clamorosaurus borealis***	***Syndyodosuchus tetricus***
	NHM MZ/ LS PW 2019/5025, /5022	**CM 8539, CMNH 11025**	**MCZ 1914**	**MCZ 1129, holo-type**	**NHMS-WP 2140 a**	**Boy (1990: Abb. 2F)**	**MHNA 15/10/62, MMG FRP1**	**PIN 1582/1**	**PIN 3950/1**	**PIN 570/40**
S_l in mm	247–270	230	333	**364**	285	160	**111**–123	182	153	162
pS_w/S_l	**0.92**	0.99	0.94	0.94	1.06	1.07	**1.**09–**10**	1.04	1.08	1.01
mS_w/S_l	0.85–91	0.89	0.94	**0.83**	0.97	**1.00**	0.88–90	0.98	0.98	0.86
aS_w/S_l	**0.**47–**52**	0.49–50	0.47	0.49	0.48	0.50	**0.38**	**0.52**	**0.52**	0.49
H_w/S_l	0.40–42	**0.56**	0.44	**0.38**	0.43	0.47	0.53–54	0.50	0.52	0.45
H_l/S_l	0.22–23	0.25–26	0.22	**0.17**	0.24	0.25	**0.**27–**28**	0.26	0.25	0.24
pS_w/H_l	3.95	3.88	4.71	**5.13**	4.45	4.28	**3.58**	3.94	4.26	4.26
PO_l/S_l	0.60–61	0.55	0.63	**0.68**	0.62	0.58	**0.53**–54	0.57	0.60	0.60
IN_w/S_l	0.24–26	0.21	0.26	0.26	0.26	0.26	**0.20**–23	0.22	0.27	**0.32**
IO_w/S_l	0.24–27	**0.29**	0.28	0.23	0.27	0.26	**0.20**–21	0.21	0.21	0.23
O_l/S_l	0.17–19	**0.**20–**21**	0.15	0.14	0.15	0.18	0.18–19	0.16	0.14	**0.12**
La_w/La_l	0.51–54	0.35–49	**0.30**	0.40	**0.62**	0.35	0.35–37	0.49	0.54	**0.30**
Po_w/Po_l	0.8–1.0	0.8–1.0	1.06	1.20	0.80	1.23	0.9–**1.3**	0.75	0.73	**0.54**
Ju_w/S_l	0.16	**0.11**	**0.23**	0.14	0.20	0.17	0.15–16	0.22	0.20	0.14
W_w/S_l	0.26	**0.20**–22	0.28	0.26	0.31	**0.32**	0.28–29	0.30	0.26	0.27
Th_l/S_l	**0.06**	**0.12**	0.07	0.09	0.08	0.10	0.08–10	0.09	0.09	0.09
Qc_l/S_l	0.20	0.16	**0.10**	**0.25**	0.18	0.21	0.11	0.17	0.22	0.14

vomer. The transverse flange of the pterygoid exhibits a low, angular expansion. In *C. borealis*, *Onchiodon* and *Actinodon*, the entire free lateral margin of the pterygoid is greatly expanded into a right-angled projection. The palatinal ramus and the elongated basipterygoid ramus are strongly curved; thus, the interpterygoid vacuities are extremely wide, especially in their anterior part. The orbitae are not concealed by the pterygoids in ventral view. These characters are shared with *C. borealis* but are unknown in other eryopids. The stereospondylomorph *Intasuchus* (Konzhukova 1956; Werneburg et al. 2020) presents similar features, but especially the anteriorly widened interpterygoid vacuities in *Clamorosaurus* contrast with *Intasuchus*. Polygonal bony plates covering the interpterygoid vacuities are not preserved. Three larger bony plates are accumulated in the anterior part of the interpterygoid vacuities (Fig. 4C, D), which may represent remains of the epipterygoid. Similar bones are known from *C. borealis* and *Syndyodosuchus* (see below).

The basicranial articulation is firmly sutured (Fig. 4C, D). The cultriform process of the parasphenoid is generally narrow in contrast to *O. labyrinthicus* and *Eryops*, in which the process is swollen in its posterior half with convex lateral margins. The basal plate has a narrow rectangular shape like in *Eryops* and *Syndyodosuchus*. The ventral surface of the parasphenoidal basal plate has curved furrows for the carotid artery below the basipterygoid pockets, but their foramina lie more anterodorsally near the pockets. A large denticle field is developed between these furrows, which may taper anteriorly like in *C. borealis* to attain a triangular shape. Numerous denticles are present on the vomer, on the palatinal ramus of the pterygoid, partly on the palatine and probably on the ectopterygoid. The basioccipital and exoccipitals were apparently not ossified in this growth stage. The articular condyle of the quadrate is transversely expanded.

The visceral skeleton and mandibles are not preserved.

Postcranium. Few bones of the anterior part of the postcranial skeleton are associated with the skulls: ribs, clavicles, scapulocoracoids and ventral scales. One narrow rib and one rib with expanded proximal and distal ends are preserved. The clavicle has a relatively narrow ventral blade with remains of dermal sculpture (Fig. 5F). The scapulocoracoid (Figs 3, 5F) has an angle of about 90° between the supraglenoid buttress and the anterior margin of the scapular blade. Such an angle is known in most *Eryops* specimens and *Stenokranio* (see discussion in Werneburg et al. 2023). This angle is less than 90° in *Glaukerpeton* and *O. labyrinthicus*.

Clamorosaurus borealis Gubin, 1983

Figs 7–9, 14C, D

Holotype. PIN 3950/1, consisting of the skull in dorsal and palatal view (skull length 15.3 cm) with associated isolated bones such as sphenethmoid, stapes and left quadrate.

Other material. None.

Occurrence. The holotypic material was found near the town of Inta (Komi Republic, Russia) in a limestone from the coal mine number nine of the Ufimian Intinskaya Svita, late Kungurian (Cisuralian, Permian) in 1961.

Diagnosis. Autapomorphies: (1) Premaxilla with only six teeth, in contrast to nine to 15 premaxillary tooth loci in all other eryopids; (2) Maxilla with only 21 teeth, in contrast to 25 to 43 maxillary tooth loci in all other eryopids; (3) Supratemporal much wider than long; (4) Cultriform process of parasphenoid much shorter than median length of vomer.

Synapomorphies with some other eryopids: (1) Density of sculpture pattern quantified as the number of pits per in^2 on frontal plus jugal range between 3.40 and 5.23, shared with *C. nocturnus*, *Glaukerpeton* and *Syndyodosuchus*, but in contrast to all other eryopids; (2) Premaxilla without alary process, shared with *Actinodon*; (3) Some teeth have a long-oval cross-section in labial-lingual direction, shared with *O. labyrinthicus* and *Eryops*; (4) Teeth four to six are the largest premaxillary teeth, in contrast to *C. nocturnus* and many other eryopids; (5) The third tooth is the largest in the maxilla, in contrast to *C. nocturnus*, and many other eryopids; (6) Lacrimal wide, its width is only exceeded in *O. thuringiensis*; (7) Internarial and interorbital width differ, shared with *Syndyodosuchus*, *Glaukerpeton*, and *E. megacephalus*, but in contrast to *C. nocturnus*; (8) Very narrow interorbital width, shared with *C. nocturnus*, *Syndydosuchus*, *Actinodon*, and *E. megacephalus*; (9) Small orbits, only *Syndyodosuchus* has relatively smaller orbits; (10) Jugal wide, shared with *C. nocturnus*, *O. thuringiensis*, and *Eryops* sp. from the Moran Formation (MCZ1914); (11) Septomaxilla is completely unsculptured and ventrally directed, shared with *C. nocturnus* and *Eryops*; (12) Elongated contact between jugal and prefrontal, shared with *O. thuringiensis*, and *E. megacephalus*; (13) No interfrontal, in contrast to *Eryops* and *Osteophorus*; (14) Tabular with elongated tabular horn, shared with *Stenokranio* and *O. thuringiensis*; (15) Quadrate condyles lie far posterior to the occipital condyles, only in *E. megacephalus* is the distance larger; (16) No lateral line sulci, in contrast to *Glaukerpeton* and *Actinodon*; (17) Interchoanal width wider than internarial width, in contrast to *C. nocturnus*; (18) Elongated and narrow palatine, much longer than wide, shared with *Syndyodosuchus* and *Actinodon*, but in contrast to *C. nocturnus*; (19) Ectopterygoid and palatine about equal in length; (20) Greatly expanded transverse flange of pterygoid into a right-angled projection, shared with *Onchiodon* and *Actinodon* and much more pronounced than in *C. nocturnus* or *Syndyodosuchus*. (21) Wide basal plate of parasphenoid, in contrast to *C. nocturnus*, *Onchiodon*, *Stenokranio* and *Glaukerpeton*; (22) Triangular denticle field, shared with *Onchiodon*.

Comparative description. *General Skull Morphology*. The dermal sculpture of the dorsal surface of the skull roof corresponds to the fine sculpture pattern known from eryopids such as *Clamorosaurus nocturnus*, *Syndyodosuchus tetricus* and *Glaukerpeton avinoffi* (Werneburg and Berman 2012) (Table 1). It consists of a reticulated pattern of small pits and valleys separated by narrow ridges on nearly all skull roof bones (Fig. 7A, B). The density of the sculpture pattern is quantified as the number of pits per in^2 (6.452 cm^2) on the frontal and jugal, which are typically well-preserved bones in eryopid skulls, and as a proportion of those counts to skull length. These intraspecific indices range between both elements of *C. borealis* between 3.40 and 5.23, and on the prefrontal this ratio is 7.84 (Table 1). The dermal sculpture of the dorsal skull roof in other eryopid specimens consists of a much coarser pattern with indices ranging from 0.4 up to 1.7. Higher indices between 1.2 and 4.3 occur only in subadult *Eryops* (Table 1).

The dorsal strutting pattern with large ridges on the skull roof is well developed (Figs 7A, B, 9A). A large longitudinal ridge extends from the lateral portion of the tabular and supratemporal to the postorbital. It then runs on the anterior skull table from the suture between prefrontal/frontal and on the lateral part of the nasal to the medial margin of the naris. A transverse ridge connects the longitudinal ridges on the frontals, and anterior and posterior to it the surface of the frontals is depressed.

The degree of skull roof ossification is probably relatively high and the bones may have the thickness commonly present in other eryopids with the exception of *Glaukerpeton* and *C. nocturnus* (see above).

The well-preserved skull of *C. borealis* allows a tentative reconstruction of the skull roof in dorsal view and of the palate in ventral view (Fig. 9). The skull is slightly wider than long (Table 2; Fig. 6B; $pS_w/S_l=1.08$). The lateral margins of the skull are convex in dorsal view. The snout margin is laterally markedly constricted at the level of the naris like in *Eryops megacephalus* and *Osteophorus*. The postorbital region of the skull roof is relatively long ($H_l/S_l=0.25$) and wide ($H_w/S_l=0.52$). The preorbital skull is relatively elongate ($PO_l/S_l=0.60$). The internarial and interorbital width differ from each other ($IN_w/S_l=0.27$, $IO_w/S_l=0.21$) with a smaller relative interorbital width. Both species of *Clamorosaurus* share with *Actinodon* ($IO_w/S_l=0.20$–0.21) the narrowest interorbital region in eryopids. The occipital margin of the skull roof is only slightly concave. The quadrate condyles lie distinctly posterior to the occipital condyles ($Qc_l/S_l=0.22$; Table 2) as in *Eryops*. The circular orbits are small compared to other eryopids ($O_l/S_l=0.14$).

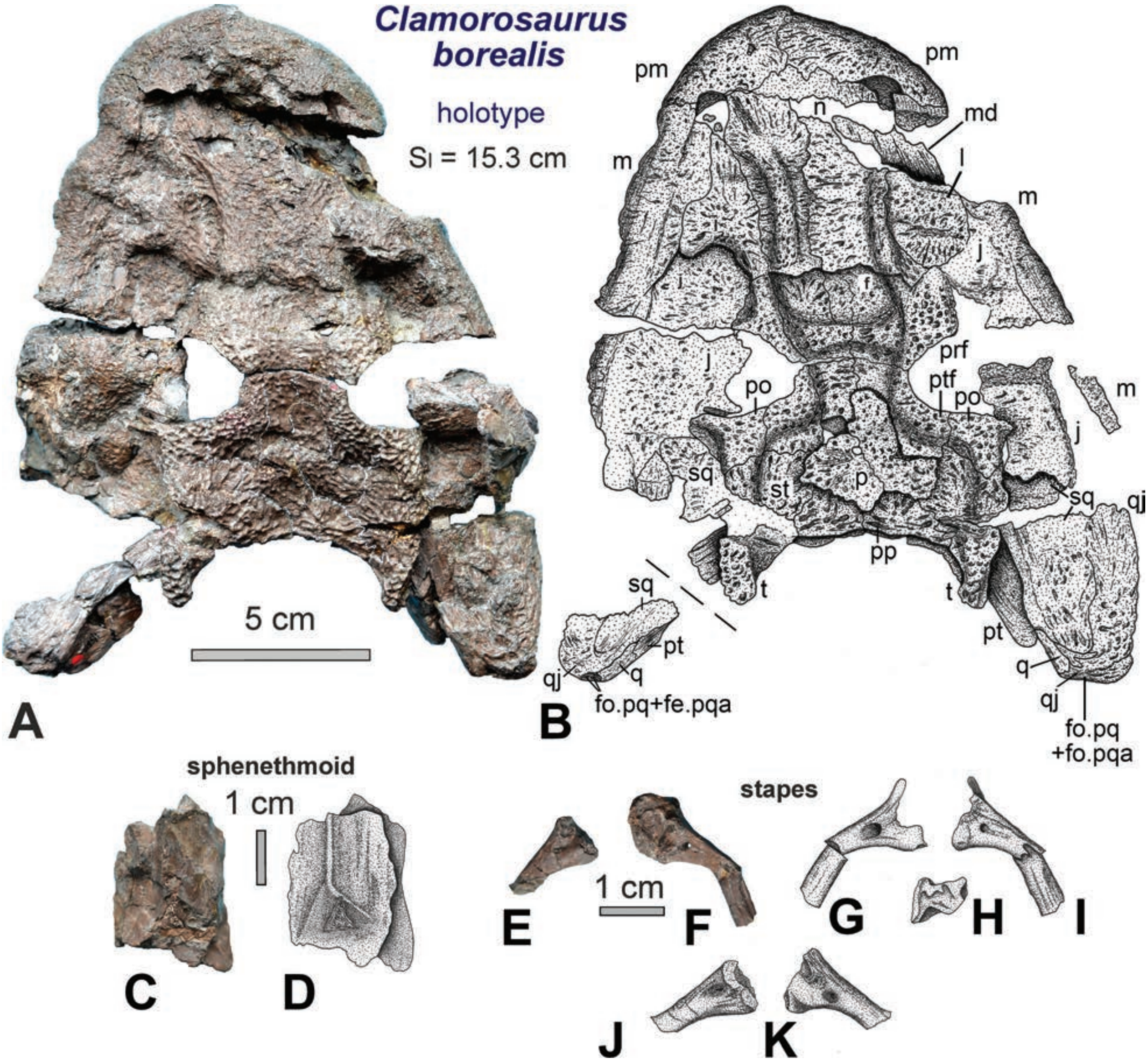

Figure 7. *Clamorosaurus borealis* Gubin, 1983, holotype PIN 3950/1 with skull roof in dorsal view (**A, B**), sphenethmoid in ventral view (**C, D**), and both stapes (**E–K**), from the Ufimian Intinskaya Svita (late Kungurian, Permian) of Inta (coal mine 9, Komi Republic, Russia). Abbreviations: f, frontal; fo.pq + fo.pqa, paraquadrate and accessory paraquadrate foramina of quadratojugal; j, jugal; l, lacrimal; m, maxilla; md, mandible; n, nasal; p, parietal; pm, premaxilla; po, postorbital; pp, postparietal; prf, prefrontal; pt, pterygoid; ptf, postfrontal; q, quadrate; qj, quadratojugal; sq, squamosal; st, supratemporal; t, tabular.

Growth stage. The single skull of *Clamorosaurus borealis* can be interpreted as adult for the following reasons: (a) The dermal sculpture consists of a dense reticulated pattern of small pits and valleys separated by narrow ridges; (b) The quadrate condyles lie far posterior to the occipital condyles; (c) The quadrate is ossified dorsally; (d) The orbits are small compared to other eryopids. Admittedly, small orbits could also represent a taxon-specific character and not necessarily an ontogenetic one. In general, however, larval and juvenile temnospondyls have proportionally larger orbits than adults, and thus the small orbits in *C. nocturnus* support our interpretation; (e) the pterygoid bears a pronounced transverse process; (f) The epipterygoid is ossified with a large plate. With a skull length of 15 cm, *C. borealis* is a middle-sized eryopid similar to *Actinodon* and *Onchiodon labyrinthicus*.

Skull roof. The interpremaxillary suture is moderately long and accounts for 11.0% of the midline length of the skull. An alary process of the premaxilla cannot be discerned, and the only other eryopid without this process is *Actinodon*. Both premaxillaries are strongly curved, leading to a narrow snout with a strongly arched tooth arcade and a lateral constriction anterior to the maxilla. The premaxilla has only six tooth loci, whereas all other eryopids have nine to 15 premaxillary tooth loci (Table 3). Similar to the small orbits, it cannot be ruled out that this is an ontogenetic character since tooth number frequently increases in temnospondyl ontogeny from larvae to adults in the context of proportional snout elongation (see e.g., Witzmann 2005b). However, this possibility is regarded as unlikely by us because (1) Boy

Table 3. Tooth places (largest and smallest values in bold), position of largest teeth (numbered from anterior) and general kind of dentition in premaxilla and maxilla of the eryopids (compare Figs 12, 13). Abbreviations. —Le, left lateral side; ri, right lateral side.

Eryopids	Premaxilla tooth places	Largest teeth	Maxilla tooth places	Largest teeth	Dentition
Clamorosaurus nocturnus (this paper)	9	8.–9.	25	6.	Small, circular cross-section
Clamorosaurus borealis (this paper)	**6**	4.–6.	**21**	3.	Large, long-oval cross-section
Syndyodosuchus tetricus (this paper)	10 (?11)	9.–10.	25 (?26)	6.–10.	Small, circular cross-section
Stenokranio boldi (Werneburg et al. 2023)	13	-	40–42	-	Small, circular cross-section
Glaukerpeton avinoffi (Werneburg and Berman 2012)	10 or 11 elong. teeth	-	37	-	Small, circular cross-section
Eryops megacephalus (Sawin 1941)	14	7.–12.	35–36	4.–7./8.	Large, long-oval cross-section
***Eryops* sp.-New Mexico** (Werneburg et al. 2010: fig. 2)	11	7.–11.	34 lat. blades	le. 4.–8., ri. 3.–10.	Large, long-oval cross-section
?*Eryops* sp.-MCZ1914 (Werneburg 2007: fig. 7b)	**14–15**	9.–14.	25–26	3.–6.	Large, long-oval cross-section
Onchiodon thuringiensis (Werneburg 2007)	12–13	-	?30–40	5.–9.	Small, circular cross-section
Onchiodon labyrinthicus (Boy 1990)	12	le. 6.–11., ri. 8.–12.	**42–43**	le. 3.–5., ri. 2.–3.	Large, long-oval cross-section
Actinodon frossardi (Werneburg and Steyer 1999)	?	?	37	3.–4.	Small, circular cross-section

(1990) did not document any increase of premaxillary teeth during ontogeny of *Onchiodon labyrinthicus*, and (2) the other characters listed here argue against a larval or juvenile state of the specimens under study. Only the first two small teeth and the following middle-sized tooth have a circular cross-section. Teeth number four to six are the largest ones and possess a long-oval cross-section in labial-lingual direction, shared with *Eryops megacephalus* and *O. labyrinthicus*.

The maxilla has a slightly wider dorsal shelf than *C. nocturnus* and it is ventrally in contact with the quadratojugal. Its tooth arcade has only about 21 tooth loci in contrast to all other eryopids having 25–43 tooth loci. All maxillary teeth are much smaller than the largest premaxillary teeth but are similar in size to the smallest premaxillary teeth. The 3rd posterior maxillary tooth is the largest one and causes a small lateral expansion of the skull margin, but this tooth is slightly smaller than the third tooth of the premaxilla. The maxillary teeth are mostly circular in cross-section with few exceptions on the right maxilla which possess a long-oval cross-section in labial-lingual direction.

The circular to oval shaped naris is relatively small as in *O. labyrinthicus*, its length comprising 8% of the midline length of the skull. The small septomaxilla is not sculptured (Fig. 7A, B) and lies ventrally directed inside the naris (shared with *Eryops* and *C. nocturnus*). The posterior margin of the naris is clearly formed by the nasal, lacrimal and maxilla (Fig. 9A).

The lacrimal is triangular with a wide posterior part (La_w/La_l=0.54). It is separated from the orbit by an elongated contact between jugal and prefrontal. The frontal is narrow like in most other eryopids and does not reach anteriorly to the level of the anterior ends of prefrontal and jugal. The jugal is wide (Ju_w/S_l=0.20) and proportionally only slightly narrower than in *C. nocturnus*. Therefore, the width of the skull at its midlength is similarly large in both species of *Clamorosaurus* (mS_w/S_l=0.98), comparable to *O. labyrinthicus* (mS_w/S_l=1.00). The postorbital is triangular in outline. The postfrontal and prefrontal clearly contact each other as in all eryopids. The prefrontal is anteriorly relatively narrow and extends further anterior than the frontal. The posteromedial part of the postfrontal is expanded. The supratemporal is much wider than long – a unique character in eryopids. The tiny parietals extend anterior to the level of the posterior orbital margin. Posteriorly, they do not reach the level of the posterior margin of the supratemporals. *C. borealis* bears a relatively short postparietal but an elongated tabular with a marked, slender tabular horn (Th_l/S_l=0.09). The cheek is narrower (W_w/S_l=0.26) than in *C. nocturnus* (Table 2). The squamosal and the quadratojugal are narrow. Similar to *C. nocturnus*, the quadratojugal reaches far posterior so that the quadrate condyle occupies a position (Qc_l/S_l=0.22) similar to *E. megacephalus*.

The dorsal exposure of the quadrate consists of a narrow, short process that is directed anteromedially between the squamosal, quadratojugal and the quadrate ramus of the pterygoid. Similar to *C. nocturnus*, a possible boss-like protuberance is developed at the ventral margin of the dorsal quadrate process (Fig. 8C). Two quadratojugal foramina are detectable close together in posterior view – the paraquadrate foramen and the accessory paraquadrate foramen (Figs 7B, 8C). Both foramina are rarely visible together in other eryopids. However, Cernansky et al. (2016) reported four internal foramina in the quadratojugal of *Eryops*, so that this feature complex is probably more variable than previously thought. Lateral line sulci are not present.

Palate and braincase. The palate is well preserved so that a reconstruction is possible (Fig. 9B). Longitudinal ridges on the palatal bones and traces of the anterior palatal fossae on the anterior part of the vomers are not preserved.

The vomer is elongated and relatively narrow. The smallest width of both vomers (=interchoanal width ICw/S_l=0.32) is wider than the smallest width between the narial openings (internarial width INw/S_l=0.27). In *C. nocturnus* both ratios are smaller and equal (0.22). The suture between vomer and palatine is much shorter than in *C. nocturnus*. The palatine is relatively narrow and elongated, much longer than wide, like in *Actinodon* and

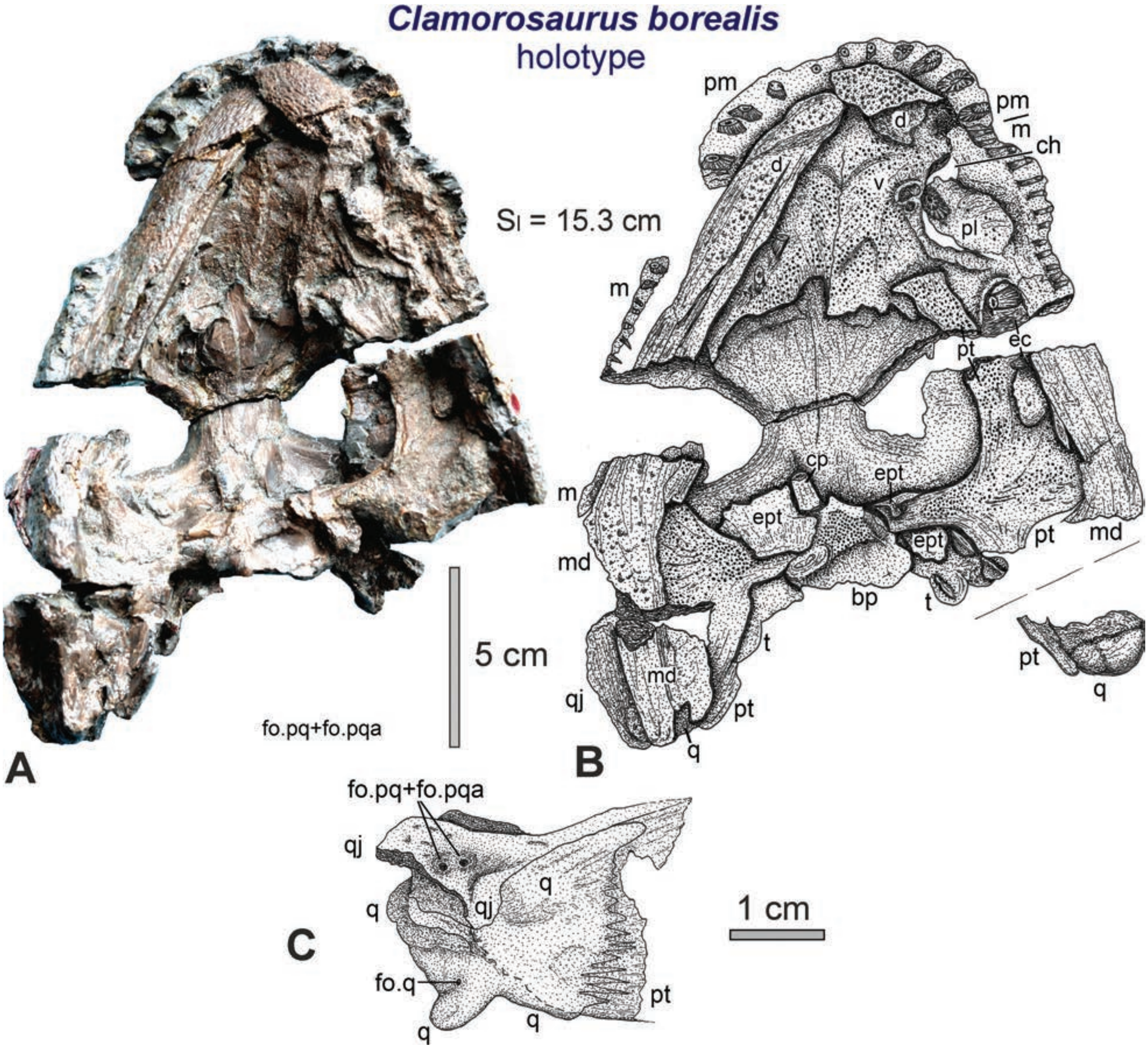

Figure 8. *Clamorosaurus borealis* Gubin, 1983, holotype PIN 3950/1 with palate and mandibles in ventral view (**A, B**), and the quadrate condyle in medial view (**C**), from the Ufimian Intinskaya Svita (late Kungurian, Permian) of Inta (coal mine 9, Komi Republic, Russia). Abbreviations: bp, basal plate of parasphenoid; ch, choane; cp, cultriform process; d, dentary; ec, ectopterygoid; ept, epipterygoid; fo.pq + fo.pqa, paraquadrate and accessory paraquadrate foramina of quadratojugal; fo.q, foramen in quadrate; m, maxilla; md, mandible; pl, palatine; pm, premaxilla; pt, pterygoid; q, quadrate; qj, quadratojugal; t, tabular; v, vomer.

Syndyodosuchus, but in contrast to the short and wide palatine in *C. nocturnus*. The ectopterygoid is longer than wide and of almost equal length as the palatine. Its posteriormost part is narrower than the adjacent part of the pterygoid.

The palatal dentition corresponds to that of *Syndyodosuchus* and differs in a few characters from that of *C. nocturnus*. The palatine bears a larger fang anteriorly and a slightly smaller fang posteriorly. The large palatine fang is smaller than the largest teeth of the premaxilla. The ectopterygoid fangs are of nearly the same size as those from the palatine. The fangs on the vomer are of equal or smaller size than those on the ectopterygoid. One fang is located anteromedial to the anterior edge of the choanae on both vomers, at the same level next to the posteriormost premaxillary teeth. A further, somewhat smaller tooth locus with two fangs on both vomers is positioned medial to the choana at its mid-length. This fang pair is located on a prominent ridge which forms the posteromedial margin of the choana and almost reaches the anterior palatine fang. This second tooth locus on the vomer medial to the choana is only known from *C. nocturnus* and *Syndyodosuchus tetricus* (however, as described in the present study, only with one fang in these species).

The large choana is longer than wide and medially expanded; it is larger than the choana of *C. nocturnus* and *S. tetricus*.

The anteriormost part of the palatinal ramus of the pterygoid is relatively broad and blunt. The transverse flange of the pterygoid is greatly expanded into a right-angled projection, which is more pronounced than in *C. nocturnus* or *Syndyodosuchus*, but similar

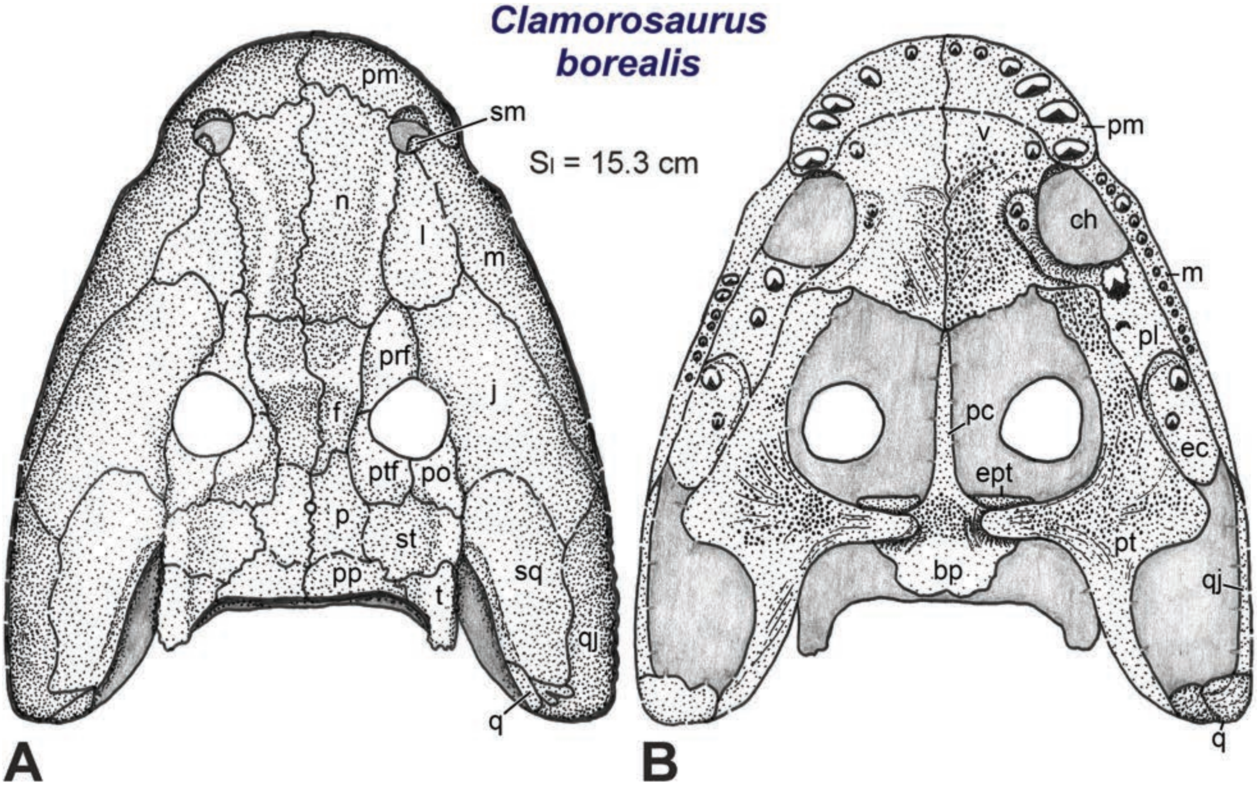

Figure 9. *Clamorosaurus borealis* Gubin, 1983, tentative reconstruction of the skull roof in dorsal view (**A**), and of the palate in ventral view (**B**). Abbreviations: bp, basal plate of parasphenoid; ch, choana; cp, cultriform process; ec, ectopterygoid; ept, epipterygoid; f, frontal; j, jugal; l, lacrimal; m, maxilla; n, nasal; p, parietal; pl, palatine; pm, premaxilla; po, postorbital; pp, postparietal; prf, prefrontal; pt, pterygoid; ptf, postfrontal; q, quadrate; qj, quadratojugal; sm, septomaxilla; sq, squamosal; st, supratemporal; t, tabular; v, vomer.

to *Onchiodon* and *Actinodon*. The palatinal ramus and the elongated basipterygoid ramus are strongly curved, leading to the great width of the interpterygoid vacuities, also in their anterior part. The orbitae are not obscured by the pterygoids in ventral view. Among eryopids, these characters are shared only with *C. nocturnus* (see above); additionally, the stereospondylomorph *Intasuchus* (Konzhukova 1956; Werneburg et al. 2020) presents similar features except for the anteriorly widened interpterygoid vacuities. Polygonal bony plates that covered the interpterygoid vacuities are not preserved.

The large bony plate lying between the basipterygoid ramus of the pterygoid plus parasphenoid on one side and the skull roof on the other side is interpreted as footplate of the epipterygoid (Fig. 8A, B). Remains of the ascending process are not preserved. A similar large footplate is known from *Eryops* (Sawin 1941: pl. 9; Schoch and Sobral 2021: fig. 6). *Syndyodosuchus* presents a similar large footplate (see description below and Fig. 11A, B).

The elongated transverse, rod-like basipterygoid process of the pterygoid overlapped the wide basipterygoid pocket of the parasphenoidal basal plate and might have formed a movable articulation (Figs 8A, B, 9B). The cultriform process of the parasphenoid is relatively narrow and much shorter than the vomer in contrast to all other eryopids. The sphenethmoid (Fig. 7C, D) is clearly wider (20 mm) than the cultriform process (5–6 mm). Its posterior part was probably attached to the underside of the skull roof in the mid-part of the interorbital region. It bears a longitudinal ridge in ventral view. The basal plate of the parasphenoid has a relatively wide rectangular shape like in *Onchiodon* but unlike *C. nocturnus*, *Eryops* and *Syndyodosuchus*. Its ventral surface has curved furrows for the carotid artery below the basipterygoid pockets, but their foramina lie more anteromedially near the pockets. A large denticle field is developed between these furrows, which has a triangular shape like in *O. labyrinthicus*. Numerous denticles are present on the vomer and on the palatinal branch of the pterygoid. The articular condyle of the quadrate is bilobed and transversely expanded. The posteromedial part of the quadrate bears a foramen near a narrow boss-like process. The basioccipital and the exoccipitals are not preserved.

Visceral skeleton. The stapes has a slender, elongated shaft without a quadrate process. It is proximally pierced by a stapedial foramen and has a wide footplate in which dorsal and ventral proximal heads can be well distinguished. In general morphology it is similar to *Glaukerpeton* (Werneburg and Berman 2012) and *E. megacephalus* (Sawin 1941), but much slenderer than in *O. thuringiensis* (Werneburg 2007).

The mandible is only partly preserved without details. No bones of the postcranial skeleton are available.

Syndyodosuchus Konzhukova, 1956

Type species. *Syndyodosuchus tetricus* Konzhukova, 1956.

Diagnosis. As for species by monotypy.

Remarks. *Syndyodosuchus* was interpreted as a basal stereospondylomorph by Konzhukova (1956); Gubin (1984) and all later workers (e.g. Shishkin et al. 2000 and Schoch and Milner 2000) followed this assignment. However, *Syndyodosuchus* bears the first four characters listed in the eryopid diagnosis (see above).

Syndyodosuchus tetricus Konzhukova, 1956

Figs 10–13, 14E, F

Holotype. PIN 570/40, consisting of the skull in dorsal and palatal view (skull length 16.2 cm).

Other material from different individuals. PIN 570/6, consisting of a right anterolateral skull edge; PIN 570/41, consisting of a right anterior dentary; PIN 570/2, consisting of a poorly preserved skull of about 17 cm length; PIN 570/3, consisting of an indeterminable bone.

Occurrence. The material of *Syndyodosuchus* was found together with that of *Intasuchus* near the 'Greater Inta River' in about 100 m depth in coal beds of a mine from the Ufimian Intinskaya Svita, late Kungurian (Cisuralian, Permian).

Diagnosis. Autapomorphies: (1) Tabular tiny in length and width; (2) Internarial width is very large (INw/Sl=0.32); (3) Postorbital very narrow (Po_w/Po_l=0.54).

Synapomorphies with some of the eryopids: (1) Density of sculpture pattern quantified as the number of pits per in^2 on frontal plus jugal ranges between 4.69 and 5.00, shared with *Glaukerpeton* and *Clamorosaurus*, but differs from all other eryopids; (2) Lateral margin of skull roof is slightly concave to straight; (3) Both premaxillae form a relatively straight snout, like in *E. megacephalus*; (4) Snout margin is laterally constricted slightly below the level of naris; (5) Premaxilla with elongated and relatively wide alary process, shared with *O. labyrinthicus*; (6) Elongated interpremaxillary suture, shared with *E. megacephalus*; (7) Premaxillary, maxillary and dentary teeth are heterodont with a circular cross-section, in contrast to *C. borealis*, *O. labyrinthicus*, and *Eryops*, but shared with *C. nocturnus*, and others; (8) In the premaxilla, teeth number nine and ten are the largest teeth, in contrast to *C. borealis*; (9) In the maxilla, teeth number six to ten are the largest teeth, in contrast to *C. borealis*, and other eryopids; (10) Lacrimal is very narrow and long, three times longer than wide, only similar in *Actinodon*; (11) Different internarial and interorbital width, in contrast to *C. nocturnus*; (12) Small orbitae, similar in *C. borealis*; (13) Very short contact between jugal and prefrontal, shared with *O. labyrinthicus*; (14) No interfrontal, in contrast to *Eryops* and *Osteophorus*; (15) Supratemporal much longer than wide, shared with *Onchiodon*, *Glaukerpeton* and *Actinodon*; (16) No lateral line sulci, in contrast to *Glaukerpeton* and *Actinodon*; (17) Occipital margin of skull roof is well concave, shared with *Glaukerpeton*, *O. labyrinthicus* and *E. megacephalus*;

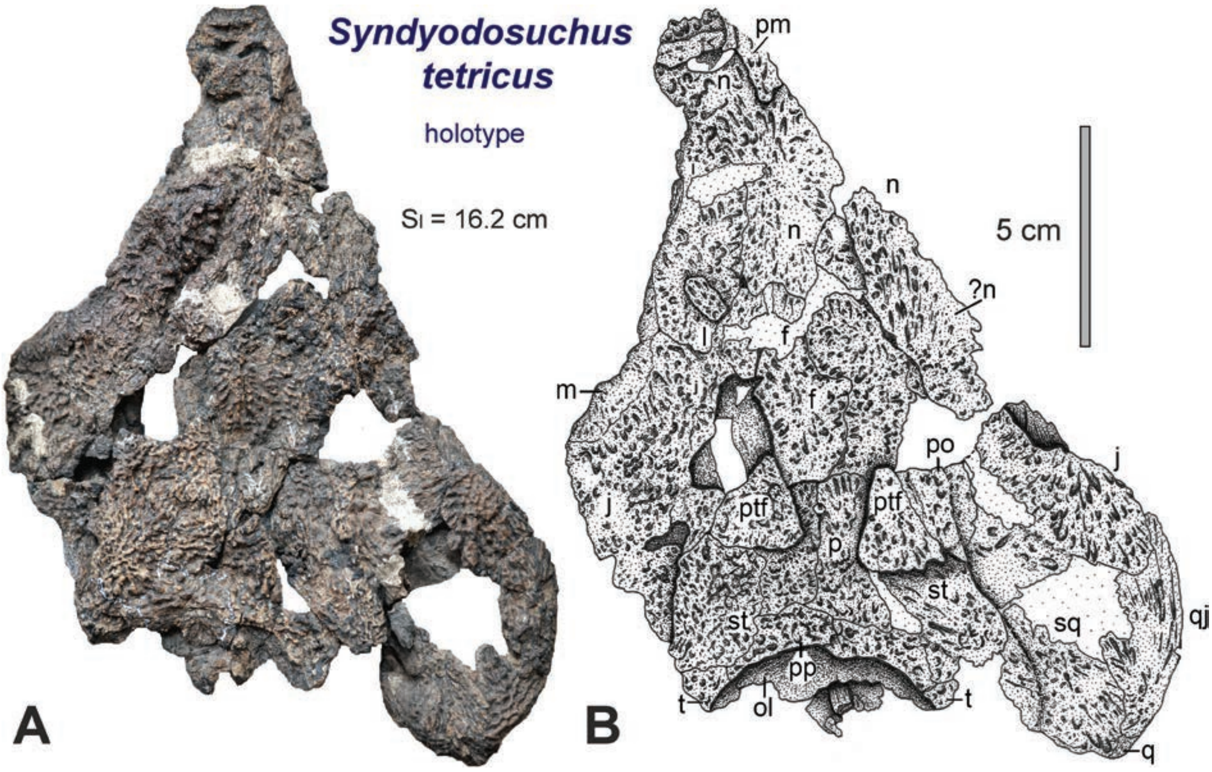

Figure 10. *Syndyodosuchus tetricus* Konzhukova, 1956, holotype PIN 570/40 with skull roof in dorsal view (**A, B**), from the Ufimian Intinskaya Svita (late Kungurian, Permian) of Inta (coal mine at 'Greater Inta River', Komi Republic, Russia). Abbreviations: f, frontal; j, jugal; l, lacrimal; m, maxilla; n, nasal; ol, occipital lamella; p, parietal; pm, premaxilla; po, postorbital; pp, postparietal; prf, prefrontal; ptf, postfrontal; q, quadrate; qj, quadratojugal; sq, squamosal; st, supratemporal; t, tabular.

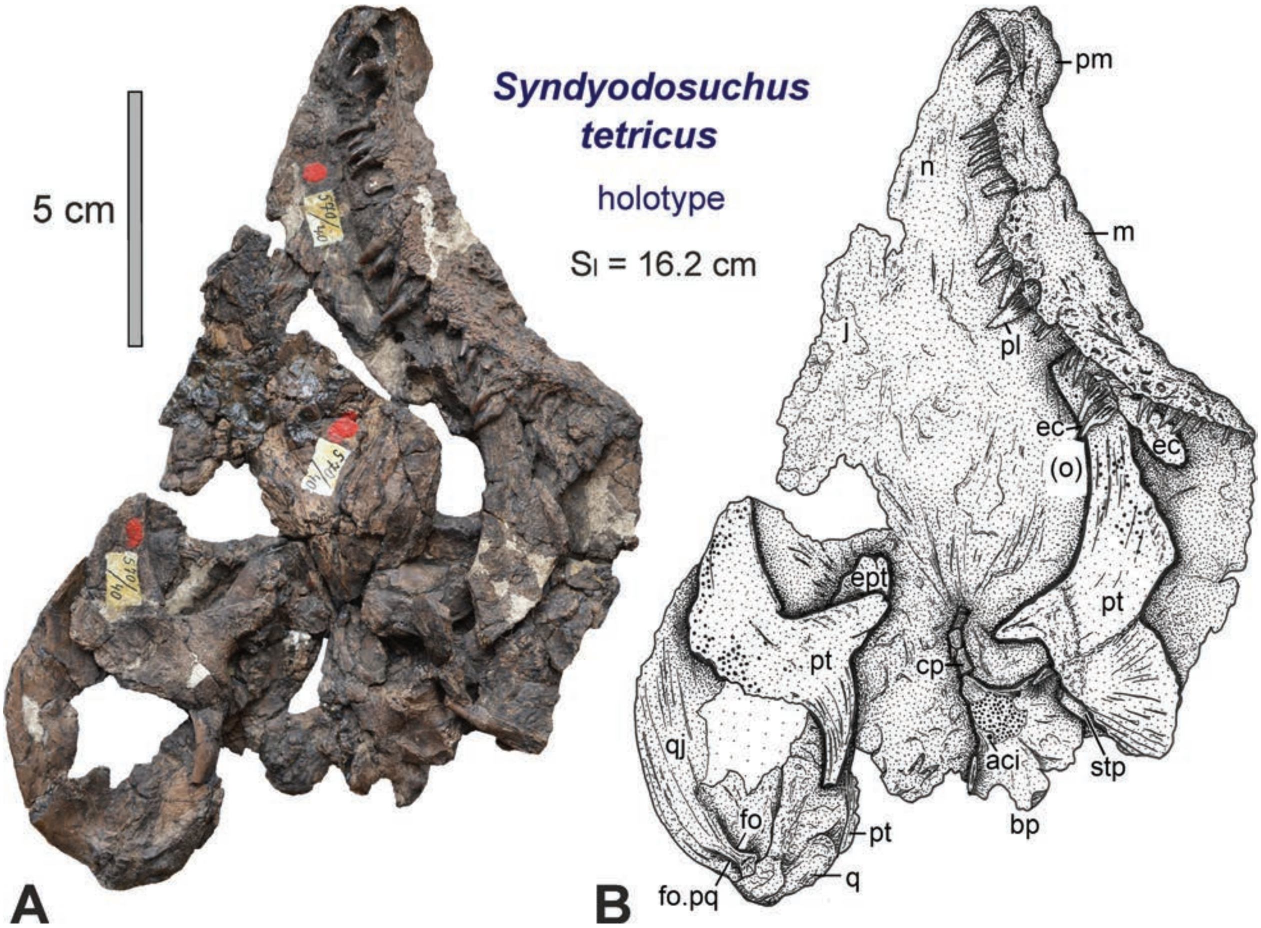

Figure 11. *Syndyodosuchus tetricus* Konzhukova, 1956, holotype PIN 570/40 with palate in ventral view and premaxilla plus maxilla in lateral view (**A, B**), from the Ufimian Intinskaya Svita (late Kungurian, Permian) of Inta (coal mine at 'Greater Inta River', Komi Republic, Russia). Abbreviations: aci, foramen for carotid artery; bp, basal plate of parasphenoid; ch, choane; cp, cultriform process; ec, ectopterygoid; ept, epipterygoid; pq, paraquadrate foramen of quadratojugal; j, jugal; m, maxilla; n, nasal; o, orbita; pl, palatine; pm, premaxilla; pt, pterygoid; q, quadrate; qj, quadratojugal; stp, stapes; v, vomer.

(18) Elongated and relatively wide palatine, much longer than wide, shared with *C. borealis* and *Actinodon*, but in contrast to *C. nocturnus*; (19) Ectopterygoid and palatine of about equal length; (20) Palatinal ramus of pterygoid relatively narrow with poorly developed transverse flange, like in *Glaukerpeton*; (21) Short basipterygoid process of pterygoid; (22) Narrow interpterygoid vacuities, in contrast to *Clamorosaurus*; (23) Orbitae are partly covered by pterygoids in ventral view, in contrast to *Clamorosaurus*; (24) Cultriform process of the parasphenoid is longer than the vomer, in contrast to *C. borealis*; (25) Narrow basal plate of parasphenoid, shared with *C. nocturnus* and *E. megacephalus*; (26) Basal plate with foramina for carotid artery in ventral view; (27) Vomer with additional fang medial to the choana, shared with *Clamorosaurus*.

Comparative description. One skull with a median length of 16 cm preserves the skull roof in dorsal and the palate in ventral view (PIN 570/40). Two right dentaries from additional individuals of the same species with heterodont dentition complete the description (Fig. 12; PIN 570/6 and PIN 570/41).

General skull morphology. The dermal sculpture of the skull roof corresponds to the fine sculpture pattern known from certain eryopids such as *Clamorosaurus*, *Syndyodosuchus* and *Glaukerpeton* (Werneburg and Berman 2012) (Table 1). It consists of a reticulated pattern of small pits and valleys separated by narrow ridges on nearly all skull roofing bones (Fig. 10A, B). The density of the sculpture pattern is quantified as the number of pits per in^2 (6.452 cm^2) on the frontal and jugal, and as a proportion of those counts to skull length. These intraspecific indices range between both elements of *S. tetricus* between 4.69 and 5.00. The dermal sculpture of the dorsal surface of the skull roof in other eryopid specimens is of much coarser sculpture pattern with indices from 0.4 up to 1.7, higher indices between 1.2 and 4.3 occur only in the subadult *Eryops* (Table 1). A dorsal strutting pattern with large ridges on the skull roof is not developed (Fig. 10).

S. tetricus and *C. nocturnus* have slightly thinner bones than the bones in other eryopids, whereas *Glaukerpeton* has 30–50% thinner skull roofing bones (Werneburg and Berman 2012).

The well-preserved skull of *S. tetricus* allows a tentative reconstruction of the skull roof in dorsal view and of the palate in ventral view (Fig. 13). The skull is as wide as long (Table 2; pS_w/S_l=1.01). The lateral margin of the

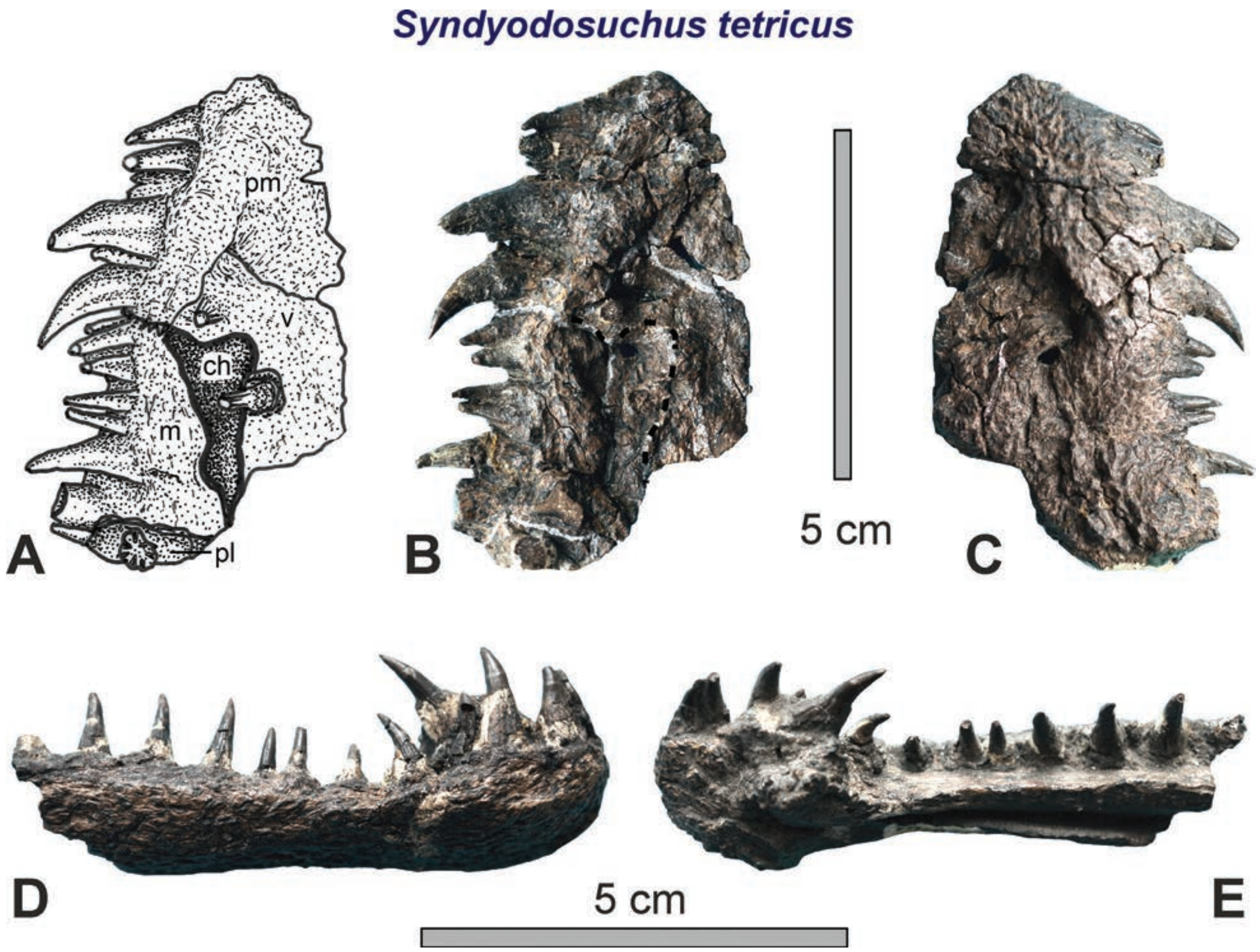

Figure 12. *Syndyodosuchus tetricus* Konzhukova, 1956, further specimens, a right-anterior part of a skull with choana (PIN 570/6) in ventral view (**A, B**), and dorsolateral view (**C**), and an anterior dentary with symphyseal tusk in labial view (**D**) and lingual view (**E**), from the Ufimian Intinskaya Svita (late Kungurian, Permian) of Inta (coal mine at 'Greater Inta River', Komi Republic, Russia) (PIN 570/41). Abbreviations: ch, choana; m, maxilla; pl, palatine; pm, premaxilla; v, vomer.

skull is slightly concave to straight in dorsal view. The snout margin is laterally constricted slightly below the level of naris but not so impressive as in *E. megacephalus*, *Osteophorus* and *Clamorosaurus*. The postorbital region of the skull roof is relatively long (H_l/S_l=0.24) and wide (H_w/S_l=0.45) (Table 2). The preorbital skull is relatively elongate (PO_l/S_l=0.60). The internarial width is very large (IN_w/S_l=0.32) and presents the largest ratio in eryopids (Table 2). The interorbital width (IO_w/S_l=0.23) is small like in *Clamorosaurus*, *Actinodon* and *E. megacephalus*. The occipital margin of the skull roof is well concave. The quadrate condyles lie distinctly posterior to the occipital condyles (Qc_l/S_l=0.14; Table 2) but not so wide posterior than in *E. megacephalus* or *C. borealis*. The long-oval orbits are the proportionally smallest ones compared to other eryopids (O_l/S_l=0.12).

Growth stage. The holotypic skull of *Syndyodosuchus tetricus* was an early adult animal, as indicated by the following features: (a) The dermal sculpture consists of a dense reticulated pattern of small pits and valleys separated by narrow ridges; (b) The quadrate condyles lie far posterior to the occipital condyles; (c) The quadrate is ossified dorsally; (d) The orbits are very small compared to other eryopids; (e) The pterygoid has a transverse process; (f) The epipterygoid is ossified with a large footplate. The skull length of 16 cm ranges in the middle-sized group of the family Eryopidae, and corresponds to *Actinodon*, *C. borealis* and *O. labyrinthicus*. However, the incomplete ossification of the occiput indicates that it was an early adult and did not reach the late adult stage.

Skull roof. The interpremaxillary suture is elongated and accounts for 13.1% of the midline length of the skull. The elongated and moderately wide alary process of the premaxilla is clearly detectable. Both premaxillae form a relatively straight snout like in *E. megacephalus*, but its lateral constriction is formed by the lateral margin of the maxilla posterior to the naris. The premaxilla has 10 or 11 tooth loci in its tooth arcade, like most other eryopids with the exception of *Clamorosaurus* which has less tooth loci (Table 3). All teeth of premaxilla, maxilla, dentary and palatal elements have a circular cross-section. The ninth and tenth teeth of the premaxilla are the largest ones. Premaxilla and maxilla have a heterodont dentition, with the size differences giving a wave-like profile of the tooth row in lateral view (Figs 11A, B, 12A–C).

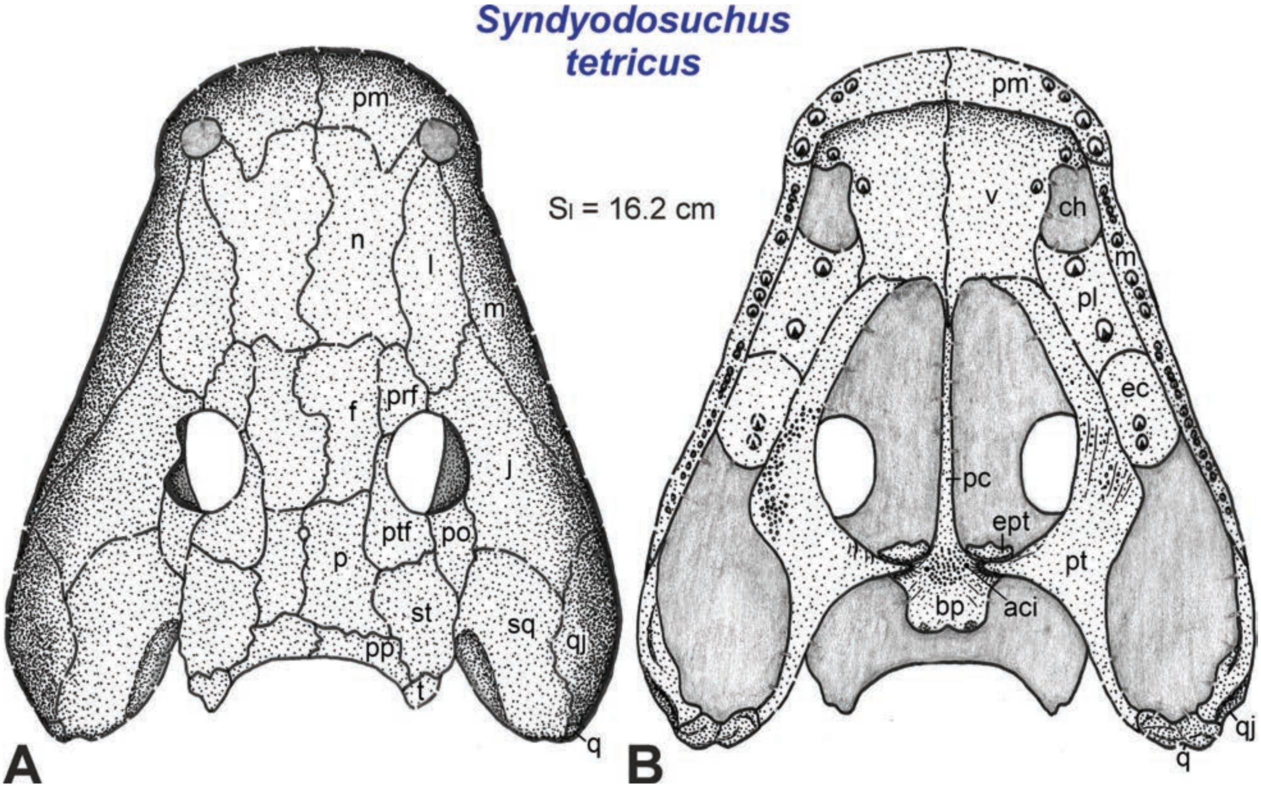

Figure 13. *Syndyodosuchus tetricus* Konzhukova, 1956, tentative reconstruction of the skull roof in dorsal view (**A**), and of the palate in ventral view (**B**). Abbreviations: aci, foramen for carotid artery; bp, basal plate of parasphenoid; ch, choane; cp, cultriform process; ec, ectopterygoid; ept, epipterygoid; f, frontal; j, jugal; l, lacrimal; m, maxilla; n, nasal; p, parietal; pl, palatine; pm, premaxilla; po, postorbital; pp, postparietal; prf, prefrontal; pt, pterygoid; ptf, postfrontal; q, quadrate; qj, quadratojugal; sm, septomaxilla; sq, squamosal; st, supratemporal; t, tabular; v, vomer.

The maxilla has a relatively narrow dorsal shelf and it is in contact ventrally with the quadratojugal. Its tooth arcade has 25 or 26 tooth loci. No maxillary tooth reaches the size of the largest premaxillary teeth, and the maxillary teeth are similar in size to the smallest premaxillary teeth. The sixth to tenth maxillary teeth are the largest ones but cause no lateral expansion of the skull margin.

The circular to oval naris is relatively small as in *C. borealis* and *O. labyrinthicus*, its length comprising 7% of the midline length of the skull. The septomaxilla is not recorded. The posterior margin of the naris is clearly formed by the nasal, lacrimal and maxilla (Fig. 13A).

The lacrimal is narrower (La_w/La_l=0.30; Table 2) and longer than the nasal, a pattern that is further present only in *Actinodon* among eryopids. It is separated from the orbit by a short contact between jugal and prefrontal. The frontal is narrow like in most other eryopids and reaches anteriorly to the level of the anterior ends of prefrontal and jugal. The jugal is relatively wide (Ju_w/S_l=0.14) and of equal width as the orbit at midlength. The left jugal constricts the orbit by a small medial expansion, whereas the orbital rim of the right jugal is not preserved in this part. The width of the skull at midlength is small (mS_w/S_l=0.86; Table 2). The postorbital is triangular in outline and much narrower than in all other eryopids (Po_w/Po_l=0.54, Table 2). The postfrontal and prefrontal clearly contact each other as in all eryopids. The prefrontal is anteriorly relatively wide and blunt (Fig. 13A). It reaches anteriorly only up to the anterior level of the frontals. The posteromedial part of the postfrontal is markedly expanded like in *C. borealis*. The supratemporal is 1.2–1.4 times longer than wide. It reaches posteriorly clearly below the level of the occipital condyle. The parietals extend anterior up to the level of the posterior orbital margin. They do not reach as wide posterior as the supratemporals. *Syndyodosuchus* bears a relatively short postparietal. The tabular is tiny – it is the proportionally smallest one in eryopids. A tabular horn is not developed. The cheek is relatively narrow (W_w/S_l=0.27; Table 2) and does not reach the relative width of the cheek in *C. nocturnus* or *Onchiodon*. Correspondingly, the squamosal and the quadratojugal are relatively narrow.

The dorsally exposed part of the quadrate between the squamosal and quadratojugal is very small, but its dorsoventral contact to the quadrate ramus of the pterygoid is extensive. Quadratojugal foramina are not visible. Lateral line sulci are not present.

Palate and braincase. The palate is well preserved and can be reconstructed (Fig. 13B). Longitudinal ridges on the palatal bones and traces of the anterior palatal fossae on the anterior part of the vomers are not preserved.

The vomers are elongated, posteriorly narrow and anteriorly widened. The smallest width of both vomers (= posterior interchoanal width ICw/S_l=0.30) is smaller

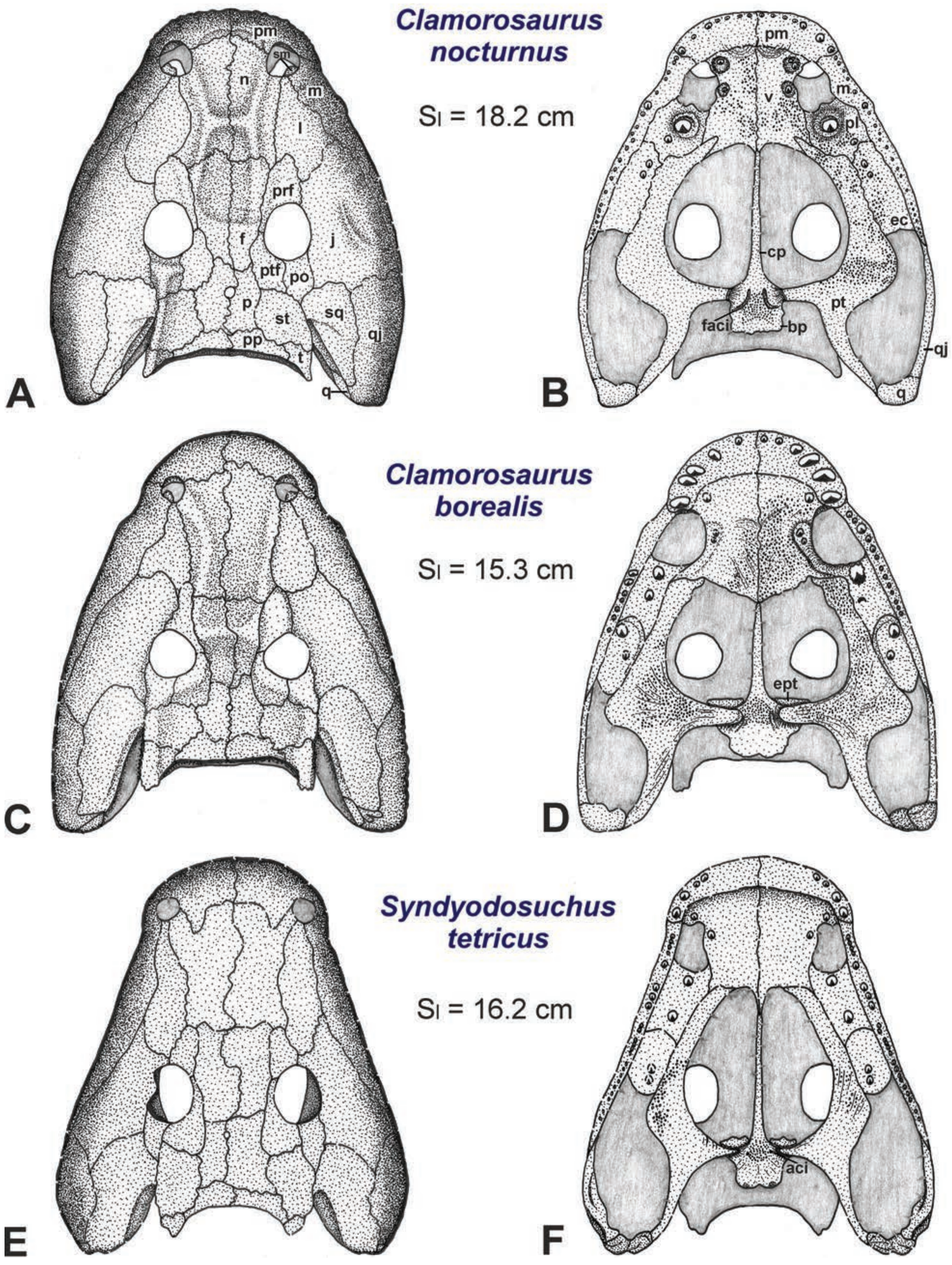

Figure 14. Comparison of the revised Russian eryopid skulls in dorsal and palatal view, *Clamorosaurus nocturnus* (**A, B**), *Clamorosaurus borealis* (**C, D**), *Syndyodosuchus tetricus* (**E, F**). Abbreviations: aci, foramen for carotid artery; bp, basal plate of parasphenoid; ch, choane; cp, cultriform process; ec, ectopterygoid; ept, epipterygoid; f, frontal; faci, furrows for carotid artery; j, jugal; l, lacrimal; m, maxilla; n, nasal; p, parietal; pl, palatine; pm, premaxilla; po, postorbital; pp, postparietal; prf, prefrontal; pt, pterygoid; ptf, postfrontal; q, quadrate; qj, quadratojugal; sm, septomaxilla; sq, squamosal; st, supratemporal; t, tabular; v, vomer.

than the smallest width between the narial openings (internarial width INw/S_l=0.32), but the anterior interchoanal width is equal to the internarial width. The suture between vomer and palatine is relatively short but longer than in *C. borealis*. The palatine is much longer than wide. The ectopterygoid is longer than wide and of almost equal length as the palatine. Its posteriormost part is wider than the neighbouring part of the pterygoid.

The palatal dentition corresponds to that of *C. borealis*. The palatine bears two relatively large fangs, one on the anterior and one on the posterior part. The palatine fangs are of similar size as the largest premaxillary teeth. The ectopterygoid bears a fang pair on its posterior part which is only slightly smaller than the fangs of the palatine. The fangs on the vomer are located on two separate tooth places and have the same size as the ectopterygoid fangs. One fang is located anterior to the choana (Fig. 12A, B). A further, somewhat larger tooth locus with one fang is positioned medial to the choana in its anterior half. This second tooth locus on the vomer, medial to the choana is otherwise only known from *C. nocturnus* and *C. borealis*.

The choana is longer than wide, but posteromedially expanded (Fig. 12A, B) like in *Actinodon*, *C. nocturnus* and *E. megacephalus*.

The palatinal ramus of the pterygoid is overall narrow. The transverse flange of the pterygoid is poorly developed like in *Glaukerpeton*. The palatinal ramus and the short basipterygoid ramus are only slightly curved and therefore, the interpterygoid vacuities are narrower than in *Clamorosaurus* and more similar to the vacuities of the other eryopids. The orbits are partially obscured by the pterygoids in ventral view, again in contrast to *Clamorosaurus*. Polygonal bony plates covering the interpterygoid vacuities are not preserved.

The large bony plate lying between the basipterygoid ramus of the right pterygoid and the skull roof is interpreted as footplate of the epipterygoid (Fig. 11A, B). Remains of the ascending process are not preserved. A similar large footplate is known from *C. borealis* (Fig. 8B) and *Eryops* (see above).

The short basipterygoid process of the pterygoid overlapped the wide basipterygoid pocket of the parasphenoidal basal plate and might have formed a movable articulation (Figs 11A, B, 13B). The cultriform process of the parasphenoid is narrow and longer than the vomer, like in all other eryopids with the exception of *C. borealis*. The basal plate of the parasphenoid has a narrow rectangular shape; its ventral surface has no clear furrows but foramina for the carotid artery between the basipterygoid pockets and the denticle field in ventral view (Fig. 11A). The large denticle field starts widened on the anterior part of the basal plate and extends anteriorly between the carotid foramina up to the base of the cultriform process. This anterior field is not clearly triangular or rounded. Further denticles are only preserved on the palatinal branch of the pterygoid. The articular condyle of the quadrate is well bilobed and transversely expanded. The posteroventral part of the quadratojugal bears a narrow bridge whose posterior boss-like end sutures with the quadrate. This bony bridge is pierced from posterolateral to anteromedial by the paraquadrate foramen (Fig. 11A). The sphenethmoid, basioccipital and exoccipitals are not recorded. The stapes of the visceral skeleton is only preserved with a small part of the shaft (Fig. 11A, B).

Mandible. The anterior part of an isolated right dentary has a heterodont dentition with a wave-like profile of the tooth series. One large symphyseal tooth and a possible tooth place are preserved (Fig. 12E).

Phylogenetic relationships

To assess the phylogenetic relationships of *Clamorosaurus nocturnus*, *C. borealis* and *Syndyodosuchus tetricus*, we included these taxa in the phylogenetic analysis of Werneburg et al. (2023), which in turn is a modified version of the analysis of Schoch (2021). We deleted *Eryops* sp. (MCZ1914) from the Moran Formation in Archer County (Texas, USA) since this taxon is still poorly known and awaits a detailed first-hand description (Werneburg 2007; Schoch and Milner 2014). This leads to a total number of 28 taxa in our analysis, with *Balanerpeton woodi*, *Dendrerpeton helogenes* (*Dendrysekos helogenes* sensu Schoch and Milner 2014) and *Cochleosaurus bohemicus* forming the operational outgroup. We modified the definition of character #5 of the original matrix (Werneburg et al. 2023) so that it reads as follows: “Snout (margin). Premaxillary snout region at the level of the external naris. Not constricted (0), constricted (1).” We added the following four new characters: character #71 (“Ratio length of external naris through length of orbit (both measured sagitally). Smaller than 0.6 (0); 0.6 or larger (1)”); character #72 (“Choanal width through orbital width (measured transversely to sagittal axis). Smaller than 0.9 (0); equal or larger than 0.9 (1)”); character #73 (“Orbits laterally obscured by pterygoids in palatal view (0); orbits completely visible in palatal view (1)”); and character #74 (“Tooth pit (with one or two fangs) medial to choana at its midlength. Absent (0); present (1)”). The complete list of characters and the character-taxon matrix are given in Suppl. material 1.

We conducted the analysis in PAUP* 4.0a169 (Swofford 2021) with all characters having equal unit weight, and used tree bisection-reconnection as a branch-swapping algorithm and 10,000 random stepwise sequences of taxon addition sequences. Tree branches were collapsed if the minimum length of any branch was zero (“amb-” option in PAUP). We then saved one tree in memory at each step during this initial stage of the tree searches. Subsequently, all trees saved from this stage were input into a new round of tree branch swappings, this time with the option of saving multiple trees. As a final step, those trees were subjected to ten successive branch swapping iterations. Neither additional nor shorter trees were obtained after these iterations. The analysis yielded 23 most parsimonious trees. The tree length is 196, the

Consistency Index CI is 0.4082, and the Retention Index is 0.7041. Fig. 17 shows the resulting strict consensus tree, and Fig. 18 shows the strict consensus of the intrarelationships of eryopids.

Additionally, we performed a second analysis with reweighted characters. Here, we reweighted characters using the maximum values of their rescaled consistency indexes obtained from the initial unweighted analysis.

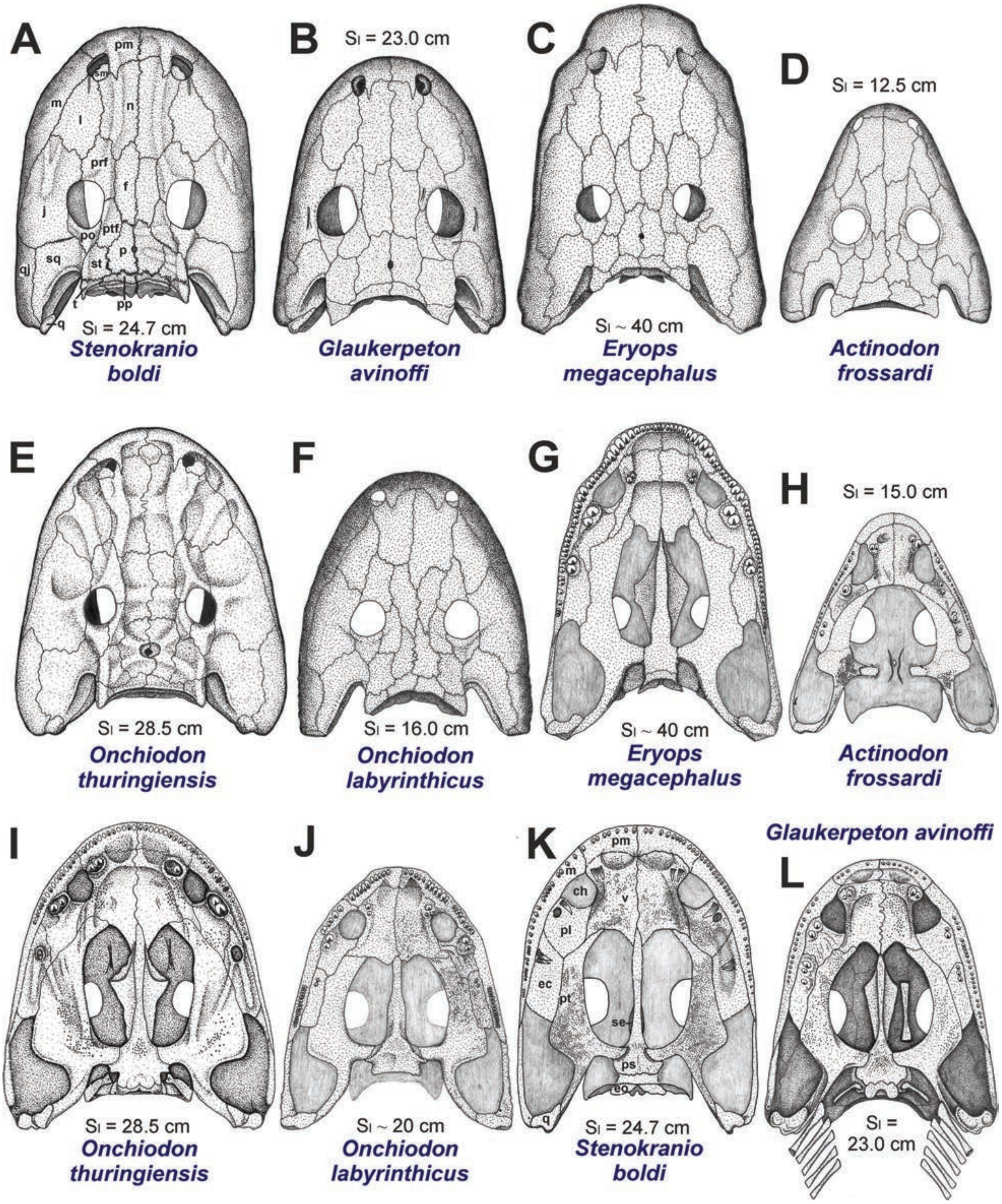

Figure 15. Comparison of related eryopid skulls in dorsal view (**A**–**F**) and palatal view (**G**–**L**); (**A, K**) after Werneburg et al. (2023); (**B, L**) after Werneburg and Berman (2012); (**C, G**) after Sawin (1941); (**D**) after Werneburg (1997); (**E, I**) after Werneburg (2007); (**F, J**) after Boy (1991); (**H**) after Werneburg and Steyer (1999). Abbreviations: ch, choane; cp, cultriform process; ec, ectopterygoid; eo, exoccipital; f, frontal; j, jugal; l, lacrimal; m, maxilla; n, nasal; p, parietal; pl, palatine; pm, premaxilla; po, postorbital; pp, postparietal; prf, prefrontal; ps, parasphenoid; pt, pterygoid; ptf, postfrontal; q, quadrate; qj, quadratojugal; se, sphenethmoid; sm, septomaxilla; sq, squamosal; st, supratemporal; t, tabular; v, vomer.

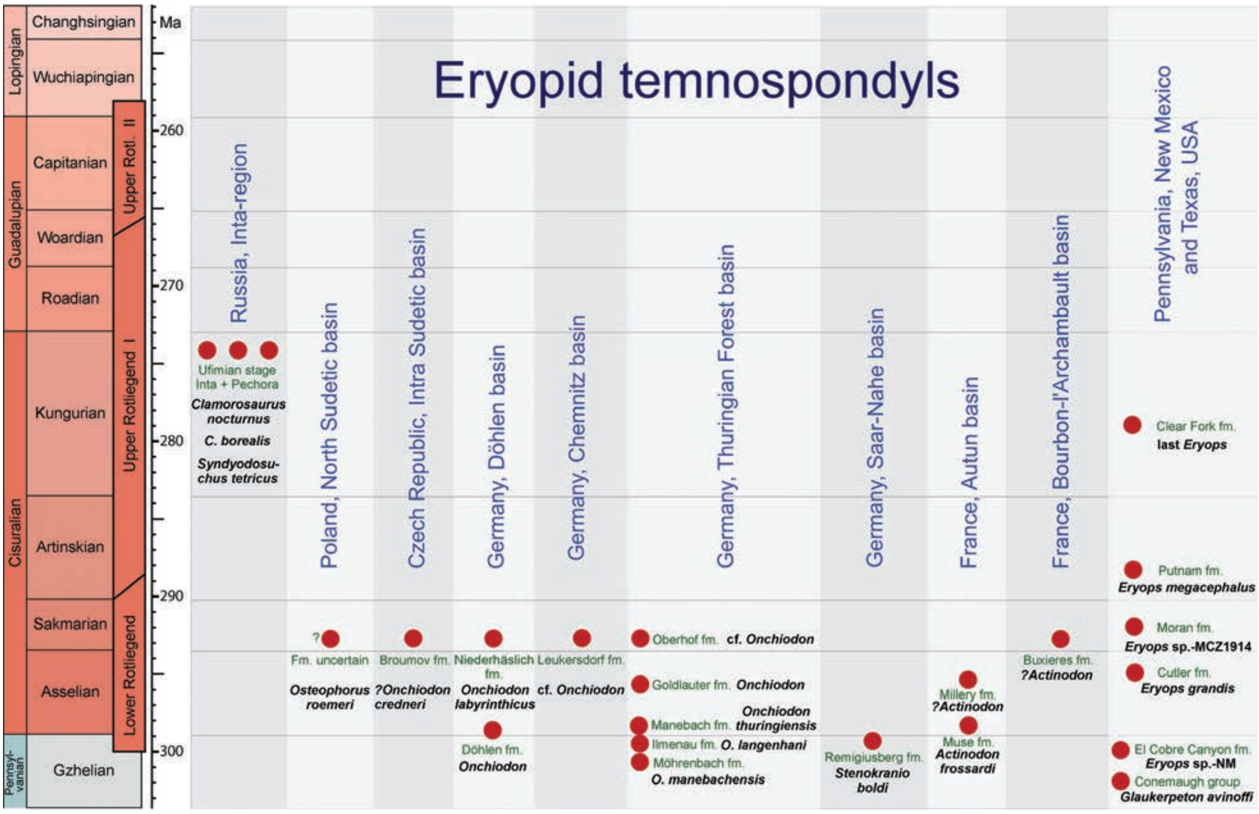

Figure 16. Eryopid temnospondyls of the world in geological time. Abbreviations: Fm, fm., formation; NM, New Mexico (after age-calibrating in Schneider et al. 2020 and Spindler 2024).

This yielded one most parsimonious tree with a tree length of 61.2911, a Consistency index CI of 0.6191, and a Retention Index of 0.8627. The intrarelationships of eryopids according to this analysis are shown in Fig. 19.

Analysis with unweighted characters

This analysis finds a monophyletic Eryopidae, similar to the analyses of Schoch (2021) and Werneburg et al. (2023), but in contrast to the latter analysis, *Actinodon frossardi* is unambiguosly an eryopid. Apart from *A. frossardi*, the clade comprises *Osteophorus roemeri*, *Syndyodosuchus tetricus*, *Glaukerpeton avinoffi*, *Onchiodon labyrinthicus*, *O. thuringiensis*, *Stenokranio boldi*, *Eryops megacephalus*, *Clamorosaurus nocturnus* and *C. borealis*. The Eryopidae as found in the present analysis are not characterized by any autapomorphic character, but supported by the following derived characters shared with *Acanthostomatops*: #17-1 (the interorbital distance being wider than the orbital width), and #29-1 (ratio length to maximum width of choana smaller than 2). *A. frossardi*, *O. roemeri* and *S. tetricus* are the basalmost eryopids, but their relationships are not resolved, thus forming a polytomy. The more advanced eryopids, comprising *G. avinoffi*, *O. labyrinthicus*, *O. thuringiensis*, *S. boldi*, *E. megacephalus*, *C. nocturnus* and *C. borealis*, are characterized by one unique derived character, the blunt anterior prefrontal end (character #15-1). The basalmost representatives of this group, *G. avinoffi* and *O. labyrinthicus* form a polytomy. The position of the remaining eryopids is resolved, with *O. thuringiensis*, *S. boldi* and *E. megacephalus* forming successive sister taxa to *Clamorosaurus*. This clade is supported by character states #21-0 (postorbital length 50% or more of the length of the postorbital skull table; it is shared with *S. tetricus* and several stereospondylomorphs, and a reversal occurs in *Clamorosaurus*), and character state #67-1 (width of interpterygoid vacuities through skull width at orbital midlength smaller than 0.5; shared with *Platyoposaurus stuckenbergi* and reversal in *Clamorosaurus*). The next grouping consisting of *S. boldi*, *E. megacephalus* and *Clamorosaurus* is characterized by one unique derived character, the choanal width through orbital width equal or larger than 0.9 (#72-1), and the following character states: the lacrimal being shorter than the nasal (character #12-1), shared with *Balanerpeton woodi*, *Micromelerpeton credneri* and several stereospondylomorphs; the ectopterygoid fangs similar to the palatine fangs (#66-0, reversal with respect to *O. thuringiensis*), the ratio skull length to posterior width of skull larger than 1 (#70-0, reversal with respect to more basal eryopids), and the ratio length of external naris through length of orbit 0.6 or larger (#71-1, shared with *P. stuckenbergi* and *Australerpeton cosgriffi*). The sister-group relationship between *E. megacephalus* and *Clamorosaurus* is supported by one unique derived character, the septomaxilla without dorsal exposure (#62-1). A further derived, but not unique character is the laterally constricted premaxillary snout region (#5-1), shared with *O. roemeri* and *Glanochthon*. Finally, *Clamorosaurus nocturnus* and *C. borealis* share the following five derived characters, neither of which is

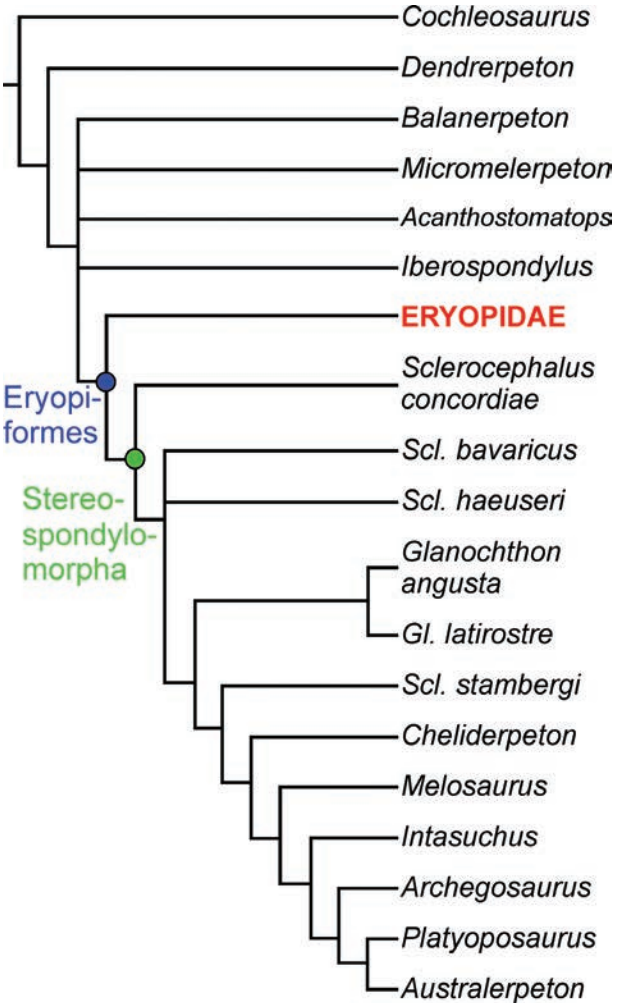

Figure 17. Phylogenetic position of the Eryopidae within temnospondyls based on the analysis with unweighted characters. Strict consensus tree of 23 most parsimonious trees. The intrarelationships of the Eryopidae based on this analysis are shown in Fig. 18.

unique: width of interpterygoid vacuities through skull width on the level of orbital midlength equal or larger than 0.5 (#67-0), and the ratio length to width of interpterygoid vacuities smaller than 1 (#68-1), both character states are shared with several taxa included in this analysis but represent a reversal with respect to the successive outgroup taxa *O. thuringiensis*, *S. boldi* and *E. megacephalus*; the ratio skull length to posterior width of skull being smaller or equal to 1 (#70-1, shared with a number of taxa, but representing a reversal with respect to *S. boldi* and *E. megacephalus*); the orbits being completely visible in ventral view (#73-1, shared with *Intasuchus silvicola*); and the presence of a tooth pit medial to the choana (#74-1, shared with *B. woodi* and *S. tetricus*).

Analysis with reweighted characters

In this second analysis, the intrarelationships of the eryopid taxa are completely resolved. Only those character changes will be listed in the following that supplement the description of the unweighted analysis. Most striking is the fact that *Actinodon frossardi* comes to lie outside Eryopidae and instead turns out to be the basalmost stereospondylomorph. This was also the result in some most parsimonious trees of the analysis conducted by Werneburg et al. (2023). This position of *A. frossardi* is supported by one unambiguous synapomorphy, the interclavicle being longer than half the skull length (#43-1), in contrast to the short interclavicle in eryopids. The basalmost taxon of the Eryopidae as found here is *Syndyodosuchus tetricus*, followed by *Osteophorus roemeri*, *Glaukerpeton avinoffi*, *Onchiodon labyrinthicus*, *O. thuringiensis*, *Stenokranio boldi* and *Eryops megacephalus* as successive outgroups of *Clamorosaurus*. Two autapomorphies characterize the Eryopidae, the length of the posterior skull table measuring 0.4–0.6 its width (#19-3) and a longer ectopterygoid than palatine (#61-1, with a reversal in *C. borealis*). The clade is further supported by the following character: a shorter frontal than nasal (#16-1, with a reversal in *G. avinoffi*, shared with *Glanochthon* and the sterospondylomorph taxa crownwards of *Sclerocephalus stambergi*). The next clade comprising *O. roemeri*, *G. avinoffi*, *O. labyrinthicus*, *O. thuringiensis*, *S. boldi*, *E. megacephalus* and *Clamorosaurus*, is characterized by one autapomorphy, the lacrimal with its lateral suture posterolaterally expanded (#13-1). *O. labyrinthicus*, *O. thuringiensis*, *S. boldi*, *E. megacephalus* and *Clamorosaurus* are united by four derived, but not unique characters: prominent ridges on the skull roof connect orbits with nares and tabular horns (#60-1, shared with *Cochleosaurus bohemicus*); infraorbital bar equal to or wider than interorbital distance (#64-1, shared with *Acanthostomatops vorax*); the ectopterygoid fangs greatly reduced in size (#66-1, reversal in *S. boldi*, *E. megacephalus* and *C. borealis*); and the distance of the choana to the interpterygoid vacuities measuring about half the length of the choana or more (#69-1, reversal in *C. borealis*, shared with *Cochleosaurus bohemicus*, *Sclerocephalus concordiae* and the long-snouted stereospondylomorphs *Archegosaurus decheni*, *Platyoposaurus stuckenbergi* and *Australerpeton cosgriffi*).

Discussion

Phylogeny of eryopids

As revealed by the analyses of Schoch (2021) and Werneburg et al. (2023), both the unweighted and the reweighted analysis in the present study finds a monophyletic Eryopiformes that is divided in two monophyletic groups, the Eryopidae and the Stereospondylomorpha. However, the intrarelationships of the basal eryopids are still not resolved, as shown by the two polytomies in the unweighted analysis. This is also indicated by the different positions of *Actinodon frossardi*, which is a basal eryopid in the unweighted analysis and a basal stereospondylomorph in the reweighted one, reflecting the similarities in skeletal morphology and proportions between basal eryopiforms. In this respect it fits well that *Syndyodosuchus tetricus*, formerly interpreted as a basal stereospondylomorph

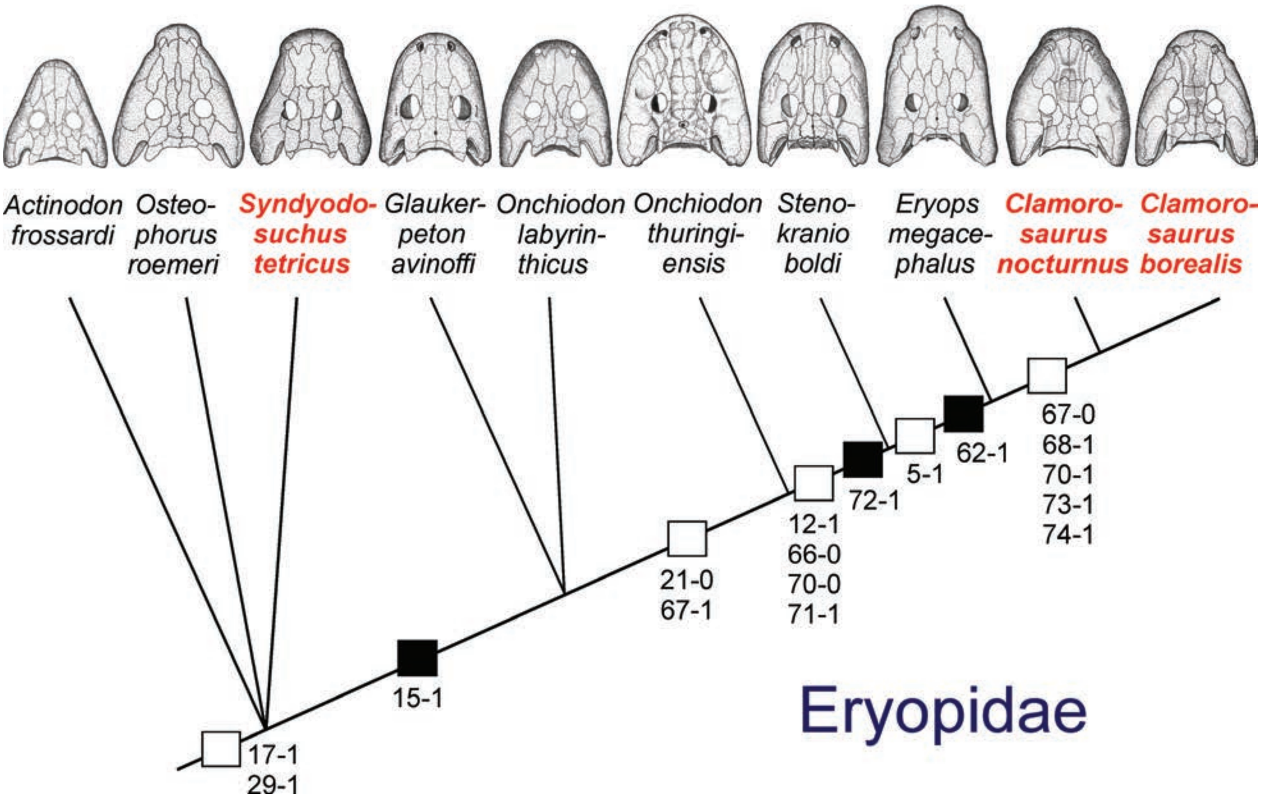

Figure 18. Intrarelationships of the different species of Eryopidae. Strict consensus tree of 23 most parsimonious trees, based on the analysis with unweighted characters. Supporting characters are mapped on nodes, with synapomorphies represented by black and homoplasies by white rectangles. The numbers refer to the characters listed in Suppl. material 1.

(Konzhukova 1956; Gubin 1984; Schoch and Milner 2000; Shishkin et al. 2000), turned out to be a basal eryopid in the present study. However, the synapomorphy uniting *A. frossardi* with stereospondylomorphs in our second analysis, the long interclavicle, is a rather ambiguous character when eryopid ontogeny is considered, which is well known in *Onchiodon labyrinthicus*. Here it has been shown that the interclavicle is an elongate element in larvae, as in stereospondylomorphs, and becomes proportionally shorter during further ontogeny (Boy 1990; Witzmann 2005a). Thus, one can easily imagine a long interclavicle as an adult character of basal eryopids. An interesting aspect of the present analyses is the fact that *Onchiodon* is not monophyletic, as first revealed by the analysis of Werneburg et al. (2023). As in the latter study, *O. thuringiensis* is more derived than *O. labyrinthicus*, here forming the sister group to *Stenokranio boldi*, *Eryops megacephalus* and *Clamorosaurus*.

The phylogenetic position of *Clamorosaurus* among the most derived eryopids is congruent with its young stratigraphic age, whereas for *S. tetricus* as a basal eryopid a long ghost lineage has to be assumed.

Palecology of the Russian eryopids

Although occurring at the same time (Ufimian, late Kungurian), *Clamorosaurus nocturnus*, *C. borealis* and *Syndyodosuchus tetricus* inhabited different environments. Both *Clamorosaurus* species were discovered in lacustrine limestones; *C. nocturnus* near the town of Pechora in the Sheshminskian Gorizont and *C. borealis* near the town of Inta in the Intinskaya Svita (Inta Formation). In contrast, *S. tetricus* was found together with *Intasuchus silvicola* in coal beds of the Ufimian Intinskaya Svita near the ‘Greater Inta River’, which can be interpreted as a habitat of a coal swamp lake comparable to that of Nýřany in the Czech Republic (Milner 1980). Following Konzhukova (1956) and Gubin (1983, 1984), Shishkin et al. (2000) regarded the temnospondyls of the Inta fauna – the eryopids described here plus the intasuchid stereospondylomorph *Intasuchus silvicola* that was found together with *Syndyodosuchus tetricus* – as terrestrial forms. Only later, in the Kazanian and early Tatarian, the composition of the temnospondyl assemblages in European Russia changed to aquatic forms like the melosaurid and archegosaurid stereospondylomorphs (Shishkin et al. 2000).

Indeed, eryopids were traditionally interpreted as terrestrial or semi-terrestrial animals (Yates and Warren 2000) mainly because of the lack of lateral line sulci and the heavily ossified postcranial skeleton at least in *Eryops megacephalus*, like the huge scapulocoracoid, the well ossified, stout limbs, and the massive ribs with hook- and blade-like uncinate processes (Miner 1925; Moulton 1974; Pawley and Warren 2006). However, the situation is not so clear cut as often claimed in the literature. Although probably capable of land excursions, these animals were certainly rather sluggish on land, and long bone histology indicates that eryopids may

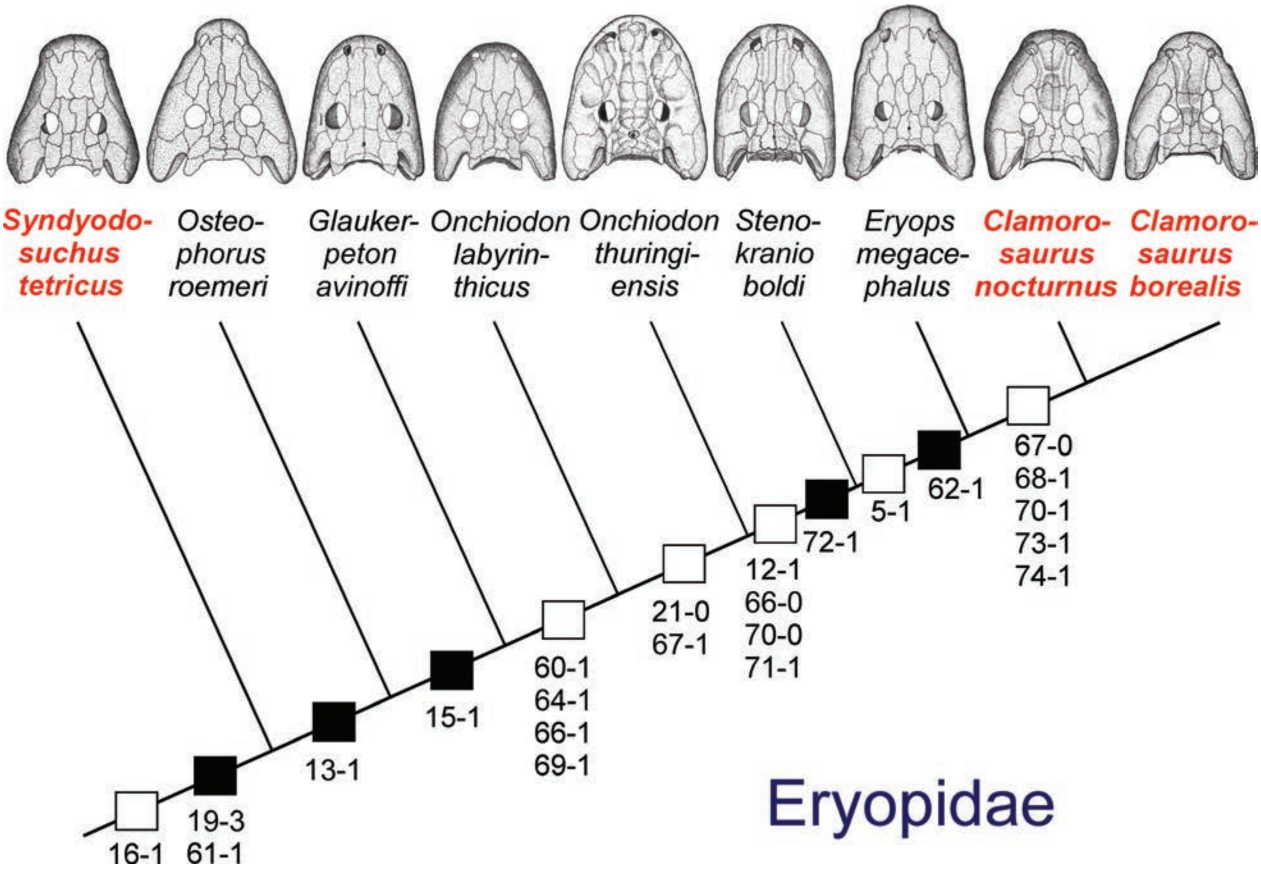

Figure 19. Intrarelationships of the different species of Eryopidae, single most parsimonious tree, based on the analysis with reweighted characters. Supporting characters are mapped on nodes, with synapomorphies represented by black and homoplasies by white rectangles. The numbers refer to the characters listed in Suppl. material 1.

have used their strong limbs for locomotion in water rather than on land (Sanchez et al. 2010; Konietzko-Meier et al. 2016). Furthermore, their fish-eater dentition suggests that eryopids searched for fishes and small tetrapods in the water (Schoch 2009, 2014). Thus, eryopids may best be designated as semi-aquatic temnospondyls (Witzmann 2016). In the specific case of *Clamorosaurus* and *Syndyodosuchus*, we have no evidence for a terrestrial mode of life as suggested by earlier authors. The fact that lateral line sulci are absent is no indication for the absence of this sense organ: the lateral line system could have been either enclosed in canals within the skull bones, as in *Eryops* (Warren 2007), or the lateral lines may have been located superficially in the skin without leaving traces on the bone surface, as in extant amphibians (Laurin et al. 2004). Furthermore, the dentition largely corresponds to that of other eryopids that have been interpreted as aquatic feeders (see above). Unfortunately, no inferences can be drawn from the postcranial skeleton since it is either completely unknown or very fragmentary in the eryopids described here.

Conclusions

Our redescription of *Clamorosaurus nocturnus*, *C. borealis* and *Syndyodosuchus tetricus* from the Ufimian-age Inta fauna (late Kungurian, Cisuralian, Permian) of the Komi Republic, Russia, confirms the eryopid assignment of *Clamorosaurus*, but moves *S. tetricus* from the base of the stereospondylomorphs to eryopids. Thus, two genera and three species of valid eryopid temnospondyls occur in Russia and are the geologically youngest known representatives of this family. The genus *Clamorosaurus* Gubin, 1983 is characterized by one autapomorphy, the very wide interpterygoid vacuities with the orbits not being obscured in palatal view. *Clamorosaurus nocturnus* Gubin, 1983, from the Sheshminskian horizon of the Pechora River has no autapomorphy but a diagnostic combination of 17 characters. *Clamorosaurus borealis* Gubin, 1983, from the Intinskaya Svita near the town of Inta is characterized by four autapomorphies: (1) only six tooth loci on the premaxilla, (2) only 21 tooth loci on the maxilla, (3) the supratemporal being much wider than long, and (4) the cultriform process of the parasphenoid being much shorter than the median length of the vomer. Although it cannot be ruled out that characters (1) and (2) are linked to ontogeny, we regard this as unlikely, as discussed above. *Syndyodosuchus tetricus* Konzhukova, 1956 from the Intinskaya Svita near the ‘Greater Inta River’ has three autapomorphies: (1) the tiny tabular, (2) the very large internarial width, and (3) the very narrow postorbital. Two phylogenetic analyses, a first one with unweighted and a second one with reweighted characters, finds a monophyletic Eryopidae. Whereas in the first analysis *Syndyodosuchus tetricus* forms a basal polytomy with *Actinodon frossardi* and *Osteophorus roemeri*, *A. frossardi* is a possible basal sterospondylomorph and *S. tetricus* forms the basalmost eryopid in the second analysis. In both analyses, *Eryops megacephalus* and a monophyletic *Clamorosaurus* form the most derived eryopids. The phylogenetic position of *Clamorosaurus* is congruent with its young stratigraphic age, whereas for *S. tetricus* as a basal eryopid a long ghost lineage has to be assumed. There is no evidence that the Russian eryopids were terrestrially adapted, as previously assumed. Rather, they can best be designated as semi-aquatic.

Acknowledgments

We are indebted to two anonymous reviewers whose comments improved the manuscript substantially. Yuri Gubin (†) and Igor Novikov (PIN, Moscow) are thanked for the possibility to work on the Permian amphibians in the PIN. The senior author started the constructive cooperation with the PIN in 1985 and continued with several stays in Moscow. Marcello Ruta, Rainer Schoch and David Marjanović are thanked for help with the phylogenetic analysis.

References

Boy JA (1990) Über einige Vertreter der Eryopoidea (Amphibia: Temnospondyli) aus dem europäischen Rotliegend (?höchstes Karbon-Perm). 3. *Onchiodon*. Paläontologische Zeitschrift 64: 287–312. https://doi.org/10.1007/BF02985720

Case EC (1911) Revision of the Amphibia and Pisces of the Permian of North America. Publications of the Carnegie Institute Washington 146: 1–179. https://doi.org/10.5962/bhl.title.56586

Čerňanský A, Witzmann F, Klembara J, Van Heteren AH (2016) The quadratojugal of *Eryops* studied by computed tomography and the morphological variability of foramina and canals in the quadratojugal of basal tetrapods. Anatomical Record 299(8): 1073–1079. https://doi.org/10.1002/ar.23373

Cope ED (1882) The rhachitomous Stegocephala. American Nature 16: 334–335. https://doi.org/10.1086/273100

Golubev VK (2005) Permian Tetrapod Stratigraphy. In: Lucas SG, Zeigler KE (Eds) The Nonmarine Permian. New Mexico Museum of Natural History and Science 30: 95–99.

Gubin YM (1983) The first eryopids from the Permian of the East-European Platform. Palaeontologiceskij Zhurnal 1983: 110–115. [in Russian]

Gubin YM (1984) On the systematic position of the intasuchids. Paleontologicheskiy zhurnal 1984(2): 118–120. [in Russian]

Gubin YM (1991) Permian archegosauroid amphibians of the USSR. Trudy Paleontologichesko Instituta Nauka SSSR 249: 1–138. [in Russian]

Jaekel O (1909) Über die Klassen der Tetrapoden. Zoologischer Anzeiger 34: 193–212.

Konietzko-Meier D, Shelton CD, Sander PM (2016) The discrepancy between morphological and microanatomical patterns of anamniotic stegocephalian postcrania from the Early Permian Briar Creek Bonebed (Texas). Comptes Rendus Palevol 15(1–2): 103–114. https://doi.org/10.1016/j.crpv.2015.06.005

Konzhukova ED (1956) The Intan Lower Permian fauna of the northern Ural region. Trudy Paleontologicheskogo Instituta Akademii Nauk SSSR 62: 5–50. [in Russian]

Laurin M, Girondot M, Loth MM (2004) The evolution of long bone microanatomy and lifestyle in lissamphibians. Paleobiology 30: 589–613. https://doi.org/10.1666/0094-8373(2004)030%3C0589:TEOLBM%3E2.0.CO;2

Linnaeus C von (1758) Systema naturae per regna tria naturae, secundum classes, ordines, genera, species, cum characteribus, differentiis, synonymis, locis. 10(1). L Salvii, Stockholm, Sweden, 823 pp. https://doi.org/10.5962/bhl.title.542

Meyer H von (1860) *Osteophorus römeri* aus dem Rothliegenden von Klein Neundorf in Schlesien. Palaeontographica 7: 1–99.

Milner AR (1980) The Tetrapod Assemblage from Nýřany, Czechoslovakia. Systematics Association Special Volume Series 15: 439–496.

Milner AR (1989) The relationships of the eryopoid–grade temnospondyl amphibians from the Permian of Europe. Acta Musei Reginaehradecensis 22: 131–137.

Milner AR (1990) Chapter 15. The radiations of temnospondyl amphibians. In: Taylor PD, Larwood GP (Eds) Major Evolutionary Radiations. Systematics Association Special Volume 42: 321–349. https://doi.org/10.1093/oso/9780198577188.003.0015

Miner RW (1925) The pectoral limb of *Eryops* and other primitive tetrapods. Bulletin of the American Museum of Natural History 51: 145–312.

Moulton JM (1974) A description of the vertebral column of *Eryops* based on the notes and drawings of A.S. Romer. Breviora 428: 1–44.

Pawley K, Warren AA (2006) The appendicular skeleton of *Eryops megacephalus* Cope, 1877 (Temnospondyli: Eryopoidea) from the Lower Permian of North America. Journal of Paleontology 80: 561–580. https://doi.org/10.1666/0022-3360(2006)80[561:TASOEM]2.0.CO;2

Romer AS (1947) Review of the Labyrinthodontia. Bulletin of the Museum of Comparative Zoology Harvard 99: 1–367.

Romer AS (1952) Late Pennsylvanian and Early Permian vertebrates in the Pittsburgh-West Virginia region. Annals of Carnegie Museum 33: 47–113. https://doi.org/10.5962/p.215221

Sanchez S, Germain D, de Ricqlès A, Abourachi A, Goussard F, Tafforeau P (2010) Limb-bone histology of temnospondyls: implications for understanding the diversification of palaeoecologies and patterns of locomotion of Permo-Triassic tetrapods. Journal of Evolutionary Biology 23: 2076–2090. https://doi.org/10.1111/j.1420-9101.2010.02081.x

Sawin HJ (1941) The cranial anatomy of *Eryops megacephalus*. Bulletin of the Museum of Comparative Zoology, Harvard College 88: 405–464.

Schneider JW, Lucas SG, Scholze F, Voigt S, Marchetti L, Klein H, Oplustil S, Werneburg R, Golubev VK, Barrick JE, Nemyrovska T, Ronchi A, Day MO, Silantiev VV, Rößler R, Saber H, Linnemann U, Zharinova V, Shen S-Z (2020) Late Paleozoic–early Mesozoic continental biostratigraphy - Links to the Standard Global Chronostratigraphic Scale. Palaeoworld 29: 186–238. https://doi.org/10.1016/j.palwor.2019.09.001

Schoch RR, Hampe O (2004) An eryopid-like temnospondyl from the Lower Rotliegend Meisenheim Formation of the Saar-Nahe Basin. Neues Jahrbuch für Geologie und Paläontologie 232: 315–323. https://doi.org/10.1127/njgpa/232/2004/315

Schoch RR (2009) Evolution of life cycles in early amphibians. Annual Review of Earth and Planetary Sciences 37: 135–162. https://doi.org/10.1146/annurev.earth.031208.100113

Schoch RR (2014) Amphibian evolution. The life of early land vertebrates. John Wiley & Sons, Chichester, UK, 264 pp. https://doi.org/10.1002/9781118759127

Schoch RR (2021) The life cycle in late Paleozoic eryopid temnospondyls: developmental variation, plasticity and phylogeny. Fossil Record 24: 295–319. https://doi.org/10.5194/fr-24-295-2021

Schoch RR, Milner AR (2000) Encyclopedia of Paleoherpetology, Part 3B, Stereospondyli. Verlag Dr. Friedrich Pfeil, Munich, 203 pp.

Schoch RR, Milner AR (2014) Encyclopedia of Paleoherpetology, Part 3A2, Temnospondyli I. Verlag Dr. Friedrich Pfeil, Munich, 150 pp.

Schoch RR, Sobral G (2021) A new species of *Sclerocephalus* with a fully ossified endocranium gives insight into braincase evolution in temnospondyls. Journal of Paleontology 95(6): 1308–1320. https://doi.org/10.1017/jpa.2021.51

Spindler F (2024) Amnioten. In: Werneburg R, Schneider JW (Eds) Rotliegend-Fauna des Thüringer Waldes: Semana Sonderveröffentlichung cap. 16: 171–183.

Swofford D (2021) PAUP* (*Phylogenetic Analysis Using PAUP). Version 4.0a169. PhyloSolutions. http://phylosolutions.com/paup-test/

Shishkin MA, Novikov IV, Gubin YM (2000) Permian and Triassic temnospondyls from Russia. In: Benton MJ, Shishkin MA, Unwin DM, Kurochkin EN (Eds) The age of dinosaurs in Russia and Mongolia. Cambridge University Press, Cambridge, UK, 35–59.

Warren AA (2007) New data on *Ossinodus pueri*, a stem tetrapod from the Early Carboniferous of Australia. Journal of Paleontology 27: 850–862. https://doi.org/10.1671/0272-4634(2007)27[850:NDOOPA]2.0.CO;2

Werneburg R (1987) Schädelrest eines sehr großwüchsigen Eryopiden (Amphibia) aus dem Unterrotliegenden (Unterperm) des Thüringer Waldes. Veröffentlichungen des Naturhistorischen Museums Schleusingen 2: 52–56.

Werneburg R (1993) *Onchiodon* (Eryopidae, Amphibia) aus dem Rotliegend des Innersudetischen Beckens (Böhmen). Paläontologische Zeitschrift 67(3/4): 343–355. https://doi.org/10.1007/BF02990287

Werneburg R (1997) Der Eryopide *Onchiodon* (Amphibia) aus dem Rotliegend des Beckens von Autun (Frankreich). Freiberger Forschungshefte C 466: 167–181.

Werneburg R (2007) Der "Manebacher Saurier" – ein neuer großer Eryopide (*Onchiodon*) aus dem Rotliegend (Unter-Perm) des Thüringer Waldes. Veröffentlichungen Naturhistorisches Museum Schleusingen 22: 3–40.

Werneburg R, Lucas S, Schneider JW, Rinehart LF (2010) First Pennsylvanian *Eryops* (Temnospondyli) and its Permian record from New Mexico. In: Lucas SG, Schneider JW, Spielmann JA (Eds) Carboniferous-Permian transition in Canõn del Cobre, northern New Mexico. New Mexico Museum of Natural History and Science, Bulletin 49: 129–135.

Werneburg R, Steyer JS (1999) Redescription of the holotype of *Actinodon frossardi* (Amphibian, Temnospondyli) from the Lower Rotliegend of the Autun Basin (Lower Permian, France). Geobios 32(4): 599–607. https://doi.org/10.1016/S0016-6995(99)80009-6

Werneburg R, Berman DS (2012) Revision of the aquatic eryopid temnospondyl *Glaukerpeton avinoffi* Romer, 1952, from the Upper Pennsylvanian of North America. Annals of Carnegie Museum 81(1): 45–72. https://doi.org/10.2992/007.081.0103

Werneburg R, Štamberg S, Steyer J-S (2020) A new stereospondylomorph, *Korkonterpeton kalnense* gen. et sp. nov., from lower Permian of the Czech Krkonoše Piedmont Basin and a redescription of *Intasuchus silvicola* from the lower Permian of Russia (Temnospondyli, Amphibia). Fossil Imprint 76(2): 217–242. https://doi.org/10.37520/fi.2020.019

Werneburg R, Witzmann F, Rinehart L, Fischer J, Voigt S (2023) A new eryopid temnospondyl from the Carboniferous–Permian boundary of Germany. Journal of Paleontology 97(6): 1251–1281. https://doi.org/10.1017/jpa.2023.58

Witzmann F (2005a) Hyobranchial and postcranial ontogeny of the temnospondyl *Onchiodon labyrinthicus* (Geinitz, 1861) from Niederhäslich (Dohlen Basin, Autunian, Saxony). Paläontologische Zeitschrift 79: 479–492. https://doi.org/10.1007/BF02988374

Witzmann F (2005b) Cranial morphology and ontogeny of the Permo-Carboniferous temnospondyl *Archegosaurus decheni* Goldfuss, 1847 from the Saar–Nahe Basin, Germany. Earth and Environmental Science Transactions of The Royal Society of Edinburgh 96(2): 131–162. https://doi.org/10.1017/S0263593300001279

Witzmann F (2013) The stratigraphically oldest eryopoid temnospondyl from the Permo-Carboniferous Saar-Nahe Basin, Germany. Paläontologische Zeitschrift 87: 259–267. https://doi.org/10.1007/s12542-012-0152-2

Witzmann F (2016) CO_2-metabolism in early tetrapods revisited: inferences from osteological correlates of gills, skin and lung ventilation in the fossil record. Lethaia 49: 492–506. https://doi.org/10.1111/let.12161

Witzmann F, Voigt S (2014) An *Eryops*-like interclavicle from the Early Permian of the Saar-Nahe Basin, and a discussion of temnospondyl interclavicle characters. Paläontologische Zeitschrift 89: 449–458. https://doi.org/10.1007/s12542-014-0235-3

Witzmann F, Scholz H, Müller J, Kardjilov N (2010) Sculpture and vascularization of dermal bones, and the implications for the physiology of basal tetrapods. Zoological Journal of the Linnean Society 160: 302–340. https://doi.org/10.1111/j.1096-3642.2009.00599.x

Yates AM, Warren AA (2000) The phylogeny of the 'higher' temnospondyls (Vertebrata: Choanata) and its implications for the monophyly and origins of the Stereospondyli. Zoological Journal of the Linnean Society 128: 77–121. https://doi.org/10.1111/j.1096-3642.2000.tb00650.x

Zittel KA von (1888–90) Handbuch der Paläontologie. 1. Abtheilung. III. Band. Paläozoologie. Vertebrata (Pisces, Amphibia, Reptilia, Aves). R. Oldenbourg, München and Leipzig, 900 pp.

Supplementary material 1

Character list and the character-taxon matrix

Authors: Ralf Werneburg, Florian Witzmann

Data type: docx

Explanation note: The supplementary information consists of two parts, the character list and the character-taxon matrix for the phylogenetic analysis.

Link: https://doi.org/10.3897/fr.27.125460.suppl1

Fossil Record 27 (3) 2024, 381–400 | DOI 10.3897/fr.27.121996

Unexpected temnospondyl diversity in the early Carnian Grabfeld Formation (Germany) and the palaeogeography of metoposaurids

Raphael Moreno[1,2], Sanjukta Chakravorti[1,2], Samuel L. A. Cooper[1,2], Rainer R. Schoch[1,2]

1 *Staatliches Museum für Naturkunde Stuttgart, Rosenstein 1, 70191 Stuttgart, Germany*
2 *Fachgebiet Paläontologie, Institute für Biologie, Universität Hohenheim, 70599 Stuttgart, Germany*

https://zoobank.org/00E2F554-551C-47A1-976A-1D9CDE52885B

Corresponding author: Raphael Moreno (raphael.moreno@smns-bw.de)

Academic editor: Florian Witzmann ♦ **Received** 29 February 2024 ♦ **Accepted** 24 June 2024 ♦ **Published** 30 December 2024

Abstract

The Middle–Late Triassic Grabfeld Formation formed in a generally arid, hostile setting with frequent evaporation under alternating sabkha and playa conditions. Here we report evidence of four temnospondyl taxa from the upper part of the sequence (‘Bunte Estherienschichten’), including (1) *Metoposaurus* sp., (2) a capitosaur, (3) *Gerrothorax* sp. and (4) *Plagiosternum* sp. This early Carnian assemblage provides the stratigraphically oldest evidence of metoposaurids and the last report of plagiosternines in the Central European Basin. The stratigraphic age of these strata and the occurrence of Metoposauridae therein sheds new light on the palaeogeographic distribution of the group and their occurrence before the Carnian Pluvial Event.

Key Words

Euryhaline, Gipskeuper, Late Triassic, *Metoposaurus*, Middle Keuper, Temnospondyli

Introduction

The Triassic Keuper sequence of the Central European Basin (CEB) is particularly noteworthy for preserving a variety of distinct, large-bodied temnospondyl amphibians (Schoch 2021). During the Triassic (251–201 Ma), temnospondyls were relatively abundant and display high levels of morphological disparity and taxonomic diversity (Schoch and Milner 2000, 2014). Temnospondyls achieved a near global distribution across the slowly rifting Pangaean supercontinent, and hence today preserve rich fossil assemblages on all continents (Schoch 2000). The diverse temnospondyl assemblage of the German Keuper (see Schoch 2021 for an overview) is comprised of capitosaurs (*Mastodonsaurus*, *Tatrasuchus*, *Capitosaurus*, *Cyclotosaurus*), plagiosaurs (*Plagiosaurus*, *Plagiosuchus*, *Gerrothorax*, *Plagiosternum*, *Megalophthalma*), trematosaurs (*Trematolestes*, *Hyperokynodon*) and metoposaurs (*Callistomordax*, *Metoposaurus*). The occurrence of often multiple taxa in these German fossil localities (Schoch and Moreno 2024) indicate stable habitation conditions, which allowed for niche partitioning among the different groups. While the large capitosaurs likely occupied the role of apex predators in these aquatic realms, the streamlined trematosaurs and related metoposaurs pursued active hunting strategies (Fortuny et al. 2017a; Kalita et al. 2022). With their flat bodies and hypothesised tolerance for changing environmental conditions (Sanchez and Schoch 2013), plagiosaurs are regarded as generalists, feeding at the bottom of lakes and fluvial systems. The stratigraphic range of capitosaurs extends from the Induan to the Rhaetian (Schoch and Milner 2000; Konietzko-Meier et al. 2019). Plagiosaurs occur from the Ladinian to the Rhaetian (Schoch and Milner 2014).

The Late Triassic family Metoposauridae Watson 1919 (Table 1) combine a near-global distribution with a relatively short stratigraphic range (Lucas 2020). Therefore, they have been considered by some authors to be a key tetrapod group for terrestrial biostratigraphic correlation (Lucas 2020). Metoposaurids were two-to-four-meter long stereospondyl temnospondyls characterised by short limbs and flat skulls with anteriorly placed orbits and needle-like teeth (Sulej 2007). Based on previously published records, the Metoposauridae of Central and Western Europe (Fig. 1A) have a brief stratigraphic range from the late Carnian to late Norian, with the oldest described CEB materials originating from the Stuttgart Formation (231 Ma; Zeh et al. 2021) in southern Germany (Sulej 2002, 2007). Outside the CEB, metoposaurids are described from the Carnian of Morocco (Jalil 1999), Madagascar (Fortuny et al. 2019) and India (Chakravorti and Sengupta 2019). Furthermore, metoposaurids occur in North America where they occupy their longest stratigraphic range from the middle Carnian to the Rhaetian (Hunt 1993). However, no records of Metoposauridae have yet been definitely identified from the base of the earliest Carnian.

Here, we review the diversity of temnospondyl remains from the Grabfeld Formation, a late Ladinian–early Carnian rock sequence of southern Germany. This formation is characterized by evaporites and mudstone-dominated sabkha and playa deposits with few fossiliferous horizons. Even temnospondyls, the most abundant tetrapod group in the German Triassic, are notoriously rare in the Grabfeld Formation and their taxonomy had long remained elusive. All specimens reviewed herein fall within the upper part of the sequence, the ‘Bunte Estherienschichten’ (Fig. 1). So far, the only described occurrence is an isolated temnospondyl clavicle tentatively assigned to *Metoposaurus* sp. by Wild (1974). However, this record has either been overlooked or rejected by subsequent review studies (Schoch and Wild 1999; Schoch 2021) as it has not been cited, and consequently the stratigraphic range of metoposaurids was figured to start in the basal part of the Stuttgart Formation (late Carnian; Schoch 2021). The objective of the present study is to examine the available body of evidence on temnospondyls from the Grabfeld Formation with particular emphasis on metoposaurids and their revised palaeobiogeographic and stratigraphic distributions.

Geological setting

Southern Germany is famous for its unique geological landscape. Among the most prominent natural regions of the South German Scarplands are the Keuper escarpments with its outcrops of Middle and Late Triassic epicontinental strata (Fig. 1).

The strata between the brackish lacustrine sediments of the Erfurt Formation (Lower Keuper) and the fluvial dominated sandstones of the Stuttgart Formation (Schilfsandstein) have historically received varying nomenclature in different regions of southern Germany (Nitsch et al. 2005). In the latter half of the 20th century the Keuper strata had been investigated more intensively (Gwinner 1980) and the general comprehension of regional correlation of these strata began to be better understood. Often confusing regional terminology was unified (see Nitsch et al. 2005 for a summary on the topic) and the term Grabfeld Formation was coined by the DEUTSCHE STRATIGRAPHISCHE KOMMISSION to define the succession (DSK 2005; Nitsch et al. 2005).

The Grabfeld Formation consists mostly of grey and occasionally coloured clays that are separated by numerous thin dolomitic banks (Nitsch 1996; Etzold and Schweizer 2005; Freudenberger 2005). Stratigraphic correlation of the formation is based mostly on these dolomitic banks that allow for basin wide correlation (Nitsch 1996). The Grabfeld Formation is wedged in by the underlying Ladinian Erfurt Formation, which encompasses a carbonate siliciclastic succession deposited in a deltaic environmental setting that is influenced by lagoonal and transgressive sequences (Mujal and Schoch 2020). The overlying Stuttgart Formation of the Middle Keuper was deposited in a similar palaeoenvironmental setting that was dominated by fluvial systems (Stollhofen et al. 2008).

The Grabfeld Formation encompasses alternating sabkha and playa deposits that formed during a transition towards a more arid climate (Nitsch et al. 2005). The sedimentary succession represents small-cycle deposits of brackish to saline ephemeral lakes.

Table 1. Spatial and temporal ranges of the family Metoposauridae.

Name	Age range	Region	Reference
Metoposaurus diagnosticus	middle Carnian	Europe	Milner and Schoch 2004
Metoposaurus krasiejowensis	late Carnian – middle/late Norian	Europe	Sulej 2007
Metoposaurus algarvensis	middle Carnian – middle/late Norian	Europe	Witzmann and Gassner 2008; Brusatte et al. 2015
Almasaurus habazzi	middle Carnian	Morocco	Jalil 1999
Dutuitosaurus ouazzoui	middle Carnian	Morocco	Jalil 1999
Arganasaurus lyazidi	middle Carnian – late Carnian	Morocco	Jalil 1999
Arganasaurus azerouali	middle Carnian – late Carnian	Morocco	Jalil 1999
“*Metoposaurus hoffmani*” *	middle Carnian – late Carnian	Madagascar	Fortuny et al. 2019
Panthasaurus maleriensis	middle Carnian – late Carnian	India	Chakravorti and Sengupta 2019
Anaschisma browni	middle Carnian – late Norian	North America	Hunt 1993
Buettnererpeton bakeri	middle Carnian – late Carnian	North America	Gee and Kufner 2022
Apachesaurus gregorii	late Carnian – Rhaetian	North America	Hunt 1993
Metoposauridae indet.	middle Carnian – Rhaetian	North America	Baird 1986; Spielmann and Lucas 2012; Heckert and Lucas 2015
Metoposauridae indet.	late Norian	Zimbabwe	Barrett et al. 2020

* this species was recently identified a *nomen dubium* by Fortuny et al. (2019).

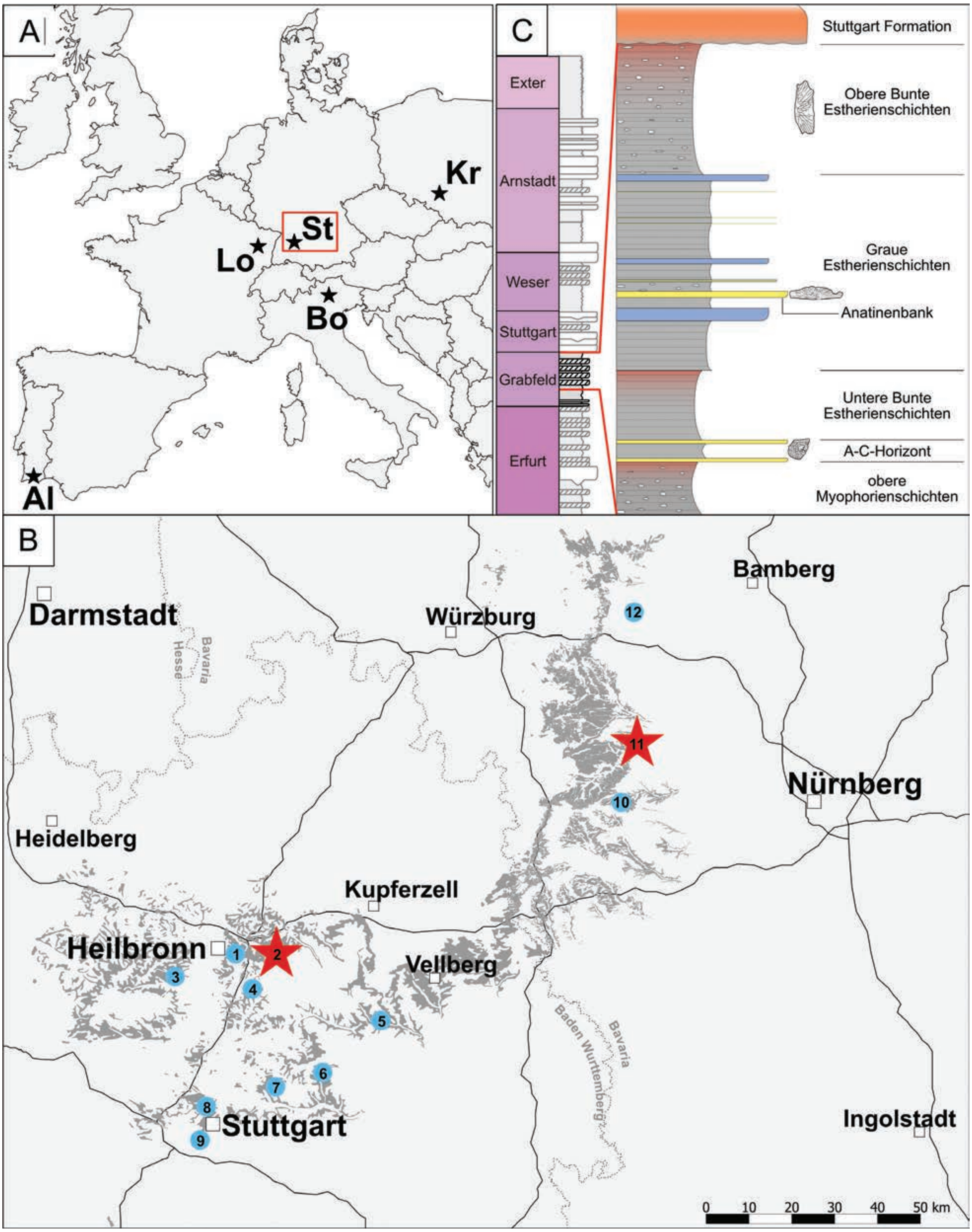

Figure 1. A. Distribution of *Metoposaurus* in Europe; **B.** *Metoposaurus*-bearing fossil localities in southern Germany. Blue circles indicate localities within the Stuttgart Formation, while red stars indicate localities with Grabfeld Formation occurrence; **C.** Stratigraphic log of the Grabfeld Formation following (Emmert et al. 1974; Nitsch et al. 2005), stratigraphic column modified from (Schoch and Moreno 2024). Lo – Lorraine, Saint-Nicolas-de-Port quarry, St – Stuttgart, Baden-Württemberg, Bo – Bolzano, Raibl beds, Kr – Krasiejów, Al – Algarve, Portugal. (1) Jägerhaus quarry Heilbronn, (2) Affaltrach, (3) Stockheim (Brackenheim), (4) Rote Wand Helfenberg, (5) Fichtenberg-Michelbächle, (6) Geißgurgelbach, (7) Winnenden Hannweiler, (8) Stuttgart Feuerbacher Heide, (9) Stuttgart Sonnenberg, (10) Markt Obernzenn–Ipsheim (Kaubenheim) area, (11) Neustadt an der Aisch, (12) Ebrach. **A–C**-Horizont – Acrodus-Corbula-Horizont.

These cyclothems are ideally tripartite and consist of a claystone–dolomite horizon (ephemeral and ingression phase), followed by an evaporitic sulphate horizon (playa phase) and an unstratified claystone–nodular sulphate horizon (palaeosol phase; Aigner and Bachmann 1992; Nitsch et al. 2005).

Thürach (1888) first divided the Grabfeld Formation into lower, middle and upper sections, a system which is still followed today. These sections of the Grabfeld Formation encompass an evaporitic-siliciclastic intercalation. In the middle Grabfeld Formation, repeated marine ingressions form thin dolomitic beds. However, a marine influence for these beds is still debated for the higher parts of the succession starting from the 'Acrodus-Corbula Horizont' (Fig. 2) (Linck 1972; Aigner and Bachmann 1992; Nitsch 1996; Nitsch et al. 2005).

Towards the southeast of the basin, the facies of the Grabfeld Formation interlocks with the marginal facies of the Vindelician Highlands. This marginal facies is represented by the Benk Formation and consists of fluvial sandstones (DSK 2005; Nitsch et al. 2005).

The cyclitic nature of the Grabfeld Formation is represented not only by fine layered mudstones and thin dolomitic layers but also by the fossil contents. Conchostracs, bivalves and rare fish remains are indicative of rapid changes in salinity from brackish to hypersaline and limnic milieus (Nitsch et al. 2005). Marine ingressions in the southern parts of the basin allowed for entry of euryhaline Tethyan taxa to invade the CEB as is documented by the presence of various sauropterygians (*Nothosaurus*, *Simosaurus*, *Psephosaurus*) in the upper Grabfeld Formation (Rieppel and Wild 1994; Nitsch et al. 2005; Schoch 2021).

While *Psephosaurus suevicus* is only known from fragmentary carapace fragments (Rieppel 2000), *Simosaurus gaillardoti* and *Nothosaurus edingerae* are each known from cranial and postcranial material (Rieppel 1994; Rieppel and Wild 1994). Until now, only few temnospondyl remains have been reported. *Capitosaurus arenaceus* Münster 1836 was the historically first mentioned temnospondyl from the marginal facies of the Grabfeld Formation, the Benker Sandstone, near Bayreuth in eastern Bavaria. Broili (1915) described the bones to be of white colour, embedded in a yellow-whiteish matrix of fine-grained sandstone. The first mention of temnospondyl remains from the basin facies of the Grabfeld Formation of Bavaria come from Emmert et al. (1974) and Wild (1974) subsequently (Fig. 1B). Schoch and Witzmann (2011) as well as Schoch and Milner (2014) mention the presence of a single osteoderm of the plagiosaurid *Gerrothorax* from the 'Anatinenbank' of Kaubenheim, Bavaria. We have located this specimen (SMNS 97109) in the collection of the State Museum of Natural History Stuttgart (SMNS). Additionally, new material has recently been recognised in the palaeontological collection of the SMNS, including fragmentary pectoral girdle elements, vertebra and a phalange, which are reported herein (Table 2). These materials originated from different localities in Baden-Württemberg and Bavaria, Germany (Fig. 1B).

Materials and methods

Metoposauridae

Three metoposaurid temnospondyl bones are described from various stratigraphic and geographic horizons of the Grabfeld Formation of southern Germany (Table 2).

A fragmentary angular, SMNS 97058, was found in 1935 by a student, G. Buck, near Affaltrach in northern Baden-Württemberg (Fig. 2A) (Linck 1972). The specimen was gifted to O. Linck and found its way to the collection of the SMNS as part of a donation in later years. This fossil was found in the 'Anatinenbank' of the 'Graue Estherienschichten' (Fig. 1C). The same horizon has yielded a mineralized phalange and a presumable caudal vertebra of indeterminate temnospondyls from Stockheim (Brackenheim), west of Heilbronn. Together with SMNS 97058, these specimens were added to the palaeontological collection as part of a donation by O. Linck.

Table 2. Examined temnospondyl material from the Grabfeld Formation of southern Germany.

Specimen	Systematic palaeontology	Material	Horizon	Locality	Reference
SMNS 97058	*Metoposaurus* sp.	isolated angular	Anatinenbank	Affaltrach, Baden-Württemberg	this study
SMNS 55899	*Metoposaurus* sp.	fragmentary clavicle	Acrodus-Corbula Horizont	Altheim, Bavaria	Wild 1974
SMNS 59770	*Metoposaurus* sp.	fragmentary interclavicle	Obere Bunte Estherienschichten	Neustadt an der Aisch, Bavaria	this study
SMNS 97109	*Gerrothorax* sp.	isolated dermal bone	Acrodus-Corbula Horizont	Kaubenheim, Bavaria	Schoch and Witzmann 2011; this study
SMNS 59771	*Plagiosternum* sp.	fragmentary interclavicle	Obere Bunte Estherienschichten	Neustadt an der Aisch, Bavaria	this study
SMNS 97123	Capitosauroidea indet.	isolated intercentrum	Grabfeld Formation	Westheim, Bavaria	this study
SMNS 97125	Temnospondyli indet.	isolated intercentrum	Anatinenbank	Stockheim, Baden-Württemberg	this study
SMNS 97124	Temnospondyli indet.	isolated phalange	Anatinenbank	Stockheim, Baden-Württemberg	this study

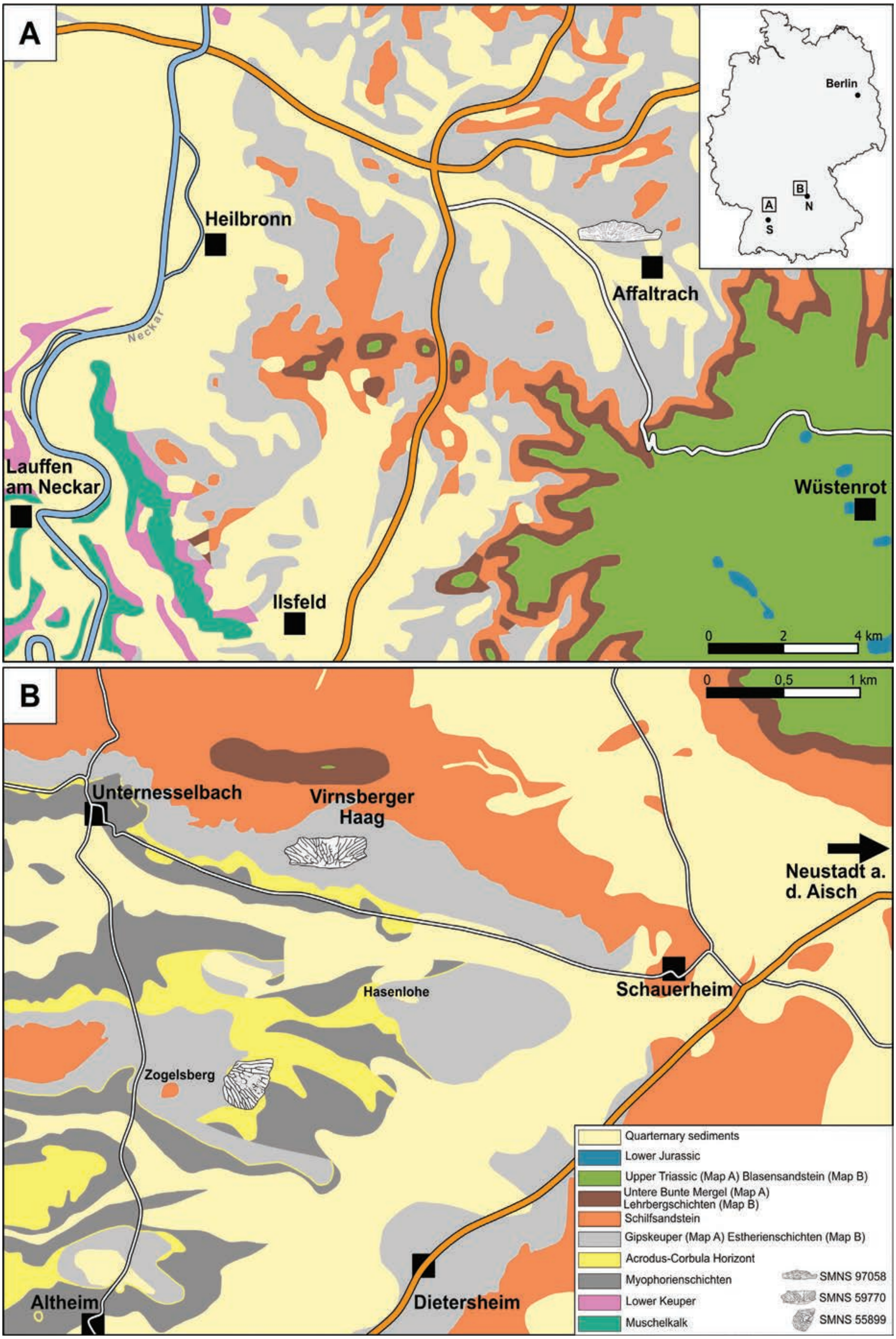

Figure 2. Geological map (redrawn from Bundesanstalt für Geowissenschaften und Rohstoffe) of the study areas. **A.** Heilbronn; **B.** Neustadt an der Aisch.

The rubblestone (*Lesestein*) specimen, SMNS 55899, described by Wild (1974) was identified as deriving from the ‘Acrodus-Corbula Horizont’ at the base of the ‘Untere Bunte Estherienschichten’ (Fig. 1B; 2B). Based on its dermal sculpture, it is identified as a partial clavicle of a metoposaurid (Wild 1974). Wild produced a mould to aid in his description of the specimen, although this could not be relocated in the SMNS. We therefore produced a new cast of the missing bone using a green latex silicone mould.

Another partial fragment, SMNS 59770, was collected in the vicinity of Neustadt an der Aisch (Fig. 1B) only a few kilometres from the collection horizon of SMNS 55899 (Fig. 2B). This specimen was collected from a field approximately 15 m north of the road connecting the municipalities of Unternesselbach and Schauerheim. This proposed fragmentary interclavicle of a metoposaurid is stratigraphically derived from the ‘Obere Bunte Estherienschichten’.

Capitosauroidea

A gently deformed isolated vertebra of an indeterminate capitosauroid was recovered from an unspecified layer within the Grabfeld Formation south of Westheim between Illesheim and Marktbergel southwest of Neustadt an der Aisch.

Plagiosauridae

SMNS 59771, an interclavicle fragment of a plagiosternine from the ‘Obere Bunte Estherienschichten’ of the same locality as SMNS 59770 consistent with finds of *Plagiosternum granulosum* from the Heldenmühle quarry at Crailsheim (Fig. 1B).

SMNS 97109, a dermal bone fragment of a plagiosaurine, consistent with *Gerrothorax pulcherrimus* from the ‘Acrodus-Corbula Horizont’ (basal part of ‘Untere Bunte Estherienschichten’, upper Grabfeld Formation) Kaubenheim, Bavaria. This specimen has wrongly been attributed to have originated from the ‘Anatinenbank’ by Schoch and Witzmann (2011) and Schoch and Milner (2014).

Institutional abbrevations: **SMNS**, Staatliches Museum für Naturkunde Stuttgart.

Results

Description

Temnospondyli Zittel, 1888
Stereospondyli Fraas, 1889
Metoposauridae Watson, 1919

***Metoposaurus* Lydekker, 1890**

Type species. *Metopias diagnosticus* (= *Metoposaurus diagnosticus*) (Meyer, 1842).

***Metoposaurus* sp.**
Fig. 3A–G

Angular (SMNS 97058)

Material. SMNS 97058, isolated angular preserved in original matrix, exposed in external lateral view (Fig. 3A).

Locality. An unspecified outcrop in the vicinity of Affaltrach, northern Baden-Württemberg (Fig. 1B).

Horizon. ‘Anatinenbank’, ‘Graue Estherienschichten’, Middle Grabfeld Formation, Middle Keuper, early Carnian, lowermost Upper Triassic (Fig. 1C).

Description. The angular (SMNS 97058) measures approximately 82 mm in anteroventral length and a maximum depth of 20 mm in height (Fig. 3A). The bone is asymmetrically elliptical with a somewhat flat ventral margin and a widely concave dorsal margin in lateral view (Fig. 3A). The bone is relatively short with a longitudinal length accounting for more than four times the bone height. The specimen is fairly well preserved albeit for the posterodorsal margin and a small section at the anteroventral side which are damaged. A small anterodorsal sulcus associated with a disarticulated suture boundary with the dentary is present. The external surface is strongly ornamented with a distinct sculpture which radiates outwards from the posteroventral margin. The posteroventral sculpture is composed of sinuously folded ridges and grooves forming a weakly polygonal texture. Radiating dorsal, dorsoanterior, and anteriorly, the sculpture forms few very well-developed elongate ridges which for the most part are straight, somewhat narrow, and neatly arranged forming a ‘striated’ appearance. Distal bifurcation of the ridges is rare but confined to only the distal extremities of the bone. This ornamentation pattern is consistent with *Metoposaurus* spp. (Sulej 2007). The ventral margin is noticeably thicker where it is developed into a weak ventral keel. The ornamented sculpture does not extend onto the ventral surface of the angular as observed in some capitosauroids including *Mastodonsaurus* (Schoch 1999).

Remarks. The shape of the bone and ornamentation pattern in SMNS 97058 are consistent with the angular in *Metoposaurus diagnosticus* from the overlaying Stuttgart Formation, as well as with *Metoposaurus krasiejowensis* from the Norian of Poland (Sulej 2007). The pattern and placement of the sculpture, notably in the presence of radiating ridges, is vastly different than the heavily reticulated, polygonal pattern of the angular of *Mastodonsaurus* (Rinehart and Lucas 2013). The isolated nature of the bone indicates that this individual was either in a late stage of decay when it was buried, or possibly represents an osteological immature individual which had not fully fused the angular to the other bones in the lower jaw.

Clavicle (SMNS 55899)

Material. SMNS 55899, incomplete clavicle preserved mostly as an external mould (Fig. 3B, C).

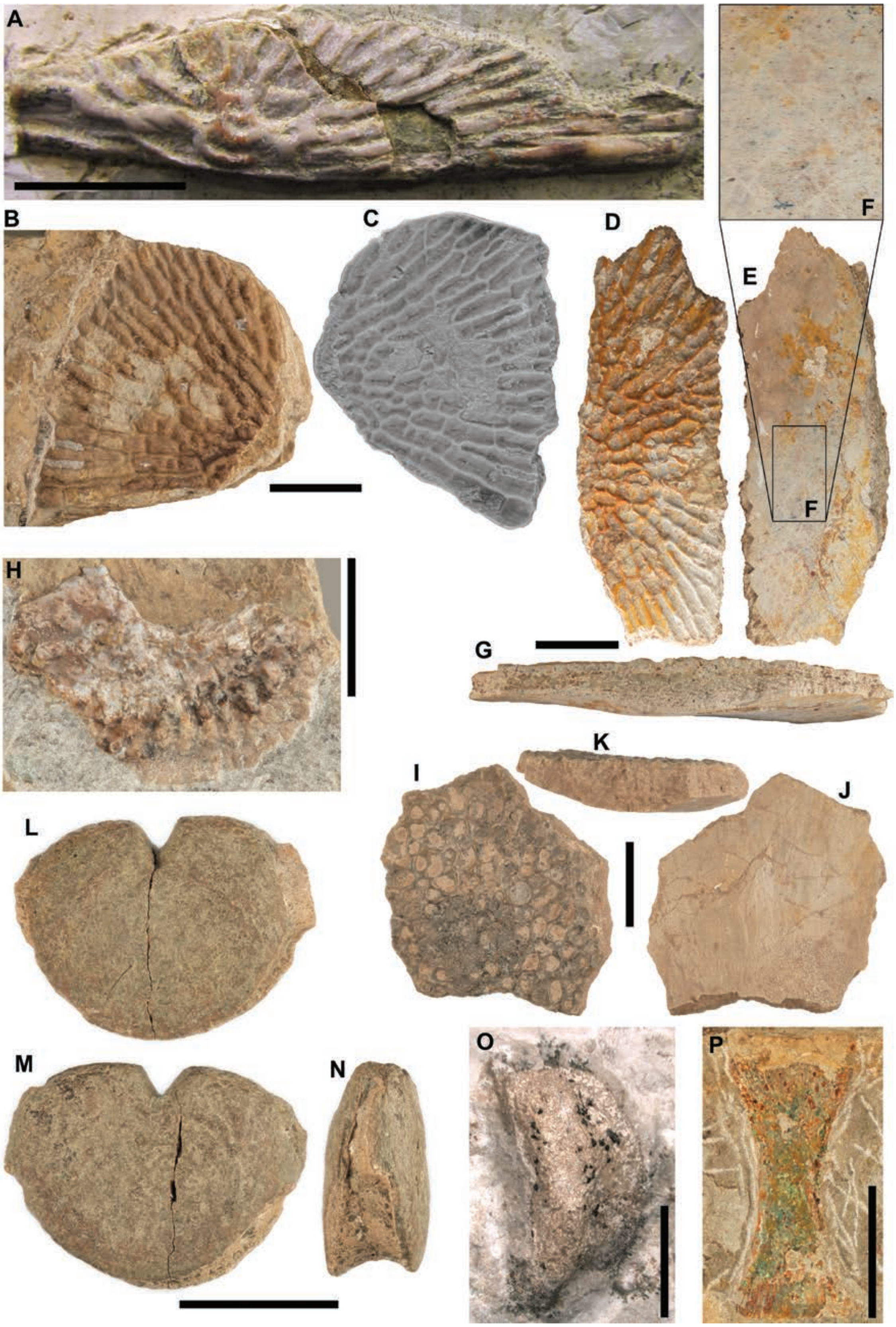

Figure 3. Fragmentary temnospondyl specimens collected from the Grabfeld Formation of southern Germany. **A.** SMNS 97058, a fragmentary angular of *Metoposaurus* sp. **B–C**, SMNS 55899, a fragmentary clavicle of *Metoposaurus* sp.; **B.** Natural mould; **C.** Silicone mould; **D–G.** SMNS 59770, a fragmentary interclavicle of *Metoposaurus* sp. in **D.** Ventral; **E.** Dorsal; **F.** Lateral view; **G.** Close-up of vascular foramina; **H.** SMNS 97109, a fragmentary dermal bone of *Gerrothorax* sp. **I–K**, SMNS 59771, a fragmentary interclavicle of *Plagiosternum* sp. in **I.** Dorsal; **J.** Lateral; **K.** Ventral view. **L–N**, SMNS 97123, an isolated capitosauroid vertebra in **L.** Anterior; **M.** Posterior, **N.** Lateral view; **O.** SMNS 97125, an isolated temnospondyl caudal vertebra in ventral view; **P.** SMNS 97124, an isolated temnospondyl phalange. Scale bars: 20 mm (**A–G, L–N, P**); 50 mm (**O**); 10 mm (**H, I–K**).

Locality. Near Altheim at the base of the Zogelsberg in the district of Neustadt an der Aisch, Middle Franconia, Bavaria (Fig. 1B, 2B).

Horizon. Collected loose from rubblestone (*Lesestein*) derived from the 'Acrodus-Corbula Horizont' at the base of the 'Untere Bunte Estherienschichten', Upper Grabfeld Formation, Middle Keuper, lowermost Upper Triassic.

Description. Marginal section of a large metoposaurid clavicle preserved mostly as an external mould (Fig. 3B) in a nodular dolostone measuring at its extremities 148 mm by 76 mm by 45 mm. The mould of the original bone, which preserves impressions of the original ventral (external) bone surface measures approximately 80 mm by 55 mm. Almost all of the original bone is absent except for a few bone splinters which are embedded around the margin of the void. An indeterminate rectangular bone is additionally preserved in cross section on the reverse margin of the matrix although the identity of the bone cannot be determined. Details of the original ornamentation are described based on a silicon mould (Fig. 3C) produced for this study.

Sculpture comprises a margin concentration of small and shallow polygonal pits arranged in a honey comb-like structure. Distally, these shallow sloped ridges radiate into mostly straight lines which proximally bifurcate in a clear 'Y' shape pattern. The area occupied by the honey comb-like polygonal pits is very narrow compared to the preserved region (and missing regions) occupied by the elongate bifurcating ridges. Collectively, all of the ridges are shallow and smooth, therefore unlike the much deeper and more deeply excavated ridges in the sculpture of Capitosauroidea (Wild 1974).

Remarks. According to Wild (1974), the area of bone represented as an external mould in SMNS 55899 derives from the posterolateral margin, likely close to the ascending process of the clavicle. The ornamentation sculpture including the small polygonal pits which are confined to a small area of the bone surface, is diagnostic of *Metoposaurus* spp. (Sulej 2002). The ornamentation of *Cyclotosaurus* distinctly differs from *Metoposaurus* by having relatively large and rhomboidal polygons (Antczak and Bodzioch 2018). The morphology of SMNS 55899 most closely matches the clavicle of *Metoposaurus diagnosticus* from the Carnian of Germany based on materials examined in the SMNS (SMNS 81981 and SMNS 81983).

Interclavicle (SMNS 59770)

Material. SMNS 59770, large isolated interclavicle fragment, likely from the posteromedial region (Fig. 3D–G).

Locality. Field exposure approximately 15 m north of the road connecting the municipalities of Unternesselbach and Schauerheim, Middle Franconia, Bavaria (Fig. 1B).

Horizon. 'Obere Bunte Estherienschichten', Upper Grabfeld Formation, Middle Keuper, lowermost Upper Triassic.

Description. A large rectangular fragment of a metoposaurid interclavicle measuring approximately 107 mm by 38 mm. The bone is broken on all sides, meaning that the precise placement of this fragment and the original size of the interclavicle cannot be reliably estimated. The bone is topographically flat and dense in cross section with a notable bulge towards the midpoint with a maximum thickness of approximately 13 mm and a minimum thickness on the lateral margins of approximately 7 mm. The ventral (external) surface (Fig. 3D) is strongly sculptured with a mosaic of shallow radiating ridges which towards the inferred midpoint of the bone, interconnect forming a regionalised polygonal network. Laterally, these polygonal ridges radiate forming thin, evenly spaced shallow ridges which do not laterally intersect one another, although proximally some display a single 'Y' shaped bifurcation. The polygonal pits formed by this medial interconnection of the ridges are fairly small and shallow throughout, with their extent appearing to be constricted to a brief regionalised area of the external sculpture. Topographically, all ridges are shallow and smooth; therefore, they distinctly differentiate from the much taller and steeper ridges and grooves in the interclavicles of capitosauroids. The dorsal (internal) surface (Fig. 3E) is smooth and irregularly concave with numerous fine vascular foramina (Fig. 3F) orientated downslope of the medial bulge (Fig. 3G). The bone is scarred with delicate cross-cutting diagenetic fractures which are responsible for the splintered margins around the edges of the bone.

Remarks. As stated above, the presence of shallow ridges and grooves, small medially localised polygonal sculpture, and thin radiating ridges strongly supports referral of SMNS 59770 to Metoposauridae rather than to Capitosauroidea. In capitosauroids, the polygonal pits are much deeper and wider with taller and steeper radiating ridges. A similar criterion had previously been used to refer SMNS 55899 (redescribed herein) to *Metoposaurus* sp. by Wild (1974). The polygonal area is tightly confined to a small area of the bone, which combined with the small size of the polygonal pits, is a character shared between *Metoposaurus krasiejowensis* from Poland and *Metoposaurus diagnosticus* from the CEB, with this character considered by many authors to be highly diagnostic of the genus *Metoposaurus* (Hunt 1993; Long and Murry 1995; Sulej 2002). The ornamentation and sculpture patterns are near enough identical in both SMNS 59770 and SMNS 55899, which despite representing different bones in the pectoral girdle, supports the hypothesis that both elements likely belong to a single metoposaurid taxon. An absence of pustules or tubercles additionally rules out either of these specimens belonging to Plagiosauridae, which are otherwise also present in the Grabfeld Formation (SMNS 59771 – this paper). The presence of a medial bulge (Fig. 3G) on the dorsal surface is consistent to that observed on the interclavicles of other metoposaurs observed in the SMNS collection. Although we have clearly demonstrated SMNS 59770 and SMNS 55899 as belonging to Metoposauridae rather than Captiosauroidea or Plagiosauridae, it is not possible to identify which species of metoposaur these fragments belong to due to their incompleteness. However, based on our current understanding of Metoposauridae palaeobiogeography, the only genus present in Europe is *Metoposaurus*: *M. diagnosticus* (Meyer 1842) (Germany), *M. krasiejowensis* (Sulej 2002) (Poland), and *M. algarvensis* (Brusatte et al. 2015) (Portugal), with the former species (*M. diagnosticus*) found in the overlaying Stuttgart Formation (Milner and Schoch 2004). We therefore tentatively refer these specimens based on the geographic location as *Metoposaurus* sp.

Plagiosauridae Abel, 1919
Plagiosaurinae Shishkin, 1986

***Gerrothorax* Nilsson, 1934**

Type species. *Gerrothorax pulcherrimus* (Fraas, 1913).

***Gerrothorax* sp.**
Fig. 3H

Dermal bone (SMNS 97109)

Referred material. SMNS 97109, an isolated dermal bone (Fig. 3H).

Locality. An unspecific outcrop near Kaubenheim, Middle Franconia, Bavaria.

Horizon. Derived from the 'Acrodus-Corbula Horizont' at the base of the 'Untere Bunte Estherienschichten', Upper Grabfeld Formation, Middle Keuper, lowermost Upper Triassic.

Description. A small fragmentary dermal bone, most closely resembling the osteoderms of *Gerrothorax*. It is embedded in a light brown dolomitic matrix (Fig. 3H). The element is damaged and measures approximately 24 mm in length and 11 mm in width. The sculpturing of the bone shows the characteristic pustular ornamentation, although most of the pustules are broken and only seen in transverse section. One margin is flat without pustules, but covered by faint ridges connecting to the pustules of the ornamented part. This resembles the marginal overlapping zone of osteoderms in *Gerrothorax*, although some transport might have worn off part of the surface in SMNS 97109.

Plagiosterninae Shishkin, 1986
***Plagiosternum* Fraas, 1896**

Type species. *Plagiosternum granulosum* (Fraas, 1889).

***Plagiosternum* sp.**
Fig. 3I–K

Plagiosternine interclavicle (SMNS 59771)

Referred material. SMNS 59771, a partial fragmentary interclavicle (Fig. 3I–K).

Locality. Field exposure approximately 15 m north of the road connecting the municipalities of Unternesselbach and Schauerheim, Middle Franconia, Bavaria (Fig. 1B).

Horizon. 'Obere Bunte Estherienschichten', Upper Grabfeld Formation, Middle Keuper, early Carnian, lowermost Upper Triassic.

Description. The specimen is a fragmentary interclavicle measuring approximately 47 mm in length and 41 mm in width, attributed to Plagiosterninae. The ventral surface (Fig. 3I) of the fragment features irregular small polygonal reticulated ornamentation with pustular structures present on nodular points. The ridges of the ornamentation are of medium height. The dorsal surface (Fig. 3J) shows a radiating pattern originating from the thickest part of the fragment. In lateral view (Fig. 3K), the height of the fragment increases towards the centre, from 5 mm to a maximum of 10 mm. The cross section is reminiscent of the medial region of the interclavicle based on *Plagiosternum* materials housed at the SMNS.

Remarks. The ornamentation of SMNS 59771 differs from that of other Plagiosauridae like *Plagiosuchus* or *Gerrothorax*, in which it primarily consists of pustules. The ornamentation further differs from the ones found in other Stereospondyli by having an overall weaker polygonal structure than Capitosauroidea, Trematosauridae and Metoposauridae. Additionally, vascular openings within the pits are not visible. Given the indistinguishable difference to comparative materials of *Plagiosternum granulosum* (SMNS 11825 and SMNS 11826; Fraas, 1889), we tentatively assign this fragmentary interclavicle to *Plagiosternum* sp.

Temnospondyli Zittel, 1888
Stereospondyli Fraas, 1889

Capitosauroidea indet.
Fig. 3L–N

Vertebra (SMNS 97123)

Referred material. SMNS 97123, a single gently deformed intercentrum (Fig. 3L–N).

Locality. An unspecified outcrop south of Westheim, Illesheim, Middle Franconia, Bavaria, (Fig. 1B).

Horizon. From an unspecified horizon within the Gipskeuper (Grabfeld Formation).

Description. The intercentrum (Fig. 3L, M) measures a width of 34 mm, height of 29 mm and anteroposterior length of 13 mm. The dorsal surface of the intercentrum is open and shows a very small "V" shaped *chorda incisure*. The pleurocentral facets are well established on the anterior side and are positioned laterally to the *chorda incisure*. Anterior and posterior surfaces of the intercentrum are very slightly concave. Paired parapophyses are found high in the lateral flank, inclined posteriorly but are broken. The flanks are highly concave as is the *tuber articularis* (Fig. 3N).

Remarks. Based on the size, morphology and position of the parapophysis and the absence of a haemal arch, we attribute the intercentrum to the posterior trunk region. It is most consistent with intercentra of early-branching capitosauroids (Schoch and Milner 2000). The intercentrum differs substantially from *Metoposaurus krasiejowensis* (Sulej 2007) by its rounder shape and higher placement of the parapophysis within the lateral flank. In conclusion, the intercentrum is more consistent with that of capitosauroids in its near circular transverse shape, the position and morphology of the parapophysis, and the more pronounced facets for the pleurocentra (Warren and Snell 1991; Schoch 1999).

Temnospondyli Zittel, 1888

Temnospondyli indet.
Fig. 3O, P

Caudal vertebra (SMNS 97125)

Referred material. SMNS 97125, a single intercentrum partially still embedded in matrix (Fig. 3O).

Locality. An unspecified outcrop in the vicinity of Stockheim (Brackenheim), northern Baden-Württemberg (Fig. 1B).

Horizon. 'Anatinenbank', 'Graue Estherienschichten', Middle Grabfeld Formation, Middle Keuper, early Carnian, lowermost Upper Triassic.

Description. The intercentrum is partially embedded in a light-grey, beige dolostone (Fig. 3O). The visible parts measure 11 mm in length and 4 mm in width. A very slight concavity is noticeable on the presumed ventral surface of the specimen.

Remarks. The small size of SMNS 97125 suggest that this intercentrum can tentatively be attributed to a vertebra of the caudal series. The concavity found on the presumed ventral surface point to this structure being the latera of the intercentrum, suggesting the dorsal part of the specimen to be covered by the matrix. Due to the size of the vertebra, it cannot be ruled out that it potentially belongs to a juvenile individual. In the absence of any diagnostic features, we refer this specimen to Temnospondyli indet.

Phalange (SMNS 97124)

Referred material. SMNS 97124, a single isolated phalange embedded in matrix (Fig. 3P).

Locality. An unspecified outcrop in the vicinity of Stockheim (Brackenheim), northern Baden-Württemberg (Fig. 1B).

Horizon. 'Anatinenbank', 'Graue Estherienschichten', Middle Grabfeld Formation, Middle Keuper, early Carnian, lowermost Upper Triassic.

Description. The specimen is an isolated phalange embedded in a light-grey, beige dolostone and is covered in a greenish mineral phase (Fig, 3P). It measures approximately 39 mm in length. The phalange has an hourglass-shape with either the dorsal or ventral side exposed. The width varies from 9 mm in the midshaft to 17 mm in the epiphyseal region. The epiphyseal regions show slight concavity on the exposed surface, whereas the bone is flat in the midshaft.

Remarks. The morphology of this phalange is indistinguishable from other stereospondyl phalanges. In comparison to the phalanges of *Nothosaurus* (Klein et al. 2022), which also occurs in the Grabfeld Formation, the hourglass-shape of the phalange is more pronounced than the constricted shaft in *Nothosaurus*. No phalanges are known from *Simosaurus* or *Psephosaurus*, the only other sauropterygians from the Grabfeld Formation of Germany (Rieppel 1994; Rieppel and Wild 1994). The present phalange resembles those of *Metoposaurus krasiejowensis* (Konietzko-Meier et al. 2020) more than those of *Nothosaurus*. We therefore attribute SMNS 97124 to Temnospondyli indet.

Discussion

Geological age correlation and constraints

To date, the Late Triassic timescale still lacks substantially detailed numerical ages for most of its stages (Lucas 2018). Given that the Late Triassic is a crucial period for the evolution and extinction of various tetrapod groups, accurately correlating geological and biotical events is vital for our understanding of these key events (Lucas 2018). In the Central European Basin (CEB), the Ladinian–Carnian boundary is indicated by the presence of the index fossil *Myophoria kefersteini okeni*, found in the 'Bleiglanzbank' in the middle of the Grabfeld Formation (Urlichs and Tichy 2000). The base of the Cordevolian (early Carnian) substage is found in the 'Estherienschichten' within the upper parts of the Grabfeld Formation and is indicated by the presence of the spinicaudatan *Laxitextella multireticulata* (Zhang et al. 2020). The 'Anatinenbank' (Fig. 1C) is extremely rich in *Laxitextella taxitexta* which is used biostratigraphically as an index for the upper Cordevolian substage (Kozur and Weems 2010; Gale et al. 2023). The Cordevolian age of the upper Grabfeld Formation is further supported by palynological evidence (Zhang et al. 2020). Another line of evidence is supported based on Milankovitch cyclicity of the fossil-bearing horizons of the Grabfeld Formation, which place the base of the Carnian at around ~237 Ma (Stollhofen et al. 2008). As the Carnian–Norian boundary has no clear Global Stratotype Section and Point (GSSP) (see Ogg 2012 as well as Lucas 2018 and references therein for in depth discussion), we are following recent results of Kohút et al. (2018) supporting the "short Norian" hypothesis. In order to contextualise the biostratigraphic and palaeobiogeographic significance of the new *Metoposaurus* materials from the Grabfeld Formation, it is necessary to evaluate the currently known global distributions of this family and the precise ages of their depositional environments.

Recent radiometric zircon dating of the Schilfsandstein (Zeh et al. 2021) indicate a delayed onset of ~3 Ma of the Carnian Pluvial Event (CPE; Dal Corso et al. 2020) in the Schilfsandstein compared to the NW Tethys region.

Following Zeh et al. (2021), the CPE begins in the Julian 2 (234 Ma) in the NW Tethys basin and in the Tuvalian 2 (231 Ma) in the Schilfsandstein of the CEB respectively and lasts until the Carnian–Norian boundary (221 Ma), indicating a probable 13 Ma duration for the CPE (Fig. 4; Zeh et al. 2021). Reliable zircon dating is an essential tool to help more precisely date occurrence points for temnospondyls in terrestrial environments. Biostratigraphically, precise dating of the temnospondyl-bearing localities of Poland are still highly debated. Szulc et al. (2015) summarized the ongoing discussions regarding the placement of the Krasiejów and Lisowice bone bearing horizon. Szulc et al. (2015) argued for a placement of the Krasiejów beds into the Norian, roughly equivalent to the lower parts of the Germanic Arnstadt Formation, while other authors suggest a Carnian age based on phytosaur occurrence (Dzik and Sulej 2007; Butler et al. 2014; Lucas 2020). In the Lisowice bone-bearing horizons, multiple lines of evidence (radiometric zircon dating (Kowal-Linka et al. 2019) as well as palynological evidence (Fijałkowska-Mader et al. 2015)) support the proposed middle–late Norian age of these bone-bearing beds. A similar co-occurrence of phytosaurs with *Metoposaurus algarvensis* in the AB2 unit of the Grés de Silves Formation of the Algarve of southern Portugal suggest a late Carnian–early Norian age of this stratum (Mateus et al. 2014; Brusatte et al. 2015).

In Morocco, the metoposaurids (*Almasaurus*, *Arganasaurus*, *Dutuitosaurus*) of the Argana basin are confined to the Irohalène (T5) member of the Timezgadiouine Formation (Jalil 1999; Buffa et al. 2019). Based on the co-occurrences of *Brachychirotherium*, *Atreipus*–*Grallator* and *Eubrontes* in the ichnoassemblages recovered from the Timezgadiouine Formation (Lagnaoui et al. 2012; Zouheir et al. 2018), the T5 member can be assigned to the early Carnian (Otischalkian) *Brachychirotherium* biozone (Klein and Lucas 2010). The base of the Otischalkian is indicated by the occurrence of parasuchids (Martz and Parker 2017) so therefore the *Brachychirotherium* biozone and hence the T5 member, are potentially of similar late Carnian age as the base of the Popo Agie Formation of Wyoming (Lovelace et al. 2023). Given these inconsistencies we assume an early–late Carnian age for the T5 member of the Timezgadiouine Formation.

The occurrence of osteoderms assigned to the phytosaur *Parasuchus* (Sharma and Kumar 2015) in the Tiki Formation of India indicates the placement of this strata into the late Carnian Otischalkian land vertebrate faunachron (LVF; Lucas 1998) in lack of radiometric dating alternatives. Furthermore, additional phytosaur material, as described and discussed by Datta et al. (2021), allow for a more detailed and global correlation of the Indian Tiki and Maleri formations. Datta et al. (2021) conclude that based on the presence of the widely used index taxa *Hyperodapedon* and *Parasuchus* in the Tiki Formation and lower Maleri Formation, these formations are considered to be late Carnian–early Norian in age. The use of these index taxa allows for additional correlation of these formations with other metoposaurid-bearing strata. Based on the occurrence of *Hyperodapedon* and *Parasuchus* the lower Maleri and Tiki formations can be correlated to the Isalo II of Madagascar (Fortuny et al. 2019), the Wolfville Formation of Nova Scotia (Sues et al. 2021), the Popo Agie Formation of Wyoming (Lovelace et al. 2023), the Camp Springs conglomerate of the Dockum Group of Texas, and the Timezgadiouine Formation of Morocco. Following Lovelace et al. (2023) and Martz and Parker (2017), the Camp Springs conglomerate contains the oldest known record of basal parasuchids, providing the base of the Otischalkian LVF (Lucas 1998). The lower Ischigualasto Formation of Argentina was successfully radioisotopically dated to 231 Ma (Martínez et al. 2012). The presence of *Hyperodapedon* in the lower Ischigualasto Formation and the radiometric dating of the purple-ochre transition of the Popo Agie Formation conclude similar ages for the other correlated strata, which places them presumably contemporaneous with the Germanic Schilfsandstein in the early Tuvalian 2 substage. The upper Maleri Formation is suggested to be Norian in age based on the disappearance of *Hyperodapedon*, *Parasuchus* and the metoposaurid *Panthasaurus* and the occurrences of more derived phytosaurs (Datta et al. 2021).

In North America, metoposaurids occur in the Late Triassic continental strata of the Chinle Group, Dockum Group and Chugwater Group of the western USA as well as the Chatham Group in the eastern part of the country (Hunt 1993). Lovelace et al. (2023) integrated the Popo Agie Formation of the Chugwater Group of Wyoming with the biostratigraphic correlations of the Chinle Group and Dockum Group (Martz and Parker 2017). On the basis of phytosaur biostratigraphy and laser ablation-inductively coupled plasma-mass spectrometry (LA-ICP-MS), the Popo Agie Formation can be placed in the Otischalkian. Additional radiometric dating suggests a maximum depositional age of the purple-ochre transition of the Popo Agie Formation of Wyoming of 230 ± 5 Ma (Lovelace et al. 2023). The following Adamanian begins at ~222 Ma with the occurrence of leptosuchomorph phytosaurs (Martz and Parker 2017; Lovelace et al. 2023).

Recent reports of indeterminate metoposaurid material from the Tashinga Formation of Zimbabwe (Barrett et al. 2020) also provided first radiometric ages for this formation, placing its depositional age around 209 Ma (late Norian). This presumable occurrence of a metoposaurid in the late Norian of southern Africa exceeds the last known record of the group in India by more than 10–15 Ma and demonstrates survivorship of Metoposauridae at high-latitudes in both Gondwana and Laurasia during the later stages of the Late Triassic.

The confirmed presence of *Metoposaurus* in the early Carnian Grabfeld Formation of southwestern Germany therefore has significant implications for the palaeogeographic distribution history (Fig. 4) of the group.

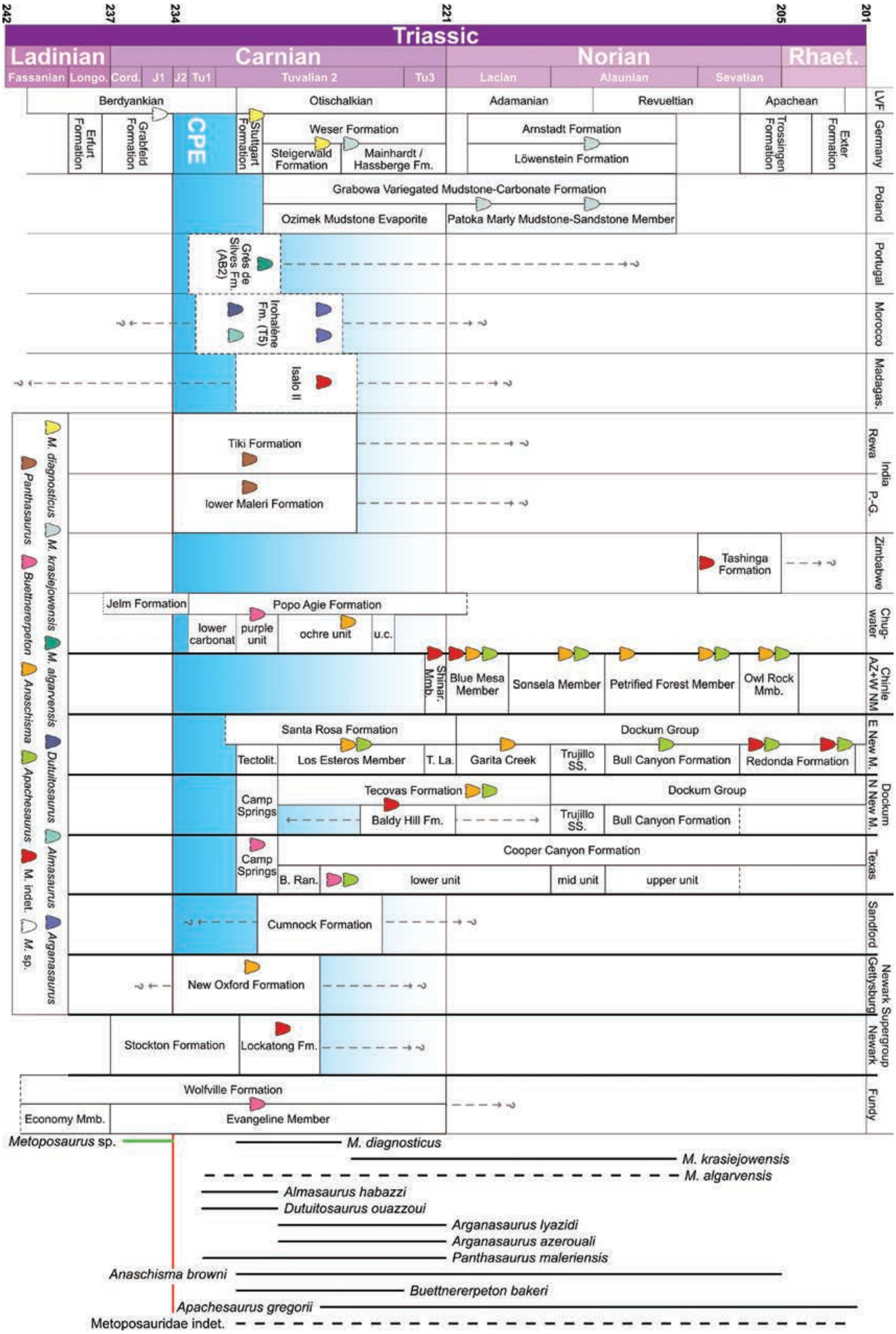

Figure 4. Stratigraphic correlation of the German Middle and Late Triassic *Metoposaurus*-bearing formations with other metoposaurid-bearing formations around the world. Correlations are based on (DSK 2005; Szulc et al. 2015; Martz and Parker 2017; Zouheir et al. 2018; Buffa et al. 2019; Datta et al. 2021; Sues et al. 2021; Zeh et al. 2021; Lovelace et al. 2023). Abbrevations: Rhaet. – Rhaetian, Longo. – Longobardian, Cord. – Cordevolian, J – Julian, Tu – Tuvalian, LVF – Land Vertebrate Faunachron, CPE – Carnian Pluvial Event, Madagas. – Madagascar, P.-G. – Pranhita-Godavari, AZ – Arizona, NM – New Mexico, TX – Texas, u.c. – upper carbonate, Shinar. – Shinarump, Mmb. – Member, Tectolit. – Tectolito, T. La. – Tres Lagunas, SS. – Sandstone, B. Ran. – Boren Ranch, Fm. – Formation.

The new *Metoposaurus* sp. materials represent the oldest known records of Metoposauridae, thereby pushing back their first occurrence in the fossil record of the CEB from the late Carnian to the early Carnian: an extension of approximately 5 million years.

Global palaeoenvironmental distribution of metoposaurids

The diversity of temnospondyls in the Grabfeld Formation is unexpectedly high given the hostile palaeoenviromental conditions. These new occurrence points therefore have novel implications for the current understanding of metoposaurid distribution and their ecosystem occupation throughout the Triassic. In Europe, three species of metoposaurids are formally recognised: (1) *Metoposaurus diagnosticus* (Meyer 1842), (2) *Metoposaurus krasiejowensis* (Sulej 2002) and (3) *Metoposaurus algarvensis* (Brusatte et al. 2015) (Table 2).

The oldest global occurrence of *Metoposaurus* sp. is from the early Carnian Grabfeld Formation (Gipskeuper) (Fig. 4; this paper), with this genus surviving throughout most of the Late Triassic within the CEB. Traditionally, *M. diagnosticus* has been recognised in the late Carnian fluvial and floodplain facies of the Stuttgart Formation (Schilfsandstein; Meyer 1842), and the lacustrine Lehrbergschichten (lower Steigerwald Formation; Seegis 1997). *M. krasiejowensis* occurs in sandstones of the Kieselsandstein or Blasensandstein (Hassberge Formation; Seegis 1997; Milner and Schoch 2004), as well as the Arnstadt Formation (Stubensandstein; Milner and Schoch 2004). The sandstones of the Kieselsandstein and Stubensandstein are clearly distinguishable by grainsize and cementation and derive from a terminal alluvial fan in the case of the Kieselsandstein, while the Stubensandstein originated from an extensive river system (Milner and Schoch 2004). Outside of the Germanic Basin, *M. krasiejowensis* is best known from the late Carnian–early Norian freshwater ephemeral marly clays of the Patoka Member of the Grabowa Formation of Poland (Bodzioch and Kowal-Linka 2012; Szulc et al. 2015; Jewuła et al. 2019). Additionally, *M. algarvensis* is recognised from the fluvial or deltaic mudstones of the AB2 beds of the Grés de Silves Formation in southern Portugal (Witzmann and Gassner 2008; Brusatte et al. 2015). Furthermore, the Raibl Schichten of the Heiligenkreuz yielded the *nomen dubium* "*M.*" *santaecrucis*, which exhibits strong morphological similarities to *M. diagnosticus* (Koken 1913). This occurrence is notable, because the specimen was found within a non-marine bed within an otherwise marine sequence (Hunt 1993).

In northern Africa the Irohalène Member (T5) of the Timezgadiouine Formation of Morocco have yielded a diverse assemblage of metoposaurids: (1) *Dutuitosaurus ouazzoui*, (2) *Almasaurus habazzi*, (3) *Arganasaurus lyazidi* and (4) *Arganasaurus azerouali* (Buffa et al. 2019). Within T5, *Dutuitosaurus ouazzoui* and *Almasaurus habazzi* occur in the lower parts of the member while *Arganasaurus lyazidi* and *Arganasaurus azerouali* co-occur in the upper parts of the formation (Jalil 1999). Hofmann et al. (2000) describe the T5 lithology as cyclically stacked sandstones with interbedded mudstones that are interpreted to have been deposited in a meandering river and floodplain system. However, Zouheir et al. (2018) describe the upper parts of the member as dry playa red beds indicating a drying-upwards trend during a transition from semiarid to arid climates.

In India the sole representative of Metoposauridae, *Panthasaurus maleriensis*, occurs in the fluvial sandstones and mudstones of the Tiki Formation and lower Maleri Formation (Chakravorti and Sengupta 2019).

Similarly, "*M. hoffmani*" of Isalo II in Madagascar, recently reappraised to Metoposauridae indet. by Fortuny et al. (2019), occurs in the fluvial sandstones and conglomerates as the only representative of the group in this region.

The metoposaurids of North America are similar across the different basins of the continent, only varying in their co-occurrence with each other. Following recent revisions of the group by Gee and Parker (2018); Gee et al. (2019); Gee and Jasinski (2021); Kufner and Gee (2021) and Gee and Kufner (2022) currently three species of metoposaurids are considered valid in North America: (1) *Anaschisma browni*, (2) *Buettnererpeton bakeri* and (3) *Apachesaurus gregorii* (Fig. 4). *Anaschisma browni* occurs in the ochre unit of the Popo Agie Formation (Kufner and Gee 2021) of Wyoming, the Bluewater Creek Formation (Heckert 1997), the Blue Mesa Member (Long and Murry 1995), Sonsela Member (Spielmann et al. 2007), Petrified Forest (Long and Murry 1995) and Owl Rock Member (Spielmann et al. 2007) of the Chinle Group in Arizona and eastern New Mexico as well as the Santa Rosa Formation (Heckert and Lucas 2015), Tecovas Formation (Hunt 1993) and Garita Creek Formation (Hunt 1993) of western New Mexico and Texas. Futhermore, *Anaschisma* is found in the New Oxford Member of the Gettysburg basin in Pennsylvania (Hunt 1993), not only extending the geographic range of the taxon tremendously but also establishing a stratigraphic range from the late Carnian–late Norian. *Apachesaurus gregorii* shows a similar stratigraphic range as *Anaschisma browni* occurring in the Bluewater Creek Formation (Heckert 2004), the Blue Mesa Member (Hunt 1993), Sonsela Member (Gee and Parker 2018), upper Petrified Forest Member (Gee and Parker 2018) and Owl Rock Member (Spielmann et al. 2007) of the Chinle Group in Arizona and eastern New Mexico as well as the Santa Rosa Formation (Hunt 1993), Tecovas Formation (Hunt 1993), Bull Canyon Formation (Hunt 1993) and Redonda Formation (Spielmann and Lucas 2012) of western New Mexico and Texas. In the Cooper Canyon Formation *Apachesaurus* was recovered from the lower unit (Hunt 1993). Currently, *Apachesaurus* has not been recovered from eastern North America, limiting its palaeobiogeographic range. *Buettnererpeton bakeri* has the shortest stratigraphic range of the North American metoposaurids as it only occurs in the purple unit of the Popo Agie Formation (Kufner and Gee 2021) and the contemporaneous Camp Springs conglomerate (Kufner and Gee 2021) of the Chinle Group. In eastern North America, *Buettnererpeton* is recovered from the Evangeline Member of the Wolfville Formation, Nova Scotia (Hunt 1993). *Buettnererpeton* shares a similar sized lateral geographic range with *Anaschisma*.

Additionally, indeterminate material of metoposaurids has been recovered from the early Carnian Lockatong Formation of the Newark basin (Baird 1986), the early Carnian Baldy Hill Formation of the Dockum Group (Heckert and Lucas 2015), the late Carnian Cumnock Formation of Sanford basin (Heckert et al. 2012), the early Norian Shinarumpa (Dubiel and Hasiotis 2011) and Bluewater Creek Formation of the Chinle Group (Heckert 1997), the late Norian Redonda Formation (Spielmann and Lucas 2012) as well as the late Norian Tashinga Formation of Zimbabwe (Barrett et al. 2020). The lithology of these strata is comprised of predominantly coarse-grained sandstones, siltstones and mudstones originating from a diverse fluvial system with interbedded floodplains and lacustrine environments (Colbert and Olsen 2001; Heckert 2004; Spielmann and Lucas 2012; Heckert and Lucas 2015; Barrett et al. 2020).

Palaeogeographic implications

Based on the correlations of metoposaurid-bearing strata (Fig. 4) and the herein reported new material from the Grabfeld Formation of southern Germany, a biogeographic distribution scenario can be assumed for the dispersal of metoposaurids across Pangea during the Late Triassic. As the material of the Grabfeld Formation is confidently placed in the early Carnian Cordevolian and Julian 1 substages, they precede the CPE and all other global occurrences of Metoposauridae at current knowledge. This suggests that the first appearance of Metoposauridae in the fossil record occurs in the CEB around the Ladinian–Carnian boundary and is further supported by the occurrence of *Callistomordax kugleri* (Schoch 2008), the sister taxon to Metoposauridae, from the Erfurt Formation of Germany. As a result of the still debated stratigraphic positions of other metoposaurid-bearing horizons of Europe the following scenario for metoposaurid distribution is proposed:

1. An initial radiation of Metoposauridae occurred with the onset of the CPE at the Julian–Tuvalian boundary in the Central European basin. From there, a first dispersal event via aquatic pathways potentially connected southern European Metoposauridae with northern Africa and eventually with India and Madagascar. The geographic distance between the Indian and other metoposaurid-bearing localities suggest emerging endemism of the group in this region due to diverging climatic conditions.
2. A second wave of radiation and dispersal started from Europe or northern Africa and connected these regions with North America. The early late Carnian occurrence of *Buettnererpton* and *Anaschisma* in different basins of the Newark Supergroup and Wyoming (Gee et al. 2019; Gee and Kufner 2022) suggest widespread aquatic pathways the group could have dispersed through.
3. The occurrence of indeterminate metoposaurid material from Zimbabwe (Barrett et al. 2020) suggest a potential third dispersal event occurring in the late Carnian–late Norian emerging from India and/or Madagascar. As Zimbabwe and these regions are found in similarly high palaeolatitudes this origin hypothesis is suggested.

The last known Metoposauridae in Europe vanish in the middle–late Norian, while the family flourishes in North America up to the Rhaetian and potentially up to the Triassic–Jurassic boundary (Fig. 4). Climatic studies of the Triassic (Sellwood and Valdes 2006; Dunne et al. 2021) have shown that the climate zones of Pangea were divided into different climatic belts and tetrapod diversity was linked to latitudinal biodiversity gradients. While Europe and North America were situated at similar palaeolatitudes in Late Triassic Pangea, potential climatic differences might not have been the trigger for the early disappearance of Metoposauridae from Europe as different groups of temnospondyls still persisted throughout the Rhaetian in this region. Palaeohistological studies of metoposaurids from Poland and India found a milder climate in these regions, compared to the climatic conditions present in Morocco (Teschner et al. 2023). Rather than climatic differences, Milner and Schoch (2004) have shown that in the case of European Metoposauridae, changes of source water and transported sediment might have an implicit impact on existing faunal components.

Physiological implications

The physiological tolerances of temnospondyls have long been debated (Laurin and Soler-Gijón 2010). While some families have been recovered from vastly different terrestrial aquatic palaeoenvironmental settings, others seem to be more restricted in their osmotic tolerance. For example, mastodonsaurids in the Middle and Late Triassic of Germany are found in freshwater fluvial, lacustrine and deltaic environments as well as in coastal or nearshore deposits (Schoch 2015). The same can be said for Plagiosauridae (*Plagiosaurus*, *Plagiosternum*, *Gerrothorax*), which are found in the same ecological range (Hagdorn and Reif 1988; Schoch and Seegis 2016) as the aforementioned capitosaurs. On the other hand, most authors concluded for Metoposauridae to have been inhabiting freshwater fluvial and lacustrine environments exclusively (Hunt 1993).

Marine affinities have been proposed for different groups of temnospondyls (DeFauw 1989). The association of temnospondyl remains with ammonoids and bivalves from the marine and nearshore deposits of the Early Triassic of Svalbard and Greenland (Scheyer et al. 2014; Kear et al. 2015) demonstrate the adaptability of the group for a wide range of potential habitats. Dutuit (1983) suggested marine migration for Metoposauridae based on the co-occurrence with phytosaurs in the Moroccan Argana Basin. The presented arguments were rejected by subsequent studies (Buffetaut and Martin 1984; Hunt 1993) showing the availability of inland connections between metoposaurid-bearing localities and the clear absence of the group from marine strata. Other studies (Laurin and Soler-Gijón 2001, 2010) report clear evidence of Palaeozoic stegocephalians from marine or saline environments, or argue specifically for the case of euryhalinity in Metoposauride (DeFauw 1989; Milner 1990) based on morphological features the group exhibits.

Until now, there has not been solid evidence for marine affinities of Metoposauridae, while Early Triassic Trematosauridae (*Aphaneramma*; Lindemann 1991; Fortuny et al. 2017b) and Plagiosauridae like *Gerrothorax* or *Plagiosternum* (Hagdorn and Reif 1988; Schoch 2021) have clearly been recovered from marine strata. While there is still no direct evidence for marine affinities of Metoposauridae, the occurrence of *Nothosaurus* and several euryhaline invertebrates (Linck 1972; Rieppel and Wild 1994) in the ‘Anatinenbank’ of the Grabfeld Formation indicates clear marine influence in this layer. The fragmentary nature of the recovered specimens might indicate an allochthonous origin. Based on the preservation of the bones (clean fractures, minimal abrasion), the temnospondyl remains have likely not been transported over a long distance and might even potentially be autochthonous. Comparisons with the autochthonous *Nothosaurus* material (Rieppel and Wild 1994) from the same layer demonstrate a ubiquitous condition of preservation with the temnospondyl remains. Had these materials been transported over a long distance or been reworked from foreign strata, one would expect the bones to be more severely abraded and rounded. Regardless, the occurrence of temnospondyls in the marine influenced ‘Anatinenbank’ opens discussion on the possibility for the osmotic tolerances of the group. The palaeoenvironment of the ‘Anatinenbank’, and Grabfeld Formation as a whole, is clearly different from the ‘typical’ palaeoenvironmental setting of other metoposaurid-bearing horizons. Further exceptions to the usual interpretation of freshwater fluvial and lacustrine habitats are known from elsewhere in Germany and Morocco: The Lehrbergschichten (Weser Formation) and Kieselsandstein (Hassberge Formation) represent playa lakes (Seegis 1997; Milner and Schoch 2004) or a terminal alluvial fan interfingering into a playa (Kern and Aigner 1997) respectively. Contrastingly, the upper parts of the T5 member of the Timezgadiouine Formation are debated to either represent a meandering river and floodplain environment (Hofmann et al. 2000) or a dry playa red bed (Zouheir et al. 2018). Seegis (1997) specifically interpreted the salinity content of the different Lehrberg lakes to vary from freshwater to euhaline (0–40‰ salinity), which falls in line with the interpretations of the salinity content for the ‘Anatinenbank’, which is referred to be «equivalent to regular sea water» (Linck 1972). Due to the cyclicity of the Grabfeld Formation, the metoposaurid material described herein were recovered from different phases within the cyclothems. The last stage, the palaeosol phase, is the least fossiliferous and interpreted as to have never been marine (Nitsch et al. 2005). The fossil occurrences of this phase are restricted to conchostracs and occasional fish remains. Additionally, this phase has yielded *Metoposaurus* sp. (SMNS 59770) and is interpreted to have the most restricted freshwater inflows and most terrestrial influence (Nitsch et al. 2005). Therefore, the presence of Metoposauridae in the early and late stages of the Grabfeld Formation cyclothems argue for a wider ecological niche of the group than previously recognised (*sensu* Hunt 1993). The occurrence of the plagiosaurids *Gerrothorax* and *Plagiosternum* in these brackish claystone-dolostones fits in line with their presumed tolerance for changing or generally higher salinity (Sanchez and Schoch 2013) as well as their occurrence in other marine-influenced depositional environments (Tverdokhlebov et al. 2003; Kear et al. 2015; Schoch 2021). Recent comparative studies on the histology of *Metoposaurus* and *Cyclotosaurus* from Poland have revealed potential differences in the mode of life and ecological niche partitioning between those taxa (Kalita et al. 2022; Teschner et al. 2023). This observation is congruent with the predominant occurrence of *Metoposaurus* in local lacustrine environments of the Stuttgart Formation, while *Cyclotosaurus* dominates the respective channel facies (Schoch and Moreno 2024). Furthermore, the scarcity of the described metoposaurid materials, as well as the small size of the *Metoposaurus* skull (SMNS 56633; Seegis 1997) combined with their higher frequency in the Lehrbergschichten, might support the indication of intraspecific variability due to environmental factors in *Metoposaurus* (Sulej 2007).

Conclusion

In the early Carnian Grabfeld Formation of southern Germany, temnospondyls have hitherto been considered to be extremely rare, in low diversity and based on largely undiagnostic material. In this study, we have presented evidence of geographically and stratigraphically widespread occurrence of this group in the upper parts of the Grabfeld Formation. Although fragmentary in nature, the presence of diagnostic temnospondyl remains across the cyclothems is indicative of their presence in this harsh environment. The ‘Estherienschichten’ formed under lacustrine conditions, with the dolomitic Corbula and Acrodus units at their base representing a limnic or lagoonal facies with siliciclastic content that connects to the marginal Benk Formation of northeastern Bavaria (Etzold and Schweizer 2005), where the historically oldest temnospondyl find, *Capitosaurus arenaceus*, was recovered (Münster 1836). This cyclotosaurid represents the only temnospondyl from this siliciclastic channel facies. The capitosauroid intercentrum reported here (SMNS 97123) adds to this picture and documents the presence of this group also in the basin facies. Surprisingly, the temnospondyl diversity was still higher in the Grabfeld Formation than in the marginal facies, as shown by the distinctive dermal bones here referred to *Plagiosternum* and *Gerrothorax*. Whereas *Plagiosternum* is known from shallow marine, coastal and lagoonal environments of the late Ladinian Meissner and Erfurt Formations (Schoch 2015), *Gerrothorax* has been characterized as a tolerant pioneer taxon that coped with a wide range of environmental conditions (Schoch and Witzmann 2011; Sanchez and Schoch 2013). Thus, these observations are consistent with the occurrence of metoposaurids and suggest the persistence of salinity-tolerant temnospondyl taxa in the Grabfeld Formation. Furthermore, the Gipskeuper *Metoposaurus* marks the earliest record of the Metoposauridae. The identification of *Gerrothorax* in the Grabfeld Formation bridges a gap between the occurrences in the Lower Keuper and overlaying Schilfsandstein in their long stratigraphic range from the Ladinian to the Rhaetian (Schoch 2021; Schoch and Moreno 2024). Likewise, the recognition of *Plagiosternum* provides new evidence of their occurrence outside of the Ladinian and thereby extending their stratigraphic range into the Late Triassic.

Although the marine influence of the 'Anatinenbank' and other dolomitic beds in the upper Grabfeld Formation is still debated (Linck 1972; Nitsch 1996), the presence of sauropterygians like *Nothosaurus* (Rieppel and Wild 1994) is clearly indicative of euryhaline and at least temporal marine conditions in the basin. While invertebrates of the formation are well studied (Linck 1972), the knowledge of vertebrates is still lacking. The supposed rarity of temnospondyls might be consequential of insufficient sampling efforts in the Grabfeld Formation, or represents general inhospitable conditions for large groups of vertebrates. Although only fragmentary, the occurrence of temnospondyls in this environment and stratigraphically wide range within the upper Grabfeld Formation demonstrates them to be a regular faunal component of this ecosystem. Palaeoenvironmental comparisons with the upper T5 member of the Timezgadiouine Formation of Morocco potentially solidify a euryhaline physiology of Metoposauridae, and while marine affinities are not directly concluded from the investigations herein, it is evident, that theories of euryhalinity in Metoposauridae and temnospondyls in general should not be dismissed.

Declaration of competing interest

The authors declare that they have no known competing financial interests or personal relationships that could have appeared to influence the work reported in this paper.

Author contributions

Raphael Moreno: Conceptualization (lead); Methodology (equal); Investigation (lead); Writing – original draft preparation (lead); Writing – review and editing (lead); Visualization (lead). Sanjukta Chakravorti: Methodology (equal); Investigation (supporting); Writing – original draft preparation (supporting); Writing – review and editing (supporting). Samuel L. A. Cooper: Methodology (equal); Investigation (supporting); Writing – original draft preparation (supporting); Writing – review and editing (supporting). Rainer Schoch: Resources (lead); Writing – review and editing (supporting); Supervision (lead).

Acknowledgments

We thank Isabell Rosin for preparation of the silicone mould used on SMNS 55899 and preparation of SMNS 97109, as well as G. Buck, A. Jansen and O. Linck for collection and donation of the specimens to the SMNS. RM was supported through a grade scholarship from the State Graduate Sponsorship Program by the Ministry of Science and Art of Baden-Württemberg. We thank the editor Florian Witzmann as well as Dorota Konietzko-Meier and an anonymous reviewer for their suggestions and comments which helped improving this manuscript.

References

Abel O (1919) Die Stämme der Wirbeltiere. Walter de Gruyter and Company, Berlin und Leipzig, 914 pp. https://doi.org/10.5962/bhl.title.2114

Aigner T, Bachmann GH (1992) Sequence-stratigraphic framework of the German Triassic. Sedimentary Geology 80: 115–135. https://doi.org/10.1016/0037-0738(92)90035-P

Antczak M, Bodzioch A (2018) Ornamentation of dermal bones of *Metoposaurus krasiejowensis* and its ecological implications. PeerJ 6: e5267. https://doi.org/10.7717/peerj.5267

Baird D (1986) Some Upper Triassic reptiles, footprints, and an amphibian from New Jersey. The Mosasaur 3: 125–153.

Barrett PM, Sciscio L, Viglietti PA, Broderick TJ, Suarez CA, Sharman GR, Jones AS, Munyikwa D, Edwards SF, Chapelle KEJ, Dollman KN, Zondo M, Choiniere JN (2020) The age of the Tashinga Formation (Karoo Supergroup) in the Mid-Zambezi Basin, Zimbabwe and the first phytosaur from mainland sub-Saharan Africa. Gondwana Research 81: 445–460. https://doi.org/10.1016/j.gr.2019.12.008

Bodzioch A, Kowal-Linka M (2012) Unraveling the origin of the Late Triassic multitaxic bone accumulation at Krasiejów (S Poland) by diagenetic analysis. Palaeogeography, Palaeoclimatology, Palaeoecology 346–347: 25–36. https://doi.org/10.1016/j.palaeo.2012.05.015

Broili F (1915) Über *Capitosaurus arenaceus* Münster. Centralblatt für Geologie und Paläontologie, 569–575.

Brusatte SL, Butler RJ, Mateus O, Steyer J-S (2015) A new species of *Metoposaurus* from the Late Triassic of Portugal and comments on the systematics and biogeography of metoposaurid temnospondyls. Journal of Vertebrate Paleontology 35: e912988. https://doi.org/10.1080/02724634.2014.912988

Buffa V, Jalil N, Steyer J-S (2019) Redescription of *Arganasaurus* (*Metoposaurus*) *azerouali* (Dutuit) comb. nov. from the Upper Triassic of the Argana Basin (Morocco), and the first phylogenetic analysis of the Metoposauridae (Amphibia, Temnospondyli). Papers in Palaeontology 5: 699–717. https://doi.org/10.1002/spp2.1259

Buffetaut E, Martin M (1984) Continental vertebrate distribution, faunal zonation and climate in the Late Triassic. In: Reif W-E, Westphal F (Eds) Third Symposium on Mesozoic Terrestrial Ecosystems, Short Papers. ATTEMPTO, Tübingen, 25–29.

Butler RJ, Rauhut OWM, Stocker MR, Bronowicz R (2014) Redescription of the phytosaurs *Paleorhinus* (‘*Francosuchus*’) *angustifrons* and *Ebrachosuchus neukami* from Germany, with implications for Late Triassic biochronology: Redescription of two phytosaurs from Germany. Zoological Journal of the Linnean Society 170: 155–208. https://doi.org/10.1111/zoj.12094

Chakravorti S, Sengupta DP (2019) Taxonomy, morphometry and morphospace of cranial bones of *Panthasaurus* gen. nov. *maleriensis* from the Late Triassic of India. Journal of Iberian Geology 45: 317–340. https://doi.org/10.1007/s41513-018-0083-1

Colbert EH, Olsen PE (2001) A new and unusual aquatic reptile from the Lockatong Formation of New Jersey (Late Triassic, Newark Supergroup). American Museum Novitates 3334: 1–24. https://doi.org/10.1206/0003-0082(2001)334%3C0001:ANAUAR%3E2.0.CO;2

Dal Corso J, Bernardi M, Sun Y, Song H, Seyfullah LJ, Preto N, Gianolla P, Ruffell A, Kustatscher E, Roghi G, Merico A, Hohn S, Schmidt AR, Marzoli A, Newton RJ, Wignall PB, Benton MJ (2020) Extinction and dawn of the modern world in the Carnian (Late Triassic). Science Advances 6: eaba0099. https://doi.org/10.1126/sciadv.aba0099

Datta D, Ray S, Bandyopadhyay S (2021) Cranial morphology of a new phytosaur (Diapsida, Archosauria) from the Upper Triassic of India: implications for phytosaur phylogeny and biostratigraphy. Papers in Palaeontology 7: 675–708. https://doi.org/10.1002/spp2.1292

DeFauw SL (1989) Temnospondyl amphibians: A new perspective on the last phases in the evolution of the Labyrinthodontia. Michigan Academician 21: 7–32.

DSK (Deutsche Stratigraphische Kommission) (2005) 253 Stratigraphie von Deutschland IV: Keuper. Schweizerbart Science Publishers, Stuttgart, Germany, 296 pp. http://www.schweizerbart.de//publications/detail/isbn/9783510613762/CFS_Courier_Forschungsinstitut_Senckenbe.

Dubiel RF, Hasiotis ST (2011) Deposystems, paleosols, and climatic variability in a continental system: The Upper Triassic Chinle Formation, Colorado Plateau, U.S.A. In: From river to rock record: The preservation of fluvial sediments and their subsequent interpretation. SEPM Society for Sedimentary Geology, 393–421. https://doi.org/10.2110/sepmsp.097.393

Dunne EM, Farnsworth A, Greene SE, Lunt DJ, Butler RJ (2021) Climatic drivers of latitudinal variation in Late Triassic tetrapod diversity. . Palaeontology 64: 101–117. https://doi.org/10.1111/pala.12514

Dutuit J-M (1983) Homogénéité et répartition des métoposauridés et phytosauridés sont-elles en relation avec les espaces marins du Trias supérieur? Comptes Rendus de l’Academie des Sciences. Séries III, Sciences de la Vie 296: 833–836.

Dzik J, Sulej T (2007) A review of the early late Triassic Krasiejów biota from Silesia. Palaeontologia Polonica 64: 1–27.

Emmert U, Bader K, Frank H, Heller F, Jerz H, Prashnowsky AA, Salger M, Schnitzer WA (1974) Geologische Karte von Bayern 1:25000 Erläuterungen zum Blatt Nr. 6429 Neustadt a. d. Aisch. Bayrisches Geologisches Landesamt, München, 143 pp.

Etzold A, Schweizer V (2005) Der Keuper in Baden-Württemberg. In: DSK (Deutsche Stratigraphische Kommission) (Ed.) Stratigraphie von Deutschland IV: Keuper. Schweizerbart Science Publishers, Stuttgart, 214–258.

Fijałkowska-Mader A, Heunisch C, Szulc J (2015) Palynostratigraphy and palynofacies of the Upper Silesian Keuper (southern Poland). Annales Societatis Geologorum Poloniae 85: 637–661. https://doi.org/10.14241/asgp.2015.025

Fortuny J, Marcé-Nogué J, Konietzko-Meier D (2017a) Feeding biomechanics of Late Triassic metoposaurids (Amphibia: Temnospondyli): a 3D finite element analysis approach. Journal of Anatomy 230: 752–765. https://doi.org/10.1111/joa.12605

Fortuny J, Arbez T, Mujal E, Steyer J-S (2019) Reappraisal of ‘*Metoposaurus hoffmani*’ Dutuit, 1978, and description of new temnospondyl specimens from the Middle–Late Triassic of Madagascar (Morondava Basin). Journal of Vertebrate Paleontology 39: e1576701. https://doi.org/10.1080/02724634.2019.1576701

Fortuny J, Gastou S, Escuillié F, Ranivoharimanana L, Steyer J-S (2017b) A new extreme longirostrine temnospondyl from the Triassic of Madagascar: phylogenetic and palaeobiogeographical implications for trematosaurids. Journal of Systematic Palaeontology 16: 675–688. https://doi.org/10.1080/14772019.2017.1335805

Fraas E (1889) Die Labyrinthodonten der schwäbischen Trias. Palaeontographica (1846–1933): 1–158.

Fraas E (1896) Die Schwäbischen Trias-Saurier nach dem Material der Kgl. Naturalien-Sammlung in Stuttgart zusammengestellt. Schweizbart, Stuttgart, 18 pp.

Fraas E (1913) Neue Labyrinthodonten aus der schwäbischen Trias. Palaeontographica (1846–1933) 60: 275–294.

Freudenberger W (2005) Der Keuper in Franken und Oberpfalz (Bayern). In: DSK (Deutsche Stratigraphische Kommission) (Ed.) Stratigraphie von Deutschland IV: Keuper. Schweizerbart Science Publishers, Stuttgart, 203–213.

Gale A, Keupp H, Schweigert G, Sell J (2023) A new phosphatic cirripede from the Carnian (Upper Triassic) of Bavaria, Germany. Neues Jahrbuch für Geologie und Paläontologie - Abhandlungen 309: 19–29. https://doi.org/10.1127/njgpa/2023/1145

Gee BM, Parker WG (2018) A large-bodied metoposaurid from the Revueltian (late Norian) of Petrified Forest National Park (Arizona, USA). Neues Jahrbuch für Geologie und Paläontologie - Abhandlungen 287: 61–73. https://doi.org/10.1127/njgpa/2018/0706

Gee BM, Jasinski SE (2021) Description of the metoposaurid *Anaschisma browni* from the New Oxford Formation of Pennsylvania. Journal of Paleontology 95: 1061–1078. https://doi.org/10.1017/jpa.2021.30

Gee BM, Kufner AM (2022) Revision of the Late Triassic metoposaurid “*Metoposaurus*” *bakeri* (Amphibia: Temnospondyli) from Texas, USA and a phylogenetic analysis of the Metoposauridae. PeerJ 10: e14065. https://doi.org/10.7717/peerj.14065

Gee BM, Parker WG, Marsh AD (2019) Redescription of *Anaschisma* (Temnospondyli: Metoposauridae) from the Late Triassic of Wyoming and the phylogeny of the Metoposauridae. Journal of Systematic Palaeontology 18: 233–258. https://doi.org/10.1080/14772019.2019.1602855

Gwinner MP (1980) Eine einheitliche Gliederung des Keupers (Germanische Trias) in Süddeutschland. Neues Jahrbuch für Geologie und Paläontologie - Monatshefte 4: 229–234. https://doi.org/10.1127/njgpm/1980/1980/229

Hagdorn H, Reif W-E (1988) "Die Knochenbreccie von Crailsheim" und weitere Mitteltrias-Bonebeds in Nordost-Württemberg - Alte und neue Deutungen. In: Hagdorn H (Ed.) Neue Forschungen zur Erdgeschichte von Crailsheim: zur Erinnerung an Hofrat Richard Blezinger. Goldschneck-Verlag, 116–143.

Heckert AB (1997) The tetrapod fauna of the Upper Triassic lower Chinle Group (Adamanian: latest Carnian) of the Zuni Mountains, west-central New Mexico. In: Lucas SG, Estep JW, Williams TE, Morgan GS (Eds) New Mexico's Fossil Record 1. New Mexico Museum of Natural History and Science Bulletin., 29–40.

Heckert AB (2004) Late Triassic microvertebrates from the lower Chinle Group (Otischalkian-Adamanian: Carnian), southwestern U.S.A. In: Heckert AB (Ed.) Late Triassic Microvertebrates. New Mexico Museum of Natural History and Science Bulletin., 1–170.

Heckert AB, Lucas SG (2015) Triassic vertebrate paleontology in New Mexico. In: Lucas SG, Sullivan RM (Eds) Fossil Vertebrates in New Mexico. New Mexico Museum of Natural History and Science Bulletin, 77–96. https://core.ac.uk/reader/345083970 [December 11, 2023]

Heckert AB, Mitchell JS, Schneider VP, Olsen PE (2012) Diverse new microvertebrate assemblage from the Upper Triassic Cumnock Formation, Sanford Subbasin, North Carolina, USA. Journal of Paleontology 86: 368–390. https://doi.org/10.1666/11-098.1

Hofmann A, Tourani A, Gaupp R (2000) Cyclicity of Triassic to Lower Jurassic continental red beds of the Argana Valley, Morocco: implications for palaeoclimate and basin evolution. Palaeogeography, Palaeoclimatology, Palaeoecology 161: 229–266. https://doi.org/10.1016/S0031-0182(00)00125-5

Hunt AP (1993) Revision of the Metoposauridae (Amphibia: Temnospondyli) and description of a new genus from western North America. Museum of Northern Arizona Bulletin 59: 67–97.

Jalil N-E (1999) Continental Permian and Triassic vertebrate localities from Algeria and Morocco and their stratigraphical correlations. Journal of African Earth Sciences 29: 219–226. https://doi.org/10.1016/S0899-5362(99)00091-3

Jewuła K, Matysik M, Paszkowski M, Szulc J (2019) The late Triassic development of playa, gilgai floodplain, and fluvial environments from Upper Silesia, southern Poland. Sedimentary Geology 379: 25–45. https://doi.org/10.1016/j.sedgeo.2018.11.005

Kalita S, Teschner EM, Sander PM, Konietzko-Meier D (2022) To be or not to be heavier: The role of dermal bones in the buoyancy of the Late Triassic temnospondyl amphibian *Metoposaurus krasiejowensis*. Journal of Anatomy 241: 1459–1476. https://doi.org/10.1111/joa.13755

Kear BP, Poropat SF, Bazzi M (2015) Late Triassic capitosaurian remains from Svalbard and the palaeobiogeographical context of Scandinavian Arctic temnospondyls. In: Kear BP, Lindgren J, Hurum JH, Milàn J, Vajda V (Eds) Mesozoic Biotas of Scandinavia and its Arctic Territories. Geological Society, London, Special Publications. The Geological Society of London, 113–126. https://www.lyellcollection.org/doi/10.1144/SP434.11 [November 8, 2023]

Kern A, Aigner T (1997) Faziesmodell für den Kieselsandstein (Keuper, Obere Trias) von SW-Deutschland: eine terminale alluviale Ebene. Neues Jahrbuch für Geologie und Paläontologie - Monatshefte 1997: 267–285. https://doi.org/10.1127/njgpm/1997/1997/267

Klein H, Lucas SG (2010) Tetrapod footprints - their use in biostratigraphy and biochronology of the Triassic. Geological Society, London, Special Publications 334: 419–446. https://doi.org/10.1144/SP334.14

Klein N, Eggmaier S, Hagdorn H (2022) The redescription of the holotype of *Nothosaurus mirabilis* (Diapsida, Eosauropterygia)—a historical skeleton from the Muschelkalk (Middle Triassic, Anisian) near Bayreuth (southern Germany). PeerJ 10: e13818. https://doi.org/10.7717/peerj.13818

Kohút M, Hofmann M, Havrila M, Linnemann U, Havrila J (2018) Tracking an upper limit of the "Carnian Crisis" and/or Carnian stage in the Western Carpathians (Slovakia). International Journal of Earth Sciences 107: 321–335. https://doi.org/10.1007/s00531-017-1491-8

Koken E (1913) Beitrage zur Kenntnis der Schichten von Heiligenkreuz (Abteital, Sudtirol). Abhandlungen der Kaiserlich-Königlichen Geologischen Reichsanstalt 16: 1–43.

Konietzko-Meier D, Teschner EM, Bodzioch A, Sander PM (2020) Pentadactyl manus of the *Metoposaurus krasiejowensis* from the Late Triassic of Poland, the first record of pentadactyly among Temnospondyli. Journal of Anatomy 237: 1151–1161. https://doi.org/10.1111/joa.13276

Kowal-Linka M, Krzemińska E, Czupyt Z (2019) The youngest detrital zircons from the Upper Triassic Lipie Śląskie (Lisowice) continental deposits (Poland): Implications for the maximum depositional age of the Lisowice bone-bearing horizon. Palaeogeography, Palaeoclimatology, Palaeoecology 514: 487–501. https://doi.org/10.1016/j.palaeo.2018.11.012

Kozur HW, Weems RE (2010) The biostratigraphic importance of conchostracans in the continental Triassic of the northern hemisphere. In: Lucas SG (Ed.) The Triassic Timescale. Geological Society, London, Special Publications. The Geological Society of London, 315–417. https://www.lyellcollection.org/doi/10.1144/SP334.13 [April 17, 2023]

Kufner AM, Gee BM (2021) Reevaluation of the holotypes of *Koskinonodon princeps* Branson and Mehl, 1929, and *Borborophagus wyomingensis* Branson and Mehl, 1929 (Temnospondyli, Metoposauridae). Journal of Vertebrate Paleontology 41: e1922067. https://doi.org/10.1080/02724634.2021.1922067

Lagnaoui A, Klein H, Voigt S, Hminna A, Saber H, Schneider JW, Werneburg R (2012) Late Triassic Tetrapod-Dominated Ichnoassemblages from the Argana Basin (Western High Atlas, Morocco). Ichnos 19: 238–253. https://doi.org/10.1080/10420940.2012.718014

Laurin M, Soler-Gijón R (2001) The oldest stegocephalian from the Iberian Peninsula: evidence that temnospondyls were euryhaline. Comptes Rendus de l'Académie des Sciences - Series III - Sciences de la Vie 324: 495–501. https://doi.org/10.1016/S0764-4469(01)01318-X

Laurin M, Soler-Gijón R (2010) Osmotic tolerance and habitat of early stegocephalians: indirect evidence from parsimony, taphonomy, palaeobiogeography, physiology and morphology. In: Vecoli M, Clément G, Meyer-Berthaud B (Eds) The terrestrialization process: modelling complex interactions at the biosphere–geosphere interface. Geological Society, London, Special Publications. The

Geological Society of London, 151–179. https://doi.org/10.1144/SP339.13 [May 4, 2022]

Linck O (1972) Die marine Fauna des süddeutschen Oberen Gipskeupers, insbesondere der sogenannten Anatinenbank (Trias, Kam, Mittl. Keuper, km1) und deren Bedeutung — Evertebraten I. Jahreshefte des Geologischen Landesamtes Baden-Württemberg 14: 145–253.

Lindemann FJ (1991) Temnospondyls and the Lower Triassic palaeogeography of Spitsbergen. In: Fifth Symposium on Mesozoic Terrestrial Ecosystems and Biota, extended abstracts. Contr. Palaeont. Mus. Univ. Oslo, 72.

Long RA, Murry PA (1995) Late Triassic (Carnian and Norian) tetrapods from the southwestern United States. New Mexico Museum of Natural History and Science Bulletin 4: 254.

Lovelace DM, Fitch AJ, Schwartz D, Schmitz M (2023) Concurrence of Late Triassic lithostratigraphic, radioisotopic, and biostratigraphic data support a Carnian age for the Popo Agie Formation (Chugwater Group), Wyoming, USA. Geological Society of America Bulletin: 20. https://doi.org/10.1130/B36807.1

Lucas SG (1998) Global Triassic tetrapod biostratigraphy and biochronology. Palaeogeography, Palaeoclimatology, Palaeoecology 143: 347–384. https://doi.org/10.1016/S0031-0182(98)00117-5

Lucas SG (2018) The Late Triassic Timescale. In: Tanner LH (Ed.) The Late Triassic World: Earth in a Time of Transition. Topics in Geobiology. Springer International Publishing, 26 pp.

Lucas SG (2020) Biochronology of Late Triassic Metoposauridae (Amphibia, Temnospondyli) and the Carnian pluvial episode. Annales Societatis Geologorum Poloniae 90: 409–418. https://doi.org/10.14241/asgp.2020.29

Lydekker R (1890) Part IV Catalogue of the fossil Reptilia and Amphibia in the British Museum of Natural History. British Museum of Natural History, London, 295 pp.

Martínez RN, Apaldetti C, Alcober OA, Colombi CE, Sereno PC, Fernandez E, Malnis PS, Correa GA, Abelin D (2012) Vertebrate succession in the Ischigualasto Formation. Journal of Vertebrate Paleontology 32: 10–30. https://doi.org/10.1080/02724634.2013.818546

Martz JW, Parker WG (2017) Revised formulation of the Late Triassic land vertebrate “faunachrons” of Western North America. In: Ziegler KE, Parker WG (Eds) Terrestrial Depositional Systems. Elsevier, 39–125. https://doi.org/10.1016/B978-0-12-803243-5.00002-9

Mateus O, Butler RJ, Brusatte SL, Whiteside JH, Steyer J-S (2014) The first phytosaur (Diapsida, Archosauriformes) from the Late Triassic of the Iberian Peninsula. Journal of Vertebrate Paleontology 34: 970–975. https://doi.org/10.1080/02724634.2014.840310

Meyer H von (1842) Letter on Mesozoic amphibians and reptiles. Neues Jahrbuch für Mineralogie, Geographie, Geologie, Paläontologie, 301–304.

Milner A (1990) The radiations of temnospondyl amphibians. In: Taylor PD, Larwood GP (Eds) Major Evolutionary Radiations. Systematics Association Special Volume. Clarendon Press, Oxford, 321–350. https://doi.org/10.1093/oso/9780198577188.003.0015

Milner AR, Schoch RR (2004) The latest metoposaurid amphibians from Europe. Neues Jahrbuch für Geologie und Paläontologie - Abhandlungen 232: 231–252. https://doi.org/10.1127/njgpa/232/2004/231

Mujal E, Schoch RR (2020) Middle Triassic (Ladinian) amphibian tracks from the Lower Keuper succession of southern Germany: Implications for temnospondyl locomotion and track preservation. Palaeogeography, Palaeoclimatology, Palaeoecology 543: 109625. https://doi.org/10.1016/j.palaeo.2020.109625

Münster G (1836) Communications addressed to Professor Bronn. Neues Jahrbuch für Mineralogie, Geognosie, Geologie und Petrefaktenkunde, 580–581.

Nilsson T (1934) Vorläufige Mitteilung über einen Stegocephalenfund aus dem Rhät Schonens. Geologiska Föreningeni Stockholm Förhandlingar 56: 428–442. https://doi.org/10.1080/11035893409444893

Nitsch E (1996) Fazies, Diagenese und Stratigraphie der Grabfeld-Gruppe Süddeutschlands (Keuper, Trias). Universität Köln.

Nitsch E, Beutler G, Hauschke N, Etzold A, Laaß M (2005) Feinstratigraphische Korrelation der Grabfeld-Formation (Keuper, Trias) zwischen Hochrhein und Ostsee. Hallesches Jahrbuch für Geowissenschaften Beiheft 19: 135–150.

Ogg JG (2012) Triassic, Chapter 25. In: Gradstein FM, Ogg JG, Schmitz MD, Ogg GM (Eds) The geologic time scale 2012. Vol. 1. Elsevier, 681–730.

Rieppel O (1994) Osteology of *Simosaurus gaillardoti* and the relationships of stem-group Sauropterygia. Fieldiana Geology, New Series 28: 1–85. https://doi.org/10.5962/bhl.title.3399

Rieppel O (2000) Sauropterygia I. Verlag Dr. Friedrich Pfeil, München, 134 pp. https://pfeil-verlag.de/en/publications/handbuch-der-palaeoherpetologie-encyclopedia-of-paleoherpetology-part-12a-sauropterygia-i-placodontia-pachypleurosauria-nothosauria-pistosauria/

Rieppel O, Wild R (1994) *Nothosaurus edingerae* Schultze, 1970: Diagnosis of the species and comments on its stratigraphical occurrence. Stuttgarter Beiträge zur Naturkunde Serie B 204: 13.

Rinehart LF, Lucas SG (2013) The functional morphology of dermal bone ornamentation in temnospondyl Amphibians. In: Tanner LH, Spielmann JA, Lucas SG (Eds) The Triassic System: New Developments in Stratigraphy and Paleontology. New Mexico Museum of Natural History and Science Bulletin. Albuquerque.

Sanchez S, Schoch RR (2013) Bone histology reveals a high environmental and metabolic plasticity as a successful evolutionary strategy in a long-lived homeostatic Triassic temnospondyl. Evolutionary Biology 40: 627–647. https://doi.org/10.1007/s11692-013-9238-3

Scheyer TM, Romano C, Jenks J, Bucher H (2014) Early Triassic marine biotic recovery: The predators’ perspective. PLOS ONE 9: e88987. https://doi.org/10.1371/journal.pone.0088987

Schoch RR (1999) Comparative osteology of *Mastodonsaurus giganteus* (Jaeger, 1828) from the Middle Triassic (Lettenkeuper: Longobardian) of Germany (Baden-Württemberg, Bayern, Thüringen). Stuttgarter Beiträge zur Naturkunde Serie B: 175.

Schoch RR (2000) Biogeography of stereospondyl amphibians. Neues Jahrbuch für Geologie und Paläontologie - Abhandlungen 215: 201–231. https://doi.org/10.1127/njgpa/215/2000/201

Schoch RR (2008) A new stereospondyl from the German Middle Triassic, and the origin of the Metoposauridae. Zoological Journal of the Linnean Society 152: 79–113. https://doi.org/10.1111/j.1096-3642.2007.00363.x

Schoch RR (2015) Amphibien und Chroniosuchier des Lettenkeupers. In: Hagdorn H, Schoch RR, Schweigert G (Eds) Der Lettenkeuper - Ein Fenster in die Zeit vor den Dinosauriern, 203–230.

Schoch RR (2021) Amphibien und Reptilien der Germanischen Trias. In: Hauschke N, Franz M, Bachmann GH (Eds) Trias: Aufbruch in das Erdmittelalter Band 1. Verlag Dr. Friedrich Pfeil, München, 324–340.

Schoch RR, Wild R (1999) Die Wirbeltier-Fauna im Keuper von Süddeutschland. In: Hauschke N, Wilde V (Eds) Trias: eine ganz andere Welt, Mitteleuropa im frühen Erdmittelalter, 395–408.

Schoch RR, Milner AR (2000) Stereospondyli: Stem-Stereospondyli, Rhinesuchidae, Rhytidostea, Trematosauroidea, Capitosauroidea. Verlag Dr. Friedrich Pfeil, München, 203 pp.

Schoch RR, Witzmann F (2011) Cranial morphology of the plagiosaurid *Gerrothorax pulcherrimus* as an extreme example of evolutionary stasis. Lethaia 45: 371–385. https://doi.org/10.1111/j.1502-3931.2011.00290.x

Schoch RR, Milner AR (2014) Temnospondyli I. Verlag Dr. Friedrich Pfeil, 150 pp.

Schoch RR, Seegis D (2016) A Middle Triassic palaeontological gold mine: The vertebrate deposits of Vellberg (Germany). Palaeogeography, Palaeoclimatology, Palaeoecology 459: 249–267. https://doi.org/10.1016/j.palaeo.2016.07.002

Schoch RR, Moreno R (2024) Synopsis on the temnospondyls from the German Triassic. Palaeodiversity 17: 9–48. https://doi.org/10.18476/pale.v17.a2

Seegis D (1997) Die Lehrbergschichten im Mittleren Keuper von Süddeutschland: Stratigraphie, Petrographie, Paläontologie, Genese. 1. Aufl. Hennecke, Remshalden, 382 pp.

Sellwood BW, Valdes PJ (2006) Mesozoic climates: General circulation models and the rock record. Sedimentary Geology 190: 269–287. https://doi.org/10.1016/j.sedgeo.2006.05.013

Sharma KM, Kumar J (2015) Phytosaurian osteoderms from the Late Triassic Tiki Formation (Shahdol District, Madhya Pradesh), India.

Shishkin MA (1986) New data on plagiosaurs from the Triassic of the USSR. Byulleten' Moskovskogo Obshchestva Ispytatelei Prirody, Otdel Geologicheskii 61: 97–102. [in Russian]

Spielmann JA, Lucas SG (2012) Tetrapod fauna of the Upper Triassic Redonda Formation, east-central New Mexico: The Characteristic Assemblage of the Apachean Land-vertebrate Faunachron. Albuquerque, 128 pp.

Spielmann JA, Lucas SG, Heckert AB (2007) Tetrapod fauna of the Upper Triassic (Revueltian) Owl Rock Formation, Chinle Group, Arizona. In: Lucas SG, Spielmann JA (Eds), The Global Triassic. New Mexico Museum of Natural History and Science Bulletin, 371–383.

Stollhofen H, Bachmann GH, Barnasch J, Bayer U, Beutler G, Franz M, Kästner M, Legler B, Mutterlose J, Radies D (2008) Upper Rotliegend to Early Cretaceous basin development. In: Littke R, Bayer U, Gajewski D (Eds) Dynamics of complex intracontinental basins: the Central European Basin System. Springer, Berlin, 181–211.

Sues H-D, Olsen PE, Fedak TJ, Schoch RR (2021) Diverse assemblage of Middle Triassic continental tetrapods from the Newark Supergroup of Nova Scotia (Canada). Journal of Vertebrate Paleontology 41: e2023168. https://doi.org/10.1080/02724634.2021.2023168

Sulej T (2002) Species discrimination of the Late Triassic temnospondyl amphibian *Metoposaurus diagnosticus*. Acta Palaeontologica Polonica 47: 535–546.

Sulej T (2007) Osteology, variability, and evolution of *Metoposaurus*, a temnospondyl from the Late Triassic of Poland. Palaeontologia Polonica 64: 29–139.

Szulc J, Racki G, Jewuła K, Środoń J (2015) How many Upper Triassic bone-bearing levels are there in Upper Silesia (southern Poland)? A critical overview of stratigraphy and facies. Annales Societatis Geologorum Poloniae 85: 587–626. https://doi.org/10.14241/asgp.2015.037

Teschner E, Garbay L, Janecki P, Konietzko-Meier D (2023) Palaeohistology helps reveal taxonomic variability in exceptionally large temnospondyl humeri from the Late Triassic Krasiejów deposit (SW Poland). Acta Palaeontologica Polonica 68: 63–74. https://doi.org/10.4202/app.01027.2022

Thürach H (1888) Übersicht über die Gliederung des Keupers im nördlichen Franken im Vergleich zu den benachbarten Gegenden. Geognostisches Jahresheft 1: 75–162.

Tverdokhlebov VP, Tverdokhlebova GI, Surkov MV, Benton MJ (2003) Tetrapod localities from the Triassic of the SE of European Russia. Earth-Science Reviews 60: 1–66. https://doi.org/10.1016/S0012-8252(02)00076-4

Urlichs M, Tichy G (2000) Correlation of the Bleiglanzbank (Gipskeuper, Grabfeld Formation) of Germany with Upper Ladinia beds of the Dolomites (Italy). Zentralblatt für Geologie und Paläontologie, Teil 1 9/10: 997–1007.

Warren AA, Snell N (1991) The postcranial skeleton of Mesozoic temnospondyl amphibians: a review. Alcheringa: An Australasian Journal of Palaeontology 15: 43–64. https://doi.org/10.1080/03115519108619009

Watson DMS (1919) The structure, evolution and origin of the Amphibia — The Orders Rhachitomi and Stereospondyli. Philosophical Transactions of the Royal Society of London, Series B 209(360–371): 1–73. https://doi.org/10.1098/rstb.1920.0001

Wild R (1974) Ein Labyrinthodonten-Rest (Amphibia) aus den Estherienschichten (Mittlerer Keuper) von Mittelfranken. Geol. Bl. NO-Bayern 24: 48–55.

Witzmann F, Gassner T (2008) Metoposaurid and mastodonsaurid stereospondyls from the Triassic – Jurassic boundary of Portugal. Alcheringa: An Australasian Journal of Palaeontology 32: 37–51. https://doi.org/10.1080/03115510701757316

Zeh A, Franz M, Obst K (2021) Zircon of Triassic Age in the Stuttgart Formation (Schilfsandstein)—Witness of Tephra Fallout in the Central European Basin and New Constraints on the Mid-Carnian Episode. Frontiers in Earth Science 9: 778820. https://doi.org/10.3389/feart.2021.778820

Zhang Y, Ogg JG, Franz M, Bachmann GH, Szurlies M, Röhling H-G, Li M, Rolf C, Obst K (2020) Carnian (Late Triassic) magnetostratigraphy from the Germanic Basin allowing global correlation of the Mid-Carnian Episode. Earth and Planetary Science Letters 541: 116275. https://doi.org/10.1016/j.epsl.2020.116275

Zittel KA (1888) Handbuch der Paläeontologie. Abteilung 1. Paläozoologie Band III. Vertebrata (Pisces, Amphibia, Reptilia, Aves). Oldenbourg, München, 900 pp.

Zouheir T, Hminna A, Klein H, Lagnaoui A, Saber H, Schneider JW (2018) Unusual archosaur trackway and associated tetrapod ichnofauna from Irohalene member (Timezgadiouine formation, late Triassic, Carnian) of the Argana Basin, Western High Atlas, Morocco. Historical Biology 32: 589–601. https://doi.org/10.1080/08912963.2018.1513506

Fossil Record 27 (3) 2024, 401–422 | DOI 10.3897/fr.27.125379

Growing giants: ontogeny and life history of the temnospondyl *Mastodonsaurus giganteus* (Stereospondyli) from the Middle Triassic of Germany

Rainer R. Schoch[1,2], Florian Witzmann[3], Raphael Moreno[1,2], Ralf Werneburg[4], Eudald Mujal[1,5]

1 *Staatliches Museum für Naturkunde, Rosenstein 1, D-70191 Stuttgart, Germany*
2 *Fachgebiet Paläontologie, Institut für Biologie, University of Hohenheim, D-70599 Stuttgart, Germany*
3 *Museum für Naturkunde, Leibniz-Institut für Evolutions- und Biodiversitätsforschung, Invalidenstraße 43, D-10015 Berlin, Germany*
4 *Naturhistorisches Museum Schloss Bertholdsburg, Burgstraße 6, D-98553 Schleusingen, Germany*
5 *Institut Català de Paleontologia Miquel Crusafont (ICP-CERCA), Universitat Autònoma de Barcelona, Edifici ICTA-ICP, c/ Columnes s/n, Campus de la UAB, E-08193 Cerdanyola del Vallès, Catalonia, Spain*

https://zoobank.org/FF6C32D8-1CB8-4779-A070-7CEB3B837EAD

Corresponding author: Rainer R. Schoch (rainer.schoch@smns-bw.de)

Academic editor: Marcello Ruta ♦ **Received** 14 April 2024 ♦ **Accepted** 29 July 2024 ♦ **Published** 30 December 2024

Abstract

The Middle Triassic capitosaur *Mastodonsaurus giganteus* was the largest temnospondyl and the dominating aquatic predator in many European freshwater to brackish ecosystems. It is represented by numerous size classes, which are described and analysed for the first time. The documented size range encompasses specimens between 12–15 mm and 1200 mm in skull length. Early growth stages are restricted to dentaries and interclavicles, whereas juveniles are represented by partial skulls, mandibles, and girdles. The smallest specimens already possessed diagnostic features of the taxon, and small juveniles also shared the dermal ornament with larger specimens. The heavy, disc-shaped intercentra were established early in the juvenile phase. Cranial proportions were remarkably conservative throughout ontogeny, with the orbits proportionately decreasing in size only very moderately, the postorbital skull becoming slightly longer and the occipital margin more concave in the largest forms. Analysis of frequency distributions of *M. giganteus* in different Lower Keuper deposits in southern Germany reflects habitat preferences in specific phases of its life cycle. The coal-bearing deposit at Gaildorf yielded unusually large specimens with relatively well-ossified appendicular skeletons. In the more common lake shore facies, only adult specimens are present. In turn, juveniles might have dwelled in calmer environments. Smaller lakes were apparently less attractive than larger or deeper water bodies that provided sufficient resources for several temnospondyls, and juvenile specimens have been identified from all of them. The diverse actinopterygian fish fauna provided prey for all growth stages of the large temnospondyl predators.

Key Words

Capitosauria, lower Keuper, ontogeny, Stereospondyli

Introduction

From the Carboniferous well into the Triassic, the temnospondyls formed a speciose clade of early tetrapods, and relic forms are known in Jurassic and Early Cretaceous strata of Asia and Australia (Warren and Hutchinson 1983; Warren et al. 1997; Schoch 2014). Temnospondyls probably include the stem-group of lissamphibians (Milner 1993; Anderson 2008; Schoch 2014), although in contrast to extant salamanders and frogs, temnospondyls were relatively large predators within or along the shores of rivers, lakes, and lagoons and many exceeded one metre in body length (Schoch and Milner 2000; Steyer and Damiani 2005). During the Triassic, a clade of large-growing and predominantly aquatic forms, the stereospondyls, diversified and populated numerous water bodies. Their robust bones form abundant finds in lacustrine and fluvial deposits around the world. The Lower Keuper (Erfurt Formation) of southern and central Germany yielded many deposits in which a variety of stereospondyls are preserved (Schoch and Seegis 2016; Schoch et al. 2022).

One of these deposits, a small coal and alum mine at Gaildorf, had yielded the historically first remains of temnospondyls (Jaeger 1828; Weber 1992). The heavy coaly siltstones contained 60 cm long skulls and articulated skeletons of the up to 5 m long capitosaur *Mastodonsaurus giganteus*, which soon became an iconic taxon for Triassic deposits (Owen 1841; Meyer and Plieninger 1844; Fraas 1889; Schoch et al. 2023). Based on the complex folds in their large fang teeth, first recognised in *Mastodonsaurus*, the temnospondyls and other early tetrapods became known as labyrinthodonts (Meyer 1842), and they were eventually recognised as relatives of extant amphibians (Quenstedt 1850). After the monographic descriptions of *M. giganteus* by Meyer and Plieninger (1844), subsequent authors added further observations on new material from Baden-Württemberg (Fraas 1889; Huene 1922; Schmidt 1928) and Thuringia (Schmidt 1931; Rühle von Lilienstern 1935), and material attributed to the genus *Mastodonsaurus* was later reported from coeval deposits of Russia (Konzhukova 1955) and Poland (Czepinski et al. 2023), as well as from Anisian lagerstaetten in Germany and arguably southern England (Schoch et al. 2023). A more complete picture of the adult skeleton of this largest temnospondyl could only emerge after new finds had accumulated (Schoch 1999). However, the ontogeny and life history of the taxon remained inadequately known.

This changed with the collection of much additional material as well as numerous data gathered during excavations. This most recent period started with the discovery of the rich fossillagerstätte exposed along a road-cut near Kupferzell-Bauersbach. Located about 22 km north of Gaildorf, this 500 m long section exposed scores of temnospondyl bones, among which were numerous skulls and postcranial remains of *M. giganteus* (Wild 1980; Urlichs 1982; Schoch et al. 2022). The same highway construction exposed further fossillagerstätten near Ilshofen and Wolpertshausen, as did housebuilding at Michelbach an der Bilz (Hagdorn et al. 2015). Finally, the Schumann limestone quarry at Vellberg-Eschenau also yielded large quantities of temnospondyl remains, among which *M. giganteus* is especially common (Schoch and Seegis 2016). The Lower Keuper also yielded material at Bedheim (Rühle von Lilienstern 1935) and Arnstadt, Thuringia (Werneburg and Witter 2005). At closer inspection, these localities preserve slightly different lake faunas, wherein *M. giganteus* is present with specimens of different sizes. These rich finds and the numerous locality data provide a unique opportunity to study the ontogeny and palaeoecology of this largest known temnospondyl. The objectives of the present study are (1) to document the ontogenetic changes in *M. giganteus* and (2) analyse the size distribution of this taxon in the different fossillagerstätten and its palaeoecological implications.

Materials and methods

Material

The material on which the present study is based was collected over a period of almost 200 years (Jaeger 1828; Weber 2013; Schoch and Seegis 2016; Schoch et al. 2022). In the 1820s to 1860s, the Gaildorf locality yielded five skulls of large to giant size (Meyer in Meyer and Plieninger 1844; Meyer 1855). One of them was associated with an articulated postcranial skeleton that was partially figured by Plieninger in Meyer and Plieninger (1844). The surviving material is housed in the collections at Tübingen (GPIT) and Stuttgart (SMNS), and the now-lost giant snout was fortunately described and figured by Meyer (1855).

The skull from Bedheim in Thuringia collected by Rühle von Lilienstern (1935) is housed in the Natural History Museum Berlin (MB), whereas the more recent finds from Arnstadt are housed in the Natural History Museum Schleusingen (NHMS).

Further material accumulated from deposits in Baden-Württemberg are now housed at the SMNS, as is the entire collection from the Kupferzell excavation of 1977 (Schoch et al. 2022). In the 1980s, finds from Michelbach an der Bilz and Wolptershausen came into the MHI collection at the Muschelkalkmuseum Ingelfingen, as did the bulk of the material collected by private collector Werner Kugler in Vellberg-Eschenau (Schoch and Seegis 2016). Since 1998, much additional material was collected by the first author and colleagues at Vellberg that is now housed at the SMNS.

Ontogeny

Analyzing ontogenetic changes in extinct taxa faces a range of challenges, such as incomplete specimens, poor preservation of small stages, taxonomic identification of all growth stages and variation of the studied samples in space and time. Even if restricted to samples collected at the same locality and within one horizon, time averaging is unavoidable in most cases (Boy 2003; Schoch 2009).

The studied material of *Mastodonsaurus giganteus* was collected at numerous localities, nine of which yielded diagnostic skull material (Gaildorf, Markgröningen, Hoheneck, Kupferzell, Vellberg, Michelbach an der Bilz, Wolpertshausen, Bedheim and Arnstadt). Among the diagnostic finds, only Vellberg and Kupferzell produced samples that are rich enough to study ontogenetic changes, whereas the other localities gave only adult or relatively large juvenile specimens. Larval specimens are known from Kupferzell K3 and Vellberg E6, whereas juvenile and subadult specimens are known from Vellberg E6 and E7.

Our focus on the ontogenetic changes in the skeleton of *M. giganteus* is therefore entirely based on the sample from Kupferzell K3, K4 and Vellberg E6 and E7. These two localities represent coeval and regionally neighbouring lake deposits, separated by 25 km distance. They both fall within the topmost units of the Untere Graue Mergel, and the lacustrine facies have been studied in detail (Schoch and Seegis 2016; Schoch et al. 2022).

All the studied specimens referred to *Mastodonsaurus giganteus* were identified on the basis of autapomorphies (see diagnosis). The samples from Vellberg (E6, E7) and Kupferzell (K3, K4) were thoroughly examined for differences between all preserved stages of ontogeny, but we identified only individual variation rather than geographically consistent clusters. We therefore conclude that the samples from Kupferzell and Vellberg, on which our ontogenetic study rests, likely represent the same species and are coeval within the limits of time averaging.

Abbreviations

Anatomical

ap, anterior process; **apv**, anterior palatal vacuity; **ch**, choana; **d**, dentary; **eo**, exoccipital; **f**, frontal; **HHL**, posterior skull length; **HHW**, posterior skull width; **IOW**, interorbital width; **ipv**, interpterygoid vacuity; **ju**, jugal; **la**, lacrimal; **m**, maxilla; **n**, nasal; **nar**, naris; **ORL**, orbit length; **p**, parietal; **pap**, parapophysis; **pf**, postfrontal; **pl**, palatine; **pm**, premaxilla; **pmf**, premaxillar fenestra; **po**, postorbital; **pop**, posterior process; **pp**, postparietal; **prf**, prefrontal; **ps**, parasphenoid; **pt**, pterygoid; **q**, quadrate; **qj**, quadratojugal; **SL**, skull length; **sq**, squamosal; **st**, supratemporal; **stf**, subtemporal fenestra; **ta**, tabular; **vo**, vomer.

Institutional

GPIT, Institut für Geologie Tübingen; **MB**, Museum für Naturkunde Berlin, Leibniz-Institut für Evolutions- und Biodiversitätsforschung; **MHI**, Muschelkalkmuseum Hagdorn Ingelfingen, **NHMS**, Naturhistorisches Museum Schloss Bertholdsburg, Schleusingen, **SMNS**, Staatliches Museum für Naturkunde Stuttgart.

Systematic Palaeontology

Temnospondyli Zittel, 1888
Eutemnospondyli Schoch, 2013
Stereospondyli Zittel, 1888
Capitosauria Yates & Warren, 2000 sensu Damiani & Yates, 2003
Capitosauroidea Säve-Söderbergh, 1935 sensu Schoch, 2008
Mastodonsauridae Lydekker, 1885

Genus *Mastodonsaurus* Jaeger, 1828

Type species. *Mastodonsaurus giganteus* Jaeger, 1828.

Diagnosis. Autapomorphies (Figs 2–6): (1) Premaxilla with openings for symphyseal tusks, set well anterior to naris; (2) orbits large, reaching one-fifth of skull length; (3) jugal slender lateral to orbit; (4) parietal elongated anterior to pineal foramen; (5) lateral line sulci very wide; (6) epipterygoid massive and complex, with six distinct processes (footplate, pr. anterior, pr. dorsalis, pr. sphenethmoidalis, pr. basalis, pr. posterior). Characters shared with other capitosaurs: (a) interclavicle with elongated anterior process; (b) elongate postglenoid area; (c) tall hamate process.

Comment. Character (1) is shared with *C. naraserluki* and *C. mordax* (Fraas 1913; Marzola et al. 2017) and also occurs in one specimen of *C. robustus* (Schoch and Moreno 2024). However, *Mastodonsaurus* differs from all these in having a more elongated premaxilla anterior to the naris and a more lateral and posterior emplacement of the opening with respect to the anterior snout margin (Schoch and Moreno 2024). Character (4) is shared with metoposaurids, but no other taxon with Capitosauroidea.

Mastodonsaurus giganteus Jaeger, 1828

1828 *Mastodonsaurus* Jaeger: p. 35, nomen imperfectum.
*1828 *Salamandroides giganteus* Jaeger: p. 38.
1841 *Labyrinthodon jaegeri* Owen: p. 227
1844 *Mastodonsaurus jaegeri* Meyer: p. 11. pls. 6–7.
1844 *Mastodonsaurus jaegeri* Plieninger: p. 57, pls. 3–7.
1850 *Mastodonsaurus giganteus* Quenstedt: p. 2.
1889 *Mastodonsaurus giganteus* Fraas: p. 32, figs 1–5.
1922 *Mastodonsaurus giganteus* Huene: p. 400, figs 1–12.
1999 *Mastodonsaurus giganteus* Schoch: p. 42, figs 8–49.
2007 *Mastodonsaurus giganteus* Moser and Schoch: p. 1245, figs 2, 3, 5–9.

Holotype. GPIT Am 678, an occiput with exoccipital condyles and posterior portion of parasphenoid, estimated skull length about 61 cm (Moser and Schoch 2007, fig. 9).

Type locality and age. Alum mine with main entrance at Parkschule north of the Kocher River, Gaildorf (Baden-Württemberg, Germany) (Meyer and Plieninger 1844). The fossiliferous sequence was locally restricted and remained poorly constrained for a long time within the Lower Keuper (Fig. 2; Weber 1992; Hagdorn et al. 2015). It encompassed coal, coaly mudstones and siltstones (Plieninger in Meyer and Plieninger 1844; Kurr 1852; Quenstedt 1880). Recent sections measured at briefly exposed outcrops in the vicinity of the type locality confirmed that the sequence was stratigraphically immediately below the Hauptsandstein or main sandstone unit of the Lower Keuper, corresponding to the Estherienschichten (Hans Hagdorn and Theo Simon, pers. comm. 2022), as had been suggested by Weber (1992). The age of the Lower Keuper is considered Longobardian (late Ladinian, late Middle Triassic).

Referred material. Fig. 2 provides an overview of the samples of *M. giganteus* studied in the present paper.

Gaildorf G2 (locus typicus, top of Estherienschichten, below Hauptsandstein). GPIT 1824, occiput (61 cm skull

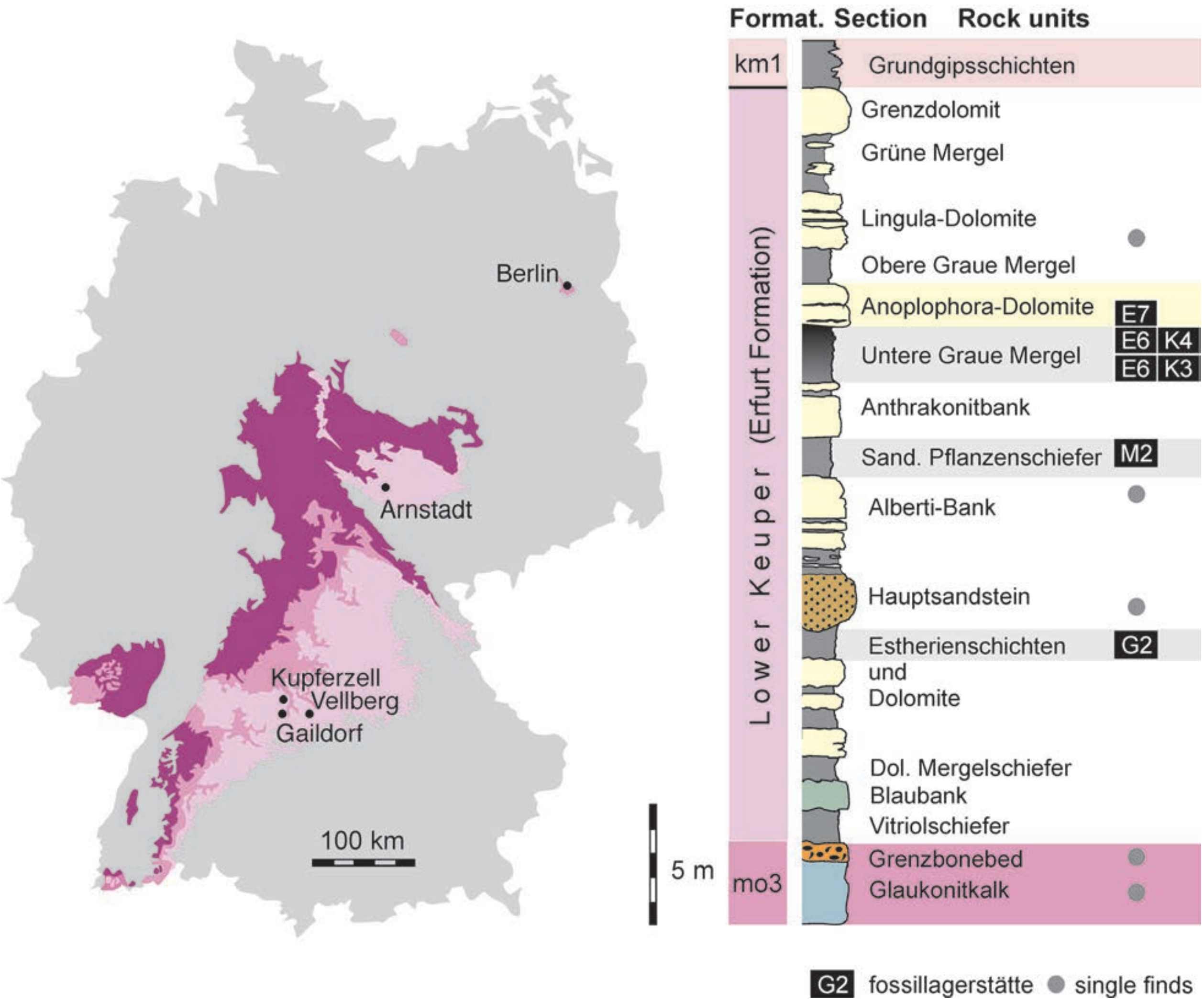

Figure 1. Localities and stratigraphic range of *Mastodonsaurus giganteus* Jaeger, 1828 in Germany. Abbreviations of major localities: G2, Gaildorf (type locality), E5, 6, 7, Vellberg-Eschenau, K3, 4, Kupferzell-Bauersbach, M2, Michelbach an der Bilz.

length). SMNS 4698, complete skull with mandibles (62 cm SL). SMNS 4707, complete skull with mandibles (68 cm SL) and anterior part of vertebral column (9 intercentra). SMNS 4938, tip of snout (estimated 65 cm SL). SMNS 54679, complete skull with mandibles (60 cm SL; this specimen was erroneously reported by Moser and Schoch (2007) as measuring 74 cm). A large snout (about 107 cm SL, described in Meyer and Plieninger 1844 and figured by Meyer 1855), reported as heavily damaged by Fraas (1889), has long been lost (Schoch 1999); here we provide an interpretation of Meyer's (1855) figure in Fig. 5D.

Michelbach an der Bilz M1 (Sandige Pflanzenschiefer, layer M1). MHI 1070, series of intercentra of juvenile specimen.

Kupferzell K3 (Untere Graue Mergel, green layer K3 of Schoch et al. 2022). SMNS 54675, complete skull (60.5 cm), almost undistorted, with perfect braincase. SMNS 54678, complete skull (54.5 cm). SMNS 80704, complete skull (55 cm) with mandible. SMNS 80889, complete skull (59 cm) with mandible. SMNS 80890, postorbital part of skull (45.5 cm). SMNS 80905, disarticulated skull (about 45 cm). SMNS 80945, disarticulated skull (60 cm). SMNS 81075, disarticulated skull (48 cm). SMNS 81310, giant specimen, including complete mandible (110 cm; 88.5 cm SL) with few remnants of the palate and a total of 28 presacral and 6 caudal vertebrae. SMNS 81368, posterior part of palate. SMNS 84030, posterior margin of skull (estimated 65 cm SL). Symphyses of tiny specimens (SMNS 97035, approx. 12–15 mm mm SL; SMNS 97036, 25 mm SL). Isolated material: supratemporal: SMNS 80886, 81153–81156; postorbital: SMNS 81161–81162; squamosal: 80946, 80947, 81164; pterygoid: SMNS 81316, 81318, 81324–81325; parasphenoid: SMNS 81326, 81328, 81330–81332; exoccipital: 80980–80988, 81002–81005, 81013, 81018–81024; interclavicle: SMNS 81282–91; clavicle: SMNS 81298; cleithrum: SMNS 81208–81209, 81257, 81264; intercentra: SMNS 84172 (13), 84173, 84194 (4), 84195, 84206, 84208, 84212 (10), 84213 (11), 84291 (5).

Kupferzell K4 (Untere Graue Mergel, yellow-brown layer K4 of Schoch et al. 2022). SMNS 54676, complete skull (56 cm). SMNS 54677, complete skull (51 cm) with mandible. SMNS 80249, posterior rim of skull (65 cm). SMNS 80878. Near-complete skull (about 65 cm) with

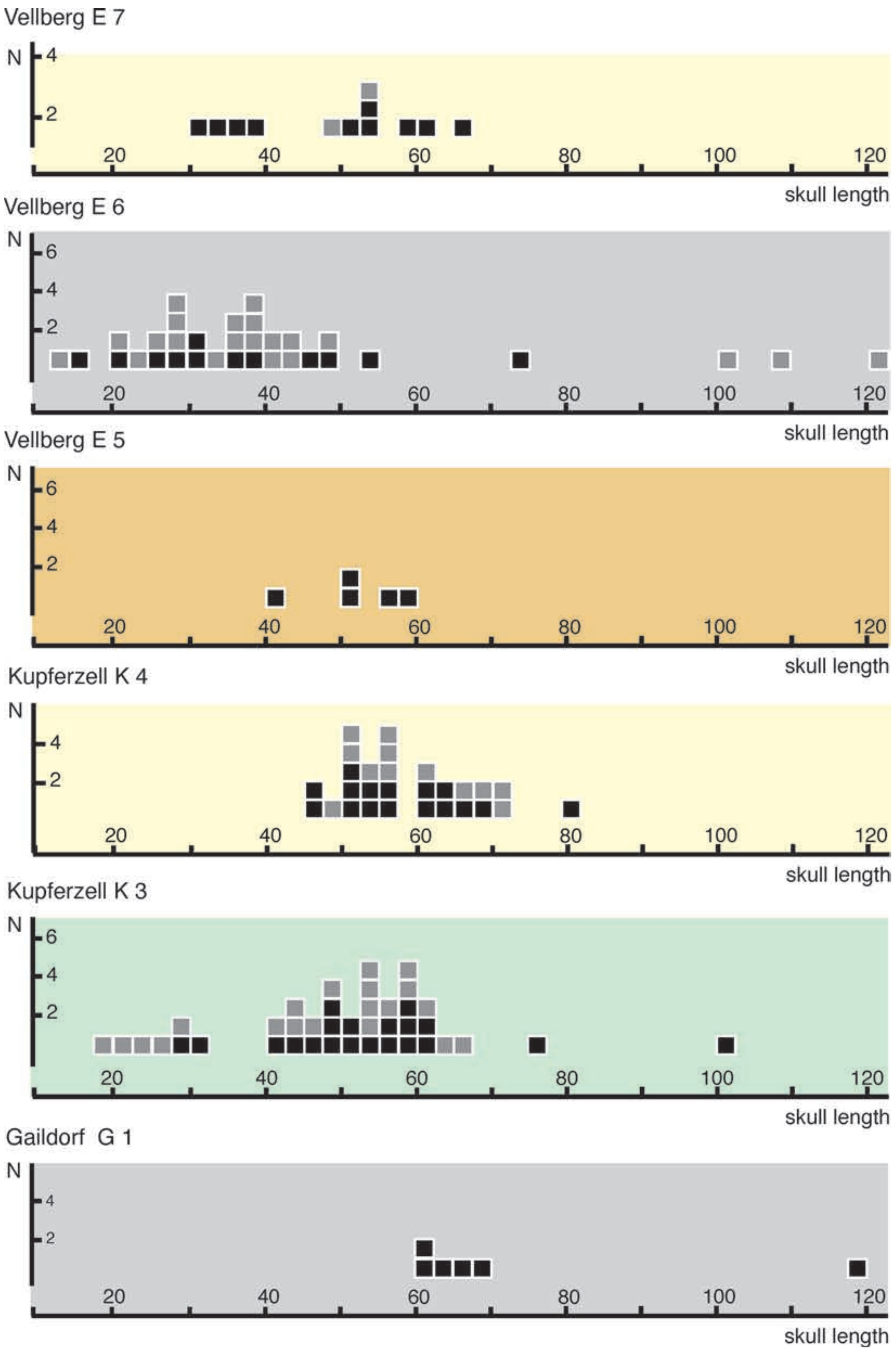

Figure 2. *Mastodonsaurus giganteus* Jaeger, 1828. Frequency and size distribution of specimens in six different localities and horizons of the Lower Keuper in northern Baden-Württemberg (Germany). Black squares: skulls or semi-articulated skeletons; Grey squares: single bones.

parts of mandible. SMNS 80887, snout fragment (54 cm SL). SMNS 80913, fragmentary skull (65 cm total length) with 28 presacral vertebrae. SMNS 83293, fragmentary skull (60 cm). SMNS 83312, fragmentary skull (45 cm). SMNS 97038–97042, skull fragments (68, 50, 47, 50, 57 cm SL, respectively). Isolated material: supratemporal: SMNS 80865, postparietal: 81000, 83260; tabular: SMNS 81091–81098; exoccipitals: SMNS 80917, 80926,

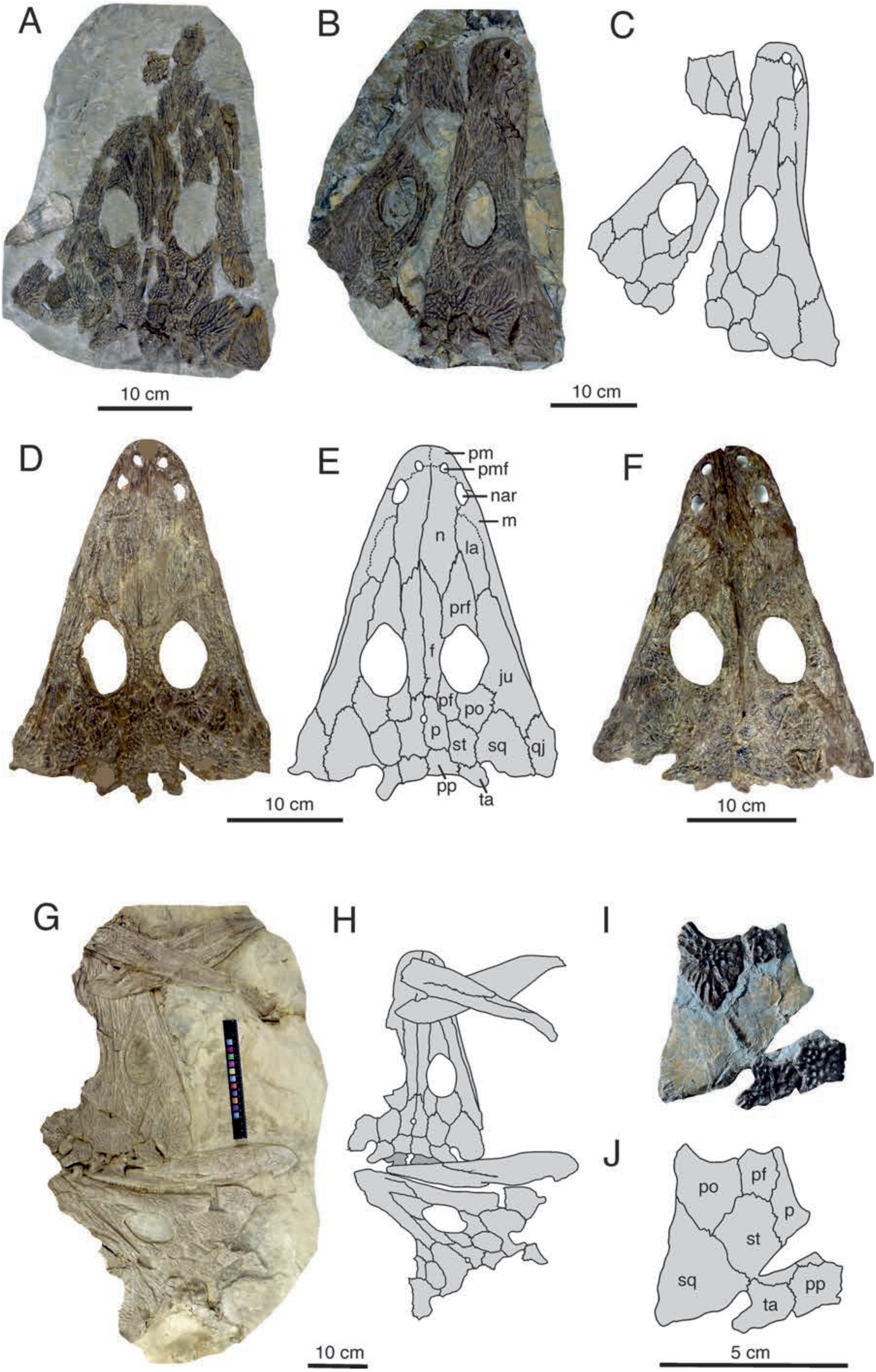

Figure 3. *Mastodonsaurus giganteus* Jaeger, 1828. **A.** MHI-Ku 1992/22 (Vellberg, E6); **B, C.** MHI-Ku 1992/21 (Vellberg, E6); **D, E.** MHI-Ku 1992/31 (Vellberg, E6); **F.** MHI-Ku 1992/42 (Vellberg, E6); **G, H.** MHI 1991-4 (Vellberg, E7); **I, J.** SMNS 97037 (Vellberg, E6).

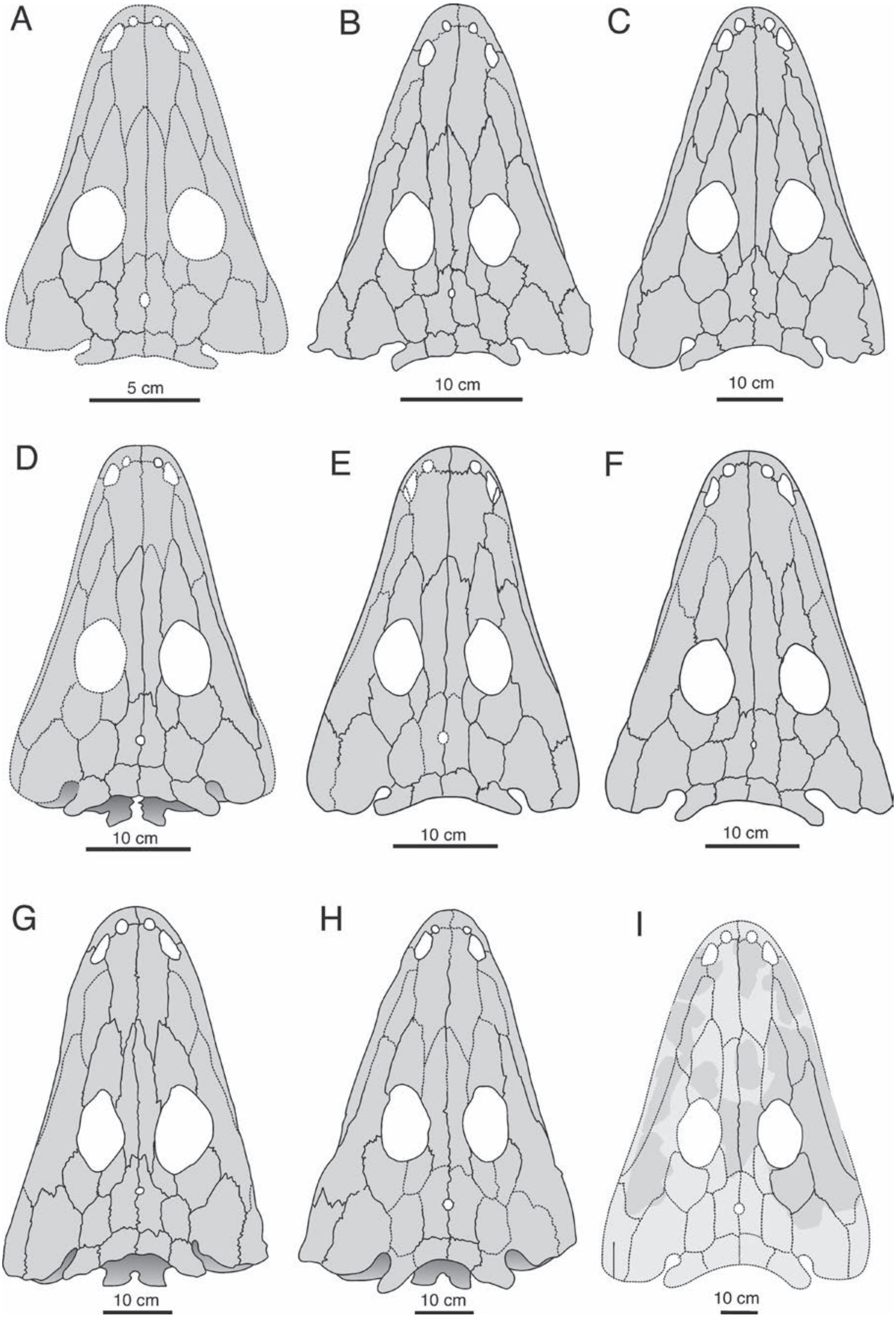

Figure 4. *Mastodonsaurus giganteus* Jaeger, 1828. Skull reconstructions in dorsal view. **A.** Restoration of incomplete specimen SMNS 97037 (Vellberg, E6); **B.** MHI-Ku 1992/31 (Vellberg, E6); **C.** SMNS 54678 (Kupferzell, K3; original figured in Schoch 1999, pl. 3); **D.** MHI-Ku 1991/4 (Vellberg, E6); **E.** MHI-Ku 1992/21 (Vellberg, E6); **F.** MHI-Ku 1992/42 (Vellberg, E6); **G.** SMNS 4698 (Gaildorf, G2; original figured in Schoch 1999, pl. 1); **H.** SMNS 54679 (Gaildorf, G2; original figured in Moser and Schoch 2007, fig. 6c); **I.** Restoration of largest skull, NHMS-WT3323-3368 (Arnstadt), restored regions in light grey.

80956, 80957, 80979, 80980, 80982, 80989, 80990, 80994, 80996, 80998, pterygoid: SMNS 81320, 81321; interclavicle: SMNS 81270–81276; cleithrum SMNS 81210, 81261, 81262; intercentra: SMNS 84138, 84139 (14), 84145 (7), 84200, 84207 (6), 84210, 84211.

Markgröningen (Fraas 1889, p. 5: "10 m above Hauptsandstein" = Untere Graue Mergel). SMNS 4974. Skull without cheek regions (71.3 cm SL).

Vellberg E5 (Untere Graue Mergel, brown layer E5 of Schoch and Seegis 2016). MHI 1991/22, complete skull (50.5 cm). MHI 1992/20, complete skull (59.5 cm). MHI 1992/41, complete skull (42 cm). MHI Ku/UC53le1 (53 cm). MHI Ku/UC53le2 (34.6 cm). SMNS 81966, complete skull (51 cm) with mandible.

Vellberg E6 (Untere Graue Mergel, grey layer E6 of Schoch and Seegis 2016). MHI 1992/1, complete large skull (72 cm) with mandible detached. MHI 1992/31, complete juvenile skull (30 cm). MHI 1992/42, complete juvenile skull (28.6 cm). MHI-Ku 1993/4, tiny interclavicle. MHI-Ku 1993/5, juvenile interclavicle. SMNS 97043, complete skull (39 cm). MHI Ku/UC54le1, mandible (24.1 cm). MHI Ku/UC54le2, mandible (20 cm). MHI Ku/UC54le3, mandible (35 cm). MHI Ku/UC1, mandible (SL approx.: 37 cm). MHI Ku/UC2, mandible (100.8 cm SL). SMNS 92128, complete, highly fractured skull (60 cm length). SMNS 97037, posterior portion of juvenile skull (15 cm SL).

Vellberg E7 (Anoplophora Dolomite, pale yellow dolostone unit E7 of Schoch and Seegis 2016). MHI 1794/3, complete, slightly deformed skull (62 cm). MHI 1991/1, complete skull in 3D with mandible (54.2 cm). MHI 1991/4, two partial skulls (32 and 34 cm). MHI 1991/5, snout (estimated 66.6 cm SL). MHI 1991/6, partial skull (53.9 cm). MHI 1991/7, snout (estimated 35 cm SL). MHI 1991/8, mandible (estimated 58.3 cm SL). MHI 1991/11, complete skull with deformed snout (38 cm). MHI Ku/UC54le, mandible (52.7 cm). MHI Ku/UC54le1, skull (54.4 cm). MHI Ku/UC, skull (54 cm).

Arnstadt (Oberes Dunkles Band, layer 42, dark coaly siltstone of Werneburg in Hagdorn et al. 2015). NHMS-WT3323-3368, partial skull and mandible (estimated 101 cm SL; Werneburg and Witter 2005).

Hoheneck H1 (Lingula-Dolomit, Hoheneck facies). SMNS 740, palate (52 cm; Fraas 1889). SMNS 4194 (66 cm; skull roof in internal view; Fraas 1889).

Diagnosis. Autapomorphies (in contrast to *M. cappelensis*, see Schoch et al. 2023): (1) Orbits with pointed anterior end and narrow interorbital distance (Figs 3, 4; IOW:SL = 0.095); (2) medial premaxillary teeth enlarged (Fig. 5C, D); (3) tusks in palate and especially in the symphysis greatly enlarged (Figs 5, 6), (4) postorbital larger than supratemporal; (5) squamosal wide to give broadened cheek; (6) interclavicle with elongate anterior process; (7) intercentra of the trunk dorsally closed in juveniles and adults (Fig. 6N–Q).

Comment. The three complete skulls from Gaildorf G2 and most specimens from Vellberg E5–7 are all heavily affected by crushing and distortion, whereas the Kupferzell specimens are preserved almost in 3d thanks to early cementation of sediment. Morphological differences especially in the squamosal embayment and cheek may therefore be caused by post-mortem processes rather than reflect morphological variation. We did not spot consistent differences between the Gaildorf G2 sample and other samples described here, therefore consider all samples as belonging to the type species.

The Kupferzell and Vellberg samples are morphologically very similar and stratigraphically well constrained (both fall within above the lagoonal deposit K1 = E4 and below the base of the Anoplophora Dolomite at the top of the Untere Grauel Mergel).

Ontogeny of *Mastodonsaurus giganteus*

Smallest growth stages

The smallest specimens comprise symphyses that were identified in screen-washed samples from Kupferzell (K3) and small elements of the pectoral girdle from Vellberg (E6). As the two localities are coeval, both yield adult specimens of *M. giganteus* that do not show consistent morphological differences, and the two lake environments were very probably interconnected, we consider the Kupferzell (K3) and Vellberg (E6) samples as part of the same species. We did not identify small growth stages of *M. giganteus* in older or younger deposits.

The symphyses are well-preserved and measure 1 mm and 2 mm in length, respectively (Fig. 6A, B). They rank among the smallest identified stereospondyl specimens worldwide, third only to *Rewanobatrachus aliciae* (Warren and Hutchinson 1988) and *Trematolestes hagdorni* (Schoch and Mujal 2022).

The smallest symphysis stems from a specimen with approximately 12–15 mm skull length (SMNS 97035, Fig. 6A). The larger symphysis (SMNS 97036, Fig. 6B) is about double the size but has proportionately similar-sized fangs. The size of the marginal teeth decreased gradually in proportion from the smallest specimen over the next larger to the juvenile and adult symphyses (Fig. 6A–D).

Both symphyses can be easily distinguished from all other temnospondyls: they differ from *Tatrasuchus* (Fig. 6E, F) by the absence of a transverse row of teeth posterior to the fangs and the larger size of these, from *Callistomordax* (Fig. 6G) in the presence of a continuous dentary tooth row anterior to the fangs and from *Trematolestes* (Fig. 6H) in the different outline of the bone, the absence of a sagittally extended symphysis and the different arrangement of the fangs with the medial one being well anterior. The symphyses of plagiosaurids are still more different, especially in the absence of tusks and the outline of the dentary (Hellrung 2003; Damiani et al. 2009; Witzmann and Schoch 2024).

Likewise, we identified a range of small and tiny interclavicles in the Vellberg (E6) sample. These

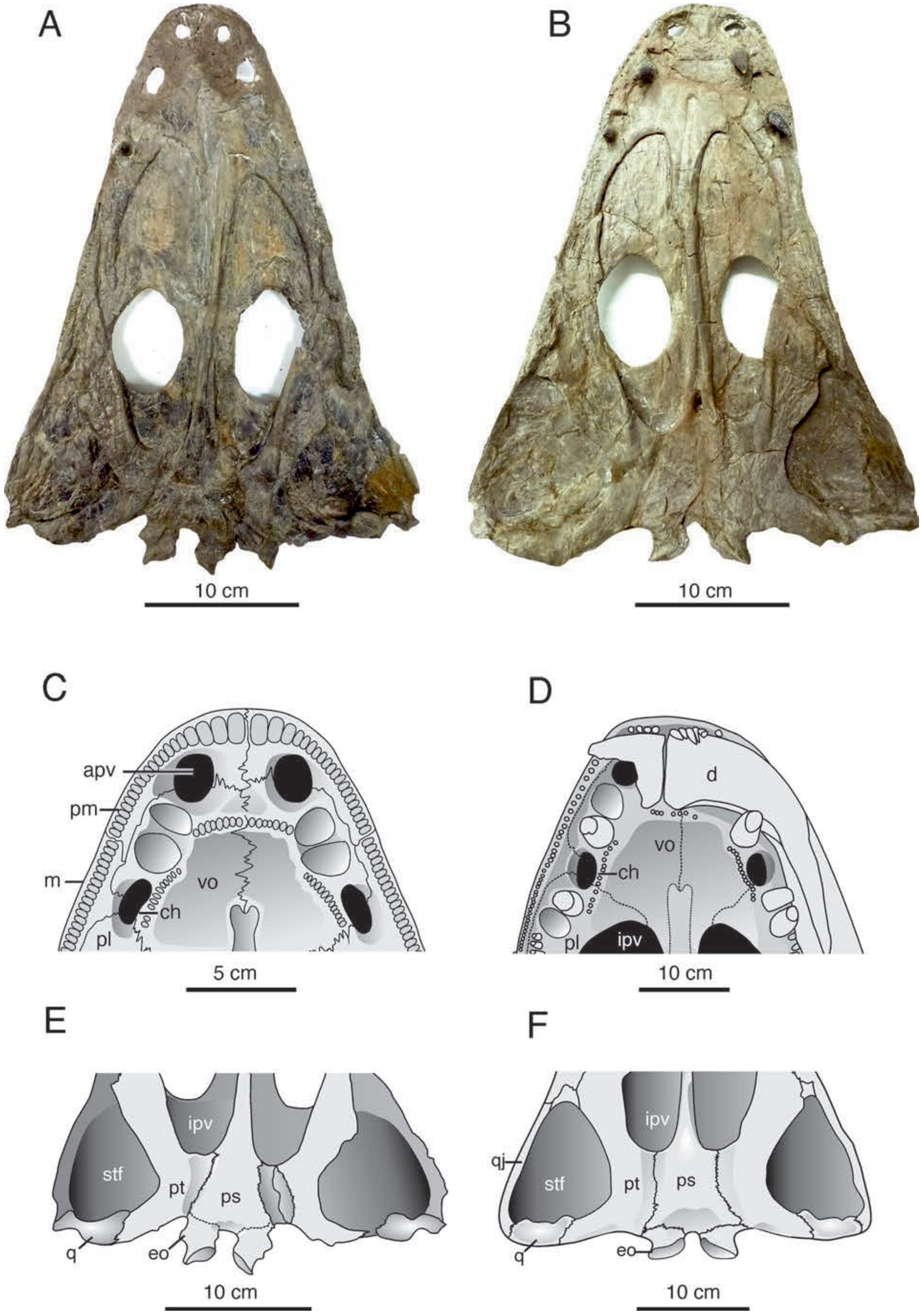

Figure 5. *Mastodonsaurus giganteus* Jaeger, 1828. Palate. **A.** MHI-Ku 1992/31 (Vellberg, E6); **B.** MHI-Ku 1991/11 (Vellberg, E6); **C.** SMNS 54678 (Kupferzell, K4); **D.** giant specimen from Gaildorf G2, based on Meyer (1855)(Gaildorf, G2); **E.** MHI-Ku 1992/42 (Vellberg, E6); **F.** SMNS 54675 (Kupferzell, K3).

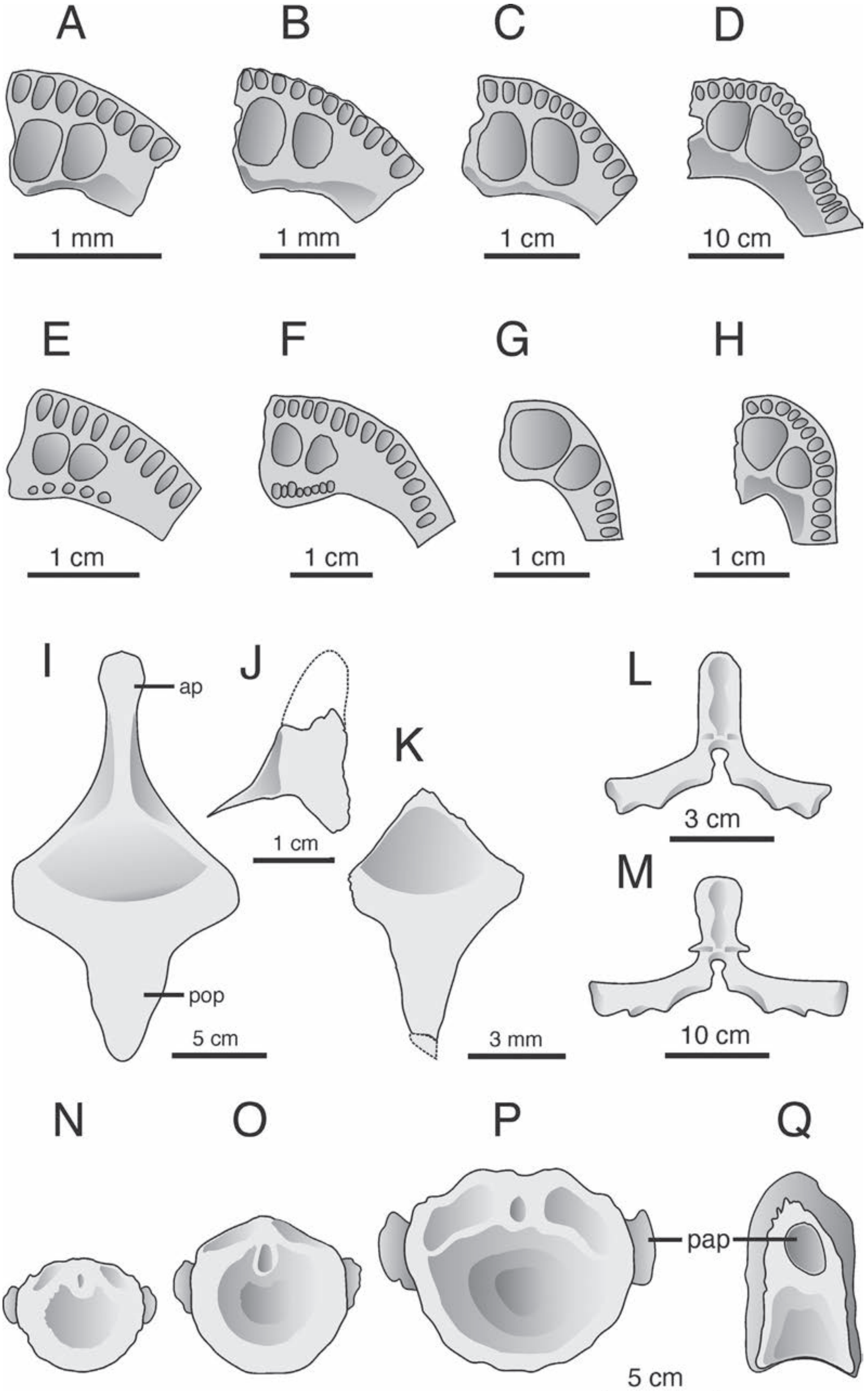

Figure 6. Mandibles and postcranial material of Lower Keuper temnospondyls. **A–H.** Symphyses. **A.** *M. giganteus*, SMNS 97035 (Kupferzell, K3); **B.** *M. giganteus*, SMNS 97036 (Kupferzell, K3); **C.** *M. giganteus*, MHI 1992/32 (Vellberg, E6); **D.** *M. giganteus*, SMNS 81310 (Kupferzell, K3); **E.** *Tatrasuchus wildi*, MHI-Ku 1992/42 (Vellberg, E6); **F.** *Tatrasuchus wildi*, SMNS 54670 (Kupferzell, K3); **G.** *Callistomordax kugleri*, SMNS 90520; **H.** *Trematolestes hagdorni*, SMNS 97034; **I.** *M. giganteus*, adult interclavicle in dorsal view, SMNS 97132 (Kupferzell, K3); **J.** *M. giganteus*, small juvenile clavicle, SMNS 97044 (Vellberg, E6); **K.** *M. giganteus*, tiny interclavicle in dorsal view, SMNS 97131 (Vellberg, E6); **L.** *M. giganteus*, adult neural arch, SMNS 80913; **M.** *M. giganteus*, giant neural arch, SMNS 81310; **N-Q.** *M. giganteus*, intercentra in anterior view; **N.** MHI 1046; **O.** MHI 1079; **P, Q.** SMNS 80913.

are consistent with juveniles and adults of *M. giganteus* in the slender posterior process and the overall proportions; they differ from small interclavicles of *Tatrasuchus* in the slenderer posterior process and from *Callistomordax* and *Trematolestes* in the greater width of the lateral process.

Despite their fragmentary nature, the small specimens here attributed to *M. giganteus* are highly informative in their great consistency with the juvenile and adult morphologies. At least regarding the interclavicle, this agrees with the ontogenetically rather conservative Palaeozoic eryopiforms (Boy 1988; Witzmann 2006).

Juveniles

The smallest juveniles are known from partial skulls, mandibles, and interclavicles (Fig. 6). Juvenile bones from other regions are also present but unambiguous referral to *M. giganteus* remains impossible because the postcranium of the closely related *Tatrasuchus wildi* remains largely unknown.

Skull roof

The best small juvenile specimen of *M. giganteus* is a partial postorbital skull (SMNS 97037) from Vellberg (E6) that preserves the left half of the posterior skull table and squamosal (Fig. 3I, J). This skull shares all features of the ornament of adults, and in comparison to other temnospondyl taxa of similar size, the bones are much thicker. This is especially obvious along the occipital margin. The small juvenile differs from all larger specimens in having a shorter squamosal and a longer supratemporal. The orbit is somewhat larger with respect to the postorbital skull compared with adult specimens; this is interesting, because larger juveniles have relatively small orbits (Fig. 8). Larger juvenile skulls, which are especially well preserved at Vellberg (E6, E7), are remarkably consistent with adults in proportions and suture topologies (Fig. 4). A few trends are apparent from morphometric analysis, in which juveniles have among the widest interorbital distances, the smallest orbit lengths and the narrowest postorbital skulls (Fig. 8). This said, there is substantial variation, especially in Vellberg E6.

Palate

The palate is well preserved in MHI 1992/31 (30 cm SL; Fig. 5A, E) and MHI 1991/11 (38 cm SL). The proportions of the palate elements are similar to those of adults, and the pattern and size of dentition is consistent with later stages. The basal plate of the parasphenoid is slightly shorter and the deltoid area in its anterior part is not yet established. However, its sutures with the pterygoid and exoccipital are consistent with the adult stages, as is the relative size of the exoccipital and its condyle.

Mandible

The Kupferzell and Vellberg localities yielded a wide range of juvenile mandibles that are readily distinguished from those of *Tatrasuchus wildi* by the following features in those of *M. giganteus*: (1) no transverse row of small teeth posterior to the symphyseal fangs, (2) larger size of the symphyseal fangs, (3) Meckelian window elongate and low, reaching 25% the length of the mandible, and (4) long and tall postglenoid area. The juvenile mandibles differ hardly from those of adults, with the postglenoid area only slightly shorter and the hamate process only gently lower in juveniles.

Vertebrae

The morphological consistency of the trunk intercentra is remarkable (Figs 6N–Q, 7K–N). In contrast to the close relative *M. cappelensis*, *M. giganteus* had closed disc-shaped intercentra already in juvenile stages. Intercentra of this type range in transverse width between 4 cm and 12 cm, representing sizes between 30 and 100 cm skull length. Smaller intercentra were found but cannot be distinguished from those of *Tatrasuchus wildi*.

Pectoral girdle

A wide range of clavicles and interclavicles were collected in Vellberg E6, spanning a full range from the smallest to various juvenile stages. These are consistent with adult interclavicles of *M. giganteus* in the slender posterior process, the much-elongated anterior process, and the shape of the clavicular facet (Fig. 7E–G). Independent of size, these features are distinct from all other temnospondyls of the Lower Keuper and especially *Tatrasuchus*. The clavicle of *M. giganteus* has a large convex dorsolateral flange anterior to the ascending process (Fig. 7H, I) that is not present in *Tatrasuchus*. In contrast to the dermal pectoral girdle, diagnostic and undisputed juvenile humeri or other limb elements have not been identified in the studied material.

Pelvic girdle

Small ilia consistent with the morphology of the adult ilium of *M. giganteus* were collected in Kupferzell K3 and figured in Schoch (1999, fig. 46), but their distinction from the yet unknown ilium of *Tatrasuchus* is unknown; the ilia of all other temnospondyls of the Lower Keuper are very different (Schoch 2006, 2008).

Adults

Here we define an arbitrary adult stage beginning with a skull length of 50 cm onwards. As depicted in Fig. 2, adult specimens ranging from 50–60 cm form the bulk of the samples Kupferzell (K3, K4) and Vellberg (E5, E6). Their morphology has been described and figured in detail by Schoch (1999).

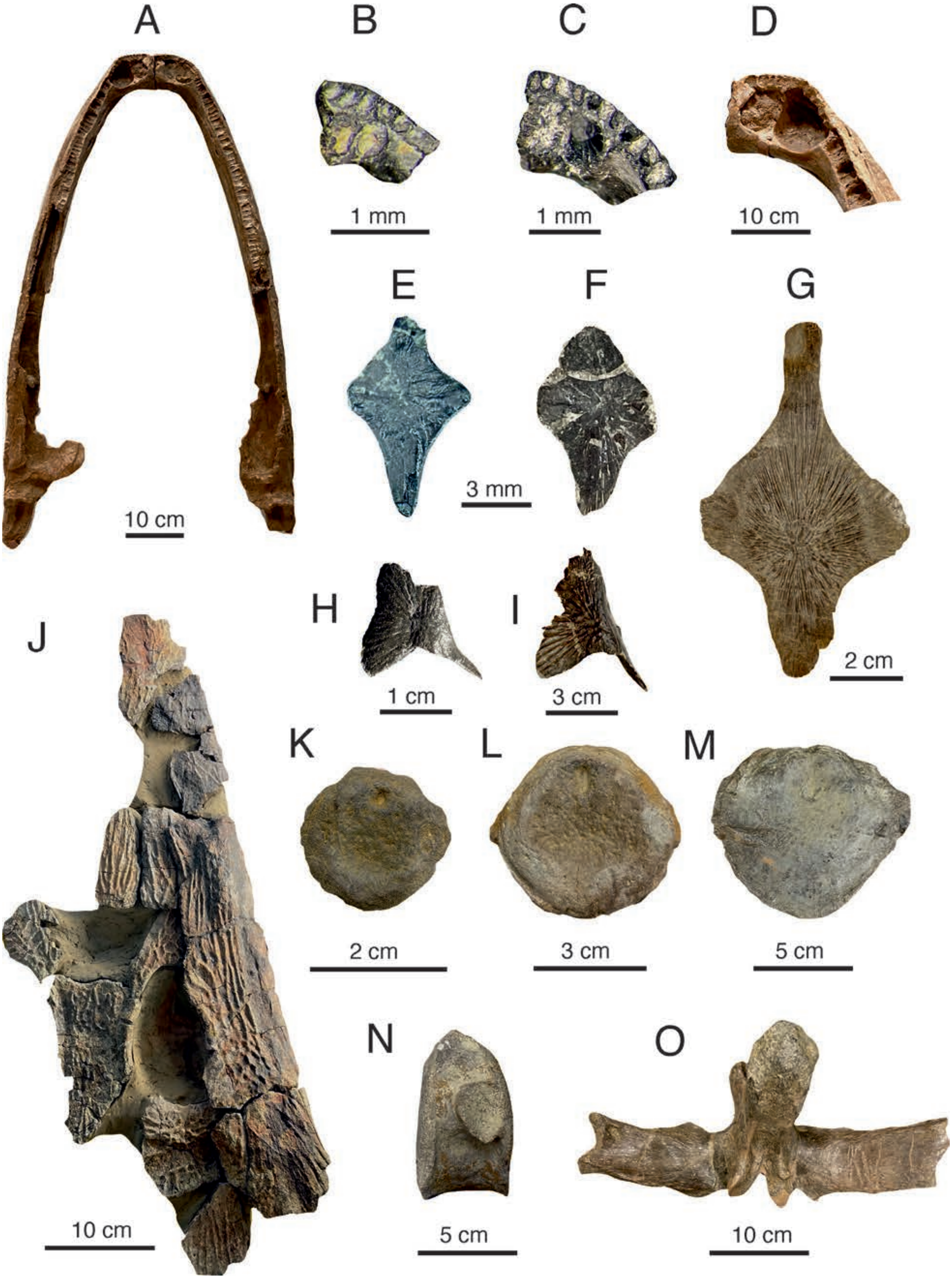

Figure 7. Original material of *Mastodonsaurus giganteus*. **A–D.** Mandibles (**B–D.** Symphyseal region in dorsal view). **A.** SMNS 81310 (Kupferzell, K3); **B.** SMNS 97035 (Kupferzell, K3); **C.** SMNS 97036 (Kupferzell, K3); **D.** SMNS 81310 (Kupferzell, K3); **E–G.** Interclavicles. **E.** SMNS 97131 (Vellberg, E6); **F.** MHI-Ku 1993/4 (Vellberg, E6); **G.** MHI-Ku 1993/5 (Vellberg, E6); **H–I.** Clavicles. **H.** SMNS 97044 (Vellberg, E6). **I.** SMNS 97044 (Vellberg, E6). **J**, large skull, NHMS-WT3323-3368 (Arnstadt). **K–N.** Intercentra (**K–M.** Anterior view; **N.** Lateral view). **K.** SMNS 97044 (Kupferzell, K3). **L.** SMNS 97044 (Kupferzell, K3). **M.** SMNS 84138 (Kupferzell, K3). **N.** SMNS 84139 (Kupferzell, K3). **O.** Neural arch, SMNS 81310 (Kupferzell, K3).

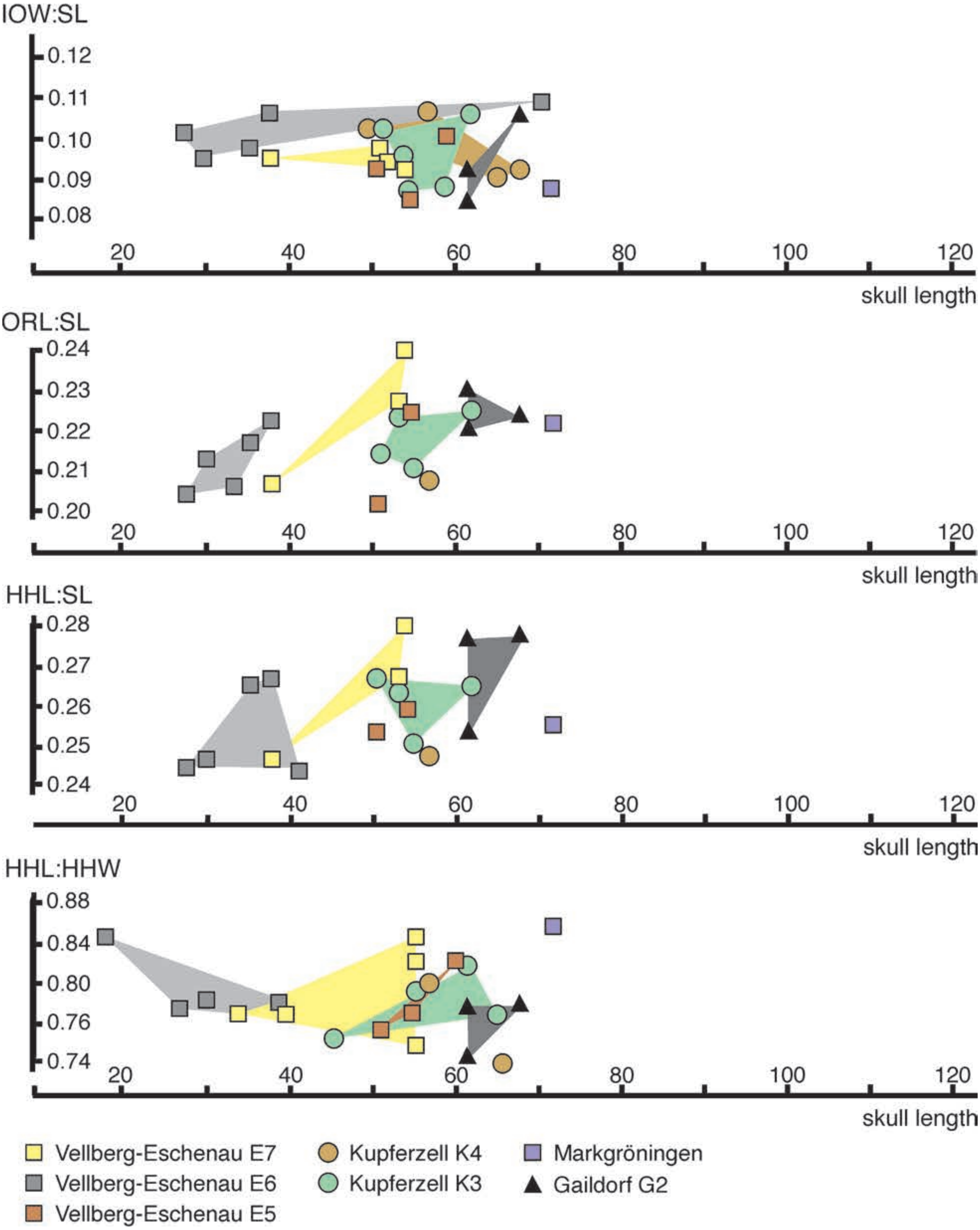

Figure 8. *Mastodonsaurus giganteus* Jaeger, 1828. Morphometrics of skull proportions in the different samples.

Giant specimens

Skull roof

The large specimens from Gaildorf (G2) were described by Meyer and Plieninger (1844), Fraas (1889) and Moser and Schoch (2007). The three complete skulls range from 60 to 68 cm skull length (Fig. 4; Moser and Schoch 2007). Fraas (1889) further described and figured a large skull without cheeks from Markgröningen (SMNS 4974), found in a dark mudstone that was roughly equivalent to the Untere Graue Mergel of Vellberg and Kupferzell.

The grey mudstones of Vellberg E6 yielded numerous isolated bones of giant specimens. These include intercentra, humeri, mandibles, and fragments of skulls in the 100–120 cm size range. It is unknown from how many specimens these bones stem, but a minimum assessment identifies at least three giant individuals collected over 30 years (Werner Kugler, pers. comm. 2016). The Kupferzell fossillagerstätte (K3) gave only a single very large skeleton, referred to as giant specimen ("Riesenexemplar", SMNS 81310). It encompasses a palatine, tabular, complete mandible and 34 vertebrae plus a series of associated ribs (Schoch 1999), representing a specimen with 88.5 cm skull length.

At a highway construction site near Arnstadt in central Thuringia (Erfurter Kreuz, see Werneburg in Hagdorn et al. 2015), a large partial skull was collected (NHMS-WT3323-3368, see Werneburg and Witter 2005) in the upper part of the Lower Keuper. The complete skull measured around 101 cm in length and preserves a good portion of the skull roof (restored in Fig. 4I). This includes portions of the preorbital, interorbital and cheek regions. It is consistent with the large Kupferzell and Vellberg material in that ornament is coarser than in 40–70 cm skulls, meaning that the size of the polygons is proportionately larger in these specimens. In turn, the ridges are low and thinner than in smaller skulls, whereas the lateral line sulci are proportionately of similar width as in smaller specimens.

The orbit of the largest skull is proportionately somewhat smaller, albeit retaining its characteristic outline with the pointed anterior end. In the other material, the length of the orbit varies broadly, with the Gaildorf and Markgröningen specimens ranking among those with the longest orbits. Such variation was also reported by Sulej (2007) on *Metoposaurus krasiejowensis*. The large size of the orbits in *M. giganteus* has been hypothesized to correlate with large adductor musculature (Schoch et al. 2023), which might explain that the size did not essentially change between juveniles and adults.

A rather clear trend was found in the length/width ratio of the postorbital skull table, which is smaller in larger specimens, except for the Markgröningen skull. Conversely, the ratio length of the postorbital skull through skull length increases slightly from juveniles to large adults (Fig. 8).

The area of the postorbital increases markedly between juveniles (30 cm) and small adults (40–50 cm) but remains constant throughout later stages. Likewise, the width of the squamosal increases between juveniles and adults. Both features are typical of adult *M. giganteus*, whereas juveniles retain the plesiomorphic condition seen in adult *M. cappelensis* (Schoch et al. 2023).

In the Thuringian and Gaildorf specimens, the postorbital is still proportionately large. The interorbital distance varies more broadly in the largest skulls, with the Markgröningen and two of the Gaildorf specimens ranking among the narrower skulls, together with K4 specimens from Kupferzell (Fig. 8). The occipital condyles are more massive than in smaller stages and the occipital margin of the postparietals is more strongly concave, especially in the Gaildorf and Markgröningen specimens.

Palate

Meyer (1855) figured the now-lost snout of a giant specimen from Gaildorf (G2) in original size, which measured approximately 107 cm in total skull length (Meyer and Plieninger 1844). Based on Meyer's drawing (modified in Fig. 5D), the marginal and vomerine teeth are throughout proportionately smaller than in 50–60 cm long skulls, whereas the fangs especially of the symphyseal region are enlarged (SMNS 81310). The choana was drawn rounded by Meyer (1855) but reported to be rather oval by Fraas (1889); we suppose that Meyer referred to the outline of the opening within the main plane of the vomer, whereas Fraas described the outline of the opening, which is more deeply emplaced in the dorsal portion of the narial capsule. At any rate, the choana is distinctly shorter and smaller in the giant Gaildorf specimen than in smaller adult stages (Fig. 5C, D).

Vertebrae

The largest vertebrae are mostly heavily crushed, sometimes even more flattened than intercentra of adults in the 50–60 cm skull range. This probably results from a higher porosity of the bones. This is particularly obvious at the top of layer K3 in Kupferzell, which contained both the giant specimen (SMNS 81310) and several smaller disarticulated vertebral columns; in the smaller specimens, the intercentra are hardly crushed at all and retained most of their 3D structure. Apart from the higher porosity, the parapophyses are proportionately larger by area in the giant specimen. The caudal vertebrae are low and wedge-shaped but very massively ossified, not as porose as the trunk vertebrae and consequently less affected by compaction. The neural arches are peculiar in giant specimens by having disproportionately large transverse processes; their length was subject to strong positive allometry from adult to giant size classes (Fig. 6L–M).

Pectoral girdle

Several huge clavicles and interclavicles are housed in the MHI and SMNS collections, among which the giant specimen (SMNS 81310) from Kupferzell (K3) permits the calibration of mandible size and interclavicle length. The proportions appear not to have changed, whereas the ornament underwent a similar coarsening as reported from the skull roof. The ontogenetic changes of the cleithrum involved a broadening of the dorsal head region and an area increase of the scapular facet, well preserved in the K3 sample (Schoch 1999, fig. 41). The humerus of large specimens differs between the Gaildorf and other samples. Large humeri in the 20–24 cm range are known from Vellberg, where they are poorly differentiated without a clear supinator and poorly defined, mostly cartilage-capped condyles. In contrast, the giant Gaildorf humerus (SMNS 4706) figured by Meyer and Plieninger (1844) has a prominent supinator process and a large fully ossified radial condyle. (Schoch 1999, fig. 43). As preserved in one Gaildorf specimen (SMNS 4706), the carpal region contained at least a few ossified carpals (Schoch 1999, p. 17 and fig. 45).

Pelvic girdle. This region is again best represented by the small Gaildorf sample, which preserves three divergent size classes. Interestingly, the smallest of these includes an ilium with attached ischium and pubis (Schoch 1999, fig. 46), being much more fully ossified than all other specimens from Vellberg and Kupferzell.

Paleoecology and life history of *Mastodonsaurus giganteus*

In Fig. 2, we mapped the frequency of *M. giganteus* in six different localities and horizons: Gaildorf (G2), Kupferzell (K3, K4) and Vellberg-Eschenau (E5, E6, E7). The basis of these distributions form registered finds of skulls, articulated skeletons, and isolated elements that together give a minimum number of individuals. To avoid counting isolated bones from the same disarticulated individual twice, we constrained the sample of single elements to the most robust and common bones, the exoccipitals. Especially at Kupferzell the number of interclavicles and mandibles, the other two common elements, matched the distribution of exoccipitals.

Lake Gaildorf G2

The Gaildorf sample is the smallest and most difficult to interpret because the locality is currently poorly accessible. It includes three complete large skulls (60–68 cm), two skull fragments (61–65 cm), one lost giant specimen (107 cm), and articulated as well as isolated postcranial bones. The minimal number of specimens is difficult to assess, because the belonging of cranial and postcranial material remains unclear. As in most other tetrapod fossillagerstätten in the Erfurt Formation, the fossiliferous horizon was restricted to a small area, and in currently accessible neighbouring outcrops it is absent.

The Gaildorf specimens of *M. giganteus* stem from a hard coaly siltstone rich in pyrite, sphalerite, and alum (Kurr 1852). This layer occurs immediately above a light grey mudstone (G1) containing a bonebed and below a 25–30 cm thick coal seam (G3) that was rich in plants, a coaly mudstone poor in fossils (G4), and a dark grey sandstone that yielded occasional plant debris and vertebrate bones (G5). This succession might have formed in a lake that provided good conditions for life, harbouring a fish fauna that is preserved in the 25 cm-thick bonebed-bearing mudstone (G1).

The 30 cm thick pyrite-rich type horizon G2 yielded the skulls and articulated skeletons of *M. giganteus*, along with a skeleton of *Plagiosuchus pustuliferus*, a skull fragment of the small capitosaur *Tatrasuchus wildi* (Schoch 1997) and mass accumulations of bivalves (*Unionites letticus*). A jaw and vertebra of the enigmatic archosauriform *Zanclodon laevis* further documents the presence of terrestrial predators (Schoch 2011), whereas isolated bones of the marine reptile *Nothosaurus* sp. (Meyer and Plieninger 1844) suggest the presence of lagoonal environments in the vicinity. The articulated state of the aquatic tetrapods in G2 indicates a calmer environment than in the preceding unit G1, and the abundant pyrite must have formed under euxinic conditions.

According to Nitsch (2015), many coal deposits of the Lower Keuper are associated with channel sandstones and probably formed in oxbow lakes. At Gaildorf, the reported sequence of mudstones, pyrite-bearing siltstones, coal, and dark grey sandstones is consistent with this interpretation. Weber (2013) cited historical sources that described the setting of the coal seam as lenticular with 1200 m longitudinal extension and 40 m width.

The lateral variation of the horizons is well documented in the three different sections that were published over a range of 36 years (Plieninger in Meyer and Plieninger 1844; Kurr 1852; Quenstedt 1880). These were probably measured in successively exposed sections of the mine.

Plieninger (1844) noted the presence of a second, thinner coal seam at the top immediately below the first sandstone unit, and he highlighted the occurrence of estherians in G1 and coaly clasts in G2 and teeth in G4. Quenstedt (1880) reported the horizons G2, G3 and G5, but noted the absence of G4 in the section available to him, he also mentioned estherians and reddish ironstone nodules in G2. In sum, these sections provide evidence of a freshwater lake environment that developed into a peat lake with calm, euxinic conditions, relatively similar to layers K1 and K2 from Kupferzell (see Schoch et al. 2022). The abundance of freshwater bivalves indicates good living conditions in G2, and the presence of four temnospondyl predators provides evidence of a rich ecosystem (*Mastodonsaurus*, *Tatrasuchus*, *Plagiosuchus*, *Trematolestes*).

Plagiosuchus probably was a bottom-dwelling sit-and-wait predator that, together with the abundance of *Unionites*, indicates a well-aerated lake floor of G2. At the same time, the abundance of pyrite and the dark colour of the sediment probably formed after seasonal poisoning of lake water, most probably by algal blooms, whereas the occurrence of coaly clasts suggest either the presence of already existing peat deposits in the vicinity or, alternatively, the input of larger quantities of plant material from the lake shore. Plieninger (Meyer and Plieninger 1844) reported that the skulls and skeletons of *M. giganteus* were found in the top of G2, with the bones reaching into the coal seam. This might indicate a drying up of Lake G2 (somewhat similar to Lake K3 in Kupferzell, see Schoch et al. 2022), followed by a peat lake preserved in the coal seam of G3 which contains *Taeniopteris*, *Calamites* and *Equisetites* (Kurr 1852).

The large size of most specimens of *M. giganteus* in G2 is remarkable; the complete skulls all fall into the 60–68 cm size range, as do most of the postcranial elements, with few bones stemming from individuals with a skull length of 50–60 cm, and several finds (humerus, ilium, fang, giant snout reported by Meyer and Plieninger 1844) of very large individuals in the 100–120 cm size range. The sample also includes three ilia of very different size, probably matching the three size classes (50, 60, and 110 cm skull length). Among all occurrences of *M. giganteus*, these finds are the most fully articulated, consistent with the find of a *Plagiosuchus* skeleton in G2 (Huene 1922).

Within this relatively small sample, the dominance of large and giant specimens is unparalleled among Lower Keuper deposits (Fig. 2). This may point at differences in life histories: either the Gaildorf population of *M. giganteus* had a longer life span or specimens reached large sizes more often than the later populations due to more favourable conditions. Two anatomical features are further noteworthy: the largest humerus is more heavily ossified than that of other samples and bears a prominent supinator process that is not developed in any other specimen, and the pelvis of some specimens includes an ossified pubis, which is unique among capitosauroid taxa except for *Sclerothorax* (Schoch et al. 2007). Ongoing analysis of bone microanatomy might shed more light on this interesting difference to the Vellberg and Kupferzell samples.

These data coincide with the occurrence of the smaller capitosauroid *Tatrasuchus*. The unusually large size of *M. giganteus* might be a result of character displacement, with *Mastodonsaurus* forming the apex predator and *Tatrasuchus* representing the guild of smaller ambush predators at this locality. At Gaildorf, *M. giganteus* appears to have invaded the lake at later ontogenetic stages and larger sizes than in other lakes, and its huge size might be a result of either plasticity or separate microevolution. Since *Tatrasuchus* probably occupied the same ecological niche as small adults of *M. giganteus*, the latter could have undergone an ontogenetic niche shift between juveniles and small adults. *M. giganteus* might have targeted larger prey and thus developed a stronger bite by proportionately increasing the area of the postorbital and the size of the squamosal (differing from *M. cappelensis*) in order to accommodate larger adductor musculature.

Lake Kupferzell K3

At Kupferzell-Bauersbach, a thick greenish mudstone (K3) has yielded a rich sample of tiny, juvenile, and adult specimens of *M. giganteus*. By the sheer quantity and density of bones, this deposit forms the richest tetrapod fossillagerstätte in the Lower Keuper and well beyond. Especially considering the excavated area, the temnospondyl specimens collected in that horizon by far outnumber those collected at the much larger excavated areas of Vellberg (E5, E6, E7). K3 yielded a loosely articulated giant specimen but otherwise contained mostly smaller adults, juveniles, and tiny specimens (Fig. 2).

The unit K3 has been interpreted as littoral facies of a lacustrine system (Schoch et al. 2022). This is also in line with the high number of bones with bite marks inflicted by the pseudosuchian archosaur *Batrachotomus kupferzellensis*, a more terrestrial predator feeding on carcasses of *M. giganteus* (Mujal et al. 2022), probably stuck in drying-up lakes (Schoch et al. 2022). Characeans and ostracods indicate well-aerated water in a basin less than 10 m deep. This water body spanned probably several km, but bone accumulations are restricted to only 500 m. The lake was subject to pulses of higher energy that produced currents, disarticulated skeletons, and transported the bones (Schoch et al. 2022). The absence of dark components and the light green colour of the sediment suggest that organic components were not as abundant as in other lakes, probably indicating a somewhat less nutrient-rich environment. Salinity fluctuations are indicated by euryhaline ostracods (Urlichs 1982) and histological evidence in bones of *Gerrothorax* point at an environment with fluctuating conditions (Sanchez and Schoch 2013). These fluctuations may have been caused by the occasional contact to a lagoonal water body in the vicinity (Schoch et al. 2022). Conversely, the poor carbonate content of the sediment was probably caused by inflowing streams that also produced channel-like erosions (Urlichs 1982). Only in the last phase of Lake K3, a diverse fish fauna (14 taxa) similar to, but not identical with E5 and E6 at Vellberg was established, and the accumulation of tetrapod bones is confined to that horizon (Schoch et al. 2022).

Despite the diverse fish assemblage, only aquatic tetrapod predators were present, *M. giganteus* and *Gerrothorax pulcherrimus*. The latter was distinctly smaller than *Plagiosuchus pustuliferus* of Gaildorf G2 and Vellberg E5. However, the abundance of this taxon in K3 concurs with the above-cited evidence of clear and well-aerated bottom water.

Within K3, the frequency distribution of *M. giganteus* is bimodal with specimens clustering in the 18–32 as well as 40–65 cm range (skull length; Fig. 2). Apart from that, tiny specimens were identified in the screen-washed fraction, and a single very large specimen (88.5 cm skull length) was found, but the giants in the range of Vellberg and Gaildorf specimens are absent. In Lake K3, *M. giganteus* must have primarily fed on *Gerrothorax* and large bony fishes such as dipnoans, actinistians and scanilepiforms.

Occasionally, *M. giganteus* may also have predated the smaller capitosaur *Tatrasuchus wildi* whose remains are always completely disarticulated and less common; this taxon probably dwelled in neighbouring habitats, and the disarticulated bones were washed in from there. The mass accumulation of bones and skulls of *M. giganteus* and *G. pulcherrimus* was probably caused by the final drying-up of Lake K3, which is documented by mud cracks; of note, bones are often found in the interface between layers K3 and K4, i.e., remaining half buried and thus exposed for a relatively prolonged time after the lake dried up (Schoch et al. 2022). At the same time, carcasses of *M. giganteus*, including that of the giant specimen, were scavenged by *Batrachotomus kupferzellensis*, which occasionally probably also actively hunted *M. giganteus* individuals (Mujal et al. 2022).

Lake Kupferzell K4

The deposit K4 encompasses yellow to brown, dolomitic marlstones. The yellow mud also fills desiccation cracks on top of layer K3, preserving equal amounts of characeans but much larger quantities of ostracods and microvertebrates than K3 (Schoch et al. 2022). Lake K4 represents a shallow, carbonate-rich environment that harboured a rich benthos. It probably formed in a more protected sub-basin that was not subject to frequent currents and therefore less siliciclastic input than K3. The oligohaline ostracod *Darwinula* was accompanied by the 14 fish taxa that also occur in K3 (Urlichs 1982; Schoch et al. 2022). The high abundance of small actinistian bones has been interpreted as evidence of a nursery ground of these fishes (Schoch et al. 2022). This lake probably existed within the same basin as K3, probably on a carbonate mudflat. Like K3, it is rich in ostracods and characeans, thus indicating the persistence of shallow water conditions.

In contrast to K3, the deposits of Lake K4 preserve skeletons rather than accumulations of single bones, indicating lower energy conditions and the preservation of skeletons after short-term droughts which are preserved as minor desiccation cracks. *Gerrothorax* was distinctly less abundant and *Tatrasuchus* more common than in K3 (Schoch 1997). In contrast to K3, *Tatrasuchus* is represented with several well-preserved skulls, suggesting that this sub-basin was inhabited by that taxon. *M. giganteus* was present with specimens in the 50–70 cm range (skull length), whereas giant specimens are entirely absent. The absence of juveniles and the slightly larger mean size compared with K3 coincide with the occurrence of *Tatrasuchus* (size range 25–40 cm skull length). Like at Gaildorf (see above), character displacement may explain this distribution (Schluter and McPhail 1992).

In K4, *M. giganteus* primarily fed on *Gerrothorax* and lungfishes such as the 2 m long *Ptychoceratodus* which is present both with skeletons and large teeth with traces of gastric acids. As in K3, *Batrachotomus kupferzellensis* primarily fed on carcasses of *M. giganteus* (Mujal et al. 2022). Littoral or marine influence in Lake K4 is indicated by the presence of a partial skeleton of *Nothosaurus* sp. (Schoch et al. 2022).

Lake Vellberg E5

In the Schumann quarry of Vellberg-Eschenau, the brown silty mudstones of E5 have been excavated by private collectors in concert with the more fossiliferous horizon E6. The horizon E5 formed in a small lake basin that developed after the retreat of a large brackish lagoon (Schoch and Seegis 2016). It is associated with autochthonous coal and roots at least in the northwestern area of its occurrence (Ummenhofen and northern Eschenau quarries). Its fauna includes a diverse fish assemblage (15 taxa) in which juvenile lungfishes and small polzbergiid actinopterygians form the bulk of the sample. Juvenile actinistians are present but much less abundant than in K4. Together with the occurrence of larval and juvenile temnospondyls (*Callistomordax*, *Trematolestes*, *Plagiosuchus*), these finds suggest the prevalence of well-structured, protected areas of a lake. The dominance of the ostracod *Speluncella* over *Darwinula* points to slightly brackish water (Schoch and Seegis 2016). The large predators in this habitat were the bottom dwelling *Plagiosuchus* and the medium-sized predator *Tatrasuchus*, both present with numerous well-preserved specimens. In contrast, *M. giganteus* is represented by relatively few skulls in the narrow range of 50–60 cm skull length (Fig. 9). This setting formed in a small lake in which *M. giganteus* was probably only occasionally present due to the dominance of competing *Tatrasuchus*. Adult *Trematolestes* and *Callistomordax* probably visited the lake only during the breeding season. In contrast to the other deposits studied by us, Lake Vellberg E5 probably could not support a population of adult *M. giganteus*.

Lake Vellberg E6

The grey clayey mudstones of E6 have been excavated over a period of 35 years and during all field seasons yielded large quantities of vertebrate remains (Schoch and Seegis 2016). They contain thin bonebeds as well as articulated skeletons and probably formed in a stratified lake (>5 km) that was at least seasonally subject to euxinic conditions.

Like in E5, baby lungfishes and two polzbergiids dominate the fish fauna, which also encompasses redfieldiids and semionotids, as well as medium-sized predators (*Saurichthys*, scanilepiforms). The high-bodied polzbergiids indicate that the lake floor was differentiated and offered protected areas, consistent with the presence of small juvenile temnospondyls (*Trematolestes*, *Callistomordax*, *Mastodonsaurus*). Layer E6 is rich in remains of the temnospondyl *Callistomordax*, an elongate eel-like form with large, keeled fangs that is only known from Vellberg. This taxon might have dwelled in protected places because it is the only aquatic tetrapod in this deposit to be preserved with fully articulated skeletons.

M. giganteus is present with specimens of all size classes, and the largest quantities of specimens fall in the 20–50 cm size range (Fig. 2). Notably, there are also remains of giant specimens up to 120 cm skull length, whereas the large adults (60–70 cm range) are much rarer than at Gaildforf G2. In contrast to *Callistomordax*, the remains of *M. giganteus* are nearly always disarticulated and often heavily damaged by predation.

In contrast, *Tatrasuchus* and *Trematolestes* are much less frequent, and only two remains of *Plagiosuchus* were found. Traces on adult remains of all taxa suggest predation by *M. giganteus* (regurgitates, bite marks, lungfish teeth and vertebral centra of temnospondyls corroded by gastric acids). Lake E6 also forms the only deposit so far to evidence cannibalism in *M. giganteus* (Schoch and Seegis

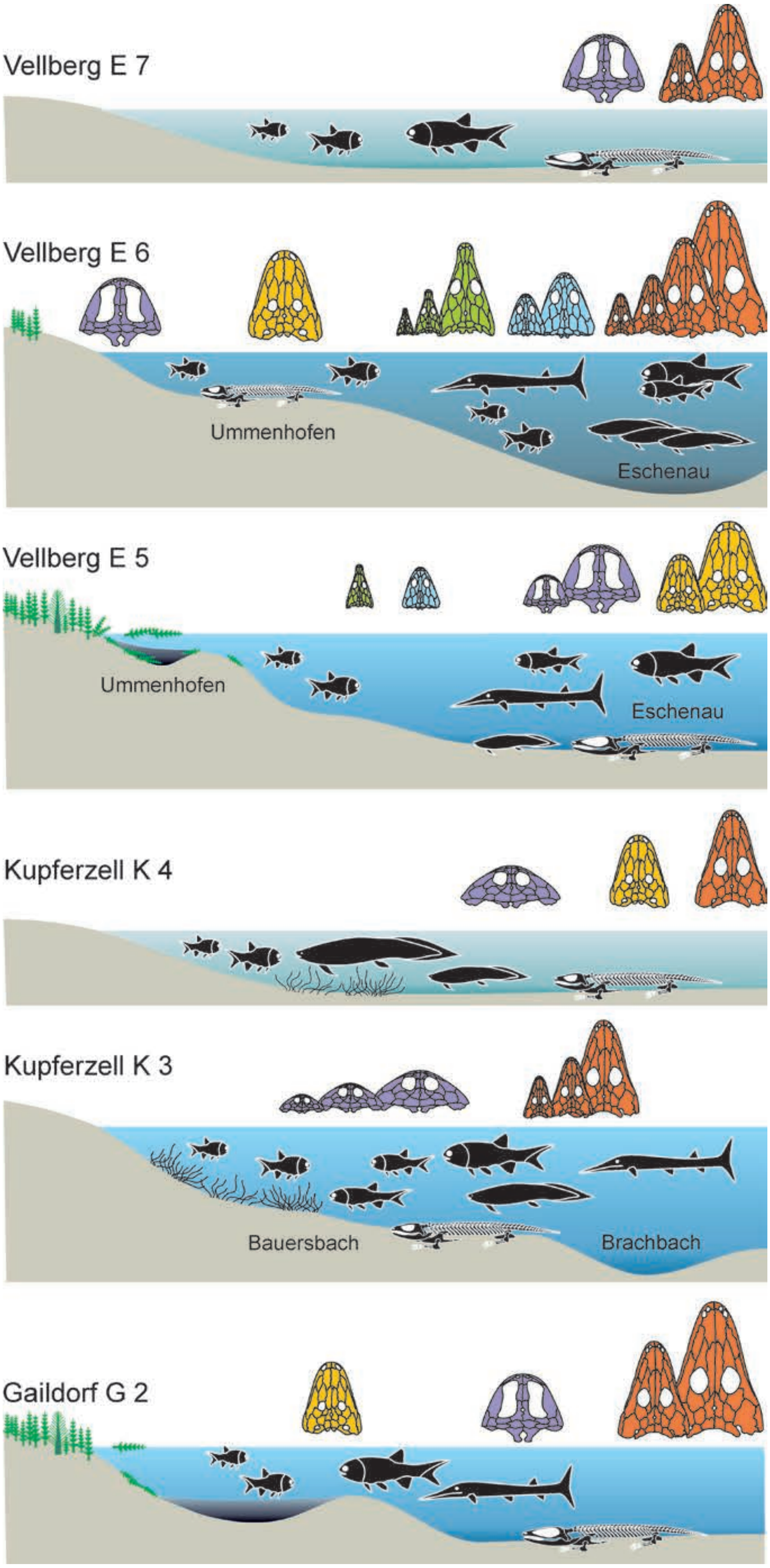

Figure 9. Faunal composition and properties of the six lake deposits with the largest samples of *M. giganteus*. Different size of skulls indicates presence of different growth stages in the same habitat.

2016; Mujal et al. 2022), including a 60 cm skull plus mandibles with bite marks of a much larger conspecific. At the same time, a reduced number of bones of *M. giganteus* display bite marks produced by *Batrachotomus kupferzellensis*, indicating scavenging as in the Kupferzell lakes, but in lesser frequency (Mujal et al. 2022), possibly because the lakes in Vellberg persisted for longer periods, so that the large pseudosuchian archosaurs could not frequently reach the large carcasses of *M. giganteus*.

These data indicate that Lake E6 formed a protected and nutrient-rich nursery ground for lungfishes and temnospondyls, with adult *Ptychoceratodus*, *Trematolestes* and *Tatrasuchus* appearing only during the mating season to lay eggs. In contrast, *Callistomordax* and *M. giganteus* were autochthonous throughout their life cycles and sufficiently different to avoid direct competition as adults. The numerous regurgitates preserved in E6 fall into two different size classes: 5–20 cm long skeletons of juvenile lungfishes and small archosauromorphs (potentially produced by *Callistomordax*) and 1–2 m long skeletons of archosauriforms (especially the amphibious *Jaxtasuchus salomoni*, Schoch and Sues 2013) and pseudosuchians (likely produced by *Mastodonsaurus*). Nevertheless, it cannot be discounted that some of the regurgitates were produced by *Batrachotomus kupferzellensis* (Mujal et al. 2022).

Lake Vellberg E7

The pale yellow micritic dolostones of E7 (Anoplophora Dolomite) form a 70–90 cm thick unit that is subdivided by thin horizons of greyish-brown mudstones. The basal unit has yielded skeletons of the terrestrial apex predator *Batrachotomus kupferzellensis* (thus the unit was coined *Batrachotomus* dolomite) skulls and disarticulated skeletons of *M. giganteus*, occasional finds of large adult *Plagiosuchus* and two juvenile skulls of *Tatrasuchus*. Fish remains are confined to single scales and teeth, with dominance of large polzbergiids (*Serrolepis*).

Like the Kupferzell facies, E7 was probably a clear water environment, although characeans have not been found. The dolostones formed under very shallow water conditions (Schoch and Seegis 2016). Like most of the aforementioned lakes, E7 developed in a sabkha-like setting, emplaced on a tidal flat that underwent frequent periods of desiccation. This is evidenced by the relative abundance of well-preserved skulls and skeletons of *M. giganteus* as well as *Batrachotomus*.

Lake Arnstadt A42

During highway construction near Arnstadt (north of the bridge at the Autobahn exit "Arnstadt Nord"), a large exposure that was open in 2003 yielded tetrapods in several horizons of the Lower Keuper (Werneburg and Witter 2005). The stratigraphically higher one yielded *M. giganteus*, among them the giant specimen restored in Fig. 4I. This horizon (Oberes Dunkles Band, Bed A42 within the upper sandstone S2o) forms a succession of dark coaly siltstones grading into dark grey mudstones. The disarticulated, large skull of *M. giganteus* was found below a bed rich in fossil wood, in a coaly and pyrite-rich layer. The preservation of bones closely resembles that of the Gaildorf specimens (Werneburg in Hagdorn et al. 2015), as does the stratigraphic association of the coaly siltstones with channel sandstones. Bed A42 also contained remains of the marine-lagoonal tetrapods *Plagiosternum* and *Nothosaurus*, as well as vertebrae of large pseudosuchians (Werneburg and Witter 2005). This setting might have formed in a lagoonally-influenced, stagnant water body with terrestrial input (reworked pseudosuchian bones). The occurrence of very large specimens of *M. giganteus* in similar facies at Gaildorf and Arnstadt is noteworthy and might either indicate a preference of swampy environments or simply a wider distribution of such giants.

Conclusions

Mastodonsaurus giganteus was a common predator in Middle Triassic freshwater environments (Hagdorn et al. 2015). The vast majority of Ladinian (Lower Keuper) occurrences stems from lake deposits, but occasional finds in river channels and lagoonal or shallow marine environments document its presence in a wide range of habitats (Schmidt 1928; Schoch 1999; Werneburg and Witter 2005). In the Lower Keuper sequence, *M. giganteus* inhabited a variety of water bodies on a large sabkha plain, including coastal and central parts of various freshwater lakes (Schoch and Seegis 2016; Schoch et al. 2022).

The currently known ontogeny of *M. giganteus* spans the enormous range of 12–15 mm to 1200 mm skull length, with a 100-fold increase in metric size. Although this range is unparalleled among temnospondyls or even lower tetrapods, it does not involve many substantial morphological changes. This agrees with the findings of Schoch and Witzmann (2024) on stereospondyl juveniles.

The smallest specimens are only known from fragmentary symphyses and interclavicles, which already show the main features of the taxon and clearly differ from small juveniles of other taxa. Proportional changes were most profound in the early juvenile phases, involving size differentiation of teeth and fangs and the size of the orbit. Early juveniles (12–20 cm skull length) already had a fully developed dermal ornament with low ridges spanning a wide network. Large adults had a longer postorbital skull table and a more deeply concave occipital margin and in giant specimens the orbit was slightly smaller, compensated by a broader jugal, and the symphyseal fangs were disproportionately large.

The frequency distribution of *M. giganteus* in the Lower Keuper provides interesting insight into the habitat preferences of this species in different phases of its life cycle. In lake shore facies (K4, E7), it was mostly present with larger specimens and juveniles are absent. These environments were probably only visited by adults because they did not provide sufficient protection for immature animals. Larvae and juveniles evidently dwelled in calmer environments within lakes. Among the latter, smaller lakes such as E5 were apparently less attractive than larger or deeper lakes such as K3 and E6. The latter evidently provided sufficient resources for breeding, and tiny specimens of *M. giganteus* have been identified in both deposits. In these rich ecosystems, a diverse actinopterygian fish fauna with taxa ranging between 3 cm (*Dipteronotus*) and 30 cm body length (scanilepiforms) provided prey for all growth stages of the large temnospondyl predators.

Adult *M. giganteus* was most common in lakes with abundant large prey, but the variation of tetrapod and sarcopterygian taxa between lakes indicates that this giant capitosaur was not restricted to a particular group of prey taxa. At Gaildorf, its most likely prey formed the relatively large *Plagiosuchus* whereas at Kupferzell (K3–4) it probably included the smaller *Gerrothorax* together with actinistians and lungfishes. At Vellberg, only adult *M. giganteus* visited the small lake E5, where *Plagiosuchus* and *Tatrasuchus* were preyed upon, as bite marks show. Heavy, predation-induced damage has been identified on several skulls of *Tatrasuchus*. *M. giganteus* also shows cannibalistic behaviours, as crushed and bite-marked skulls and mandibles indicate. At the same time, *M. giganteus* carcasses fed the pseudosuchian archosaur *Batrachotomus kupferzellensis*.

Mastodonsaurus giganteus was not only flexible enough to feed on a wide range of prey taxa, but also occurred in divergent habitats (Fig. 9). This is best exemplified by its abundance at both Kupferzell K3 and Vellberg E6. In these very different water bodies, its babies hatched and grew up to large adult size, whereas in Kupferzell K4 and Vellberg E7, it visited the habitats only during well-defined phases of juvenile and adult life. We conclude that its presence was apparently more restricted by the presence of competitors than by the stability of living conditions. Probably the question of which capitosaur first settled in a lake made the difference. In rich habitats, *M. giganteus* managed to partition niches with *Tatrasuchus*, whereas in most others it failed to do so.

Acknowledgments

We are indebted to Isabell Rosin, Andreas Radecker, and Norbert Adorf for their organisation of field work and their skilful preparation. Werner Kugler, Traugott and Ute Haubold, Frank Ullmann, Brigitte Rozynek and Fabian Mohl donated many specimens to the SMNS, which is gratefully acknowledged. We also thank Dieter Seegis for his long-term help with field work and discussions. Hans Hagdorn and Rupert Wild helped with making material accessible to study, by many thoughtful discussions and by sharing their observations. Finally we thank the two reviewers and the editor for their helpful reviews and suggestions.

References

Anderson JS (2008) Focal review: the origin(s) of modern amphibians. Evolutionary Biology 35: 231–247. https://doi.org/10.1007/s11692-008-9044-5

Boy JA (1988) Über einige Vertreter der Eryopoidea (Amphibia: Temnospondyli) aus dem europäischen Rotliegend (? höchstes Karbon – Perm). 1. *Sclerocephalus*. Paläontologische Zeitschrift 62: 107–132. https://doi.org/10.1007/BF02989838

Boy JA (2003) Paläoökologische Rekonstruktion von Wirbeltieren: Möglichkeiten und Grenzen. Paläontologische Zeitschrift 77: 123–152. https://doi.org/10.1007/BF03004564

Czepiński L, Pawlak W, Rytel A, Tałanda M, Szczygielski, Sulej T (2023) A new Middle Triassic vertebrate assemblage from Miedary (southern Poland). Journal of Vertebrate Paleontology 43: e2265445. https://doi.org/10.1080/02724634.2023.2265445

Damiani R, Schoch RR, Hellrung H, Werneburg R, Gastou S (2009) The plagiosaurid temnospondyl *Plagiosuchus pustuliferus* (Amphibia: Temnospondyli) from the Middle Triassic of Germany: anatomy and functional morphology. Zoological Journal of the Linnean Society 155: 348–373. https://doi.org/10.1111/j.1096-3642.2008.00444.x

Fraas E (1889) Die Labyrinthodonten der schwäbischen Trias. Palaeontographica 36: 1–158.

Hagdorn H, Schoch RR, Seegis D, Werneburg R (2015) Wirbeltierlagerstätten im Lettenkeuper. In: Hagdorn H, Schoch RR, Schweigert G (Eds) Der Lettenkeuper – Ein Fenster in die Zeit vor den Dinosauriern. Palaeodiversity Sonderband 2015: 325–358.

Hellrung H (2003) *Gerrothorax pustuloglomeratus*, ein Temnospondyle (Amphibia) mit knöcherner Branchialkammer aus dem Unteren Keuper von Kupferzell (Süddeutschland). Stuttgarter Beiträge zur Naturkunde B 330: 1–130.

Huene F von (1922) Beiträge zur Kenntnis der Organisation einiger Stegocephalen der schwäbischen Trias. Acta Zoologica 3: 395–460. https://doi.org/10.1111/j.1463-6395.1922.tb01025.x

Jaeger GF (1828) Ueber die fossile [sic] Reptilien, welche in Württemberg aufgefunden worden sind. Metzler, Stuttgart, 48 pp. https://doi.org/10.5962/bhl.title.4689

Konzhukova ED (1955) Permskiye i triasovyye labirintodonty Povolzh'ya i Predural'ya. Trudy Paleontologicheskogo Instituta AN SSSR 49: 5–88.

Kurr J (1852) Natürliche Beschaffenheit. In: Beschreibung des Oberamts Gaildorf. J.B. Müller, Stuttgart, 3–27.

Lydekker R (1885) Indian Pre-Tertiary Vertebrata. The labyrinthodont from the Bijori group. Palaeontologia Indica 4(1): 1–16.

Marzola M, Mateus O, Shubin NH, Clemmensen LB (2017) *Cyclotosaurus naraserluki*, sp. nov., a new Late Triassic cyclotosaurid (Amphibia, Temnospondyli) from the Fleming Fjord Formation of the Jameson Land Basin (East Greenland). Journal of Vertebrate Paleontology 73: e1303501. https://doi.org/10.1080/02724634.2017.1303501

Meyer H von (1842) Briefliche Mitteilung an Prof. Bronn gerichtet, Neues Jahrbuch für Mineralogie, Geologie und Paläontologie 1842: 301–304.

Meyer H von (1855) Zur Fauna der Vorwelt. Die Saurier des Muschelkalks, mit Rücksicht auf die Saurier aus buntem Sandstein und Keuper. Keller, Frankfurt am Main, 167 pp.

Meyer H von, Plieninger T (1844) Beiträge zur Paläontologie Württemberg's, enthaltend die fossilen Wirbeltierreste aus den Triasgebilden mit besonderer Rücksicht auf die Labyrinthodonten des Keupers. Schweizerbart, Stuttgart, 132 pp.

Milner AR (1993) The Paleozoic relatives of lissamphibians. Herpetological Monographs 7: 8–27. https://doi.org/10.2307/1466948

Moser M, Schoch RR (2007) Revision of the type material and nomenclature of *Mastodonsaurus giganteus* (Jaeger) (Temnospondyli) from the Middle Triassic of Germany. Palaeontology 50: 1245–1266. https://doi.org/10.1111/j.1475-4983.2007.00705.x

Mujal E, Foth C, Maxwell EE, Seegis D, Schoch RR (2022) Feeding habits of the Middle Triassic pseudosuchian *Batrachotomus kupferzellensis* from Germany and palaeoecological implications for archosaurs. Palaeontology 65: e12597. https://doi.org/10.1111/pala.12597

Nitsch E (2015) Fazies und Ablagerungsräume. In: Hagdorn H, Schoch RR, Schweigert G (Eds) Der Lettenkeuper – Ein Fenster in die Zeit vor den Dinosauriern. Palaeodiversity Sonderband 2015: 285–324.

Owen R (1841) On the teeth of species of the genus Labyrinthodon (*Mastodonsaurus salamandroides* and *Phytosaurus*) of Jaeger, from the German Keuper and sandstone of Warwick and Leamington. Proceedings of the Geological Society of London 3: 357–360.

Quenstedt FA (1850) Die Mastodonsaurier im grünen Keupersandstein Württtemberg's sind Batrachier. Laupp und Siebeck, Stuttgart, 48 pp.

Quenstedt FA (1880) Begleitworte zur Geognostischen Specialkarte von Württemberg. Atlasblatt Hall, Stuttgart, 40 pp.

Rühle von Lilienstern H (1935) *Mastodonsaurus acuminatus* E. Fraas aus der Lettenkohle. Aus der Heimat 48: 176–178.

Säve-Söderbergh G (1935) On the dermal bones of the head in labyrinthodont stegocephalians and primitive Reptilia. Meddelelser om Grønland 98(5): 1–211.

Sanchez S, Schoch RR (2013) Bone histology reveals a high environmental and metabolic plasticity as a successful evolutionary strategy in a long-lived homeostatic Triassic temnospondyl. Evolutionary Biology 40: 627–647. https://doi.org/10.1007/s11692-013-9238-3

Schluter D, McPhail JD (1992) Ecological character displacement and speciation in sticklebacks. American Naturalist 140: 85–108. https://doi.org/10.1086/285404

Schmidt M (1928) Die Lebewelt unserer Trias. Ferdinand Rau, Öhringen, 461 pp.

Schmidt M (1931) Labyrinthodonten und Reptilien aus den Thüringischen Lettenkohleschichten. Geologische und Paläontologische Abhandlungen, Neue Serie 18: 229–276.

Schoch RR (1997) A new capitosaur amphibian from the Upper Lettenkeuper (Triassic: Ladinian) of Kupferzell (Southern Germany). Neues Jahrbuch für Geologie und Paläontologie Abhandlungen 203: 239–272. https://doi.org/10.1127/njgpa/203/1997/239

Schoch RR (1999) Comparative osteology of *Mastodonsaurus giganteus* (Jaeger, 1828) from the Middle Triassic (Lettenkeuper: Longobardian) of Germany (Baden-Württemberg, Bayern, Thüringen). Stuttgarter Beiträge zur Naturkunde B 278: 1–175.

Schoch RR (2009) Evolution of life cycles in early amphibians. Annual Reviews in Earth and Planetary Sciences 37: 135–162. https://doi.org/10.1146/annurev.earth.031208.100113

Schoch RR (2011) New archosauriform remains from the German Lower Keuper. Neues Jahrbuch für Geologie und Paläontologie Abhandlungen 203: 239–272. https://doi.org/10.1127/njgpa/203/1997/239

Schoch RR (2013) The major clades of temnospondyls: an inclusive phylogenetic analysis. Journal of Systematic Palaeontology 11: 673–705. https://doi.org/10.1080/14772019.2012.699006

Schoch RR (2014) Amphibian Evolution. The Life of Early Land Vertebrates. Wiley, New Jersey, 288 pp. https://doi.org/10.1002/9781118759127

Schoch RR, Milner AR (2000) Encyclopedia of Paleoherpetology, Part 3B, Stereospondyli. Verlag Dr. Friedrich Pfeil, Munich, 203 pp.

Schoch RR, Mujal E (2022) Ontogeny and adult osteology of the Middle Triassic temnospondyl *Trematolestes hagdorni*. Neues Jahrbuch für Geologie und Paläontologie 306: 265–286. https://doi.org/10.1127/njgpa/2022/1106

Schoch RR, Moreno R (2024) Synopsis on the temnospondyls from the German Triassic. Paleodiversity 17: 9–48. https://doi.org/10.18476/pale.v17.a2

Schoch RR, Witzmann F (2024) The evolution of larvae in temnospondyls and the stepwise origin of metamorphosis. Biological Reviews. https://doi.org/10.1111/brv.13084

Schoch RR, Seegis D (2016) A Middle Triassic palaeontological gold mine: The vertebrate deposits of Vellberg (Germany). Palaeogeography, Palaeoclimatology, Palaeoecology 459: 249–267. https://doi.org/10.1016/j.palaeo.2016.07.002

Schoch RR, Seegis D, Mujal E (2022) The Middle Triassic vertebrate deposits of Kupferzell (Germany): Palaeoenvironmental evolution of complex ecosystems. Palaeogeography, Palaeoclimatology, Palaeoecology 603: p.111181. https://doi.org/10.1016/j.palaeo.2022.111181

Schoch RR, Sues HD (2013) A new archosauriform reptile from the Middle Triassic (Ladinian) of Germany. Journal of Systematic Palaeontology 12: 113–131. https://doi.org/10.1080/14772019.2013.781066

Schoch RR, Milner AR, Witzmann F, Mujal E (2023) A revision of *Mastodonsaurus* from the Anisian of Germany, and the evolutionary history of mastodonsaurid temnospondyls. Neues Jahrbuch für Geologie und Paläontologie 309: 123–140. https://doi.org/10.1127/njgpa/2023/1154

Steyer JS, Damiani RJ (2005) A giant brachyopoid temnospondyl from the Upper Triassic or Lower Jurassic of Lesotho. Bulletin de la Societe géologique de France 176: 243–248. https://doi.org/10.2113/176.3.243

Urlichs M (1982) Zur Stratigraphie und Fossilführung des Lettenkeupers (Ob. Trias) bei Schwäbisch Hall (Baden-Württemberg). Jahresberichte und Mitteilungen des Oberrheinischen Geologischen Vereines 64: 213–224. https://doi.org/10.1127/jmogv/64/1982/213

Warren AA, Hutchinson MN (1983) The last labyrinthodont? A new brachyopoid (Amphibia, Temnospondyli) from the Early Jurassic Evergreen Formation of Queensland, Australia. Philosophical Transactions of the Royal Society of London B 303: 1–62. https://doi.org/10.1098/rstb.1983.0080

Warren AA, Hutchinson MN (1988) A new capitosaurid from the Early Triassic of Queensland and the ontogeny of the capitosaur skull. Palaeontology 31: 857–876.

Warren AA, Rich TH, Vickers-Rich PV (1997) The last last labyrinthodonts? Palaeontographica A 247: 1–24. https://doi.org/10.1127/pala/247/1997/1

Weber H (1992) Frühe Stratigraphie im Lettenkeuper des Hohenloher Landes (nördliches Baden-Württemberg) im 19. Jahrhundert (Alberti und Kurr). Jahresberichte und Mitteilungen des Oberrheinischen Geologischen Vereines 74: 173–190. https://doi.org/10.1127/jmogv/74/1992/173

Weber H (2013) Spurensuche zum Virtiolbergbau bei Gaildorf (Landkreis Schwäbisch Hall, nördliches Baden-Württemberg). Gesellschaft für Naturkunde in Württemberg, Sonderbände 3: 291–316.

Werneburg R, Witter W (2005) Fossillagerstätten im Unteren Keuper Thüringens (Erfurt-Formation, Mittel-Trias). Teil 2: ICE-Trasse südlich der BAB 71-Ausfahrt „Arnstadt-Nord“. Veröffentlichungen des Naturhistorischen Museums Schleusingen 20: 57–75.

Wild R (1980) The vertebrate deposits of Kupferzell. Mesozoic Vertebrate Life 1: 15–18.

Witzmann F (2006) Morphology and palaeobiology of the Permo-Carboniferous temnospondyl amphibian *Archegosaurus decheni* Goldfuss, 1847 from the Saar-Nahe Basin, Germany. Transactions of the Royal Society of Edinburgh, Earth Sciences 96: 131–162. https://doi.org/10.1017/S0263593300001279

Witzmann F, Schoch RR (2006) The postcranium of *Archegosaurus decheni*, and the phylogenetic analysis of temnospondyl postcrania. Palaeontology 49: 1211–1235. https://doi.org/10.1111/j.1475-4983.2006.00593.x

Witzmann F, Schoch RR (2024) Osteology and phylogenetic position of *Plagiosaurus depressus* (Temnospondyli: Plagiosauridae) from the Late Triassic of Germany and the repeated loss of dermal bones in plagiosaurids. Zoological Journal of the Linnean Society 2024: zlae014. https://doi.org/10.1093/zoolinnean/zlae014

Yates A, Warren AA (2000) The phylogeny of the ‘higher’ temnospondyls (Vertebrata: Choanata) and its implications for the monophyly and origins of the Stereospondyli. Zoological Journal of the Linnean Society 128: 77–121. https://doi.org/10.1111/j.1096-3642.2000.tb00650.x

Zittel KA von (1888) Handbuch der Paläontologie. 1. Abtheilung. III. Band. Paläozoologie. Vertebrata (Pisces, Amphibia, Reptilia, Aves). R. Oldenbourg, München and Leipzig, 900 pp.

Fossil Record 27 (3) 2024, 423–443 | DOI 10.3897/fr.27.135664

Osteology and revised diagnosis of *Cherninia denwai* from the Middle Triassic Denwa Formation, Satpura Gondwana Basin, Central India

Pummy Roy[1], Sanjukta Chakravorti[2], Dhurjati Prasad Sengupta[1]

1 *Geological Studies Unit, Indian Statistical Institute, 203 Barrackpore Trunk Road, Kolkata 700108, India*
2 *Staatliches Museum für Naturkunde, Stuttgart, Rosenstein 1, Stuttgart 70191, Germany*

https://zoobank.org/91AE9CD7-5B92-43F3-9013-A47FD8B54BE9

Corresponding author: Sanjukta Chakravorti (sanjukta.chakravorti@smns-bw.de)

Academic editor: Nadia Fröbisch ♦ **Received** 27 August 2024 ♦ **Accepted** 11 December 2024 ♦ **Published** 30 December 2024

Abstract

The Middle Triassic Denwa Formation located within the Satpura Gondwana basin of Central India exhibits a significant presence of temnospondyl amphibians classified under the family Mastodonsauridae. Prior investigations have documented two taxa of the Mastodonsauridae family, namely *Cherninia denwai* and *Paracyclotosaurus crookshanki*, from the Denwa Formation. These prior accounts were predominantly predicated upon two holotype skull specimens, thereby neglecting other specimens contained within the collection as well as various associated post-cranial materials. Recently, a diverse assortment of novel specimens pertaining to *C. denwai* has been unearthed from the Denwa Formation. Utilizing both the newly acquired specimens and previously overlooked specimens, this study presents a redescription of *C. denwai*. The newly discovered specimens comprise a partial skull, a mandible, clavicles, interclavicles, vertebrae, neural arches and spines, ulnae, an ilium, a femur, and a fibula, all of which are described herein for the first time. An extensive osteological analysis of the skull and mandible is conducted. It is noted that *C. denwai* coexists temporally with *C. megarhina*, and both taxa exhibit distinct synapomorphies; however, they are recognized as separate and unique species.

Key Words

Capitosauridae, Gondwana, India, Middle Triassic, Temnospondyl

Introduction

Temnospondyls were highly diverse amphibians having nearly 200 genera and 290 species showing high disparity and diversity. They range in size from a few centimeters to more than 6 meters (Schoch 2013) and remain one of the most demanding groups to understand organic evolution. The appearance of temnospondyls dates back to the Early Carboniferous (Milner and Sequeira 1993) and their radiation in the Early Triassic is an important faunal recovery after the Permo-Triassic mass extinction event. During the Late Triassic, tough competition with the neosuchian crocodylomorphs in non-marine ecosystems resulted in their decline, however, *Cyclotosaurus*, a mastodonsaurid, persisted in the Late Triassic (Fortuny et al. 2019). McHugh (2012) attempted a phylogenetic study of Temnospondyli involving 99 taxa and 297 morphological characters. The Mastodonsauridae, within the superfamily Capitosauroidea, is the largest family of amphibians in the earth's history, particularly in the Early and Middle Triassic, dominating the Mesozoic aquatic to semi-aquatic habitats such as lakes, rivers, and swamps. *Mastodonsaurus giganteus* was the first discovered temnospondyl and the largest amphibian to date (Damiani 2001).

The mastodonsaurids are the most widely distributed temnospondyls present in most of the vertebrate-bearing strata of the Triassic (Cosgriff and Defauw 1987; Schoch and Milner 2000). However, mastodonsaurid phylogeny has always remained a fairly debatable issue over the years. The first systematic grouping of the mastodonsaurids had been done by Ochev (1966). Welles (1965) attempted grouping of different capitosauroids through the measurements and / or their ratios of several skull parameters. Primary phylogenetic analyses of the capitosauroids have been done by Ingavat and Janvier (1981) and (Milner 1990). Jupp and Warren (1986) suggested some identifying characters of the mandibles of the capitosauroids and Warren and Snell (1991) worked on the postcranial elements. Meanwhile Shishkin (1980), suggested the concept of a diphyletic origin of the otic fenestra in capitosauroids, and Morales and Kamphausen (1984) described a new taxon, *Odenwaldia heidelbergensis* that appeared to confirm that hypothesis. Almost thirty-five years later, Schoch and Milner (2000) and Damiani (2001) reviewed Capitosauroidea and the latter study performed a cladistic analysis based on a larger dataset involving computer-aided software such as PAUP and MacClade. Both studies came up with contrasting ideas (Schoch and Milner 2000; Damiani 2001). Damiani (2001) proposed the family name Mastodonsauridae. Steyer (2003) and Schoch (2008) also dealt with the characters and phylogeny of mastodonsaurids (Steyer 2003; Schoch 2008, 2013); Schoch (2008) however preferred to retain the family ‘Capitosauridae’. Most of the mastodonsaurid (Bandyopadhyay and Ray) characters, apart from the diagnostic features of *Cherninia denwai* described herein are taken from the above references. Some of the characters of the genus *Cherninia* are noted from *C. megarhina* from the Middle Triassic Ntawere Formation of Zambia (Chernin 1970). It is to be noted that Damiani (2001) assumed an Anisian age for *Cherninia* and Roy [2024, unpublished Ph.D. thesis] regarded *Paracyclotosaurus* from Denwa as Ladinian in age.

The Middle Triassic Denwa Formation of Satpura Gondwana Basin, Central India (Fig. 1), is well known for its mastodonsaurid content (Mukherjee and Sengupta 1998; Bandyopadhyay and Sengupta 1999). The Denwa Formation constitutes a significant component of the Satpura Valley basin, which is recognized as one of the four principal Gondwana basins located in India. The Middle Triassic Denwa Formation is predominantly characterized by heterolithic deposits that encompass sequences of sandstone and mudstone. Positioned above the Early Triassic Panchmarhi Formation and beneath the Jurassic

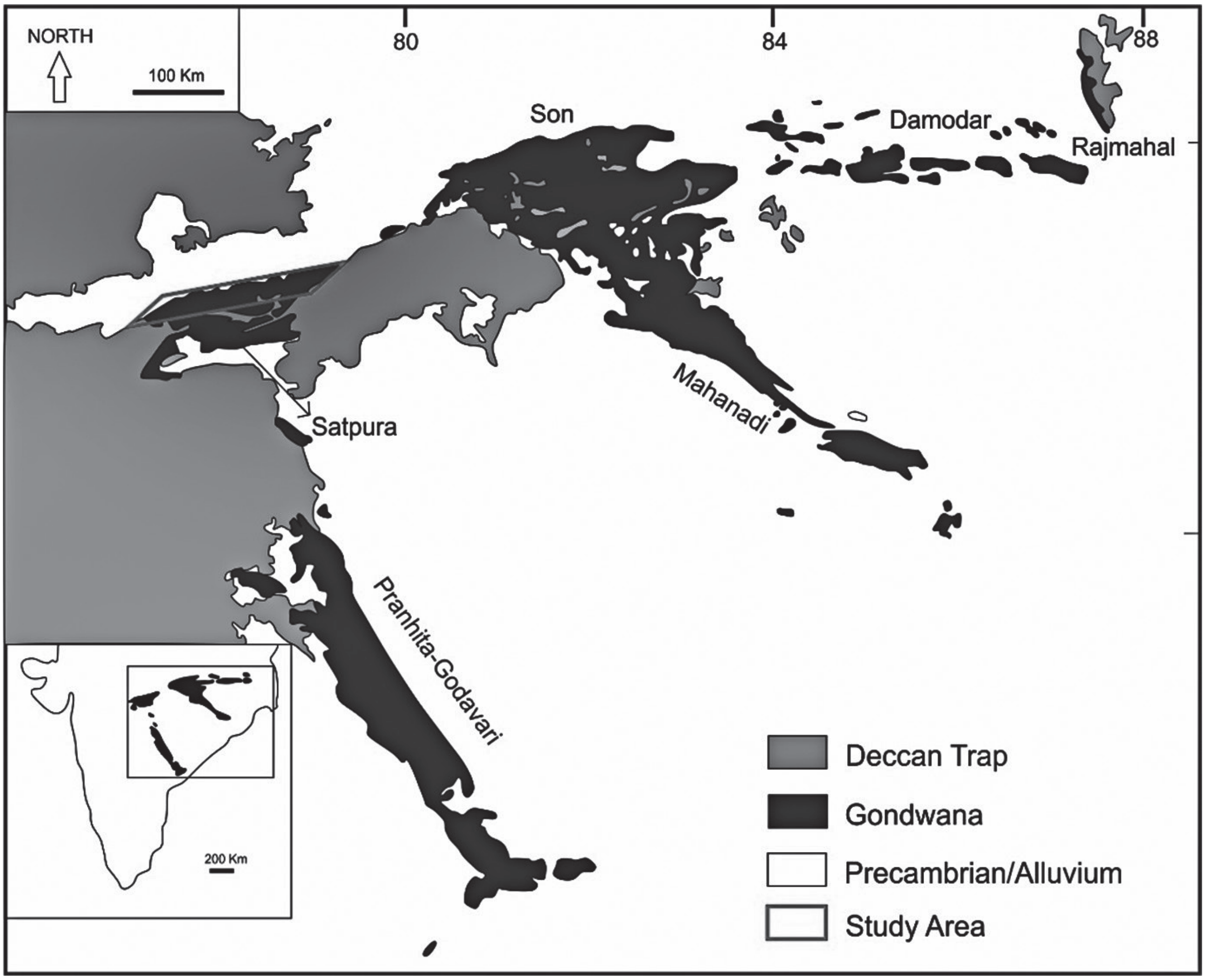

Figure 1. Map of India showing the Gondwana basins of peninsular India (after Bandyopadhyay 1999). The red box marks the Satpura basin.

Bagra Formation, the Middle Triassic Denwa Formation is notable for its abundance of Triassic vertebrate fossils, which include a variety of fish fossils, temnospondyls, and the renowned *Shringasaurus indicus*, a horned archosauromorph, among others (Bandyopadhyay and Ray 2020; Sengupta and Sengupta 2021). The prevailing palaeo-environment of the Denwa Formation is characterized as fluvio-lacustrine in nature, contributing to a larger braided river system (Dasgupta 2021).

Two mastodonsaurids, *Cherninia denwai* and *Paracyclotosaurus crookshanki* have already been described (Mukherjee and Sengupta 1998; Damiani 2001) from the Denwa Formation (Fig. 2). The identifications and descriptions were solely based on two skulls designated as holotypes (ISI A 54 and ISI A 55, respectively). Those descriptions were done mainly on the basis of material collected by the late R.N. Mukherjee of the Geological Studies Unit, Indian Statistical Institute, Kolkata. In the existing description, the figures representing the occipital views of those two taxa were inadvertently swapped (see Mukherjee and Sengupta 1998). However, not all the material collected by him has been used in the existing descriptions. Moreover, in subsequent years, many new specimens were excavated by the present authors which included several postcranial elements so far unknown in *Cherninia denwai* from the Middle Triassic Denwa Formation, therefore, a comprehensive osteological description of *C. denwai* is now possible. The present work, thus, emends the diagnosis of the taxon *C. denwai*, providing a detailed osteology of the skull and postcranial skeleton with the help of new specimens. The mandible and the postcranial elements of *C. denwai* are described here for the first time.

Materials and methods

A cumulative total of approximately 80 skeletal elements have now been documented and ascribed to *Cherninia denwai* (Suppl. material 1: table S1). One of the specimens, a fragmented cranium (ISI A 207), exceeds one meter in length, while a mandible (ISI A 208) approaches 96 cm. Both of these specimens have been unearthed by the senior author DPS from the central stratigraphic section of the Denwa Formation, specifically from violet-hued mudstones, thereby indicating that the central section of Denwa served as a sanctuary for colossal temnospondyls that attained lengths of 4 to 5 meters.

Abbreviations

Anatomical abbreviations: **AC:** Anterior coronoid; **AF**: Adductor fossa; **AN:** Angular; **APV:** Anterior palatal vacuity; **AR:** Articular; ***Cm*:** Crista muscularis; **CT:** Cultriform process; **D:** Dentary; **ECT:** Ectopterygoid; **EO:** Exoccipital; **F:** Frontal; **FM:** Foramen magnum; **GF:** Glenoid fossa; ***IJ*:** Insulae jugalis; **IN:** Internal nares; **ITPV:** Interpterygoid vacuity; **J:** Jugal; **L:** Lacrimal; **MC:** Middle coronoid; **MS:** Mandibular sulcus; **MX:** Maxilla; **N:** Narial; **NA:** Naris; **O:** Orbit; **P:** Parietal; **PAL:** Palatine; **PAR:** Prearticular; **PC:** Posterior coronoid; **PF:** Postfrontal; **PMF:** Posterior Meckelian foramen; **PMX:** Premaxilla; **PNF:** Pineal foramen; **PO:** Postorbital; **POSP:** Postsplenial; **PP:** Postparietal; **PQF:** Paraquadrate foramen; **PRF:** Prefrontal; **PSP:** Parasphenoid; **PT:** Pterygoid; **PTF:** Post temporal fenestra; **Q:** Quadrate; **QB:** Quadrate boss; **QJ:** Quadratojugal; **SA:** Surangular; **SMX:** Septomaxilla; **SP:** Splenial; **SQ:** Squamosal; **ST:** Supratemporal; **STV:** Subtemporal vacuity; **T:** Tabular; **V:** Vomers.

Institutional abbreviations: **ISI:** Indian Statistical Institute, Kolkata (Geological Studies Unit).

Systematic Palaeontology

Temnospondyli von Zittel, 1887–1890
Stereospondyli von Zittel, 1887–1890
Capitosauroidea Watson, 1920
[nom. Trans. (Säve-Söderbergh 1935) ex. Capitosauridae (Watson 1920) emend (Schoch and Milner 2000)]
Mastodonsauridae Damiani, 2001
Genus: *Cherninia* Damiani, 2001

Species: *Cherninia denwai* Damiani, 2001
Figs 2–13

(= '*Parotosuchus*' *denwai* Mukherjee & Sengupta, 1998).

Type horizon. Denwa Formation (Middle Denwa Formation).

Age. Anisian, Middle Triassic.

Locality. Purtala village, Madhya Pradesh, Central India (22°35'38.6"N, 78°32'17.0"E).

Holotype. ISI A 54, a near complete skull (Fig. 2).

Referred specimens. A posterior portion of skull found near Kohpani village (ISI A 207; Fig. 3), nearly complete left mandible near Jhirpa village (ISI A 208; Figs 3, 4), vertebral elements (ISI A 218 to 225, 226a and b, 227 to 234; Figs 5, 6), ribs (ISI A 235, 238 to 266; Fig. 7), cleithra (ISI A 275 to 280; Fig. 8), interclavicles and clavicles (ISI A ISI A 267, 268, 272 to 274; Fig. 9), Ulnae (ISI A 182/3, 182/4, 281, 282; Fig. 10), ilium (ISI A 283; Fig. 11), femur (ISI A 284; Fig. 12) and fibula (ISI A 285, Fig. 13). The postcranial bones are mostly fragmentary and collected from the villages of Purtala, Jhirpa and Kohpani.

Diagnosis. Synapomorphies with Mastodonsauridae.

Pre-orbital part of skull (snout) elongated with orbits placed at the posterior half of the dorsal skull roof; orbital margins raised above the dorsal surface of the skull roof; posterolateral corners of the cheek anterior to the level of the posterior edge of the tabular horns; well-developed zone of intensive growth on the preorbital and cheek region of the skull; infraorbital sensory canal forms a

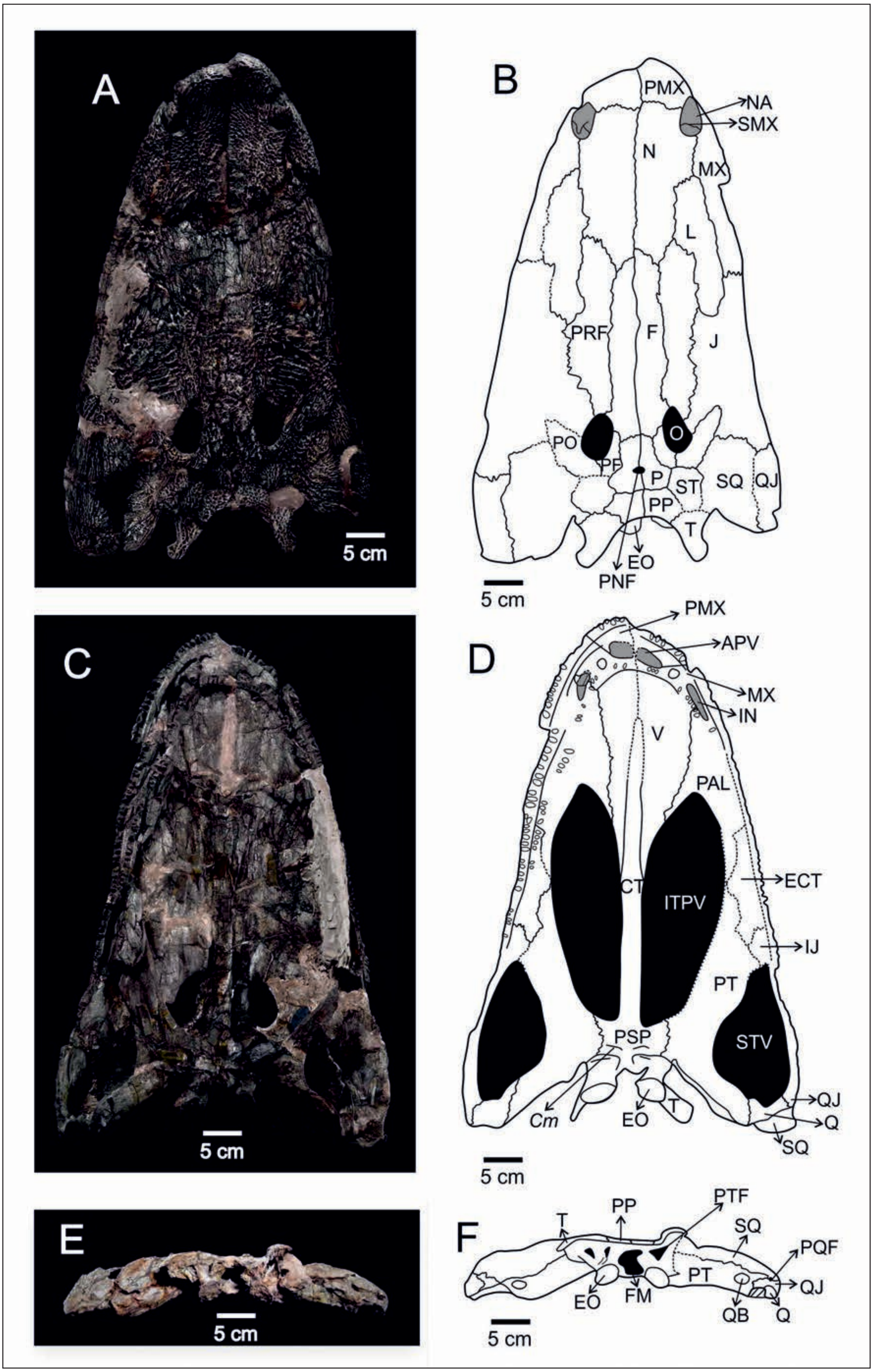

Figure 2. A, C, E. The skull roof of *Cherninia denwai* (Holotype ISI A 54) from the middle part of the Middle Triassic Denwa Formation in dorsal, ventral and occipital views, respectively; **B, D, F.** Line drawing of the same.

Z-shaped loop on the lacrimal bone, the lacrimal flexure; deeply incised otic notch; occipital condyles anterior to quadrate condyles; well-developed, lappet-like tabular horns which are partly supported from below by muscular cristae from the paroccipital process; elongated preorbital projection of the jugal, extending to the lateral border of the snout; supratemporal bone excluded from the border of the otic notch; postorbital antero-laterally expanded ('hooked'); ***crista muscularis*** of the parasphenoid levels with the posterior border of the pterygoid-parasphenoid suture; unbroken chain of teeth on the vomer-palatine-ectopterygoid series; occipital face of the pterygoid bears a tall, narrow, crest-like flange of bone, the oblique ridge of the pterygoid; posttemporal fenestra triangular in shape; mandible with an antero-posteriorly expanded symphysis; a short accessory sensory sulcus dorsal to the oral sulcus present.

Synapomorphies with *Cherninia* sp.

Pterygoid-parasphenoid suture short, less than the width of the corpus of the parasphenoid; occiput moderately shallow; skull margins moderately concave lateral to the orbits so that the cheek region is flared; prefenestral division of the palate (the region of the palate anterior to the interpterygoid vacuities) markedly elongated; anterior palatal vacuity paired but set in an oval depression so that the vacuities lie below the plane of the palate; elongated and broad snout so that parts of the anterior lateral margin of the skull on both sides are almost parallel to each other; skull roof with conspicuous, paired, forked ridges anterior to the orbits; anterior rim of the otic notch angular; temporal sensory canal extending posteriorly to the tips of the tabular horns; internal nares (choanae) are placed extremely far forward with respect to the interpterygoid vacuities.

Cherninia denwai can be distinguished from *Cherninia megarhina*, the second known species of *Cherninia*, by short and narrow postparietals, the presence of a septomaxilla, both anteriorly and posteriorly pointed interpterygoid vacuities, lack of parasphenoid groove, lack of occipital sensory canal, posteriorly directed and distally recurved tabular horns, the deeply concave occipital margin of the skull and the posteriorly broad otic.

Autapomorphies of *Cherninia denwai*

Skull margins moderately concave lateral to the orbits such that the cheek region is flared; elongated and moderately broad snout; lateral margins of the middle part of the skull anteromedially aligned. The skull roof has conspicuous, paired and forked ridges anterior to the orbits on both sides of the skull. Anterior rim of the otic notch angular (40–60 degrees), tabular horns posteriorly directed and recurved distally, postparietals antero-posteriorly compressed and narrow, deeply concave occipital margin of skull, well expressed lateral line sensory canals, septomaxilla present (Mukherjee and Sengupta 1998). The pterygoid-parasphenoid suture is short and the interpterygoid vacuities pointed both anteriorly and posteriorly. The skull table is shallow, the region of the palate anterior to the interpterygoid vacuities is elongated, anterior palatal vacuity paired but set in an oval depression so that the vacuities lie below the plane of the palate, cultriform process merges with the vomers and the occiput is moderately shallow. The mandible is slender and long (the largest measuring almost 96 cm in length), distinct post glenoid area (PGA) is present, hamate process of prearticular is well developed. It is pointed and sharp and its height is almost equal to the length of the PGA. The labial wall of adductor chamber is dorsally horizontal, prearticular is separated from splenial by dentary and coronoid series, glenoid facet lies below the dorsal surface of dentary.

Osteology. Skull roof (Figs 2, 3). The detailed osteological description of the dorsal part of the skull roof is as follows:

Premaxillae. The anterior-most rim of the snout is formed by the premaxillae. The premaxillae suture with the maxillae laterally, with the nasals posteriorly, and form the anteromedial part of the nasal rim. In ventral view, they contact the vomers posteriorly, the maxillae laterally, and form the anterior rim of the anterior palatal vacuity. The ornamentation is made up of pits and grooves (Figs 2, 3).

Maxillae. The anterior one-third of the lateral skull margin is formed by the maxillae, commencing from the posterolateral rim of the nares. Septomaxillae were figured by Mukherjee and Sengupta (1998), however, they are ill-preserved. Anteriorly, the maxillae are sutured with the premaxillae, medially by the nasals and the lacrimals, and posteriorly by the jugals. In ventral view, the maxillae border the premaxillae anteromedially, and suture medially with the vomers and the palatines. The anterolateral rim of the choanae is formed by the maxillae. Very faint pit and groove ornamentation is present in the anterior part (Figs 2, 3).

Nasal. The nasals are quite broad, and form a major part of the anterior skull roof medially (Figs 2, 3). They contact the premaxillae anteriorly. The nasals form a triple junction posteriorly, contacting the frontals posteromedially and the prefrontals posterolaterally. The nasals are bordered by the maxillae behind the nares and contact the lacrimals laterally. The nasals form the posteromedial rims of the nares. Pit and groove ornamentation is present in the anterior-most part and ridge and furrow ornamentation in the posterior part.

Lacrimal. The lacrimals are tear-drop shaped, suturing with the maxillae anterolaterally, the nasal medially, the prefrontal posteriorly, and the jugal posterolaterally (Figs 2, 3). Pit and groove ornamentation is present in the anterior part and ridge and furrow ornamentation in the posterior part. The lacrimals do not enter the orbit margin.

Jugal. The jugals form the majority of the cheek regions. Anteriorly, they contact the maxilla and anteromedially the lacrimal. Medially, the jugals are sutured anteriorly and in their middle part with the prefrontal and posteriorly with the postorbital. The jugal forms a narrow process and enters the orbit, thereby separating

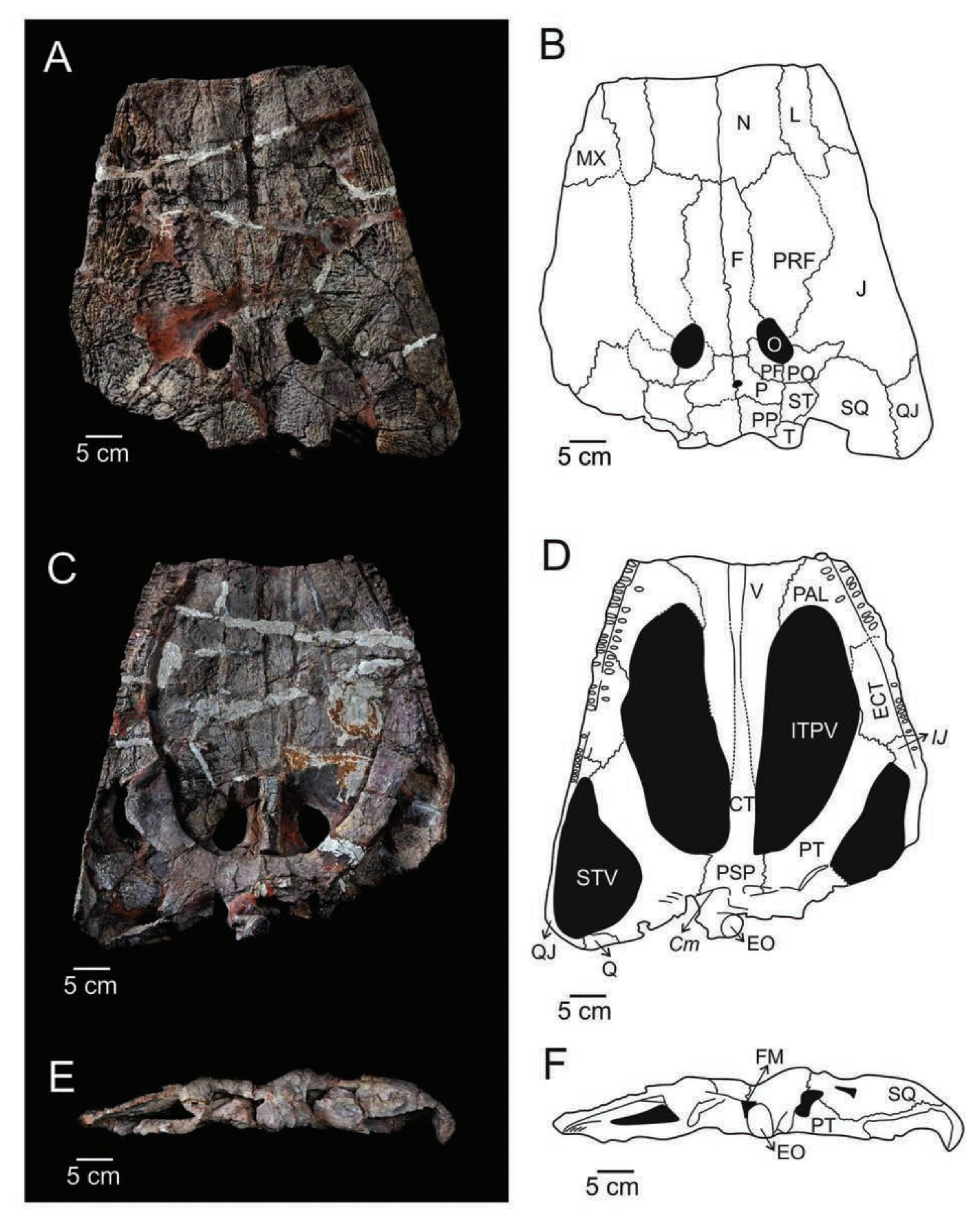

Figure 3. A, C, E. The skull roof of *Cherninia denwai* (Paratype ISI A 207) from the middle part of the Middle Triassic Denwa Formation in dorsal, ventral and occipital views respectively; **B, D, F.** Line drawing of the same.

the prefrontal and the postorbital. Posteriorly, the jugals suture with the squamosal medially and the quadratojugal laterally. Pit and groove ornamentation occur in the posterior part and ridges and furrows are present in the anterior part (Figs 2, 3).

Prefrontal. The elongate prefrontals suture with the nasals and lacrimals anteromedially and anterolaterally, respectively (Figs 2, 3). Medially, towards the midline, they suture with the frontals and towards the lateral margin with the jugals and form the anterior most rim of the orbits. Ridge and furrow-like ornamentation is present on their surface.

Frontal. The frontals are conspicuous, elongate bones that are anteriorly subtriangular in shape (Figs 2, 3). They run from the middle part of the snout region to the interorbital region. Anteriorly, they are bounded by the nasals, laterally by the prefrontals, posteriomedially by the parietals, posterolaterally by the postfrontals and form a part of the rim of the orbit projecting between the prefrontals and the postorbitals. Ornamentation in the anterior part is feeble but in the posterior part pit and groove ornamentation is present.

Postfrontal. The postfrontals are pentagonal in outline and form the posteromedial margin of the orbits. Anteriorly, they suture with the frontals, posteromedially with the parietals, posteriorly with the supratemporals, and laterally with the postorbitals (Figs 2, 3). Pit and groove ornamentations is present throughout.

Postorbital. The postorbitals are wing-like projections, contributing to the posterolateral rim of the orbits (Figs 2, 3). The postorbitals contact the postfrontals medially, and the supratemporals posteromedially and project into the jugals anterolaterally. The postorbitals contact the squamosals posterolaterally. Like on the postorbitals, pit and groove ornamentation are present throughout.

Quadratojugals. The quadratojugals form the cheeks and the lateral-most part of the skull (Figs 2, 3). Dorsally, they have a sub-rectangular outline, contacting the jugals anteriorly and the squamosals medially. On the ventral side, they contact the quadrates medially. They form a larger part of the lateral and posterior rims of the subtemporal vacuities. In the occipital view, the quadratojugals suture with the quadrates medially and the squamosals dorsally. Quadratojugals have ridge and furrow ornamentation throughout.

Parietals. The parietals contact each other medially and resemble a trapezium in outline. They enclose the parietal (pineal) foramen along the medial suture towards the posterior half of the bone. The parietals suture with the frontals anteriorly, the postfrontals and the supratemporals laterally, and the postparietals posteriorly (Figs 2, 3). Pit and groove ornamentations are present throughout.

Supratemporals. The supratemporals are polygonal in outline and contact the postorbitals and postfrontals anteriorly, the parietals anteromedially, and the postparietals posteromedially. The supratemporals suture with the squamosals laterally and posteriorly with the tabulars. The supratemporal does not contribute to the rim of the otic notch (Figs 2, 3). Pit and groove ornamentation is present throughout.

Squamosals. The squamosals are located between the quadratojugals and the tabulars. They form the postero-lateral rim of the skull and almost half the anterior and lateral margin of the otic notch. The squamosals are bordered by the postorbitals and the jugals anteriorly, the supratemporals medially, and the quadratojugals laterally (Figs 2, 3). Squamosals suture with the tabulars posteromedially. Pit and groove ornamentation is present near the rim of the otic notch which gradually grades into radially oriented ridges and furrows radially at the postero-lateral corner.

Postparietals. The polygonal postparietals form the posterior concavity of the dorsal rim of the skull. The postparietals suture with the parietal anteriorly, the supratemporals anterolaterally and the tabulars laterally. They are much shorter than the parietals (Figs 2, 3). Pit and groove ornamentations are present throughout.

Tabulars. The tabulars are elongated, polygonal in shape and have posterolaterally directed horns (Figs 2, 3). The tabulars form the medial margin of the otic notch. They contact the supratemporals anteriorly, the postparietals medially, and the squamosals anterolaterally. The tabulars do not suture with the squamosal laterally thereby forming a small embayment between the tabular and the squamosal. In dorsal view, the tabular horns have a concave lateral margin. Pit and groove ornamentation is there throughout.

Lateral Line Sulci. The lateral line sulci are present as pairs of supraorbital, infraorbital, and postorbital sulci. They are more evident laterally, especially in the posterior part of the skull, and weakly impressed medially, and again pronounced across the snout. However, all the lateral line sulci are discernible. The supraorbital sulci arise from the anterior region of the snout and traverse medially to the nares. They meander anteroposteriorly from the nasals to the prefrontals, running along the prefrontal-lacrimal suture reaching the posterior half of the frontals before terminating on the postfrontals near the orbital midline (Figs 2, 3). The infraorbital sulci begin lateral to the nares and meander anteroposteriorly on the maxillae before bending acutely onto the lacrimals forming a Z-flexure and terminating atop or parallel to the jugal-maxilla sutures. The postorbital sulci originate from the postorbital rim of the orbits. They run in a sigmoid form onto the jugals and quadratojugals first, then along the squamosal-quadratojugal sutures, terminating at the posterior border of the skull.

Palate (Figs 2C, D, 3C, D).

Vomers. The vomers are elongated bones tapering posteriorly (Figs 2C, D, 3C, D). Anteriorly, the vomers suture with the premaxillae, forming the posterior margin of the anterior palatal vacuity. Immediately, behind this opening, the vomers bear a transversely arranged row of teeth. The vomers also bear palatal tusks, which are circular in cross-section. Anterolaterally, the vomers contact the maxillae and laterally contact the palatines. The vomers contribute to the medial choanal margin at the left side of the skull ISI A 54 and to most of the medial rim of the palatal vacuities. At their contact along the interpterygoid vacuities, the vomers form a V-shaped ridge that projects ventrally. The posterior part of the vomer, while bordering a considerable portion of the anteromedial borders of the interpterygoid vacuities, forms a fork-shaped extension keeping the cultriform process of the parasphenoid in between. This posterior extension is more elongate than in other mastodonsaurids. This seems to be more pronounced in ISI A 207. However, in that specimen, the palate is not well preserved. Hence, the discovery of more well-preserved specimens can only shed some light on this character state.

Palatines. The palatines are crescent in shape and bear the second pair of palatal tusks. The palatines form the posterior rim of the choanae and contact the maxillae anteriorly. The palatine-maxilla sutures run posterolaterally from the choanae to the ectopterygoid and form the anterolateral rim of the interpterygoid vacuity. The palatine has a discontinuous row of teeth more or less becoming larger anteriorly (Figs 2C, D, 3C, D).

Pterygoids. The pterygoids have a bow-like structure extending between the interpterygoid vacuities and the subtemporal vacuities and form parts of their respective rims (Figs 2C, D, 3C, D). Anterolaterally, the pterygoids contact the ectopterygoids and establish point contact with the ***insulae jugalis***. Posteriorly, the pterygoids contact the quadrates and form part of the posterior margin of the skull. The pterygoids contact the parasphenoid medially by a serrated suture. The pterygoids do not contact the palatines. The pterygoids suture with the exoccipitals ventrally. The palatine ramus of the pterygoid bears feeble ornamentation.

Parasphenoid. The parasphenoid is an unpaired bone present in the middle of the palate (Figs 2C, D, 3C, D). The cultriform process of the parasphenoid projects beyond the anterior margin of the interpterygoid vacuities. The parasphenoid-exoccipital suture has a flat and long ‘M’ shaped outline. The ***crista muscularis*** of the parasphenoid runs transversely. Laterally, the parasphenoid sutures with the pterygoids. The parasphenoid-pterygoid sutures are as long as the width of the parasphenoid basal plate. The parasphenoid forms the posteromedial rim of the interpterygoid vacuities. The basal plate of parasphenoid is short and parasphenoid pockets are present entirely on the ventral surface of the palate. The cultriform process of the parasphenoid gradually merges with the vomers anteriorly (Figs 2C, D, 3C, D).

Ectopterygoids. The ectopterygoids are longitudinal bones. Posteromedially, the ectopterygoid sutures with the pterygoid, posteriorly with the ***insula jugalis***, and anteriorly with the palatines (Figs 2C, D, 3C, D). The ectopterygoid bears a number of laterally compressed teeth. Ectopterygoids contribute a small portion to the rim of the interpterygoid vacuities (Figs 2C, D, 3C, D).

Insulae Jugalis. The ***insulae jugalis*** are triangular bones forming a point contact with the pterygoids posteriorly. Anteromedially, the ***insula jugalis*** is bound by the ectopterygoid and posteriorly forms a part of the anterior rim of the subtemporal vacuity (Figs 2C, D, 3C, D).

Quadrates. The quadrates are polygonal-shaped bone and contact the pterygoids medially and the quadratojugals laterally (Figs 2C, D, 3C, D). Anteriorly, the quadrates contribute to the posterior rim of the subtemporal vacuity, and posteriorly form the posterior margin of the skull. A prominent quadrate boss is present on the occipital face (Figs 2C, D, 3C, D).

Skull openings. Skull openings from the holotype ISI A 54 are listed below:

The nares are the tear-drop-shaped dorsal openings with a maximum length of 4.33 cm and maximum width 2.52 cm for the left and maximum length 4.76 cm and maximum width of 2.63 cm for the right opening. A small bone, the septomaxilla, is present at the inside of the anterolateral margin of the nares. The orbits are positioned at the posterior half of the skull with a maximum length of 5.70 cm and 5.85 cm and a maximum width of 3.76 cm and 3.30 cm respectively for left and right and they are elliptical in outline. The orbits are slightly elevated with respect to the plane of the skull roof. The pineal foramen is subcircular; its long axis is 1.68 cm and short axis is 1.03 cm, and is completely enclosed by the parietals. The otic notch is wide open posteriorly and is bounded by the squamosal and the tabular. The anterior rim of the otic notch is angular, the angles between the squamosals and the tabulars are 41 and 62 degrees in the left and right otic notch respectively. The anterior palatal vacuities are subdivided and laterally stretched with a maximum length of 2.5 cm and width of 7 cm. The left one measures 2.08 × 3.22 cm and the right one measures 1.46 × 3.49 cm. It is enclosed by the premaxillae and the vomers. The anterior palatal vacuity is bean-shaped with a constriction in between. The choanae are two slit-like cavities in the anterior part of the palate. The left and right choanae are quite deformed (taphonomically) with dimensions of 3.49 × 1.28 cm and 5.07 × 1.21 cm, respectively. The interpterygoid vacuities are the largest openings of the palate, with a ‘D’-shaped outline, they measure 28.93 × 8.08 cm and 28.91 × 9.60 cm on left and right respectively. The lateral rims have a parabolic curvature with the posterior curvature being more acute than the anterior one. The marginal rims are almost straight. The interpterygoid vacuities are enclosed by the vomers, the palatines, the pterygoids, the parasphenoid and a small portion of the ectopterygoids. The cultriform process of the parasphenoid forms most of the medial margin. The subtemporal vacuities are the posterior most vacuities in the palate. The vacuities are arch shaped with a gentle lateral convexity and a more acute medial concavity. The maximum length measured parallel to the midline is 17.30 cm, and the maximum width is 7.90 cm for the left one and 17.47 cm and 9.01 cm respectively for the right one. The subtemporal vacuities are enclosed by the pterygoids, the quadrates, the quadratojugals and the ***insulae jugalis***. The tip of the anterior projection of the subtemporal vacuity does not reach the level of the midpoint of the interpterygoid vacuities.

Occiput (Figs 2E, F, 3E, F). The occipital process contacting postparietal and tabular is extremely short and stout dorso-ventrally in occipital view. The pterygoid oblique ridge is exceptionally short and dorsomedially oriented, located just anterior to the otic notch and approaching the ***crista falciformis*** of the squamosal. The descending ramus of the squamosal partially covers the lateral sections of the pterygoid and quadrate and extends dorsolaterally to the paraquadrate foramen at the quadrate. From its posterior corner, the quadratojugal produces a narrow but thicker flange that extends medially for a short distance along the rear surface of the quadrate. The quadrate bears a prominent quadrate boss. The post temporal fenestra is triangular in outline. The torsion in the quadrate is visible in occipital view.

Exoccipitals. The exoccipitals project posteriorly to establish the atlas-exoccipital articulation and diverge dorsally to encompass the ventral portion of the foramen magnum. They suture with the parasphenoid anteriorly. The posterior projection of the exoccipitals lies anterior to the projection of the quadrates. The posterior contact surfaces of the exoccipitals with the atlas are sub-oval in shape and are flat and narrow.

***Mandible* (Fig. 4).** A well-preserved right mandibular ramus of *Cherninia denwai* (ISI A 208) was recovered from the Baki-Nala section near the village of Jhirpa, measuring almost 96 cm in length (Fig. 4). The curvature of the mandible exactly fits with the skull outline of *C. denwai*. Moreover, skull fragments of *C. denwai* are found from the same locality.

Dentary. The dentary forms the dorsal and parts of the labial and lingual surface of the anterior part of the ramus (Fig. 4). The dentary is bound ventrally by the splenials and angular in labial view; posteriorly the dentary tapers to a point and projects into the surangular. In lingual view, it is bound by the splenial and the coronoids ventrally, while it forms the anterior margin of the adductor fossa posteriorly. The dentary and the splenial are present in the anterior symphysis. The main marginal teeth are located on the dorsal surface. The symphysial region of the dentary has one large tusk.

***Splenial and postsplenia*l.** In labial view, the splenial and postsplenial lie ventral to the dentary with the splenial located anteriorly. The region of the posterior Meckelian foramen is broken. The ventral surface is not fully preserved (Fig. 4).

Angular. The angular forms the remaining bone in the ventrolabial and some part of the ventrolingual surface (Fig. 4). It is bound by the dentary anterodorsally, by the postsplenial anteroventrally, and by the surangular dorsally in labial view. In lingual view, it is bound by the prearticular dorsally and articular posteriorly.

Surangular. The surangular forms most of the posterodorsal part of the labial surface, including that of the postglenoid area. In labial view, the surangular sutures with the angular ventrally and with the dentary anteriorly. In lingual view, it sutures with the articular posteriorly and with the angular ventrally and anteriorly with the prearticular. In dorsal view, the surangular sutures with the dentary anteriorly; lingually it sutures with the articular and forms the lingual margin of the adductor fossa (Fig. 4).

Coronoid series. The coronoid series consists of anterior, middle and posterior coronoid on the lingual surface of the mandible. They are placed ventral to the dentary and extend from shortly behind the symphysis to the leading edge of the adductor fossa. The anterior coronoid sutures with the splenial ventrally, the middle coronoid sutures with the postplenial and some part of the splenial and the posterior coronoid with the prearticular. No dentition is present in the coronoid series nor is there any process present in the coronoids (Fig. 4).

Prearticular. In lingual view, the prearticular forms the posterior half of the ramus. It sutures with the postsplenial anteriorly and dorsally with the middle and posterior coronoids. The prearticular forms the lingual margin of the adductor fossa and the lingual edge of the glenoid fossa. The prearticular does not form part of the postglenoid area and it does not suture with the splenial because it is separated by the coronoid (Fig. 4).

Articular. The articular is an endoskeletal bone that completely forms the glenoid fossa. Anterodorsally, the articular forms the posterior border of the adductor fossa. The articular is enclosed labially by the surangular and lingually by the prearticular. Ventrally, the articular is overlain by the angular. Posteriorly the articular enters the postglenoid area. The posterior extremity of the articular is not completely ossified.

Other important features of mandible (Fig. 4). The hemi-mandible is low except for its posterior area, which is dorsally straight along the posterior two-thirds and slightly curved in the anterior part. In labial view, the angular shows well-defined ornamentation that becomes less evident in the postsplenial. A highly developed mandibular sulcus is found in the back of the hemi-mandible, and the marked oral sulcus extends all the way to the dentary. There is also a tiny accessory sulcus that runs from the mandibular sulcus to the surangular. The posterior Meckelian foramen is not preserved and the anterior Meckelian foramen is absent. The adductor fossa is quite large, with an oval shape and dimensions of 21.2 cm along the long axis and 2.3 cm along the short axis. The lingual border of the articular, the labial border of the surangular, the antero-labial border of the dentary, the antero-lingual border of the posterior coronoid, and the posterior border of the glenoid fossa all encircle the adductor fossa. One anterior tusk and multiple teeth with elliptical bases can be seen in the dentary. As is characteristic in many temnospondyls, both the dentary and the splenial are a part of the symphyseal area. The articular and surangular (but not the prearticular) are located in the postglenoid region, which is considerably extended. The angular is extended to the ventral side of the articular. The ***foramen chorda tympani*** are situated more on the labial side of the post-glenoid region (dorsal). Although Jupp and Warren (1986) discussed the lower jaw anatomy of temnospondyls and stated that mastodonsaurids mostly have Type I post glenoid area, the morphology of the post– glenoid area of *C. denwai* cannot be clearly placed in any of the two types defined by Jupp and Warren (1986). It shares with Type I the following features: the prearticular does not extend into the postglenoid area, the articular is the major component of the postglenoid area and the angular lies ventral to the articular. On the other hand, as in Type II, the angular lies labial to the articular and the postglenoid area is slightly elongated. The prearticular hamate process is highly developed, huge, and spatulate. In comparison to the hamate process, the quadrate trochlea is shorter. There were two separate processes called the ***crista articularis*** and ***crista medialis***. Underneath the dentary's dorsal surface is the

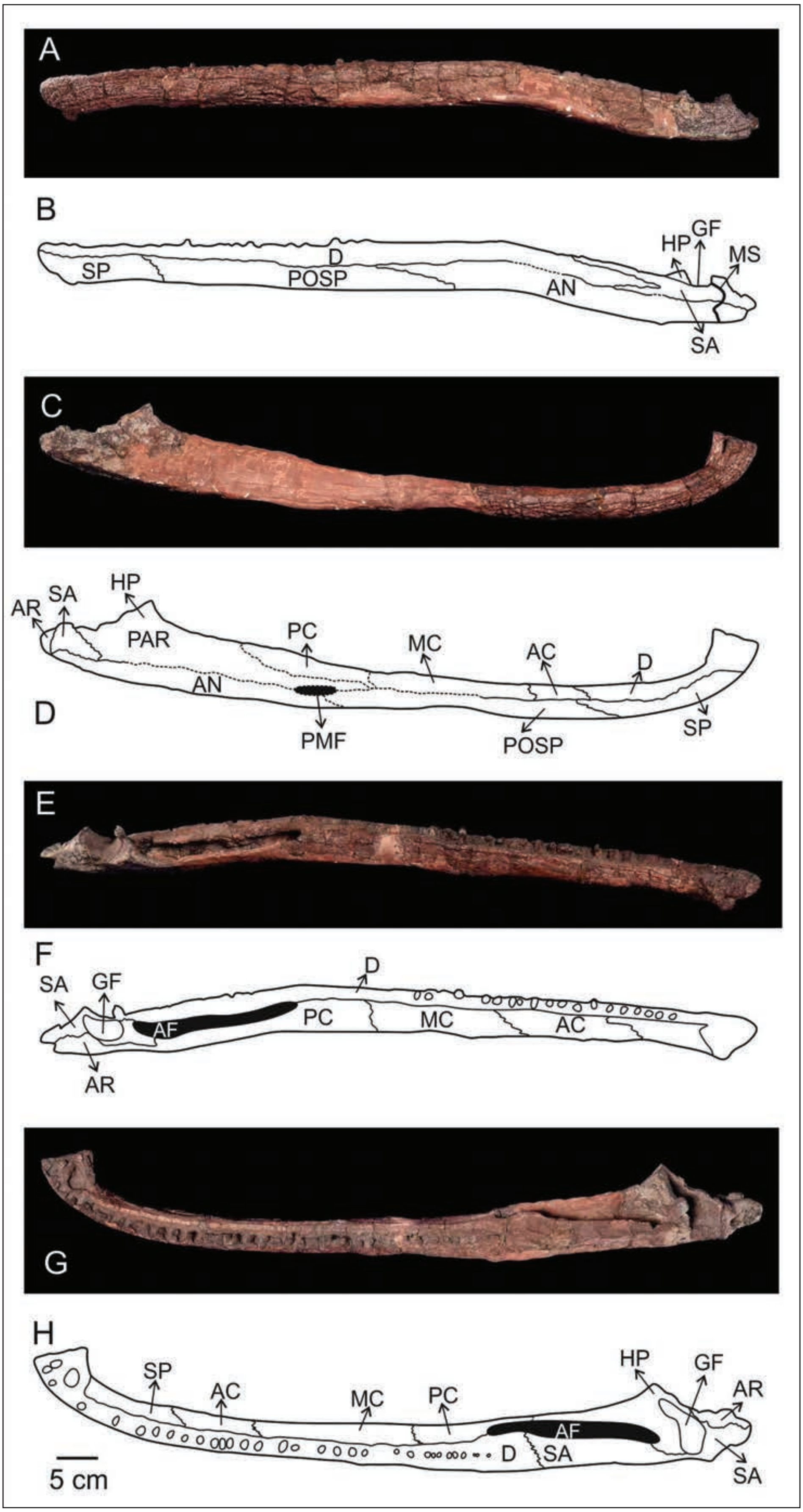

Figure 4. A, C, E, G. The right mandibular ramus of *Cherninia denwai* (ISI A 208) from the middle part of the Middle Triassic Denwa Formation in labial, lingual, dorsal, and dorso-lingual view respectively; **B, D, F, H.** Line drawing of the same.

glenoid fossa. The elliptical, sizable adductor fossa has a horizontal and straight labial wall. The ***torus arcuata*** (muscle scar near the hamate process) is prominent and the muscle insertion area is comparatively large (Fig. 4). The shape of the glenoid fossa is rectangular. The adductor fossa's anterior process is elevated and conspicuous.

Postcranium (Figs 5–13). All postcranial elements were retrieved from the middle part of the Denwa Formation. They are assigned to the taxon *Cherninia denwai*, as they were discovered either in association or in very close proximity (almost together) to the cranial fragments of the taxon. The postcranial elements were mainly collected from Purtala, Kohpani and Jhirpa villages and adjoining areas of the state of Madhya Pradesh (Central provinces), India. In Purtala and in Kohpani, they are either associated with the skull or found in close proximity, sometimes within a meter or so, in the same bed and at the same level. In Jhirpa they are associated with the mandible of *C. denwai* which is unique in its curvature, proportion of dentigerous area with respect to the adductor fossa and the postglenoid area. The said proportions are different from that of the brachyopids and the trematosaurid mandibles. Brachyopids and trematosaurids are the other two groups that are present in the Middle Denwa. The postcranial elements, particularly the vertebrae, of these two groups are also different from those of the mastodonsaurids (Warren and Snell 1991).

The Vertebral column. The preserved vertebral elements mainly encompass the intercentra, neural arches, and neural spines (Fig. 5). The post-atlantal and presacral neural arches are different. The presacral neural arches have less developed posterior zygapophyses with shorter neural spines than the post-atlantal arches. The neural spines of the post-atlantal vertebrae have erect

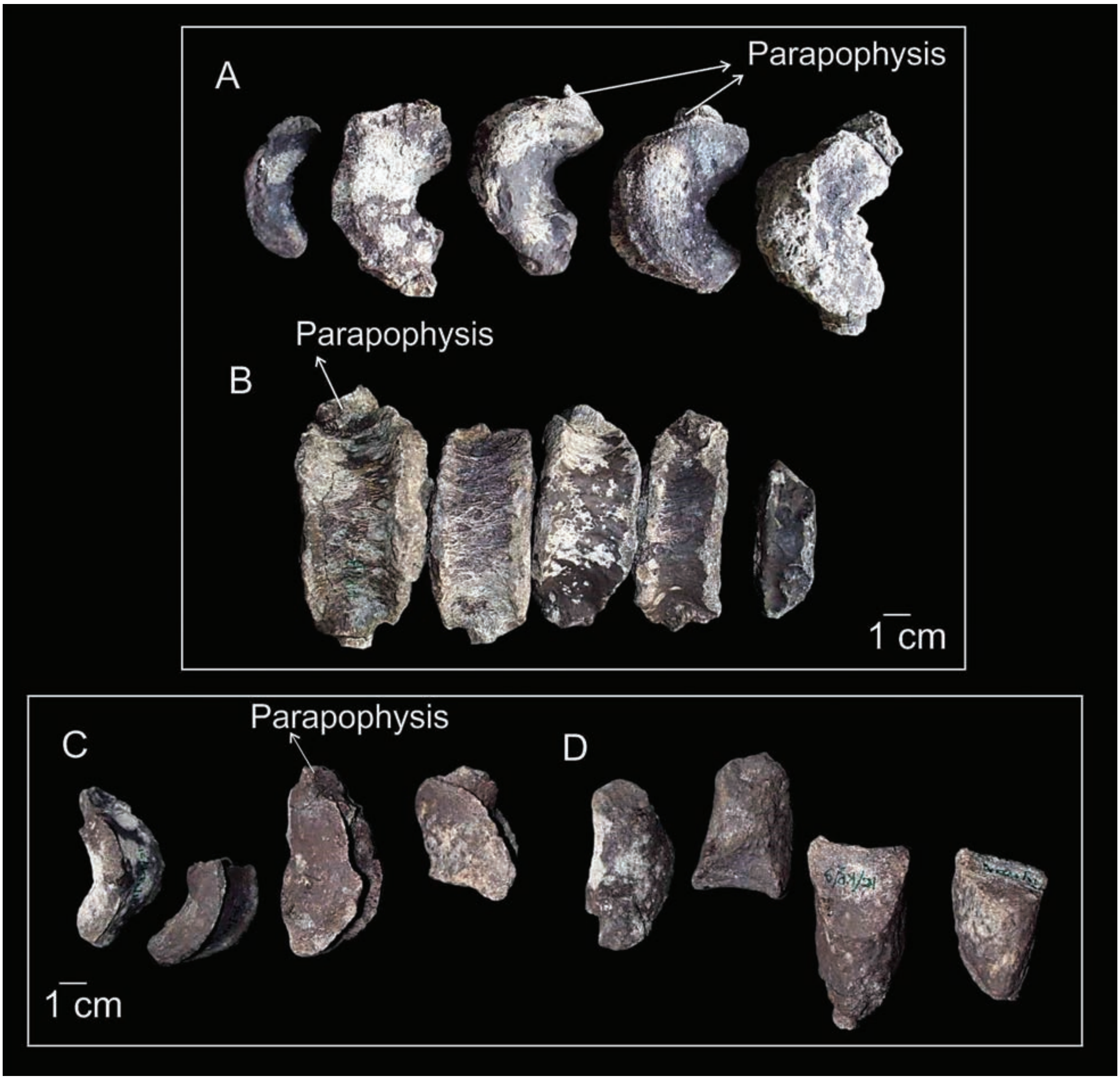

Figure 5. Intercentra (ISI A 214–217) of *Cherninia denwai* from the middle part of the Middle Triassic Denwa Formation in anterior and ventral views respectively. **A, B.** Anterior intercentra (ISI A 209–213); C, D. Posterior intercentra

spines. Most of the neural arches and neural spines were incomplete and broken in *C. denwai*. Atlas and axis are not present in the collection.

The intercentra are wedge-shaped in lateral view and crescentic or heart-shaped in anterior and posterior views. Distinctly, two types of intercentra are present, type 1 in the anterior part and type 2 in the posterior part. The anterior intercentra are massive, quite thick, and robust. The dorsal most part is blunt. The ventrolateral surface of the intercentrum is concave with two raised rims at the anterior and posterior borders. The parapophysis is well developed. Five anterior intercentra are preserved (ISI A 209–213). The posterior intercentra are flattened ventrally and the lateral surfaces are more distinct from the ventral face. They are shallower and less ossified than the anterior ones. The parapohyses were directed more ventrally, thus their lower edges project below the ventral line with a triangular outline. There are four posterior intercentra preserved (ISI A 214–217) (Fig. 5).

Neural arch and neural spine. Neural arch and neural spines (Fig. 6) are broken in the specimens from the middle part of the Denwa Formation. The body of the neural arch extends laterally. A rectangular facet, the area of attachment of the pleurocentrum (Watson 1958) is present. At the distal end of the transverse process, a squarish facet is present which is the diapophysis.

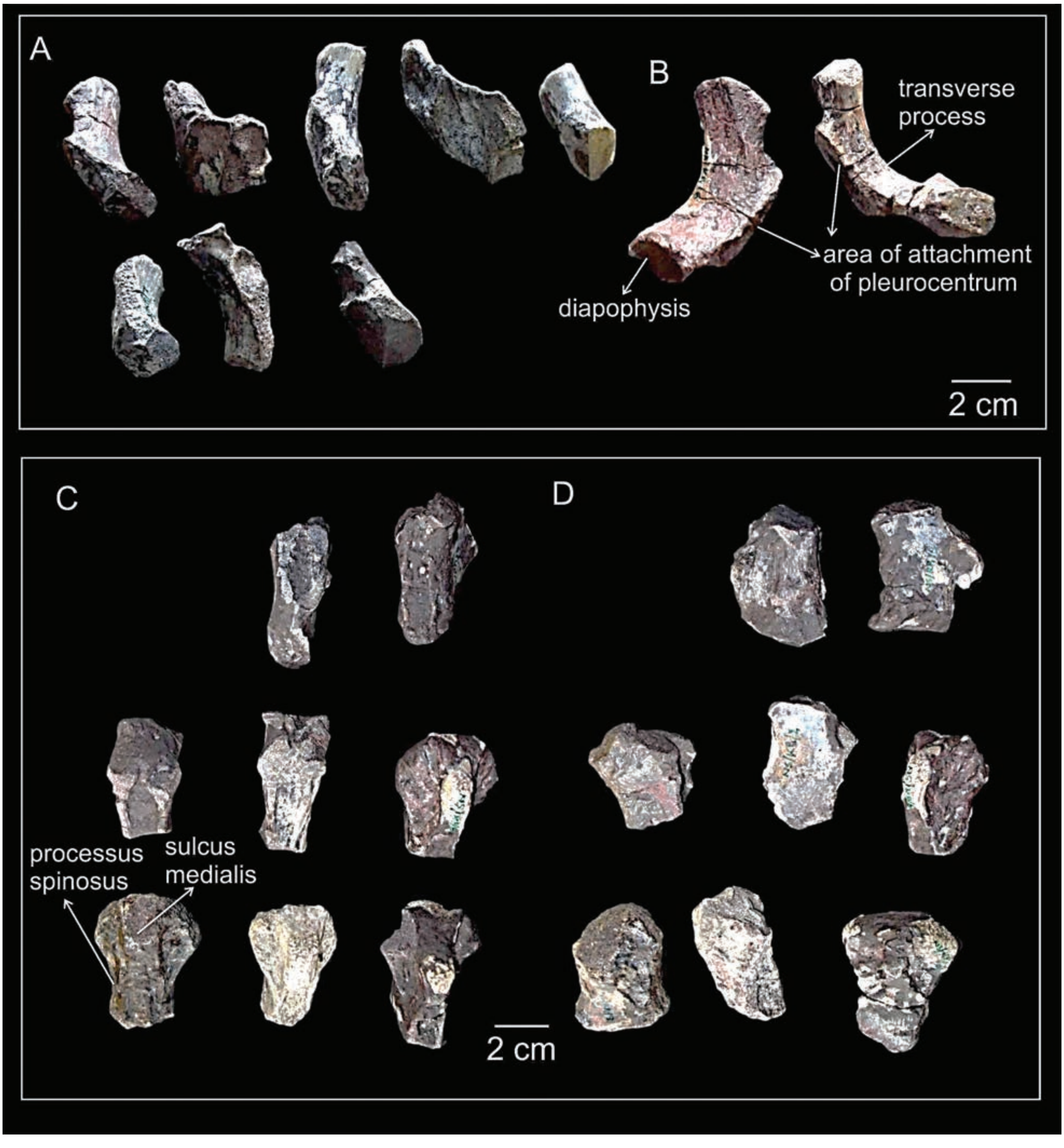

Figure 6. Neural arches of *Cherninia denwai* from the middle part of the Middle Triassic Denwa Formation in anterior view. **A.** Neural arch (ISI A 218–225); B. Two lateral halves of a neural arch (ISI A 226a&b).

Neural spines were detached from the bodies of the neural arches. They are short and stout. Eight single broken neural arches (ISI A 218–225) and two broken lateral halves of a neural arch (ISI A 226a & b) are preserved. Eight neural spines have been detected (ISI A 227–234).

No haemal arches are preserved.

Ribs. A total of 30 rib fragments and one almost complete rib are present (Fig. 7). The ribs show distinct variation in morphology. The position of the ribs has been determined by the existing literature of temnospondyls ribs (Dutuit 1976; Dutuit 1978; Sengupta 2002; Sulej 2007).

The cervical ribs have two separate rib facets. The anterior thoracic rib **(**ISI A 235; ISI A 238–250) heads were elliptical in cross-section with a narrow extension for attachment of capitulum and tuberculum. The distal end of the anterior thoracic rib is expanded and plate-like. The posterior thoracic ribs (ISI A 251–266) are cylindrical and have elliptical proximal heads and rounded distal ends (Fig. 8). Sacral ribs are expanded both proximally and distally and are short and stout (ISI A 236–237).

No caudal ribs are preserved.

Pectoral girdle. Two almost complete and three fragmented interclavicles (ISI A 267 & 268), one complete left and one fragmented left and one fragmented right clavicle (ISI A 272–274) and six fragmented cleithra (ISI A 275–280) are present. The interclavicles are large and robust and their thickness varies from 3 to 5 cm. The clavicles have a long dorsal process originating at the posterolateral corner of the clavicular blade. The dorsal

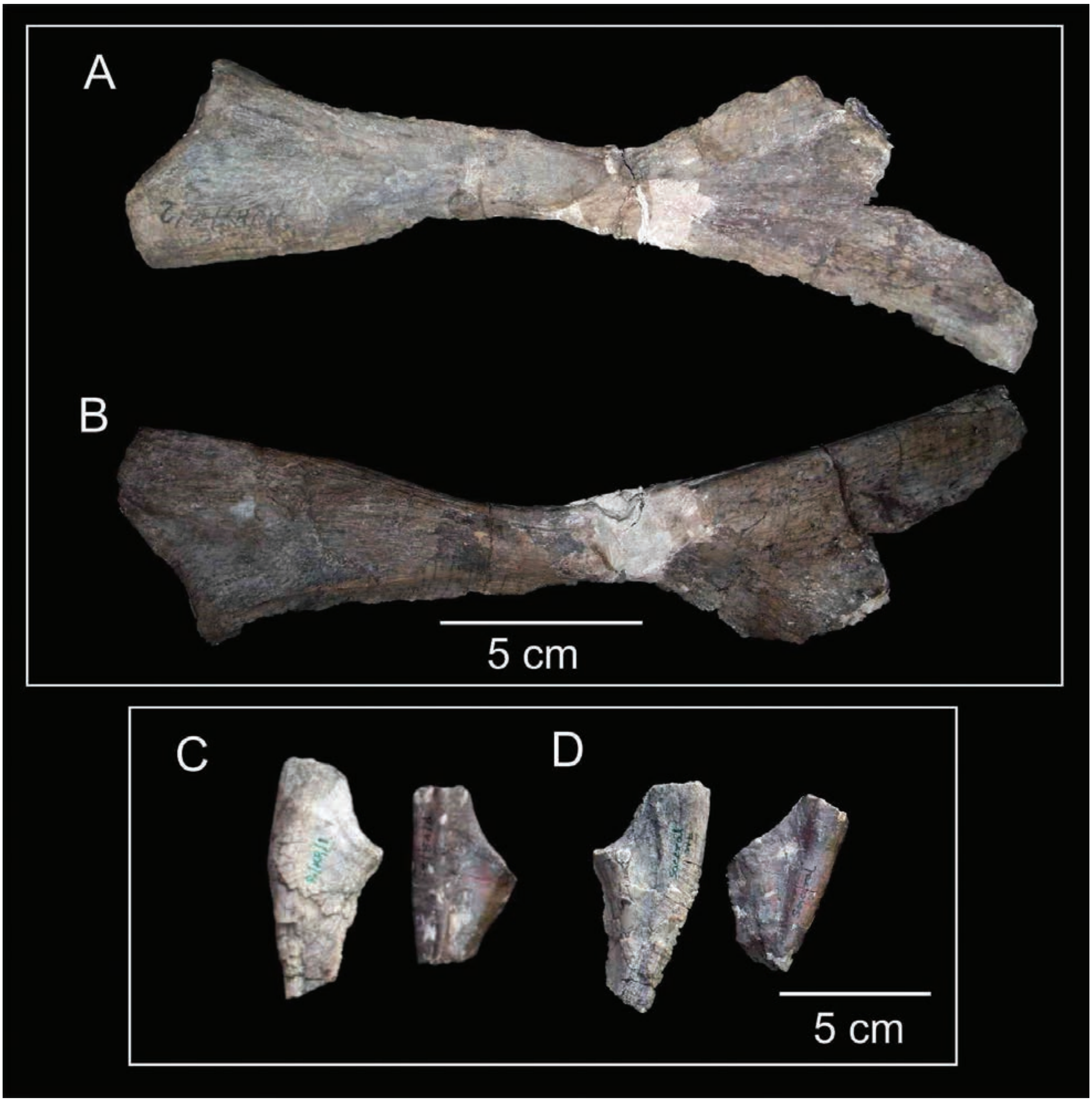

Figure 7. Ribs of *Cherninia denwai* from the middle part of the Middle Triassic Denwa Formation. **A, B.** Anterior thoracic ribs (ISI A 235) in dorsal view; **C, D.** Sacral ribs (ISI A 236–237) in ventral view.

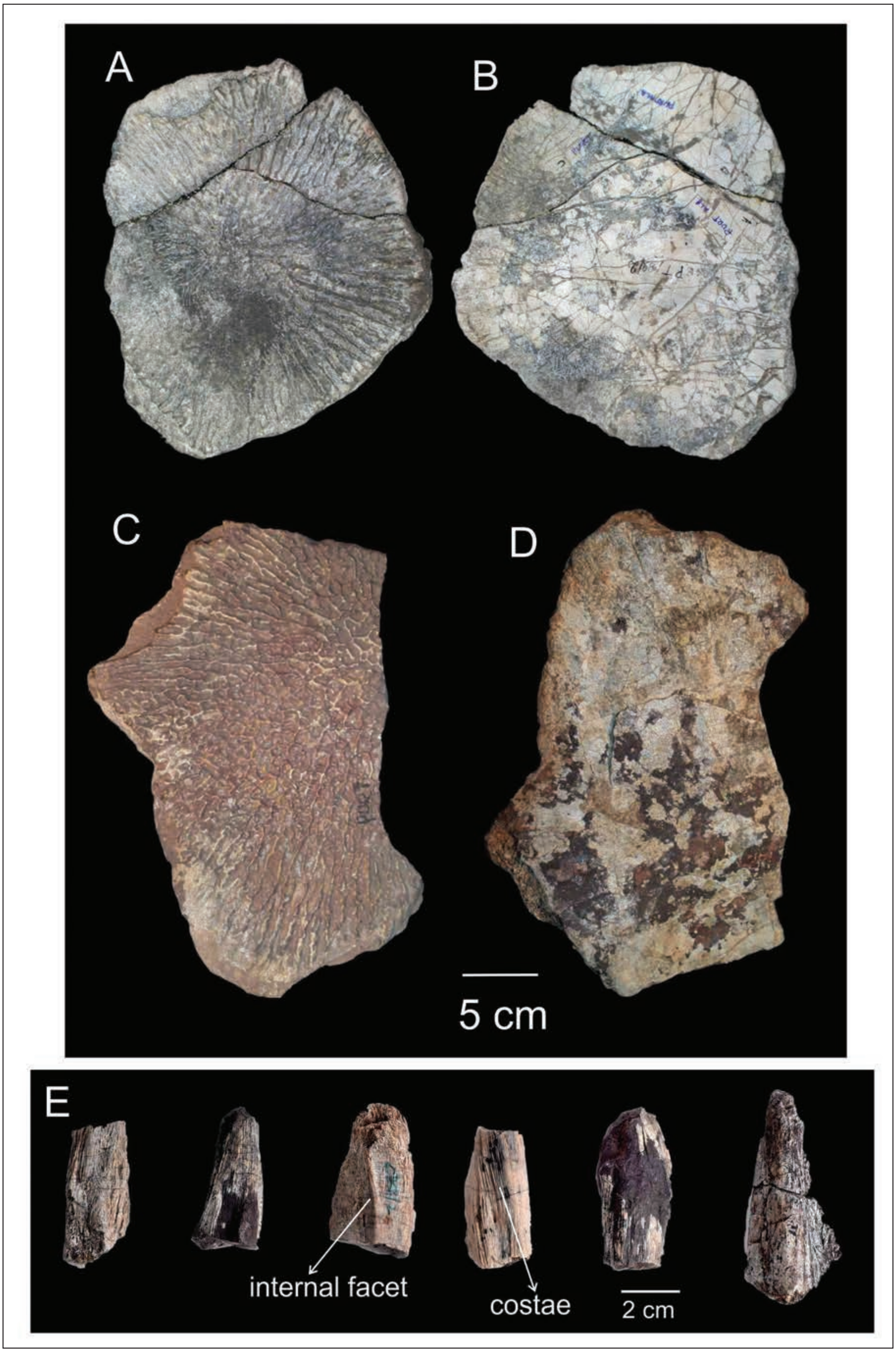

Figure 8. Claviculae of *Cherninia denwai* from the middle part of the Middle Triassic Denwa Formation. **A–C.** Left clavicle (ISI A 272) in dorsal, ventral and posterior views, respectively; **D–G.** Left clavicle (ISI A 273) in dorsal, ventral, lateral and posterior views respectively; **H, I.** Right clavicle (ISI A 274) in dorsal and ventral views respectively.

process is slender and twisted. The clavicular blades are slender and spatulate (Fig. 8).

Cleithra are slender processes having low ridges on their surfaces. A scapular crest is present at its head. The shaft's external surface is convex. The internal facet has a concave attachment area for the clavicle and a convex attachment area for the scapula (Sulej 2007). All the cleithra are broken (Fig. 9).

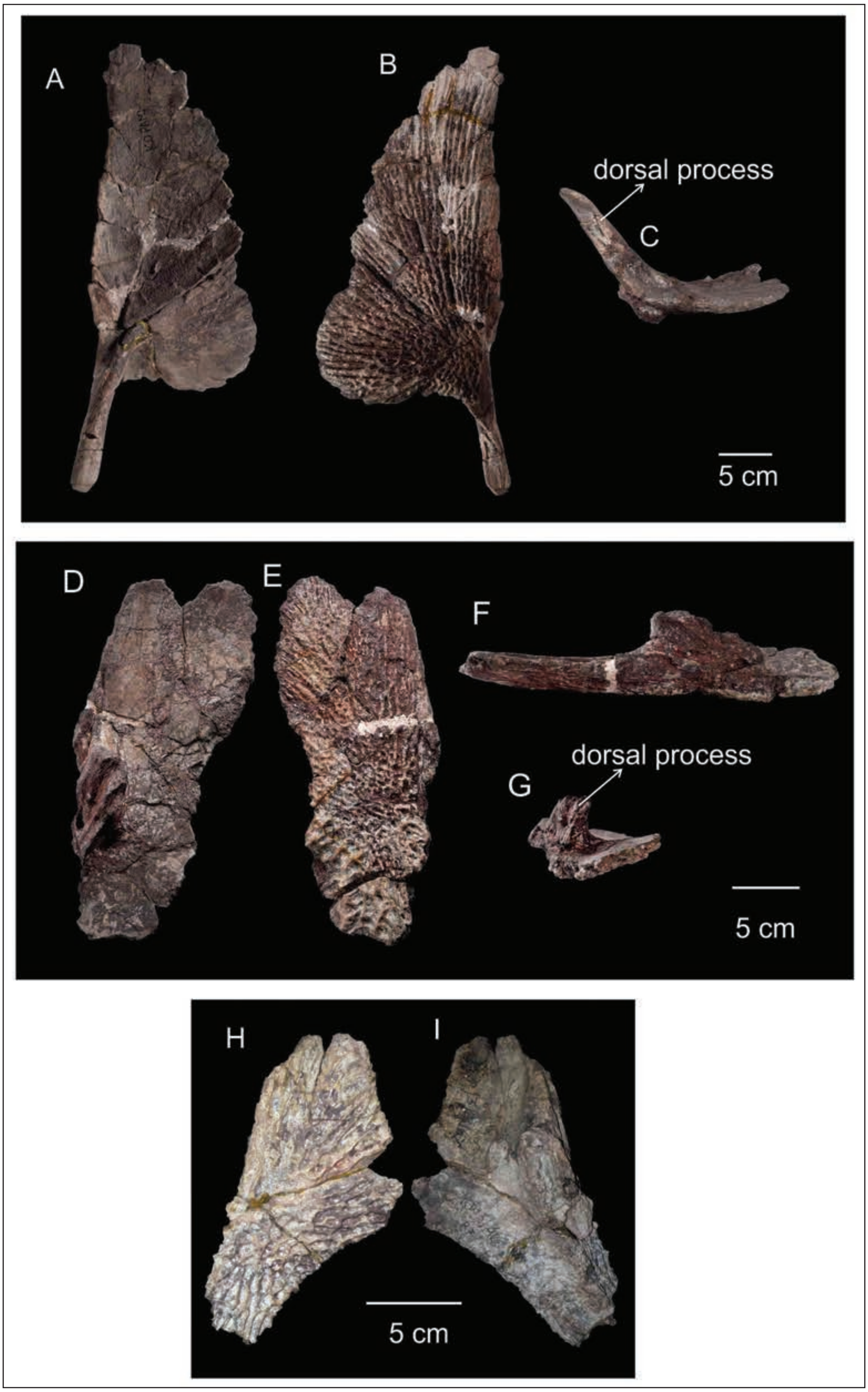

Figure 9. A–D. Interclaviculae of *Cherninia denwai* from the middle part of the Middle Triassic Denwa Formation. **A, B.** Interclavicle (ISI A 267) in ventral view; **C, D.** Interclavicle (ISI A 268) in dorsal view; **E.** Cleithrum (ISI A 275–280) of *Cherninia denwai* from the middle part of the Middle Triassic Denwa Formation.

Forelimb. From the forelimb, only the proximal and distal heads of the ulna are preserved in the present collection (ISI A 182/3 & 4; ISI A 281–282, Fig. 10). The specimen ISI A 182/4 was interpreted as the distal shaft of the ulna by Mukherjee et al. (2020), but the olecranon process is distinct in the specimen, so that it can be regarded as the proximal shaft of the right ulna. The proximal and distal ends of the ulna are expanded towards the radius. The proximal head is rhombohedral in outline and the posterolateral corners of the head are raised with the olecranon process. On the posterior surface, a low crest is present. The distal heads bear a laterally flattened articulation surface for ulnare and intermedium.

Pelvic girdle. The pelvic girdle comprises only the left ilium as no other elements are preserved (Fig. 11). Overall, the ilium is cylindrical with a convex ventral

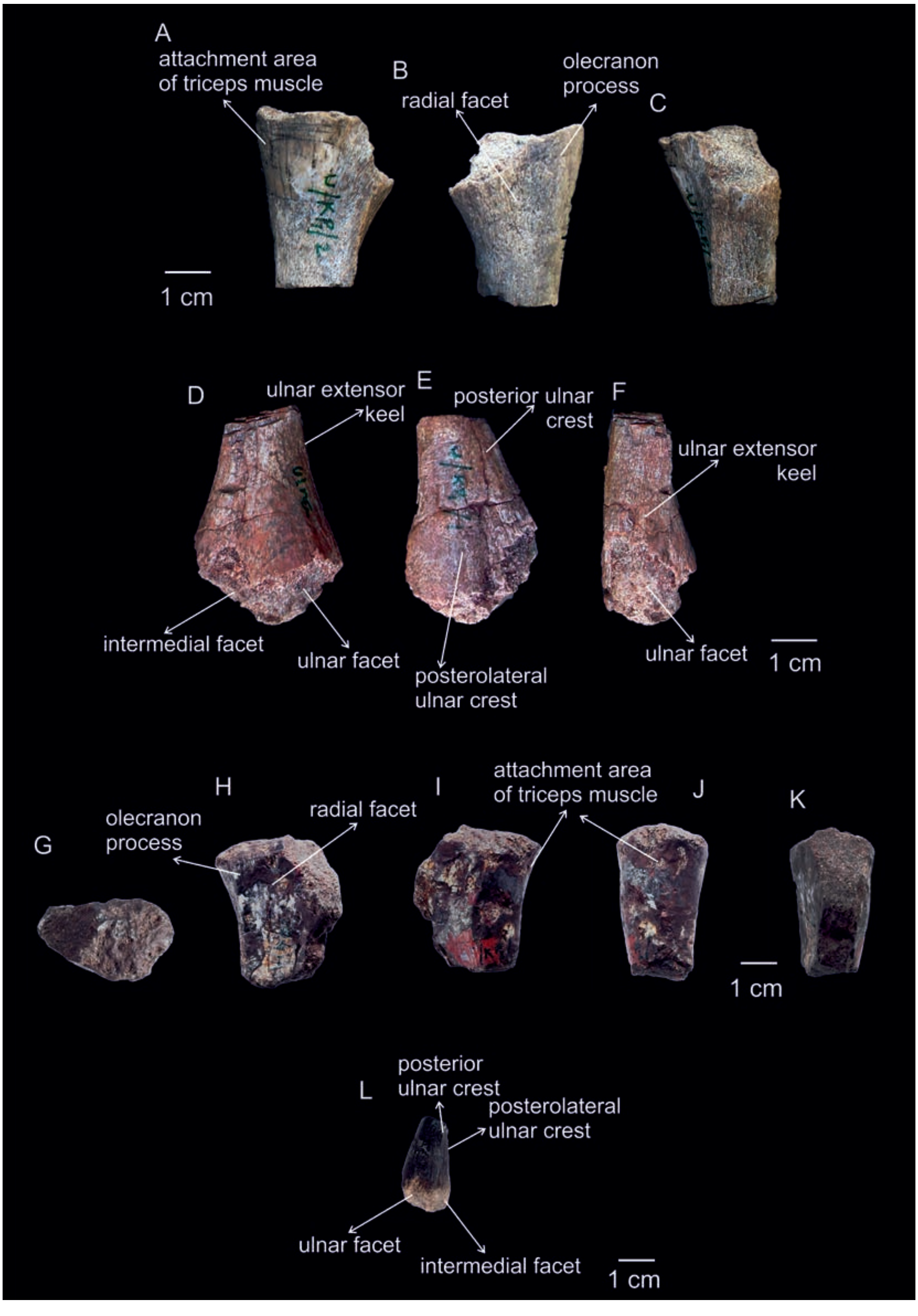

Figure 10. Ulna of *Cherninia denwai* from the middle part of the Middle Triassic Denwa Formation. **A–C.** Proximal shaft of left ulna (ISI A 182/4) in anterior, posterior and flexor views respectively; **D–F.** Distal shaft of left ulna (ISI A 182/3) in anterior, posterior, and extensor views respectively.

margin that tends to meet the puboischiadic blade (ISI A 283). A depression at the posterior part of the ilium is the area of attachment of the acetabulum head which is mostly cartilaginous. The acetabular buttress is thicker anteriorly and laterally projected. The acetabulum is bounded by two notches. The anterior supracetabular notch is slenderer and dorsally placed while the posterior acetabular notch is ventrally placed. The iliac blade is robust and cylindrical and bears some striations for attachment of muscles. The shaft is oval in cross-section.

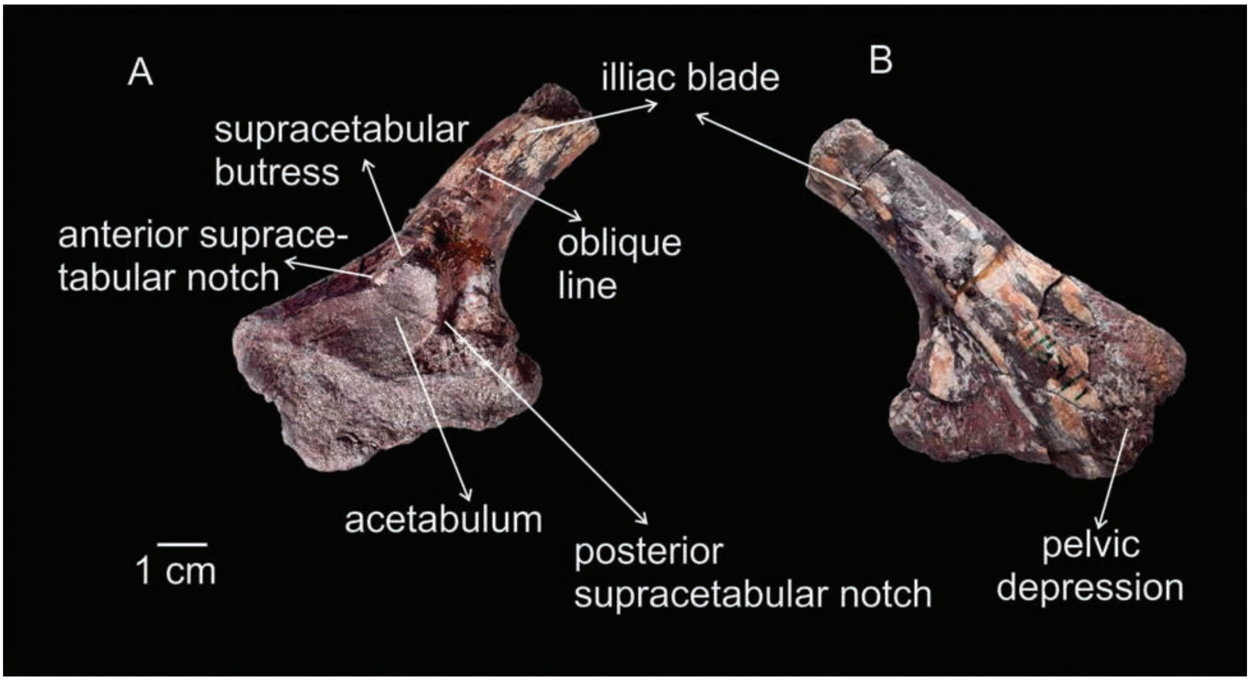

Figure 11. Left ilium (ISI A 283) of *Cherninia denwai* from the middle part of the Middle Triassic Denwa Formation. **A.** Ventrolateral view; B. Dorsomedial view.

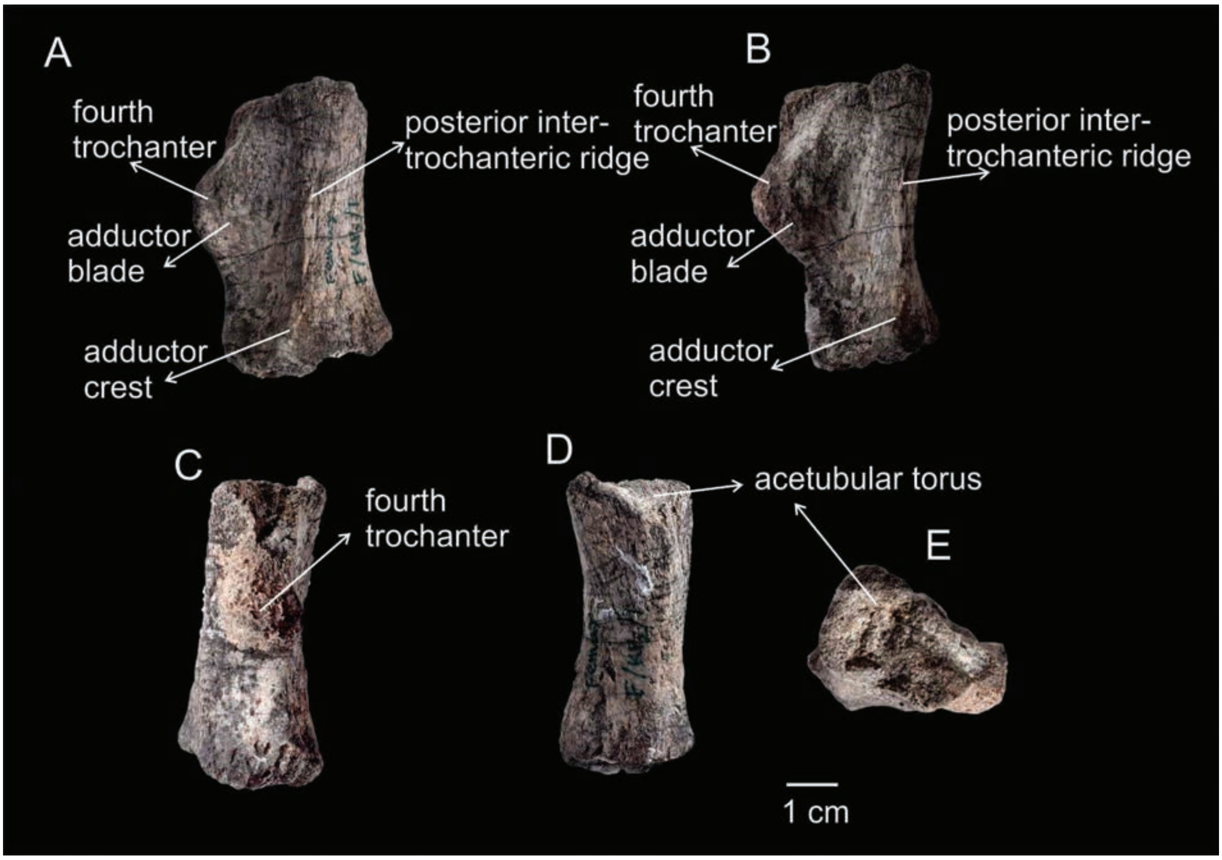

Figure 12. Proximal shaft of right femur (ISI A 284) of *Cherninia denwai* from the middle part of the Middle Triassic Denwa Formation. **A.** Ventral view; **B.** Ventrolateral view; **C.** Anterior view; **D.** Posterior view; **E.** Proximal view. .

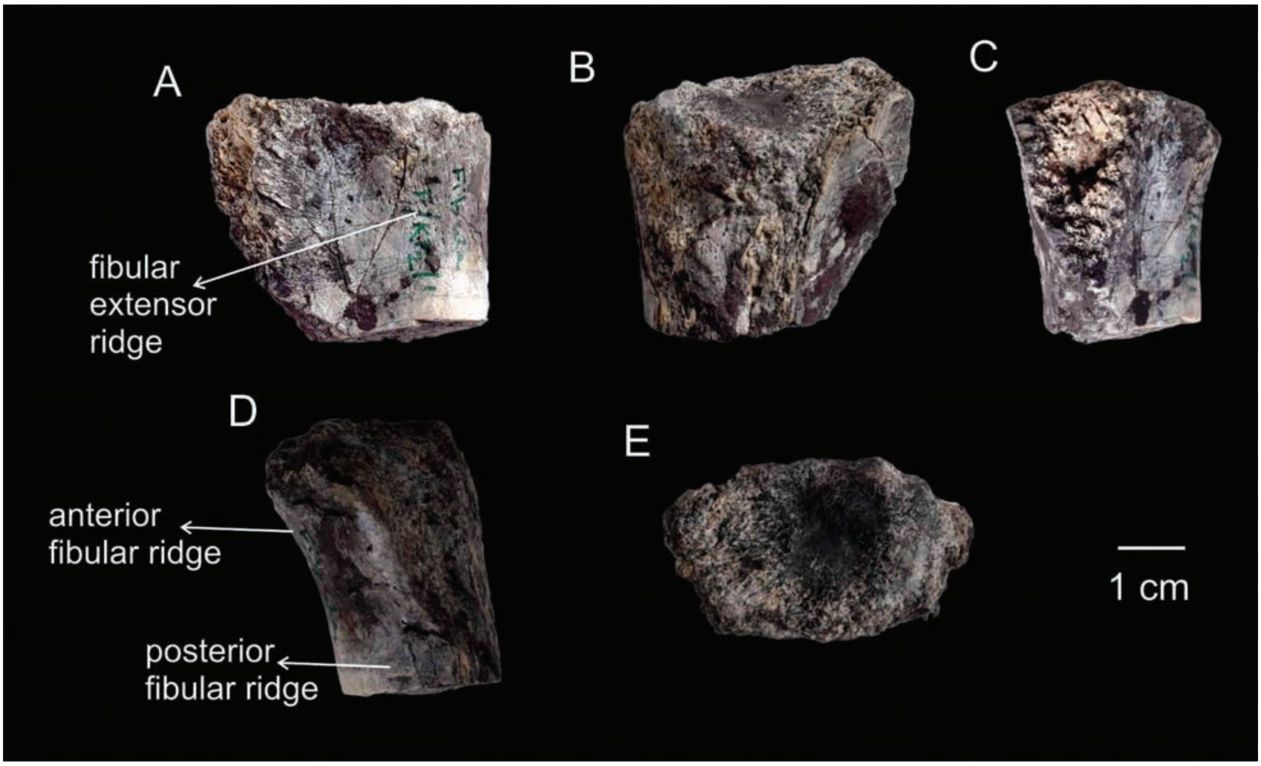

Figure 13. Left fibula (ISI A 285) of *Cherninia denwai* from the middle part of the Middle Triassic Denwa Formation. **A.** Extensor view; **B.** Flexor view; **C.** Posterior view; **D.** Anterior view; **E.** Proximal view.

Hind limbs. From the hindlimbs, the proximal shaft of a right femur and the proximal shaft of left fibula is preserved. The tibia is not present in the collection. The proximal shaft of the right femur (Fig. 12) shows concave anterior and posterior margins. The bone is strong and stout with a medial ridge. The adductor blade is present housing the fourth trochanter. The proximal articular surface is oval in outline (ISI A 284).

The fibula is dorsoventrally flattened, with a trapezoidal outline of the proximal head (Fig. 13). The anterior margin is concave. The well-developed posterior fibular ridge is visible, which is bordered by a furrow in the front and a raised surface made by two short parallel ridges in the back (ISI A 285).

No digit bones were found.

Discussion

Supported by the new material, an emended diagnosis and a new reconstruction of the skull of *C. denwai* is presented here (Fig. 14). New specimens including a partial skull, a mandible, clavicles, interclavicles, vertebrae, neural arches and spines, ulnae, an ilium, a femur and a fibula were also described for the first time. A detailed osteological description of the skull and the mandible was provided. It was noted that the skull roof has conspicuous, paired and forked ridges anterior to the orbits and the otic notch is angular, the tabular horns posteriorly directed and recurved distally. The mandible is slender with a distinct post glenoid area (PGA) and a well-developed, hamate process. The prearticular is separated from the splenial by the dentary and the coronoid series. The PGA is a combination of type 1 and type 2 (*sensu* Jupp and Warren 1986). The hemi-mandible is low. In the labial view, the angular shows well-defined ornamentation that becomes feeble on the postsplenial. A well-developed mandibular sulcus is found in the posterior part of the hemi-mandible, and the oral sulcus extends all the way to the dentary. All those characters are the diagnostic characters of *Cherninia denwai*.

Conclusion

The hitherto undescribed limb bones of *C. denwai* add to our knowledge on mastodonsaurid limb bones. This is important as stereospondyl specimens are mostly represented by skulls that are heavy and flat with better preservation potential than the long bones. The limbs of the mastodonsaurids are rarely found and are not very diverse (Warren and Snell 1991). However, they are not suited for terrestrial locomotion. The vertebrae, however, have functional significances. Carter et al. (2021) studied the evolution and functional significance of the intercentral traits within temnospondyls, which, they said, were repeatedly converging on distinct forms in terrestrial and aquatic taxa, with little overlap between. Their geometric morphometric study revealed relationships between vertebral shape and environmental preferences and a strong relationship between habitat preference and intercentrum shapes (Carter et al. 2021). The same publication

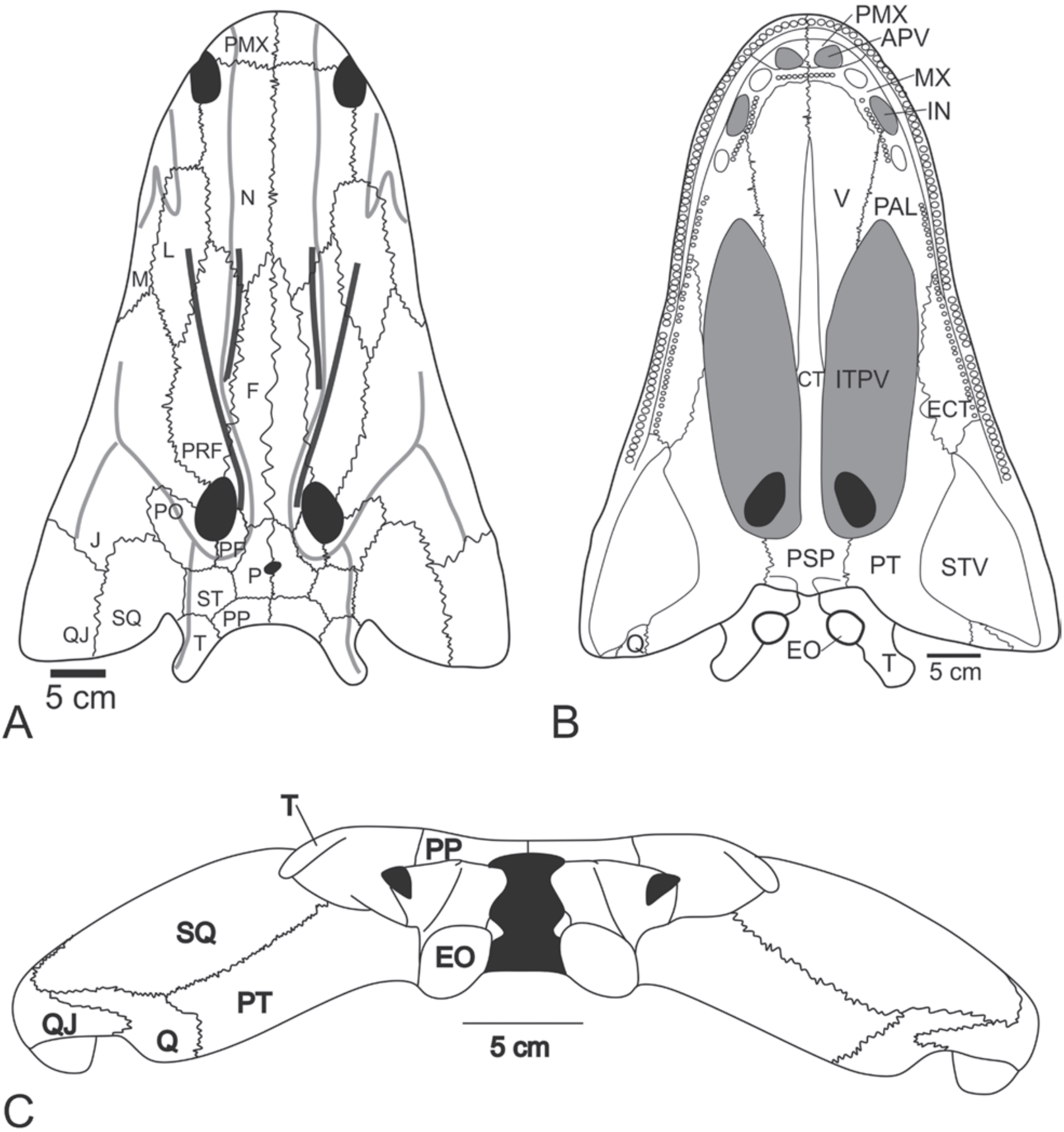

Figure 14. Skull reconstruction of *Cherninia denwai* based on the new emended diagnosis presented herein. **A.** Dorsal view; **B.** Palatal view; **C.** Occipital view.

considered the capitosauroids with wedge-shaped intercentra as noticed in *C. denwai* as semiaquatic.

Mukherjee et al. (2020) noticed stable fibrolamellar bone tissue associated with growth marks later in ontogeny in the limb bone histology of *C. denwai*. This suggests that the growth slowed down later in ontogeny. The growth of *C. denwai* was susceptible to seasonal fluctuations. The same observed that *Cherninia* inhabited the bottom of the water column and acted as a passive benthic predator. The triangular skull of *Cherninia* with almost parallel lateral margins and wide cheek and snout regions indicate a primarily aquatic life style. On the other hand, heavy interclavicles may have served as ballast in bottom-dwelling aquatic forms; this was at least the case in *Metoposaurus* (Kalita et al. 2022). The primitive and small limb bones in comparison with the heavily built skulls are also indicative of a mostly aquatic habitat. The specimen ISI A 182/4 was noted as the distal shaft of an ulna by Mukherjee et al. (2020). However, it was found to be the proximal shaft of the right ulna in this study. The proximal head of the ulna is rhombohedral and the posterolateral corners of the head are raised with the olecranon process. The acetabulum is bounded by two notches. The anterior supracetabular notch is slenderer and dorsally placed while the posterior acetabular notch is ventrally placed.

The detailed osteology and the emended diagnosis of *C. denwai* is the first step to systematically study the huge array of temnospondyls that are present in the Anisian Denwa Formation of Central India. This detailed osteology presented here will act as a prelude to a further revised phylogenetic analysis of mastodonsaurids considering all the newer taxa and features that have been recorded so far. The emended diagnosis of *Cherninia denwai* presented herein reflects a future need of a detailed phylogeny of the superfamily Capitosauroidea. Schoch (2018) in his detailed revision of *Parotosuchus nasutus* has retained the superfamily Capitosauroidea (Säve-Söderbergh 1935), and established *Cherninia denwai* in Parotosuchidae. Also, according to Schoch (2018) *Cherninia* is closely related to *Xenotosuchus* on one hand and also to *Odenwaldia* on the other hand. The phylogenetic status of *Cherninia* thus, largely depends on the inclusion of *Odenwaldia* and *Xenotosuchus* in a phylogenetic analysis. Therefore, so far, the status of *Cherninia* is debatable and calls for a separate stand-alone phylogenetic analysis including all Mastodonsauridae which is a work in progress. Herein, so far, Mastodonsauridae (Damiani 2001) still remains to be a valid family and thus, *Cherninia* would be included in the family Mastodonsauridae, until any further amendment of the family status of *Cherninia*.

Acknowlegements

The present work was carried out with the financial support from the Indian Statistical Institute, Kolkata (ISI Kolkata). The authors are grateful to the Geological Studies Unit, Indian Statistical Institute for the laboratory and financial support. We acknowledge Mr. Pushpal Kundu of Photography and Reprography Unit, ISI, Kolkata for all the photography assistance provided and preparator Mr. Lakshman Mahankur for his assistance in preparation of the specimens. We also acknowledge Mr. Swapan Aich, Mr. Ashok Saha and Mr. Sasanka Sekhar Sahu of the Transport unit of ISI, Kolkata for transport and driving assistance during field-work in the Satpura basin. The authors sincerely thank Prof. Rainer Schoch and the two anonymous peer-reviewers whose comments have significantly helped to develop the manuscript further.

References

Bandyopadhyay S, Ray S (2020) Gondwana vertebrate faunas of India: their diversity and intercontinental relationships. Episodes 43: 438–460. https://doi.org/10.18814/epiiugs/2020/020028

Bandyopadhyay S, Sengupta DP (1999) Middle triassic vertebrates of India. Journal of African Earth Sciences 29: 233–241. https://doi.org/10.1016/S0899-5362(99)00093-7

Carter AM, Hsieh ST, Dodson P, Sallan L (2021) Early amphibians evolved distinct vertebrae for habitat invasions. PLOS ONE 16: e0251983. https://doi.org/10.1371/journal.pone.0251983

Chernin S (1970) Capitosaurid amphibians from the upper Luangwa Valley, Zambia. http://hdl.handle.net/10539/16048

Cosgriff J, Defauw S (1987) A capitosaurid labyrinthodont from the Early Scythian of Tasmania. Alcheringa 11: 21–41. https://doi.org/10.1080/03115518708618977

Damiani RJ (2001) Cranial anatomy of the giant Middle Triassic temnospondyl Cherninia megarhina and a review of feeding in mastodonsaurids.

Dasgupta S (2021) A review of stratigraphy, depositional setting and Paleoclimate of the Mesozoic Basins of India. In: Banerjee S, Sarkar S (Eds) Mesozoic Stratigraphy of India: A Multi-Proxy Approach. Society of Earth Scientists Series. Springer, Cham, 1–37. https://doi.org/10.1007/978-3-030-71370-6_1

Dutuit J-M (1976) Introduction à l'étude paléontologique du Trias continental marocain. Description des premiers stegocephales recueillis dans le couloir d'Argana (Atlas occidental).

Dutuit J (1978) Description de quelques fragments osseux provenant de la région de Folakara (Trias supérieur malgache). Bulletin de Museum Nationale d'Histoire naturelle, Paris Series III 516: 79–89.

Fortuny J, Arbez T, Mujal E, Steyer JS (2019) Reappraisal of '*Metoposaurus hoffmani*' Dutuit, 1978, and description of new temnospondyl specimens from the Middle–Late Triassic of Madagascar (Morondava Basin). Journal of Vertebrate Paleontology 39: e1576701. https://doi.org/10.1080/02724634.2019.1576701

Ingavat R, Janvier P (1981) *Cyclotosaurus* cf. *posthumus* Fraas (Capitosauridae, Stereospondyli) from the Huai Hin Lat Formation (Upper Triassic), Northeastern Thailand: with a note on capitosaurid biogeography. Geobios 14: 711–725. https://doi.org/10.1016/S0016-6995(81)80149-0

Jupp R, Warren A (1986) The mandibles of the Triassic temnospondyl amphibians. Alcheringa 10: 99–124. https://doi.org/10.1080/03115518608619164

Kalita S, Teschner EM, Sander PM, Konietzko-Meier D (2022) To be or not to be heavier: The role of dermal bones in the buoyancy of the Late Triassic temnospondyl amphibian *Metoposaurus krasiejowensis*. Journal of Anatomy 241: 1459–1476. https://doi.org/10.1111/joa.13755

McHugh JB (2012) Temnospondyl ontogeny and phylogeny, a window into terrestrial ecosystems during the Permian-Triassic mass extinction. The University of Iowa.

Milner A (1990) The Radiations of Temnospondyl Amphibians. In: Taylor PD, Larwood GP (Eds) Major Evolutionary Radiations, 321–349. https://doi.org/10.1093/oso/9780198577188.003.0015

Milner A, Sequeira S (1993) The temnospondyl amphibians from the Viséan of east Kirkton, West Lothian, Scotland. Earth and Environmental Science Transactions of the Royal Society of Edinburgh 84: 331–361.https://doi.org/10.1017/S0263593300006155

Morales M, Kamphausen D (1984) *Odenwaldia heidelbergensis*, a new benthosuchid stegocephalian from the Middle Buntsandstein of the Odenwald, Germany. Neues Jahrbuch für Geologie und Paläontologie Monatshefte, 673–683. https://doi.org/10.1127/njgpm/1984/1984/673

Mukherjee D, Sengupta DP, Rakshit N (2020) New biological insights into the Middle Triassic capitosaurs from India as deduced from limb bone anatomy and histology. Papers in Palaeontology 6: 93–142. https://doi.org/10.1002/spp2.1263

Mukherjee RN, Sengupta DP (1998) New capitosaurid amphibians from the Triassic Denwa Formation of the Satpura Gondwana basin, central India. Alcheringa 22: 317–327. https://doi.org/10.1080/03115519808619330

Ochev V (1966) Systematics and phylogeny of capitosauroid labyrinthodonts. Izdatel'stvo Saratovskogo Universiteta, Saratov 184: 73–87.

Säve-Söderbergh G (1935) On the Dermal Bones of the Head in Labyrinthodont Stegocephalians and Primitive Reptilia: With Special Reference to Eotriassic Stegocephalians from East Greenland: Treaarsexpeditionen Til Christian Den X's Land 1931–34 Under Ledelse Af Lauge Koch. Reitzel.

Schoch RR (2008) The Capitosauria (Amphibia): characters, phylogeny, and stratigraphy. Palaeodiversity 1: 189–226.

Schoch RR (2013) The evolution of major temnospondyl clades: an inclusive phylogenetic analysis. Journal of Systematic Palaeontology 11: 673–705. https://doi.org/10.1080/14772019.2012.699006

Schoch RR (2018) The temnospondyl *Parotosuchus nasutus* (v. Meyer, 1858) from the early triassic middle Buntsandstein of Germany. Palaeodiversity 11: 107–126. https://doi.org/10.18476/pale.11.a6

Schoch RR, Milner AR (2000) Stereospondyli: Stem-Stereospondyli, Rhinesuchidae, Rhytidostea, Trematosauroidea, Capitosauroidea: with 106 Figures and 16 Plates. F. Pfeil.

Sengupta DP (2002) Indian metoposaurid amphibians revised. Paleontological Research 6: 41–65.

Sengupta S, Sengupta DP (2021) Taphonomy and depositional setting of the *Shringasaurus indicus* (Archosauromorpha: Allokotosauria) bonebed from the Middle Triassic Denwa Formation, Satpura Gondwana Basin, India. Palaios 36: 339–351. https://doi.org/10.2110/palo.2021.013

Shishkin M (1980) The Luzocephalidae, a new Triassic labyrinthodont family. Paleontological Journal 14: 88–101.

Steyer JS (2003) A revision of the early Triassic "capitosaurs" (Stegocephali, Stereospondyli) from Madagascar, with remarks on their comparative ontogeny. Journal of Vertebrate Paleontology 23: 544–555. https://doi.org/10.1671/1740

Sulej T (2007) Osteology, variability, and evolution of Metoposaurus, a temnospondyl from the Late Triassic of Poland. Palaeontologia Polonica 64: 29–139.

von Zittel KA (1887) Handbuch der Paläontologie. 1. Paläozoologie: 3. Vertebrata:(pisces, amphibia, reptilia, aves). Oldenbourg.

Warren A, Snell N (1991) The postcranial skeleton of Mesozoic temnospondyl amphibians: a review. Alcheringa 15: 43–64. https://doi.org/10.1080/03115519108619009

Watson DMS (1920) I. The structure, evolution and origin of the amphibia.-The" orders' rachitomi and stereospondyli. Philosophical Transactions of the Royal Society of London Series B, Containing Papers of a Biological Character 209: 1–73. https://doi.org/10.1098/rstb.1920.0001

Watson DMS (1958) A new labyrinthodont (Paracyclotosaurus) from the Upper Trias of New South Wales. Bulletin of the British Museum of Natural History, London (Geology) 3: 233–263.

Welles SP (1965) A revision of the labyrinthodont family Capitosauridae and a description of *Parotosaurus peabodyi*, n. sp. from the Wupatki member of the Moenkopi Formation of northern Arizona. University of California Publications in Geological Sciences 54: 1–148.

Zittel K (1888) Handbuch der Paläontologie, Abtheilung Palaeozologie, Band III, Vertebrata (Pisces, Amphibians, Reptilia, Aves): München y Leipzig. Germany, R. Oldenbourg.

Supplementary material 1

List of specimens assigned as *Cherninia denwai*

Authors: Pummy Roy, Sanjukta Chakravorti, Dhurjati Prasad Sengupta

Data type: docx

Explanation note: The data is a list of all the specimens occuring in the geology museum of the Indian Statistical Institute, Kolkat, that has now been assigned as *Cherninia denwai*.

Link: https://doi.org/10.3897/fr.27.135664.suppl1

Fossil Record 27 (3) 2024, 445–471 | DOI 10.3897/fr.27.133803

Evolution of the tetrapod skull: a systematic review of bone loss

Kim Julia Kean[1], Marylène Danto[2], Celeste Pérez-Ben[2,3], Nadia Belinda Fröbisch[1,2]

1 *Institut für Biologie, Humboldt Universität zu Berlin, Berlin, Germany*
2 *Museum für Naturkunde, Leibniz-Institut für Evolutions- und Biodiversitätsforschung, Berlin, Germany*
3 *Laboratorio de Biología Integral de Sistemas Evolutivos, IEGEBA, FCEN, UBA / CONICET, CABA, Argentina*

https://zoobank.org/65576914-26C6-47D6-8A71-7EAA354B1970

Corresponding author: Kim Julia Kean (kimjulia.kean@mfn.berlin)

Academic editor: Florian Witzmann ♦ **Received** 2 August 2024 ♦ **Accepted** 20 October 2024 ♦ **Published** 30 December 2024

Abstract

The simplification of the tetrapod skull occurred convergently in various tetrapod lineages from the Devonian into the Mesozoic, leading to some groups (e.g. lissamphibians) to retain only 19 of the original 41 dermal roof bones present in stem-tetrapods. Despite the potential to shed light on the functional adaptations and developmental mechanisms behind skull simplification, little work has been done on the distribution of bone loss across tetrapod phylogeny. We conducted maximum likelihood ancestral state reconstructions for the presence/absence of temporal and median dermatocranial bones using two large composite trees that placed Lissamphibia either within Temnospondyli or Lepospondyli, reflecting the ongoing debate on lissamphibian origins. Our results indicate that the temporal series did not form a developmental module, as the loss of these bones was quite variable. With the exception of Sauropsida, the intertemporal bone was lost first, followed by the supratemporal, and then the tabular and/or postparietal. In Sauropsida, the tabular and/or postparietal was the second bone to be lost. The supratemporal was lost and regained repeatedly, and was found to be the most variable element, while the nasal, frontal, and parietal were the least variable. Interestingly, the ontogenetic timing of ossification does not correlate with the propensity for a certain bone to be re-acquired or lost. No obvious relationship was found between skull simplification and lifestyle or body size. In summary, the simplification of the dermatocranium is a more complex process than previously thought, and likely involved a mixture of developmental, ecological, and functional drivers.

Key Words

Ancestral state reconstruction, dermatocranium, lepospondyl, lissamphibians skull simplification, temnospondyl, tetrapod

Introduction

The skull is one of the most complex and versatile components of the vertebrate body plan. In addition to housing the sensory organs that allow vertebrates to navigate and interact with the world, this anatomical unit is also used in feeding (Heiss et al. 2018), locomotion (Wake 1993), combat (Farke et al. 2009), and sexual display (Knell et al. 2013). The main components of the skull include the (1) endocranium (chondrocranium and neurocranium) which protects the brain, the (2) viscerocranium (gill arches and splanchnocranium) which originates from the branchial arches, and (3) the dermatocranium, which acts as a vault for these structures (Walker et al. 2000). The complexity and multifunctional nature of the skull is a direct result of selection pressures applied to these individual components over evolutionary time.

One of the most significant moments in the evolution of the skull was the water-to-land transition in Tetrapodomorpha (the clade made up of extant tetrapods and extinct species more closely related to them than to lungfish) during the Devonian, which was a time of rapid change, morphological innovation, and ecological radiation (Long and Gordon 2004; Clack 2009, 2012). Previous studies have already outlined some of the morphofunctional shifts in the skull during this period, including the evolution of the tetrapod otic region, and adaptations associated with feeding and breathing on land (Coates and Clack 1991; Clack 1992, 1994, 1998; Clack et al. 2003; Brazeau and Ahlberg 2006; Schoch and Witzmann 2011). Another key change that occurred at this transition was the apparent reduction of bone elements in the dermal skull. This can first be seen in *Acanthostega* and *Ichthyostega* which lack the extrascapular and operculogular bones present in finned tetrapodomorphs such as *Eusthenopteron* (Andrews and Westoll 1970; Jarvik 1980). The loss of the extrascapulars was a pivotal moment in tetrapodomorph evolutionary history, marking the origin of the neck as the skull became detached from the dermal pectoral girdle (Clack 2002; Sefton et al. 2016; Maddin et al. 2020) (note, a functional 'neck' has been reported in the tetrapodomorph fish *Mandageria fairfaxi* (Johanson et al. 2003)).

The trend towards a simplified skull continued after the Devonian and can be observed throughout tetrapod evolutionary history, occurring independently (i.e. convergently) in several lineages with a diversity of skull morphologies and functional adaptations (Rawson et al. 2022) (Fig. 1). Skull simplification has been extensively documented in reptiles (Williston 1925; Lee et al. 2020), birds (Smith-Paredes et al. 2018; Plateau and Forth 2020; Asakura and Kawabe 2022), synapsids (Sidor 2001), and lissamphibians (caecilians, salamanders, and frogs), with the latter only retaining 19 of the original 41 bony elements found in many stem-tetrapod skulls (Fig 1; Shoch 2014). Interestingly, the convergent bone loss across tetrapod lineages is not only seen in the overall number of elements lost, but also in the consistent loss of particular bones, the intertemporals being a prime example (at least as separately ossified elements). In contrast, bones such as the parietals have been conserved for over 400 million years from the first osteichthyans to extant tetrapods (Fig. 1). This would suggest that there is a commonality in the evolutionary pathways towards skull simplification, regardless of morphofunctional differences in cranial construction. Surprisingly, the distribution of bone loss across tetrapod phylogeny has received little attention. Research has instead been largely focused on quantifying simplification in terms of changes in complexity through network analyses (Esteve-Altava et al. 2013, 2014; Lee et al. 2020; Plateau and Forth 2020; Asakura and Kawabe 2022; Rawson et al. 2022; Strong et al. 2022), and determining the mode of loss in extant taxa through fate mapping (Maddin et al. 2016), histological (Arnaout et al. 2022), and embryological studies (Koyabu et al. 2012; Smith-Paredes et al. 2018).

At the developmental level, bone loss in the skull is known to occur in one of two ways: either through (1) fusion or (2) lack of ossification. Fusion of adjacent bones can occur when ossification centres merge with neighbouring ones early in development due to the premature closure of suture joints, or when the cartilaginous anlagen fuse before the suture joint develops. This then forms a composite bone which is made up of multiple ossification centres, and thus gives the impression that a bone element has been lost (Koyabu et al. 2012; Esteve-Altava et al. 2013; Schoch et al. 2014). The mammalian interparietal is an example of such a composite bone, consisting of four fused ossification centres thought to be homologous to the postparietals and tabulars (Koyabu et al. 2012). The second developmental mechanism of skull bone loss is the failure of ossification centres to form, often caused by heterochronic truncation. This typically affects those bones that form in the final stages of ancestral skull ossification, as the shortened ontogenetic trajectory prevents them from forming (Schoch 2014). In other words, ossification fails to occur in bones which, primitively, tend to ossify in the later stages of skull development. The missing dermal bones in the skulls of extant lissamphibians, for instance (e.g. the postfrontal, postorbital, and tabular), are those that form late in the ontogeny of temnospondyls (Schoch 2002), the putative stem group of Lissamphibia (Carroll 2007; Ruta and Coates 2007; Anderson 2007, 2008; Schoch et al. 2020). However, dermal bones can also fail to ossify if the minimum population size of stem cells in the mesenchymal tissue layer where these bones form is not reached (Atchley and Hall 1991), as may be the case in instances of miniaturised body size (Pérez-Ben et al. 2018; see below).

Various functional adaptations have been proposed as potential evolutionary drivers of cranial simplification. For example, it has been hypothesised that a reduction in the number of bony elements would increase the degree of connectivity in the individual remaining cranial bones (Strong et al. 2022), which in turn would lead to a more robust skull capable of withstanding the biomechanical stresses associated with certain lifestyles such as crevice dwelling (e.g. in extant lepidosaurians) (Herrel et al. 2007) and head-first burrowing (e.g. in recumbirostran microsaurs, caecilians, amphisbaenids, dibamids, and scolecophidian snakes) (Pardo et al. 2015; Szostakiwskyj et al. 2015; Pardo and Anderson 2016; Strong et al. 2022). In the case of batrachians (frogs and salamanders), Schoch (2014) suggested that the skull morphology and bone reduction may have been driven by the rearrangement of jaw musculature related to skull flattening. The study proposed that a highly fenestrated skull morphology and the emargination of the cheek region in salamanders and frogs (via the loss of the postfrontal, postorbital, jugal, postparietal, supratemporal, and tabular) would allow for an extension of the muscles onto the dorsal surface of their flattened skull. In synapsids, it has been hypothesised that skull simplification occurred as an adaptation to strengthen the skull in response to biomechanical forces applied to the skull roof by jaw abductor muscles (Sidor 2001). An alternative argument was presented by Koyabu (2023) who posited that skull simplification in synapsids may be the by-product of increasing brain size over the evolution of the clade instead of a functional adaptation. Evidence supporting this hypothesis comes from the presence of genes such as Dlx5 and Lmx1b which are known to influence both brain expansion and suture closure in the skulls of mammals (Koyabu 2023).

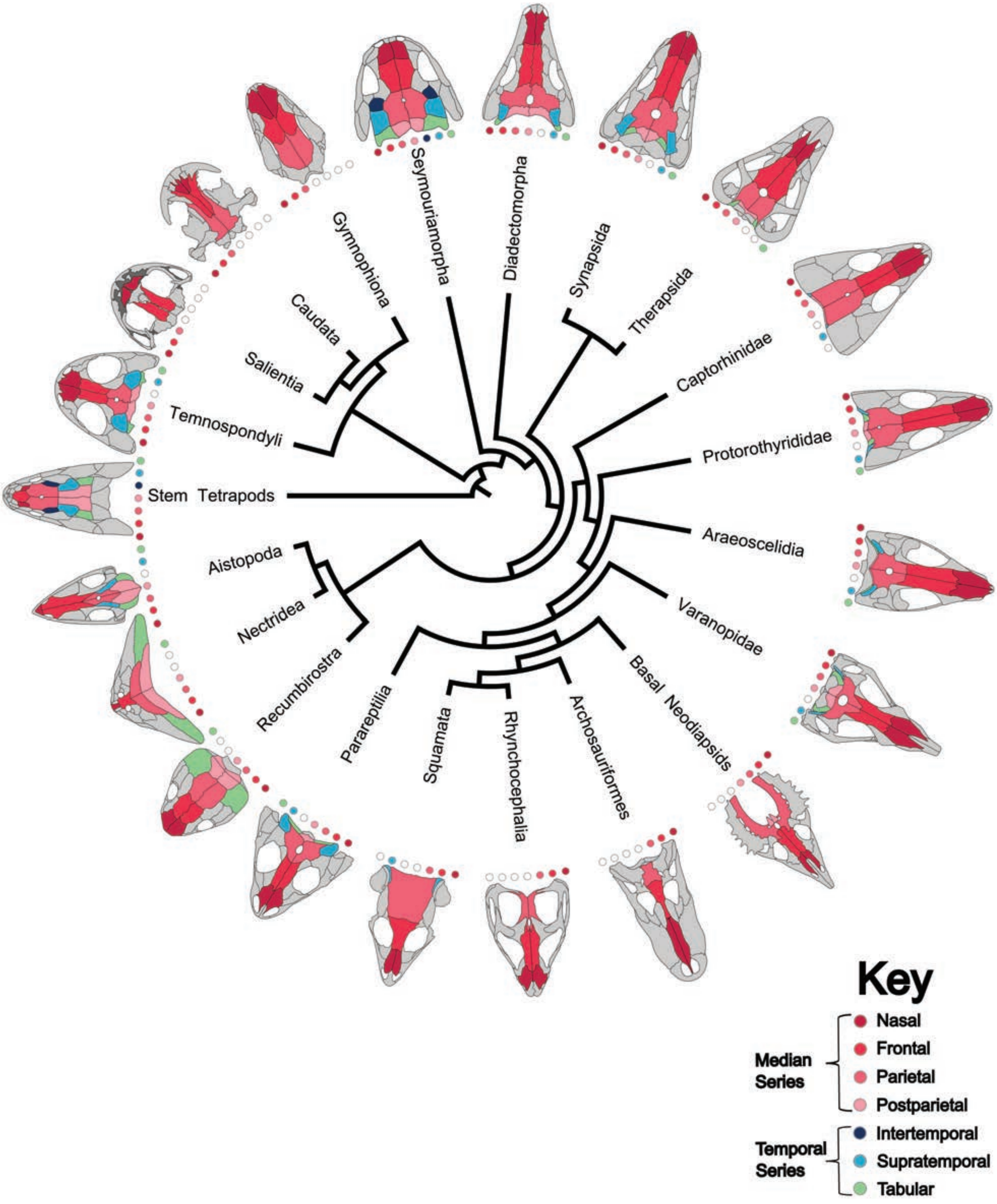

Figure 1. Summary of the changes in composition of the median and temporal series in tetrapods. For a more detailed overview of the presence/absence of median and temporal series elements see Fig. 2. (Stem tetrapod = *Eusthenopteron* (Carroll 1988); Temnospondyli = *Apateon* (Schoch and Milner 2014); Salientia = *Bombina* (Maglia and Púgener 1998); Caudata = *Cryptobranchus* (Elwood and Cundall 1994); Gymnophiona = *Ichthyophis* (Wilkinson et al. 2014); Seymouriamorpha = *Seymouria* (Berman et al. 2000); Diadectomorpha = *Tseajaia* (Berman et al. 1992); Synapsida = *Eothyris* (Reisz et al. 2009); Therapsida = *Suminia* (Rybczynski 2000); Captorhinidae = *Captorhinus* (Fox and Bowman 1966); Protorothyrididae = *Paleothyris* (Carroll 1969); Araeoscelidia = *Petrolacosaurus* (Reisz 1981); Varanopidae = *Mesenosaurus* (Reisz and Berman 2001); Basal Neodiapsida = *Weigeltisaurus* (Pritchard et al. 2021); Archosauriformes = *Alligator* (Jollie 1962); Rhynchocephalia = *Sphenodon* (Jones et al. 2009); Squamata = *Cordylus* (Evans 2008); Parareptilia = *Macroleter* (Tsuji 2006); Recumbirostra = *Eryodus* (Carroll and Gaskill 1978); Nectridea = *Diplocaulus* (Carroll et al. 1998); Aïstopoda = *Pseudophlegethontia* (Anderson 2003).

Miniaturisation is another developmental change linked to skull bone loss; this is the evolution of an adult body size so small that it surpasses a threshold at which dramatic changes in morphology, physiology, and ecology can occur (Hanken and Wake 1993; Yeh 2002; Pérez-Ben et al. 2018). Different explanations have been given to link extremely small body sizes to skull simplification. On the one hand, bone loss might occur as a by-product of ontogenetic truncation, which seems to be a frequent mechanism for the evolutionary reduction of body size, as miniaturised species typically resemble the juvenile stages of related non-miniaturised taxa (Hanken and Wake 1993). In this regard, miniaturised species lack bones that form late in the ontogeny of these larger species (Hanken and Wake 1993; Yeh 2002; Schoch and Rubidge 2005; Schoch 2013a; Scherz et al. 2019). Whereas skull simplification by ontogenetic truncation is related to the causes of miniaturisation, the small body size itself may impose developmental constraints that lead to bone loss (Yeh 2002; Pérez-Ben et al. 2018). As discussed above, it has been suggested that the minimum number of mesenchymal cells required to induce bone formation cannot be reached at extremely small body sizes, thus preventing bones from ossifying (Atchley and Hall 1991; Pérez-Ben et al. 2018).

Physical and functional constraints may also play a role. For example, certain structures, such as the eye, require a minimum size to be functional and are therefore proportionally much larger in small species. Consequently, the need to retain functionality in a sense organ might lead to major morphological rearrangements of the skull to accommodate the organ within a miniaturised structure. One instance of this is found in geckos, which are thought to have lost their postorbital and supratemporal because of the space taken up by their large eyes (Herrel et al. 2007). Together, all these proposed evolutionary drivers highlight the complexities of skull bone reduction and show that the evolutionary underpinnings of this trend might not be uniform among clades.

In addition to providing insight on the functional and developmental drivers of skull evolution, the simplification of the dermal skull roof has also been used in phylogenetic studies that address the relationships of early tetrapods. Many such studies have utilised the absence of specific cranial roof bones as 'loss characters' which have been central to ongoing discussions surrounding the origin of lissamphibians. Currently there are two main lines of thought: (1) the Temnospondyl Hypothesis (TH) which is favoured by most authors and states that lissamphibians form a monophyletic group within temnospondyls and are nested within Dissorophoidea, likely with Amphibamidae (Anderson 2007, 2008; Carroll 2007; Ruta and Coates 2007; Schoch et al. 2020) but Branchiosauridae have also been suggested as putative lissamphibian relatives (Milner 1993; Anderson 2007; Carroll 2007; Ruta and Coates 2007), and (2) the Lepospondyl Hypothesis (LH) which suggests that a monophyly is formed between lissamphibians and lepospondyls (Laurin 1998; Vallin and Laurin 2004; Marjanović and Laurin 2008, 2009; Laurin et al. 2022). There are some variants of the TH, Pardo et al. (2017a), for instance, hypothesised that caecilians are derived from stereospondyls, while frogs and salamanders are nested within dissorophoids. Previously, a third hypothesis had also been considered to explain lissamphibian origins, namely the Polyphyly Hypothesis, which placed frogs and salamanders with temnospondyls, and caecilians with lepospondyls (Carroll 2001, 2009; Anderson et al. 2008a; Lee and Anderson 2006); this has received very little attention, though, in more recent analyses.

The first step to unravelling the evolutionary factors that underlie the convergent evolution of bone loss is to identify any patterns of loss and regain. This presents a challenge, however, as determining whether or not a bone has been truly lost or has simply fused with others is often impossible, in particular when dealing with fossil forms. Establishing whether or not the loss of a specific bone is comparable across the phylogeny is, therefore, quite complicated. Another limitation is that the presence/absence of these skull bones are often used as characters in phylogenetic analyses based on morphological data. Consequently, mapping the presence/absence of these bones on phylogeny to study their evolution is somewhat circular. Nonetheless, quantifying patterns of loss and regain can still provide helpful insights into the comparable evolvability of certain bones, and whether convergent bone loss (even if by fusion) occurred in a modular manner (i.e. bones are lost together and not independently).

In light of this, we present the first reconstruction of the evolutionary history of bone loss in the tetrapod skull. We aim to set a framework for future discussions and to detect if there are distinct patterns of presence/absence, or loss/regain of bones that have not been recognised in previous studies due to more limited taxonomic samples or focus on specific groups.

Materials and methods

The skull morphology of 313 extinct and extant tetrapod taxa were examined. The material includes finned and limbed stem-tetrapods, as well as extant tetrapods (lissamphibians plus amniotes) and their closest extinct relatives (Figs 2, 3; Suppl. material 1). The species sampling was designed to represent the phylogenetic and morphological diversity within tetrapods. We have focused solely on bones in the median and temporal series in the dermatocranium for two reasons: (1) the dorsal bones of the dermatocranium are typically the best-preserved skull bones in the fossil record, and (2) the median and temporal series represent the most and least stable series of the dermatocranium, respectively. The median series is largely involved with protecting the brain and other sensory organs, it includes the nasal, frontal, parietal and postparietal (sometimes referred to as the interparietal (Koyabu et al. 2012)). The temporal series, on the other hand, is variably made of the intertemporal, supratemporal, and tabular. The supratemporal and tabular are associated with the otic region of the skull (Clack et al. 2003), and the tabular along with the postparietal act as attachment sites for muscles associated with the neck (Carstens 2023).

Two composite trees were constructed by hand in Mesquite (Maddison and Maddison 2021) which showed the relationships of all major stem and crown tetrapod groups with Lissamphibia either nested within Temnospondyli or Lepospondyli (Figs 2, 3; Suppl. materials 2, 3). While the phylogenetic position of several major clades is not well clarified, we chose to only consider the alternative hypotheses on the origin of lissamphibians (i.e. Temnospondyl and Lepospondyl Hypotheses) because: (1) the position of Lissamphibia radically affects the phylogenetic structure of early tetrapod relationships, and (2) as mentioned previously, the use of 'loss characters' to construct the Temnospondyl and Lepospondyl Hypothesis phylogenies impacts the interpretation of the loss of cranial bones.

The backbone of the trees was taken from the comprehensive and highly cited (e.g. Anderson et al. 2008b; Pyron 2011; Pardo et al. 2017b; Marjanović and Laurin 2019) strict consensus tree found by Ruta and Coates (2007), the stem tetrapods, Nectridea, and Aistopoda sections of the tree was left unchanged. Other portions of the tree, however, were altered. The microsaur topology was taken from MacDougall et al. (2021); the temnospondyl branch was replaced with trees recovered by Schoch (2013b) and Schoch (2022). The lissamphibian topology was taken from Jones et al. (2022), while the branch leading to the Reptiliomorpha was replaced by the tree from Ford and Benson (2020). For our purposes, the neodiapsid section of the Ford and Benson (2020) tree was not exhaustive enough as it only includes six taxa, all of which are extinct. To address this, the neodiapsid portion was replaced with that from Simoes et al. (2018). The position of Testudinata shown in the Simoes et al. (2018) tree, however, was altered so that it was a member of Archelosauria, as proposed by Crawford et al. (2015). The placement of Saurosphargidae was also updated from that shown in Simoes et al. (2018) to follow the position in Wang et al. (2022) which places them as sister to Sauropterygia. Within therapsids, the topology recovered by Huttenlocker et al. (2021) was used as a backbone, while the topology from Fraser-King et al. (2019) was used for Biarmosuchia, Anomodontia, Gorgonopsia, and Dinocephalia, and the topologies from Huttenlocker (2009) and Wallace et al. (2019) were used for Therocephalia and Cynodontia, respectively.

The trees were later time calibrated in R using the 'timePaleoPhy' function in the 'paleotree' package (Bapst 2012), with 'randres' set to TRUE to allow polytomies to be randomly resolved and using the 'minMax' date treatment. 'minMax' was chosen over other treatments such as 'firstLast' because it incorporates uncertainty by randomly assigning an age to a species within the provided time data (Bapst and Wagner 2022). This is often necessary when dealing with the vertebrate fossil record as it is rarely possible to provide precise first and last appearance dates, especially given that so many of the clades in the composite tree are poorly sampled. The minimum and maximum ages of the first appearance datum (FADs) for each tip were provided for the time calibration. The FAD ages were taken from the age of the rock formations that the oldest known specimen of each tip or clade was found in. There were four exceptions where it was not possible to ascertain the age of a tip based on geology, in these cases ages were taken from palynological analyses (Clack et al. 2019), estimations from molecular clock methods (van Tuinen and Dyke 2004), time calibrated phylogenetic analyses (Joyce et al. 2013), and biogeographically calibrated phylogenies (Leavitt et al. 2007) (see Suppl. material 4).

Presence/absence data for the bones in the temporal and median series in the skull roof were gathered for each of the 313 tips in the composite tree and scored as a binary trait. Where possible, presence/absence data was gathered from first hand examination of specimens, but this was not feasible in the majority of cases, and so data was largely taken from the literature (see Suppl. material 1). A bone element was defined based on its sutures separating it from its neighbours, therefore, any reported embryonic bones were marked as absent, except for the homology hypothesis for Mammaliaformes mentioned below. In instances where there are mixed reports on the presence/absence of a given bone, such as the intertemporal in *Greererpeton* and the temnospondyl *Micromelerpeton*, the bone was coded as absent as its presence is rare and its identity uncertain. Birds and frogs, which have frontoparietals (although see Arnaout et al. (2022) as there is still some debate on the homology of the frontal in birds), were coded as having both the frontal and parietal.

To ensure that uncertainties on bone homology were taken into account, several alternative hypotheses were collated from the literature, and a separate dataset was constructed for each with alternative coding for the relevant taxa. These different hypotheses of homology are shown in Table 2 and were based on: (1) the temporal series of the Early Jurassic stem-caecilian, *Eocaecilia*, which has a single bone that is presumed to be either the supratemporal or tabular (Jenkins et al. 2007); (2) the single interparietal in mammals, whose embryological data suggests may be composed of paired postparietals fused to the tabulars, instead of just the paired postparietals (Koyabu et al. 2012); (3) the median series in extant birds, which is composed of two bones that are either the frontal and parietal, or the frontoparietal and postparietal (Maddin et al. 2016; Arnaout et al. 2022); (4) the temporal series of the Permian nectridean, *Diplocaulus*, which is composed of a single bone that is either the supratemporal or tabular (Olson et al. 1951; Carroll et al. 1998), and (5) the uncertainty in the presence of a supratemporal in the stem testudines *Odontochelys* and *Proganochelys* (Gaffney and Meeker 1983; Li et al. 2008; Scheyer et al. 2022).

Table 1. Presence/Absence data in Hypothesis A of tips associated with alternative homology hypotheses.

Affected Tips	Presence/Absence Data in Hypothesis A
Eocaecilia micropodia	supratemporal = 0; tabular = 1
Mammaliaformes	tabular = 0
Gallus domesticus	postparietal = 1
Diplocaulus magnicornis	supratemporal = 0; tabular = 1
Proganochelys quenstedtii	supratemporal = 1
Odontochelys semitestacea	supratemporal = 1

Table 2. Alternative analyses based on uncertainties in homology.

Hypothesis	Affected Tips	Changes in Presence/ Absence Data
b	*Eocaecilia micropodia*	supratemporal = 1; tabular = 0
c	Mammaliaformes	tabular = 1
d	*Gallus domesticus*	postparietal = 0
e	*Diplocaulus magnicornis*	supratemporal = 1; tabular = 0
f	*Proganochelys quenstedtii*	supratemporal = 0
g	*Odontochelys semitestacea*	supratemporal = 0
h	*Proganochelys quenstedtii* and *Odontochelys semitestacea*	supratemporal = 0

Maximum likelihood ancestral state reconstructions were conducted for each bone, except for the nasals, frontals, and parietals, as these were found to be present in all taxa. Analyses were performed on the different datasets considering the different homology hypotheses, and alternatively under the temnospondyl and lepospondyl phylogenetic hypotheses for the origin of Lissamphibia. The reconstructions were performed in R using the 'ace' function from the 'ape' package (Paradis and Schliep 2019). The weights and AICs (Akaike Information Criterion) from ancestral state reconstructions using the ER (Equal Rates, i.e., all possible character state transitions occur at the same rate) and ARD (All Rates Different, i.e., all possible character state transitions can occur at a different rate) models were compared for each bone, and it was determined that the ARD model was the most appropriate to use for all the bones (see Suppl. material 5). Plots showing the ancestral state reconstructions with the ARD model for each bone under Homology Hypothesis A in both the Temnospondyl and Lepospondyl Hypothesis can be found in the supplementary, along with the data and R script used (Suppl. materials 6–23). To reconstruct the ancestral states in nodes (i.e. presence or absence of the bones), the ratio of the likelihoods of two estimates is used to gauge the level of support for the maximum likelihood estimate. A likelihood ratio of 7.4:1 is commonly employed as a rough minimum threshold to determine the likely state of a node (Schulter et al. 1997; Rüber et al. 2004; Dalerum 2007). With this threshold, gains and losses of bones were identified by manually tracing character changes in the branches. At each node the presence % likelihood returned from the analysis was multiplied by 7.4, if this value was less than the absence % likelihood at that node, then the bone in question was deemed to be absent. If a transition was thought to have occurred at a node (e.g. from present to absent), then a second calculation was undertaken to determine if the character change was statistically significant or not. A transition threshold was calculated by dividing the absence % likelihood by 7.4, if this value was equal to or greater than the presence % likelihood then the transition from present to absent was statistically significant.

Results

Pattern of bone loss

Our analyses indicate that the intertemporal is the first bone to be lost; in stem-tetrapods it is lost multiple times, for instance in *Acanthostega*, *Ichthyostega*, *Ossinodus*, and at the node leading to Colosteidae, adelospondyls, and *Acherontiscus* (Figs 2, 3A). Within the lissamphibian stem-group (temnospondyls), the intertemporal bone is lost convergently numerous times and is only present in basal temnospondyls such as Edopoidea and most Dvinosauria (Figs 2, 3A). Following the intertemporal, the supratemporal is the next bone that is lost; once within stem-tetrapods at the node leading to the adelospondylids, and once at the lissamphibian node (Figs 2, 3A). After the supratemporal is lost, the tabular and/or postparietal can be lost. These bones are both lost twice within Lissamphibia, once in Gymnophiona (caecilians), and once at the Batrachia node. In Batrachia, the supratemporal is surprisingly regained in the karaurid stem-salamanders *Karaurus*, *Marmorerpeton*, and *Kokartus* (Figs 2, 3A). In Gymnophiona, the exact position of the loss of the tabular and postparietal is uncertain as only a partial jaw of the stem-caecilian *Rubricaecilia* has been described (Evans and Sigogneau-Russell 2001). As the stem-caecilian *Eocaecilia* retains the tabular and postparietal, the loss of these bones either occurs at the node leading to *Rubricaecilia*, *Epicrionops*, and *Ichthyophis* (Figs 2, 3A), or the node leading to *Ichthyophis* and *Epicrionips* (Suppl. material 24). It is also possible that the tabular and postparietal are lost at the lissamphibian node and are regained in *Eocaecillia* (Suppl. material 24). In Homology Hypothesis B, where *Eocaecilia* is coded as having a supratemporal and no tabular, the presence/absence of the supratemporal is ambiguous at the node leading to *Rubricaecilia*, *Epicrionops*, and *Ichthyophis*. At the node leading to *Epicrionops*, and *Ichthyophis* the supratemporal is absent. The state of the tabular, on the other hand, is ambiguous at node Gymnophiona, and is absent at the node leading to *Rubricaecilia*, *Epicrionops*, and *Ichthyophis*.

As in stem-tetrapods and temnospondyls, the intertemporal is the first bone that is lost in the stem-amniotes, followed by the supratemporal (Figs 2, 3B). The intertemporal is lost once, at the base of the tree, the supratemporal is then either lost at the base of

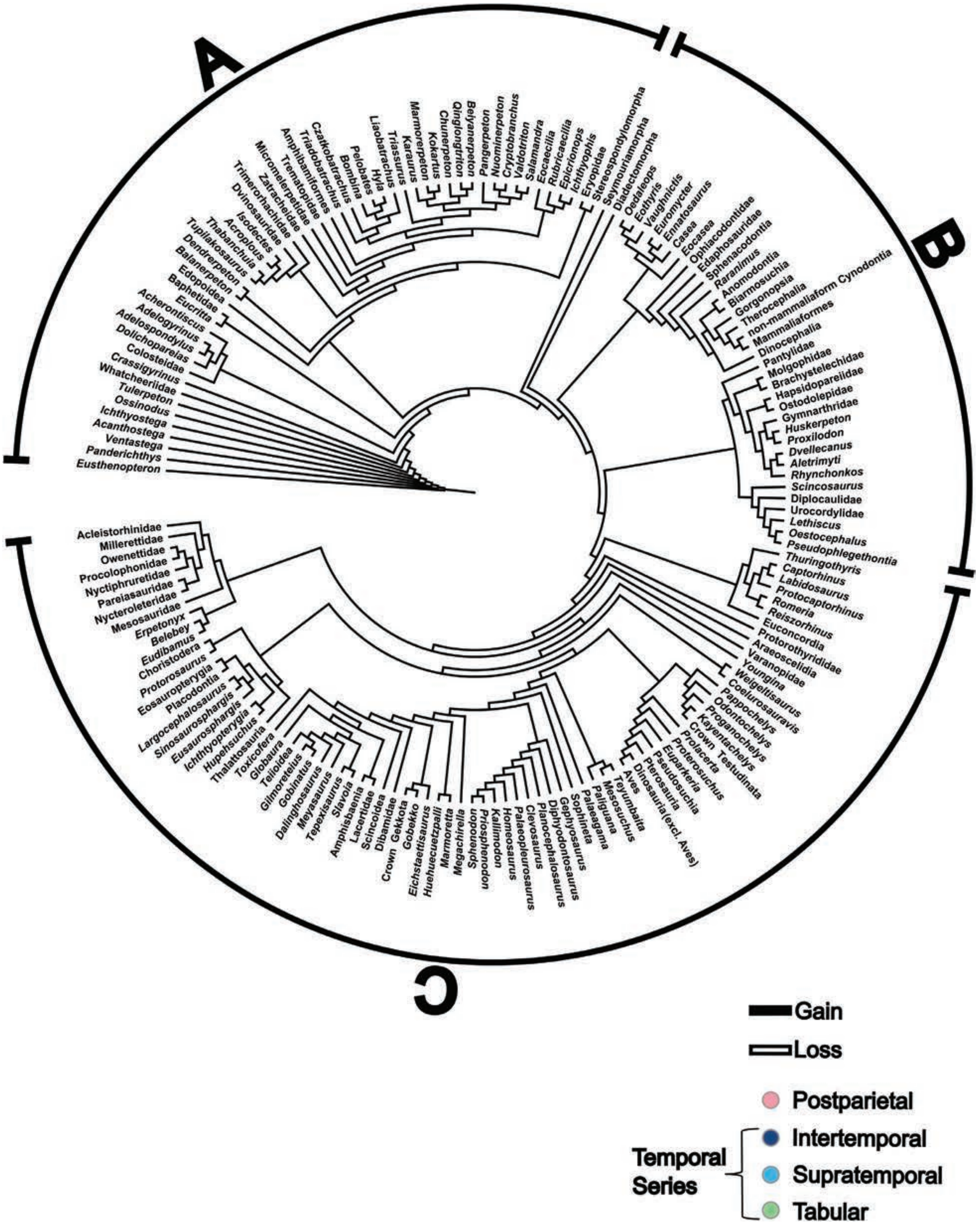

Figure 2. Maximum likelihood ancestral state reconstruction of the presence/absence of the postparietal, intertemporal, supratemporal, and tabular (see key for colour associations) under Temnospondyl Hypothesis a. At the nodes, a filled in quadrant = presence; empty quadrant = absence; striped quadrant = presence/absence is ambiguous. On the branches, empty rectangle = loss of element; filled rectangle = gain of element. At the branch tips, filled in circle = presence of element; empty circle = absence of element; half-filled circle = mixed presence/absence of element. Tree A = Tetrapodomorpha, Temnospondyli, and Lissamphibia. Tree B = Seymouriamorpha, Diadectomorpha, Synapsida, and Lepospondyli. Tree C = Captorhinidae, Protorthyrididae, Araeoscelidia, Varanopidae, Neodiapsida, and Parareptilia.

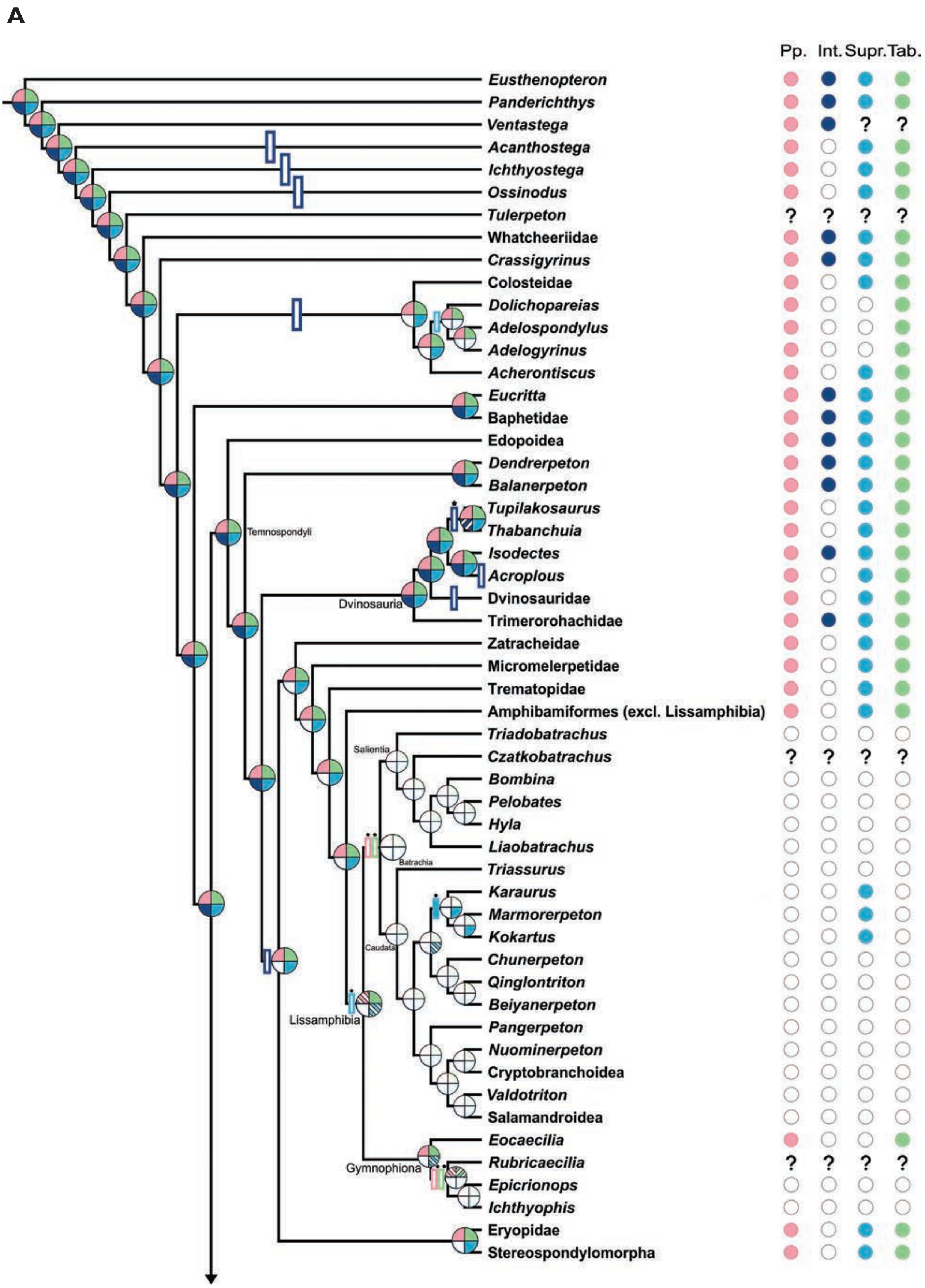

Figure 2. Continued.

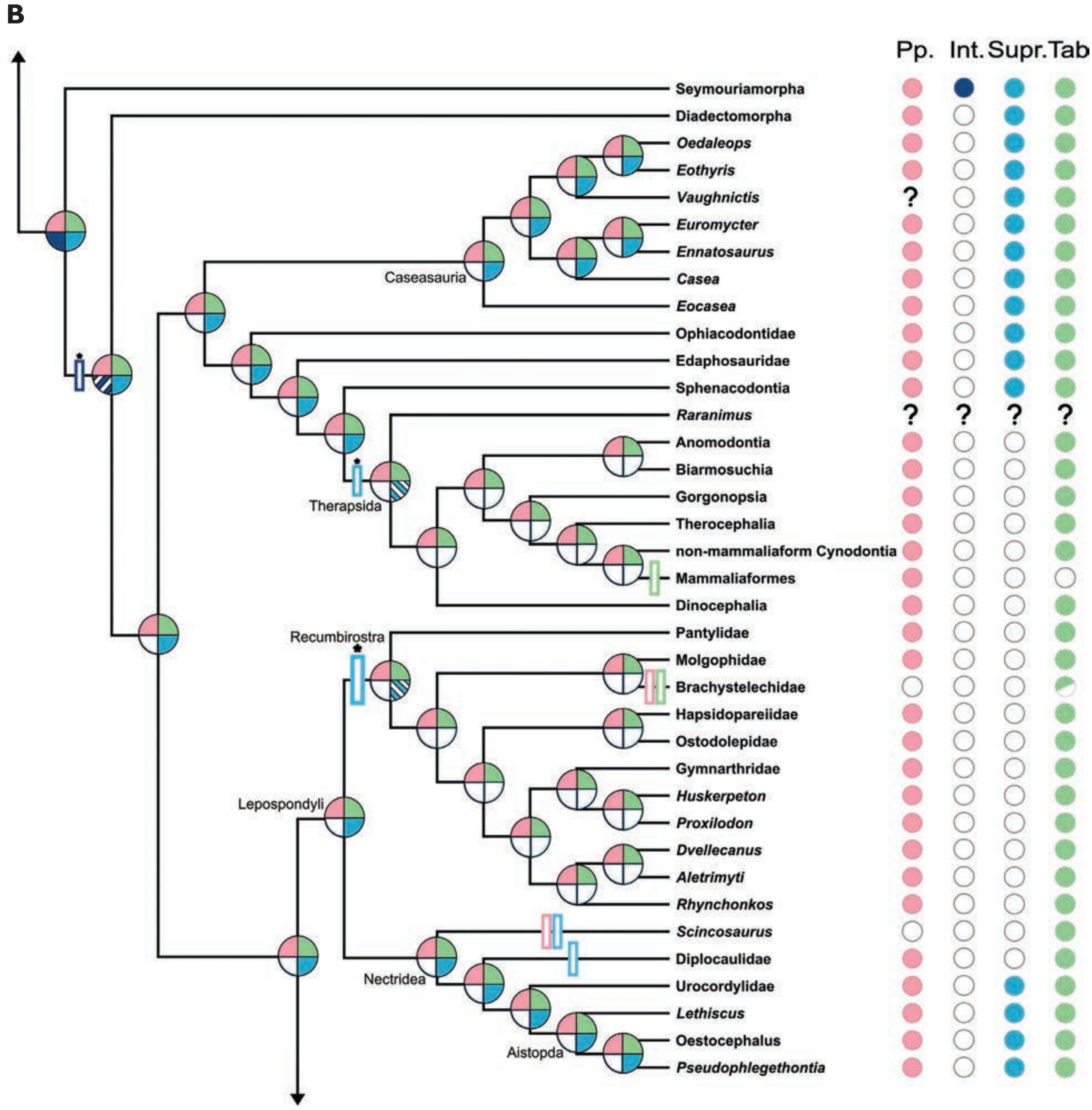

Figure 2. Continued.

Therapsida (Suppl. material 24) or within Therapsida (Figs 2, 3B). The uncertainty again is due to a lack of data, this time in *Raranimus* which is considered to be the basal-most therapsid, and is only known from a partial snout (Liu et al. 2009; Huttenlocker et al. 2021). With the exception of Mammaliaformes which lose their tabular, all other therapsids maintain this temporal series bone (Figs 2, 3B). The tabular is present at all nodes in Therapsida, irrespective of whether or not it is coded as present or absent in Mammaliaformes (Homology Hypothesis C). There is a little more variety in the composition of the temporal series in lepospondyls. Here, the intertemporal is absent, the supratemporal and postparietal are lost multiple times, and the tabular is present in all taxa besides some brachystelechids (namely *Quasicaecilia*, *Diabloroter*, and *Carrolla*; Suppl. material 1). The supratemporal is lost in the nectridean *Scincosaurus*, and at the node Diplocaulidae. It is also potentially lost at the node leading to Recumbirostra. The postparietal is lost with the tabular in Brachystelechidae, and with the supratemporal in *Scincosaurus*, which marks the only point at which the postparietal is not lost on its own, or with the tabular (Figs 2, 3B). The coding of *Diplocaulus* as having a supratemporal and no tabular (Homology Hypothesis E) has no effect on the results, as the supratemporal is still lost at node Diplocaulidae and the tabular remains present.

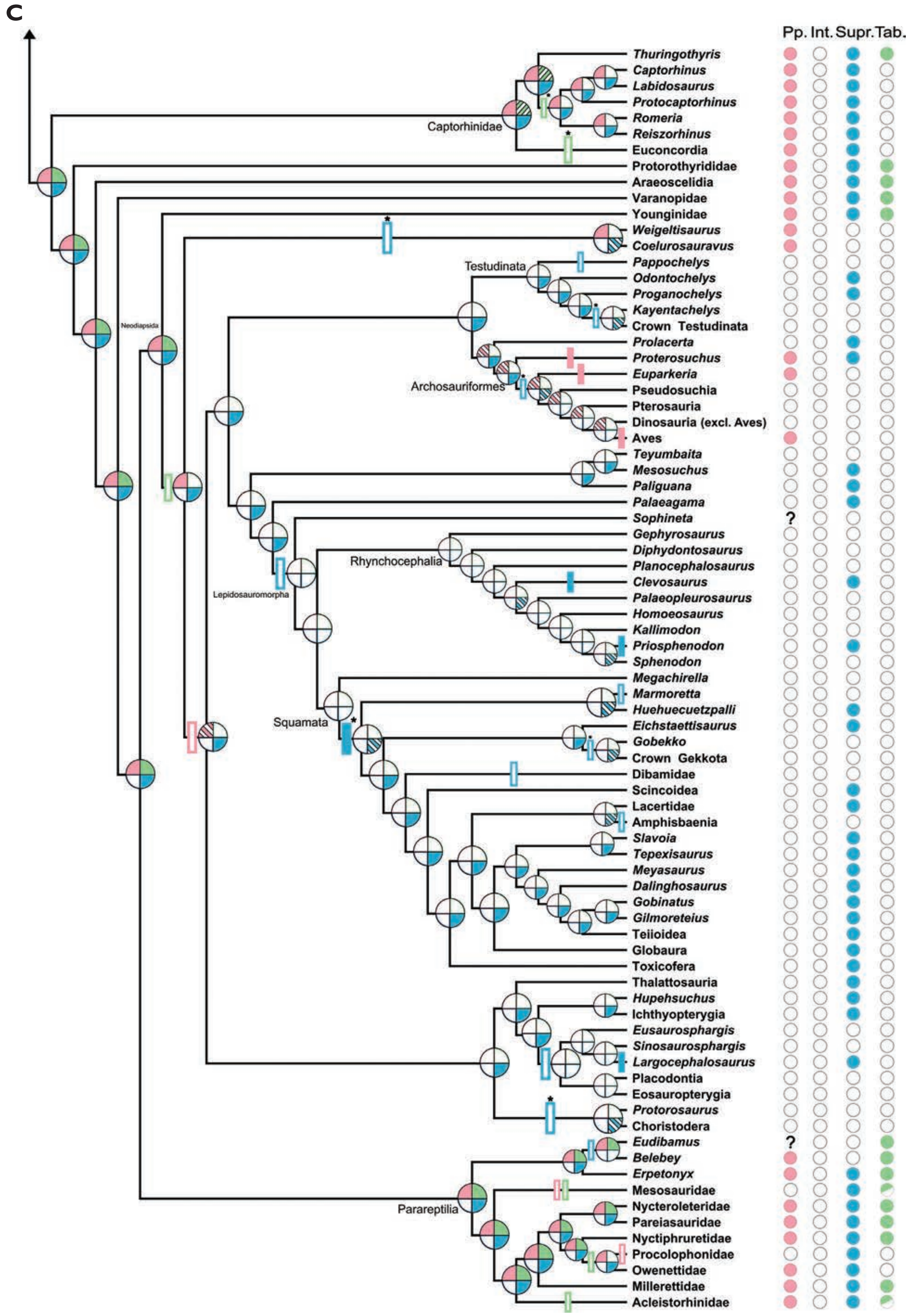

Figure 2. Continued.

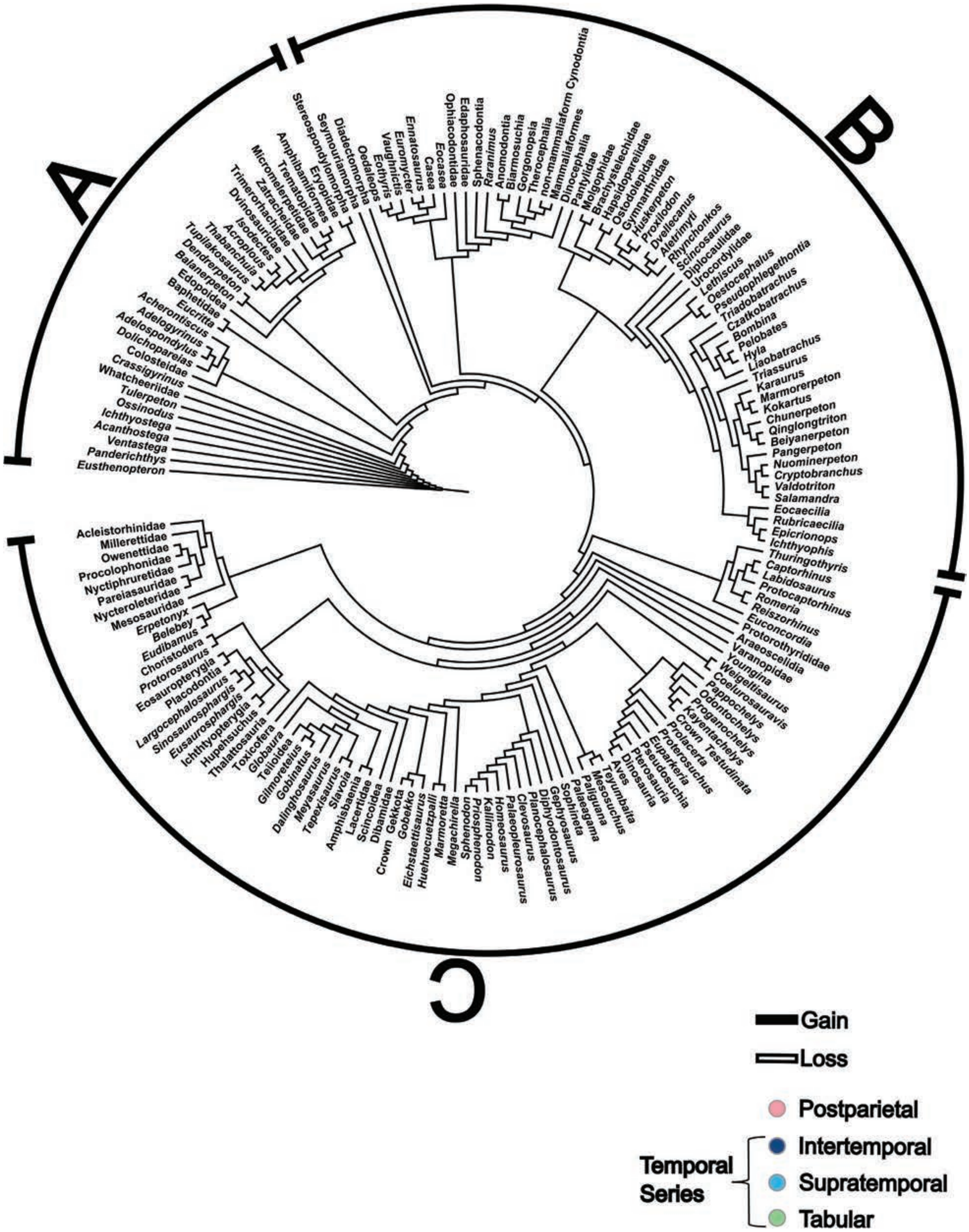

Figure 3. Maximum likelihood ancestral state reconstruction of the presence/absence of the postparietal, intertemporal, supratemporal, and tabular (see key for colour associations) under Lepospondyl Hypothesis a. At the nodes, a filled in quadrant = presence; empty quadrant = absence; striped quadrant = presence/absence is ambiguous. On the branches, empty rectangle = loss of element; filled rectangle = gain of element. At the branch tips, filled in circle = presence of element; empty circle = absence of element; half-filled circle = mixed presence/absence of element. Tree A = Tetrapodomorpha and Temnospondyli. Tree B = Seymouriamorpha, Diadectomorpha, Synapsida, Lepospondyli, and Lissamphibia. Tree C = Captorhinidae, Protorthyrididae, Araeoscelidia, Varanopidae, Neodiapsida, and Parareptilia.

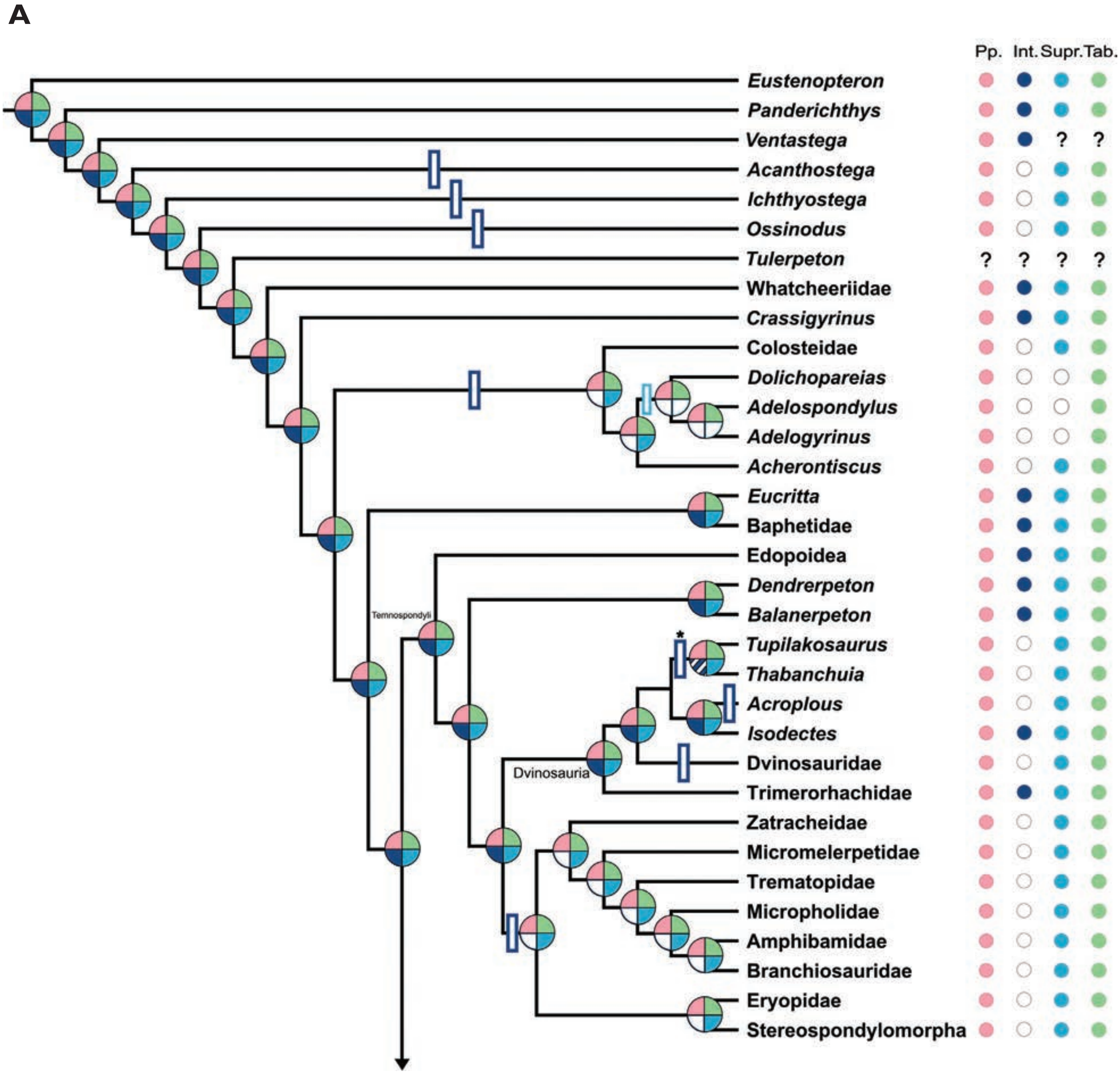

Figure 3. Continued.

In reptiles the pattern of bone loss becomes more heterogenous, especially in Eureptilia (the "true reptiles" and sister group to Parareptilia). Unlike in all the other groups, in Eureptilia the tabular is the second bone to be lost after the intertemporal, followed by the postparietal and then the supratemporal. In Captorhinidae the supratemporal is maintained, while the tabular is either lost twice (Figs 2, 3C), or once at the base of Captorhinidae and is regained in *Thuringothyris* (Suppl. material 24). In neodiapsids the tabular is lost at the base of the tree, shortly followed by the postparietal, although the supratemporal is lost in Weigeltisauridae while the postparietal is retained. The postparietal is regained convergently three times in archosauriformes in *Proterosuchus*, *Euparkeria*, and in Aves. Coding the postparietal as absent in Aves (Homology Hypothesis D) has little effect as the presence/absence of the postparietal remains ambiguous at all nodes in Archosauriformes. The supratemporal is lost a total of 12 times in Neodiapsida, namely at node Weigeltisauridae, node *Kayentachelys*-Crown Testudinata, node Choristodera-*Proterosaurus*, in Archosauriformes, node Lepidosauromorpha, and node Saurosphargidae-Placodontia-Eosauropterygia. Given the uncertainty in the presence of the supratemporal in the stem testudines *Odontochelys* and *Proganochelys* (Gaffney and Meeker 1983; Li et al. 2008; Scheyer et al. 2022), it is possible that the supratemporal is lost up to three times in Testudinata, or is even regained. In Hypothesis A the supratemporal is coded as present for both *Odontochelys* and *Proganochelys*. With this configuration, the supratemporal is present at all testudine nodes besides that leading to *Kayentachelys* and Crown Testudinata, where it is ambiguous. The supratemporal is therefore lost twice, once in *Pappochelys*, and once at the *Kayentachelys*-Crown Testudinata node. In Homology Hypothesis F the supratemporal is coded as present in *Odontochelys* and absent in *Proganochelys*, here the supratemporal is lost convergently three times,

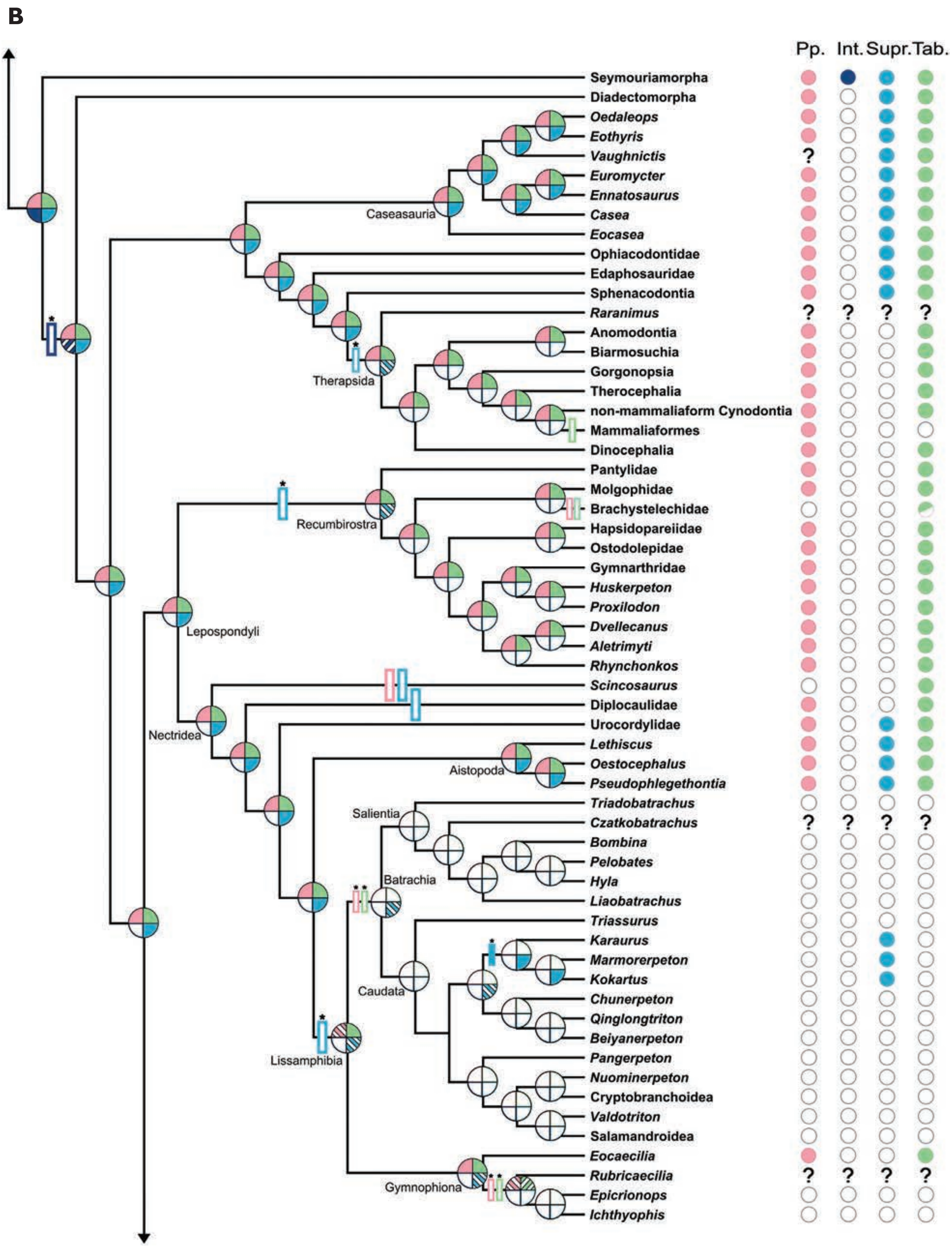

Figure 3. Continued.

once in *Pappochelys*, once in *Proganochelys*, and once at the *Kayentachelys*-Crown Testudinata node. In Homology Hypothesis G the supratemporal is coded as absent in *Odontochelys* and present in *Proganochelys*, similarly to Homology Hypothesis F, the supratemporal is also lost three individual times under this scenario, in *Pappochelys*, at the node leading to *Odontochelys*, *Proganochelys*, *Kayentachelys*, and Crown Testudinata, and at the *Kayentachelys*-Crown Testudinata node. However, the supratemporal is then also regained in

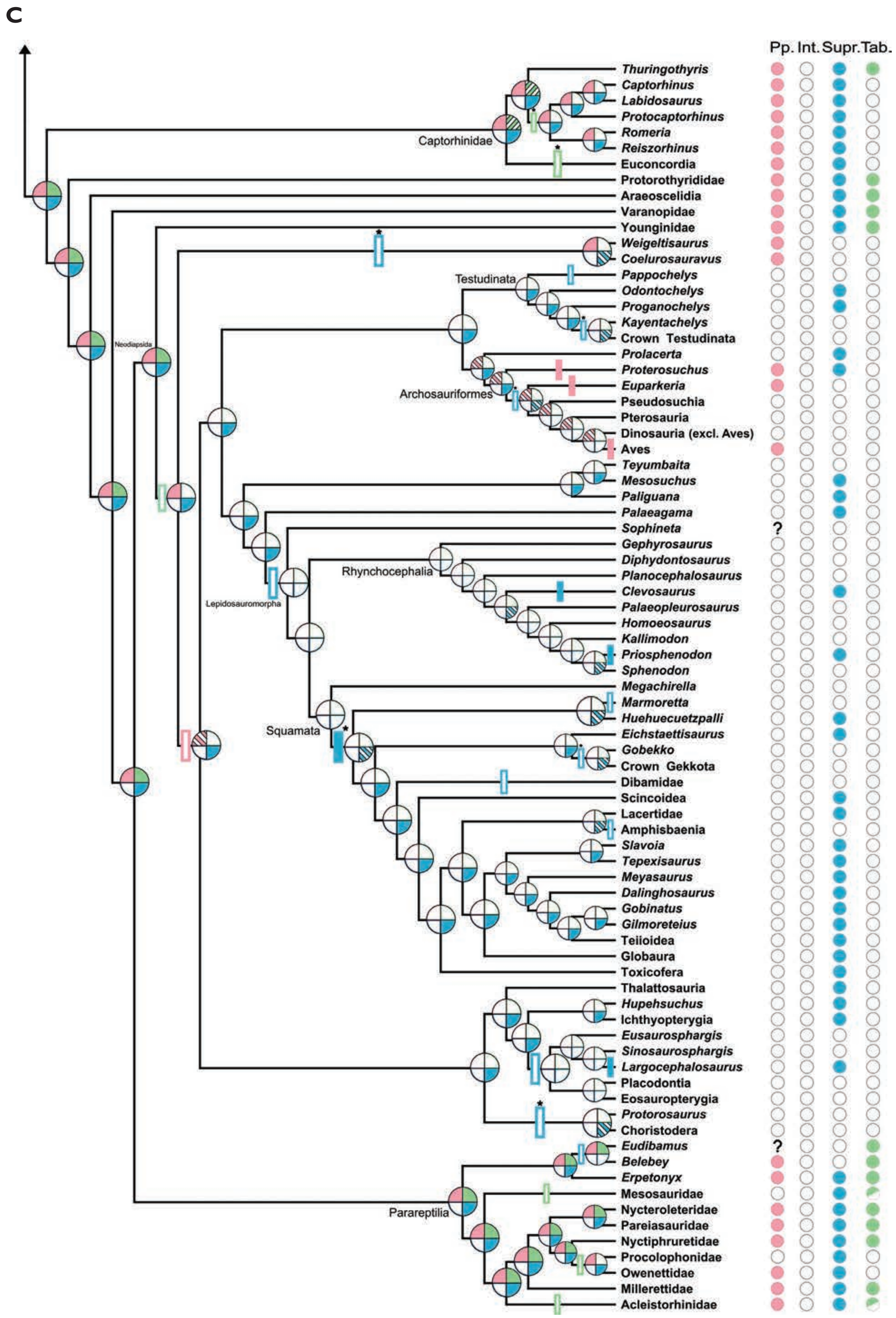

Figure 3. Continued.

Proganochelys. In Homology Hypothesis H, the supratemporal is coded as absent in both *Odontochelys* and *Proganochelys*, in this case the supratemporal is lost once at the Testudinata node. In Squamata the supratemporal is lost four times after being regained at the node leading to Squamata excluding *Megachirella*. The supratemporal is also regained twice within Rhynchocephalia (Figs 2, 3C).

In Parareptilia the pattern of loss observed in stem-tetrapods, temnospondyls, therapsids, and lepospondyls, is only seen in the bolosaurids *Eudibamus* and *Belebey* which lose the supratemporal while retaining the postparietal and tabular (the intertemporal having been lost further down the tree in the stem-amniotes). However, in other parareptiles the postparietal is the second bone to be lost, and not the supratemporal, as is the case in Mesosauridae where the supratemporal is retained, but the postparietal is lost in both *Stereosternum* and *Mesosaurus*, while the tabular is only lost in *Stereosternum* (Suppl. material 1). In Procolophonidae, Owenettidae, and some acleistorhinids (e.g. *Colobomycter*), however, the tabular is the second bone to be lost. In Procolophonidae the postparietal is also lost (Figs 2, 3C).

Placing Lissamphibia with lepospondyls instead of temnospondyls has only a minor effect on where the losses occur along the tree. Both hypotheses have the same number of losses and regains: the intertemporal is lost 9 times, the supratemporal is lost 18 times and regained 5 times, the tabular is lost 9–10 times and possibly regained once, and the postparietal is lost 7 times and regained 3 times. The main difference between the two hypotheses is that temnospondyls only lose the intertemporal and retain the rest of their temporal series and all of their median series elements as these are all lost in lissamphibians. A minor difference is that the presence/absence of the supratemporal at node Batrachia is ambiguous in the Lepospondyl Hypothesis, while it is absent in the Temnospondyl Hypothesis.

Discussion

Pattern of bone loss

Four general principles of loss of the temporal and median series can be gleaned from the results detailed above: (1) the intertemporal is always the first bone to be lost; (2) in general, the supratemporal is the second element to be lost (except in Sauropsida), when this is not the case (i.e. when the tabular is lost before the supratemporal), the supratemporal is largely retained and if lost may be regained; (3) when the supratemporal is the second bone to be lost, the postparietal and tabular are often, but not always, lost together; and (4) the presence/absence of

Table 3. Composition of median and temporal series in groups with reported miniaturisation.

Clade	Frontal	Parietal	Postparietal	Intertemporal	Supratemporal	Tabular
Amphibamidae	1	1	1	0	1	1
Lissamphibia	1	1	1	0	0	0
Mammaliaformes	1	1	1	0	0	0
Squamata	1	1	0	0	1	0
Aves	1	1	0	0	0	0
Recumbirostra	1	1	1	0	0	1
Phlegethontia	1	1	1	0	1	1

Table 4. Composition of median and temporal series in groups associated with terrestrial, aquatic, and semi-aquatic ecologies.

			Terrestrial			
Clade	**Frontal**	**Parietal**	**Postparietal**	**Intertemporal**	**Supratemporal**	**Tabular**
Mammaliaformes	1	1	1	0	0	1
Parareptilia	1	1	1	0	1	1
Aistopoda	1	1	1	0	1	1
Lepidosauria	1	1	0	0	0	0
Gorgonopsia	1	1	1	0	0	1
			Aquatic			
Clade	**Frontal**	**Parietal**	**Postparietal**	**Intertemporal**	**Supratemporal**	**Tabular**
Diplocaulidae	1	1	1	0	0	1
Dvinosauria	1	1	1	1	1	1
Discosauriscus	1	1	1	1	1	1
Branchiosauridae	1	1	1	0	1	1
Acanthostegidae	1	1	1	0	1	1
			Semi-Aquatic			
Clade	**Frontal**	**Parietal**	**Postparietal**	**Intertemporal**	**Supratemporal**	**Tabular**
Crocodylia	1	1	0	0	1	0
Testudinata	1	1	0	0	1*	0
Batrachia	1	1	0	0	0	0

* note the ambiguity in the presence of the supratemporal in stem testudines (Scheyer et al. 2022).

the tabular is not dictated by the presence/absence of the postparietal and vice versa.

The variability we observed in the sequential bone loss in the temporal series across tetrapod phylogeny would indicate that these bones did not form an evolutionary module, and therefore the developmental pathways that control the presence/absence of the individual temporal series bones were not strongly integrated. However, this cannot be confirmed until further work is done to understand the mechanisms of loss undergone by individual bones across the skull, and until we have a clearer consensus on what constitutes bone loss with regards to skull simplification (see below for further discussion). It is also worth noting that the variability in the sequential loss of the supratemporal is restricted to Sauropsida (Eureptilia and Parareptilia, Figs 2, 3C), the group where the diapsid skull morphology appears.

Interestingly, the order in which the temporal series bones are lost does not correspond with the order in which they ossify during development as would be expected. In both the skulls and limbs of lissamphibians, it has been shown that bones are typically lost in reverse order of development, i.e. the last bones to ossify in the sequence are usually the first to be lost (Alberch and Gale 1985; Yeh 2002; Schoch 2014). In fossil tetrapods, the pattern of ossification has mainly been studied in temnospondyl species, in particular in the branchiosaurid *Apateon*, and the stereospondylomorph *Sclerocephalus* (Schoch 1992, 2004; Werneburg et al. 2023; Schoch and Witzmann 2024). These studies show that the ossification of the median series starts with the frontal, followed by the parietal, postparietal, and then the nasal. The ossification sequence of the temporal series has only been described for the branchiosaurid *Apateon*. In this taxon, the supratemporal is the first bone to ossify, followed by the tabular. The tabular ossifies after all other median and temporal series elements. However, contrary to what one would expect given the sequence of ossification during ontogeny, our results show the tabular as often being the last element to be lost, and never the first. This suggests that the pattern of simplification is not driven by a simple heterochronic truncation of the ontogenetic trajectory, but that more complex underlying factors and constraints affect the evolution of skull simplification.

Among the bones analysed here, the supratemporal was shown to be the most evolvable as it was lost and regained the most often (lost 18 times and regained 5 times). In terms of independent losses, the tabular follows suit with a total of 9–10 losses, then the intertemporal with 9 losses, and the postparietal with 7 losses. The postparietal, however, was regained 2–3 times depending on if Aves are coded with a present postparietal or not. The tabular may have been regained once, depending on how the loss of the tabular in Captorhinidae is interpreted (i.e. is it lost twice (in *Euconcordia* and the node leading to Captorhinidae excluding *Euconcordia* and *Thuringothyris*), or is it lost once at the base of Captorhinidae and regained in *Thuringothyris*). In contrast to these elements, the nasal, frontal and parietal of the median series occur at every tip in the tree, suggesting that these were the most stable bones investigated. Neither the relative stability of the median and temporal series bones, nor the order in which these elements are ossified during ontogeny shows a simple correlation with the observed pattern of loss in tetrapodomorphs, again highlighting that more complex evolutionary drivers are at play in the simplification of the skull.

Phylogenetic insights and future directions of study

While the composition of the temporal series can be used to some extent to predict the relative position of groups (e.g. the intertemporal is only present in more basal clades, while the tabular is typically absent in the most derived clades), the loss or regain of the bones reported here are too variable to be useful as phylogenetic characters. This is in large part due to our current understanding of homology in the dermatocranium, and a lack of consensus on what ‘true’ bone loss involves. To date, skull simplification has only been quantified based on the number of individual bone elements defined by clear sutures in adult specimens, and not on embryological data. However, given the difficulties in assessing loss homology in the fossil record, in addition to the prevalence of skull simplification and the variability in the pattern of loss in different tetrapod groups, it is critical that future embryological studies investigate the methods of loss affecting individual bones across the tetrapod phylogeny.

This work has already begun in mammals, as demonstrated by Koyabu et al. (2012) who showed that the mammalian tabular fuses to the postparietal to form the composite interparietal early in development. A possible embryonic tabular was also identified in the archosauriform *Euparkeria capensis* which would have likely later become part of the interparietal (Sookias et al. 2020). A discrete supratemporal was identified in a hatchling of *Sphenodon punctatus* by Rieppel (1992) who concluded that the bone would have later fused with either the parietal or squamosal. In anurans it was proposed that the tabular fuses with the squamosal, and the supratemporal fuses with the frontoparietal (Alcalde and Basso 2013), whereas in Caudata it has been suggested that the supratemporal fuses with the squamosal (Schoch 2014). In avians, a fate-mapping study conducted by Maddin et al. (2016) showed that the frontal and parietal may have fused together to form a frontoparietal, and that the element traditionally referred to as the parietal, is most likely the postparietal. However, a histological study on *Gallus domesticus* did not find evidence of a suture being present between the two ossification centres of Maddin et al.’s (2016) frontoparietal element, which may imply that this bone is in fact just a frontal and not a composite bone (Arnaout et al. 2022), or that two elements are mapped as individual units only early in cellular development, but in later phases of tissue development are not detectable as such anymore.

We would argue that loss by fusion is not 'true' bone loss as the ossification centres are still present. Instead, we agree with the definition of 'true' bone loss as used by Schoch (2014), which requires the ossification centres of the lost bone to have failed to form, often due to heterochronic processes truncating the developmental trajectory. With this in mind, it is necessary to reassess not only how we measure skull simplification, but also how composite bones are named, and how we define bone elements in the context of skull simplification. By not doing so, we run the risk of missing important complexities of skull simplification and potentially having an overly restricted view of the degree to which the skull has been simplified in tetrapod evolutionary history. To avoid this, it may be worthwhile for future studies to focus on re-evaluating tetrapod skull homology across the phylogeny, including fossil clades where possible, and providing revised definitions and new names for composite bones that are formed from fusions, as was done with the mammalian interparietal (Koyabu et al. 2012). This is particularly relevant for phylogenetic analyses, especially those that utilise 'loss characters' as is the case with the Temnospondyl and Lepospondyl Hypotheses for lissamphibian origins. In doing so it would be easier to capture the complexity of skull simplification and perform more detailed versions of the analyses presented here that can attempt to trace evolutionary mechanisms of simplification across tetrapod phylogeny more effectively. It would also make comparisons between the evolutionary lability of individual bones clearer. Although our results indicate that the supratemporal is the most evolutionarily labile bone out of those analysed, while the nasal, frontal and parietal are the least labile, future analyses that are able to incorporate embryological information, and therefore define bone elements based on the presence of their ossification centres may tell a different story.

Phylogenetic inference

Despite the growing number of lissamphibians found in the fossil record, there is still much discourse surrounding the interrelationships of this group, as well as their origin (or origins) (Laurin and Reisz 1997; Meyer and Zardoya 2003; Ruta et al. 2003; Schoch and Milner 2004; Ruta and Coates 2007; Sigurdsen and Green 2011; Marjanovic and Laurin 2013; Schoch 2014; Pardo et al. 2017a, b). The earliest known fossil salamanders (Middle Jurassic *Marmorerpeton* (Jones et al. 2022)), frogs (Early Triassic *Triadobatrachus* (Ascarrunz et al. 2016)), and caecilians (Late Triassic *Funcusvermis* (Kligman et al. 2023)) already display a highly derived morphology, which implies that they radiated from a common ancestor sometime before the Triassic (San Mauro et al. 2005; Zhang et al. 2005; Pardo et al. 2017a; Jones et al. 2022; Kligman et al. 2023). The strong differences in morphology, in addition to the temporal gap between members of the Mesozoic lissamphibian stem-group and Palaeozoic early tetrapods make it harder to determine the origins of lissamphibians. This complication is further augmented by the diversity of developmental mechanisms and life history patterns in early tetrapods, which results in a large number of homoplastic characters and uncertain character polarisations, all of which are similar to the challenges faced when assessing modern amphibian systematics (Wake 1991; Wiens et al. 2005; Schoch 2009; Schoch 2013a).

As previously discussed, there are currently two main hypotheses that explain the origins of lissamphibians, namely the Temnospondyl Hypothesis (TH) and the Lepospondyl Hypothesis (LH). The Temnospondyl Hypothesis argues that lissamphibians form a monophyletic clade and are derived from dissorophoid temnospondyls (Ruta et al. 2003; Schoch and Milner 2004; Caroll 2007; Ruta and Coates 2007; Sigurdsen and Bolt 2010; Sigurdsen and Green 2011; Maddin et al. 2012; Kligman et al. 2023). The Lepospondyl Hypothesis, on the other hand, places lissamphibians within lepospondyls (Laurin and Reisz 1997; Laurin 1998; Vallin and Laurin 2004; Marjanovic and Laurin 2008, 2009, 2013; Laurin et al. 2022).

For all of these cladistic analyses, the reduction in the number of skull bones is used as a character trait to assess the relationships between lissamphibians and stem-tetrapods. However, as we have already noted, the losses of these bones may not be homologous as we cannot determine which developmental processes were responsible for bone loss in fossils. This possible lack of homology highlights not only the complexity of evolutionary processes, but also the potential pitfalls this may create in phylogenetic analyses.

Drivers of loss

A number of ecological and functional selection pressures, developmental mechanisms, and various physical constraints have been proposed in the literature as potential drivers of skull simplification (Atchley and Hall 1991; Hanken and Wake 1993; Sidor 2001; Yeh 2002; Herrel et al. 2007; Esteve-Altava et al. 2013; Schoch 2013a; Schoch 2014; Pardo et al. 2015; Szostakiwskyj et al. 2015; Pardo and Anderson 2016; Pérez-Ben et al. 2018; Strong et al. 2022; Koyabu 2023). One of the most widely cited functional selection pressures concerns the biomechanical stresses on the skull roof associated with biting (Sidor 2001), and specialised ecologies such as headfirst burrowing (Herrel et al. 2007; Pardo et al. 2015; Szostakiwskyj et al. 2015; Pardo and Anderson 2016; Strong et al. 2022). Bone loss linked to the evolution of small body size (and sometimes even true miniaturisation) within a lineage has also been heavily reported (Hanken and Wake 1993; Yeh 2002; Schoch 2013b; Pérez-Ben et al. 2018). Miniaturisation has been documented in dissorophoid temnospondyls (Fröbisch and Schoch 2009), Lissamphibia (Hanken and Wake 1993; Yeh 2002), Mammaliaformes, Squamata (Rieppel

1996; Glaw et al. 2021), Aves (Ocampo et al. 2018), Recumbirostra (Maddin et al. 2011), and Aistopoda (Anderson 2002). Miniaturised body size can also impose physical constraints that may contribute to the loss of skull bones (e.g. large gecko eyes resulting in the loss of the postorbital and supratemporal (Herrel et al. 2007)). Another physical constraint linked to skull simplification is the relative degree of connectivity of individual bones in the skull. A network analysis conducted by Esteve-Altava et al. (2014) on a range of different tetrapod groups showed that poorly connected bones (i.e. bones in direct contact with comparatively few neighbouring bones) were more likely to be lost randomly compared to well-connected bones, which were more likely to be lost by selective fusion. These composite bones made of several ossification centres were themselves less likely to be lost than less complex bones made of a single ossification centre. This is because the more complex bones have a larger role in shaping skull architecture, and the space that they would leave behind if they were lost would be more difficult to fill than that of a less complex and poorly connected bone (Esteve-Altava et al. 2013).

Both functional and developmental selection pressures impose constraints that often result in characteristic, homoplastic anatomical skull morphologies. Therefore, one may expect to see a correlation between skull simplification and lifestyle or miniaturised body size. Tables 3, 4, however, illustrate that the loss of bones in the median and temporal series has no obvious relationship with ecology or an evolutionary decrease in body size in a clade. Nonetheless, more detailed investigations focused on body size and lifestyle are necessary to definitively identify or refute a correlation between these drivers and skull simplification in different tetrapod clades. It is also worth noting the difficulties in detangling the effects of ecological selection pressures versus phylogeny on simplification. For example, from the comparisons of median and temporal series composition in terrestrial and aquatic clades shown in Table 4, it is possible to conclude that aquatic clades are more likely to have a supratemporal than terrestrial clades. However, this could just be a relic of the relative phylogenetic positions of these clades as aquatic groups are often more basal in the phylogeny than their terrestrial relatives.

In the absence of an obvious relationship between skull simplification and lifestyle, it would be pertinent to assume that the evolutionary simplification of the median and temporal series in both anamniotes and amniotes is largely the result of developmental processes and intrinsic evolutionary drivers. In reality though, skull simplification is likely caused by complex combinations of developmental, ecological, and functional factors unique to specific tetrapod lineages, which may also act differently in various tetrapod lineages and at different times in their evolutionary history. What these developmental, ecological, and functional factors may be, we do not yet know, but it is important to consider that the loss of bones (no matter the process), is much more likely than the (re)appearance of additional elements in the dermal skull roof. With this in mind, it may not be surprising that skull simplification is so prevalent in tetrapods.

Conclusions

In summary, the simplification of the dermatocranium is a well-documented yet poorly understood phenomenon which began in the Devonian and evolved parallelly in various tetrapod lineages into the Mesozoic. By conducting ancestral state reconstructions on the presence/absence of the median and temporal series, we have shown that the evolutionary loss of bones in the dermatocranium was much more complex than initially thought, and likely involved a mixture of developmental, ecological, and functional drivers. As no obvious correlation was found between skull simplification and lifestyle or body size, further work will be required to determine what these factors may be and how they interact with one another both in individual lineages, and across the evolutionary history of different tetrapod lineages. Our analyses also showed that the temporal series did not form an evolutionary module, and consequently that the developmental pathways influencing the presence/absence of these individual bones were unlikely to be strongly integrated as the loss of these bones is quite variable. In general though, the intertemporal is lost first, then followed by the supratemporal, then the tabular and/or postparietal. However, although most groups seem to follow this pattern of loss, this was not the case in Sauropsida (i.e. Eureptilia and Parareptilia) where the tabular or postparietal was the second bone to be lost and not the supratemporal. Of the bones studied, the supratemporal was the most evolvable given that it was lost and regained the most often, while the nasal, frontal, and parietal were the least evolvable as they were always present. Interestingly, the sequence in which the temporal and median series bones were lost did not reflect the order in which they ossify in ontogeny.

The analyses presented here demonstrate that the evolution of skull simplification is much more complex than previously realised. Further work is needed to fully capture the intricacies involved, and we would encourage future studies to focus on reassessing skull homology across tetrapodomorphs, and to apply embryological methods to determine the mode of bone loss in the skulls of extant groups.

Acknowledgements

The authors would like to thank Marcello Ruta and Torsten Scheyer for their kind and constructive reviews which helped improve the manuscript. KJK would like to thank Johannes Müller and Mark MacDougal for helpful discussions on amniotes, and parareptile and recumbirostran phylogeny respectively; Davide Foffa for providing help with R; Antoine Verrière for giving advice both on R and on the figures presented here; and Yara Haridy for proof reading. This work is part of KJK's PhD project and was funded by the Deutsche Forschungsgemeinschaft (grant number 442217617) awarded to MD.

References

Alberch P, Gale EA (1985) A developmental analysis of an evolutionary trend: digital reduction in amphibians. Evolution 39: 8–23. https://doi.org/10.2307/2408513

Alcalde L, Basso NG (2013) Old and new hypotheses about the homology of the compound bones from the cheek and otico-occipital regions of the anuran skull. Zoology 116: 232–245. https://doi.org/10.1016/j.zool.2013.03.002

Anderson JS (2002) Revision of the aïstopod genus *Phlegethontia* (Tetrapoda: Lepospondyli). Journal of Paleontology 76: 1029–1046. https://doi.org/10.1666/0022-3360(2002)076%3C1029:ROTAGP%3E2.0.CO;2

Anderson JS (2003) A new aïstopod (Tetrapoda: Lepospondyli) from Mazon Creek, Illinois. Journal of Vertebrate Paleontology 23: 79–88. https://doi.org/10.1671/0272-4634(2003)23[79:ANATLF]2.0.CO;2

Anderson JS (2007) Incorporating ontogeny into the matrix: a phylogenetic evaluation of developmental evidence for the origin of modern amphibians. In: Anderson JS, Sues HD (Eds) Major transitions in vertebrate evolution. Bloomington: Indiana University Press, Indiana.

Anderson JS (2008) Focal review: the origin (s) of modern amphibians. Evolutionary Biology 35: 231–247. https://doi.org/10.1007/s11692-008-9044-5

Anderson JS, Reisz RR, Scott D, Fröbisch NB, Sumida SS (2008a) A stem batrachian from the Early Permian of Texas and the origin of frogs and salamanders. Nature 453: 515–518. https://doi.org/10.1038/nature06865

Anderson JS, Henrici AC, Sumida SS, Martens T, Berman DS (2008b) *Georgenthalia clavinasica*, a new genus and species of dissorophoid temnospondyl from the Early Permian of Germany, and the relationships of the family Amphibamidae. Journal of Vertebrate Paleontology 28: 61–75. https://doi.org/10.1671/0272-4634(2008)28[61:GCANGA]2.0.CO;2

Andrews SM, Westoll TS (1970) IX.—The postcranial skeleton of *Eusthenopteron foordi* Whiteaves. Earth and Environmental Science Transactions of the Royal Society of Edinburgh 68(9): 207–329. https://doi.org/10.1017/S008045680001471X

Arnaout B, MacKenzie EM, Lantigua KE, Brzezinski K, McKinnell IW, Maddin HC (2022) The histology of sutures in chicken skulls: Types, conservation, and ontogeny. Journal of Anatomy 240: 503–515. https://doi.org/10.1111/joa.13574

Asakura Y, Kawabe S (2022) Anatomical network analyses reveal evolutionary integration and modularity in the lizards skull. Scientific Reports 12: 14429. https://doi.org/10.1038/s41598-022-18222-8

Ascarrunz E, Rage JC, Legreneur P, Laurin M (2016) *Triadobatrachus massinoti*, the earliest known lissamphibian (Vertebrata: Tetrapoda) re-examined by µCT scan, and the evolution of trunk length in batrachians. Contributions to Zoology 85: 201–234. https://doi.org/10.1163/18759866-08502004

Atchley WR, Hall BK (1991) A model for development and evolution of complex morphological structures. Biological Reviews 66: 101–157. https://doi.org/10.1111/j.1469-185X.1991.tb01138.x

Bapst DW (2012) Paleotree: An R package for paleontological and phylogenetic analyses of evolution. Methods in Ecology and Evolution 3: 803–807. https://doi.org/10.1111/j.2041-210X.2012.00223.x

Babst DW, Wagner PJ (2022) Package 'paleotree'. [pdf] CRAN. http://cran.fhcrc.org/web/packages/paleotree/paleotree.pdf

Berman DS, Sumida SS, Lombard RE (1992) Reinterpretation of the temporal and occipital regions in *Diadectes* and the relationships of diadectomorphs. Journal of Paleontology 66: 481–499. https://doi.org/10.1017/S0022336000034028

Berman DS, Henrici AC, Sumida SS, Martens T (2000) Redescription of *Seymouria sanjuanensis* (Seymouriamorpha) from the Lower Permian of Germany based on complete, mature specimens with a discussion of paleoecology of the Bromacker locality assemblage. Journal of Vertebrate Paleontology 20: 253–268. https://doi.org/10.1671/0272-4634(2000)020[0253:ROSSSF]2.0.CO;2

Brazeau MD, Ahlberg PE (2006) Tetrapod-like middle ear architecture in a Devonian fish. Nature 439(7074): 318–321. https://doi.org/10.1038/nature04196

Carroll RL (1969) A Middle Pennsylvanian Captorhinomorph, and the Interrelationships of Primitive Reptiles. Journal of Paleontology 43: 151–170.

Carroll R, Gaskill P (1978) The Order Microsauria. Memoirs of the American Philosophical Society 126: 1–211.

Carroll RL (1988) Vertebrate Paleontology and Evolution. WH Freeman, New York.

Carroll RL, Bossy KA, Milner AC, Andrews SM, Wellstead CF (1998) Handbook of paleoherpetology part 1. Lepospondyli. München, Germany: Verlag Dr. Friedrich Pfeil.

Carroll RL (2001) The origin and early radiation of terrestrial vertebrates. Journal of Paleontology 75: 1202–1213. https://doi.org/10.1666/0022-3360(2001)075%3C1202:TOAERO%3E2.0.CO;2

Carroll RL (2007) The Palaeozoic ancestry of salamanders, frogs, and caecilians. Zoological Journal of the Linnean Society 150: 1–140. https://doi.org/10.1111/j.1096-3642.2007.00246.x

Carroll RL (2009) The Rise of Amphibians: 365 Million Years of Evolution. Johns Hopkins University Press, Baltimore.

Carstens MH (2023) The Neck: Development and Evolution. In: Carstens MH (Ed.) The Embryologic Basis of Craniofacial Structure: Developmental Anatomy, Evolutionary Design, and Clinical Applications. Springer, Cham, 781–940. https://doi.org/10.1007/978-3-031-15636-6_10

Clack JA (1992) The stapes of *Acanthostega gunnari* and the Role of the Stapes in Early Tetrapods. In: Webster DB, Popper AN, Fay RR (Eds) The Evolutionary Biology of Hearing. Springer, New York, 405–420. https://doi.org/10.1007/978-1-4612-2784-7_24

Clack JA (1994) Earliest known tetrapod braincase and the evolution of the stapes and fenestra ovalis. Nature 369(6479): 392–394. https://doi.org/10.1038/369392a0

Clack JA (1998) A new Early Carboniferous tetrapod with a mélange of crown-group characters. Nature 394(6688): 66–69. https://doi.org/10.1038/27895

Clack JA (2002) The dermal skull roof of *Acanthostega gunnari*, an early tetrapod from the Late Devonian. Earth and Environmental Science Transactions of the Royal Society of Edinburgh 93(1): 17–33. https://doi.org/10.1017/S0263593300000304

Clack JA, Ahlberg PE, Finney SM, Dominguez Alonso P, Robinson J, Ketcham RA (2003) A uniquely specialized ear in a very early tetrapod. Nature 425(6953): 65–69. https://doi.org/10.1038/nature01904

Clack JA (2009) The fish–tetrapod transition: new fossils and interpretations. Evolution: Education and Outreach 2: 213–223. https://doi.org/10.1007/s12052-009-0119-2

Clack JA (2012) Gaining Ground: The Origin and Evolution of Tetrapods. Second Edition. Indiana University Press, Indiana.

Clack JA, Ruta M, Milner AR, Marshall JE, Smithson TR, Smithson KZ (2019) *Acherontiscus caledoniae*: the earliest heterodont and durophagous tetrapod. Royal Society Open Science 6: 182087. https://doi.org/10.1098/rsos.182087

Coates MI, Clack JA (1991) Fish-like gills and breathing in the earliest known tetrapod. Nature 352(6332): 234–236. https://doi.org/10.1038/352234a0

Crawford NG, Parham JF, Sellas AB, Faircloth BC, Glenn TC, Papenfuss TJ, Henderson JB, Hansen MH, Simison WB (2015) A phylogenomic analysis of turtles. Molecular Phylogenetics and Evolution 83: 250–257. https://doi.org/10.1016/j.ympev.2014.10.021

Dalerum F (2007) Phylogenetic reconstruction of carnivore social organizations. Journal of Zoology 273: 90–97. https://doi.org/10.1111/j.1469-7998.2007.00303.x

Elwood JRL, Cundall D (1994) Morphology and behavior of the feeding apparatus in *Cryptobranchus alleganiensis* (Amphibia: Caudata). Journal of Morphology 220: 47–70. https://doi.org/10.1002/jmor.1052200106

Esteve-Altava B, Marugán-Lobón J, Botella H, Rasskin-Gutman D (2013) Structural constraints in the evolution of the tetrapod skull complexity: Williston's law revisited using network models. Evolutionary Biology 40: 209–219. https://doi.org/10.1007/s11692-012-9200-9

Esteve-Altava B, Marugán-Lobón J, Botella H, Rasskin-Gutman D (2014) Random loss and selective fusion of bones originate morphological complexity trends in tetrapod skull networks. Evolutionary Biology 41: 52–61. https://doi.org/10.1007/s11692-013-9245-4

Evans SE, Sigogneau-Russell D (2001) A stem-group caecilian (Lissamphibia: Gymnophiona) from the Lower Cretaceous of North Africa. Palaeontology 44: 259–273. https://doi.org/10.1111/1475-4983.00179

Evans SE (2008) The Skull of Lizards and Tuatara. Biology of the Reptilia 20: 1–347.

Farke AA, Wolff EDS, Tanke DH (2009) Evidence of Combat in *Triceratops*. PLOS ONE 4: e4252. https://doi.org/10.1371/journal.pone.0004252

Ford DP, Benson RB (2020) The phylogeny of early amniotes and the affinities of Parareptilia and Varanopidae. Nature Ecology & Evolution 4: 57–65. https://doi.org/10.1038/s41559-019-1047-3

Fox RC, Bowman MC (1966) Osteology and relationships of *Captorhinus aguti* (Cope) (Reptilia: Captorhinomorpha). University of Kansas Paleontological Contributions 15: 1–80.

Fraser-King, SW, Benoit J, Day MO, Rubidge BS (2019) Cranial morphology and phylogenetic relationship of the enigmatic dinocephalian *Styracocephalus platyrhynchus* from the Karoo Supergroup, South Africa. Palaeontologia Africana 54: 14–29.

Gaffney ES, Meeker LJ (1983) Skull morphology of the oldest turtles: a preliminary description of *Proganochelys quenstedtii*. Journal of Vertebrate Paleontology 3: 25–28. https://doi.org/10.1080/02724634.1983.10011953

Glaw F, Köhler J, Hawlitschek O, Ratsoavina FM, Rakotoarison A, Scherz MD, Vences M (2021) Extreme miniaturization of a new amniote vertebrate and insights into the evolution of genital size in chameleons. Scientific Reports 11: 1–14. https://doi.org/10.1038/s41598-020-80955-1

Hanken J, Wake DB (1993) Miniaturization of Body Size; Organismal Consequences and Evolutionary Significance. Annual Review of Ecology and Systematics 24: 501–519. https://doi.org/10.1146/annurev.es.24.110193.002441

Heiss E, Aerts P, Van Wassenbergh S (2018) Aquatic-terrestrial transitions of feeding systems in vertebrates: a mechanical perspective. Journal of Experimental Biology 221: jeb154427. https://doi.org/10.1242/jeb.154427

Herrel A, Schaerlaeken V, Meyers JJ, Metzger KA, Ross CF (2007) The evolution of cranial design and performance in squamates: consequences of skull-bone reduction on feeding behavior. Integrative and Comparative Biology 47: 107–117. https://doi.org/10.1093/icb/icm014

Huttenlocker A (2009) An investigation into the cladistic relationships and monophyly of therocephalian therapsids (Amniota: Synapsida). Zoological Journal of the Linnean Society 157: 865–891. https://doi.org/10.1111/j.1096-3642.2009.00538.x

Huttenlocker AK, Singh SA, Henrici AC, Sumida SS (2021) A Carboniferous synapsid with caniniform teeth and a reappraisal of mandibular size-shape heterodonty in the origin of mammals. Royal Society Open Science 8: 211237. https://doi.org/10.1098/rsos.211237

Jarvik E (1980) Basic Structure and Evolution of Vertebrates. Academic Press, London.

Jenkins F.A, Walsh DM, Carroll RL (2007) Anatomy of *Eocaecilia micropodia*, a limbed caecilian of the Early Jurassic. Bulletin of the Museum of Comparative Zoology 158: 285–365. https://doi.org/10.3099/0027-4100(2007)158[285:AOEMAL]2.0.CO;2

Johanson Z, Ahlberg P, Ritchie A (2003) The Braincase and Palate of the Tetrapodomorph Sarcopterygian *Mandageria fairfaxi*: Morphological Variability near the Fish-Tetrapod Transition. Palaeontology 46: 271–293. https://doi.org/10.1111/1475-4983.00298

Jollie M (1962) Chordate Morphology. Reinhold, New York. https://doi.org/10.5962/bhl.title.6408

Jones ME, Curtis N, O'Higgins P, Fagan M, Evans SE (2009) The head and neck muscles associated with feeding in *Sphenodon* (Reptilia: Lepidosauria: Rhynchocephalia). Palaeontologia Electronica 12.

Jones ME, Benson RB, Skutschas P, Hill L, Panciroli E, Schmitt AD, Walsh SA, Evans SE (2022) Middle Jurassic fossils document an early stage in salamander evolution. Proceedings of the National Academy of Sciences 119: e2114100119. https://doi.org/10.1073/pnas.2114100119

Joyce WG, Schoch RR, Lyson TR (2013) The girdles of the oldest fossil turtle, *Proterochersis robusta*, and the age of the turtle crown. BMC Evolutionary Biology 13: 1–9. https://doi.org/10.1186/1471-2148-13-266

Kligman BT, Gee BM, Marsh AD, Nesbitt SJ, Smith ME, Parker WG, Stocker MR (2023) Triassic stem caecilian supports dissorophoid origin of living amphibians. Nature 614: 102–107. https://doi.org/10.1038/s41586-022-05646-5

Knell RJ, Naish D, Tomkins JL, Hone DWE (2013) Sexual selection in prehistoric animals: detection and implications. Cell Press 28: 38–47. https://doi.org/10.1016/j.tree.2012.07.015

Koyabu D, Maier W, Sánchez-Villagra MR (2012) Paleontological and developmental evidence resolve the homology and dual embryonic origin of a mammalian skull bone, the interparietal. Proceedings of the National Academy of Sciences 109: 14075–14080. https://doi.org/10.1073/pnas.1208693109

Koyabu D (2023) Evolution, conservatism and overlooked homologies of the mammalian skull. Philosophical Transactions of the Royal Society B 378: 20220081. https://doi.org/10.1098/rstb.2022.0081

Laurin M, Reisz RR (1997) A new perspective on tetrapod phylogeny. In: Sumida SS, Martin KLM (Eds) Amniote Origins: Completing the Transition to Land. Academic Press, Inc, San Diego, 9–59. https://doi.org/10.1016/B978-012676460-4/50003-2

Laurin M (1998) The importance of global parsimony and historical bias in understanding tetrapod evolution. Part II. Vertebral centrum, costal ventilation, and paedomorphosis. Annales des Sciences Naturelles - Zoologie et Biologie Animale 19: 99–114. https://doi.org/10.1016/S0003-4339(98)80004-X

Laurin M, Lapauze O, Marjanović D (2022) What do ossification sequences tell us about the origin of extant amphibians? Peer Community Journal 2: e12. https://doi.org/10.24072/pcjournal.89

Leavitt DH, Bezy RL, Crandall KA, Sites Jr JW (2007) Multi-locus DNA sequence data reveal a history of deep cryptic vicariance and habitat-driven convergence in the desert night lizard *Xantusia vigilis* species complex (Squamata: Xantusiidae). Molecular Ecology 16: 4455–4481. https://doi.org/10.1111/j.1365-294X.2007.03496.x

Lee MS, Anderson JS (2006) Molecular clocks and the origin (s) of modern amphibians. Molecular Phylogenetics and Evolution 40: 635–639. https://doi.org/10.1016/j.ympev.2006.03.013

Lee HW, Esteve-Altava B, Abzhanov A (2020) Evolutionary and ontogenetic changes of the anatomical organization and modularity in the skull of archosaurs. Scientific Reports 10: 16138. https://doi.org/10.1038/s41598-020-73083-3

Li C, Wu XC, Rieppel O, Wang LT, Zhao LJ (2008) An ancestral turtle from the Late Triassic of southwestern China. Nature 456: 497–501. https://doi.org/10.1038/nature07533

Liu J, Rubidge B, Li J (2009) New basal synapsid supports Laurasian origin for therapsids. Acta Palaeontologica Polonica 54: 393–400. https://doi.org/10.4202/app.2008.0071

Long JA, Gordon MS (2004) The greatest step in vertebrate history: a paleobiological review of the fish-tetrapod transition. Physiological and Biochemical Zoology 77: 700–719. https://doi.org/10.1086/425183

MacDougall MJ, Seeger R, Gee B, Ponstein J, Jansen M, Scott D, Bevitt JJ, Reisz RR, Fröbisch J (2021) Revised description of the early Permian recumbirostran “microsaur” *Nannaroter mckinziei* based on new fossil material and computed tomographic data. Frontiers in Ecology and Evolution 9: 739316. https://doi.org/10.3389/fevo.2021.739316

Maddin HC, Olori JC, Anderson JS (2011) A redescription of *Carrolla craddocki* (Lepospondyli: Brachystelechidae) based on high-resolution CT, and the impacts of miniaturization and fossoriality on morphology. Journal of Morphology 272: 722–743. https://doi.org/10.1002/jmor.10946

Maddin HC, Jenkins Jr FA, Anderson JS (2012) The braincase of *Eocaecilia micropodia* (Lissamphibia, Gymnophiona) and the origin of caecilians. PLOS ONE 7: e50743. https://doi.org/10.1371/journal.pone.0050743

Maddin HC, Piekarski N, Sefton EM, Hanken J (2016) Homology of the cranial vault in birds: new insights based on embryonic fate-mapping and character analysis. Royal Society Open Science 3: 160356. https://doi.org/10.1098/rsos.160356

Maddin HC, Piekarski N, Reisz RR, Hanken J (2020) Development and evolution of the tetrapod skull-neck boundary. Biological Reviews 95: 573–591. https://doi.org/10.1111/brv.12578

Maddison WP, Maddison DR (2021) Mesquite: a modular system for evolutionary analysis. Version 3.7. http://www.mesquiteproject.org

Maglia AM, Púgener LA (1998) Skeletal development and adult osteology of *Bombina orientalis* (Anura: Bombinatoridae). Herpetologica 54: 344–363.

Marjanović DM, Laurin M (2008) A reevaluation of the evidence supporting an unorthodox hypothesis on the origin of extant amphibians. Contributions to Zoology 77: 149–199. https://doi.org/10.1163/18759866-07703002

Marjanović D, Laurin M (2009) The origin(s) of modern amphibians: a commentary. Evolutionary Biology 36: 336–338. https://doi.org/10.1007/s11692-009-9065-8

Marjanović D, Laurin M (2013) The origin (s) of extant amphibians: a review with emphasis on the “lepospondyl hypothesis”. Geodiversitas 35: 207–272. https://doi.org/10.5252/g2013n1a8

Marjanović D, Laurin M (2019) Phylogeny of Paleozoic limbed vertebrates reassessed through revision and expansion of the largest published relevant data matrix. PeerJ 6: e5565. https://doi.org/10.7717/peerj.5565

Meyer A, Zardoya R (2003) Recent advances in the (molecular) phylogeny of vertebrates. Annual Review of Ecology, Evolution, and Systematics 34: 311–338. https://doi.org/10.1146/annurev.ecolsys.34.011802.132351

Milner AR (1993) The Paleozoic relatives of lissamphibians. Herpetological Monographs 7: 8–27. https://doi.org/10.2307/1466948

Ocampo D, Barrantes G, Uy JAC (2018) Morphological adaptations for relatively larger brains in hummingbird skulls. Ecology and Evolution 8: 10482–10488. https://doi.org/10.1002/ece3.4513

Olson EC, Roy SK, Ross LA (1951) *Diplocaulus*: a study in growth and variation. Fieldiana: Geol 11: 57–149. https://doi.org/10.5962/bhl.title.3527

Paradis E, Schliep K (2019) ape 5.0: an environment for modern phylogenetics and evolutionary analyses in R. Bioinformatics 35: 526–528. https://doi.org/10.1093/bioinformatics/bty633

Pardo JD, Szostakiwskyj M, Anderson JS (2015) Cranial morphology of the brachystelechid ‘microsaur’ *Quasicaecilia texana* Carroll provides new insights into the diversity and evolution of braincase morphology in recumbirostran ‘microsaurs’. PLOS ONE 10: e0130359. https://doi.org/10.1371/journal.pone.0130359

Pardo JD, Anderson JS (2016) Cranial morphology of the Carboniferous-Permian tetrapod *Brachydectes newberryi* (Lepospondyli, Lysorophia): new data from µCT. PLOS ONE 11: e0161823. https://doi.org/10.1371/journal.pone.0161823

Pardo JD, Small BJ, Huttenlocker AK (2017a) Stem caecilian from the Triassic of Colorado sheds light on the origins of Lissamphibia. Proceedings of the National Academy of Sciences 114: E5389–E5395. https://doi.org/10.1073/pnas.1706752114

Pardo JD, Szostakiwskyj M, Ahlberg PE, Anderson JS (2017b) Hidden morphological diversity among early tetrapods. Nature 546: 642–645. https://doi.org/10.1038/nature22966

Pérez-Ben CM, Schoch RR, Báez AM (2018) Miniaturization and morphological evolution in Paleozoic relatives of living amphibians: a quantitative approach. Paleobiology 44: 58–75. https://doi.org/10.1017/pab.2017.22

Plateau O, Foth C (2020) Birds have peramorphic skulls, too: anatomical network analyses reveal oppositional heterochronies in avian skull evolution. Communications Biology 3: 195. https://doi.org/10.1038/s42003-020-0914-4

Pritchard AC, Sues HD, Scott D, Reisz RR (2021) Osteology, Relationships and Functional Morphology of *Weigeltisaurus jaekeli* (Diapsida, Weigeltisauridae) based on a Complete Skeleton from the Upper Permian Kupferschiefer of Germany. PeerJ 9: e11413. https://doi.org/10.7717/peerj.11413

Pyron RA (2011) Divergence time estimation using fossils as terminal taxa and the origins of Lissamphibia. Systematic Biology 60: 466–481. https://doi.org/10.1093/sysbio/syr047

Rawson JR, Esteve-Altava B, Porro LB, Dutel H, Rayfield EJ (2022) Early tetrapod cranial evolution is characterized by increased complexity, constraint, and an offset from fin-limb evolution. Science Advances 8: eadc8875. https://doi.org/10.1126/sciadv.adc8875

Reisz RR (1981) A diapsid reptile from the Pennsylvanian of Kansas. Occasional Papers of the Museum of Natural History, University of Kansas 7B: 1–74. https://doi.org/10.5962/bhl.title.8440

Reisz RR, Berman DS (2001) The skull of *Mesenosaurus romeri*, a Small Varanopseid (Synapsida: Eupelycosauria) from the Upper Permian of the Mezen River Basin, Northern Russia. Annals-Carnegie Museum Pittsburgh 70: 113–132. https://doi.org/10.5962/p.215145

Reisz RR, Godfrey SJ, Scott D (2009) *Eothyris* and *Oedaleops*: do these Early Permian synapsids from Texas and New Mexico form a clade? Journal of Vertebrate Paleontology 29: 39–47. https://doi.org/10.1671/039.029.0112

Rieppel O (1992) The skull in a hatchling of *Sphenodon punctatus*. Journal of Herpetology 26: 80–84. https://doi.org/10.2307/1565028

Rieppel O (1996) Miniaturization in Tetrapods: Consequences for Skull Morphology. In: Miller PJ (Ed.) Miniature Vertebrates: The Implications of Small Body Size. Oxford Academic, Oxford, 47–61. https://doi.org/10.1093/oso/9780198577874.003.0003

Rüber L, Britz R, Tan HH, Ng PK, Zardoya R (2004) Evolution of mouthbrooding and life-history correlates in the fighting fish genus Betta. Evolution 58: 799–813. https://doi.org/10.1111/j.0014-3820.2004.tb00413.x

Ruta M, Coates MI, Quicke DL (2003) Early tetrapod relationships revisited. Biological Reviews 78: 251–345. https://doi.org/10.1017/S1464793102006103

Ruta M, Coates MI (2007) Dates, nodes and character conflict: addressing the lissamphibian origin problem. Journal of Systematic Palaeontology 5: 69–122. https://doi.org/10.1017/S1477201906002008

Rybczynski N (2000) Cranial anatomy and phylogenetic position of *Suminia getmanovi*, a basal anomodont (Amniota: Therapsida) from the Late Permian of Eastern Europe. Zoological Journal of the Linnean Society 130: 329–373. https://doi.org/10.1111/j.1096-3642.2000.tb01634.x

San Mauro D, Vences M, Alcobendas M, Zardoya R, Meyer A (2005) Initial diversification of living amphibians predated the breakup of Pangaea. The American Naturalist 165: 590–599. https://doi.org/10.1086/429523

Scherz MD, Hutter CR, Rakotoarison A, Riemann JC, Rödel MO, Ndriantsoa SH, Glos J, Hyde Roberts S, Crottini A, Vences M, Glaw F (2019) Morphological and ecological convergence at the lower size limit for vertebrates highlighted by five new miniaturised microhylid frog species from three different Madagascan genera. PLOS ONE 14: e0213314. https://doi.org/10.1371/journal.pone.0213314

Scheyer TM, Klein N, Evers SW, Mautner AK, Pabst B (2022) First evidence of *Proganochelys quenstedtii* (Testudinata) from the Plateosaurus bonebeds (Norian, Late Triassic) of Frick, Canton Aargau, Switzerland. Swiss Journal of Palaeontology 141: 17. https://doi.org/10.1186/s13358-022-00260-4

Schluter D, Price T, Mooers AØ, Ludwig D (1997) Likelihood of ancestor states in adaptive radiation. Evolution 51: 1699–1711. https://doi.org/10.2307/2410994

Schoch RR (1992) Comparative ontogeny of early Permian branchiosaurid amphibians from southwestern Germany. Developmental stages. Palaeontographica, Abteilung A, Paläozoologie, Stratigraphie 222: 43–83.

Schoch RR (2002) The early formation of the skull in extant and Paleozoic amphibians. Paleobiology 28: 278–296. https://doi.org/10.1666/0094-8373(2002)028%3C0278:TEFOTS%3E2.0.CO;2

Schoch RR (2004) Skeleton formation in the Branchiosauridae: a case study in comparing ontogenetic trajectories. Journal of Vertebrate Paleontology 24: 309–319. https://doi.org/10.1671/1950

Schoch RR, AR Milner (2004) Structure and implications of theories on the origins of lissamphibians. In: Arratia G, Wilson MV, Cloutier R (Eds) Recent advances in the origin and early radiation of vertebrates. Verlag Dr. Friedrich Pfeil, München, 345–377.

Schoch RR, Rubidge BS (2005) The amphibamid *Micropholis* from the Lystrosaurus assemblage zone of South Africa. Journal of Vertebrate Paleontology 25: 502–522. https://doi.org/10.1671/0272-4634(2005)025[0502:TAMFTL]2.0.CO;2

Schoch RR (2009) Evolution of life cycles in early amphibians. The Annual Review of Earth and Planetary Sciences 37: 135–162. https://doi.org/10.1146/annurev.earth.031208.100113

Schoch RR, Witzmann F (2011) Bystrow's Paradox–gills, fossils, and the fish-to-tetrapod transition. Acta Zoologica 92(3): 251–265. https://doi.org/10.1111/j.1463-6395.2010.00456.x

Schoch RR (2013a) How body size and development biased the direction of evolution in early amphibians. Historical Biology 25: 155–165. https://doi.org/10.1080/08912963.2012.724796

Schoch RR (2013b) The evolution of major temnospondyl clades: an inclusive phylogenetic analysis. Journal of Systematic Palaeontology 11: 673–705. https://doi.org/10.1080/14772019.2012.699006

Schoch RR (2014) Amphibian skull evolution: the developmental and functional context of simplification, bone loss and heterotopy. Journal of Experimental Zoology Part B: Molecular and Developmental Evolution 322: 619–630. https://doi.org/10.1002/jez.b.22599

Schoch RR, Milner AR (2014) Handbook of Paleoherpetology part 3A2. Temnospondyli I. Verlag Dr. Friedrich Pfeil, München.

Schoch RR, Werneburg R, Voigt S (2020) A Triassic stem-salamander from Kyrgyzstan and the origin of salamanders. Proceedings of the National Academy of Sciences 117: 11584–11588. https://doi.org/10.1073/pnas.2001424117

Schoch RR (2022) Phylogeny of the amphibamiform temnospondyls: the relationship of taxa known by adults, larvae and neotenes. Journal of Systematic Palaeontology 20: 1–30. https://doi.org/10.1080/14772019.2022.2113831

Schoch RR, Witzmann F (2024) The evolution of larvae in temnospondyls and the stepwise origin of amphibian metamorphosis. Biological Reviews 99: 1613–1637. https://doi.org/10.1111/brv.13084

Sefton EM, Bullar B-AS, Mohaddes Z, Hanken J (2016) Evolution of the head-trunk interface in tetrapod vertebrates. eLife 5: e09972. https://doi.org/10.7554/eLife.09972

Sidor CA (2001) Simplification as a trend in synapsid cranial evolution. Evolution 55: 1419–1442. https://doi.org/10.1111/j.0014-3820.2001.tb00663.x

Sigurdsen T, Bolt JR (2010) The Lower Permian amphibamid *Doleserpeton* (Temnospondyli: Dissorophoidea), the interrelationships of amphibamids, and the origin of modern amphibians. Journal of Vertebrate Paleontology 30: 1360–1377. https://doi.org/10.1080/02724634.2010.501445

Sigurdsen T, Green DM (2011) The origin of modern amphibians: a re-evaluation. Zoological Journal of the Linnean Society 162: 457–469. https://doi.org/10.1111/j.1096-3642.2010.00683.x

Simoes TR, Caldwell MW, Tałanda M, Bernardi M, Palci A, Vernygora O, Bernardini F, Mancini L, Nydam RL (2018) The origin of squamates revealed by a Middle Triassic lizard from the Italian Alps. Nature 557: 706–709. https://doi.org/10.1038/s41586-018-0093-3

Smith-Paredes D, Núñez-León D, Soto-Acuña S, O'Connor J, Botelho, JF, Vargas AO (2018) Dinosaur ossification centres in embryonic birds uncover developmental evolution of the skull. Nature Ecology & Evolution 2: 1966–1973. https://doi.org/10.1038/s41559-018-0713-1

Sookias RB, Dilkes D, Sobral G, Smith RM, Wolvaardt FP, Arcucci AB, Bhullar BAS, Werneburg I (2020) The craniomandibular anatomy of the early archosauriform *Euparkeria capensis* and the dawn of the archosaur skull. Royal Society Open Science 7: 20011. https://doi.org/10.1098/rsos.200116

Strong CR, Scherz MD, Caldwell MW (2022) Convergence, divergence, and macroevolutionary constraint as revealed by anatomical network analysis of the squamate skull, with an emphasis on snakes. Scientific Reports 12: 14469. https://doi.org/10.1038/s41598-022-18649-z

Szostakiwskyj M, Pardo JD, Anderson JS (2015) Micro-CT study of *Rhynchonkos stovalli* (Lepospondyli, Recumbirostra), with description of two new genera. PLOS ONE 10: e0127307. https://doi.org/10.1371/journal.pone.0127307

Tsuji LA (2006) Cranial anatomy and phylogenetic affinities of the Permian parareptile *Macroleter poezicus*. Journal of Vertebrate Paleontology 26: 849–865. https://doi.org/10.1671/0272-4634(2006)26[849:CAAPAO]2.0.CO;2

van Tuinen M, Dyke GJ (2004) Calibration of galliform molecular clocks using multiple fossils and genetic partitions. Molecular Phylogenetics and Evolution 30: 74–86. https://doi.org/10.1016/S1055-7903(03)00164-7

Vallin G, Laurin M (2004) Cranial morphology and affinities of *Microbrachis*, and a reappraisal of the phylogeny and lifestyle of the first amphibians. Journal of Vertebrate Paleontology 24: 56–72. https://doi.org/10.1671/5.1

Wake DB (1991) Homoplasy: The Result of Natural Selection, or Evidence of Design Limitations? The American Naturalist 138: 543–567. https://doi.org/10.1086/285234

Wake MH (1993) The skull as a locomotor organ. In: Hanken J, Hall BK (Eds) The Skull. University of Chicago Press, Chicago, 197–240.

Walker W, Bemis W, Liem K, Grande L (2000) Functional Anatomy of the Vertebrates: An Evolutionary Perspective. Third Editon. Harcourt College Publishers, Fort Worth.

Wallace RV, Martínez R, Rowe T (2019) First record of a basal mammaliamorph from the early Late Triassic Ischigualasto Formation of Argentina. PLOS ONE 14: e0218791. https://doi.org/10.1371/journal.pone.0218791

Wang W, Shang Q, Cheng L, Wu XC, Li C (2022) Ancestral body plan and adaptive radiation of sauropterygian marine reptiles. Iscience 25: 105635. https://doi.org/10.1016/j.isci.2022.105635

Werneburg R, Witzmann F, Rinehart L, Fischer J, Voigt S (2023) A new eryopid temnospondyl from the Carboniferous–Permian boundary of Germany. Journal of Paleontology 97: 1251–1281. https://doi.org/10.1017/jpa.2023.58

Williston SW (1925) The Osteology of the Reptiles. Harvard University Press. https://doi.org/10.5962/bhl.title.6573

Wilkinson M, Presswell B, Sherratt E, Papadopoulou A, Gower DJ (2014) A new species of striped *Ichthyophis* Fitzinger, 1826 (Amphibia: Gymnophiona: Ichthyophiidae) from Myanmar. Zootaxa 3785: 45–58. https://doi.org/10.11646/zootaxa.3785.1.4

Wiens JJ, Bonett RM, Chippindale PT (2005) Ontogeny discombobulates phylogeny. Systematic Biology 54: 91–110. https://doi.org/10.1080/10635150590906037

Yeh J (2002) The effect of miniaturized body size on skeletal morphology in frogs. Evolution 56: 628–641. https://doi.org/10.1111/j.0014-3820.2002.tb01372.x

Zhang P, Zhou H, Chen YQ, Liu YF, Qu LH (2005) Mitogenomic perspectives on the origin and phylogeny of living amphibians. Systematic Biology 54: 391–400. https://doi.org/10.1080/10635150590945278

Supplementary material 1

Notes and references for presence/absence data

Authors: Kim Julia Kean, Marylène Danto, Celeste Pérez-Ben, Nadia Belinda Fröbisch

Data type: xlsx

Explanation note: Presence/absence data with notes and references.

Link: https://doi.org/10.3897/fr.27.133803.suppl1

Supplementary material 2

Temnospondyl Hypothesis composite tree

Authors: Kim Julia Kean, Marylène Danto, Celeste Pérez-Ben, Nadia Belinda Fröbisch

Data type: tre

Link: https://doi.org/10.3897/fr.27.133803.suppl2

Supplementary material 3

Lepospondyl Hypothesis composite tree

Authors: Kim Julia Kean, Marylène Danto, Celeste Pérez-Ben, Nadia Belinda Fröbisch

Data type: tre

Link: https://doi.org/10.3897/fr.27.133803.suppl3

Supplementary material 4

Notes and references for FADs

Authors: Kim Julia Kean, Marylène Danto, Celeste Pérez-Ben, Nadia Belinda Fröbisch

Data type: xlsx

Link: https://doi.org/10.3897/fr.27.133803.suppl4

Supplementary material 5

AICs and weights of ARD and ER models in Temnospondyl and Lepospondyl Hypothesis

Authors: Kim Julia Kean, Marylène Danto, Celeste Pérez-Ben, Nadia Belinda Fröbisch

Data type: xlsx

Link: https://doi.org/10.3897/fr.27.133803.suppl5

Supplementary material 6

R script

Authors: Kim Julia Kean, Marylène Danto, Celeste Pérez-Ben, Nadia Belinda Fröbisch

Data type: R

Explanation note: R Script used for maximum likelihood ancestral state reconstructions.

Link: https://doi.org/10.3897/fr.27.133803.suppl6

Supplementary material 7

TH-LHa data

Authors: Kim Julia Kean, Marylène Danto, Celeste Pérez-Ben, Nadia Belinda Fröbisch

Data type: csv

Explanation note: Homology Hypothesis A data.

Link: https://doi.org/10.3897/fr.27.133803.suppl7

Supplementary material 8

TH-LHb data

Authors: Kim Julia Kean, Marylène Danto, Celeste Pérez-Ben, Nadia Belinda Fröbisch

Data type: csv

Explanation note: Homology Hypothesis B data.

Link: https://doi.org/10.3897/fr.27.133803.suppl8

Supplementary material 9

TH-LHc data

Authors: Kim Julia Kean, Marylène Danto, Celeste Pérez-Ben, Nadia Belinda Fröbisch
Data type: csv
Explanation note: Homology Hypothesis C data.

Link: https://doi.org/10.3897/fr.27.133803.suppl9

Supplementary material 10

TH-LHd data

Authors: Kim Julia Kean, Marylène Danto, Celeste Pérez-Ben, Nadia Belinda Fröbisch
Data type: csv
Explanation note: Homology Hypothesis D data.

Link: https://doi.org/10.3897/fr.27.133803.suppl10

Supplementary material 11

TH-LHe data

Authors: Kim Julia Kean, Marylène Danto, Celeste Pérez-Ben, Nadia Belinda Fröbisch
Data type: csv
Explanation note: Homology Hypothesis E data.

Link: https://doi.org/10.3897/fr.27.133803.suppl11

Supplementary material 12

TH-LHf data

Authors: Kim Julia Kean, Marylène Danto, Celeste Pérez-Ben, Nadia Belinda Fröbisch
Data type: csv
Explanation note: Homology Hypothesis F data.

Link: https://doi.org/10.3897/fr.27.133803.suppl12

Supplementary material 13

TH-LHg data

Authors: Kim Julia Kean, Marylène Danto, Celeste Pérez-Ben, Nadia Belinda Fröbisch
Data type: csv
Explanation note: Homology Hypothesis G data.

Link: https://doi.org/10.3897/fr.27.133803.suppl13

Supplementary material 14

TH-LHh data

Authors: Kim Julia Kean, Marylène Danto, Celeste Pérez-Ben, Nadia Belinda Fröbisch
Data type: csv
Explanation note: Homology Hypothesis H data.

Link: https://doi.org/10.3897/fr.27.133803.suppl14

Supplementary material 15

FAD data

Authors: Kim Julia Kean, Marylène Danto, Celeste Pérez-Ben, Nadia Belinda Fröbisch
Data type: csv

Link: https://doi.org/10.3897/fr.27.133803.suppl15

Supplementary material 16

THa postparietal

Authors: Kim Julia Kean, Marylène Danto, Celeste Pérez-Ben, Nadia Belinda Fröbisch
Data type: pdf

Link: https://doi.org/10.3897/fr.27.133803.suppl16

Supplementary material 17

THa intertemporal

Authors: Kim Julia Kean, Marylène Danto, Celeste Pérez-Ben, Nadia Belinda Fröbisch
Data type: pdf

Link: https://doi.org/10.3897/fr.27.133803.suppl17

Supplementary material 18

THa supratemporal

Authors: Kim Julia Kean, Marylène Danto, Celeste Pérez-Ben, Nadia Belinda Fröbisch
Data type: pdf

Link: https://doi.org/10.3897/fr.27.133803.suppl18

Supplementary material 19

THa tabular

Authors: Kim Julia Kean, Marylène Danto, Celeste Pérez-Ben, Nadia Belinda Fröbisch
Data type: pdf

Link: https://doi.org/10.3897/fr.27.133803.suppl19

Supplementary material 20

LHa postparietal

Authors: Kim Julia Kean, Marylène Danto, Celeste Pérez-Ben, Nadia Belinda Fröbisch
Data type: pdf

Link: https://doi.org/10.3897/fr.27.133803.suppl20

Supplementary material 21

LHa intertemporal

Authors: Kim Julia Kean, Marylène Danto, Celeste Pérez-Ben, Nadia Belinda Fröbisch
Data type: pdf

Link: https://doi.org/10.3897/fr.27.133803.suppl21

Supplementary material 22

LHa supratemporal

Authors: Kim Julia Kean, Marylène Danto, Celeste Pérez-Ben, Nadia Belinda Fröbisch
Data type: pdf

Link: https://doi.org/10.3897/fr.27.133803.suppl22

Supplementary material 23

LHa tabular

Authors: Kim Julia Kean, Marylène Danto, Celeste Pérez-Ben, Nadia Belinda Fröbisch
Data type: pdf

Link: https://doi.org/10.3897/fr.27.133803.suppl23

Supplementary material 24

Alternative transitions

Authors: Kim Julia Kean, Marylène Danto, Celeste Pérez-Ben, Nadia Belinda Fröbisch
Data type: tiff

Link: https://doi.org/10.3897/fr.27.133803.suppl24

Fossil Record 27 (3) 2024, 473–497 | DOI 10.3897/fr.27.137860

Terrestrialisation and the cranial architecture of tetrapods

Ingmar Werneburg[1,2]

1 *Paläontologische Sammlung, Senckenberg Centre for Human Evolution and Palaeoenvironment (SHEP) an der Universität Tübingen, Sigwartstraße 10, 72076 Tübingen, Germany*

2 *Fachbereich Geowissenschaften, Universität Tübingen, Hölderlinstraße 12, 72074 Tübingen, Germany*

https://zoobank.org/D94F687E-FD99-4793-841C-D59747269AD8

Corresponding author: Ingmar Werneburg (ingmar.werneburg@senckenberg.de)

Academic editor: Florian Witzmann ♦ **Received** 25 September 2024 ♦ **Accepted** 27 October 2024 ♦ **Published** 30 December 2024

Abstract

Using four extinct land vertebrate species as examples, I discuss ontogenetic strategies as well as the potential influence of bite- and other external forces on the formation of the land vertebrate skull. In principle, areas under biomechanical stress are strongly ossified, whereas regions with little or no stress show only weak or no ossification. In this regard, all plates, arcades and openings of the skull – even in that of the multi-fenestrated dinosaurs – can be explained. I trace the changes in feeding mode and body posture at the transition from semi-aquatic to fully terrestrial tetrapods and discuss changes in the position of bite points. Through evolution, an increasing bite force is argued to have a crucial influence on the formation of new skull openings, such as the supratemporal and the antorbital fenestrae in archosaurs, by changing the direction of stress flows in the skull. The conquest of land was also associated with the appearance of novel types of behaviour such as inter- and intraspecific combats. Horns and other cranial weapons were formed repeatedly, which are shown to alter skull construction when receiving external forces. Changes in the skull biomechanics are associated with body posture and postcranial skeletal anatomy. Additionally, vice versa, the neck muscles are shown to have an important impact on the differentiation of the tetrapod skull. Finally, a new hypothesis is provided for the evolution of the temporal openings, based on biomechanical considerations. I argue that the synapsid (infrafenestral) morphotype was ancestral to amniotes related to a strong anterior bite in the mouth. Along the reptilian lineage – such as in many parareptiles, captorhinids and turtles – temporal fenestration was repeatedly closed by stiffening the temporal region in response to external forces. In addition, I argue that the upper temporal opening evolved first and that the diapsid (bifenestral) morphotype is secondary. The “triapsid” morphotype in ceratopsid dinosaurs is shown to be related to concentrated forces on the animal’s neck frill.

Key Words

Bite performance, biomechanics, fenestration, stresses, ossification

The story of the vertebrate land conquerors

The conquest of the terrestrial realm is considered to be one of the major “key innovations” in vertebrate evolution. Several physiological and anatomical adaptations were necessary for the animals outside the aquatic milieu (e.g. Laurin (2010); Clack (2012); Maier and Werneburg (2014); Schoch (2014a); Dial et al. (2015); Molnar et al. (2022a, 2022b)). These included, amongst others, the development of specialised skins to avoid dehydration and the exclusive use of lungs to process atmospheric oxygen. Skeletal reorganisation evolved in response to gravity and limbs emerged, as documented by a well-resolved series of Devonian tetrapodomorph fossils (Clack 2012). Many early tetrapod groups (e.g. Temnospondyli) had a biphasic lifestyle with an early, larval stage in water and a later, adult stage on land – similar to their extant representatives, the lissamphibians (Gymnophiona, Caudata, Anura) (Schoch 2014a). Perhaps already some of the earliest reptiliomorphs (e.g. Diadectomorpha) (Berman 2013), as well as the undisputed members of Amniota (Synapsida and Reptilia *sensu* Modesto and Anderson (2004)) completely skipped the aquatic phase of development and completed their early phase of ontogeny within the cleidoic (amniotic) egg. This prevents dehydration of the egg and embryo on land. The larval stage, as such, was transferred into a "test tube" environment, much more independent from the outside world with consequences also on skull development. This ontogenetic innovation permitted amniotes to conquer the most extreme regions on land, including deserts and mountains (Zhang et al. 2024).

Some of the most conspicuous structural remodelling at the water-to-land transition affected the skull. Ancestrally, it was a massive structure in aquatic fish-like vertebrates which both afforded protection for the brain and sensory organs against predation and hydrostatic pressure in the water column and during swimming (Liem et al. 2001). Sarcopterygian fishes adapted to near-shore environments (Werneburg et al. 2024a) with a tendency to flatten their skull, such as is evident in early tetrapodomorphs. Such a flattened skull enabled a faster sidewards movement during hunting, because of less water resistance when compared to taller skulls (Hohn-Schulte et al. 2013; Preuschoft 2022). In addition to a lower water column, more terrestrial food was available. The feeding strategy has changed from the generalised fish-like suction feeding to a hunting behaviour (Bramble and Wake 1985; Schwenk 2000), in which the jaws were increasingly used as weapons (in the sense of Hülsmann and Wahlert (1972)) or as manipulating tools (see also Natchev et al. (2015)).

With the stepwise conquest of the terrestrial environment, shoulders separated from the skull (Preuschoft and Gudo 2005; Daeschler et al. 2006; Ahlberg 2018; Cloutier et al. 2020). Originally, shoulders and fins assisted in balancing the head during swimming and enabled updrift (Liem et al. 2001). In sarcopterygian fish, muscularised limbs pushed the heavy head forward in densely vegetated waters near the shore. When walking on land, force lines in the body were largely rearranged: shoulders and limbs now mainly had to handle the vertical weight force of the body stem (Preuschoft et al. 2022) and the connection to the skull became looser. A neck region evolved which enabled a more flexible head movement (Diogo et al. 2008; Diogo and Abdala 2010; Diogo and Abdala 2011; Clement 2019). The skull had to be lifted against gravity and the resulting strain had to be taken up by shoulders and limbs. As a consequence, the originally massive skull was lightened. This was enabled by reducing the number (Williston 1925; Gregory 1935) and thickness (Abel et al. 2022a, 2022b) of skull bones. In this context, the expansion and arrangement of skull bones experienced an enormous diversification in land vertebrates, particularly in the crown tetrapods: Lissamphibia (Schoch 2014b) and Amniota (Abel and Werneburg 2021, 2024). However, several skull reductions already and independently occurred amongst early tetrapod clades (Schoch 2014a; Abel and Werneburg 2021; see also the contribution of Kean et al. in this volume).

In this paper, I discuss potential factors that influenced the diversification of skull construction at the transition from early land vertebrates to well-established amniotes. I will, firstly, (A) discuss the ontogenetic preconditions for skull formation and, secondly, (B) the influence of external forces on skull construction. The latter will be separated into (B1) bite-related forces and (B2) forces resulting from body posture and, if present, from cranial armour. To explain the biomechanical principles, I selected four taxa:

(1) The Early Triassic temnospondyl *Parotosuchus helgolandicus* (Schroeder 1913) has a rather ancestral tetrapodomorph skull anatomy (Lautenschlager et al. 2016; Witzmann and Werneburg 2017) (Fig. 1). It will be used to mainly discuss anterior perpendicular bite, i.e. the bite force that is vertically acting on the frontal teeth.
(2) The Late Carboniferous, early reptiliomorph *Anthracosaurus russelli* (Huxley 1863; Panchen 1977; Clack 1987) has distinct temporal fenestration similar to the condition in the synapsid amniotes (Kemp 2005) and many parareptiles (Tsuji and Müller 2009) (Fig. 2). It will mainly serve as an example to illustrate the influence of strong anterior and low posterior perpendicular bite forces. Additionally, the influence of neck muscles will be discussed in this species, as they are considered relevant to stiffening the back of the skull.
(3) The condition of a diapsid reptile with a strong posterior bite is exemplified by the Early Triassic archosauriform *Euparkeria capensis* (Broom 1913a; Broom 1913b; Sookias et al. 2020) (Fig. 3). Additionally, the influence of transversal bite forces will be briefly discussed in this species.
(4) Finally, using the Late Cretaceous dinosaur *Protoceratops andrewsi* (Granger and Gregory 1923) (Fig. 4), I explore the implications of body posture and cranial armour (Section B2) on the skull construction of land vertebrates.

All species show very complex patterns of skull formation in evolution, which cannot be discussed in detail. In the chosen examples, only the biomechanical principles will be illustrated. These will be used as basis to reconstruct the evolution of temporal openings – an old topic in comparative anatomy (Abel and Werneburg 2021, 2024).

A. Ontogenetic preconditions for skull formation

A1. From larva to adult

The lungfishes (Dipnoi) are the closest living relatives of Tetrapodomorpha and a detailed observation of dipnoan development allows deep insights into the ancestral ontogeny of land vertebrates (Long 2011; Clack 2012;

Schoch 2014a). Adult lungfishes plesiomorphically have a head fully covered by dermal bones. The jaw adductor muscles close the mouth when feeding. They are inserted into the lower jaw, but arise from the lateral surface of the braincase and the interior surface of the temporal bones (Diogo and Abdala 2011). The "temple" is the area behind the eye (Werneburg 2019; Abel and Werneburg 2021; Werneburg and Abel 2022; Abel and Werneburg 2024).

The free-living and feeding larvae of lungfishes do not have a fully formed dermal skeleton yet and the temporal bones are loosely located on the head's surface (Ziermann et al. 2018). To be able to feed, the larvae's jaw musculature only originates from the braincase, which is already formed very early in development (de Beer 1937). Later in development, the dermal bones grow, become connected to each other and encompass the whole head externally. This can be interpreted as an adaptation to increased water pressure on the skull in the faster and deeper swimming adults (see above). With the formation of the full temporal skull cover, the jaw musculature expands laterally from the braincase to the internal surface of the temporal bones (Ziermann et al. 2018; Werneburg 2019). In that arrangement, which involves additional muscle fibres (i.e. a larger physiological cross-section), a greater bite force can be generated in the adult compared to the larva. This developmental process can be expected to have happened also in early tetrapods, including the temnospondyls, lepospondyls and most stem-amniote reptiliomorphs (e.g. Seymouriamorpha) with direct development from larva to adult.

Close to the origin of Lissamphibia, within dissorophoid temnospondyls, metamorphosis evolved, which includes remarkable reorganisations of the body (Schoch 2014a). The palate is largely reorganised at metamorphosis, whereas the skull roof undergoes changes related to other developmental processes (Schoch 2014b), as follows. The lissamphibian skulls are largely considered paedomorphic in relation to the original temnospondyl skulls. Several bones that appear late in the ontogeny of temnospondyls (postfrontal, postorbital, jugal, tabular) fail to form in the shortened ontogeny of lissamphibians (comparable to snakes in relation to lizards: Werneburg and Sánchez-Villagra (2015); cf. Fig. 5K). Bones that reach only a "half-way-development" compared to the ancestral dissorophoid (i.e. branchiosaurid) condition (parietal, prefrontal, squamosal, quadratojugal, parasphenoid, palatine, pterygoid), either remain small or fuse with each other (Schoch 1992). As a result, the skull of lissamphibians is extremely reduced in overall ossification and largely excavated in the cheek region (Schoch 2014b; Abel and Werneburg 2021). The large jaw adductor muscles fill the emarginated cheek region and can even expand – with more fibres (i.e. involving greater bite force) – on top of the skull roof bones (Schoch 2014b) because no temporal bones block them laterally.

I argue that the ancestral ontogenetic condition described for lungfish larvae above (Ziermann et al. 2018) is, by paedomorphosis, retained in modern Batrachia (caudates and anurans). The flattened skulls of batrachians result in longer muscle fibres (Schoch 2014b), which allow a larger gape when compared to the shorter fibres in the fully encapsulated skull of ancestral tetrapods. The fossorial adaptation of caecilians resulted in the secondary stiffening of the skull (Schoch 2014a) and already the oldest known caecilian representatives had a typically stiffened skull (Evans and Sigogneau-Russell 2001). Developmental evidence suggests a similarity between early batrachian and caecilian skull development (Müller et al. 2005). Moreover, as in batrachians, their jaw musculature solely originates on the braincase in larvae (Edgeworth 1935; Kleinteich and Haas 2007; Kleinteich 2009) and adults (Lowie et al. 2023), representing the ancestral larval stage of the lungfish (Ziermann et al. 2018).

With the emergence of the cleidoic egg in amniotes, the free-living larval stage was skipped and the hatchling more closely resembles the adult. That means that the amniote embryo does not need to develop the functional muscle arrangement of a free-living larva that is otherwise seen in non-amniote vertebrates (Werneburg 2019). In particular, the jaw muscles do not attach to the braincase in the early development of amniotes (Edgeworth 1935). Similar to the temporal bones, the developing jaw musculature is not functional in the embryo yet and associates with the skull bones only late in development (Rieppel 1987). The late emerging association is related to the particular functional needs of the post-hatching animal (Werneburg 2019; also sensu Maier (1999)). This pre-adaptation must be understood as an evolutionary consequence of a genetically fixed ontogenetic penetration (Schlindwein et al. 2022).

There are two major routes of feeding behaviour with several modifications and combinations. These two feeding adaptations are typified in early amniotes. Synapsida concentrate on a bite anterior in the mouth with higher bite forces in this region; Diapsida (within Reptilia), in contrast, concentrate on a bite more posterior in the snout. Both conditions will be discussed below (Sections B1-3 and B1-4).

A2. Sensory organs and skull bone arrangement

In early embryology, the brain and the sensory organs are amongst the first cranial structures to develop (Schoenwolf and Mathews 2007; Werneburg 2009). Cranial bones emerge only late in embryogenesis as small ossification centres (Rieppel 1994; Sánchez-Villagra et al. 2008; Werneburg et al. 2009; Weisbecker and Mitgutsch 2010; Mitgutsch et al. 2011; Spiekman and Werneburg 2017). Only later in development do the bones arrange into the typical skull architecture (Werneburg et al. 2015c; Werneburg 2019; Xing et al. 2022). Muscles become active and promote specific ossification modes and at hatching or birth, the feeding apparatus must be functional (Maier 1999; Schlindwein et al. 2022). In addition to the brain, skull bones developmentally arrange around the pre-existing sensory organs, including the nose, eyes and the

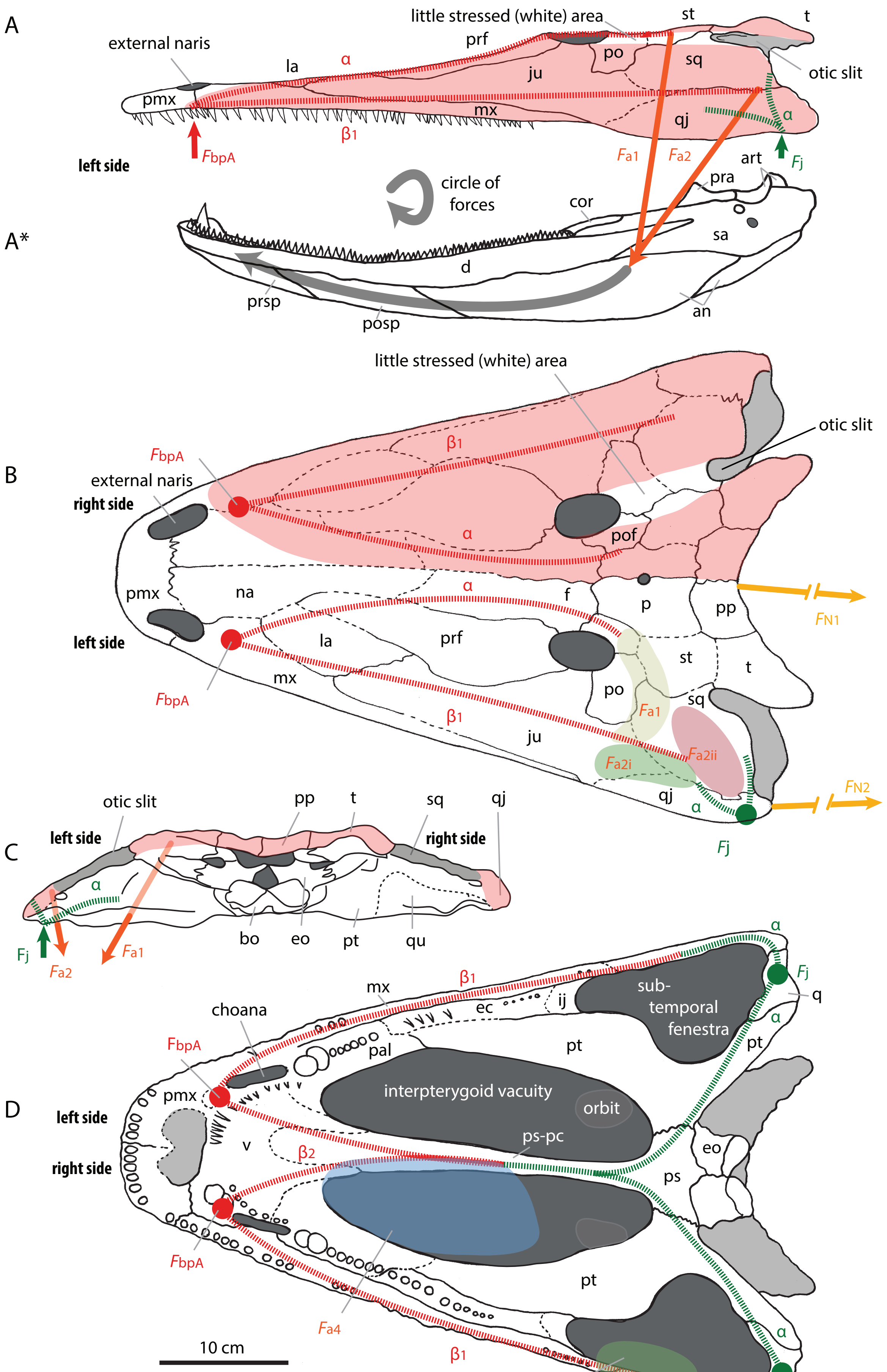
A
little stressed (white) area
st
t
external naris
prf
po
sq
otic slit
la
α
ju
pmx
mx
qj
α
β1
FbpA
Fa1
Fa2
Fj
left side
art
pra
circle of forces
cor
A*
sa
d
prsp
posp
an
little stressed (white) area
otic slit
β1
FbpA
B
external naris
right side
α
pof
pmx
na
f
p
pp
FN1
α
left side
la
prf
st
t
mx
po
Fa1
sq
FbpA
β1
ju
Fa2ii
Fa2i
qj
α
FN2
Fj
otic slit
pp
t
sq
qj
left side
right side
C
α
Fj
Fa2
Fa1
bo
eo
pt
qu
α
β1
Fj
mx
ec
ij
sub-temporal fenestra
q
choana
α
pal
pt
pt
FbpA
pmx
interpterygoid vacuity
orbit
D
left side
ps-pc
eo
v
β2
right side
ps
FbpA
pt
Fa4
α
10 cm
β1
Fa2i
Fj
α

labyrinth organ (Sánchez-Villagra et al. 2008; Werneburg et al. 2009; Weisbecker and Mitgutsch 2010; Koyabu et al. 2014), which, therefore, provide a crucial spatial constraint to skull shape. When an animal bites, stress flows (i.e. resultants of the force) distribute in the head, which over evolutionary time, contributes to forming ossified areas around the brain and the sensory organs. This process can be traced in late-term embryos/foetuses, in which the specific jaw movements are already present (Werneburg and Maier 2019) and bones are arranged along the stress flows (Spiekman and Werneburg 2017; Werneburg 2019).

B. The influence of external forces on skull construction

Recently, Werneburg and Preuschoft (2024) provided a basic biomechanical discussion on skull construction in land vertebrates. They showed that the point of attack, the amount of bite force in the mouth and the handling of the food items are important aspects to consider when interpreting temporal bone architecture. Feeding mode was discussed as an overwhelming driving factor in altering the shape of the temporal skull region in evolution and the phylogenetic value of this anatomical region must be regarded as informative only on selected taxonomic levels with similar trophic adaptations. Two principal considerations are important (e.g. sensu Preuschoft (2022)): 1. Only those areas of the head that are under biomechanical stress form bone, whereas unstressed areas result in openings in the skull. 2. Stresses are taken up by jaw musculature (F_a), neck musculature (F_N) and the scruff of the neck (F_S) to guide the stresses back to the point of attack – i.e. in a "circle of forces" – via the lower jaw or via the postcranial skeleton and the soil that the animal and the food item (prey or plant) share.

In the present paper, I summarise the approach of Werneburg and Preuschoft (2024) and expand on their study. Here, I discuss the general skull construction of the four selected early tetrapods from the Paleozoic and Mesozoic eras in terms of their specific vacuities and ossified areas. These include their snout, palatal and occipital skull regions, as well as their lower jaw. This study aims to provide an overview of forces acting on the skull during feeding (Section B1) and enlighten the evolutionary "precondition" for the later success of taxa with the related cranial adaptations. However, I argue that not only bite-related forces, but also further external forces (Section B2) – induced by neck posture and cranial weapons (e.g. horns) – need to be considered for a more comprehensive understanding of tetrapod skull construction. This paper can only touch upon the surface of the highly complex patterns of skull formation in land vertebrates. I developed stress flow diagrams as graphical reconstructions. This is an exclusive qualitative, not a quantitative approach. Such basic considerations, however, are largely under-represented in the literature and, in my opinion, need more attention. Providing experiments, such as finite element system syntheses (FESS) or -analyses (FESA) (Witzel and Preuschoft 2005; Rayfield 2007), was beyond the scope of this article, but they will be important in future work seeking to test and elaborate the arguments discussed herein.

The major effects of each stress – compression or tension – is indicated as α or β, respectively, although complex stress patterns are present in the actual skull as shown by finite element analyses, depending on the internal bone anatomy, architectural integration in the skull and stress flows from other forces. In particular, the stresses induced by the obliquely orientated neck muscles will result in a complex combination of tensional (backwards) and compressional (midwards) stress patterns. Those are indicated as γ in the figures. Stresses received also numbers, which are just descriptive to refer to them in the figures and texts and do not necessarily indicate 'homologies'.

B1. Bite related forces

B1-1. Otic notch

The early semi-aquatic tetrapods, including many temnospondyls and stem amniotes, were characterised by a rather flat skull with an otic notch at the posterior border of the temporal region (Figs 1, 2, 5A). It has been shown that this notch is spatially related to the ancestral vertebrate spiracle (i.e. 1st pharyngeal slit), which changed its functionality from breathing towards a hearing-related organ (Schoch 2014a; Fröbisch and Witzmann 2019; Gai et al. 2022). The exact position and extent of the spiracular openings in the dorsolateral parts of the skull vary amongst taxa (Figs 1, 2). Noteworthy, the spiracle does not have an elongated dorsoventral orientation in gnathostomes, which is different from the orientation of the adjacent gill openings. This can be partly explained by the original articulation of the hyomandibula and the

Figure 1. Skull (**A, B–D**) and lower jaw (**A***) of the temnospondyl *Proterosuchus helgolandicus* in left lateral (**A, A***), dorsal (**B**), posterior (**C**) and ventral (**D**) views; after Granger and Gregory (1923). Stress flows (i.e. resulting forces) are illustrated as dashed lines. Simplified scheme of anterior perpendicular bite (F_{bpA}) with the resulting stress along the whole snout (red shaded area; Fig. 1A–C). This stress distribution, indicated by compressive (red α) and tensional (red β) stress lines, passes the eye dorsally and ventrally. In the "shadow of the eye", in the temporal region, less stress is present (not shaded). Here, the otic slit can form. The main stress lines are taken up by the jaw musculature ($F_{a1\text{-}2i/ii}$). In addition to the anterior bite, compressive stress from the jaw joint (F_j; green α) is indicated. The jaw muscles redirect the stresses to the lower jaw, where they distribute towards the point of attack. In this way, the circle of forces is closed (grey arrow in **A**). The stress lines from the anterior bite also travel along the palate (**D**) and are also taken up by jaw muscles (F_{a4+a2i}). Neck muscles ($F_{N1\text{-}2}$) are indicated, but do not have the same mechanical importance on the skull as in the reptiliomorphs (Figs 2–4) and, hence, no post-temporal bar is formed by them.

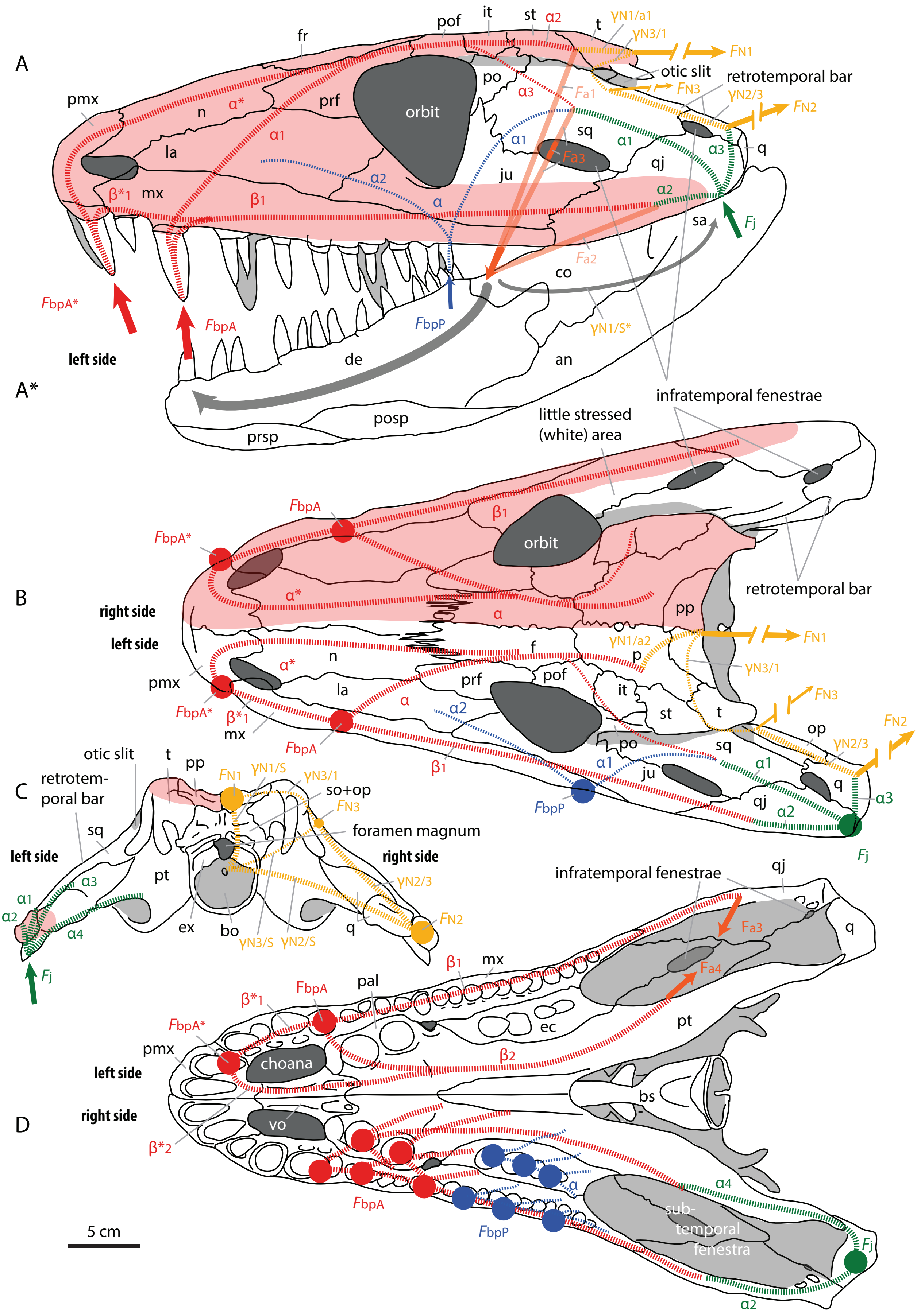
A
pmx
fr
pof
it
st
α2
t
γN1/a1
γN3/1
FN1
n
α*
prf
orbit
po
otic slit
retrotemporal bar
α3
Fa1
FN3
γN2/3
FN2
α1
la
α1
sq
α1
q
α3
β*1
mx
α2
Fa3
ju
qj
β1
α
α2
sa
Fj
Fa2
co
FbpA*
FbpA
FbpP
γN1/S*
left side
de
an
A*
infratemporal fenestrae
posp
prsp
little stressed
(white) area
β1
FbpA
FbpA*
orbit
retrotemporal bar
B
α*
right side
α
pp
left side
γN1/a2
FN1
f
p
n
γN3/1
α*
pof
pmx
prf
la
it
FN3
α
FbpA*
α2
st
t
β*1
mx
FN2
FbpA
op
β1
po
sq
γN2/3
α1
α1
ju
q
FbpP
α3
qj
α2
Fj
otic slit
t
pp
C
retrotem-
poral bar
FN1
γN1/S
γN3/1
so+op
FN3
sq
foramen magnum
left side
right side
α3
pt
α1
γN2/3
α2
α4
ex
bo
q
FN2
γN3/S
γN2/S
Fj
infratemporal fenestrae
qj
q
Fa3
β1
mx
Fa4
pal
β*1
FbpA
FbpA*
ec
pt
pmx
choana
β2
left side
bs
right side
D
vo
β*2
α
α4
FbpA
FbpP
sub-
temporal
fenestra
Fj
α2
5 cm

palatoquadrate leaving only the upper part of their intervening space (i.e. the spiracle) and no full gill slit open. In tetrapodomorphs, the hyomandibular of the hyoid apparatus and the upper jaw (palatoquadrate) became decoupled (Clack 2012; Schoch 2014a), which could have enabled a downward expansion of the external spiracle opening similar to the other pharyngeal slits in fish-like vertebrates – but it did not. Similar to the sensory organs described above, the skull bones are arranged around this developmentally pre-existing structure (i.e. pharyngeal opening). I argue that the specific architecture of bones around this opening depends on specific types of bite behaviour as outlined in the following.

A shift from the primarily fish-like suction to a primarily or exclusively prey-hunting feeding mode of tetrapods is obvious by the size reduction of the hyoid apparatus and by the large fangs in many temnospondyls (Fig. 1A*) and other early tetrapod groups such as whatcheeriids, baphetids and colosteids. Fangs of the lower jaw may leave a recess or an opening in the upper jaw (light grey shade in Fig. 1D). When the animal bites anteriorly, the snout has to withstand the external bite force (red F_{bpA} in the figures) and ossified areas are formed. Stress distributes along the whole snout (reddish shade in Figs 1A, B, 2A, B). Dorsally in the snout, there is compressive stress (red α in the Figures), whereas ventrally, tensional stress occurs (red β_1). As mentioned above, the sensory organs are formed early in ontogeny. Hence, when biting, the stress flows have to travel around the eye as visible in *Parotosuchus* (Fig. 1A, B) and *Anthracosaurus* (Fig. 2A, B). As a consequence, the area behind the eye is under little stress (“in the shadow of the eye”) resulting in less potential to ossify (Figs 1A–C, 2A–C, 5A).

In *Anthracosaurus*, the cheek region is even spatially recessed from the skull table (Fig. 2A–C). This unstressed recess area corresponds to the skull hinge of early sarcopterygian fishes (Kemp 1980; Abel and Werneburg 2021; Abel et al. 2022a; Werneburg and Abel 2022); but see Panchen (1964)). To manipulate some food items, anterior bite was present in addition to suction feeding, but this was to a much smaller extent when compared to the more advanced tetrapods. Similar to early sarcopterygian fishes, the spiracle “finds its position” within the posterior part of the mechanically unstressed “hinge area”, i.e. inside the otic notch of early tetrapods. This notch is lost in all undisputed amniotes (Figs 3, 4, 5B/C).

Based on the considerations above, I suggest that, in *Protoceratops*, the anterior bite is primarily concentrated on the animal’s beak ($F_{bpA/A*}$; Figs 4A, B, 5O). The associated compressive stress in the dorsal part of the skull (red $\alpha_{1/2}$) will be very high and extended, resulting in a specialised occiput with a crest-bearing elongated parietal ossification. This is similar to the condition seen in other “beaked” amniotes, such as turtles and anomodont synapsids with their supraoccipital crests and/or their broad parietal- and squamosal expansions in the back of the skull (Kemp 1980; Werneburg 2011, 2012, 2013a; Kammerer et al. 2014). In birds, no crest develops because of the roundish and compact braincase of these animals, which distributed forces more evenly (similar to the tube-like nose in mammals: see Preuschoft and Witzel (2002)).

B1-2. Circle of forces

Stresses increase along the skull (Werneburg and Preuschoft 2024) and, to avoid breakage, they are guided to close the “circle of forces”. In an animal exhibiting a perpendicular bite (shown on the left skull side in the Figures) without moving the head, the jaw adductor muscles (F_a) assist in guiding the stresses (α, β) from the temporal region back to the lower jaw and from there back to the point of attack (grey arrows in Figs 1A, A*, 4B*; only indicated in Fig. 3A*). Related to the differentiation of the temporal and palatal region, the jaw musculature is separated into different portions and muscle heads (dark orange F_{a1-5} in Figs 1, 3, 4) (Holliday and Witmer 2007; Diogo and Abdala 2010; Daza et al. 2011; Werneburg 2011, 2013a; Ferreira and Werneburg 2019; Ziermann et al. 2019).

By correspondence with traces of muscle attachments on the bones, Witzmann and Werneburg (2017) reconstructed the jaw muscles of *Parotosuchus* (here simplified as F_{a1}, F_{a2i}, F_{a2ii}). They aligned with the stress flows from the anterior bite (Fig. 1). In *Euparkeria* and *Protoceratops*, the jaw muscle heads originated on the temporal bars (F_{a2-3}) and the skull roof (F_{a1}; Figs 3A–C, 4A, B, D). Additionally, *Anthracosaurus* might have shown a similar complex differentiation of the jaw adductor musculature related to its differentiated temporal region (hinge and temporal opening; Fig. 2A).

B1-3. Infratemporal opening

At the jaw joint, i.e. between articular (art) and quadrate (q), compressive stress develops (green α), because of the force generated here (F_j) when biting. In early tetrapods, such as in *Parotosuchus* (Fig. 1), the force intensity at the

Figure 2. Skull (**A–D**) and lower jaw (**A***) of the early reptiliomorph *Anthracosaurus russelli* (Huxley 1863) in left lateral (**A, A***), dorsal (**B**), posterior (**C**) and ventral (**D**) views; after Panchen (1977) and Clack (1987). In addition to the processes shown in Fig. 1, strong anterior (F_{bpA}) and most anterior (F_{bpA}*) perpendicular bites (red) as well as weak posterior perpendicular (F_{bpP}, blue) bites are illustrated. The latter influences, together with the compressive stresses (green α_{1-3}) from the jaw joint (F_j), the shaping of the temporal region. The strong lateral neck muscle F_{N2} induces stress ($\gamma_{N2/3}$) in the retrotemporal part of the temporal region. The stress induced by F_{N3} ($\gamma_{N3/2}$) was not large enough to strongly shape the posttemporal region in the “shadow of the eye”, and a minute otic slit persisted. In the ventral view (**D**), the meaning of several teeth in the palate is indicated: Many bite points result in a mesh of stresses that result in the closure of palatal openings. A differentiation of three jaw adductor muscle portions (Fa_{1-3}) in the temple are hypothesised to correlate to the edges of the temporal opening and the upper temporal “hinge”-area (**A, A***).

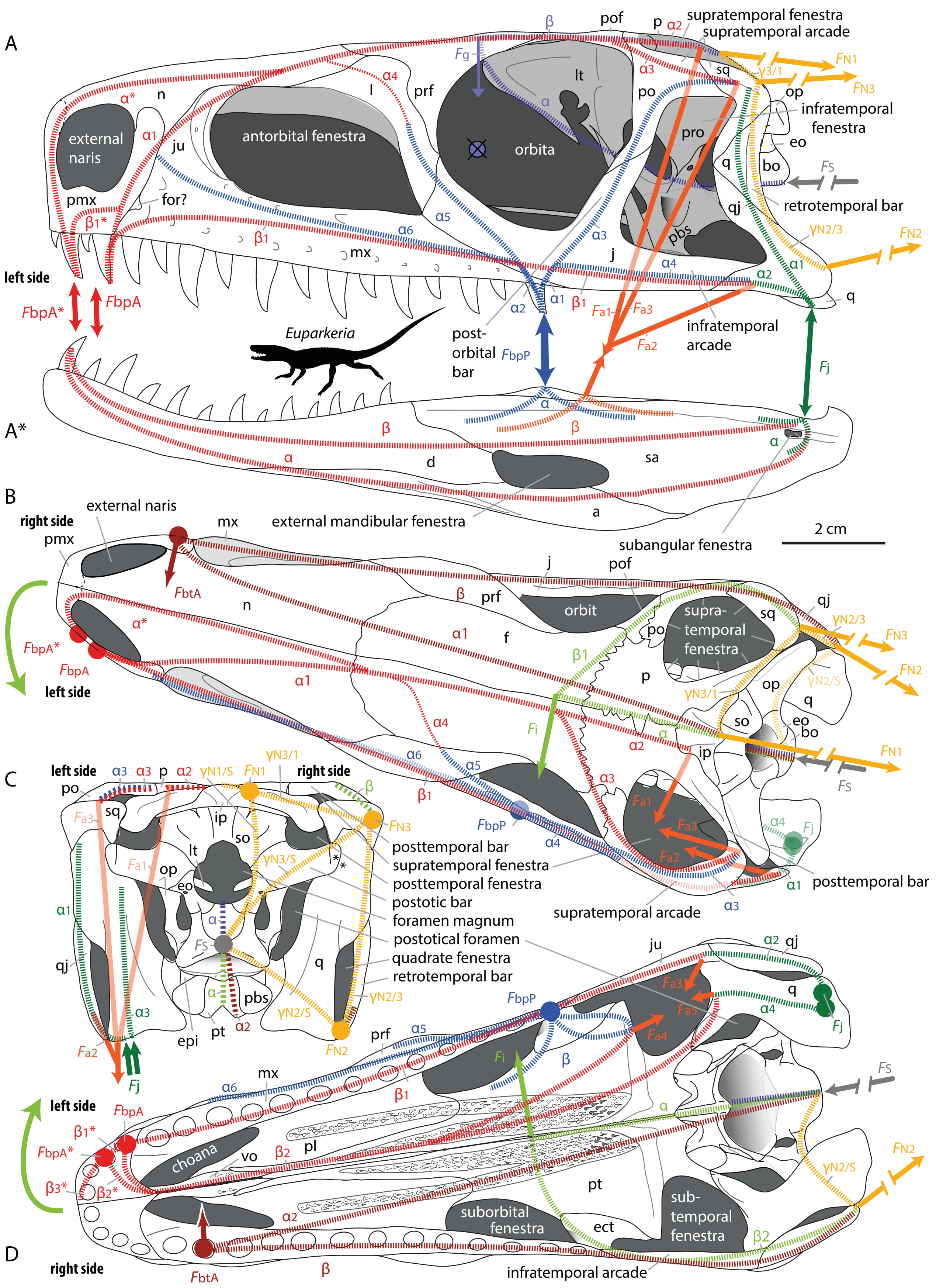
A
β
pof
p
α2
supratemporal fenestra
supratemporal arcade
Fg
α*
n
α4
l
prf
lt
α3
sq
FN1
γ3/1
FN3
po
op
infratemporal
fenestra
external
naris
α1
ju
antorbital fenestra
α
orbita
pro
eo
q
bo
Fs
pmx
for?
qj
retrotemporal bar
α5
α3
pbs
γN2/3
FN2
β1*
β1
α6
mx
j
α4
α1
α2
q
left side
α2
α1
β1
Fa1
Fa3
FbpA*
FbpA
Euparkeria
post-
orbital
bar
FbpP
Fa2
infratemporal
arcade
Fj
A*
α
β
β
α
α
d
sa
a
B
external naris
external mandibular fenestra
right side
mx
pmx
subangular fenestra
2 cm
FbtA
j
pof
n
β
prf
orbit
qj
α*
α1
f
supra-
temporal
fenestra
sq
γN2/3
FN3
FbpA*
po
FbpA
β1
left side
α1
p
FN2
γN2/S
op
γN3/1
q
Fi
α4
so
eo
bo
α
α2
ip
FN1
C
left side
α3
α3
p
α2
γN1/S
FN1
right side
α6
α5
Fs
po
γN3/1
β
β1
sq
ip
FN3
FbpP
α3
Fa1
Fa3
α4
Fj
so
α4
Fa3
lt
posttemporal bar
Fa1
op
γN3/S
supratemporal fenestra
Fa2
eo
posttemporal fenestra
α1
posttemporal bar
postotic bar
α
foramen magnum
supratemporal arcade
α3
α1
postotical foramen
ju
Fs
qj
q
quadrate fenestra
α2
qj
retrotemporal bar
α
pbs
γN2/3
Fa3
q
α3
α2
γN2/S
FbpP
Fa5
α4
pt
Fa4
Fj
Fa2
epi
FN2
prf
α5
Fi
β
Fj
mx
Fs
α6
β1
left side
FbpA
α
β1*
FbpA*
choana
vo
β2
pl
γN2/S
FN2
β3*
β2*
pt
α2
sub-
temporal
fenestra
suborbital
fenestra
ect
β2
D
right side
FbtA
β
infratemporal arcade

jaw joint may have been low, because of the joint's long distance to the major, pterygoid-related jaw muscle (F_{a4}) (Olson 1961). Stress from F_j (dark green $\alpha_{1\text{-}2}$) contributed to an enforcement of the cheek region. Here it was taken up by the jaw musculature ($F_{a2i/ii}$, Fig. 1B, D). The stress also travelled along the posterior border of the cheek, which is usually formed by quadratojugal (qj) and squamosal (sq) (dark green α_1; Fig. 1A).

Force at the jaw joint (F_j) is larger, when the jaw muscles are placed more posteriorly in the adductor chamber, because of the shorter lever arm to the joint (Olson 1961). A proportionally larger muscle mass posterior in the adductor chamber is associated with taller skulls to provide more area for muscle attachment. This is generally the case in Reptiliomorpha, including *Anthracosaurus* (Fig. 2) and amniotes (Figs 3, 4, 5C).

Please note that the here chosen species *Anthracosaurus russelli* is very special amongst Anthracosauridae (Embolomeri) in having a temporal fenestration similar to the amniote Synapsida and several parareptiles. It had a relatively high skull when compared to other early tetrapods and very large teeth on the jaws and on the palate (Fig. 1A, D), which distinguishes this animal as a specialised hunter with high bite forces (see also Porro et al. (2024)). This example also illustrates the large degree of convergences in the formation of temporal fenestrations amongst land vertebrates and strengthens the assessment that this character is not very informative in phylogenetic reconstructions (Abel and Werneburg 2021).

A retrotemporal bar is formed in fenestrated taxa. It is mainly established by the lateral neck musculature (F_{N2}), which is – because of higher neck mobility – much more strongly developed in reptiliomorphs (Fig. 5B) compared to early tetrapods (Starck 1979–1982; Kardong 2008). It inserts into the posterolateral angle of the skull. Amongst early reptiliomorphs, *A. russelli* might be interpreted as a transitional taxon in regard to a stronger neck development. A movement of the head, enabled by contraction of F_{N2}, induced a resulting stress flow (yellow $\gamma_{2/3}$) along the posterior border of the cheek region (Werneburg and Preuschoft 2024). The spatial relation of the insertion of F_{N2} to the jaw joint (Fig. 2) or even a transversal jaw movement may have resulted in different stress flows as in *A. russelli*, which, hence, developed two infratemporal openings (Fig. 2A, B, D). This, however, is a highly unusual case.

Recently, Werneburg and Bronzati (in press) have argued that, in crown diapsids, a great bite force would be correlated with the crescent- or crosier-shaped retrotemporal bar, which is unique to this clade and exemplified by *Euparkeria* herein (Fig. 3). The dorsal part of the retrotemporal bar (upper section of squamosal) aligned with the (blue and red) stress flows in their supratemporal arcade (see Section B1–4), whereas the ventral part (lower part of quadratojugal) aligned with the tensional stress flow of the infratemporal arcade. The re-orientation of the retrotemporal bar was related to a separation of the columella, which ancestrally served as a mechanical brace of the skull flank, but became integrated into the hearing system. Embryonically, the re-orientation of the retrotemporal bar results in a tissue separation from the quadrate anlage to contribute to the extracolumella cartilage, which enhances the sound transmission in the middle ear of crown diapsids (Werneburg and Bronzati, in press).

In ceratopsid dinosaurs (Fig. 4), the presence of a specialised, laterally exposed and posteriorly decoupled cheek region, which can be interpreted as a kind of armour (see Section B2), likely resulted in a re-orientation of the tensional stress from the anterior bite (F_{bpA}) away from the retrotemporal "edge" of the skull. In that configuration, the cheek-associated jaw musculature (F_{a2}) was separated from the remaining jaw muscle portions (F_{a1+3}) and inserted laterally into the dentary. The muscle (F_{a2}) might have allowed transversal, chewing-like movements and might have served as a soft cheek to prevent food from falling off the mouth during feeding (Varriale 2016). As such, it is equivalent to the musculus (m.) masseter in mammals (Schumacher 1985) and the m. zygomaticomandibularis in trionychian turtles (Werneburg 2011, 2013a; Rollot et al. 2024). A reorganisation of the lower temporal part of the skull frequently results in the separation of a lateral muscle also known for parrots (Tokita 2004) and lizards (Rieppel 1980; Werneburg 2013b).

My interpretation is close to older interpretations regarding the insertion of the chewing muscle (F_{a2}) to the lower jaw in ceratopsids (Haas 1955; Ostrom 1964, 1966; Holliday 2009). How far anterior or posterior the muscle originated at the skull flank can only be specified using muscle-associated riffling on the bones' surfaces (sensu Holliday (2009); Witzmann and Werneburg (2017)). Given the deep and long insertion groove in the dorsal face of the dentary (Ostrom 1964: fig. 5; see also Hatcher et al. (1907)), an origin at the upper jaw, also anterior to the tooth row, is quite plausible (Fig. 4A, B: F_{a2*}). My reconstruction of the cheek muscle differs from that of Nabavizadeh (2020a, b, 2023) and Nabavizadeh and Weishampel (2023), who did not discuss particular stress distributions in the skulls. However, the other muscle reconstructions provided by these authors can be confirmed by the considerations of the present paper (i.e. F_{a1+3}).

Figure 3. Skull (**A–D**) and lower jaw (A*) of the early archosauriform diapsid *Euparkeria capensis* (Broom 1913a) in left lateral (**A, A***), dorsal (**B**), posterior (**C**) and ventral (**D**) views; after Sookias et al. (2020). In addition to the processes shown in Figs 1, 2, the influence of a very strong posterior perpendicular bite (F_{bpP}) on the formation of the supratemporal, antorbital and mandibular fenestrae is indicated. With the establishment of an upper temporal bar, a clear separation of a new muscle portion is present (F_{a2}) [but it might have been present in *Anthracosaurus russelli* already, Fig. 2]. In **B–D**, transversal anterior bite forces (F_{btA}) as well as lateral movement of the head (large light green arrow) with the related inertia force (F_i) are illustrated. Half of the resulting stress flows take diagonal courses (light green $\beta_{1/2}$ + brown $\alpha_{1/2}$), which contribute to the shaping of the skull, such as the orientation of the supratemporal bar. ** in **C** indicates the pleurokinetic articulation.

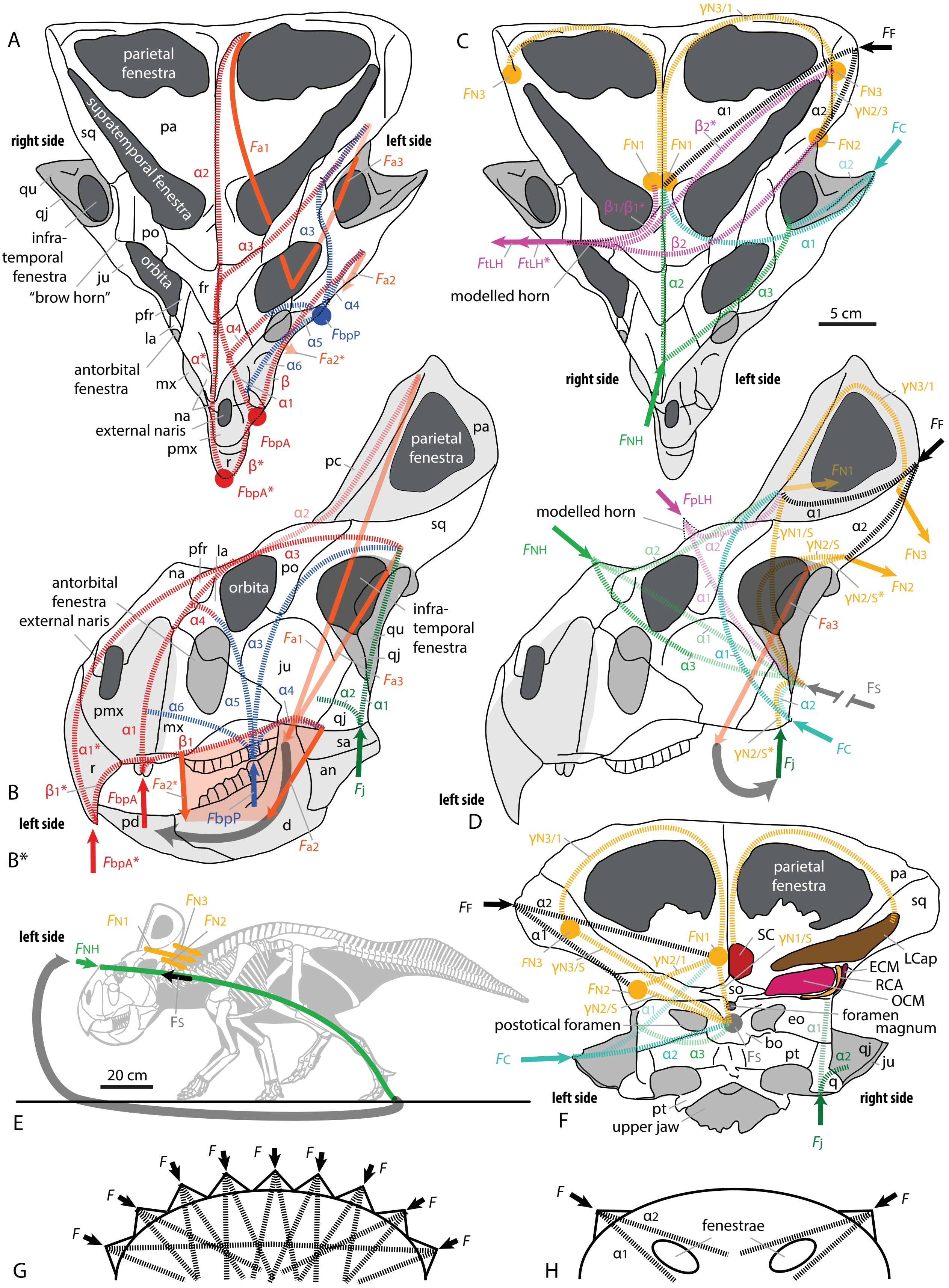
A
parietal fenestra
supratemporal fenestra
right side
left side
sq
pa
qu
qj
infra-temporal fenestra
po
orbita
ju
"brow horn"
fr
pfr
la
antorbital fenestra
mx
na
external naris
pmx
r
Fa1
Fa3
α2
α3
Fa2
α4
FbpP
α5
Fa2*
α6
β
α1
FbpA
β*
FbpA*
α*
C
FF
γN3/1
FN3
γN2/3
FC
FN1
FN2
β2*
β1/β1*
β2
FtLH
FtLH*
modelled horn
5 cm
right side
left side
FNH
B
pa
parietal fenestra
pc
sq
pfr
la
na
po
orbita
antorbital fenestra
external naris
infra-temporal fenestra
qu
qj
ju
pmx
mx
sa
an
d
pd
r
β1*
β1
α1*
FbpA
Fa2*
FbpP
Fa2
Fj
left side
B*
FbpA*
D
modelled horn
FpLH
FNH
γN1/S
γN2/S
γN2/S*
FN3
FN2
FN1
Fa3
FS
FC
Fj
left side
E
left side
FN1
FN3
FN2
FNH
FS
20 cm
F
γN3/1
parietal fenestra
pa
sq
FF
FN1
SC
γN1/S
LCap
ECM
RCA
OCM
FN3
γN3/S
γN2/1
FN2
γN2/S
so
postotical foramen
eo
foramen magnum
bo
FS
pt
FC
qj
ju
q
left side
right side
pt
upper jaw
Fj
G
F
H
F
α2
α1
fenestrae

A high anterior bite force can also be found in crocodiles. The related stress flows can be related to a very strong ossification in the skull roof and on the skull side. As a result, the genetically fixed upper and temporal fenestrations are suppressed in a way that the postorbital bar is retracted to a more medial position in the head and that the upper temporal openings are almost or completely closed. In such a way, a "pseudosynapsid" (or pseudoinfrafenestral) morphotype emerges "on top" of the diplapsid morphotype (Fig. 5L; Werneburg and Fernandez Blanco, in prep.).

B1-4. Supratemporal opening

As mentioned before, a greater bite force (blue F_{bpP}) can be generated posteriorly in the snout because of the shorter lever arm to the jaw joint (Preuschoft and Witzel 2002). Whereas synapsid amniotes originally favoured anterior bites with large fangs to pierce the skin of their large prey (Kemp 1982), diapsid amniotes (Fig. 3) originally developed posterior bites to crack the chitinous exoskeletons of their arthropod prey (Gregory and Adams 1915; Evans 2008; Werneburg and Preuschoft 2024).

A posterior bite along the snout (blue F_{bpP}) results in compressive stress below the eye (blue α). One part of this stress travels posterior to the eye (blue α_1), along the postorbital bar, which is built of jugal and postorbital (Fig. 2A). Here, this stress flow comes in contact with the compressive stress from the anterior perpendicular bite (red α_1) and both influence and redirect each other (Werneburg and Preuschoft 2024). The anterior stress flow (red α_1) separates into two sections above the eye (red α_{2+3}) and the lower part (red α_2) aligns with the re-orientated dorsal aspect of the postorbital part (blue α_1) of the posterior bite-related compression flow. In *Anthracosaurus*, it contributed to the stiffening of the upper cheek region (postorbital, squamosal) and the otic slit fell in between the separated stress flows of the anterior compressive stress (red α_{2+3}; Fig. 2A, B).

With increased neck mobility along the amniote stem, the otic slit was closed (Fig. 5B). This is because, between the original neck muscles (F_{N1} and F_{N2}), a new muscle portion has been established related to the now taller skull (F_{N3}; Figs 2–4). The contraction of this muscle portion results in a stress flow along the posterior part of the dorsal temporal region (yellow $\gamma_{\mathrm{N3/1}}$; Fig. 2A–C). When the posterior bite (F_{bpP}) is large enough, as visible in *Euparkeria* (Fig. 3B), the separation of the dorsal anterior stress flow (red α_1) becomes very distinct. The area in between these two sub-flows (red α_2+α_3) and the F_{N3}-induced enforcement of the skull (yellow $\gamma_{\mathrm{N3/1}}$) may then result in the formation of an upper temporal fenestra, posteriorly bordered by the post-temporal bar (Fig. 3A, B). This is a typical construction in almost all members of the Diapsida clade (Benton 2005). I refer to this group as 'Suprafenestralia' – not to replace the well-established name of the clade but: 1. to hint at its unique, non-diapsid (i.e. non-bifenestral sensu Abel and Werneburg (2021)) morphotype and 2. to also draw attention to the disputed interrelationship of the weakly-preserved earliest members of this group. Related to this, I introduce the terms "Fossafenestralia" (cf. sensu Maisch (2020)) and "Diplapsida" (cf. sensu Werneburg (2019)) to distinguish between the two major morphotypes in the advanced eureptiles (see Fig. 5).

In addition to the supratemporal fenestra, the early ceratopsian dinosaur *Protoceratops* had a parietal fenestra (Fig. 4A, B). Its medial border, the parietal, was much elongated to the frill. The bone still served, around its median crest, as the origin site of the medialmost jaw muscle portion (F_{a1}; Figs 4A, 5O). The elongation of the parietal evolved in response to the medially concentrated anterior-most bite force ($F_{\mathrm{bpA*}}$) at the peak of the rhamphotheca (r) and its related dorsal compressive stress (red α_{1*}/α_2) in the skull (Fig. 4A, B). The presence of the parietal fenestra (Fig. 5O) in addition to the supratemporal one is related to another external force, which will be discussed in Section B2–3.

As in other diapsid reptiles, the posterior extension of the dorsolateral muscle portion (F_{a3}), which takes up the stress from the posterior (blue α_3) and anterior bite (red α_3) in the upper temporal arcade, does not go much beyond the articulation of the squamosal with the quadrate in *Protoceratops* (cf. Nabavizadeh (2023)). The more posterior extension of the supratemporal fenestra is associated with the external forces (F_{F}, $F_{\mathrm{tLH*}}$) discussed in Section B2. Holliday et al. (2020) comprehensively discussed the filling of the extended supratemporal fossa with typical soft tissue like fat or blood vessels (e.g. for changing colouration or temperature in the animal's display).

B1-5. Orbita and naris

The naris and the orbit were already discussed as being related to the early presence of nose and eye organs in the embryo (Section A2). The dermal bones develop later and arrange around these organs (Rieppel 1993a, b). The orbit is originally surrounded by bones that are associated with the stress flows of anterior (F_{bpA}: red α, β_1 in Fig. 1) and posterior bites (F_{bpP}: blue $\alpha_{1/2}$ in Fig. 2, blue $\alpha_{3/5}$ in Fig. 3).

The nasal is surrounded by stress flows from anterior bites in the snout. Posteriorly, it is bordered by the

Figure 4. Skull (**A–D, F**) and lower jaw (**B***) of the early ceratopsid dinosaur *Protoceratops andrewsi* (Granger and Gregory 1923) in slightly rotated dorsal (**A, C**), in left lateral (**B, B*, D**) and in posterior (**F**) views; after Weishampel et al. (2004). **E.** Whole skeleton of the species in left lateral view (after Scott Hartmann, Wikimedia Commons, license: CC BY 4.0). **G, H.** Schematic view on the posterior edge of the skull (**G**) with external forces acting on several osteoderms or (**H**) just on one osteoderm on each side with one concentrated external force each. Only in the latter, parietal fenestrae can form. Note that stress from the neck muscles can be taken up by the jaw musculature, which is then guided to the lower jaw and the scruff of the neck (F_{S}). This is illustrated in **D** for F_{N2} only with its stress flow $\gamma_{\mathrm{N2/S*}}$ (see also Fig. 2A: $\gamma_{\mathrm{N1/S*}}$). Sutures in the basicranium in F are only tentatively drawn.

compressive stress (red α / red α_1 in the Figures) that was discussed above concerning the anterior perpendicular bite (F_{bpA}). This bite, however, only relates to the largest, the canine-like tooth. More anteriorly, at the incisor-like teeth, a further anterior bite force (F_{bpA*}) can develop. It introduces similar stress patterns as the canine-related bite (F_{bpA}) with a dorsal compression (red α^*/α^*_1) and a ventral tensional (red β^*/β^*_1) stress flow, which relate to bone structures anterior, dorsal and ventral to the naris – i.e. the premaxilla (Higashiyama et al. 2021) (Figs 2A, B, 3A, B, D, 4A, B).

In birds, the orbits and visual cortex of the brain are largely expanded, which results in a roundish braincase and a compressed temporal region of an infrafossal morphotype (Abel and Werneburg 2021). Additionally, the unique jaw mechanisms induced comprehensive changes of this area (Fig. 5M) (Bock 1964).

B1-6. Transversal bite

Pure perpendicular bite is rarely performed amongst tetrapods. Often the head is passively moved by fleeing prey or is actively moved to tear off food items. This results in transversal bite forces (F_{bt}), which distribute differently in the skull when compared to the perpendicular bite (F_{bp}). This typical condition is illustrated herein only for the anterior bite pointing to the mid-line of the skull (brown F_{btA} in Fig. 3B, D; i.e. on the right skull side). Further scenarios with other bite modalities were reconstructed by Werneburg and Preuschoft (2024) in detail.

The anterior transversal bite (F_{btA}) results in two stress flows. Tensional stress (brown β_1 in Fig. 3B, D) travels along the skull sides, along maxillary, jugal as well as quadratojugal and quadrate in *Euparkeria* – similar to the tensional stress of the perpendicular anterior bite (red β). The tensional stress from transversal biting (brown β) is then taken up by the lateral neck musculature (orange F_{N2}). Dorsally in the skull, compressive stress (brown α) develops from the point of attack and travels along the nasal, frontal, parietal and interparietal in *Euparkeria* (Fig. 3B). This stress flow is taken up by the medialmost neck musculature (yellow F_{N1}).

The medial and lateral neck muscles guided the stress along the neck, to the shoulder and the forelimbs, to finally close the "circle of forces" via the soil that *Euparkeria* and its prey shared (illustrated for the lateral direction of anterior and posterior transversal bite forces in fig. 4k of Werneburg and Bronzati, in press).

In situations where the head is passively swept to the side – a situation engendered by struggling prey (illustrated by the green bent arrow in front of the head in Fig. 3B, D) – inertia force (F_i) is applied at the centre of mass of the skull. This transversal force (F_i) also resulted in two stress flows (light green α and β in Fig. 3). The compressive stress (light green α) was also taken up by the medialmost neck musculature (F_{N1}). The tensional stress (light green β) was taken up by a lateral neck muscle (e.g. F_{N2}). Together with transversal bite forces in the back of the mouth (F_{btP}; not illustrated here, but see Werneburg and Preuschoft (2024)), the inertia force (F_i) contributed to shaping the orientation of the upper and lower temporal arcade.

When the head was actively pulled to the side, i.e. when tearing off food items, the resulting stresses from the inertia force (F_i) took different courses, further altering the orientation and architecture of the temporal region (see Werneburg and Preuschoft (2024) for further scenarios).

In the remaining parts of Section B1, I will elaborate upon the above explanations on the influence of the feeding mode on skull formation. Anterior and posterior perpendicular and transversal bites, as well as inertia force, help explain much of the architecture of the snout, the palate and the occipital region, all of which were not discussed by Werneburg and Preuschoft (2024) before.

B1-7. The antorbital fenestra

Most reptiles of the diapsid clade Archosauriformes (including birds, but excluding crocodiles) process an antorbital fenestra anterior to the orbit (Sookias et al. 2020) and there has been a variety of hypotheses on how to explain the presence of this opening (Witmer 1997; Werneburg et al. 2019). Certainly, several factors are likely to have acted simultaneously, resulting in the origin and remodelling of this fenestra. Amongst them, feeding-related forces are most important to consider.

The early archosauriform *Euparkeria* established the first adaptations to very powerful biting "on its way" towards the hypercarnivorous dinosaurs. In a recent contribution, Sookias et al. (2020) studied all cranial material of *Euparkeria* to reconstruct its skull anatomy in great detail. In their article, the authors inferred, using Anatomical Network Analysis (AnNA) (Esteve-Altava et al. 2011; Rasskin-Gutman and Esteve-Altava 2014), on the modularity of the skull bones and provided functional interpretations. Compared to the skull integration of other land vertebrates, including a theropod dinosaur and a crocodile (Werneburg et al. 2019), *Euparkeria* was shown to have possessed a flexible skull "well adapted to feeding on swift preys, but with a clear tendency towards more carnivorous behaviour, placing the taxon at the interface between ancestral diapsid and crown archosaur ecomorphology, corresponding to increases in brain size, visual sensitivity, upright locomotion and metabolism around this point in archosauriform evolution" (Sookias et al. 2020: p. 2).

As I have shown above (Section B1-4, the compressive stress (dark blue α) of the posterior perpendicular bite force (F_{bpP}) was distributed posterior to the orbit (dark blue α_1 in Fig. 2). With the formation of a distinct infratemporal arcade, as in *Euparkeria*, it was separated into two stress flows (dark blue α_{3+4}) to align with the major stress flows from the anterior bite (red α_3 and red β in Fig. 3).

Anterior to the eye, in the snout, the stress flow of the posterior bite (blue α_2 of Fig. 2A) took a steep course along the anterior border of the eye when an animal like *Euparkeria* bit hard (Fig. 3A). This process was further triggered by a strong anterior bite (F_{bpA}), with the related compression (red α_1) and tension (red β_1) stresses. They split and redirected the posterior perpendicular bite-related stress in front of the snout (blue α_2) into a dorsal (blue α_5) and a ventral (blue α_6) section, leaving the unstressed antorbital fenestra of the snout in between (Figs 3A, 5G). A similar splitting process was discussed in connection with the formation of the supratemporal fenestra above (Section B1-4).

The steep dorsal stress flow (blue α_5) was associated with the ossification in front of the orbit, i.e. the anterodorsal wing of the jugal and the lacrimal in *Euparkeria* (Fig. 3A). Around the lacrimal, it deflected a part of the compressive stress from the anterior bite (red α_4). The ventral part of the posterior bite-related stress flow (blue α_6) aligned with the tensional stress from the anterior bite (red β_1) along the maxillary.

The anterior and dorsal borders of the antorbital fenestra, formed by a dorsal wing of the maxilla and the nasal in *Euparkeria*, were associated with the compression flow of the anterior bite stress only (red α_1 in Fig. 3A).

The antorbital fenestra of the archosaur *Protoceratops* (Fig. 4) was narrower than in *Euparkeria* (Fig. 3) because of the influence of the beak, the height of the skull and fight-related forces (Section B2).

In general, the shape and size of the bars and fenestrae amongst taxa depend on the strengths and specific distributions of all the stresses discussed in this paper (Figs 1–5). Factors related to the general proportions, like brain and eye size or to other aspects of functional morphology, like chewing or suckling in mammals (Fig. 5J; Maier 1999; Herring et al. 2001), are worth considering. Specifying this further, however, goes beyond the scope of the present article.

B1-8. Palate

The palate of the early tetrapods was plesiomorphically formed by elongated bones, inherited from fish-like ancestors. In most species, the bite forces were not strong enough to induce a full closure of the palate region yet. The interpterygoid vacuities (Fig. 1D; Witzmann and Werneburg 2017; Witzmann and Ruta 2018) were filled with membranes, which were spanned in between the bony bars surrounding these vacuities. The membranes were considered to be related to suction breathing in the past (Schoch 2014a). However, in a recent study on extant batrachians, it has been shown that their function is more likely to be related to the transport of food (Witzmann et al. 2019). In any case, a functional constraint might have hindered the closure of the palate. Moreover, the flattening of the skull resulted in the expansion of different skull areas, which also partly explains the wide palatal vacuities in the temnospondyls (Fig. 1).

The palate of early reptiliomorphs and amniotes shows remarkable diversity (Lakjer 1927). Some taxa have vacuities (Fig. 3D), partly inherited from their early tetrapod ancestors. Others have more or less closed palates (Fig. 2D). According to Lautenschlager et al. (2016), I argue that the position and shape of the palatal bones also largely relate to the stress flows when feeding (D-panels in Figs 1–3).

Within the palate, the lateral stress flow of the anterior bite (F_{bpA}, red β_1 in Fig. 1) travelled along the maxillary, jugal and squamosal/quadratojugal in *Parotosuchus*. It was passed to the lower jaw via the jaw adductor musculature (Fig. 1D; $F_{a2i/ii}$; see also Fig. 1B).

The medial stress (red β_2) flow travelled medial to the choana in *Parotosuchus* (Fig. 1D). This skull opening was inherited from the fish-like precursors of tetrapods and corresponded to the internal (mouth) opening of the nasal organ. As with all sensory organs, it developed early in embryology and posed a spatial constraint for the skull architecture. The medial stress flow (red β_2) was then distributed along the vomer (v) and the cultriform process of the parasphenoid (ps-pc) in *Parotosuchus* (Fig. 1D). Here the stress was taken up by the anterior jaw musculature (F_{a4}). The compressive stress (dark green α_4) that developed from the jaw joint (F_j) might have also travelled along the posterior part of the palate and been taken up by the same jaw musculature. The posterior jaw adductors ($Fa_{1,2i+ii}$) extended to the lower jaw through the subtemporal fenestra. In between both openings, the subtemporal fenestra and the interpterygoid vacuity, the pterygoid braced to the braincase. It could also transmit stresses from posterior perpendicular biting as illustrated for the right skull sides of *Anthracosaurus* (Fig. 2D) and *Euparkeria* (Fig. 3D; blue F_{bpP}).

The tensional stress from the more anterior bite at the tip of the snout (F_{bpA*}) distributed laterally along the premaxillary (red β^*_1) and medially along the vomer (red β^*_2), surrounding the choana anteriorly as shown in *Anthracosaurus* (Fig. 3D).

The posterior bite force (F_{bpP}, dark blue β) was not only distributed laterally along the skull flank (Figs 2A, B, 3A, B, 4A, B), but also medially to the palate, where it corresponded with particular ossifications such as the ectopterygoid (ec) (Figs 2D, 3D, left skull sides). Part of the posterior stress flow was taken up by the jaw adductor musculature (F_{a4}; i.e. "pterygoideus muscle"; Fig. 3D).

Many early tetrapods showed extensive palatal dentition (Benton 2005; Clack 2012; Schoch and Milner 2014). The small denticles on the pterygoid and palatine bones served in the fixation and processing of food (Sues 2000), suggesting different points and magnitudes of the anterior and posterior bites ($F_{bpA} + F_{bpP}$) and their related stresses resulting in different shapes of the palate. This becomes obvious in *Anthracosaurus* with its almost fully closed palate (Fig. 2D).

Additionally, the temporal arches can be shaped by palatal bite. The early synapsid *Edaphosaurus*, for example, was a herbivore with extended palatal dentition. The skull has a fossafenestral morphotype (different from the infrafenestral morphotype in its close relative *Dimetrodon*; Abel and Werneburg (2021, 2024); Werneburg and Preuschoft (2024)) and the suborbital fenestra is fully closed (Sues and Reisz 1998; Sues 2000), suggesting an extremely high posterior bite force on the palate.

As in the case of the temporal region (Werneburg and Preuschoft 2024), transversal stresses play a role in shaping the palate. A bite force directed to the mid-line of the skull (F_{btA}) led to tensional stress along the maxillary, jugal and quadratojugal, as shown in *Euparkeria* (brown β in Fig. 3D, right skull side) and was taken up by the lateral neck muscle (F_{N2}). Compressive stress was distributed more medially (brown α_2 in Fig. 3D) along the palatine, the pterygoid and the basicranium to reach the occipital condyle (F_S). In the described direction of the stress flow, mass inertia pointed to the direction of the opposite skull side (F_i). The medial stress flow from the F_i (light green α in Fig. 3D) reached the occipital condyle medially (F_S) and the lateral stress flow (light green β_2) travelled towards the lateral neck muscle (F_{N2}), passing the pterygoid, ectopterygoid, jugal and quadratojugal. Taking it all together, the suborbital fenestra in *Euparkeria* was surrounded and internally built by different stress lines, which aligned along maxillary, palatine, pterygoid and ectopterygoid (Fig. 3D).

The chewing behaviour in *Protoceratops* (Varriale 2016) did not result in a closure of the palate. In mammals, chewing also does not influence the formation of the secondary palate – milk-sucking behaviour, in contrast, is most important for that (Maier 1999).

B1-9. Fenestrae of the lower jaw

As in most Archosauriformes (Fig. 5G, L–N), a mandibular fenestra can be found in *Euparkeria capensis* (Fig. 3A*). A mandibular fenestra is usually associated with a rather elongated lower jaw, which is exposed to high bending loads and strong symphyses (see Lessner et al. (2019)). Similar to the snout discussed above, the anterior bite resulted in compressive (red α) and tensile (red β) stresses in *Euparkeria*, which flowed along the ventral and dorsal borders of the lower jaw. In between those stress flows, an unstressed area existed. As a result, a mandibular foramen could form along the sutures between dentary, surangular and angular.

More posteriorly, in *Euparkeria*, a subangular fenestra is present (Fig. 3A*). As with the more posterior infratemporal opening in *Anthracosaurus russelli* (Fig. 2A, B), specific jaw movement abilities might have been responsible for the formation of this area without biomechanical stress. Modelling different amounts and directions of forces on the jaw joint will help understanding altering morphotypes.

The mandibular fenestra was secondarily closed in the archosaur *Protoceratops* (Fig. 5O), likely as a result of the influence of the jaw musculature (F_{a2}) inserting into the dorsal and lateral face of the mandible (Fig. 4B*).

B1-10. Small openings in the skull

Whereas I discussed the major fenestrae of most tetrapods above, other cranial openings require brief comments. These include several foramina with little stresses, which permit the passage of nerves and vessels (e.g. Demes (1985)), particularly in the neurocranium, but also in other parts of the skull.

In *Euparkeria*, the median pineal foramen (Smith et al. 2018), below which the parietal organ usually receives information on light intensity in land vertebrates, was absent. It is, however, plesiomorphically present in reptiles (Evans 2008). Menaker et al. (1997) correlated the absence of the foramen with a potential nocturnality in *Euparkeria*. The foramen, however, is clearly visible in the extant mostly nocturnal tuatara (Jones et al. 2011; Cree 2014).

Feeding-related stresses in the skull would rather support the fusion of median openings in the skull; however, the physiological importance of the pineal organ requires the pineal foramen to stay open from the early beginning with bone formation in late embryonic development (Rieppel 1992; Zhang et al. 2022), similar to the other sensory organs discussed.

The tuatara also has a frontonasal fontanelle (Jones et al. 2011). It appears to be related to its unique functional feeding morphology. Werneburg et al. (2019) found a complex separation of anterior (incl. nasal and prefrontal) and posterior (incl. frontal) functional snout modules in tuatara, which might support a rather loose connection of the skull roof in this area (sensu Werneburg and Abel (2022)), perhaps also related to some degree of mesokinetic mobility (at least in the juveniles, see Rieppel (1992); Jones et al. (2011); Yaryhin and Werneburg (2019); Zhang et al. (2022)).

In turtles, the parietal foramen is closed, presumably due to the strong neck retraction-related forces exerted on the skull roof (Werneburg et al. 2021).

B2. Further external forces acting on the skull

B2-1. Cranial weapons

During the terrestrialisation process, not only feeding, but also inter- and intraspecific combat behaviour changed. In several land vertebrates, cranial weapons evolved for defence. At foremost, these include horns and exposed osteoderms, but also expansions of cranial regions, such as the frill of ceratopsian dinosaurs or the wide cheek expansions of the diplocaulid nectrideans. In the latter, in particular, multiple functions of such structures are plausible including the use for swimming (e.g. Cruickshank and Skews (1980); Skews (2016)). Amongst temnospondyls, small horns are known for zatracheids (e.g. *Acanthostomatops*, *Zatrachys*; Schoch (1997); Witzmann and Schoch (2006)) and the dissorophoid *Stegops* (R. Werneburg et al. 2023). Amongst amniotes, taxa with cranial armour can be found amongst reptiles and mammals (e.g. Bovidae) with horns, antlers, osteoderms or just keratinised spines (Bubenik and Bubenik 1990; Hall 2015; Gates et al. 2016; Nabavizadeh 2023).

There are several studies on the evolution and function of the cranial armour of ceratopsians, comprehensively reviewed by Nabavizadeh (2023) and I already discussed some adaptations of the jaw musculature related to it (Section B1-3). Fig. 4 shows my interpretations of the biomechanics of the ceratopsian skull exemplified by *Protoceratops*. The initial cranial armour in ceratopsian evolution consisted of a vaulted beak, a nasal protuberance and a cheek extension as visible in *Psittacosaurus*, for example, followed by the frill, a medial nasal horn, large paired horns above the eye and, finally, large osteoderms at the edge of the frill (Nabavizadeh 2020b, 2023). *Protoceratops* already showed a well-developed frill and close relatives would evolve a nasal horn. Above the eyes, small protuberances "foreshadowed" the lateral horns of more advanced species such as *Triceratops horridus* (Hatcher et al. 1907). True cranial horns were not present in *Protoceratops*, although its protuberances likely already had a similar functional meaning. As such, I modelled the horns as dashed lines in Fig. 4C, D (F_{NH}, F_{pLH}, $F_{tLH/tLH*}$) to better illustrate my principle thoughts as outlined below.

B2-2. Nasal horn

The unpaired nasal protuberance of *Protoceratops* received an external force (F_{NH}), which resulted in a comprehensive distribution of compressive stresses. One of them (light green α_1) travelled along the anteroventral margin of the braincase [visible through the infratemporal fenestra in Fig. 4D] and was received by the scruff of the neck (F_S). A second one (light green α_2) travelled along the skull roof and was received by the medial neck muscle (F_{N1}; i.e. m. spinalis capitis, SC, sensu Tsuihiji (2010)); Fig. 4C, D). This pattern was similar to the stresses induced by the skull weight (F_g) as reconstructed by Werneburg and Preuschoft (2024: fig. 2) and as illustrated for *Euparkeria* herein (Fig. 3A: purple $\alpha+\beta$). A third stress (light green α_3) flow developed around the anterior curvature of the eye and found its way along the nasal, lacrimal, jugal and medial to the exposed cheek, along the pterygoid towards the occipital condyle (F_S) (Fig. 4C, D, F).

Stress distributions within the skulls of rhinoceroses might be similar to that of *Protoceratops* with broad insertions of the nape muscles (F_{N1}) on the skull. The pre-orbital stress flow (light green α_3) of rhinoceroses certainly distributed along the strong infratemporal bar to reach the occiput.

B2-3. Parietal fenestra

In case a force (*F*F) acted on the posterolateral edge of the frill in *Protoceratops* (Fig. 4C, D, F, H), the resulting stresses travelled (as black α_1) toward the medial-most neck muscle (F_{N1}) and (as black α_2) towards the neck muscle posterior to the posterodorsal corner of the infratemporal fenestra (F_{N3}; i.e. m. longissimus capitis Pars articuloparietalis, LCap, sensu Tsuihiji (2010)). In between them, the posterior half of the supratemporal fenestra was situated as an unstressed area. Posteriorly, the supratemporal fenestra corresponded to the external force related to combat (*F*F). The anterior part of the fenestra, however, was related to the stress flows of anterior and posterior perpendicular bite (Section B1-4; dark blue α_3 and red α_{2+3} in Fig. 4A, B). As discussed for *Anthracosaurus* and *Euparkeria* above (Section B1-3), the action of the lateral most muscle (F_{N3}) resulted in the formation of the post-temporal bar (yellow $\gamma_{N3/1}$), which mainly distributes along the posterior border of the broad parietal in *Protoceratops*. The parietal itself had its own fenestra, which spanned between the neck muscle-related stress flow (yellow $\gamma N_{3/1}$) of the post-temporal bar and the stress flow from combat-/fight-related forces (F_F, F_{tLH} – see Section B2-5, for the latter). Noteworthy, the parietal fenestra was formed within one single bone, whereas all other openings of the skull are formed at least in between two bones.

The frill in Ceratopsida experienced a great diversification, with some taxa having parietal openings and some not (Nabavizadeh 2023). I hypothesise that this was largely related to the appearance of the frill as a weapon. A weaponry with many spines, such as in *Triceratops horribilis* (Hatcher et al. 1907), evenly distributed several external forces at the frill and the many resulting stress flows hindered the formation of a parietal foramen (Fig. 4G). This is mechanically similar to the use of many palatal teeth in taxa with closed palatines (Fig. 2D). Single salient osteoderms (i.e. "epiossifications" after Loewen et al. (2024)) or frill edges as in *Protoceratops* (Fig. 4C, D, F), concentrated the stress of a single external force (*F*F) and resulted in clear-cut borders of a frill foramen (Fig. 4H).

In this context, I wish to mention the origin of turtles. Recently, a series of cranial "horn cores" (cf. Fig. 4G) have been discovered in the Late Triassic *Proganochelys* (Scheyer et al. 2022), one of the earliest representatives of the anapsid (labelled as 'infrafossal' in Fig. 5) Testudinata (Joyce 2007). This does not come as a surprise given the spiny osteoderms of this species on the dorsal side of the neck and it fits into the general picture of early turtle defensive behaviour, which includes the formation of a fully formed shell (Gaffney 1990; Werneburg et al. 2015a). Cranial armour is known from other stem turtles (e.g. *Meiolania*; Gaffney (1983)) and was likely used in intraspecific combats (Jannel 2015).

Turtles are currently considered to have derived from diapsid ancestors, based on molecular and morphological data (Rieppel 2008; Wang et al. 2013; Simões et al. 2022; Werneburg et al. 2024b) and, hence, must have closed their temporal openings in one way or another. In previous works, I developed an evolutionary scenario whereby the influence of neck retraction resulted in the reorganisation and secondary closure of the temporal region in turtle ancestors (Werneburg 2015; Werneburg et al. 2015a; Werneburg et al. 2015b; Böhmer and Werneburg 2017; Cordero and Werneburg 2018; Ferreira and Werneburg 2019; Werneburg 2019; Werneburg and Maier 2019; Ferreira et al. 2020; Werneburg 2020; Abel and Werneburg 2021; Werneburg et al. 2021; Werneburg and Abel 2022; Werneburg and Preuschoft 2023; Werneburg et al. 2024b). Given the discovery of osteoderms in *Proganochelys* (Scheyer et al. 2022), I would expand these thoughts (Fig. 5: "D+F+H"). When external forces were taken up by the osteoderms, broad compressive stresses were added to the posterior edge of the skull. To withstand, the temporal opening(s) might have closed. As such, the stresses from the horns were more evenly distributed into the skull (cf. Fig. 4G). A hypothesis of early turtles showing a fossorial lifestyle and stiffening the temporal opening by digging (similar to caecilians), can be excluded because a slender rather than a roundish, shell-related trunk would be required for such behaviour (discussed by Werneburg et al. (2024b)).

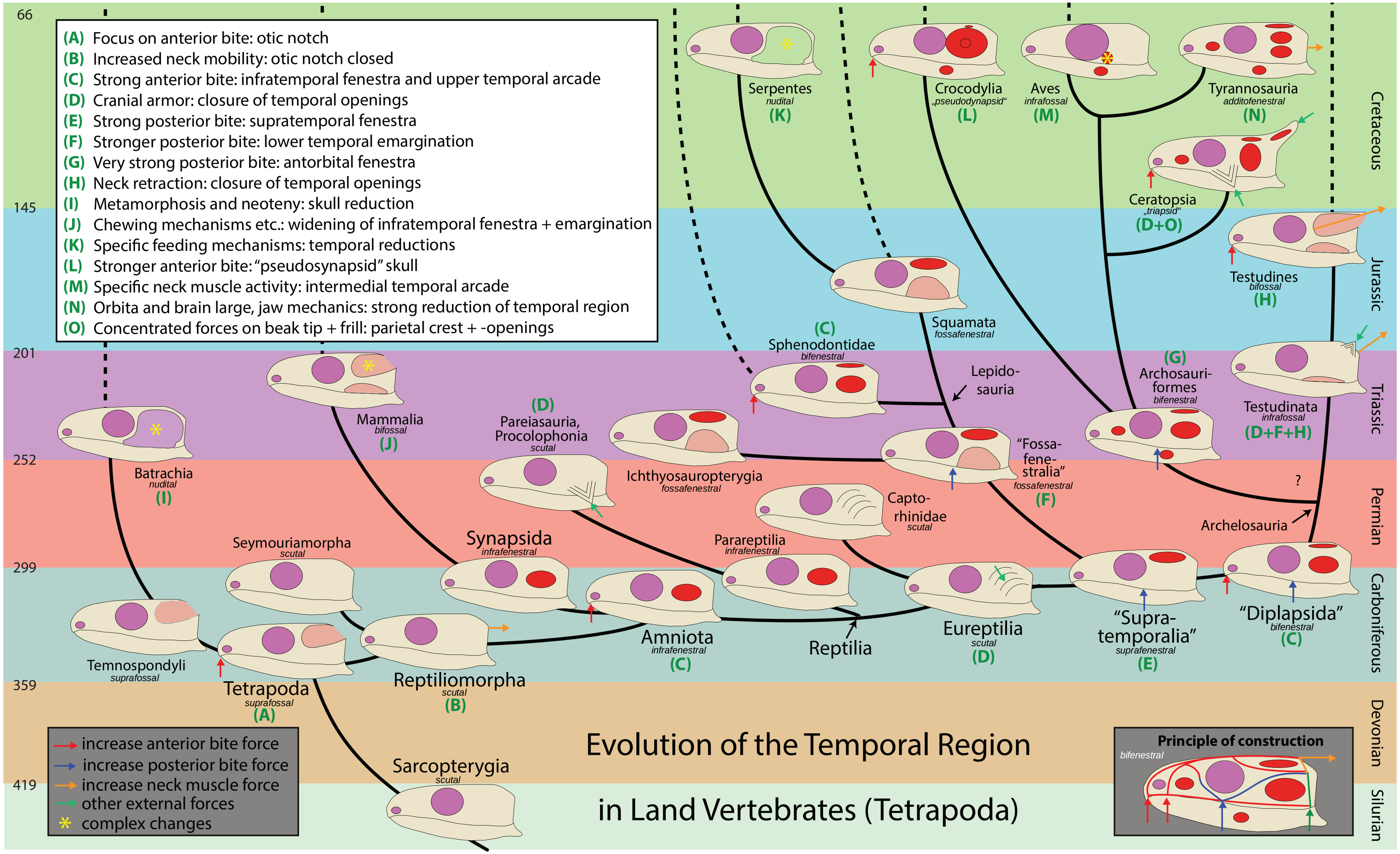
66
145
201
252
299
359
419
Cretaceous
Jurassic
Triassic
Permian
Carboniferous
Devonian
Silurian
(A) Focus on anterior bite: otic notch
(B) Increased neck mobility: otic notch closed
(C) Strong anterior bite: infratemporal fenestra and upper temporal arcade
(D) Cranial armor: closure of temporal openings
(E) Strong posterior bite: supratemporal fenestra
(F) Stronger posterior bite: lower temporal emargination
(G) Very strong posterior bite: antorbital fenestra
(H) Neck retraction: closure of temporal openings
(I) Metamorphosis and neoteny: skull reduction
(J) Chewing mechanisms etc.: widening of infratemporal fenestra + emargination
(K) Specific feeding mechanisms: temporal reductions
(L) Stronger anterior bite: "pseudosynapsid" skull
(M) Specific neck muscle activity: intermedial temporal arcade
(N) Orbita and brain large, jaw mechanics: strong reduction of temporal region
(O) Concentrated forces on beak tip + frill: parietal crest + -openings
Serpentes
nudital
(K)
Crocodylia
„pseudodynapsid"
(L)
Aves
infrafossal
(M)
Tyrannosauria
additofenestral
(N)
Ceratopsia
„triapsid"
(D+O)
Testudines
bifossal
(H)
Squamata
fossafenestral
(C)
Sphenodontidae
bifenestral
Lepido-
sauria
(G)
Archosauri-
formes
bifenestral
Testudinata
infrafossal
(D+F+H)
Mammalia
bifossal
(J)
(D)
Pareiasauria,
Procolophonia
scutal
Batrachia
nudital
(I)
Ichthyosauropterygia
fossafenestral
"Fossa-
fene-
stralia"
fossafenestral
(F)
?
Capto-
rhinidae
scutal
Archelosauria
Seymouriamorpha
scutal
Synapsida
infrafenestral
Parareptilia
infrafenestral
Temnospondyli
suprafossal
Amniota
infrafenestral
(C)
Reptilia
Eureptilia
scutal
(D)
"Supra-
temporalia"
suprafenestral
(E)
"Diplapsida"
bifenestral
(C)
Tetrapoda
suprafossal
(A)
Reptiliomorpha
scutal
(B)
Sarcopterygia
scutal
Evolution of the Temporal Region
in Land Vertebrates (Tetrapoda)
increase anterior bite force
increase posterior bite force
increase neck muscle force
other external forces
complex changes
Principle of construction
bifenestral

B2-4. Cheek weapons

External force (F_C) on the lateral cheek extensions (cheek wings) of *Protoceratops* was guided, firstly (light blue α_1), at the skull's surface along quadratojugal, jugal, postorbital and frontal/parietal towards the central nape muscle (F_{N1}; Fig. 4D, F). A second major stress flow (light blue α_2) extended medially along the jugal/quadratojugal and the pterygoid and was taken up by the scruff of the neck at the occipital condyle (F_S; Fig. 4D, F). The orientation of the cheek weapon, which could have been equipped with a distinct horn, resulted in changed directions of the stress flows and, hence, different patterns of skull ossifications (Fig. 5D). This is well visible in the skull of the therapsid *Estemmenosuchus* as well as in most parareptilian Procolophonia (incl. Pareiasauromorpha and Procolophonidea). In the latter, distinct horns developed on the cheekbones (Fig. 5) and a "deformation" of the whole temporal region is visible (e.g. MacDougall and Reisz (2014)). Likely this led to the closure of the infratemporal fenestration that is otherwise visible in other parareptiles and other early amniotes, such as *Mesosaurus*, *Eunotosaurus*, Millerosauria and Bolosauridae, as well as many procolophonids without cheek armour. The influence of the cheek armour may even help explain the peculiar extension of the orbit above the cheek-wing and into the temporal region of many procolophonids.

In this regard, the evolutionary origin of temporal fenestration in amniotes might be briefly discussed (see also Abel and Werneburg (2021, 2024); Werneburg (2024)). Except for very few species (e.g. *Anthracosaurus russelli*, Fig. 2), most non-amniotic Reptiliomorpha had an anapsid skull condition, which is often considered ancestral for early Reptilia (Fig. 5B). In contrast, all undisputed synapsids have an infratemporal opening (Fig. 5). Reconstructions of early amniote phylogeny often result in contradicting scenarios for the origin of temporal openings (Ford and Benson 2020; Simões et al. 2022). In this regard, I wish to mention the contested monophyly and ingroup relationships of the early reptilian parareptiles, many of which have fenestrated temporal regions (Cisneros et al. 2004; Modesto et al. 2009; Piñeiro et al. 2012; MacDougall and Reisz 2014); see also this debate: (Laurin and Piñeiro 2017; Laurin and Piñeiro 2018; MacDougall et al. 2018).

Throughout all of their life, most early amniotes faced a completely different, i.e. harder food supply outside the aquatic milieu when compared to non-amniotic tetrapods. It is well imaginable that the earliest amniotes primarily made use of their ancestral focus on anterior bite (see Figs 1, 2), which resulted – in association with the formation of the neck muscle-related retrotemporal bar (yellow α_{N3}; Section B1-3) – in the formation of an infratemporal opening (Fig. 5C). External forces acting on the head – resulting from combat or fossorial behaviour – might have resulted in the closure of the infratemporal opening in Eureptilia (Fig. 5D), as also discussed for Procolophonia above. In this regard, the heavily sculptured skull ossification of the eureptilian captorhinids (Fig. 5); (Abel et al. 2022b) and *Brouffia* (Fox and Bowman 1966; Abel et al. 2022a; Klembara et al. 2024) is worth mentioning. With more gracile skulls – related to a less exposed lifestyle (maybe in an arboreal habitat) – early diapsids might have re-evolved the infratemporal fenestration (Fig. 5) – in addition to their posterior bite-related supratemporal opening (cf. Fig. 5E) to feed on (tree-dwelling) arthropods (see Section B1-4; Fig. 5).

B2-5. Lateral horns

Protoceratops already had distinct "brow" protuberances above the eye (Fig. 4A). As mentioned in the Introduction, I use the *Protoceratops* model to discuss a condition as if it would have had well-exposed lateral horns above the eye (dotted horn in Fig. 4C, D) that otherwise many ceratopsids had. When an external force (F_{pLH}) directly acted on such a horn (Fig. 4D), the compressive stress flows (pink α_{1+2}) were transmitted toward the medial neck muscle (F_{N1}) and the scruff of the neck (F_S).

In case the horn was pulled to the side (e.g. inside the belly of a tyrannosaur), transversal forces acted on the skull. The principle is similar as explained with different scenarios by Werneburg and Preuschoft (2024) for transversal bite force and briefly discussed for *Euparkeria* above (Section B1-6). Here, in Fig. 4C, I illustrate only two cases in which the external force on the lateral horn is directed away from the skull ($F_{tLH/tLH*}$; cf. Werneburg and Preuschoft (2024): fig. 8b, d, f). If the force was large (F_{tLH}), then one tensional stress flow (pink β_1) travelled along the parietal and was taken up by the medial neck muscle (F_{N1}). A second major stress flow (pink β_2) travelled to the other side of the skull, along the parietals, the postorbital and the squamosal to the lateralmost neck muscle (F_{N2}). If the transversal force on the lateral horn was small (F_{tLH*}), then the angle between the major stress flows was smaller. The first stress flow (pink β_1*) was taken up by the medial neck muscle (F_{N1}) again, whereas the second one (pink β_2*) took a different course, along the parietals, towards the muscle in between F_{N1} and F_{N2},

Figure 5. Hypothesis on land vertebrate interrelationships and skull evolution, based on biomechanical considerations, with a focus on the temporal region. Morphotypes (mainly sensu Abel and Werneburg (2021)) are indicated below the taxon names. Apomorphic and convergent traits are listed in the figure. Specific discussion of these traits can be found in the text of (**A**) Section B1-1, (**B**) Section B1-3, (**C**) Sections B1-3 and B2-4, (**D**) Sections B2-3 and -4, (**E**) Section B1-4, (**F**) Werneburg and Preuschoft (2024) and Section B1-3, (**G**) Section B1-7, (**H**) Sections B2-7 and B2-3, (**I**) Section A1, (**J**) Werneburg and Preuschoft (2024) and Preuschoft et al. (in press), (**K**) Section A1, (**L**) Section B1-3, (**M**) Section B1-5, (**N**) Section B2-7, (**O**) Section B2-3. See also Werneburg (2024). The idiosyncratic names for advanced eureptile groups are based on the hypothesised evolution of the temporal region and do not necessarily represent phylogenetic relationships (sensu Werneburg (2019)). However, please note the uncertainties of the interrelationship of early eureptilian taxa in the literature. By spatial restriction, the Late Cretaceous Ceratopsia had to be placed to the lower part of green field.

namely F_{N3} (Fig. 4C), which then transferred the stress into the body (see Section B1-6). The strength, the preferred transversal direction (e.g. medial or lateral) of the external force, as well as the size and the orientation of the lateral horns contributed to an altering shape of the lateral border of the parietal. In that way, also the shapes of the supratemporal, as well as the parietal fenestrae, were defined.

B2-6. Body posture

For all forces not related to perpendicular bites ($F_{bpA/A*/P}$), namely the transversal bites ($F_{btA/A*/P}$) and the cranial armour-related forces (F_F, F_C, F_{pLH}, F_{tLH}), the resulting stresses (a/β) were taken up by the vertebral column (scruff of the neck, F_S), as well as by the neck muscles ($\mathrm{F}_{N1\text{-}3}$). The postcranial skeleton assisted in closing the circle of forces (Section B1-6).

In those cases where a medial force (F_{NH}) acted on the beak or the medial horn (Fig. 4C, D), the resulting stresses (light green $\alpha_{1\text{-}3}$) were transferred to the vertebral column and further along the skeleton to the hind limbs (Fig. 4E, green arrow), which supported the body against the ground and guided back the forces – via the soil (Fig. 4E, grey arrow) – towards the origin of the initial force (F_{NH}) that acted on the skull.

In those cases where external forces acted transversally to the skull ($F_{btA/A*/P}$, F_F, F_C, F_{pLH}, F_{tLH}), transversal stress flows reached the postcranium. First, they were taken up by the transversal processes/ribs of the neck vertebrae (Preuschoft et al. 2022). Then the stresses continued in the transversal direction towards the shoulder and to the sprawled forelimbs in reptiles and early synapsids or to the splayed-out forelimbs in horned and antlered mammals. After that, the stresses reached the ground to eventually close the circle of forces (Preuschoft and Gudo 2005; Werneburg and Bronzati, in press).

In summary, the postcranial bones were structured and arranged not only in relation to locomotion, but also in response to the forces acting on the skull. This is particularly clear in ceratopsids, which have more or less upright hind limbs to support a pushed-back body and the forelimbs could be sprawled in the lateral direction to prevent the body from falling over to the side when fighting (Preuschoft and Gudo 2006: fig. 9). Animals with less transversal forces on the head, namely without cranial armour and a rather perpendicular bite, tend to have less transversal processes/ribs and less sprawled fore-limbs (Preuschoft et al. 2022; Preuschoft et al., in press). This is the case for mammals with their modified teeth, which reduced transversal bite behaviour (Preuschoft et al., in press). Additionally, shoulder anatomy depends on head posture and movements as outlined in all the cited works of Holger Preuschoft.

Three major neck muscles ($F_{N1\text{-}3}$) have been discussed in this paper (Fig. 4E). Of course, in reality, there are more to take up specific stresses from the skull (see right side of Fig. 4F). The second major function of the dorsal neck muscles is to lift the skull above the ground. Partly stiff tendons and ligaments can develop to save energy (e.g. in horses). The weight of the head, therefore, plays a crucial role also for the reshaping of the dorsal vertebrae with some taxa having very high and bent neural processes in their vertebrae and shoulder humps may develop (e.g. bison).

B2-7. Occipital region

Posterior views of the skulls are shown in the C-panels of Figs 1–3 and in Fig. 4F. Pulling neck muscles also directly influence the shape of the occipital region and the adjacent skull parts. Werneburg and Preuschoft (2024: fig. 13b, c) have shown that some of the stresses are taken up by parts of the jaw musculature, which transmit them towards the lower jaw. These stresses are then transferred to the jaw joint (F_j) and from there to the occipital condyle (F_S) to close the circle of forces (Fig. 2A: $\gamma_{N1/S*}$; 4D: $\gamma_{N2/S*}$).

As explained above, the compressive stress induced by F_{N3} is associated with the formation of the posttemporal arcade ($\gamma_{N3/1}$), which not only borders the supratemporal fenestra posteriorly, but also the posttemporal fenestra at its dorsal side (Fig. 3C). The ventral border of the post-temporal fenestra, in contrast, is formed by the ancestral pleurokinetic joint (** in Fig. 3C) between palatoquadrate (i.e. via its quadrate part) and neurocranium (Natchev et al. 2016; Werneburg and Maier 2019).

The stress flow resulting from F_{N2} and with that the posteroventral margin of the skull in most species, pointed towards the middle of the skull ($\gamma_{N2/S}$) and connected the quadrate and the pterygoid with the braincase in *Euparkeria* (Fig. 3C), leaving an unstressed area below the pleurokinetic joint, the foramen postoticum. With the structural reorganisations related to the frill, the stresses of the neck muscles were reorientated in *Protoceratops* (Fig. 4F).

A quadrate fenestra was formed between quadrate medially and quadratojugal laterally in *Euparkeria* and was associated with the compressive stress flows (dark green α) from the force acting in the jaw joint (F_j; Fig. 3C). If such a quadrate fenestra has formed, a complex jaw movement can be expected (indicated by two dark green arrows in Fig. 3C).

The stress flows from the bite points and the cranial weapons reached the occiput dorsomedially, ventrolaterally and dorsolaterally and were transmitted by the respective neck muscle (F_{N1}, F_{N2} and F_{N3}). It is apparent in the palatal and occipital views of the skull (Figs 2C, 3C, D, 4F) that several stress flows culminated in the occipital condyle. They were already mentioned in the previous Sections and should be kept in mind when interpreting occiput architecture. In this context, it is worth noting that reptiles only have one condyle, whereas therapsid synapsids and advanced temnospondyls have two. This condition can be explained by the high transverse forces in carnivorous taxa associated with different transversal stress directions that reach the occiput at different places. Towards Mammalia, i.e. amongst synapsids, the condyles shift more dorsally to assume a more lateral place in relation to the foramen magnum. This prohibits or at least makes difficult the lateral rotation of the head and so facilitates the formation of an atlas-axis system (pers. comm. Holger Preuschoft in 2023).

Although mainly receiving stresses from external forces on the skull, neck muscles (as well as the jaw muscle) will also induce some stresses into the skull, beyond the occipital region. Great pulling of the dorsal neck muscles ($F_{N1/2}$) has been discussed for the neck retraction mode of turtles, which influences the shaping of the temporal region and might even have contributed to the closure of the temporal openings in turtle ancestors (see Section B2-3) (Werneburg 2015). The movement and the posture of the neck contribute to the strengthening of the temporal arches, behind which the major neck muscles insert.

In this regard, the additofenestral condition of tyrannosaurids may be mentioned (Fig. 5N) (Plateau and Foth 2020). They have a temporal bar within the infratemporal fenestra which develops from the occipital regions. I discussed the unique functional morphology of *Tyrannosaurus* feeding elsewhere (Werneburg et al. 2019), and here I suggest that specific neck movements during feeding resulted in a stress flow that is taken up – via this unique temporal bar – to a separate muscle portion in these dinosaurs.

This final Section on the occipital region illustrates, again, that skull architecture needs to be analysed in a holistic manner, whereby distinct biomechanical conditions need to be considered in the context of the animal's behaviour as well as its life history mode. The four species exemplarily discussed herein may serve as a starting point for future more sophisticated technical assessments of skull biomechanics, such as the use of finite element analyses.

Conclusions

The present contribution is a novel approach to understanding the enormous cranial diversity of land vertebrates. It takes both comparative anatomy as well as biomechanical considerations into account to provide a comprehensive picture of skull formation in time and space. Moreover, developmental and behavioural aspects of extant and extinct animals are incorporated to draw a comprehensive picture of skull evolution.

The evolution of cranial openings in tetrapods is, firstly, largely related to ontogenetic strategies with differences in directly developing and metamorphosing animals on one hand and larval and non-larval life histories on the other hand. Secondly, modulations of anterior and posterior bite points, the bite intensity, as well as the presence of cranial armour, such as horns and cheek wings (e.g. pareiasaurs, procolophonids, turtles, ceratopsids, bovids) or just bone thickenings (e.g. early eureptiles) correspond to the presence or closure of cranial openings. A scenario for the evolution of temporal skull openings is provided (Fig. 5).

It is shown that a strong bite anterior in the snout, as well as breathing behaviour, originally influenced the formation of the otic slit and the interpterygoid formamen in the earliest tetrapods. With increased terrestrialisation in the amniote stem group, neck muscles became very important for skull formation and their tension resulted in the formation of a straight border at the posterior edge of the skull. An infratemporal fenestra appears to be ancestral to amniotes (Fig. 5C) – at least from a biomechanical point of view.

A preference for biting posteriorly in the jaw resulted in the formation of an upper temporal fenestra (and a ventral temporal excavation). Increased posterior bite force triggered the formation of an antorbital and a mandibular fenestra in Archosauriformes (Fig. 5G). The lower temporal bar of diapsid reptiles corresponds with a strengthened anterior bite.

Jaw muscles mainly relate to perpendicular bites. Neck muscles, in contrast, take up the stresses from transversal bite as well as from all other external forces acting on the skull. This leads to comprehensive responses in the postcranial skeleton to close the circle of forces. However, skeletal responses to neck muscle tension also appear in the occiput and other regions of the skull. This is most obvious in turtle evolution with neck retraction largely altering the skull anatomy.

The present paper may serve as a framework for future quantitative biomechanics that take a holistic view of the skull, in which ontogenetic, evolutionary, as well as comprehensive morphological aspects of skull architecture, will be considered.

Acknowledgements

I am grateful to Florian Witzmann (Berlin) for discussion and the invitation to contribute to this Special Issue on "The fish-to-tetrapod transition and the conquest of land by vertebrates". Marcello Ruta (Bristol) and Stephanie Woodgate (Berlin) are thanked for their useful comments on the manuscript. I also thank Holger Preuschoft (Bochum), Felix Augustin, Pascal Abel (Tübingen) and Marc E. H. Jones (London) for discussions. The study was supported by the grant WE 5440/6-1 of Deutsche Forschungsgemeinschaft.

References

Abel P, Pommery Y, Ford DP, Koyabu D, Werneburg I (2022a) Skull sutures and cranial mechanics in the Permian stem-reptile *Captorhinus aguti* and the evolution of the temporal region in early amniotes. Frontiers in Ecology and Evolution 10: 1–28. https://doi.org/10.3389/fevo.2022.841784

Abel P, Pommery Y, Ford DP, Koyabu D, Werneburg I (2022b) 3D models related to the publication: Skull sutures and cranial mechanics in the Permian reptile *Captorhinus aguti* and the evolution of the temporal region in early amniotes. MorphoMuseuM 8: 1–2. https://doi.org/10.18563/journal.m3.167

Abel P, Werneburg I (2021) Morphology of the temporal skull region in tetrapods: research history, functional explanations, and a new comprehensive classification scheme. Biological Reviews 96: 2229–2257. https://doi.org/10.1111/brv.12751

Abel P, Werneburg I (2024) The temporal region of the tetrapod skull: a textbook example on integrative morphology. Revue de Paleobiologie 43: 101–118.

Ahlberg PE (2018) Follow the footprints and mind the gaps: a new look at the origin of tetrapods. Earth and Environmental Science Transactions of the Royal Society of Edinburgh 109: 115–137. https://doi.org/10.1017/S1755691018000695

Benton MJ (2005) Vertebrate Palaeontology. Blackwell Publishing, Malden, Oxford, Carlton.

Berman DS (2013) Diadectomorphs, amniotes or not? New Mexico Museum of Natural History and Science Bulletin 60: 22–35.

Bock WJ (1964) Kinetics of the avian skull. Journal of Morphology 114: 1–42. https://doi.org/10.1002/jmor.1051140102

Böhmer C, Werneburg I (2017) Deep time perspective on turtle neck evolution: chasing the *Hox* code by vertebral morphology. Nature Scientific Reports 7: 1–14. https://doi.org/10.1038/s41598-017-09133-0

Bramble D, Wake D (1985) Feeding Mechanisms of Lower Tetrapods. In: Hildebrand M, Bramble D, Liem K, Wake D (Eds) Functional Vertebrate Morphology. Harvard University Press, Cambridge, 230–261. https://doi.org/10.4159/harvard.9780674184404.c13

Broom R (1913a) Note on *Mesosuchus browni*, Watson, and on a new South African Triassic pseudosuchian (*Euparkeria capensis*). Records of the Albany Museum 2: 394–396.

Broom R (1913b) On the South-African pseudosuchian *Euparkeria* and allied genera. Proceedings of the Zoological Society of London 83: 619–633. https://doi.org/10.1111/j.1469-7998.1913.tb06148.x

Bubenik GA, Bubenik AB [Eds] (1990) Horns, Pronghorns, and Antlers: Evolution, Morphology, Physiology, and Social Significance. Vol. Springer-Verlag, New York. https://doi.org/10.1007/978-1-4613-8966-8

Cisneros JC, Damiani R, Schultz C, da Rosa Á, Schwanke C, Neto LW, Aurélio PLP (2004) A procolophonoid reptile with temporal fenestration from the Middle Triassic of Brazil. Proceedings of the Royal Society of London, B 271: 1541–1546. https://doi.org/10.1098/rspb.2004.2748

Clack JA (1987) Two new specimens of *Anthracosaurus* (Amphibia: Anthracosauria) from the Northumberland Coal Measures. Palaeontology 30: 15–26.

Clack JA (2012) Gaining Ground. The Origin and Evolution of Tetrapods. Second Edition. Indiana University Press, Bloomington, 544 pp. https://www.jstor.org/stable/j.ctt16gz91r

Clement AM (2019) Sarcopterygian Fishes, the "Lobe-Fins". In: Ziermann JM, Diaz Jr RE, Diogo R (Eds) Heads, Jaws, and Muscles: Anatomical, Functional, and Developmental Diversity in Chordate Evolution. Springer International Publishing, Cham, 119–142. https://doi.org/10.1007/978-3-319-93560-7_6

Cordero GA, Werneburg I (2018) Reconstructing the Evolution of Neck Retraction. In: Hirayama R, Kuratani S, Takahashi A, Nakajima Y, Sonoda T, Nishioka Y, Yoshida M (Eds) 6th Turtle Evolution Symposium, Tokyo, 26-2852018. Scidinge Hall Verlag, Tübingen, 26–29.

Cree A (2014) Tuatara: Biology and Conservation of a Venerable Survivor. Canterbury University Press, Christchurch, New Zealand, 583 pp.

Cruickshank ARI, Skews BW (1980) The Functional-Significance of Nectridean Tabular Horns (Amphibia, Lepospondyli). Proceedings of the Royal Society Series B-Biological Sciences 209: 513–537. https://doi.org/10.1098/rspb.1980.0110

Daza JD, Diogo R, Johnston P, Abdala V (2011) Jaw adductor muscles across lepidosaurs: a reappraisal. The Anatomical Record 294: 1765–1782. https://doi.org/10.1002/ar.21467

de Beer GR (1937) The Development of the Vertebrate Skull. Oxford University Press, New York, [xxiv+] 552 pp.[+143 plates pp.]

Demes B (1985) Biomechaniscs of the Primate Skull Base. In: Dunker HR, Fleischer DG (Eds) Functional Morphology in Vertebrates Forschriftte der Zoologie 30. Gustav Fischer, Jena, 139–143.

Dial KP, Shubin N, Brainerd EL [Eds] (2015) Great Transformations in Vertebrate Evolution. Vol. University of Chicago Press, Chicago. https://doi.org/10.7208/chicago/9780226268392.001.0001

Diogo R, Abdala V (2010) Muscles of Vertebrates. CRC Press / Science Publishers, Boca Bacon, New York, Oxon / Enfield. https://doi.org/10.1201/9781439845622

Diogo R, Abdala V (2011) The Head Muscles of Dipnoans—A Review on the Homologies and Evolution of these Muscles within Vertebrates. In: Jørgensen JM, Joss J (Eds) The Biology of Lungfishes. CRC Press, Enfield, 169–218.

Diogo R, Abdala V, Lonergan N, Wood B (2008) From fish to modern humans – comparative anatomy, homologies and evolution of the head and neck musculature. Journal of Anatomy 213: 391–424. https://doi.org/10.1111/j.1469-7580.2008.00953.x

Daeschler EB, Shubin NH, Jenkins Jr FA (2006) A Devonian tetrapod-like fish and the evolution of the tetrapod body plan. Nature 440(7085): 757–763. https://doi.org/10.1038/nature04639

Cloutier R, Clement AM, Lee MS, Noel R, Bechard I, Roy V, Long JA (2020) Elpistostege and the origin of the vertebrate hand. Nature 579(7800): 549–554. https://doi.org/10.1038/s41586-020-2100-8

Edgeworth FH (1935) The Cranial Muscles of Vertebrates. Cambridge University Press, London.

Esteve-Altava B, Marugan-Lobon J, Botella H, Rasskin-Gutman D (2011) Network Models in Anatomical Systems. Journal of Anthropological Sciences 89: 175–184.

Evans SE (2008) The Skull of Lizards and Tuatara. In: Gans C, Gaunt AS, Adler K (Eds) Morphology H The Skull of the Lepidosauria. Society for the Study of Amphibians and Reptiles, Salt Lake City, 1–347.

Evans SE, Sigogneau-Russell D (2001) A stem-group caecilian (Lissamphibia: Gymnophiona) from the Lower Cretaceous of North Africa. Palaeontology 44: 259–273. https://doi.org/10.1111/1475-4983.00179

Ferreira GS, Lautenschlager S, Evers SW, Pfaff C, Kriwet J, Raselli I, Werneburg I (2020) Feeding biomechanics suggests progressive correlation of skull architecture and neck evolution in turtles. Scientific Reports 10: 5505. https://doi.org/10.1038/s41598-020-62179-5

Ferreira GS, Werneburg I (2019) Evolution, diversity, and development of the craniocervical system in turtles with special reference to jaw musculature. In: Ziermann JM, Diaz Jr RE, Diogo R (Eds) Heads, Jaws, and Muscles. Springer, 171–206. https://doi.org/10.1007/978-3-319-93560-7_8

Ford DP, Benson RB (2020) The phylogeny of early amniotes and the affinities of Parareptilia and Varanopidae. Nature Ecology & Evolution 4: 57–65. https://doi.org/10.1038/s41559-019-1047-3

Fox RC, Bowman MC (1966) Osteology and relationships of *Captorhinus aguti* (Cope) (Reptilia: Captorhinomorpha). The University of Kansas Paleontological Contributions Vertebrata 11: 1–79. https://hdl.handle.net/1808/3815

Fröbisch NB, Witzmann F (2019) Early tetrapods had an eye on the land. Nature 574: 494–495. https://doi.org/10.1038/d41586-019-03107-0

Gaffney ES (1983) The cranial morphology of the extinct horned turtle, *Meiolania platyceps*, from the Pleistocene of Lord Howe Island, Australia. Bulletin of the American Museum of Natural History 175: 361–480.

Gaffney ES (1990) The comparative osteology of the Triassic turtle *Proganochelys*. Bulletin of the American Museum of Natural HIstory 194: 1–263. http://hdl.handle.net/2246/884

Gai ZK, Zhu M, Ahlberg PE, Donoghue PCJ (2022) The evolution of the spiracular region from jawless fishes to tetrapods. Frontiers in Ecology and Evolution 10: 887172. https://doi.org/10.3389/fevo.2022.887172

Gates TA, Organ C, Zanno LE (2016) Bony cranial ornamentation linked to rapid evolution of gigantic theropod dinosaurs. Nature Communications 7: 12931. https://doi.org/10.1038/ncomms12931

Granger W, Gregory WK (1923) *Protoceratops andrewsi*, a pre-ceratopsian dinosaur from Mongolia. American Museum of NaturalHistory Novitates 72: 1–9.

Gregory WK (1935) 'Williston's law' relating to the evolution of skull bones in the vertebrates. American Journal of Physical Anthropology 20: 123–152. https://doi.org/10.1002/ajpa.1330200202

Gregory WK, Adams LA (1915) The temporal fossæ of vertebrates in relation to the jaw muscles. SCIENCE 41: 763–765. https://doi.org/10.1126/science.41.1064.763

Haas G (1955) The jaw musculature in *Protoceratops* and in other ceratopsians. American Museum Novitates: 1–24.

Hall BK (2015) Bones and Cartilage: Developmental and Evolutionary Skeletal Biology (2nd edition). Elsevier Academic Press, San Diego, [xxxviii +] 760 pp.

Hatcher JB, Marsh OC, Lull RS (1907) The Ceratopsia. Government Printing Office, Washington. https://doi.org/10.5962/bhl.title.60500

Herring SW, Rafferty KL, Liu ZJ, Marshall CD (2001) Jaw muscles and the skull in mammals: the biomechanics of mastication. Comparative Biochemistry and Physiology Part A 131: 207–219. https://doi.org/10.1016/S1095-6433(01)00472-X

Higashiyama H, Koyabu D, Hirasawa T, Werneburg I, Kuratani S, Kurihara H (2021) Mammalian face as an evolutionary novelty. Proceedings of the National Academy of Sciences of the United States of America 118(44): e2111876118. https://doi.org/10.1073/pnas.2111876118

Hohn-Schulte B, Preuschoft H, Witzel U, Distler-Hoffmann C (2013) Biomechanics and functional preconditions for terrestrial lifestyle in basal tetrapods, with special consideration of *Tiktaalik roseae*. Historical Biology 25: 167–181. https://doi.org/10.1080/08912963.2012.755677

Holliday CM (2009) New insights into dinosaur jaw muscle anatomy. The Anatomical Record 292: 1246–1265. https://doi.org/10.1002/ar.20982

Holliday CM, Porter WR, Vliet KA, Witmer LM (2020) The frontoparietal fossa and dorsotemporal fenestra of archosaurs and their significance for interpretations of vascular and muscular anatomy in dinosaurs. Anatomical Record-Advances in Integrative Anatomy and Evolutionary Biology 303: 1060–1074. https://doi.org/10.1002/ar.24218

Holliday CM, Witmer LM (2007) Archosaur adductor chamber evolution: integration of musculoskeletal and topological criteria in jaw muscle homology. Journal of Morphology 268: 457–484. https://doi.org/10.1002/jmor.10524

Hülsmann E, Wahlert Gv (1972) Das Schädelkabinett - Eine erklärende Naturgeschichte der Wirbeltiere. Basilius Presse, Basel.

Huxley TH (1863) Description of *Anthracosaurus russelli*, a new labyrinthodont from the Lanarkshire coal-field. Quarterly Journal of the Geological Society 19: 56–68. https://doi.org/10.1144/GSL.JGS.1863.019.01-02.11

Jannel A (2015) Neck mobility, grazing habits, and intraspecific combat behaviour in the Giant Pleistocene horned turtle *Meiolania platyceps*. Uppsala Universitet.

Jones MEH, Curtis N, Fagan MJ, O'Higgins P, Evans SE (2011) Hard tissue anatomy of the cranial joints in *Sphenodon* (Rhynchocephalia): sutures, kinesis, and skull mechanics. Palaeontologia Electronica 14: 1–92.

Joyce WG (2007) Phylogenetic relationships of Mesozoic turtles. Bulletin of the Peabody Museum of Natural History 48: 3–102. https://doi.org/10.3374/0079-032X(2007)48[3:PROMT]2.0.CO;2

Kammerer CF, Angielczyck KD, Fröbisch J (2014) Early Evolutionary History of the Synapsida. Springer, Dortrecht. https://doi.org/10.1007/978-94-007-6841-3

Kardong KV (2008) Vertebrates: Comparative Anatomy, Function, Evolution. McGraw–Hill Primis.

Kean KJ, Danto M, Pérez-Ben C, Fröbisch N (2024) Evolution of the tetrapod skull: a systematic review of bone loss. Fossil Record 27(3): 445–471. https://doi.org10.3897/fr.27.133803

Kemp T (1980) Origin of the mammal-like reptiles. Nature 283: 378–380. https://doi.org/10.1038/283378a0

Kemp TS (1982) Mammal-like reptiles and the origin of mammals. Academic Pr.

Kemp TS (2005) The Origin and Evolution of Mammals. University Press, Oxford. https://doi.org/10.1093/oso/9780198507604.001.0001

Kleinteich T (2009) The evolution of intrauterine feeding in the Gymnophiona (Lissamphibia): A comparative study on the morphology, function, and development of cranial muscles in oviparous and viviparous species. Universität Hamburg, Hamburg.

Kleinteich T, Haas A (2007) Cranial Musculature in the larva of the caecilian, *Ichthyophis kohtaoensis* (Lissamphibia:Gymnophiona). Journal of Morphology 268: 74–88. https://doi.org/10.1002/jmor.10503

Klembara J, Ruta M, Anderson J, Mayer T, Hain M, Valaška D (2024) A redescription of *Brouffia orientalis* Carroll & Baird, 1972 from the Upper Carboniferous of the Czech Republic and the status and affinities of protor othyridid amniotes. Swiss Journal of Palaeontology 143: 33. https://doi.org/10.1186/s13358-024-00329-2

Koyabu D, Werneburg I, Morimoto N, Zollikofer CPE, Forasiepi AM, Endo H, Kimura J, Ohdachi SD, Son NT, Sanchez-Villagra MR (2014) Mammalian skull heterochrony reveals modular evolution and a link between cranial development and brain size. Nature Communications 5: 3625. https://doi.org/10.1038/ncomms4625

Lakjer T (1927) Studien über die Gaumenregion bei Sauriern im Vergleich mit Anamniern und primitiven Sauropsiden. Zoologische Jahrbücher 49: 57–356.

Laurin M (2010) How Vertebrates Left the Water. University of California Press, Berkeley, Los Angeles, London, 216 pp. https://doi.org/10.1525/9780520947986

Laurin M, Piñeiro G (2018) Response: Commentary: A reassessment of the taxonomic position of mesosaurs, and a surprising phylogeny of early amniotes. Frontiers in Earth Science 6: 220. https://doi.org/10.3389/feart.2018.00220

Laurin M, Piñeiro GH (2017) A reassessment of the taxonomic position of mesosaurs, and a surprising phylogeny of early amniotes. Frontiers in Earth Science 5: 88. https://doi.org/10.3389/feart.2017.00088

Lautenschlager S, Witzmann F, Werneburg I (2016) Palate anatomy and morphofunctional aspects of interpterygoid vacuities in temnospondyl cranial evolution. Science of Nature 103: 79. https://doi.org/10.1007/s00114-016-1402-z

Lessner EJ, Gant CA, Hieronymus TL, Vickaryous MK, Holliday CM (2019) Anatomy and ontogeny of the mandibular symphysis in *Alligator mississippiensis*. The Anatomical Record 302: 1696–1708. https://doi.org/10.1002/ar.24116

Liem KF, Bemis WE, Walker WF, Grande L (2001) Functional Anatomy of the Vertebrates - An Evolutionary Perspective. Harcourt College Publishers, 703 pp.

Loewen MA, Sertich JJW, Sampson S, O'Connor JK, Carpenter S, Sisson B, Ohlenschlaeger A, Farke AA, Makovicky PJ, Longrich N, Evans DC (2024) *Lokiceratops rangiformis* gen. et sp. nov. (Ceratopsidae: Centrosaurinae) from the Campanian Judith River Formation of Montana reveals rapid regional radiations and extreme endemism within centrosaurine dinosaurs. PeerJ 12. https://doi.org/10.7717/peerj.17224

Long JA (2011) The Rise of Fishes. 500 Million Years of Evolution (2nd edition). John Hopkins University Press, Baltimore.

Lowie A, De Kegel B, Wilkinson M, Measey J, O'Reilly JC, Kley NJ, Gaucher P, Adriaens D, Herrel A (2023) The anatomy of the head muscles in caecilians (Amphibia: Gymnophiona): Variation in relation to phylogeny and ecology? Journal of Anatomy 242: 312–326. https://doi.org/10.1111/joa.13763

MacDougall MJ, Modesto SP, Brocklehurst N, Verrière A, Reisz RR, Fröbisch J (2018) Commentary: A reassessment of the taxonomic position of mesosaurs, and a surprising phylogeny of early amniotes. Frontiers in Earth Science 6: 99. https://doi.org/10.3389/feart.2018.00099

MacDougall MJ, Reisz RR (2014) The first record of a nyctiphruretid parareptile from the Early Permian of North America, with a discussion of parareptilian temporal fenestration. Zoological Journal of the Linnean Society 172: 616–630. https://doi.org/10.1111/zoj.12180

Maier W (1999) On the evolutionary biology of early mammals - with methodological remarks on the interaction between ontogenetic adaptation and phylogenetic transformation. Zoologischer Anzeiger Festschrift D Starck 238: 55–74.

Maier W, Werneburg I [Eds] (2014) Schlüsselereignisse der organismischen Makroevolution. Scidinge Hall Verlag, Zürich.

Maisch MW (2020) The evolution of the temporal region of placodonts (Diapsida: Placodontia) – a problematic issue of cranial osteology in fossil marine reptiles. Palaeodiversity 13: 57–68. https://doi.org/10.18476/pale.v13.a6

Menaker M, Moreira L, Tosini G (1997) Evolution of circadian organization in vertebrates. Brazilian Journal of Medical and Biological Research 30: 305–313. https://doi.org/10.1590/S0100-879X1997000300003

Mitgutsch C, Wimmer C, Sanchez-Villagra MR, Hahnloser R, Schneider RA (2011) Timing of ossification in duck, quail, and zebra finch: lntraspecific variation, heterochronies, and life history evolution. Zoological Science 28: 491–500. https://doi.org/10.2108/zsj.28.491

Modesto SP, Anderson JS (2004) The phylogenetic definition of Reptilia. Systematic Biology 53: 815–821. https://doi.org/10.1080/10635150490503026

Modesto SP, Sues H-D, Scott DM, Reisz RR (2009) A new parareptile with temporal fenestration from the Middle Permian of South Africa. Canadian Journal of Earth Sciences 46: 9–20. https://doi.org/10.1139/E09-001

Molnar JL, Diogo R, Werneburg I, Boisvert CA (2022a) Tetrapod water-land transition: Reconstructing soft tissue anatomy and function. Frontiers Media SA, Lausanne. https://doi.org/10.3389/978-2-88976-787-8

Molnar JL, Diogo R, Werneburg I, Boisvert CA (2022b) Editorial: Tetrapod water-land transition: Reconstructing soft tissue anatomy and function. Frontiers in Ecology and Evolution 10: 1–3. https://doi.org/10.3389/fevo.2022.968979

Müller H, Oommen OV, Bartsch P (2005) Skeletal development of the direct-developing caecilian *Gegeneophis ramaswamii* (Amphibia: Gymnophiona: Caeciliidae). Zoomorphology 124: 171–188. https://doi.org/10.1007/s00435-005-0005-6

Nabavizadeh A (2020a) Cranial musculature in herbivorous dinosaurs: A survey of reconstructed anatomical diversity and feeding mechanisms. Anat Rec (Hoboken) 303: 1104–1145. https://doi.org/10.1002/ar.24283

Nabavizadeh A (2020b) New reconstruction of cranial musculature in ornithischian dinosaurs: implications for feeding mechanisms and buccal anatomy. Anatomical Record 303: 347–362. https://doi.org/10.1002/ar.23988

Nabavizadeh A (2023) How *Triceratops* got its face: An update on the functional evolution of the ceratopsian head. Anatomical Record 306: 1951–1968. https://doi.org/10.1002/ar.25196

Nabavizadeh A, Weishampel DB (2023) An illustrated guide to dinosaur feeding biology. John Hopkins University Press, Baltimore. https://doi.org/10.56021/9781421445878

Natchev N, Handschuh S, Lukanov S, Tzankov N, Naumov B, Werneburg I (2016) Contributions to the functional morphology of caudate skulls: kinetic and akinetic forms. PeerJ 5: 1–15. https://doi.org/10.7717/peerj.2392

Natchev N, Tzankov N, Werneburg I, Heiss E (2015) Feeding behaviour in a 'basal' tortoise provides insights on the transitional feeding mode at the dawn of modern land turtle evolution. PeerJ 3: 1–23. https://doi.org/10.7717/peerj.1172

Olson EC (1961) Jaw mechanisms: rhipidistians, amphibians, reptiles. Integrative and Comparative Biology 1: 205–215. https://doi.org/10.1093/icb/1.2.205

Ostrom JH (1964) A functional analysis of jaw mechanics in the dinosaur *Triceratops*. Postilla 88: 1–35.

Ostrom JH (1966) Functional morphology and evolution of the ceratopsian dinosaurs. Evolution 20: 290–308. https://doi.org/10.2307/2406631

Panchen AL (1964) The cranial anatomy of two Coal Measure anthracosaurs. Philosophical Transactions of the Royal Society of London B: Biological Sciences 247: 593–636. https://doi.org/10.1098/rstb.1964.0006

Panchen AL (1977) On *Anthracosaurus russelli* Huxley (Amphibia: Labyrinthodontia) and the family Anthracosauridae. Philosophical Transactions of the Royal Society of London B, Biological Sciences 279: 447–512. https://doi.org/10.1098/rstb.1977.0096

Piñeiro G, Ferigolo J, Ramos A, Laurin M (2012) Cranial morphology of the Early Permian mesosaurid *Mesosaurus tenuidens* and the evolution of the lower temporal fenestration reassessed. Comptes Rendus Palevol 11: 379–391. https://doi.org/10.1016/j.crpv.2012.02.001

Plateau O, Foth C (2020) Birds have peramorphic skulls, too: anatomical network analyses reveal oppositional heterochronies in avian skull evolution. Communications Biology 3: 195. https://doi.org/10.1038/s42003-020-0914-4

Porro LB, Martin-Silverstone E, Rayfield EJ (2024) Descriptive anatomy and three-dimensional reconstruction of the skull of the tetrapod *Eoherpeton watsoni* Panchen, 1975 from the Carboniferous of Scotland. Earth and Environmental Science Transactions of the Royal Society of Edinburgh 2024: 1–21. https://doi.org/10.1017/S175569102300018X

Preuschoft H (2022) Understanding Body Shapes of Animals: Shapes as Mechanical Constructions and Systems Moving on Minimal Energy Level. Springer, Cham, 581 pp. https://doi.org/10.1007/978-3-030-27668-3

Preuschoft H, Gudo M (2005) Der Schultergürtel der Wirbeltiere: Biomechanische Überlegungen zum Verständnis der Lokomotionsweisen von Tetrapoden. Zentralblatt für Geologie und Paläontologie, Teil II: 339–361.

Preuschoft H, Krahl A, Werneburg I (2022) From sprawling to parasagittal locomotion in Therapsida: A preliminary study of historically collected museum specimens. Vertebrate Zoology 72: 907–936. https://doi.org/10.3897/vz.72.e85989

Preuschoft H, Martin T, Werneburg I (in press) Remarks on the functional morphology of the earliest mammals. Mammalian Biology. https://doi.org/10.1007/s42991-024-00437-z

Preuschoft H, Witzel U (2002) Biomechanical investigations on the skulls of reptiles and mammals. Senckenbergiana lethaea 82: 207–222. https://doi.org/10.1007/BF03043785

Rasskin-Gutman D, Esteve-Altava B (2014) Connecting the dots: anatomical network analysis in morphological EvoDevo. Biological Theory 9: 178–193. https://doi.org/10.1007/s13752-014-0175-x

Rayfield EJ (2007) Finite element analysis and understanding the biomechanics and evolution of living and fossil organisms. Annual Review of Earth Planetary Science 35: 541–576. https://doi.org/10.1146/annurev.earth.35.031306.140104

Rieppel O (1980) The trigeminal jaw adductor musculature of *Tupinambis*, with comments on the phylogenetic relationship of the Teiidae (Reptilia, Lacertilia). Zoological Journal of the Linnean Society 69: 1–29. https://doi.org/10.1111/j.1096-3642.1980.tb01930.x

Rieppel O (1987) The development of the trigeminal jaw adductor musculature and associated skull elements in the lizard Podarcis sicula. Journal of Zoology 212: 131–150. https://doi.org/10.1111/j.1469-7998.1987.tb05120.x

Rieppel O (1992) The skull in a hatchling of *Sphenodon punctatus*. Journal of Herpetology 26: 80–84. https://doi.org/10.2307/1565028

Rieppel O (1993a) Patterns of Diversity in the Reptilian Skull. In: Hanken J, Hall BK (Eds) The Skull, Volume 2: Patterns of Structural and Systematic Diversity. University of Chicago Press, Chicago, 344–389.

Rieppel O (1993b) Studies on skeleton formation in reptiles. v. Patterns of ossification in the skeleton of *Alligator mississippiensis* DAUDIN (Reptilia, Crocodylia). Zoological Journal of the Linnean Society 109: 301–325. https://doi.org/10.1111/j.1096-3642.1993.tb02537.x

Rieppel O (1994) Studies on skeleton formation in reptiles - patterns of ossification in the skeleton of *Lacerta agilis exigua* Eichwald (Reptilia, Squamata). Journal of Herpetology 28: 145–153. https://doi.org/10.2307/1564613

Rieppel O (2008) The relationships of turtles within amniotes. In: Wyneken J, Godfrey MH, Bels V (Eds) Biology of Turtles. CRC Press, Boca Raton, London, New York, 345–353. https://doi.org/10.1201/9781420004977

Rollot Y, Evers SW, Ferreira GS, Girard LC, Werneburg I, Joyce WG (2024) Skull osteology, neuroanatomy, and jaw-related myology of the pig-nosed turtle *Carettochelys insculpta* (Cryptodira, Trionychia). Anatomical Record 307: 2966–3020. https://doi.org/10.1002/ar.25411

Sánchez-Villagra MR, Goswami A, Weisbecker V, Mock O, Kuratani S (2008) Conserved relative timing of cranial ossification patterns in early mammalian evolution. Evolution & Development 10: 519–530. https://doi.org/10.1111/j.1525-142X.2008.00267.x

Scheyer TM, Klein N, Evers SW, Mautner AK, Pabst B (2022) First evidence of *Proganochelys quenstedtii* (Testudinata) from the bonebeds (Norian, Late Triassic) of Frick, Canton Aargau, Switzerland. Swiss Journal of Palaeontology 141: 17. https://doi.org/10.1186/s13358-022-00260-4

Schlindwein X, Yaryhin O, Werneburg I (2022) Discrete embryonic character variation uncovers hidden ecological adaptations in lacertid lizards. Development Growth & Differentiation 64: 178–191. https://doi.org/10.1111/dgd.12777

Schoch RR (1992) Comparative ontogeny of early Permian brachiosaurid amphibians. Developmental stages. Palaeontographica A222: 43–83.

Schoch RR (1997) Cranial anatomy of the Permian temnospondyl amphibian *Zatrachys serratus* Cope 1878, and the phylogenetic position of the Zatrachydidae. Neues Jahrbuch für Geologie und Paläontologie - Abhandlungen 206: 223–248. https://doi.org/10.1127/njgpa/206/1997/223

Schoch RR (2014a) Amphibian Evolution: The Life of Early Land Vertebrates. Wiley Blackwell, Hobroken. https://doi.org/10.1002/9781118759127

Schoch RR (2014b) Amphibian skull evolution: The developmental and functional context of simplification, bone loss and heterotopy. Journal of Experimental Zoology Part B: Molecular and Developmental Evolution 322(8): 619–630. https://doi.org/10.1002/jez.b.22599

Schoch RR, Milner AR (2014) Temnospondyli. In: Sues H-D (Ed.) Handbook of Paleoherpetology Vol 3A2. Verlag Friedrich Pfeil, München, 1–150.

Schoenwolf GC, Mathews WW (2007) Atlas of Descriptive Embryology. Pearson Education, San Francisco.

Schroeder H (1913) Ein Stegocephalen-Schädel von Helgoland. Jahrbuch der Preussischen geologischen Landesanstalt 33: 232–264.

Schumacher GH (1985) Comparative Functional Anatomy of Jaw Muscles in Reptiles and Mammals. In: Dunker/Fleischer (Ed.) Fortschritte der Zoologie / Vertebrate Morphology. Gustav Fischer Verlag, Stuttgart, New York, 203–212.

Schwenk K [Ed.] (2000) Feeding: Form, Function and Evolution in Tetrapod Vertebrates. Vol. Academic Press, San Diego.

Simões TR, Kammerer CF, Caldwell MW, Pierce SE (2022) Successive climate crises in the deep past drove the early evolution and radiation of reptiles. Science Advances 8: eabq1898. https://doi.org/10.1126/sciadv.abq1898

Skews BW (2016) Hydrodynamics of an extinct amphibian. Journal of Applied Fluid Mechanics 9: 2899–2903. https://doi.org/10.29252/jafm.09.06.25634

Smith KT, Bhullar BAS, Köhler G, Habersetzer J (2018) The only known jawed vertebrate with four eyes and the Bauplan of the pineal complex. Current Biology 28: 1101–1107. https://doi.org/10.1016/j.cub.2018.02.021

Sookias RB, Dilkes D, Sobral G, Smith RMH, Wolvaardt FP, Arcucci AB, Bhullar BAS, Werneburg I (2020) The craniomandibular anatomy of the early archosauriform *Euparkeria capensis* and the dawn of the archosaur skull. Royal Society Open Science 7. https://doi.org/10.1098/rsos.200116

Spiekman SNF, Werneburg I (2017) Patterns in the bony skull development of marsupials: high variation in onset of ossification and conserved regions of bone contact. Nature Scientific Reports 7: 1–11. https://doi.org/10.1038/srep43197

Starck D (1979–1982) Vergleichende Anatomie der Wirbeltiere - auf evolutionsbiologischer Grundlage, Band 1–3. Springer-Verlag, Berlin, Heidelberg, New York. https://doi.org/10.1007/978-3-642-68421-0_1

Sues H-D, Reisz RR (1998) Origins and early evolution of herbivory in tetrapods. TREE 13: 141–145. https://doi.org/10.1016/S0169-5347(97)01257-3

Sues HD [Ed.] (2000) Evolution of Herbivory in Terrestrial Vertebrates. Perspectives from the Fossil Record. Vol. University Press, Cambridge. https://doi.org/10.1017/CBO9780511549717

Tokita M (2004) Morphogenesis of parrot jaw muscles: Understanding the development of an evolutionary novelty. Journal of Morphology 259: 69–81. https://doi.org/10.1002/jmor.10172

Tsuihiji T (2010) Reconstructions of the axial muscle insertions in the occipital region of dinosaurs: evaluations of past hypotheses on Marginocephalia and Tyrannosauridae using the extant phylogenetic bracket approach. Anatomical Record 293: 1360–1386. https://doi.org/10.1002/ar.21191

Tsuji LA, Müller J (2009) Assembling the history of the Parareptilia: phylogeny, diversification, and a new definition of the clade. Fossil Record 12: 71–81. https://doi.org/10.1002/mmng.200800011

Varriale FJ (2016) Dental microwear reveals mammal-like chewing in the neoceratopsian dinosaur *Leptoceratops gracilis*. PeerJ 4. https://doi.org/10.7717/peerj.2132

Wang Z, Pascual-Anaya J, Zadissa A, Li W, Niimura Y, Huang Z, Li C, White S, Xiong Z, Fang D, Wang B, Ming Y, Chen Y, Zheng Y, Kuraku S, Pignatelli M, Herrero J, Beal K, Nozawa M, Li1 Q, Wang J, Zhang H, Yu L, Shigenobu S, Wang J, Liu J, Flicek P, Searle S, Wang J, Kuratani S, Yin Y, Aken B, Zhang G, Irie N (2013) The draft genomes of soft-shell turtle and green sea turtle yield insights into the development and evolution of the turtle-specific body plan. Nature Genetics 45: 701–706. https://doi.org/10.1038/ng.2615

Weisbecker V, Mitgutsch C (2010) A large-scale survey of heterochrony in anuran cranial ossification patterns. Journal of Zoological Systematics and Evolutionary Research 48: 332–347. https://doi.org/10.1111/j.1439-0469.2010.00570.x

Weishampel DB, Dodson P, Osmolska H [Eds] (2004) The Dinosauria. Second edition. Vol. University of California Press, Berkeley, Los Angeles & London, [i–xviii,] 861 pp.

Werneburg I (2009) A standard system to study vertebrate embryos. PLOS ONE 4(6): e5887. https://doi.org/10.1371/journal.pone.0005887

Werneburg I (2011) The cranial musculature in turtles. Palaeontologia Electronica 14: 15a. [99 pp] https://palaeo-electronica.org/2011_2/254/254.pdf

Werneburg I (2012) Temporal bone arrangements in turtles: an overview. The Journal of Experimental Zoology B 318: 235–249. https://doi.org/10.1002/jez.b.22450

Werneburg I (2013a) Jaw musculature during the dawn of turtle evolution. Organisms, Diversity & Evolution 13: 225–254. https://doi.org/10.1007/s13127-012-0103-5

Werneburg I (2013b) The tendinous framework in the temporal skull region of turtles and considerations about its morphological implications in amniotes: a review. Zoological Science 31: 141–153. https://doi.org/10.2108/zsj.30.141

Werneburg I (2015) Neck motion in turtles and its relation to the shape of the temporal skull region. Comptes Rendus Palevol 14: 527–548. https://doi.org/10.1016/j.crpv.2015.01.007

Werneburg I (2019) Morphofunctional categories and ontogenetic origin of temporal skull openings in amniotes. Frontiers in Earth Science 7: 13. https://doi.org/10.3389/feart.2019.00013

Werneburg I (2020) Konsequenzen der Panzer-Produktion auf die Radkettenmechanik und deren Wirkung auf terminale Greifarm-Effizienz bei Schildkröten. In: Werneburg I, Betz O (Eds) Phylogenie, Funktionsmorphologie und Bionik Schriften zum 60 Phylogenetischen Symposium in Tübingen. Scidinge Hall Verlag, Tübingen, 277–316.

Werneburg I (2024) Biomechanische Grundlagen der Schläfenevolution bei Landwirbeltieren. Jahreshefte der Gesellschaft für Naturkunde in Württemberg 180. [in press]

Werneburg I, Abel P (2022) Modeling skull network integrity at the dawn of amniote diversification with considerations on Functional morphology and fossil jaw muscle reconstructions. Frontiers in Ecology and Evolution 9: 799637. https://doi.org/10.3389/fevo.2021.799637

Werneburg I, Bronzati M (in press) Trifold origin of the reptilian ear ossicle and its relation to the evolutionary modification of the temporal skull region. Journal of Anatomy 00: 1–13. https://doi.org/10.1111/joa.14105

Werneburg I, Esteve-Altava B, Bruno J, Torres Ladeira M, Diogo R (2019) Unique skull network complexity of *Tyrannosaurus rex* among land vertebrates. Scientific Reports 9: 1520. https://doi.org/10.1038/s41598-018-37976-8

Werneburg I, Evers SW, Ferreira G (2021) On the “cartilaginous rider” in the endocasts of turtle brain cavities. Vertebrate Zoology 71: 403–418. https://doi.org/10.3897/vz.71.e66756

Werneburg I, Hinz JK, Gumpenberger M, Volpato V, Natchev N, Joyce WG (2015a) Modeling neck mobility in fossil turtles. Journal of Experimental Zoology, Part B, Molecular and Developmental Evolution 324: 230–243. https://doi.org/10.1002/jez.b.22557

Werneburg I, Hoßfeld U, Levit G (2024a) Darwin, Haeckel, and the »Mikluskan gas organ theory«. Developmental Dynamics 253: 370–389. https://doi.org/10.1002/dvdy.661

Werneburg I, Hugi J, Müller J, Sánchez-Villagra MR (2009) Embryogenesis and ossification of *Emydura subglobosa* (Testudines, Pleurodira, Chelidae) and patterns of turtle development. Developmental Dynamics: an official publication of the American Association of Anatomists 238: 2770–2786. https://doi.org/10.1002/dvdy.22104

Werneburg I, Krahl A, Zhang Z (2024b) Chelonia: Morphology of a Stiffened Body. In: Joger U (Ed.) Reptilia Volume 1: General Biology, Archosauria. Walter de Gruyter GmbH, Berlin/Boston, 201–233. https://doi.org/10.1515/9783110367256-010

Werneburg I, Maier W (2019) Diverging development of akinetic skulls in cryptodire and pleurodire turtles: an ontogenetic and phylogenetic study. Vertebrate Zoology 69: 113–143.

Werneburg I, Polachowski KM, Hutchinson MN (2015c) Bony skull development in the Argus monitor (Squamata, Varanidae, *Varanus panoptes*) with comments on developmental timing and adult anatomy. Zoology 118: 255–280. https://doi.org/10.1016/j.zool.2015.02.004

Werneburg I, Preuschoft H (2023) Biomechanical basics for the evolution of cranial openings in amniotes. Anatomical Record Special Issue: Abstracts of ICVM2023, Cairns/Australia: 231–232.

Werneburg I, Preuschoft H (2024) Evolution of the temporal skull openings in land vertebrates: A hypothetical framework on the basis of biomechanics. Anatomical Record-Advances in Integrative Anatomy and Evolutionary Biology 307: 1559–1593. https://doi.org/10.1002/ar.25371

Werneburg I, Sánchez-Villagra MR (2015) Skeletal heterochrony is associated with the anatomical specializations of snakes among squamate reptiles. Evolution 69: 254–263. https://doi.org/10.1111/evo.12559

Werneburg I, Wilson LAB, Parr WCH, Joyce WG (2015b) Evolution of neck vertebral shape and neck retraction at the transition to modern turtles: an integrated geometric morphometric approach. Systematic Biology 64: 187–204. https://doi.org/10.1093/sysbio/syu072

Werneburg R, Witzmann F, Schneider JW, Rössler R (2023) A new basal zatracheid temnospondyl from the early Permian Chemnitz Fossil Lagerstatte, central-east Germany. Palz 97: 105–128. https://doi.org/10.1007/s12542-022-00624-8

Williston SW (1925) The Osteology of the Reptiles. Harvard University Press, Cambridge. https://doi.org/10.5962/bhl.title.6573

Witmer LM (1997) The evolution of the antorbital cavity of archosaurs: A study in soft-tissue reconstruction in the fossil record with an analysis of the function of pneumaticity. Journal of Vertebrate Paleontology 17: 1–73. https://doi.org/10.1080/02724634.1997.10011027

Witzel U, Preuschoft H (2005) Finite-element model construction for the virtual synthesis of the skulls in vertebrates: case study of *Diplodocus*. The Anatomical Record 283: 391–401. https://doi.org/10.1002/ar.a.20174

Witzmann F, Ruta M (2018) Evolutionary changes in the orbits and palatal openings of early tetrapods, with emphasis on temnospondyls. Earth and Environmental Science Transactions of the Royal Society of Edinburgh 109: 333–350. https://doi.org/10.1017/S1755691018000919

Witzmann F, Schoch RR (2006) Skeletal development of the temnospondyl from the Lower Permian Dohlen Basin of Saxony. Transactions of the Royal Society of Edinburgh-Earth Sciences 96: 365–385. https://doi.org/10.1017/S0263593300001358

Witzmann F, Werneburg I (2017) The palatal interpterygoid vacuities of temnospondyls and the implications for the associated eye-and jaw musculature. The Anatomical Record 300: 1240–1269. https://doi.org/10.1002/ar.23582

Witzmann F, Brainerd EL, Konow N (2019) Eye movements in frogs and salamanders—testing the palatal buccal pump hypothesis. Integrative Organismal Biology 1(1): obz011. https://doi.org/10.1093/iob/obz011

Xing LD, Niu KC, Ma WS, Zelenitsky DK, Yang TR, Brusatte SL (2022) An exquisitely preserved theropod dinosaur embryo sheds light on avian-like prehatching postures. Iscience 25(1): 103516. https://doi.org/10.1016/j.isci.2021.103516

Yaryhin O, Werneburg I (2019) The origin of orbitotemporal diversity in lepidosaurs: insights from tuatara chondrocranial anatomy. Vertebrate Zoology 69: 169–181. https://doi.org/10.26049/Vz69-2-2019-04

Zhang Z, Cordero AG, Werneburg I (2024) Embryology and Life history of Reptilia with a Focus on the Organogenesis of Squamates. In: Joger U (Ed.) Handbuch der Zoologie, Reptilia 1. DeGruyter, Berlin, 13–37. https://doi.org/10.1515/9783110367256-002

Zhang ZT, Yaryhin O, Koyabu D, Werneburg I (2022) Morphological association between muscle attachments and ossification sites in the late cartilaginous skull of tuatara embryos. Journal of Morphology 283: 908–931. https://doi.org/10.1002/jmor.21474

Ziermann JM, Clement AM, Ericsson R, Olsson L (2018) Cephalic muscle development in the Australian lungfish,. Journal of Morphology 279: 494–516. https://doi.org/10.1002/jmor.20784

Ziermann JM, Diaz RE, Diogo R (2019) Heads, Jaws, and Muscles. Anatomical, Functional, and Developmental Diversity in Chordate Evolution. Springer, Cham. https://doi.org/10.1007/978-3-319-93560-7

Appendix 1

Abbreviations:

an, angular; **bo**, basioccipital; **bs**, basisphenoid; **co**, coronoid; **de**, dentary; **ec**, ectopterygoid; **eo**, exoccipital; **ECM**, m. episternocleidomastoideus; **f**, frontal; $\boldsymbol{F}$, force; $\boldsymbol{F}_{\mathbf{a1}}$, force of the medial most jaw adductor muscle portion; $\boldsymbol{F}_{\mathbf{a2}}$, force of the lateral most jaw adductor muscle portion; $\boldsymbol{F}_{\mathbf{a2}}$*****, possible anterior insertion of the "chewing" muscle in *Protoceratops*; $\boldsymbol{F}_{\mathbf{a3}}$, force of the jaw adductor muscle portion in between F_{a1} and F_{a2}; $\boldsymbol{F}_{\mathbf{bpA}}$, anterior perpendicular bite force (at the "caninus"-position); $\boldsymbol{F}_{\mathbf{bpA*}}$, most anterior perpendicular bite force (at the "incicivus"-position; $\boldsymbol{F}_{\mathbf{bpP}}$, posterior perpendicular bite force (at the "caninus"-position); $\boldsymbol{F}_{\mathbf{btA}}$, anterior transversal bite force in the back of the mouth; $\boldsymbol{F}_{\mathbf{C}}$, force acting laterally on the cheek extension; $\boldsymbol{F}_{\mathbf{i}}$, inertia force; $\boldsymbol{F}_{\mathbf{F}}$, force acting laterally on the frill; $\boldsymbol{F}_{\mathbf{N1}}$, force of the medial most dorsal neck muscle; $\boldsymbol{F}_{\mathbf{N2}}$, force of the neck muscle that inserts lateral most to the skull; $\boldsymbol{F}_{\mathbf{N3}}$, force of the neck muscle placed between F_{N1} and F_{N2}; $\boldsymbol{F}_{\mathbf{NH}}$, force acting on the nasal horn; $\boldsymbol{F}_{\mathbf{pLH}}$, force acting perpendicularly on the lateral horn; $\boldsymbol{F}_{\mathbf{pLH}}$, large pulling force acting transversally away from the lateral horn; $\boldsymbol{F}_{\mathbf{pLH*}}$, small pulling force acting transversally away from the lateral horn; $\boldsymbol{F}_{\mathbf{S}}$, force at the scruff of the neck (neck vertebra vs. occipital condyle); **ij**, insula jugalis; **ip**, interparietal; **it**, intertabular; **ju**, jugal; **la**, lacrimal; **LCap**, m. longissimus capitis Pars articuloparietalis; **lt**, laterosphenoid; **mx**, maxilla; **n**, nasal; **oc**, occipital; **OCM**, m. obliquus capitis magnus; **op**, opisthotic; **p**, parietal; **pbs**, parabasisphenoid; **pc**, parietal crest; **pd**, predental; **po**, postorbital; **pof**, postfrontal; **prf**, prefrontal; **pmx**, premaxilla; **po**, paroccipital; **posp**, postsplenial; **pp**, postparietal; **prsp**, presplenial; **ps**, parasphenoid; **ps-pc**, cultriform process of parasphenoid; **pt**, pterygoid; **q**, quadrate; **qj**, quadratojugal; **r**, rhamphoteca; **RCA**, m. rectus capitis anterior; **sa**, surangular; **SC**, m. spinalis captitis; **so**, supraoccipital; **sq**, squamosal; **t**, tabular; **v**, vomer, **α**, compressive stress; **β**, tensional stress.

Colour code for forces (*F*) and related stresses (dashed lines):

blue (dark), posterior bite; **blue (light)**, external force on the cheek; **brown**, transversal anterior bite; **green (dark)**, jaw joint; **green (light) in Fig. 3B–D**, inertia force and direction of skull move to the left side; **green (light) in Fig. 4D–F**, nasal horn; **orange (dark)**, jaw adductor muscles; **orange (light)**, neck muscles; **pink**, transversal force(s) on the lateral horn; **red**, anterior bite(s); **black**, external force(s) on the frill/posterior edge of the skull table; **yellow**, neck muscle related. Dashed lines indicate stress flows of merely compressive (α), tensional (β), or mixed (γ) stress.